
A Study on the Effect of Heavy Metals and Leachates on Engineering Behaviour of Bentonite

*A thesis submitted in partial fulfilment of the requirement
for the award of the degree of*

Doctor of Philosophy

by

SASWATI RAY



**Department of Civil Engineering
Indian Institute of Technology Guwahati
Guwahati – 781 039, Assam, India**

May 2021

A Study on the Effect of Heavy Metals and Leachates on Engineering Behaviour of Bentonite

*A thesis submitted in partial fulfilment of the requirement
for the award of the degree of*

Doctor of Philosophy

by

SASWATI RAY



**Department of Civil Engineering
Indian Institute of Technology Guwahati
Guwahati – 781 039, Assam, India**

May 2021



Dedicated

to

Maa and Baba

*For lifting me up during my hardest times with their unconditional love and
care...*





Department of Civil Engineering
Indian Institute of Technology Guwahati
Guwahati – 781039
Assam, India

Candidate's Declaration

This is to certify that the thesis entitled “**A study on the effect of heavy metals and leachates on the engineering behaviour of bentonite**”, submitted by me to the Indian Institute of Technology Guwahati, for the award of the degree of Doctor of Philosophy, is a Bonafede work carried out by me. The contents of this thesis, in full or in parts, have not been submitted to any other University or Institute for the award of any degree or diploma.

Date: 12-01-2021

Saswati Ray

Registration No.: 156104018



Department of Civil Engineering
Indian Institute of Technology Guwahati
Guwahati – 781039
Assam, India

Dr. Anil Kumar Mishra

Associate Professor

Email: anilmishra@iitg.ac.in

Phone: +91-361-258-2435

Dr. Ajay Kalamdhad

Professor

Email: kajay@iitg.ac.in

Phone: +91-361-258-2431

Certificate

This is to certify that the thesis entitled “**A study on the effect of heavy metals and leachates on the engineering behaviour of bentonite**”, submitted by Saswati Ray (156104018), a Research scholar in the Department of Civil Engineering, Indian Institute of Technology Guwahati, for the award of the degree of Doctor of Philosophy, is a record of an original research work carried out by her under our supervision and guidance. The thesis has fulfilled all requirements as per the regulations of the institute and in our opinion has reached the standard needed for submission. The results embodied in this thesis have not been submitted to any other University or Institute for the award of any degree or diploma.

Date:

Place: IIT Guwahati

Dr. Anil Kumar Mishra

Dr. Ajay Kalamdhad

Acknowledgements

The work completed in this thesis could not have been done without the help of many individuals over the past five years. First and foremost, I am extremely grateful to my supervisor, **Dr. Anil Kumar Mishra**, for his guidance, patience, motivation, answering my endless stream of questions regarding expansive soil and immense knowledge. I am also profoundly grateful that he gave me the opportunity to travel, meet people in the profession, and gain knowledge and expertise outside the bounds of my dissertation research. I will forever benefit from these experiences. It has been an honour and a privilege to work with a great professor and a great person.

I would like to express my gratitude to my co-supervisor, **Dr. Ajay Kalamdhad**, who has been a mentor, for offering support and direction on this research. This document is the culmination of five years of effort and would not have been possible without him. He has been an effective mentor, and I will carry the lessons I have learned from him, especially management skills, for years to come. I am grateful for the principles he instilled in me and his guidance. Apart from research, he constantly motivates me and prepares me for building leadership qualities and professional competence.

Besides my supervisors, I would like to thank the chairman of my Doctoral Committee **Dr. Pranab K. Ghosh** and other members **Dr. T. V. Bharat** and **Dr. Chivakula Sastri**, for their valuable, insightful comments and encouragement. Their suggestions incited me to widen my research from various perspectives.

I would take this opportunity to thank the Director of IIT Guwahati for providing necessary facilities and conducive academic environment. I sincerely thank the Ministry of Human Resource Development, India for providing necessary financial support. I am equally grateful to the Department of Physics, Central Instruments Facility, and Central Library, IIT G, to provide me state of the art infrastructure for advanced research level.

I would also like to extend my sincerest thanks to Head of the Department, Civil Engineering for providing me with necessary laboratory and research facilities. My utmost thanks to the technical staffs of the Civil Department for their support in administration work. I gratefully acknowledge the generous help provided by Mr Chitaranjan Medhi, Mr Hari Ram Upadhyaya and Mr Pathak during all phases of my research work.

I express my gratitude towards all the present and past lab members in the Civil Engineering Department for their technical support, understanding and encouragement in

my moments of crisis. I cannot list all names here, but you are always on my mind. I need to thank all the cheerful group members of the Waste Management Research Group (WMRG) for their precious support and stimulating discussions. It was my great pleasure to associate with the members of WMRG.

My utmost thanks and regards to Dr. Anuj Kumar Baruah, Dr. Devanand Pathak, and Ms. Pallabita B Chowdhury for their constant support and motivation.

I owe my goodwill in research and personal life to my brother and best friend Mr. Siddhant Dash for his constant help and support through thick and thin. I will always remain indebted to my friend Dr. Amalesh Jana for his continuous support and motivation. My discussions and argument with him gave me hope and inspiration.

I extend a special acknowledgement to Dr. Subrat Mallick, Dr. Srikanth Vadlamudi, Mr. Chandra Bhanu Gupt, Mr. Arun Satyan, Mr. Ankur Pandey, Mr. Venkatesh Reddy and Ms. Payal Mazumder for their extending help and scholarly interactions. I am very thankful to my friends Ms. Gargi Majumder, Dr. Jyoti Kainthola, Ms. Priyanka Kotoky, Ms. Shinjini Paul Choudhury, Ms. Aritra Das, Ms. Swati Sarkar, Ms. Aparajita Dutta, Mr. Ankit Goswami, Dr. Vinay Kumar Gadi and Mr. Nuthalapati Mahesh Babu for making me feel homely and joyful during my stay in Campus. I will never forget all the conversations and lovely moments I shared with my friends.

I am most grateful to my dear brother, Dr. Soumik Ray for the ceaseless love and motivation. His strength and support in my life cannot be quantified. I am also thankful to my friend and sister-in-law, Ms. Bisakha Bakshi for her invaluable life advice and care.

Finally, I must express my very profound gratitude to my amazing parents, **Mrs. Nandini Ray** and **Shri Tanay Kumar Ray** for providing me with unfailing support, continuous encouragement, unconditional love and blessing throughout my years of study and through the process of researching and writing this thesis. This accomplishment would not have been possible without them.

Above all, I would like to thank the Almighty for giving me the wisdom, health, strength and the perseverance to complete this research.

Date: 12-01-2021

Saswati Ray

Abstract

A rapid increase in industrialization is leading to the generation of high metal toxicity to the ecosystem. Landfilling has been carried out as the most preferred method of waste disposal around the globe. Leachates generated from wastes inside the landfills decrease the efficiency of the liner material. These leachates can also migrate toward the surrounding environment and groundwater, and pollute it. Therefore, a low-permeable liner is provided at the bottom of the landfill to separate the waste and groundwater. Bentonite is an inexpensive natural resource refined from volcanic ash consisting mostly of montmorillonite mineral can be used as a liner material in landfills due to its low hydraulic conductivity, high adsorption capacity, high cation exchange capacity and capacity to retard the percolation of pollutant through sorption.

Due to the presence of harmful chemicals, the properties of liner materials may alter. Since the bentonite varying in their mineralogical and chemical properties performs differently with different metal contaminants, hence, it is also needed to compare the change in behaviour of bentonites in the presence of various metal contaminants. In the present study, two bentonites of different mineralogical composition were considered. Bentonite-1 possessed higher liquid limit, montmorillonite content, specific surface area (SSA), and cation exchange capacity (CEC) than Bentonite-2, and thus, was marked as a superior quality bentonite. Both bentonites were studied for their change in the index properties, swelling, swelling potential, swelling pressure, hydraulic conductivity, consolidation parameters, shear strength properties and sorption characteristics in the presence of different heavy metals of various concentrations and different leachates. In the present study, two bentonites of different mineralogical composition were studied for their change in the index properties, swelling, swelling potential, swelling pressure, hydraulic conductivity, consolidation parameters, shear strength properties and sorption characteristics in the presence of different heavy metals of various concentrations and different leachates. Different isotherm models were used to determine the best-fit equilibrium isotherms. Kinetic models were fitted to investigate the kinetics and mechanisms of metal sorption on both the bentonites. Field emission scanning electron microscopy (FESEM) and Fourier Transform Infrared (FTIR) studies were conducted to analyze the change in surface morphology and alteration in FTIR pattern in both the bentonites before and after sorption of heavy metals.

The results showed that the liquid limit, free swelling, swelling potential and swelling pressure of the bentonites decreased with an increase in the heavy metal ion concentration and the presence of leachates. The reduction in these parameters is attributed to the decrease in the diffuse double layer thickness. Results also indicated that compression index (C_c) and time required for the 90% of consolidation (t_{90}) decreased. In contrast, the coefficient of consolidation (c_v) and hydraulic conductivity (k) increased in the presence of heavy metals and leachates. Both the bentonites showed a reduction in the Unconfined Compression Strength in the presence of heavy metals and leachates, yet, lying within the recommended value of $>200\text{kPa}$. The study showed that pH influenced the adsorption of heavy metals for both bentonites. Isotherms' investigation reveals that both the isotherm model fits well with equilibrium data. Kinetic studies followed the Pseudo-second order model.

A comparison between the two bentonites showed that metals and leachates have a significant effect on Bentonite-1. Bentonite-1, which has a high liquid limit, swelling capacity, SSA, CEC and montmorillonite content, undergoes a massive change in the liquid limit, free swelling, swelling pressure and hydraulic conductivity due to the presence of the various permeants.

The results showed that the sorption capacity of Bentonite-1 was found to be higher than Bentonite-2 under the same initial concentration in the presence of all the metals and leachates. The leachates had a considerable effect on the liquid limits, swelling pressure, and swelling potential of both the bentonites, compared to an individual heavy metal solution. This study concluded that the effect of the metal contaminants on the properties of the bentonites depends on the factors such as type and concentration of metal and composition of bentonite. Similarly, the study also concluded that physical and mineralogical properties, i.e., specific surface area, montmorillonite content, swelling capacity, and cation exchange capacity, exhibit potential usage of bentonite as an adsorbent.

Keywords: Bentonite; Heavy metals; Leachates; Consolidation; Adsorption; Diffuse double layer; Swelling potential; Swelling pressure; Hydraulic conductivity; Compressibility.

Contents

| | Page No. |
|--|---------------------|
| ACKNOWLEDGEMENTS | iii |
| ABSTRACT | v |
| LIST OF FIGURES | xiii |
| LIST OF TABLES | xxi |
| ABBREVIATIONS | xxv |
| SYMBOLS USED | xxvii |
| 1 INTRODUCTION | 1 |
| 1.1. General | 1 |
| 1.2. Thesis Organization | 4 |
| 2 BACKGROUND AND LITERATURE REVIEW | 5 |
| 2.1. Context | 5 |
| 2.2. General | 5 |
| 2.3. Present Situation of Waste Management and Disposal | 6 |
| 2.4. Landfill liners | 7 |
| 2.5. Landfill design method adopted in different countries | 9 |
| 2.6. Design parameters for landfill liners | 10 |
| 2.6.1. Hydraulic conductivity | 10 |
| 2.6.2. Shear strength | 12 |
| 2.6.3. Volumetric shrinkage | 12 |
| 2.7. Use of Bentonite as a liner material | 12 |
| 2.7.1. Introduction | 12 |
| 2.7.2. Structure of montmorillonite | 13 |
| 2.7.3. Swelling behaviour of bentonite | 15 |
| 2.7.3.1. Inner-crystalline swelling | 15 |
| 2.7.3.2. Osmotic swelling | 16 |
| 2.8. Diffuse double layer | 18 |

| | |
|--|----|
| 2.8.1. Factors affecting diffuse double layer (DDL) thickness | 19 |
| 2.9 Engineering properties of bentonite | 20 |
| 2.9.1. Swelling pressure | 20 |
| 2.9.2. Swelling potential | 21 |
| 2.9.3. Compressibility | 21 |
| 2.9.4. Hydraulic conductivity | 22 |
| 2.9.4.1. Influence of salt on hydraulic conductivity of clay | 23 |
| 2.9.4.2. Effect of bentonite waste interaction on hydraulic conductivity | 23 |
| 2.9.5. Adsorption | 24 |
| 2.10. Review of published work on salt Solutions | 25 |
| 2.11. Heavy metals | 29 |
| 2.11.1. Sources and Impact of heavy metal | 30 |
| 2.11.2. Disposal of waste containing heavy metal in the landfills | 32 |
| 2.11.3. Impact of heavy metal on liner material | 34 |
| 2.11.4. Impact of heavy metal on engineering behaviour of liner material | 35 |
| 2.11.4.1. Atterberg limits | 35 |
| 2.11.4.2. Free swelling | 36 |
| 2.11.4.3. Hydraulic conductivity | 36 |
| 2.11.4.4. Compressibility | 36 |
| 2.11.4.5. Shear strength | 36 |
| 2.11.4.6. Consolidation characteristics | 37 |
| 2.12. Review of published work on metal solutions | 37 |
| 2.13. Review of published work on adsorption of Pb^{2+} | 40 |
| 2.14. Review of published work on adsorption of Cu^{2+} | 43 |
| 2.15. Review of published work on adsorption of Zn^{2+} | 45 |
| 2.16. Generation of leachate from MSW | 47 |
| 2.16.1. Composition of leachate | 47 |
| 2.16.2. Effect of leachate on liner material | 48 |
| 2.17. Review of published works on various leachates | 48 |
| 2.18. Summary and critical appraisal of literature review | 50 |
| 2.19. Research gap | 51 |
| 2.20. Objectives of the study | 51 |

| | |
|--|-----------|
| 2.21. Scope of the thesis | 52 |
| 3 MATERIALS AND METHODOLOGY | 53 |
| 3.1. Context | 53 |
| 3.2. Design of research work | 53 |
| 3.3. Procurement of bentonites and their characterization | 56 |
| 3.4. Permeant liquid | 60 |
| 3.4.1. Metal preparation | 60 |
| 3.4.2. Leachate preparation | 61 |
| 3.5. Determination of hydraulic conductivity and consolidation characteristics | 64 |
| 3.6. Estimation of swelling potential and swelling pressure | 67 |
| 3.7. Unconfined compression test | 68 |
| 3.8. pH study | 69 |
| 3.9. Batch study | 70 |
| 3.10. Sorption isotherm study | 71 |
| 3.11. Kinetic study | 72 |
| 4 INFLUENCE OF HEAVY METALS ON THE BEHAVIOUR OF BENTONITES | 75 |
| 4.1. Introduction | 75 |
| 4.2. Results and Discussion | 77 |
| 4.2.1. Influence of heavy metals on liquid limits | 77 |
| 4.2.2. Influence of heavy metals on Free swelling | 78 |
| 4.2.3. Influence of heavy metals on swelling pressure | 79 |
| 4.2.4. Influence of heavy metals on swelling potential | 80 |
| 4.2.5. Influence of heavy metals on Time swelling relationship | 81 |
| 4.2.6. Influence of heavy metals on Hydraulic conductivity | 85 |
| 4.2.7. Influence of heavy metals on compressibility behaviour of bentonite | 88 |
| 4.2.8. Coefficient of consolidation (c_v) | 91 |
| 4.2.9. Time for 90% of consolidation (t_{90}) | 93 |
| 4.2.10. Compression index (C_c) | 96 |
| 4.2.11. Unconfined compressive strength (UCS) of bentonites | 96 |
| 4.2.12. pH study | 101 |

| | |
|--|------------|
| 4.2.13. Batch adsorption study | 104 |
| 4.2.14. Isotherm study | 109 |
| 4.2.15. Dose study | 113 |
| 4.2.16. Contact time | 117 |
| 4.2.17. Kinetic study | 119 |
| 4.2.18. FESEM study | 123 |
| 4.2.19. FTIR study | 130 |
| 4.3. Summary | 136 |
| | |
| 5 EFFECT OF MSW AND SYNTHETIC MSW ON THE BEHAVIOUR OF BENTONITES | 141 |
| 5.1. Introduction | 141 |
| 5.2. Results and Discussions | 144 |
| 5.2.1. Effect of MSW and synthetic MSW leachates on Liquid limit | 144 |
| 5.2.2. Effect of MSW and synthetic MSW leachates on Free swell | 145 |
| 5.2.3. Effect of MSW and synthetic MSW leachates on Swelling potential and Swelling pressure of bentonites | 146 |
| 5.2.4. Effect of MSW and synthetic MSW leachates on Time swelling relationship | 147 |
| 5.2.5. Effect of MSW and synthetic MSW leachates on Hydraulic conductivity | 149 |
| 5.2.6. Void ratio-pressure (e -log P) relationships in the presence of leachates | 151 |
| 5.2.7. Influence of leachates on Coefficient of consolidation (c_v) | 152 |
| 5.2.8. Influence of leachates on Time for 90% of consolidation (t_{90}) | 154 |
| 5.2.9. Influence of leachates on Compression index (C_c) of bentonites | 155 |
| 5.2.10. Influence of leachates on Unconfined compressive strength of both bentonites | 156 |
| 5.2.11. Adsorption of MSW and synthetic MSW leachate | 157 |
| 5.2.12. Effect of MSW and synthetic MSW leachate on dose of bentonites | 161 |
| 5.2.13. Kinetic study of MSW and synthetic MSW leachate | 169 |
| 5.2.13.1. Effect of contact time | 169 |
| 5.2.13.2. Kinetic model | 172 |
| 5.3. Summary | 183 |

| | | |
|-----------|---|------------|
| 6 | INFLUENCE OF VARIOUS LEACHATES ON THE BEHAVIOUR OF BENTONITES | 185 |
| 6.1. | Introduction | 185 |
| 6.2. | Results and Discussions | 187 |
| 6.2.1. | Impact of leachates on liquid limit and free swell | 187 |
| 6.2.2. | Impact of leachates on swelling pressure and swelling potential | 188 |
| 6.2.3. | Impact of synthetic leachates on Time-swelling plot | 189 |
| 6.2.4. | Impact of leachates on Hydraulic conductivity | 192 |
| 6.2.5. | Impact of leachates on compressibility behaviour of bentonites | 194 |
| 6.2.6. | Impact of leachates on Coefficient of consolidation (c_v) of bentonites | 196 |
| 6.2.7. | Impact of leachates on t_{90} of bentonites | 198 |
| 6.2.8. | Impact of leachates on Compression index (C_c) of bentonites | 200 |
| 6.2.9. | Impact of leachates on UCS of bentonites | 200 |
| 6.2.10. | Adsorption of various leachates on bentonites | 203 |
| 6.2.11. | Effect of leachates on various bentonite doses | 207 |
| 6.2.12. | Kinetic study of various leachates | 220 |
| 6.2.12.1. | Effect of contact time | 220 |
| 6.2.12.2. | Kinetic model | 224 |
| 6.3. | Summary | 238 |
| 7 | CONCLUSIONS AND FUTURE SCOPE OF WORK | 239 |
| 7.1. | Conclusions | 239 |
| 7.2. | Scientific contributions and practical applications of the research | 240 |
| 7.3. | Scope for the future work | 241 |
| | REFERENCES | 243 |
| | LIST OF PUBLICATIONS | 269 |



List of Figures

| Figure No. | Caption | Page No. |
|------------------|--|----------|
| Chapter 2 | | |
| 2.1 | Cross section of a typical waste disposal site | 8 |
| 2.2 | Liner systems specified in Europe and America | 10 |
| 2.3 | Japanese liner systems | 10 |
| 2.4 | The effect of compaction water content (w) and dry density on the orientation of the soil fabric | 11 |
| 2.5 | Acceptable zone for hydraulic conductivity | 11 |
| 2.6 | Structure of montmorillonite | 14 |
| 2.7.a | Inner-crystalline swelling of sodium montmorillonite. | 16 |
| 2.7.b | The structure of water molecule | 16 |
| 2.8.a | Two negatively charged clay layers with ion cloud. | 18 |
| 2.8.b | Negatively charged clay surface, ions in the diffuse double layer and ions in the pore water. | 18 |
| 2.9 | Gouy-Chapman diffuse double layer model | 19 |
| Chapter 3 | | |
| 2.10 | Mechanism of the swelling pressure of compacted bentonite | 20 |
| 3.1 | Design of research work | 55 |
| 3.2 | Bentonite images | 57 |
| 3.3 | XRD plot for Bentonites-1 and -2 | 58 |
| 3.4 | FTIR plot of both the bentonites | 59 |
| 3.5 | FESEM images of the bentonites | 60 |
| 3.6 | Consolidation setup in the laboratory and its schematic diagram | 65 |
| 3.7 | Taylor's square root-of-time fitting method | 66 |
| 3.8 | Determination of swelling pressure and swelling potential | 68 |
| 3.9 | Unconfined compressive strength (UCS) testing machine | 69 |
| 3.10 | Batch adsorption study | 70 |

Chapter 4

| | | |
|------|--|----|
| 4.1 | Liquid limits of Bentonite-1 and -2 in the presence of different concentrations of heavy metals | 78 |
| 4.2 | Plots for the free swelling of Bentonite-1 and -2 in the presence of different concentrations of heavy metals | 79 |
| 4.3 | Time–swelling plot for Bentonite-1 compacted at MDD-OMC in the presence of various Pb^{2+} concentration | 82 |
| 4.4 | Time–swelling plot for Bentonite-2 compacted at MDD-OMC in the presence of various Pb^{2+} concentration | 82 |
| 4.5 | Time–swelling plot for Bentonite-1 compacted at MDD-OMC in the presence of various Zn^{2+} concentration | 83 |
| 4.6 | Time–swelling plot for Bentonite-2 compacted at MDD-OMC in the presence of various Zn^{2+} concentration | 83 |
| 4.7 | Time–swelling plot for Bentonite-1 compacted at MDD-OMC in the presence of various Cu^{2+} concentration | 84 |
| 4.8 | Time–swelling plot for Bentonite-2 compacted at MDD-OMC in the presence of various Cu^{2+} concentration | 84 |
| 4.9 | Void ratio-hydraulic conductivity plots for Bentonite-1 and -2 compacted at MDD-OMC in presence of various concentration of Pb^{2+} | 85 |
| 4.10 | Void ratio-hydraulic conductivity plots for Bentonite-1 and -2 compacted at MDD-OMC in presence of various concentration of Cu^{2+} | 86 |
| 4.11 | Void ratio-hydraulic conductivity plots for Bentonite-1 and -2 compacted at MDD-OMC in the presence of various concentrations of Zn^{2+} | 86 |
| 4.12 | Void ratio-pressure plots for Bentonite-1 and -2 in the presence of various Pb^{2+} concentration at OMC-MDD | 89 |
| 4.13 | Void ratio-pressure plots for Bentonite-1 and -2 in the presence of various Cu^{2+} concentration at OMC-MDD | 90 |
| 4.14 | Void ratio-pressure plots for Bentonite-1 and -2 in the presence of various Zn^{2+} concentration at OMC-MDD | 90 |
| 4.15 | Plot between the coefficient of consolidation and pressures of Bentonite-1 and -2 in the presence of various concentrations of Pb^{2+} | 92 |

| | | |
|------|--|-----|
| 4.16 | Plot between the coefficient of consolidation and pressures of Bentonite-1 and -2 in the presence of various concentrations of Cu^{2+} | 92 |
| 4.17 | Plot between the coefficient of consolidation and pressures of Bentonite-1 and -2 in the presence of various concentrations of Zn^{2+} | 93 |
| 4.18 | Plot between the time for 90% of consolidation and consolidation pressures of Bentonite-1 and -2 in the presence of various concentrations of Pb^{2+} | 94 |
| 4.19 | Plot between the time for 90% of consolidation and consolidation pressures of Bentonite-1 and -2 in the presence of various concentrations of Cu^{2+} | 95 |
| 4.20 | Plot between the time for 90% of consolidation and consolidation pressures of Bentonite-1 and -2 in the presence of various concentrations of Cu^{2+} | 95 |
| 4.21 | Unconfined compressive strength (UCS) of Bentonite-1 and-2 in the presence of DI water and heavy metals | 97 |
| 4.22 | Axial stress (kPa) vs. strain (%) relationship of the Bentonite-1 in the presence of various concentrations of Cu^{2+} | 98 |
| 4.23 | Axial stress (kPa) vs. strain (%) relationship of the Bentonite-2 in the presence of various concentrations of Cu^{2+} | 99 |
| 4.24 | Axial stress (kPa) vs. strain (%) relationship of the Bentonite-2 in the presence of various concentrations of Pb^{2+} | 99 |
| 4.25 | Axial stress (kPa) vs. strain (%) relationship of the Bentonite-2 in the presence of various concentrations of Pb^{2+} | 100 |
| 4.26 | Axial stress (kPa) vs. strain (%) relationship of the Bentonite-1 in the presence of various concentrations of Zn^{2+} | 100 |
| 4.27 | Axial stress (kPa) vs. strain (%) relationship of the Bentonite-2 in the presence of various concentrations of Zn^{2+} | 101 |
| 4.28 | Effect of pH on Pb^{2+} sorption on bentonites | 102 |
| 4.29 | Effect of pH on Cu^{2+} sorption on bentonites | 102 |
| 4.30 | Effect of pH on Zn^{2+} sorption on bentonites | 103 |
| 4.31 | Effect of initial concentration of Pb^{2+} on bentonites | 105 |
| 4.32 | Effect of initial concentration of Cu^{2+} on bentonites | 106 |
| 4.33 | Effect of initial concentration of Zn^{2+} on bentonites | 106 |

| | | |
|------|--|-----|
| 4.34 | Percentage removal of the Pb^{2+} at various initial concentrations | 108 |
| 4.35 | Percentage removal of the Cu^{2+} at various initial concentrations | 108 |
| 4.36 | Removal percentage of the Zn^{2+} at different initial concentrations | 109 |
| 4.37 | Linearized Langmuir and Freundlich isotherms for Pb^{2+} removal by bentonites | 110 |
| 4.38 | Linearized isotherm models for Cu^{2+} removal by bentonites | 111 |
| 4.39 | Linearized isotherm models for Zn^{2+} removal by bentonites | 112 |
| 4.40 | Removal percentage of the Pb^{2+} at different bentonite dosage | 114 |
| 4.41 | Removal percentage of the Cu^{2+} at different bentonite dosage | 114 |
| 4.42 | Removal percentage of the Zn^{2+} at different bentonite dosage | 115 |
| 4.43 | Quantity of Pb^{2+} adsorbed at various bentonite dose | 116 |
| 4.44 | Quantity of Cu^{2+} adsorbed at various bentonite dose | 116 |
| 4.45 | Quantity of Zn^{2+} adsorbed at various bentonite dose | 117 |
| 4.46 | Adsorption kinetics for Pb^{2+} | 118 |
| 4.47 | Adsorption kinetics for Cu^{2+} | 118 |
| 4.48 | Adsorption kinetics for Zn^{2+} | 119 |
| 4.49 | Kinetic study of bentonites in presence of Pb^{2+} | 120 |
| 4.50 | Kinetic study of bentonites in presence of Cu^{2+} | 121 |
| 4.51 | Kinetic study of bentonites in the presence of Zn^{2+} | 122 |
| 4.52 | FESEM images of bentonites in presence of Cu^{2+} | 125 |
| 4.53 | FESEM images of bentonites in presence of Pb^{2+} | 127 |
| 4.54 | FESEM images of bentonites in presence of Zn^{2+} | 129 |
| 4.55 | FTIR Spectra for both bentonites in DI water and Cu^{2+} solutions | 133 |
| 4.56 | FTIR Spectra for both bentonites in DI water and Pb^{2+} solutions | 134 |
| 4.57 | FTIR Spectra for both bentonites in DI water and Zn^{2+} solutions | 135 |

Chapter 5

| | | |
|-----|---|-----|
| 5.1 | Liquid limit of bentonites in the presence of leachates | 144 |
| 5.2 | Free swell of bentonites in presence of leachates | 145 |
| 5.3 | Time–swelling plot in the presence of leachates | 147 |
| 5.4 | Hydraulic conductivity of bentonites in the presence of leachates | 149 |
| 5.5 | Void ratio and Pressure relationship of bentonites in the presence of leachates | 151 |

| | | |
|------|---|-----|
| 5.6 | Coefficient of consolidation (c_v) and pressure relationship for bentonites in the presence of leachates | 153 |
| 5.7 | Time for 90% consolidation (t_{90}) and pressure relationship for bentonites in the presence of leachates | 155 |
| 5.8 | Axial stress (kPa) vs strain (%) relationship of the bentonites in the presence of leachates | 156 |
| 5.9 | Removal of heavy metal from MSW and synthetic MSW leachate by bentonites | 158 |
| 5.10 | Removal % of MSW leachate at different bentonite dosage for Bentonite-1 | 162 |
| 5.11 | Removal % of MSW leachate at different bentonite dosage for Bentonite-2 | 162 |
| 5.12 | Removal % of synthetic MSW leachate at different bentonite dosage for Bentonite-1 | 163 |
| 5.13 | Removal % of synthetic MSW leachate at different bentonite dosage for Bentonite-2 | 163 |
| 5.14 | Amount of MSW leachate adsorbed by Bentonite-1 at various bentonite dose | 165 |
| 5.15 | Amount of MSW leachate adsorbed by Bentonite-2 at various bentonite dose | 166 |
| 5.16 | Amount of synthetic MSW leachate adsorbed by Bentonite-1 at various bentonite dose | 167 |
| 5.17 | Amount of synthetic MSW leachate adsorbed by Bentonite-2 at various bentonite dose | 169 |
| 5.18 | Adsorption kinetics for MSW leachate in the presence of Bentonite-1 | 170 |
| 5.19 | Adsorption kinetics for MSW leachate in the presence of Bentonite-2 | 170 |
| 5.20 | Adsorption kinetics for synthetic MSW leachate in the presence of Bentonite-1 | 171 |
| 5.21 | Adsorption kinetics for synthetic MSW leachate in the presence of Bentonite-2 | 171 |
| 5.22 | Kinetic study of Bentonite-1 in the presence of MSW leachate | 174 |
| 5.23 | Kinetic study of Bentonite-2 in the presence of MSW leachate | 176 |
| 5.24 | Kinetic study of Bentonite-1 in the presence of synthetic MSW leachate | 178 |

| | | |
|------|--|-----|
| 5.25 | Kinetic study of Bentonite-2 in the presence of synthetic MSW leachate | 180 |
|------|--|-----|

Chapter 6

| | | |
|------|--|-----|
| 6.1 | Time–swelling plot for Bentonite-1 in presence of synthetic leachates | 190 |
| 6.2 | Time–swelling plot for Bentonite-2 in presence of synthetic leachates | 190 |
| 6.3 | Hydraulic conductivity of Bentonite-1 in presence of synthetic leachates | 193 |
| 6.4 | Hydraulic conductivity of Bentonite-2 in presence of leachates | 193 |
| 6.5 | Void ratio and Pressure relationship of bentonites in presence of leachates | 195 |
| 6.6 | Void ratio and Pressure relationship of bentonites in presence of leachates | 195 |
| 6.7 | Coefficient of consolidation (c_v) and pressure relationship for Bentonite-1 in presence of leachates | 197 |
| 6.8 | Coefficient of consolidation (c_v) and pressure relationship for Bentonite-2 in presence of leachates | 197 |
| 6.9 | Time for 90% consolidation (t_{90}) and pressure relationship for Bentonite-1 in presence of leachates | 199 |
| 6.10 | Time for 90% consolidation (t_{90}) and pressure relationship for Bentonite-2 in presence of leachates | 199 |
| 6.11 | Axial stress (kPa) vs strain (%) relationship of the bentonites in the presence of various leachates | 202 |
| 6.12 | Removal of heavy metal from fly ash leachate by bentonites | 203 |
| 6.13 | Removal of heavy metal from sewage sludge leachate by bentonites | 204 |
| 6.14 | Removal of heavy metal from paper mill leachate by bentonites | 204 |
| 6.15 | Removal % of fly ash leachate at different bentonite dosage for Bentonite-1 | 208 |
| 6.16 | Removal % of fly ash leachate at different bentonite dosage for Bentonite-2 | 209 |
| 6.17 | Removal % of sewage sludge leachate at different bentonite dosage for Bentonite-1 | 210 |
| 6.18 | Removal % of sewage sludge leachate at different bentonite dosage for Bentonite-2 | 211 |

| | | |
|------|--|-----|
| 6.19 | Removal % of paper mill leachate at different bentonite dosage for Bentonite-1 | 212 |
| 6.20 | Removal % of paper mill leachate at different bentonite dosage for Bentonite-2 | 213 |
| 6.21 | Amount of fly ash leachate adsorbed by Bentonite-1 at various bentonite dose | 214 |
| 6.22 | Amount of fly ash leachate adsorbed by Bentonite-2 at various bentonite dose | 215 |
| 6.23 | Amount of sewage sludge leachate adsorbed by Bentonite-1 at various bentonite dose | 216 |
| 6.24 | Amount of sewage sludge leachate adsorbed by Bentonite-2 at various bentonite dose | 217 |
| 6.25 | Amount of paper mill leachate adsorbed by Bentonite-1 at various bentonite dose | 218 |
| 6.26 | Amount of paper mill leachate adsorbed by Bentonite-2 at various bentonite dose | 219 |
| 6.27 | Adsorption kinetics for fly ash leachate in presence of Bentonite-1 | 221 |
| 6.28 | Adsorption kinetics for fly ash leachate in presence of Bentonite-2 | 221 |
| 6.29 | Adsorption kinetics for sewage sludge leachate in presence of Bentonite-1 | 222 |
| 6.30 | Adsorption kinetics for sewage sludge leachate in presence of Bentonite-2 | 222 |
| 6.31 | Adsorption kinetics for paper mill leachate in presence of Bentonite-1 | 223 |
| 6.32 | Adsorption kinetics for paper mill leachate in presence of Bentonite-2 | 223 |
| 6.33 | Kinetic study of Bentonite-1 in presence of fly ash leachate | 226 |
| 6.34 | Kinetic study of Bentonite-2 in presence of fly ash leachate | 228 |
| 6.35 | Kinetic study of Bentonite-1 in presence of sewage sludge leachate | 230 |
| 6.36 | Kinetic study of Bentonite-2 in presence of sewage sludge leachate | 231 |
| 6.37 | Kinetic study of Bentonite-1 in presence of paper mill leachate | 233 |
| 6.38 | Kinetic study of Bentonite-2 in presence of paper mill leachate | 235 |



List of Tables

| Table No. | Caption | Page No. |
|------------------|--|----------|
| Chapter 2 | | |
| 2.1 | Summary of interaction of clay with salt solutions | 27 |
| 2.2 | Summary of interaction of clay with heavy metals | 38 |
| 2.3 | Summary of interaction of clay with Pb^{2+} | 41 |
| 2.4 | Summary of interaction of clay with Cu^{2+} | 44 |
| 2.5 | Summary of interaction of clay with Zn^{2+} | 46 |
| 2.6 | Summary of interaction of clay with leachates | 49 |
| Chapter 3 | | |
| 3.1 | Chemical and mineralogical properties of Bentonites | 56 |
| 3.2 | Elemental composition expressed as weight percent of major element of both the bentonites | 57 |
| 3.3 | pH values of individual metal solutions | 61 |
| 3.4 | pH values of metal solutions with bentonites | 61 |
| 3.5 | Composition of MSW leachate | 62 |
| 3.6 | Composition of synthetic MSW leachate | 63 |
| 3.7 | Composition of Fly ash leachate | 63 |
| 3.8 | Composition of Paper mill leachate | 63 |
| 3.9 | Composition of sewage sludge leachate | 64 |
| 3.10 | pH values of different leachate solutions | 64 |
| Chapter 4 | | |
| 4.1 | Swelling Pressure of Bentonite-1 and -2 in the presence of heavy metals | 79 |
| 4.2 | Swelling potential of Bentonite-1 and -2 in the presence of heavy metals | 81 |
| 4.3 | Hydraulic conductivity of bentonites at a void ratio of 1.3 for Pb^{2+} | 87 |
| 4.4 | Hydraulic conductivity values of bentonites at a void ratio of 1.3 for Zn^{2+} | 87 |
| 4.5 | Hydraulic conductivity of bentonites at a void ratio of 1.1 for Cu^{2+} | 88 |
| 4.6 | Compression index of Bentonite-1 and -2 for various concentrations of Zn^{2+} , Cu^{2+} and Pb^{2+} solution | 96 |

| | | |
|------|--|-----|
| 4.7 | Unconfined compression test of bentonite in presence of heavy metals | 98 |
| 4.8 | Metal ion characteristic parameters | 105 |
| 4.9 | The sorption isotherms parameters for different models for Pb^{2+} , Cu^{2+} and Zn^{2+} | 113 |
| 4.10 | Parameters for adsorption of heavy metals on Bentonites derived from the pseudo-first- and second-order kinetic models | 123 |
| 4.11 | FTIR spectra bands of Bentonite-1 before and after adsorption of heavy metals | 131 |
| 4.12 | FTIR spectra bands of Bentonite-2 before and after adsorption of heavy metals | 132 |

Chapter 5

| | | |
|-----|--|-----|
| 5.1 | Swelling Potential and Swelling Pressure of bentonite in the presence of leachates. | 146 |
| 5.2 | Initial swelling (IS) and Primary swelling (PS) of bentonites in the presence of leachates | 148 |
| 5.3 | Hydraulic conductivity of bentonites at a void ratio 1.2 for leachates | 150 |
| 5.4 | Compression index of Bentonites-1 and -2 in presence of various leachate | 155 |
| 5.5 | Unconfined compressive strength of both bentonites in the presence of leachates | 157 |
| 5.6 | Removal of heavy metal from MSW leachate by bentonites | 159 |
| 5.7 | Removal of heavy metals from synthetic MSW leachate by bentonites | 160 |
| 5.8 | Parameters for adsorption of heavy metals present in MSW leachate on bentonites derived from the pseudo-first- and second-order kinetic models | 181 |
| 5.9 | Parameters for adsorption of heavy metals present in synthetic MSW leachate on bentonites derived from the pseudo-first- and second-order kinetic models | 182 |

Chapter 6

| | | |
|-----|---|-----|
| 6.1 | Liquid limit and free swell of bentonites in presence of synthetic leachates | 187 |
| 6.2 | Swelling Potential and Swelling Pressure of bentonites in presence of synthetic leachates | 189 |
| 6.3 | Initial swelling (IS) and Primary swelling (PS) of bentonites in presence of leachates | 191 |

| | | |
|------|--|-----|
| 6.4 | Hydraulic conductivity of bentonites at a void ratio of 1.2 for synthetic leachates | 194 |
| 6.5 | Compression index of bentonites in presence of synthetic leachates. | 200 |
| 6.6 | Unconfined compressive strength of bentonites in presence of synthetic leachates | 201 |
| 6.7 | Removal of heavy metal from Fly ash leachate by bentonites | 205 |
| 6.8 | Removal of heavy metal from sewage sludge leachate by bentonites | 206 |
| 6.9 | Removal of heavy metal from paper mill leachate by bentonites | 207 |
| 6.10 | Parameters for adsorption of heavy metals present in fly ash leachate on bentonites derived from the pseudo-first- and second-order kinetic models | 236 |
| 6.11 | Parameters for adsorption of heavy metals present in sewage sludge leachate on bentonites derived from the pseudo-first- and second-order kinetic models | 236 |
| 6.12 | Parameters for adsorption of heavy metals present in paper mill leachate on bentonites derived from the pseudo-first- and second-order kinetic models | 237 |



List of Abbreviations

| | |
|----------|---|
| L | Litre |
| mL | Millilitre |
| ppm | Parts per million |
| mg | Milligram |
| g | Gram |
| kg | Kilogram |
| N | Normality |
| MC | Moisture Content |
| MSW | Municipal Solid Waste |
| DDL | Diffuse Double Layer |
| SSA | Specific Surface Area |
| CEC | Cation Exchange Capacity |
| ESP | Exchangeable Sodium Percentage |
| GCL | Geosynthetic Clay Liner |
| OMC | Optimum Moisture Content |
| MDD | Maximum Dry Density |
| ASTM | American Society for Testing and Materials |
| EGME | Ethylene glycol mono-ethyl ether |
| XRD | X-ray diffraction |
| XRF | X-ray fluorescence |
| SAR | Sodium Absorption Ratio |
| DI water | De-ionized water |
| ppm | Parts per million |
| AAS | Atomic Absorption Spectrophotometer |
| WHO | World Health Organization |
| FESEM | Field emission scanning electron microscopy |
| EDX | Energy Dispersive X-Ray |
| FTIR | Fourier Transform Infrared |
| USEPA | United States Environmental Protection Agency |
| IS | Indian Standards |
| DWL | Dye waste leachate |
| MWL | Metal waste leachate |
| TSW | Tannery solid waste |
| CRT | Cathode ray tube |
| HDPE | High Density Poly Ethylene |
| UNEP | United Nations Environment Programme |
| RPM | Revolutions per minute |



Symbols Used

| | |
|---------------|---|
| k | Hydraulic conductivity |
| γ_d | Dry density |
| m_v | Coefficient of volume change |
| c_v | Coefficient of consolidation |
| t_{90} | Time for 90% of consolidation |
| C_c | Compression index |
| ΔP | Change in pressure |
| Δe | Change in void ratio |
| T_v | Time factor |
| γ_w | Unit weight of the pore fluid |
| G | Specific gravity of soil solid particles |
| S | Specific surface area of soil |
| d | Half distance between the parallel clay plates |
| M | Molar concentration of ions in pore fluid |
| k | Boltzmann's constant (1.38×10^{-23} J/K) |
| T | Temperature in Kelvin |
| v | Valency of exchangeable cation |
| ξ | Distance function |
| ε | Dielectric constant of the pore fluid |
| e' | Elementary electric charge (4.8×10^{-10} esu) |
| σ_c | Unconfined compressive strength |
| C_0 | Initial Concentration |
| C_e | Equilibrium Concentration |
| M | Mass |
| PR | Percentage Removal |
| q_e | Amount of metal ion adsorbed on adsorbent |



*Today's trend ends up in
tomorrow's landfill*

- David Amram

1

Introduction

1.1. General

Intense industrialization has interfered with the natural environment by heavy discharge of effluents rich in heavy metals. These heavy metals, when present in trace quantities, benefit in the proper functioning of human catalytic. However, when these elements accumulate in the natural environment as a result of anthropogenic activities and are found in excess amounts, they conduce to the disturbance of human metabolism (Tchounwou et al., 2012). Various human-made sources of heavy metals exist; one such significant source is the leachates generated from wastes in the landfills. The world, in recent years, has witnessed a considerable elevation in the generation of municipal solid wastes (MSWs) as a result of enormous population growth coupled with improvised standards of living. This has increased the pressures on the landfills as most of the wastes generated get disposed of into landfills. This is primarily because landfilling is the most suitable and extensively employed technique for waste disposal (Qian et al., 2001). Over time, these wastes undergo biological as well as chemical transformations inside the landfills, thereby producing leachate (Kjeldsen et al., 2002). This leachate, when it comes in contact with rainwater, migrate into the sub-surface layer and thus contaminate the groundwater as well as the surrounding environment. Therefore, an impermeable clay liner

is usually provided at the bottom of a landfill to avoid groundwater and soil contamination in the proximate region (Daniel, 1984).

Various studies have been conducted in the past, proving that bentonite is one of the most suitable landfill liner materials for the prevention of leachate percolation to the sub-surface strata (Daniel, 1984; Dutta and Mishra, 2016a, b; Pawar et al., 2016). Properties of bentonite such as high swelling tendency, high specific surface area, lower hydraulic conductivity, high cation exchange capacity and high sorption capacity aid in achieving such high appropriateness as a liner material. Montmorillonite, consisting of phyllosilicate, forms the primary component of bentonite. It is comprised of one octahedral unit sandwiched between two tetrahedral units. The layers are bound together by weak van der Waals force of attraction, which allows the water to easily infiltrate, thus resulting in the formation of a diffuse double layer (DDL) followed by the swelling of bentonite (Madsen and Müller-Vonmoos, 1989; Mitchell and Soga, 2005; Norrish, 1954; Norrish and Quirk, 1954).

Metals present in the leachate is of the most significant concern since it can cause detrimental impacts on the ecosystem. The existence of heavy-metal pollutants in the leachates disturbs the pore-fluid chemistry of the bentonite clay particles and affects the DDL. Besides, due to the presence of metal solution, the mineral composition of bentonite also gets altered, which consequently affects the swelling and influences the hydraulic conductivity (Dutta and Mishra, 2016a). The most critical parameters that must be considered while designing a liner system for the landfill are hydraulic conductivity, compressibility, shear strength and adsorption. Harmful pollutants present inside the landfill may alter the properties of the liner material, causing a reduction in efficiency. As a result, the flow path opens, and consequently, the hydraulic conductivity rises. Hence, it is essential to investigate the change in hydraulic behaviour in the presence of various pollutants present in the leachates. Numerous research groups have focused on the hydraulic characteristics of bentonite clays and their uses in landfills as a barrier material in the presence of several chemicals (Dutta and Mishra, 2015; Dutta and Mishra, 2016a; Ören and Akar, 2017).

Furthermore, estimation of the settlement of the liner material is predicted by its compressibility. The liner system gets compressed, and eventually, settle as a result of the overloading of the wastes at the disposal sites. However, bentonite, being a highly compressible material, can get consolidated substantially. Physico-chemical and mechanical factors measure the compressibility nature of the clay particles (Bolt, 1956).

Physical properties control the short-range particle interactions such as sliding, rolling and bending. However, long-range particle interactions through the DDL thickness are controlled by the physico-chemical properties (Mitchell and Soga, 2005). Various consolidation parameters of bentonite such as coefficient of consolidation (c_v), coefficient of volume change (m_v), compression index (C_c) and time for 90% consolidation (t_{90}) are in much concern among investigators due to their significance on consolidation behaviour. Many works of literature have proposed that the liner material usually retains a meagre shear strength value (Graham et al., 1989; Wan et al., 1990).

Like hydraulic conductivity, shear strength and compressibility, adsorption is a significant parameter assisting in the evaluation of the adsorption capacity of the liner. Various reports citing methodologies for the removal of metals are available; membrane filtration, coagulation, adsorption, solvent extraction and electrochemical operations being a few of them. Some of these technologies are expensive, while others have their limitations in terms of their environmental impacts and their efficacies in real-world applications (Pawar et al., 2016). Amongst all the available methods for heavy metal removal, adsorption is the most preferred technique owing to its high efficiency of eliminating contaminants and the use of non-toxic and relatively inexpensive materials (Azad et al., 2015; Lee and Tiwari, 2013). The major drawback, however, remains the high price of the adsorbent material. Thus, selecting a more reasonable adsorbent for the adsorption process makes it very suitable for practical applications. Bentonite, an economical material derived from the volcanic ashes, has been found to have excellent adsorbing capacity. This is primarily due to its pore structure and chemical nature (Brigatti et al., 2006). Numerous well-documented investigations have reported effective removal of heavy metals such as Cu^{2+} (Freitas et al., 2017; Glatstein and Francisca, 2015; Karapinar and Donat, 2009), Pb^{2+} (Baylan and Meriçboyu, 2016; Deka and Sekharan, 2017; Pawar et al., 2016), Zn^{2+} (Araujo et al., 2013; Kaya and Ören, 2005; Kubilay et al., 2007) and Ni^{2+} (Futalan et al., 2011; Liu and Zhou, 2010; Vhahangwele and Mugeru, 2015; Vieira et al., 2010) employing bentonite.

In the past, very few investigations have been reported on the effect of various metals, leachate and mineralogical parameters on swelling, hydraulic conductivity, compressibility, shear strength and sorption behaviour of bentonite together. Most previous studies have primarily focused on the study of the hydraulic conductivity of bentonite and sorption of bentonite only. Hence, this investigation aims at studying the effect of various concentrations of heavy metals as well as different leachates on the swelling, hydraulic conductivity, consolidation, shear strength and adsorption behaviour of bentonite.

Bentonites were studied for their change in the index properties, swelling, swelling potential, swelling pressure, hydraulic conductivity, consolidation parameters, shear strength properties and sorption characteristics under different conditions, i.e., the presence of different heavy metals of various concentrations and for different leachates.

1.2. Thesis Organization

The thesis is organized into seven chapters, as described below:

Chapter 1 provides an insight into the introduction to the problem statement and the relevance of its outcome. It also provides a chapter plan where the entire thesis organization has been discussed.

Chapter 2 deals with the background of the study, with a comprehensive literature review on bentonite used in liners and their interaction with various chemicals present in various leachates. The objectives of the study and its significance are also presented in this chapter.

Chapter 3 introduces the materials and experimental procedures used in the research while performing the study. A detailed research work plan in the form of a flowsheet has been represented in this chapter.

Chapter 4 investigates the effects of heavy metals (Zn^{2+} , Pb^{2+} and Cu^{2+}) of varying concentrations on free swelling, liquid limit, hydraulic conductivity, swelling potential, swelling pressure, various consolidation parameters such as compression index (C_c), coefficient of volume change (m_v), coefficient of consolidation (c_v) and time to complete 90% of the consolidation (t_{90}), shear strength and adsorption capacity of two bentonites of different mineralogical composition and swelling capacity.

Chapter 5 examines and compares the effect of Municipal Solid Waste (MSW) leachate and synthetic MSW leachate on the free swelling, liquid limit, hydraulic conductivity, swelling potential, swelling pressure consolidation parameters, shear strength and adsorption capacity of the two bentonites.

Chapter 6 studies the effect of various synthetic leachates (fly ash, sewage sludge and paper mill sludge leachate) on the two different bentonites.

Chapter 7 includes the concluding remarks of the present study and details the scope for future work, which can be carried out as an extension to this study.



*You have to dream
before your dreams can
come true.*

*- Bharat Ratna
Dr. A.P.J. Abdul Kalam*

2

Background and Literature Review

2.1. Context

This chapter explains in detail the particulars of the published works of literature, which helped in identifying gaps in the research and thereby, framing the design of the study.

2.2. General

The primary function of a compacted clay liner is to provide a barrier between the leachates generated from the waste and the groundwater. The reason of bentonite is being used as a barrier material at the waste disposal site to control the migration of contaminated leachate into the surrounding environment is attributed to its low hydraulic conductivity, higher swelling capacity and contaminant adsorption ability (Daniel, 1984).

Bentonite can form a diffuse double layer (DDL) with water, which in turns leads to higher swelling capacity and lower hydraulic conductivity (Norrish and Quirk, 1954; Olson and Mesri, 1970). However, an opposite scenario is observed when contaminants present

in the leachate (Olson and Mesri, 1970). Hence, studying the behaviour of bentonite in the presence of various chemicals present in the leachate is necessary to design the clay liner.

2.3. Present situation of waste management and disposal

Rapid urbanization and industrialization lead to the production of enormous amounts of wastes that degrade the quality of geo-environment and groundwater. Improved standard of living and affluence has led to an alarming increasing of wastes produced by the developed and developing countries of the world. The ever-increasing amount of wastes produced by cities have become a significant concern over the past years. Landfilling is the most widely accepted method of solid waste disposal in various countries around the world. Though implementation of waste reduction, recycling, and transformation technologies have decreased landfill burdens, landfills remain an essential tool of an integrated solid waste management strategy. Landfill liners protect the surrounding environment, including soil, surface water and groundwater against contamination.

Waste can be broadly categorized as municipal solid waste (MSW) and industrial waste. The industrial waste includes burnt residue, sewage, waste oils, waste acid and alkali, waste plastics, waste paper, wood waste, waste textile, animal and plant residues, waste rubber, waste metal, glass waste, concrete waste and pottery waste, slag, debris, animal faeces and urine, dead animal, ash dust, and wastes generated after the treatment of aforementioned industrial waste.

MSW indicate wastes that are generated mainly from household besides human waste and also include the wastes from business activities in offices and restaurants. Wastes that are derogatory to health and environment because of being explosive, toxic and/or infectious. These wastes are classified with “specially controlled MSW” or “specially controlled industrial wastes”. Such wastes are strictly controlled in all steps of collection to disposal.

The total amount of waste generated worldwide is more than 4 billion tons per year. Global urban MSW production, which has nearly doubled in the last ten years, is projected to double again in the next 15 years, increasing from 1.3 billion tons a year in 2010 to 2.2 billion tons a year in 2025 (Hoornweg and Bhada-Tata, 2012). The combination of high urbanization rates and economic development has led to a rapid increase in waste generation in developing countries. In developing countries, the per capita waste generation

rate ranges from 0.4 to 1.1 kg per day, reaching in some urban areas 2.4 kg per day and more in tourist areas.

The estimated quantity of MSW generated worldwide is 1.7 – 1.9 billion metric tons. In many cases, MSW is not well managed in developing countries, as cities and municipalities cannot cope with the accelerated pace of waste production. More than 50 % of the collected waste is often disposed of through uncontrolled landfilling, and about 15 per cent is processed through unsafe and informal recycling (Chalmin and Gaillochet, 2009). The United States generates the most significant amount of MSW in the world as it accumulates yearly of around 387 million tonnes of MSW (Themelis and Mussche, 2013).

2.4. Landfill liners

The design of waste disposal facilities typically involves some form of the barrier which separates the waste from the groundwater. This barrier is intended to minimize the migration of contaminants from the facility; thus, the environmental impact of the facility is intimately related to its design and long term performance. Natural clayey deposits or compacted clayey liners frequently represent a crucial component of these barriers.

These days, barriers usually include one or more of the following types:

- (i) Natural clayey soils such as lacustrine clay or clayey till;
- (ii) Compacted clayey liners;
- (iii) Cut-off walls;
- (iv) Natural bedrock;
- (v) Composite liner system consisting of geomembranes

Out of the types mentioned above generally compacted clayey liners and composite liner system with geomembranes are used at the waste disposal site. Landfilling employs an engineered method of disposing MSW on land in a manner that minimizes any environmental hazards. A landfill liner is relatively a thick structure of compacted natural clayey soil or manufactured material (i.e. geomembrane or geosynthetic clay liners) which serves as a barrier between leachate and groundwater to control the movement of leachate that reaches or mixes with the groundwater.

Cross section of a typical waste disposal site

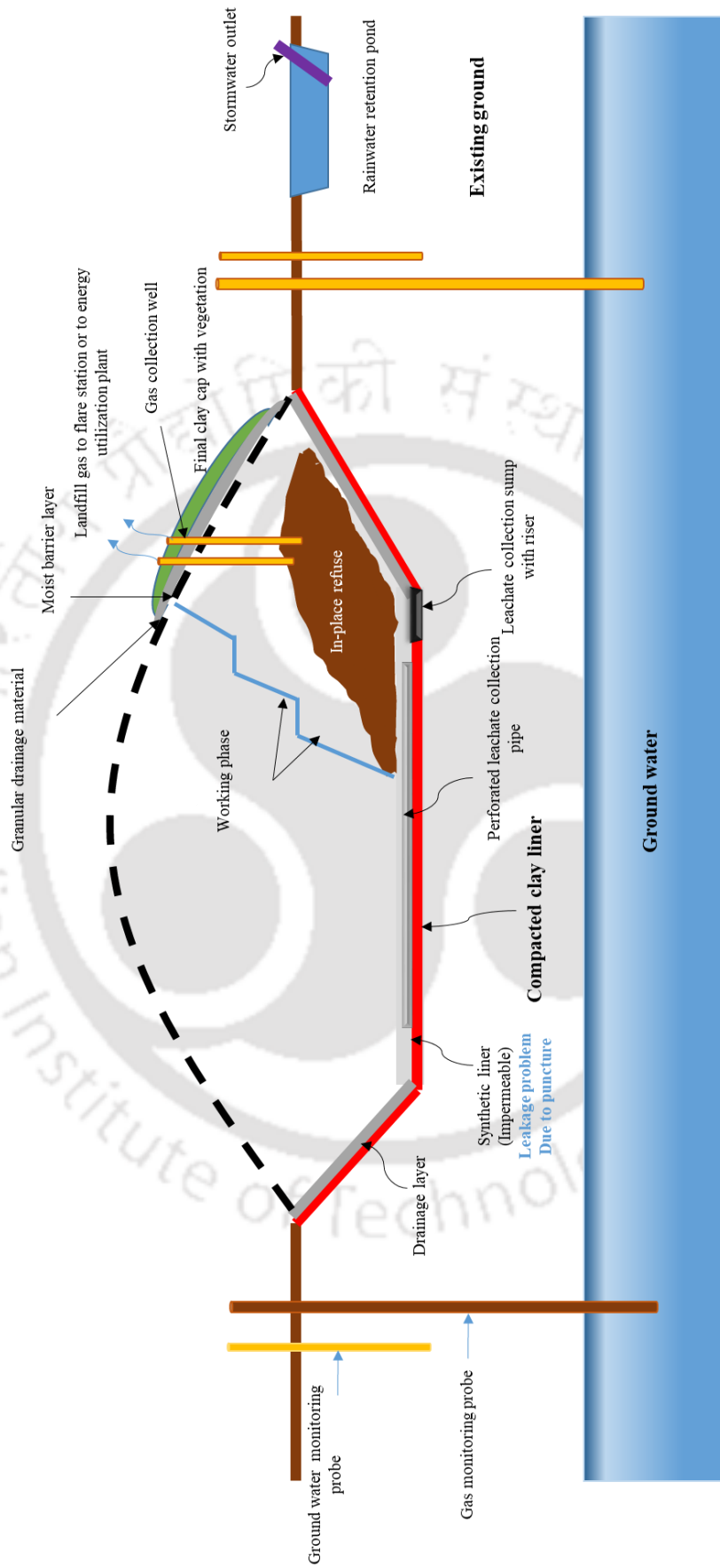


Fig. 2.1. Cross-section of a typical waste disposal site

Fig. 2.1. shows the cross-section of a typical waste disposal site. Clay liners are frequently installed at waste disposal sites to prevent contaminant migration and to minimize or eliminate the risk of groundwater contamination owing to their low hydraulic conductivity and adsorption capability of the liner material. The liner may be required for one or two reasons; firstly, if the natural soil is fractured clayey soil then the liner may be necessary to retard movement of contaminant along with the fractures, secondly, if the surrounding natural soil does not have a low enough hydraulic conductivity to provide an adequate barrier, a liner is provided. Some conceptual designs may not involve sufficient confidence in having any or negligible effect on groundwater quality. Under these circumstances, an additional level of protection in the form of a secondary leachate collection system or hydraulic control layer may be provided.

2.5. Landfill design method adopted in different countries

In the late 1980s, the European Commission began to draft the Council Directive on the Landfill of Waste. The Directive went through many iterations until it was finally agreed in 1999 and proposed that landfill liner should satisfy at least one of the hydraulic conductivity and thickness requirements for the protection of soil, groundwater and surface water:

Landfill for hazardous waste:

Hydraulic conductivity (k) $< 1 \times 10^{-9}$ m/sec; thickness > 5 m

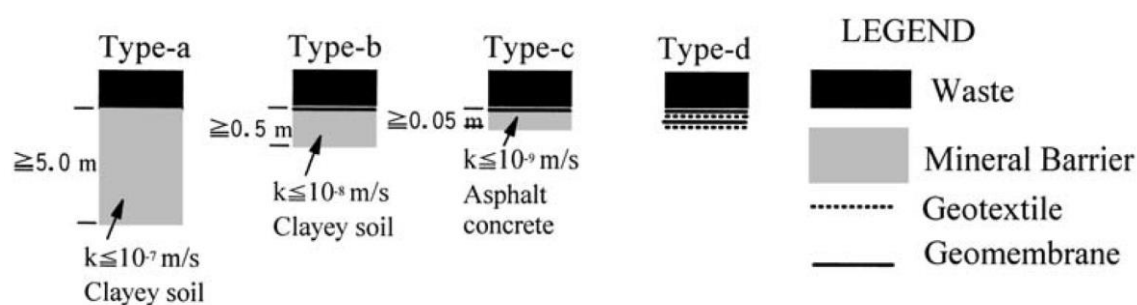
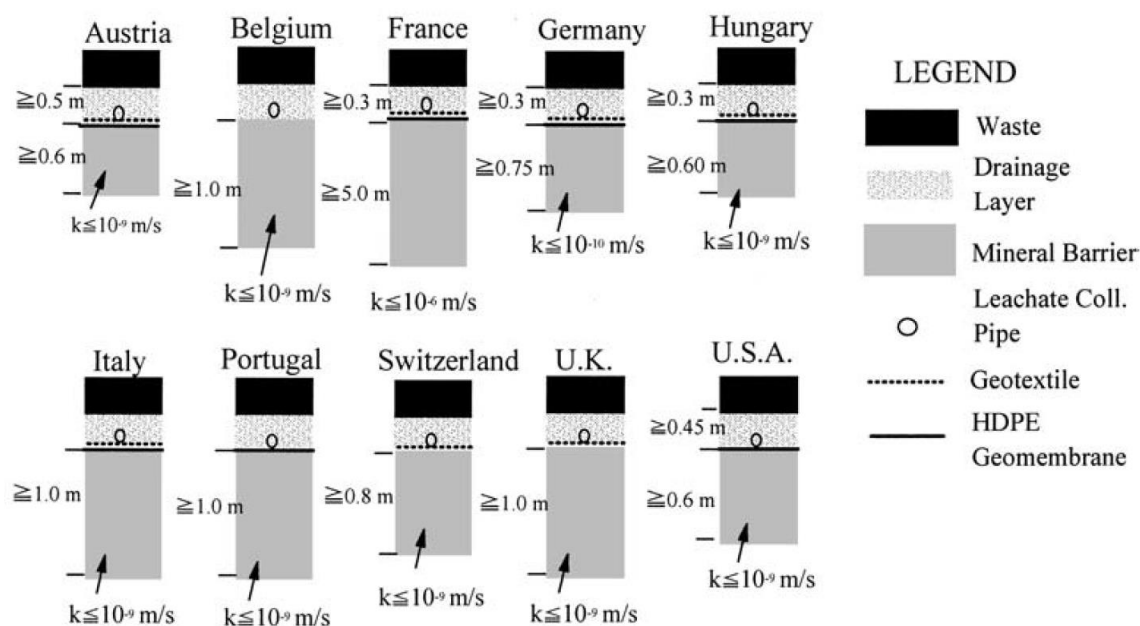
Landfill for non-hazardous waste:

Hydraulic conductivity (k) $< 1 \times 10^{-9}$ m/sec; thickness > 1 m

Landfill for inert waste:

Hydraulic conductivity (k) $< 1 \times 10^{-7}$ m/sec; thickness > 1 m

The thickness and hydraulic conductivity criteria of the mineral barrier used in liners vary from country to country and are shown in Figs. 2.2 and 2.3 The thickness of the barrier to be used should be less than 0.6 m and 1 m for USA and UK respectively, and the hydraulic conductivity (k) should be less than 10^{-9} m/sec. For Japan, the thickness of the barrier should be less than 5 m, and k should be less than 10^{-9} m/sec.



2.6. Design parameters for landfill liners

2.6.1. Hydraulic conductivity

The primary concern about liners is its hydraulic conductivity. A well-designed clay liner must have a low hydraulic conductivity to minimize leakage of leachate. (Mitchell and Jaber, 1990) stated that moisture content and dry density affect a soil's ability to restrict the transmission of flow. Placement conditions that result in a high dry density and a moisture content wet of optimum leads to the lowest values of hydraulic conductivity (k) because the soil particles are arranged in a dispersed pattern. In contrast, a dry side of compaction produces a flocculated pattern (as shown in Fig. 2.4), which offers better paths for the flow of water leading to a higher k . Wet of optimum, the clay can be easily

remoulded, clods and macropores are broken up. Since hydraulic conductivity through clay micropores is very low, the overall hydraulic conductivity is also low.

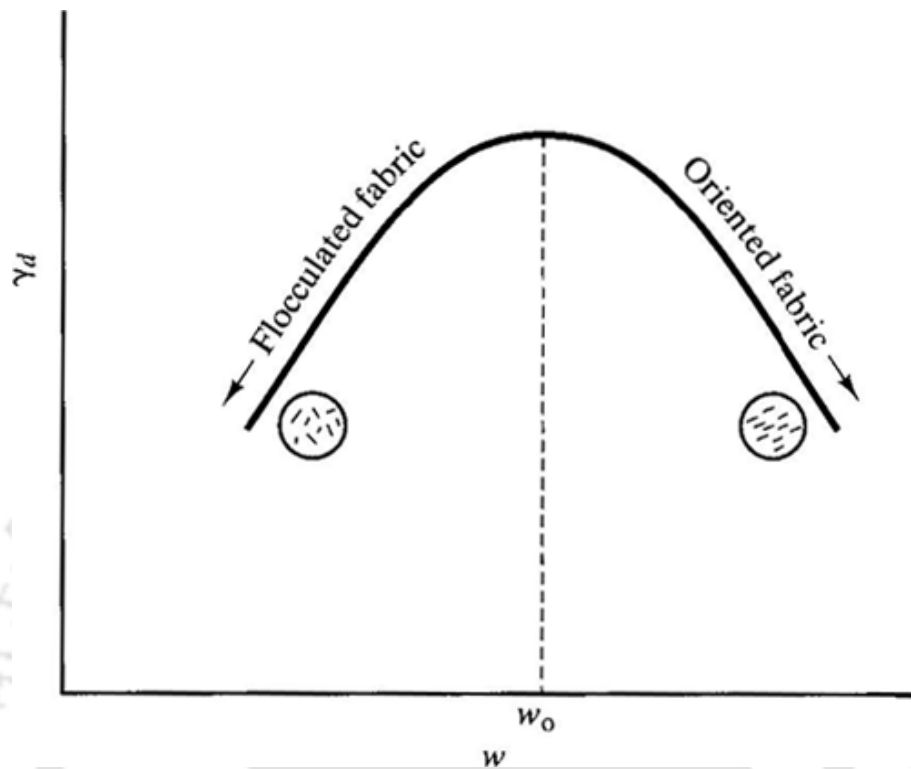


Fig. 2.4. The effect of compaction water content (w) and dry density on the orientation of the soil fabric (Lambe, 1958)

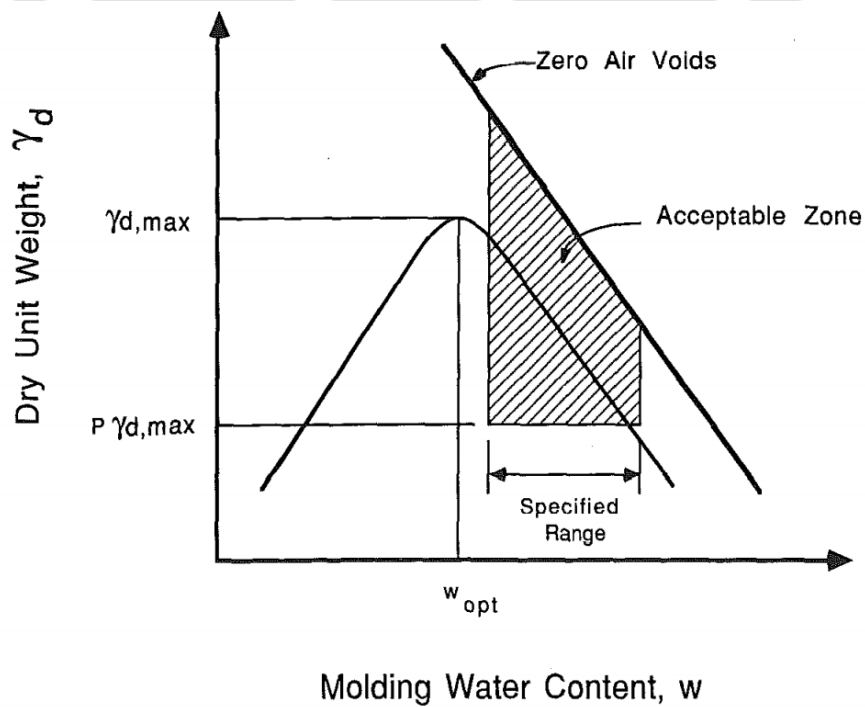


Fig. 2.5. Acceptable zone for hydraulic conductivity (Daniel and Benson, 1990)

The line of optimums can be plotted on water content vs dry density graph by performing modified standard and reduced proctor tests. The acceptable zone for hydraulic conductivity may be defined with the line of optimums as the bottom boundary and zero air voids curve as the top limit (Fig. 2.5).

2.6.2. Shear Strength

Clay liners should have adequate strength to maintain the integrity of the liner against the overburden stress imposed by the material above it and to make the liner stable when employed on slopes, for example, in the sidewall of a waste containment facility. The required strength for a clay liner to support the maximum bearing stress in a landfill project was calculated to be 30 psi or 200 kPa (Daniel and Wu, 1993).

2.6.3. Volumetric shrinkage

Clay soils used in liners are typically placed and compacted at the wet of optimum moisture content to minimize the hydraulic conductivity of the compacted soil. As the moulding water content of compacted soil is increased, the shrinkage potential of the soil increases as well. Desiccation or shrinkage cracking can occur if liners are exposed to the atmosphere in hot weather and can result in an increase in the hydraulic conductivity by many folds. Daniel and Wu (1993) investigated a clayey soil in West Texas in 1993 and concluded that the volumetric shrinkage upon drying should be less than or equal to 4%.

2.7. Use of bentonite as a liner material

2.7.1. Introduction

Bentonite is widely used as a backfill material during the construction of slurry trench walls, as a soil admixture for the construction of seepage barriers, as a grout material, as a sealant for piezometer installations and various other civil engineering construction techniques. It is an absorbent aluminium phyllosilicate, essentially impure clay, formed as a deposit of volcanic ashes at shallow wet sites in various location of the world (Grimm and Güven, 1978). These deposits are variable, depending on the nature of the volcanic ashes and the salinity of the water into which they were deposited. Since the bentonite is a natural material, its mineral composition, chemical state, and grain size distribution varies considerably from one source to another. Different parameters such as mineralogical

composition (i.e. amount and type of montmorillonite), type of exchangeable cations, surface area and the surface charge density affect the behaviour of bentonite considerably.

Bentonite is primarily composed of the smectite group of minerals, most common among which is montmorillonite $(Al_{1.7}Mg_{0.3})[Si_4O_{10}(OH)_2]^{-0.3}(M)^{+0.3}$, where M represents the exchangeable cation (Mitchell and Soga, 2005). The behaviour of bentonite primarily is governed by montmorillonite which has characteristics like a large specific surface area (as high as 800 m²/g), high charge deficiency (0.5-1.2 per unit cell), high cation exchange capacity (80-150 cmol_c/kg), and the ability for interlayer swelling. These factors contribute to the increased swelling, low hydraulic conductivity and contaminants adsorption ability of the bentonite.

2.7.2. Structure of Montmorillonite

Clays are the particles with an effective diameter smaller than 2µm and phyllosilicates as its main mineralogical components. These phyllosilicates are made of silica (SiO₂) tetrahedral sheets and Aluminium (Al³⁺) or magnesium (Mg²⁺) oxides octahedral sheets. Montmorillonite has a prototype structure similar to that of pyrophyllite consisting of an octahedral sheet sandwiched between two tetrahedral sheets (2:1 mineral) and diagrammatically in three dimensions (Fig. 2.6). The silica and gibbsite sheets are combined in such a way that the tips of the tetrahedron of each silica sheet and one of the hydroxyl layers of octahedral sheet form a standard layer and all the tips of the tetrahedral point toward the centre of the unit cell. The oxygen forming the tips of the tetrahedral is shared with the octahedral sheet as well. The anions in the octahedral sheet that falls directly above and below the hexagonal holes formed by the bases of the silica tetrahedral are hydroxyls. Bonding between successive layers is by van der Waal's forces and by cations that balance charge deficiencies in the structure. These bonds are weak, and water or other polar liquids can quickly enter between the layers, causing them to expand significantly. It has a lateral dimension of 1000 to 5000 Å and thickness 10 to 50 Å.

The layers formed in this way are continuous in 'a' and 'b' directions and stacked one above the other in the 'c' direction. Bonding between successive layers is by van der Waal's forces and by cations that balance the charge deficiencies in the structure. These bonds are weak and easily separated by cleavage or adsorption of water or other polar liquids. The basal spacing in the c direction, d (001), is variable, ranging from about 0.96 nm (1 nm = 10⁻⁶ mm) to complete separation.

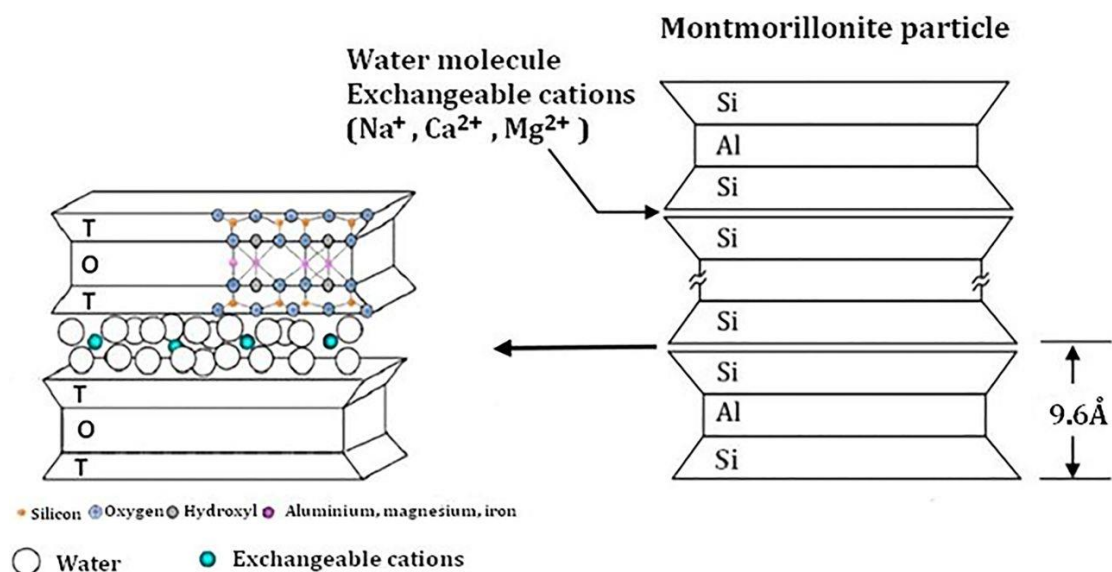


Fig. 2.6. Structure of montmorillonite

The montmorillonite is the primary mineral of bentonite. In the dry state, a particle of montmorillonite resembles a closed book composed of many thin crystalline sheets held together by weak van der Waal's forces and by cations. Each sheet has charge deficiencies within its crystal structure and is neutralized by the presence of cations held loosely to the surface of the sheets. When the dry bentonite and water are mixed, water is drawn into the montmorillonite particles to hydrate the surface of the elemental sheets and the cations. For the combination of sodium montmorillonite and freshwater, the fluid that enters the particles forms thick, viscous diffuse ionic layers around the layer, causing the montmorillonite particles to swell, possibly to the extent of complete separation of the sheets. The fabric of freshwater, low salt, sodium bentonite resembles a pile of crumpled paper. For the combination of dry sodium bentonite and a saline solution, less fluid is required to neutralize the negatively charged sheets, and if the ion concentration is large or the valence of the cations are large, the separation distance between sheets will remain small, and the montmorillonite particles will remain in the form of closed books. The fabric of bentonite, in this case, will consist of swollen but intact montmorillonite particles surrounded by thin, viscous diffuse ionic layers, in an arrangement resembling a pile of fallen books. A third case is that of calcium bentonite, an example of bentonite in which dominant exchangeable cations is polyvalent. The calcium cation is very useful in holding together the montmorillonite sheets, and therefore calcium bentonite has the small potential to swell, even when mixed with fresh water. Calcium bentonite behaves similarly to sodium bentonite in a high salt state, and its permeability properties are about the same.

2.7.3. Swelling behaviour of bentonite

The swelling of bentonite takes place in two stages, inner-crystalline swelling and osmotic swelling (Norrish and Quirk, 1954).

2.7.3.1. Inner-crystalline swelling

In inner-crystalline swelling, water molecules enter the interlayer region of the montmorillonite to hydrate the exchangeable cations located there. The cations upon contact with water order themselves on a plane halfway between the clay layers which lead to a widening of the spacing between the layers. The volume of montmorillonite can double in the process of inner-crystalline swelling. The polarity of the water molecule is an essential factor in the inner-crystalline swelling of clay. When cations hydrate, the water molecules orient their negative dipoles towards the cation and thus weaken the electrostatic interaction between the negatively charged layers and the interlayer cations. Inner-crystalline swelling, which has also been referred to as Type I swelling, is a process, whereby, expandable 2:1 phyllosilicate sequentially intercalate one, two, three or four discrete layers of H₂O molecules between the mineral interlayers (Norrish, 1954). In this process, the swelling occurs before osmotic (Type II) swelling, which is associated with longer range electrical diffuse double layer effects. Fig. 2.7. a and 2.7.b shows inner-crystalline swelling of sodium montmorillonite.

In inner-crystalline swelling, there is a balance between attractive and repulsive forces operating between adjacent interlayer surfaces (Kittrick, 1969; Norrish, 1954; Van Olphen, 1965). Electrostatic attraction between the exchange cations and the basal surfaces of the clay dominates the net potential energy of interaction (Laird, 1996, 2006). The positively charged cations provide links or are like charge bridges between adjacent negatively charged clay layers. On the other hand, the hydration energy of the exchange cations dominates the net potential energy of repulsion. Net forces of attraction are dominant for unsaturated conditions or saturated conditions with high electrolyte concentrations, while net forces of repulsion are dominant in case of fully saturated conditions of low electrolyte concentration.

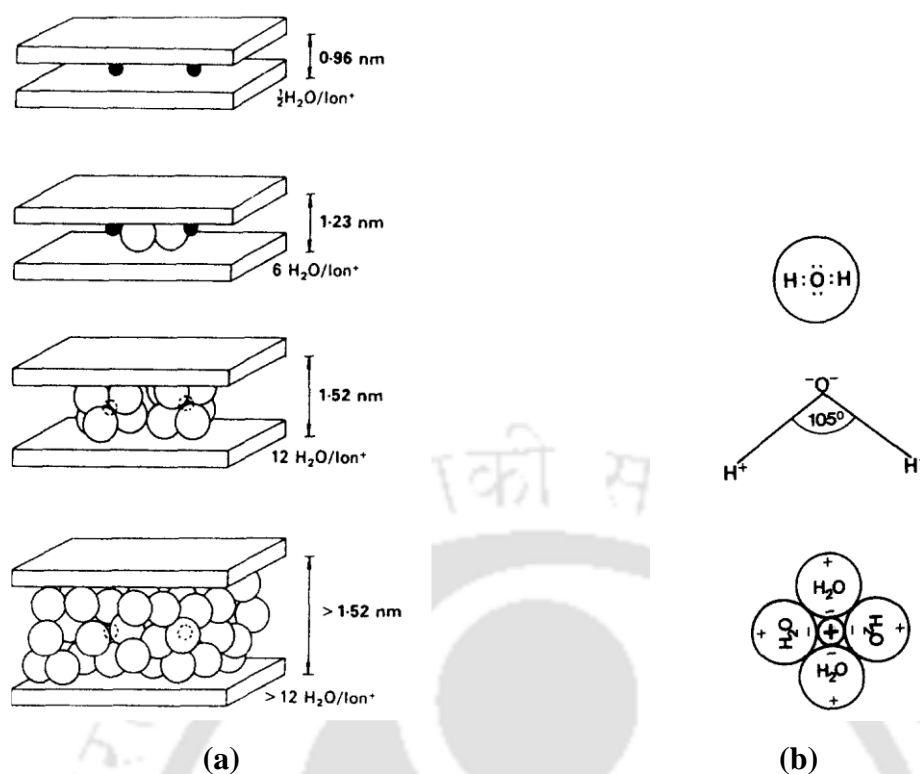


Fig. 2.7. a. Inner-crystalline swelling of sodium montmorillonite. Given are the layer distances and the maximum number of water molecules per sodium ion.

b. The structure of water molecule.

2.7.3.2. Osmotic swelling

The osmotic phase of swelling follows the hydration phase but occurs only when the exchange sites contain monovalent cations (Jellander et al., 1988; Mc Bride, 1994; Norrish and Quirk, 1954; Prost et al., 1998). The interlayer region retains numerous layers of water molecules during the osmotic phase. The number of layers of water molecules at equilibrium is proportional to the cation concentration in the bulk water (Norrish, 1954; Onikata et al., 1999; Zhang et al., 1995). Accordingly, when the bulk water contains a low concentration of monovalent cations, and monovalent cations occupy the exchange sites, a larger fraction of the total water is bound, and less mobile water is available for flow resulting in a lower value of hydraulic conductivity. This condition is commonly observed when sodium-montmorillonite are hydrated and/or permeated with DI water (Alther et al., 1985; Gleason et al., 1997; Lutz and Kemper, 1959; Petrov and Rowe, 1997; Ruhl and Daniel, 1997; Shackelford et al., 2000). When polyvalent cations occupy the exchange sites, only the hydration phase occurs. The interlayer expands until it contains four monolayers of water and then expands no further (Jellander et al., 1988; Mc Bride, 1994;

Norrish and Quirk, 1954; Posner and Quirk, 1964; Prost et al., 1998). There are several explanations for the lack of additional interlayer swelling when polyvalent cations occupy the exchange sites, but consensus does not exist regarding which explanation is correct (Mc Bride, 1994). Nevertheless, the absence of the osmotic phase is well documented experimentally in the literature (Mc Bride, 1994; Norrish and Quirk, 1954; Posner and Quirk, 1964; Prost et al., 1998). Lack of an osmotic phase is evident in the free swelling of calcium-montmorillonite (i.e., bentonites where Ca^{2+} cations occupy the exchange sites), which typically is about 3 mL/2g even when DI water is the hydrating liquid. In contrast, the free swelling of sodium-montmorillonite typically exceeds 30 mL/2g in dilute monovalent solutions or DI water (Egloffstein, 2020; Lin and Benson, 2000).

In sodium-montmorillonite, the swelling can result in the complete separation of the layers. The driving force for the osmotic swelling is the large difference in concentration between the ions electrostatically held close to the clay surface and the ions in the pore water of the rock (Fig. 2.8.a). Irregularities in the crystal lattice are manifested by an excess negative charge, which must be compensated by positive ions close to the surface of the clay. The concentration of positive ions close to the surface is thus too high, while that of negative ions is very small. The positive ion concentration decreases with increasing distance from the surface, whereas the concentration of negative ions increases. The negatively charged clay surface and the cloud of ions form the diffuse electric double layer (Fig. 2.8 b). A high negative potential exists directly at the surface of the clay layer. The value of this potential is reduced, with increasing distance from the surface and reaches zero in the pore water. When two such negative potential fields overlap, they repel each other and cause the observed swelling in clay. The profile of the potential curves, and therefore the repulsion at a given distance varies with the valence and the radius of the counter-ions in the double layer and with the concentration of electrolytes in the pore water. A transformation of sodium montmorillonite into its calcium form or an increase in the electrolyte concentration in the pore water results in the decrease in the double layer thickness and a reduction in the swelling stress.

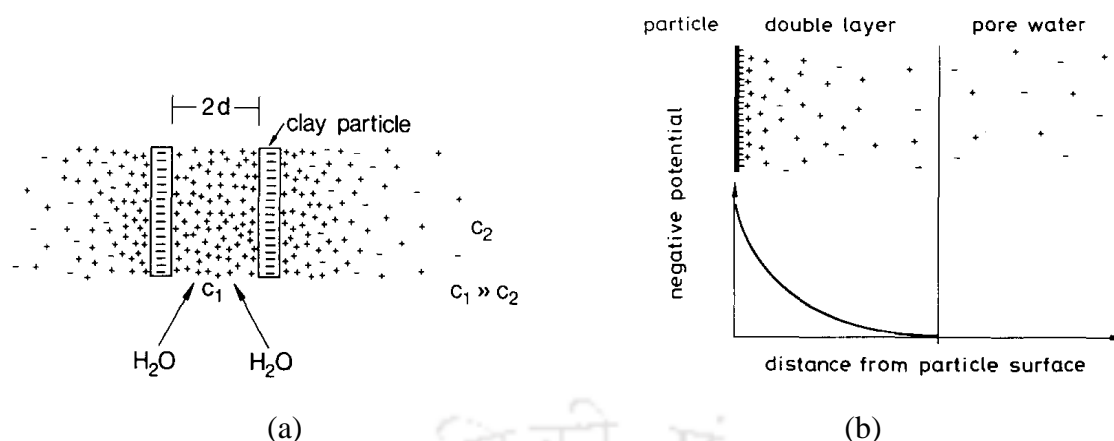


Fig. 2.8. a. Two negatively charged clay layers with ion cloud. The ion concentration C_1 between the layers is much higher than the ion concentration C_2 in the pore water. An equilibration of the concentration can only be reached through the penetration of water into the space between clay layers, since the interlayer cations are fixed electrostatically by the negative charge of the layers (osmotic swelling) (Van Olphen, 1965).

b. Negatively charged clay surface, ions in the diffuse double layer and ions in the pore water. The distribution of the negative potential changes with the valence and the radius of the ions in the double layer and with the electrolyte concentration in the pore water

2.8. Diffuse Double Layer

In dry clay, the negative charge is balanced by exchangeable cations like Ca^{2+} , Mg^{2+} , Na^+ , and K^+ surrounding the particles being held by electrostatic attraction. Cations in excess of those needed to neutralize the electronegativity of the clay particles and associated anions are present as salt precipitates. When water is added, the precipitates can go into solution. The interlayer cations within the clay particles, due to electrostatic attraction of the negatively charged surfaces, pull water molecules because of their hydration energy upon wetting. Highly concentrated cations along the charged surfaces try to diffuse away from the surfaces in order to equalize concentration throughout the clay water solution. The action of two opposing tendencies leads to a specific ion distribution along the clay particles in the clay water suspension. The concentration of the counter ions near the particle surface is high and it decreases with the increase in the distance from the surface. The charged surface and the distributed charge in the adjacent phase are together termed as the diffuse double layer.

Gouy (Gouy, 1910) and Chapman (Chapman, 1913) introduced diffuse double layer model, as shown in Fig. 2.9, in which the potential decreases exponentially away from the clay surface.

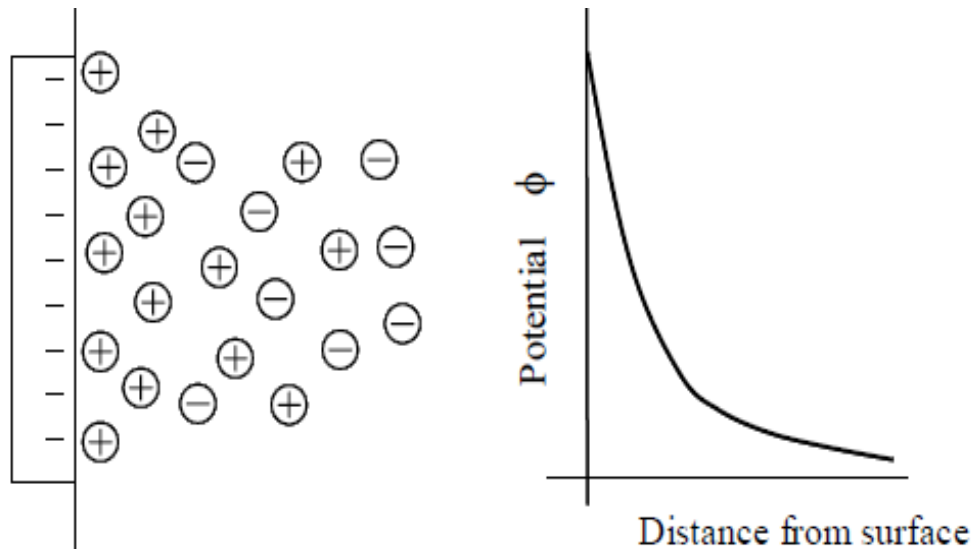


Fig. 2.9. Gouy-Chapman diffuse double layer model

2.8.1. Factors affecting diffuse double layer (DDL) thickness

Factors such as electrolyte concentration, ion valence, di-electric constant, temperature, size of hydrated ions, pH and anion adsorption affects the thickness of diffuse double layer.

- **Electrolyte concentration:** Thickness of DDL varies inversely to the square root of pore water concentration. An increase in electrolyte concentration decreases the surface potential for the condition of constant surface charge, and the potential decays rapidly with distance and the diffuse layer gets reduced. As concentration increases, the mid-plane concentration and electric potential for interacting parallel plates (clay particles) at a given spacing decrease and the interparticle repulsive forces decrease.
- **Cation valence:** Thickness of DDL varies inversely to the valence of cation. An increase in valence reduces the mid-plane concentration and potential between interacting plates, thus leading to a decrease in inter-plate repulsion.
- **Di-electric constant:** Thickness of DDL varies directly to square root of the di-electric constant.
- **Size of hydrated ions:** Thickness of DDL varies directly to size of the hydrated cation.
- **Temperature:** Thickness of DDL varies directly to square root of the temperature.

2.9. Engineering properties of bentonite

2.9.1. Swelling pressure

The swelling pressure of a soil is the external pressure that needs to be placed over the soil to prevent its volume from increasing. Swelling pressure can also be defined as the pressure required to compress a specimen, which has been soaked and completely swollen under seating pressure, back to its original configuration (i.e. before swelling) (Sridharan et al., 1986). Swelling pressure is a helpful index indicating the trouble potential of an expansive soil. When the bentonite contains a significant percentage of montmorillonite, it swells more in presence of water since larger number of water molecules intercalate in between the clay mineral sheets. Thus a larger pressure is required to prevent volume increase which gives rise to a higher swelling pressure for high swelling bentonites.

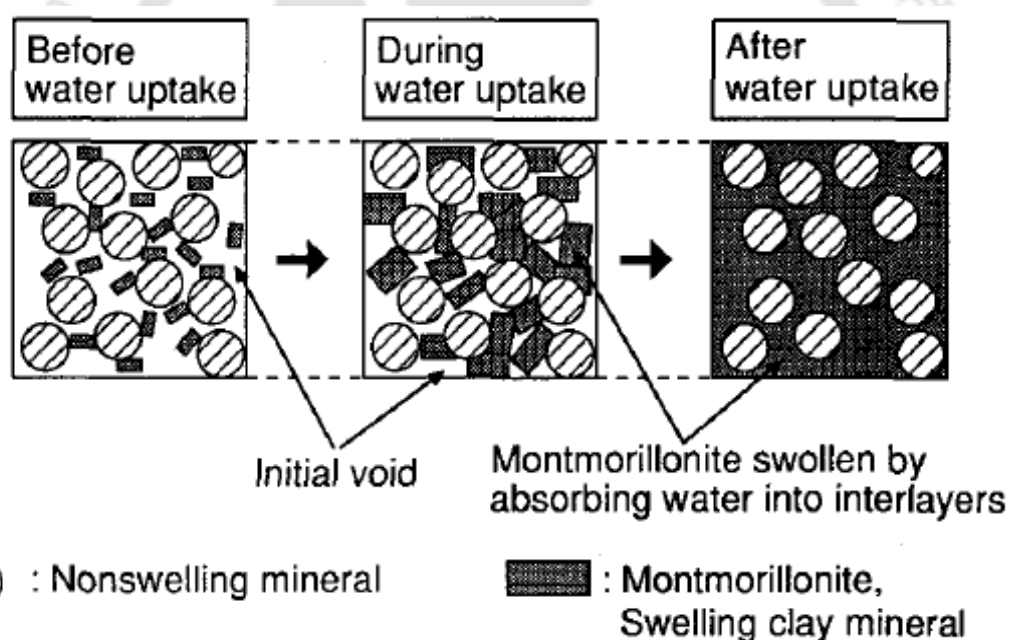


Fig. 2.10. Mechanism of the swelling pressure of compacted bentonite (Komine and Ogata, 1996)

Fig. 2.10 represents mechanism of swelling pressure of bentonite. Bentonite consists of montmorillonite minerals, non-swelling minerals and voids. Before bentonite imbibes water, the voids are mainly occupied by air and free water. After water gets absorbed into the interlayers of montmorillonite, the mineral present in the bentonite, the volume of montmorillonite increases and thus the volume of compacted bentonite increases until the swelling pressure of the montmorillonite minerals equals the vertical pressure. If the total

volume of compacted bentonite is restrained, the montmorillonite minerals swell and fill the voids in the compacted bentonite maintaining the overall constant volume of the bentonite. The volume of montmorillonite minerals cannot change in the compacted bentonite after the voids are filled, and the pressure caused by the swelling of montmorillonite minerals is measured as the swelling pressure of the compacted bentonite.

2.9.2. Swelling potential

The swelling potential is defined as the percentage swelling of a compacted, laterally confined sample, which has been soaked in liquid under a surcharge pressure of 4.9 kPa. The ratio of the maximum swell height of a soil sample to the initial height of the sample is defined as the swelling potential of the soil.

The tendency of expansive soils to increase their volume when they come in contact with water is quantified by the swelling potential and swelling pressure parameters (Rao, 2006). The Atterberg limits and swell potentials of clays depend on the quantity of water that clay can imbibe. High swelling soils imbibe greater quantum of water and hence greater would be its swelling potential.

2.9.3. Compressibility

Similar to the hydraulic conductivity, compressibility is one of the most important properties of clayey soils which need to be studied for settlement analysis. Since the bentonite is a highly compressible material, the liner gets compressed due to the increase in the overburden waste.

The compressibility of the bentonite is controlled by the mechanical and physicochemical effect. High swelling soils develop a larger thickness of diffuse double layer when it interacts with water. When subjected to an overburden pressure, a high swelling soil expels more water resulting in a higher compressibility value. Thus a high swelling bentonite affects its compressibility significantly.

The compressibility of clays under external load is governed by not only the mechanical properties of clay minerals but also the ion concentration, cation valence, dielectric constant and temperature of the pore fluid (Bolt, 1956; Olson and Mesri, 1970; Sridharan and Rao, 1973). The concentration of ions in the pore fluid significantly affects the compressibility behaviour of clays. According to double layer theory, the double layer is compressed due an increase in ion concentration. The compressibility of clays also depends on the chemical

composition of the interstitial liquid or the soil solution. For instance, the replacement of calcium ion in the soil solution of bentonite by sodium ion increases the compression index of the bentonite many times, but the mechanical properties of the solid soil constituents remain unchanged (Salas and Serratosa, 1953). However, the compressibility of clays may be influenced by both mechanical and physico-chemical effects depending on the clay mineralogy, saturating cation and pore fluid. Mechanical effects control the compressibility of kaolinite and illite, whereas, the compressibility of montmorillonite is controlled by physicochemical effects (Robinson and Allam, 1998).

2.9.4. Hydraulic conductivity

The low hydraulic conductivity of the bentonite is due to the accumulation of the water molecules associated with the cations in the interlayer and external surface of the montmorillonite particles, which is manifested as swelling at the macroscale (Mc Bride, 1994; Mitchell and Soga, 2005; Olphen, 1977). These water molecules are tightly held by electrical forces in the interlayer region (i.e. the water molecules are “bound”) and are hydraulically immobile (Mc Bride, 1994; Olphen, 1977). When modest confinement exists, the pores containing free (hydraulically mobile) water becomes compressed and more tortuous as bound water accumulates. As a result, lower hydraulic conductivity occurs as the fraction of the bound water increases (Egloffstein, 1997; Jo et al., 2001; Kashir and Yanful, 2001; Mesri and Olson, 1971; Mitchell and Soga, 2005; Shackelford et al., 2000).

Hydraulic conductivity generally increases when the permeating fluid has a higher unit weight. Similarly, a more viscous fluid will result in a lower hydraulic conductivity. Temperature also affects hydraulic conductivity as temperature variations can change viscosity. These variations are explicable for coarse grained soils. For clays, other factors such as physico-chemical interactions of clay particles also significantly affect the hydraulic conductivity.

The hydraulic conductivity of the clays depends on a number of factors including soil composition, permeant characteristics, void ratio and structure (Lambe, 1955). The saturated hydraulic conductivity is affected by compaction dry density, temperature, montmorillonite content and type of exchangeable cation. (Haug and Boldt-Leppin, 1994) reported that the hydraulic conductivity of a sand-bentonite mixture with 76% montmorillonite was almost 400 times higher than the mixture containing a bentonite with 95% montmorillonite content. Similarly, Martin et al. (1964) concluded from their study

that the hydraulic conductivity of soil has a definite relationship with the exchangeable sodium percentage (ESP) at different pH levels.

2.9.4.1. Influence of salt on hydraulic conductivity of clay

The low hydraulic conductivity of the bentonite is due to imbibing of the water molecules associated with the cations in the interlayer and external surface of the montmorillonite particles, which is manifested as swelling at the macroscale (Mc Bride, 1994; Mitchell and Soga, 2005; Olphen, 1977). Water in the pores of bentonite is of both mobile and immobile type. Mobile water is the freely flowing bulk water that is free to move under a hydraulic gradient. Immobile water is bound to the external and internal (i.e. interlayer) mineral surfaces by strong electrical forces, and act similar to the solid phase in terms of affecting flow. This immobile water is known as diffuse double layer (DDL). When the DDL in the system increases, the fraction of the pore space comprised of freely flowing bulk water decreases and pathways for flow become smaller and more tortuous. With an increase in the volume of bound water, the swell volume increases and the hydraulic conductivity decreases (McNeal et al., 1966; Mesri and Olson, 1971). However, chemicals present in the leachate suppress the thickness of diffuse double layer which in turn shrinks the bentonite. As the bentonite shrink, the flow path becomes open and the hydraulic conductivity increases.

2.9.4.2. Effect of bentonite waste interaction on hydraulic conductivity

Hydraulic conductivity is a one of the key parameter in the design of landfill liners since leachate from waste disposal site influence soil properties. The contaminants affect the hydraulic conductivity of the clays in the following three ways;

- Dissolution of soil minerals- Acids and bases in the contaminant fluids may reduce certain soil minerals into liquid forms by dissolution. For e.g., acids dissolve aluminium and iron, alkali metals, bases dissolve silica in the soils. As a large amount of alumina is present in clay minerals, they get partially dissolved by acids. The solubility of clays in acids depends upon the nature of the acid, the acid concentration, the acid to clay ratio, the temperature and duration of treatment (Grim, 1968). The fines formed by dissolution migrate with the contaminant fluids and cause hydraulic conductivity to decrease due to plugging of the soil pores. However, after a considerable time, this

migration of fines may cause increase in hydraulic conductivity due to piping and channel formation within the soil.

- Changes in clay structure- The clay structure changes due to the changes in its exchange complex or by the replacement of adsorbed water by contaminant fluids. The concentration and valence of cations affect the electrical forces between the clay mineral layer sheets. When cation concentration or valence increases, the net repulsive forces decrease. Thus, a dispersed clay structure changes into flocculated and exhibits an open card house type of structure which increases the hydraulic conductivity. With an increase in Ca^{2+} concentration, replacement of Na^+ with Ca^{2+} takes place and the clay particles become flocculated. On the other hand, when the Na^+ concentration increases, the clay structure gets dispersed, resulting in a lower hydraulic conductivity. In presence of calcium ions, the increase in hydraulic conductivity can be attributed to a decrease in the DDL thickness due to replacement of the monovalent sodium ions by divalent calcium ions and formation of quasicrystals between exchangeable calcium ions and a pair of opposing siloxane cavities (Sposito, 1984). Among the smectite minerals, more changes occur in montmorillonite because of its greater SSA and CEC. The increase in hydraulic conductivity varies depending upon the quality of bentonite to be used in waste containment systems.
- Precipitation- The precipitation of heavy metals, salts and carbonates bring changes in hydraulic conductivity. This precipitation blocks the soil pores and decrease the hydraulic conductivity. However, when the pH, solute concentration, temperature changes, the precipitation reverted.

2.9.5. Adsorption

Adsorption is the phenomenon of accumulation of large number of molecular species at the surface of liquid or solid phase in comparison to the bulk. The process of adsorption arises due to presence of unbalanced or residual forces at the surface of liquid or solid phase. These unbalanced residual forces have tendency to attract and retain the molecular species with which it comes in contact with the surface. Adsorption is essentially a surface phenomenon. Adsorption process involves two components adsorbent and adsorbate. Adsorbent is the substance on the surface of which adsorption takes place. Adsorbate is the substance, which is being adsorbed on the surface of adsorbent. Adsorption process takes place by adsorbate getting adsorbed on adsorbent. Forces of attraction exist between

adsorbate and adsorbent and due to these forces of attraction, heat energy is released. Therefore, adsorption is an exothermic process. Adsorption on solid- solution interface is an important means for controlling the extent of pollution due to heavy metal ion.

2.10. Review of published works on salt solutions

Petrov and Rowe (1997) examined influence of NaCl on the hydraulic conductivity value of bentonite and found that hydraulic conductivity value of bentonite raised from 10^{-9} to $\sim 10^{-6}$ cm/s with the rise in concentration from 0 (DI water) to 2 N. Shackelford et al. (2000) examined the hydraulic conductivity of GCLs infused with salt solutions like ZnCl₂, CaCl₂ and NaCl and concluded that permeant solution containing high concentration of monovalent cations along with low concentration of divalent cations causes substantial rise in the hydraulic conductivity value. Jo et al. (2001) investigated the swelling characteristics and hydraulic conductivity value of non-prehydrated GCLs containing granular bentonite infused with salt solution of NaCl, KCl, CaCl₂, LiCl, MgCl₂, CuCl₂, ZnCl₂, HCl, and NaOH. They reported that with the rise in electrolyte concentration and cation valency of the pore fluid the hydraulic conductivity value of bentonite increased. Castellanos et al. (2008) examined the swelling, compressibility and hydraulic conductivity value of compacted FEBEX bentonite in presence of saline fluid (CaCl₂ and NaCl). From the investigation they concluded that swelling capacity of bentonite decreases & the hydraulic conductivity of bentonite increases when high salinity permeants were used. Mishra et al. (2009) examined the influence of different concentration of CaCl₂ and NaCl on hydraulic conductivity and liquid limit of different mixtures of bentonite and basalt soil and found that due to the infusion of CaCl₂ and NaCl solution, the bentonite of superior quality which is categorized by an exchangeable sodium percentage, high swelling capacity and liquid limit experiences considerable variation in the hydraulic conductivity value. Thammathiwat and Chim-oye (2010) studied the impact of monovalent, divalent and trivalent salt solutions on hydraulic behaviour and swelling of geosynthetic clay liners (GCLs) and reported that for similar concentration, divalent and trivalent cation solutions shows less swelling and higher hydraulic conductivity value as compared to monovalent cations.

Shirazi et al. (2011) studied the swelling characteristics of compacted bentonite in presence of saline solution (NaCl) and reported that rate of swelling is influenced by the

concentration of NaCl more as compared to loading impact and initial dry density. Impact of different inorganic salts such as NaCl, MgCl₂ and CaCl₂ was investigated by Shariatmadari et al. (2011) on the compressibility behaviour bentonite–clay admixtures and concluded that with the rise in the concentration of salt, the C_c of that reduced. Xue et al. (2012) investigated the influence of KCl, NaCl, MgCl₂ and CaCl₂ on hydraulic behaviour of Geosynthetic Clay Liner materials and concluded that hydraulic conductivity value of the liner material increased two orders of magnitude when saturated with salt solutions in comparison with water. Zhu et al. (2013) examined the impact of NaCl and CaCl₂ solutions on the hydraulic conductivity value and swelling pressure of compacted bentonite. From the investigation they concluded that the hydraulic conductivity value increased and the swelling pressure of the bentonite reduced with rising concentration of permeants. Weimin et al. (2014) studied the influence of various concentration of NaCl solution on the swelling strain, hydraulic conductivity, compression index and secondary consolidation coefficient of highly compacted GMZ01 bentonite. They reported that swelling strain, compression index and secondary consolidation coefficient reduced and hydraulic conductivity value increased with the rise in concentration of NaCl solution. Dutta and Mishra (2015) examined the alteration in properties of bentonites in the existence of various salt solutions and they found a direct correlation between the NaCl and CaCl₂ concentration and hydraulic conductivity, while an inverse correlation was established with swelling pressure, swelling volume, liquid limit. Dutta and Mishra (2016a) investigated the influence of NaCl and CaCl₂ on the alteration in consolidation parameters of compacted bentonites and concluded that the compression index (C_c), coefficient of volume change (m_v) and time for 90% consolidation (t_{90}) of the bentonites decreased, whereas, coefficient of consolidation (c_v) increased with the increase in salt concentration.

Table 2.1. Summary of interaction of clay with salt solutions

| Sr. No | Author & year | Salt solutions | Properties | Conclusion |
|---------------|---------------------------|------------------------------------|---|--|
| 1. | Petrov and Rowe (1997) | NaCl | Hydraulic conductivity | Hydraulic conductivity of bentonite increased from $\sim 10^{-11}$ to $\sim 10^{-8}$ m/s with an increase in the NaCl concentration from 0 to 2N. |
| 2. | Shackelford et al. (2000) | NaCl & CaCl ₂ | Hydraulic conductivity | High concentration of monovalent cations as well as low concentration of divalent cations causes significant increase in the hydraulic conductivity. |
| 3. | Jo et al. (2001) | Single and divalent salt solutions | Hydraulic conductivity | Hydraulic conductivity of bentonite increased with the increase in valency of the cations of the pore fluid. |
| 4. | Castellanos et al. (2008) | CaCl ₂ and NaCl | Swelling capacity, hydraulic conductivity | Swelling capacity of bentonite decreases & the hydraulic conductivity of bentonite increases when high salinity permeants were used. |
| 5. | Mishra et al. (2009) | NaCl & CaCl ₂ | Liquid limit, hydraulic conductivity | Liquid limit of the mixtures decreases and hydraulic conductivity increases with an increase in the salt concentration. |

| | | | | |
|-----|----------------------------------|--|--|--|
| 6. | Thammathiwat and Chim-oye (2010) | Monovalent (LiCl, NaCl and KCl), divalent (CaCl ₂ , MgCl ₂ and CuCl ₂) and trivalent cation (FeCl ₃) | Hydraulic conductivity | A higher value of hydraulic conductivity was observed for GCLs permeated with solutions containing divalent or trivalent cations in comparison with monovalent cations or distilled water. |
| 7. | Shirazi et al. (2011) | NaCl | Swelling volume, liquid limit | Liquid limit decreased remarkably from 497 % to 112 % when the testing liquid changed from DI water to 0.5 M NaCl solution |
| 8. | Shariatmadari et al. (2011) | NaCl, CaCl ₂ and MgCl ₂ | Swelling volume, liquid limit & hydraulic conductivity | Increasing the salt concentration, the swelling volume and liquid limit of the mixtures decreased whereas the hydraulic conductivity increased. |
| 9. | Xue et al. (2012) | MgCl ₂ , CaCl ₂ , NaCl and KCl | Hydraulic conductivity | Hydraulic conductivity was found to be in the order CaCl ₂ > MgCl ₂ > KCl > NaCl. |
| 10. | Zhu et al. (2013) | NaCl and CaCl ₂ | Swelling pressure and hydraulic conductivity | Swelling pressure of the bentonite decreased with increasing concentration of infiltrating solutions. |

| | | | | |
|-----|--------------------------|----------------------------|---|--|
| 11. | Dutta and Mishra (2015) | NaCl and CaCl ₂ | Liquid limit, swelling characteristics & hydraulic conductivity | Liquid limit, free swelling, swelling potential and swelling pressure of the bentonites decreased with an increase in the salt concentration. The hydraulic conductivity of the bentonite increased with an increase in the inorganic salt concentrations. |
| 12. | Dutta and Mishra (2016a) | NaCl and CaCl ₂ | Consolidation parameter | At constant pressure, with rise in concentration, DDL decreases, Hydraulic conductivity increases (expulsion of water fast), c_v increases, t_{90} decreases, m_v increases Increase in pressure Clay particle come closer c_v decreases, t_{90} increases m_v decreases |

2.11. Heavy Metals

Heavy metals are commonly found in several kinds of wastes, landfill leachates and accounted for much of the contamination found at hazardous waste sites. Concentration of heavy metals ranges from 0 to 100 ppm in municipal solid waste and residual agricultural waste and from 100 to 10000 ppm in sewage sludge, mining waste and industrial wastes (Yong and Di Perno, 1991).

The heavy metals commonly found in landfill leachate include Pb, Cd, Cu, Ni, Fe and Se. Although the actual number and concentration of heavy metals in the leachate varies

from one landfill to another, the concentration of most of the heavy metals are considerably above the allowable concentrations.

Metal species in leachate is of utmost concern because of the dangerous effects of heavy metals on the geo-environment. Heavy metals do not get degraded or destroyed and a small extent of them generally enters human and animal bodies via food, drinking water, and air. In trace amounts, some heavy metals (e.g., copper, nickel, zinc) are good for all organisms, to accomplish specific catalytic functions. However, when it exceeds the permissible limits, all metals can disturb the metabolism by binding non-specifically to biomolecules and inflicting oxidative damage, due to their ability to catalyse redox reactions, which may result in damage to cellular structures (especially membranes), and DNA modification (mutagenesis). If human beings are exposed to high levels of metals it can cause acute toxicity symptoms, while long-term exposure to lower levels can cause allergies and even cancers.

2.11.1. Sources and Impact of heavy metal

In recent years, human exposure has risen dramatically because of an exponential increase in the use of heavy metal in several industrial, agricultural, domestic and technological applications (Bradl, 2005). Sources of heavy metals in the environment include geogenic, industrial, agricultural, pharmaceutical, domestic effluents, and atmospheric sources (He et al., 2005). In point source areas such as mining, foundries and smelters, and other metal-based industrial operations environmental pollution is very prominent (Bradl, 2005; Ferguson, 1990; He et al., 2005).

Human exposure to heavy metals result from anthropogenic activities such as mining and smelting operations, industrial production and use, and domestic and agricultural use of metals and metal-containing compounds (Goyer and Clarkson, 1996; He et al., 2005; Herawati et al., 2000; Shallari et al., 1998).

Metals such as cobalt (Co), copper (Cu), iron (Fe), magnesium (Mg), manganese (Mn), nickel (Ni), and zinc (Zn) are essential nutrients that are required for various biochemical and physiological functions. Inadequate supply of these micronutrients results in a variety of deficiency diseases or syndromes (WHO/FAO/IAEA, 1996).

Excessive exposure to zinc causes various health issues in human body, generally entering through three ways; inhalation, dermal exposure and oral exposure. Some of the ill effects include lethargy and focal neuronal deficits (brain), disorders in (respiratory tracts) after inhalation of zinc smoke and fumes, nausea, vomiting, epigastric pain and

diarrhoea (gastrointestinal tracts), and elevated risks of prostate cancer (prostate) (Plum et al., 2010). Additionally, the zinc contamination is not only limited to human health disorders, it also adversely affects fish mortality and physiology when in excess amounts in the water environment (Giardina et al., 2009), decreases the bacterial diversity in soil thereby diminishing the effective fertility (Hiroki, 1992; Moffett et al., 2003), and seriously altering the earthworm population in soil (Spurgeon et al., 1994; Spurgeon and Hopkin, 1996). Hence, zinc contamination is considered a serious concern in the field of environmental engineering, owing to the diversifying ill-effects on various components of the natural ecosystem. Cadmium is often used in various industrial activities. Production of alloys, pigments, and batteries are the major industrial applications of cadmium (Wilson, 1988). Although the use of cadmium in batteries has shown substantial growth in recent years. Other sources of cadmium comprise emissions from industrial activities, including mining, smelting, and manufacturing of batteries, pigments, stabilizers, and alloys (ATSDR, 2008). Chronic inhalation exposure to cadmium particulates is generally associated with changes in pulmonary function and chest radiographs that are consistent with emphysema (Davison et al., 1988). Similarly, lead has many different industrial, agricultural and domestic applications. It is currently used in the production of lead-acid batteries, ammunitions, metal products (solder and pipes), and devices to shield X-rays. An estimated 1.52 million metric tons of lead were used for various industrial applications in the United States in 2004. Of that amount, lead acid batteries production accounted for 83 percent, and the remaining usage covered a range of products such as ammunitions (3.5 percent), oxides for paint, glass, pigments and chemicals (2.6 percent), and sheet lead (1.7 percent) (Gabby, 2006; Norseth, 1986). The nervous system is the most vulnerable target of lead poisoning. Headache, poor attention span, irritability, loss of memory and dullness are the early symptoms of the effects of lead exposure on the central nervous system (ATSDR, 1999; Harvey, 2002). In the human body, the greatest percentage of lead is taken into the kidney, followed by the liver and the other soft tissues such as heart and brain, however, the lead in the skeleton represents the major body fraction (Flora et al., 2006).

Copper is one of the main constituents of discharge from mining, smelting, and various other chemical plants as well as landfill leachates (Ding et al., 2009; Kjeldsen et al., 2002). In trace amount, copper is considered essential for all organisms to perform their complete catalytic functions (WHO, 1996); however, amounts exceeding desirable limits can seriously disturb the metabolism and cause cellular damage and DNA modification (Bonsignore et al., 2018). Excessive exposure to copper has been linked to cellular damage

leading to Wilson disease in humans (Dorsey and Ingerman, 2004; Tchounwou et al., 2008).

2.11.2. Disposal of waste containing heavy metal in the landfills

In landfill leachate, the presence of heavy metals poses a threat to the environment. Different kinds of wastes i.e., electronic waste, painting waste and utilized batteries are responsible for the increment of heavy metals in the landfills (Aderemi et al., 2011). Leachate are extracted, dissolved or suspended materials, which permeated through solid waste. Mostly it enters into the landfills through external sources, such as rainfall, surface drainage, and water from underground springs and percolates through solid wastes that are undergoing decomposition. Depending on the age of the landfill and the events before the time of sampling the chemical composition of the leachate will differ significantly (Tchobanoglous et al., 1993). The recent increase in use and disposal of electronic gadgets like mobile phones and computers bring up the issue about the amount of metals they contain in waste disposal sites and their fate in the environment especially because such gadgets chiefly contain mercury, arsenic, lead, cadmium, copper, zinc and others (Agamuthu and Fauziah, 2010). Thus, heavy metals present in leachate can migrate a long way from the disposal site limits and may constitute a genuine contamination danger for the water table and the soil around the landfill (Yoshida et al., 2002; Zai et al., 2004).

Approximately 50% of the cadmium load was in the form of plastics as pigments or stabilizing agents (Prudent et al., 1996). However, data that is more recent shows that 75% of the cadmium in MSW today is in the form of batteries (Boehme and Panero, 2003). The presence of copper in landfill was mostly due to non-ferrous metal or metal scrap but also was associated with fine particles, paper and cardboard (inks). Chromium was mostly in the form of non-ferrous metal scrap but perhaps 25% of the load in waste was in leather. Nickel was found to be mostly associated with scrap metal, but also with glass and fine particles. Zinc and lead were mostly in the form of scrap metal (Prudent et al., 1996). In the year 2000, 65% of the lead in products discarded in MSW was in the form of lead-acid batteries, 30% was in consumer electronics, and 4% was in glass, ceramics, and plastics was estimated (USEPA, 1989). Mercury in waste is supposed to exist primarily within disposed products including batteries, fluorescent bulbs, thermostats and other switches, and measuring and control devices such as thermometers (NJDEP, 2002).

In electronic devices toxic chemicals are used which include metals and Metalloids (e.g., arsenic, cadmium, chromium, copper, lead, And mercury) and organic chemicals such as

brominated Flame retardants (FWI, 2001; Hedemalm et al., 1995). Toxic chemicals will leach when these devices are disposed (Lee et al., 2000; Young, 2012). The printed wire boards also referred to as circuit boards may contain arsenic, cadmium, chromium, lead, and mercury are mostly found in e-waste (FWI, 2001; Hedemalm et al., 1995). One of most common component of discarded electronic is cathode ray tubes in computer monitors & television. Cathode ray tubes (CRTs) may contain barium, cadmium, Copper, lead, zinc, and several rare earth metals (FWI, 2001). Due to their growing magnitude in municipal solid waste (MSW) & their role as a major source of lead in MSW, CRTs are facing disposal problem. Musson et al. (2006) reported that Lead leached from the CRT samples at an average concentration of 18.5 mg/L. This exceeded the regulatory limit of 5.0 mg/L. Lead is one heavy metal with known toxic properties that is found in large amounts in many electronic devices (Hedemalm et al., 1995). Electronic Devices, along with lead-acid batteries, are the major Contributors of lead in the municipal solid waste stream (USEPA, 1989) Discarded electronic devices are characterised as hazardous waste due to the presence of lead (Spalvins et al., 2008). Other devices such as computers, cell phones, and electronic parts contain elements that can cause threat to human health and the environment at prominent exposure (Widmer et al., 2005; Wong et al., 2007). A plentiful of toxic chemicals are present in these devices comprising mercury, silver, cadmium, and flame-retardants. Spalvins et al. (2008) determined the lead concentrations ranging from 7 to 66 µg/L in the columns containing electronic waste. In India, leather tanning is a major industrial sector. This sector produces tons of solid waste every year and that waste are dumped in the open field and landfills. The presence of hexavalent chromium (Cr), a well-known mutagenic carcinogenic metal, has already been reported in tannery waste-contaminated soils (IARC, 1990; Thangavel et al., 2002). The leachates from tannery solid waste (TSW), a major environmental pollutant. The chemical analysis of TSW samples revealed that the chief constituents were chromium and nickel, which may cause genetic abnormalities (Chandra et al., 2004). Chandra et al. (2005) revealed that both metal waste leachate (MWL) and dye waste leachate (DWL) contained high concentrations of chromium, nickel and iron that significantly induced cytogenetic alterations. Heavy metal composition from different sources as observed by different researchers have been summarized in Table 2.2.

2.11.3. Impact of heavy metal on liner material

a. Sorption

Clay minerals are good adsorbents for metal ions from aqueous solutions, owing to their high cation exchange capacity and high specific surface area associated with their small particle sizes, and have the advantage of being abundant and inexpensive; therefore they can find application as low-cost, effective materials for the removal of metal ions from various effluents, such as industrial and processing waters and wastewaters, or extracts resulting from the treatment of contaminated soils by soil washing (Adeyemo et al., 2017; Pawar et al., 2016).

The key constituent of bentonites is montmorillonite, which is a 2:1 mineral with one octahedral sheet and two silica sheets, forming a layer. Layers are held together by van der Waals forces. Because of these weak forces and some charge deficiencies in the structure, water can easily penetrate these layers and cations balance the deficiencies. Sorption of metal ions by bentonite depends on charge characteristics of the adsorbent, including surface charge magnitude, type of charge (permanent or variable) and point of origin from tetrahedral or octahedral substitution in the case of a permanent charge (Baylan and Meriçboyu, 2016; Galindo et al., 2013) On the other hand, properties of metal ions like charge, ionic radius and their soft-hard acid-based characteristics are also known to regulate metal affinity for reactive bentonite surfaces. Other factors such as metal concentration, pH, ionic strength, type and concentration of competing ions, the liquid: solid ratio and temperature also affect sorption processes (Baylan and Meriçboyu, 2016; Pawar et al., 2016)

b. Impacts of heavy metal on bentonite in terms of DDL

Clay soils that are used in landfill liners get exposed to physicochemical attacks by the leachates generated from the wastes. Metal species in leachate is of utmost concern because of the harmful impacts of heavy-metal contaminants on the geoenvironment. The presence of heavy-metal contaminants in the leachates affects the pore-fluid chemistry and controls the diffuse double layer (DDL) thickness of the clay particles.

Although landfill leachates usually contain only modest concentrations, i.e., from traces to 1,000 mg/L (Kanmani and Gandhimathi, 2013; Prudent et al., 1996) of heavy-metal contaminants, it is quite essential for a geotechnical engineer to understand the engineering properties of clayey soils in the presence of contaminants. Because of their high contaminant adsorption capacity and low hydraulic conductivity, bentonites are frequently

used as a liner material at waste disposal sites. When montmorillonite, a dominant mineral present in bentonite, reacts with water, DDL develops (Mitchell and Soga, 2005), resulting in the swelling of bentonite. However, the presence of various contaminants in the leachate decreases the DDL thickness, resulting in a change in the swelling behavior of bentonite (Norrish and Quirk, 1954).

As the thickness of the DDL is primarily controlled by factors such as clay mineralogical composition and concentration and type of salt present in the pore water (Bolt, 1956; Mitchell and Soga, 2005; Sridharan and Rao, 1973; Young, 2012), these same factors may affect the various consolidation parameters such as C_c , m_v , c_v , and t_{90} of the bentonite undergoing compression. Many investigations have been carried out in the past to study the influence of heavy metals on the behaviour of bentonite. Bentonites with different mineralogical composition may behave differently in the presence of heavy-metal contaminants, it is quite important to compare the behaviour of different bentonites in the presence of heavy metal contaminants.

The heavy metal contaminants present in the leachates of the wastes affects the pore-fluid chemistry and diffuse double layer (DDL) thickness of the clay particles. The heavy-metal contaminants suppress the DDL thickness of bentonite, resulting in a decrease in its swelling capacity.

2.11.4. Impact of heavy metals on engineering behaviour of liner material

2.11.4.1. Atterberg limits

The liquid limit of the bentonite decreased with increasing heavy metal concentrations (Dutta and Mishra, 2016b). Increasing the metal ion concentration decreases the inter-particle repulsion that makes the particles free to move at lower inter-particle distances, resulting in the decrease in the liquid limit (Sridharan, 1975; Warkentin, 1961).

The plastic limit of the bentonites decreased marginally with increasing heavy metal concentrations (Dutta and Mishra, 2016b). In plastic state, in order to take up a new position, the soil particles should be able to move or slide past one another and retain this new equilibrium position; however, the cohesion between the particles should be low enough to permit this movement of the particles and strong enough to hold the particles in its new equilibrium position (Young, 2012).

2.11.4.2. Free swelling

The free swelling of bentonite was found to be decreased significantly due to the increase in the metal ion concentration. A higher reduction in the free swelling of bentonite can be attributed to the significant reduction in the DDL thickness due to the addition of heavy metal solutions.

2.11.4.3. Hydraulic conductivity

Hydraulic conductivity of bentonites depends on a number of factors including mineral composition, permeant characteristics, void ratio, and structure of soil fabrics (Lambe, 1958). Hydraulic conductivity of the bentonite increased with an increase in the heavy metal concentrations (Dutta and Mishra, 2016b).

2.11.4.4. Compressibility

Compressibility of the liner material is one of the most important properties that help in analysing the settlement of the clay liner (Mishra et al., 2010). As bentonite is a very highly compressible material, it gets compressed significantly because of the weight of the waste stacked in a waste disposal site. Consolidation is a process defined as compression that results when a surcharge load is applied to a saturated clay. The consolidation of a soil gives rise to a settlement, the magnitude of which is determined after the complete dissipation of the generated pore-water pressure (Young, 2012).

The compressibility behavior of bentonite can be derived by using the DDL theory, as the compressibility of bentonite is primarily controlled by the physicochemical stresses generated in a clay-water system (Bolt, 1956; Sridharan and Jayadeva, 1982). The DDL theory was first proposed by Gouy (1910), and then it was modified by Chapman (1913). This theory was further derived and used by many researchers (Bolt, 1956; Dutta and Mishra, 2016a; Olphen, 1977; Ouhadi et al., 2006; Sridharan and Jayadeva, 1982) to analyse the compressibility of bentonite in the presence of various electrolyte solutions.

2.11.4.5. Shear strength

A liner should be strong enough to withstand the load exerted by the overlying body of waste.

2.11.4.6. Consolidation characteristics

Heavy metal contaminants can also influence the consolidation parameters such as coefficient of volume change (m_v), coefficient of consolidation (c_v), compression index (C_c), and time requires for the completion of 90% of consolidation (t_{90}) in the presence. The C_c , m_v , and t_{90} of the bentonites decreased, whereas, the c_v increased with the increase in heavy-metal contaminants concentration (Dutta and Mishra, 2017).

2.12. Review of published works on metal solutions

Li and Li (2001) explored the impact of metal on bentonite–spruce bark, sand–bentonite and sand–bentonite–forest soil and observed that that forest soil admixture showed higher sorption capacity. Soil admixtures permeated with heavy metals exhibited higher hydraulic conductivity value in comparison to the blank solution (water). Abollino et al. (2003) examined sorption of seven heavy metals on bentonite and concluded that the sorption capacity of heavy metal declines with the decrease in pH. Li (2003) studied the adsorption capacity of kaolinite clay mineral in the presence of various combinations of cadmium, copper and zinc and observed that binary and ternary solutions of heavy metal ion showing lower adsorption capacity compared to the individual metal solution. Lo et al. (2004) studied the migration of cadmium lead and zinc in and Ottawa sand and bentonite-soil admixture and concluded that the hydraulic conductivity of bentonite-soil admixture increases noticeably when it is infused with the metal solution. Ouhadi et al. (2006) studied the consolidation behaviour of bentonite in the presence of heavy metal at different pH and observed that at low pH and high metal concentration the microstructural change in the soil occurs. They also concluded that heavy metals have the different onset of precipitation and the rheological performance of soil is controlled by the osmotic phenomenon. Nakano et al. (2008) conducted various tests to determine hydraulic conductivity and lead adsorption behaviour of three Japanese and one U.S. bentonite and concluded that carbonate precipitate as $PbCO_3$ on the bentonites and it also shows a leading role in the low lead solution. Du et al. (2015) investigated the influence of various levels of lead concentration on calcium–bentonite backfills/bentonite clay and concluded that with the increase in the concentration of lead, the pH, liquid limit and compression index of the soil decreases. Bentonites with different mineralogical compositions were also examined by Dutta and Mishra (2016b) under varying concentration of heavy metals (Pb^{2+} , Cu^{2+} and Zn^{2+}). It was

found that with the rise in the concentration of the metal solution, Atterberg limits, free swelling, swelling pressure, and swelling potential of the soil decreased and the hydraulic conductivity increased. Dutta and Mishra (2017) examined the impact of various heavy metals of varying concentration on the consolidation parameters of bentonite. They concluded that coefficient of consolidation (c_v) increases while, C_c , coefficient of volume change (m_v), and time to achieve 90% of consolidation (t_{90}) of the bentonites decreases with the rise in heavy metal concentration.

Table 2.2. Summary of interaction of clay with heavy metals

| Sr. No | Author & year | Heavy metals | Properties | Conclusion |
|--------|------------------------|---|---|--|
| 1 | Li and Li (2001) | Cd, Pb, and Cu | Sorption and Hydraulic conductivity behaviour of three types of bentonite admixes | Soil used: sand bentonite, sand bentonite forest soil, sand bentonite spruce bark. Sand bentonite spruce bark: highest retention capacity and lowest hydraulic conductivity. |
| 2 | Abollino et al. (2003) | Cd, Cr, Cu, Mn, Ni, Pb and Zn | Adsorption | Adsorption of metal ion decreases with decreasing in pH. |
| 3 | Li (2003) | Cd, Pb, and Cu binary Pb^{2+} + Cu^{2+} , Pb^{2+} + Cd^{2+} , Cu^{2+} + Cd^{2+} and ternary Pb^{2+} + Cu^{2+} + Cd^{2+} | Adsorptivity of heavy metal ions | The adsorptivity of heavy metal ions was slightly lower in binary and ternary solutions than for single ion species in the solution. Soil used : kaolinite |
| 4 | Lo et al. (2004) | Pb, Zn, and Cd | Batch sorption and column tests | That the permeability of the compacted sand to be of six |

| | | | | |
|---|--------------------------|--|---|---|
| | | | | orders of magnitude higher than that of bentonite soil admixture |
| 5 | Ouhadi et al. (2006) | Pb ²⁺ , Zn ²⁺ | Mechanical behaviour of bentonite soil | pH variation in the presence of HMs has more effect on the compressibility behaviour of soil. |
| 6 | Nakano et al. (2008) | Pb ²⁺ | Batch adsorption test, and hydraulic conductivity . | Carbonate plays a major role at low Pb solution concentration and precipitate as PbCO ₃ . Hydraulic conductivity: US bentonite was lowest in comparison to the Japanese bentonite due to its highest montmorillonite content and swelling capacity. Soil used: 3 Japanese bentonite, 1 US bentonite. |
| 7 | Du et al. (2015) | Pb ²⁺ | Liquid limit, compression index, hydraulic conductivity & pH | Liquid limit, compression index & pH decreased and the hydraulic conductivity increases as the Pb concentration increased. |
| 8 | Dutta and Mishra (2016b) | Zn ²⁺ , Pb ²⁺ , and Cu ²⁺ | Liquid limit, swelling characteristics & hydraulic conductivity | Increase in the heavy metal concentration the liquid limit, free swelling, swelling pressure, and swelling potential of the bentonite decreased and the hydraulic conductivity increased. |
| 9 | Dutta and Mishra (2017) | Zn ²⁺ , Pb ²⁺ , and Cu ²⁺ | Consolidation parameter | At constant pressure, with rise in concentration, DDL decreases, Hydraulic conductivity increases (expulsion of water fast), c_v |

increases, t_{90} decreases, m_v
 increases
 Increase in pressure
 Clay particle come closer
 c_v decreases, t_{90} increases
 m_v decreases

2.13. Review of published works on adsorption of Pb^{2+}

Gong et al. (2006) studied adsorption capacity at various pH and kinetic model of Pb^{2+} and Cu^{2+} onto the organo-bentonite modified by 4-methyl benzo-15-crown-5 (MB15C5) and observed that with the increase in pH, adsorption of both the metal increased and stated that pseudo-second-order kinetic model fitted well in all cases. Ayari et al. (2007) investigated on retention of Pb^{2+} by using bentonite as an adsorbent and observed a greater potential of bentonite to adsorb Pb^{2+} . Zhang and Hou (2008) investigated the adsorption of Pb^{2+} by using montmorillonite and reported that adsorption of Pb^{2+} is dependent on the pH of the solution, and the adsorption capacity upsurges with the increase in pH. Hefne et al. (2008) studied kinetic and isotherm study of sorption of Pb^{2+} by natural and treated bentonites. From the investigation they concluded that the adsorption of Pb^{2+} on the bentonite reaches equilibrium time after 5 min, and the data were fitted well by a Langmuir isotherm model. Gupta and Bhattacharyya (2008) examined the immobilization of Pb^{2+} , Ni^{2+} and Cd^{2+} on montmorillonite and kaolinite clay and found that the adsorption capacity of heavy metals was in range of 21.1–31.1 mg/g for montmorillonite and 6.8–11.5 mg/g for kaolinite respectively. Adsorption of Pb^{2+} was investigated by Kul and Koyuncu (2010) by activated and native bentonites. They reported that with the increase in temperature the adsorption efficiency of both the bentonites were found to be increased. Fernández-Nava et al. (2011) examined the removal of Pb^{2+} , Cd^{2+} and Hg^{2+} using granular bentonite and found an adsorption capacity of 19.45, 13.05 and 1.7 mg/g for Pb^{2+} , Cd^{2+} and Hg^{2+} respectively for an initial capacity of 100 mg/L, respectively. Hamidpour et al. (2011) studied the use of the natural bentonite and zeolite for the sorption of Pb^{2+} and reported that removal of Pb^{2+} was higher for zeolite as compared to natural bentonite due to high CEC and specific surface area for zeolite. Pawar et al. (2016) studied removal of Pb^{2+} and Cu^{2+} by using bentonite as an adsorbent and concluded that removal of metal ions was favoured

by increases in the pH, heavy metal concentrations, contact time, and bentonite dosage. Baylan and Meriçboyu (2016) examined the adsorption study on bentonite and grapeseed activated carbon in the presence of single and binary solutions of copper and lead and observed a higher sorption capacity of bentonite in comparison to grapeseed activated carbon. They also concluded a greater affinity for Pb^{2+} in comparison to the Cu^{2+} solution. Deka and Sekharan (2017) investigated the contaminant retention characteristics of bentonite, fly ashes, and bentonite-fly ash mixes in the presence of Pb^{2+} and observed a good removal percentage (>90%) of Pb^{2+} for bentonite and all fly ash–bentonite mixes. Khan et al. (2017) examined the adsorption study on bentonite in the presence of lead and reported that maximum adsorption occurs within 5 minutes. Experimental data were fitted well to the Langmuir adsorption isotherm. The maximum lead removal was attained at 6 g/L of bentonite clay at pH of 4. Zhu and Qin (2017) studied the sorption capacity of natural and composite bentonite in existence of lead aqueous solution and found that sorption of both the bentonites intensely governed by the pH values of the mixture.

Table 2.3. Summary of interaction of clay with Pb^{2+}

| Sr. No | Author & Year | Heavy metal | Properties | Conclusion |
|--------|----------------------|-------------|--|--|
| 1. | Gong et al. (2006) | Pb, Cu | Adsorption & Isotherm study For Pb- pH-5, 0.4-10 mmol/L For Cu- pH-5, 0.2-6 mmol/L | The adsorption of Cu^{2+} and Pb^{2+} increases with increasing pH and the adsorption of Cu^{2+} and Pb^{2+} reaches a maximum at pH 3.5–6. Experimental data were fitted well to the Langmuir adsorption isotherm. The kinetics of sorption processes were best described by a pseudo-second-order kinetic model. |
| 2. | Zhang and Hou (2008) | Pb | Adsorption & Isotherm study pH-6, 0-400 mg/L | Adsorption is dependent on the pH value of the medium, and the uptake of Pb(II) increases with the pH increasing in the pH range of 2.0–10.0. The adsorption kinetics is in better agreement with pseudo-second order kinetics, and the |

| | | | |
|----|--------------------------------|--|---|
| | | | adsorption data is a good fit with Langmuir isotherm. |
| 3. | Hefne et al. (2008) | Pb Isotherm, & Kinetic study pH-6, 500-1000 mg/L | The equilibrium time for Pb (II) adsorption on bentonite was 5 min, the processes conforming to second order kinetics. Experimental data were fitted well to the Langmuir adsorption isotherm. The kinetics of sorption processes were best described by a pseudo-second-order kinetic model. |
| 4. | Gupta and Bhattacharyya (2008) | Pb Isotherm, & Kinetic study pH-5.7, 10-50 mg/L | The uptake is rapid with maximum adsorption being observed within 180 min. The data fitted well with both Langmuir and Freundlich isotherms. The kinetics of sorption processes were best described by a pseudo-second-order kinetic model. |
| 5. | Kul and Koyuncu (2010) | Pb Isotherm & Kinetic study 5-10 mg/L | The kinetics of sorption processes were best described by a pseudo-second-order kinetic model. Langmuir, Freundlich and Dubinin–Redushkevich (D–R) isotherm models were used to represent the experimental data, and the models fitted well. |
| 6. | Hamidpour et al. (2011) | Pb Adsorption, Isotherm, & Kinetic study 5-10 mg/L | The experimental data showed that bentonite used in this study exhibited a reasonable sorption capacity for Pb, and thus may be useful for the immobilization of Pb from polluted sites. |
| 7. | Pawar et al. (2016) | Pb, Cu Adsorption, Isotherm study | Removal of these metal ions was favored by increases in the pH, initial metal concentrations, contact time, and |

| | | | | |
|-----|-----------------------------|--------|--|---|
| | | | and Kinetic study pH-5, 1-20 mg/L | dose of the adsorbents. The data fitted well with both Langmuir and Freundlich isotherms. The adsorption process was fast and the kinetic data fit better to the pseudo-second order kinetic model. |
| 8. | Baylan and Meriçboyu (2016) | Pb, Cu | Adsorption pH-5, 50-800 mg/L | The total adsorption capacity values of bentonite in binary ion system was lower than that of single Pb^{2+} ion system and was higher than that of single Cu^{2+} ion system. |
| 9. | Deka and Sekharan (2017) | Pb | Adsorption & Isotherm study pH-5, 1.39-987 ppm | A good removal efficiency (>85%) was observed for bentonite. The data fitted well with both Langmuir and Freundlich isotherms. |
| 10. | Khan et al. (2017) | Pb | Adsorption & Isotherm study pH-6.7, 1-180 mg/L | Maximum adsorption occurs in within 5 minutes. Experimental data were fitted well to the Langmuir adsorption isotherm. |
| 11. | Zhu and Qin (2017) | Pb | Adsorption & Isotherm study pH-4, 50-1000 mg/L | Adsorption of bentonites strongly depended on the pH values of the solution The data fitted well with both Langmuir and Freundlich isotherms |

2.14. Review of published works on adsorption of Cu^{2+}

Al-Qunaibit et al. (2005) studied the adsorption of Cu^{2+} ions by Saudi clay mineral (bentonite) and found that the highest adsorption capacity attained was 909 mg Cu^{2+} /g clay. Karapinar and Donat (2009) investigated the adsorption of Cu^{2+} and Cd^{2+} on bentonite and concluded that bentonite can efficiently be used for the removal of metal ions by opting adsorption process. Ding et al. (2009) examined the sorption capacity of Na- and Ca-bentonite to eliminate Cu^{2+} under various conditions and concluded that the process of adsorption was intensely depending on pH of the solution, initial metal concentration and bentonite dosage. They reported that the maximum adsorption capacity was 26 mg/g and

12 mg/g for of Na- and Ca-bentonite, respectively. Liu and Zhou (2010) conducted adsorption study on Na-bentonite in the presence of single and binary copper and nickel solution and observed that at same pH a higher percentage of adsorption was observed for Cu^{2+} as compared to Ni^{2+} . Olu-Owolabi and Unuabonah (2010) investigated adsorption kinetic and thermodynamic study of Zn^{2+} and Cu^{2+} by phosphate and sulphate modified bentonite clay and concluded that the process of adsorption was spontaneous in nature for both the heavy metals onto the bentonites. Maramis et al. (2012) studied the sorption of Cu^{2+} ions using modified bentonite at different temperature and at pH 5 and concluded that the Sips equation performs satisfactorily to represent the sorption equilibrium data. Aljlil and Alsewailem (2014) tested the capacity to adsorb copper (Cu^{2+}) and nickel (Ni^{2+}) by bentonite clay and concluded that the highest adsorption capacity achieved was 13.22 mg g^{-1} (Cu^{2+}) and 9.29 mg g^{-1} (Ni^{2+}). The equilibrium data fitted satisfactory with Langmuir, Freundlich and Langmuir-Freundlich isotherms.

Table 2.4. Summary of interaction of clay with Cu^{2+}

| Sr. No | Author & Year | Heavy metal | Properties | Conclusion |
|--------|----------------------------|-------------|--|--|
| 1. | Al-Qunaibit et al. (2005) | Cu | Adsorption & Isotherm study 60-100 ppm | The sorption processes were relatively fast in the first few minutes and then became slow after reaching 80% of the total sorption. The maximum adsorption obtained was 909 mg Cu^{2+} /g clay. The sorption of Cu^{2+} on the clay surface can be described by the high-affinity Langmuir isotherm. |
| 2. | Karapinar and Donat (2009) | Cu | Adsorption & Isotherm study pH-3, 50-300 mg/L | The experimental results indicated that natural bentonite could be successfully used for the adsorption of Cd^{2+} and Cu^{2+} from aqueous solutions. The adsorption patterns of metal ions onto followed the Langmuir, Freundlich and Dubinin–Radushkevich isotherms. |

| | | | | |
|----|----------------------------------|--------|--|---|
| 3. | Ding et al. (2009) | Cu | Adsorption & Isotherm study pH-5.66, 10-100 mg/L | The results show that the adsorption process of bentonite accorded with the Freundlich isotherm model and that the sorption results of Na bentonite are better than those of Ca-bentonite. Adsorption behavior of both bentonites was strongly depending on pH, initial concentration and additional amounts of bentonites. |
| 4. | Liu and Zhou (2010) | Cu | Adsorption, Isotherm, & Kinetic study 5-10 mg/L | The adsorption equilibrium for nickel and copper onto Na-bentonite is reached in 200 min. The kinetic process of adsorption can be described by the pseudo-second-order kinetic equation excellently and the adsorption isotherm be fitted to the Langmuir model |
| 5. | Olu-Owolabi and Unuabonah (2010) | Cu, Zn | Adsorption & Kinetic study pH-5.5 ± 0.2, 200 mg/L | The adsorption process for both metal ions onto the adsorbents was spontaneous in nature. kinetic data were found to show very strong fit to the pseudo-second order kinetic model. |
| 6. | Aljlil and Alsewailem (2014) | Cu | Adsorption & Isotherm study 50-1000 ppm | The maximum adsorption capacity was 13.22 mg g ⁻¹ for copper. The data fitted well with Langmuir, Freundlich and Langmuir-Freundlich isotherms. |

2.15. Review of published works on adsorption of Zn²⁺

Kaya and Ören (2005) investigated the adsorption of zinc by Na-enriched and natural bentonite and concluded that pH is an important factor which strongly influence the adsorption behaviour. They reported that basic mechanism is an ion exchange process occurs between pH 4 and 7. Kubilay et al. (2007) studied adsorption properties of bentonite in the presence of Cu²⁺, Zn²⁺ and Co²⁺ at a concentration range from 15 to 70 mg/L at various pH and concluded that at 20 °C the order of adsorptivity was found to be Zn²⁺>

$\text{Cu}^{2+} > \text{Co}^{2+}$ at pH 3.0, 5.0 and 7.0 and $\text{Zn}^{2+} > \text{Co}^{2+} > \text{Cu}^{2+}$ at pH 9.0 on bentonite respectively. Sen and Gomez (2011) determined the adsorptive properties of natural bentonite in the removal Zn^{2+} and found that the adsorption was very rapid initially and the maximum adsorption could be attained within 20 minutes. They also reported that at an optimum pH of 6.76 the maximum adsorption of Zn^{2+} takes place. Araujo et al. (2013) examined the equilibrium and kinetic study of zinc on by Brazilian bentonite clay and concluded that it can eliminate zinc ion and it can replace other expensive adsorbent. They also reported that the equilibrium data are well fitted the Langmuir isotherm model. Freitas et al. (2017) studied adsorption capacity on Verde-lodo bentonite in the presence of the binary solution of silver and copper and observed that copper possessed greater adsorption capacity as compared to silver.

Table 2.5. Summary of interaction of clay with Zn^{2+}

| Sr. No | Author & Year | Heavy metal | Properties | Conclusion |
|--------|-----------------------|-------------|--|---|
| 1. | Kaya and Ören (2005) | Zn | Adsorption & Isotherm study pH-4, 12.5-100 mg/L | The rate of zinc removal depends also on the solid concentration of the suspension. Reducing the slurry concentration allows particles to get in the more dispersed form, resulting higher available sorption sites for zinc. The adsorption performance of Na-enriched bentonite is better than the natural bentonite in all physical and chemical changes. The data were fitted both Langmuir and Freundlich isotherms. |
| 2. | Kubilay et al. (2007) | Zn, Cu, Co | Adsorption and Isotherm study pH-7, 15-70 mg/L | The order of adsorption of metals on bentonite at 20 °C is $\text{Zn(II)} > \text{Cu(II)} > \text{Co(II)}$ at pH 3.0, 5.0 and 7.0; $\text{Zn(II)} > \text{Co(II)} > \text{Cu(II)}$ at pH 9.0. Adsorption isotherms are obtained and they are well described by the Langmuir and Freundlich equation. |

| | | | | |
|----|----------------------|----|---|--|
| 3. | Sen and Gomez (2011) | Zn | Adsorption, Isotherm and Kinetic study pH-6.64, 10-90 mg/L | The maximum adsorption takes place at an optimum pH of 6.76. The process is very fast initially and maximum adsorption is obtained within 20 min. Zinc adsorption process followed pseudo second-order kinetics. Langmuir isotherm is more applicable compared to Freundlich isotherm. |
| 4. | Araujo et al. (2013) | Zn | Adsorption, Isotherm and Kinetic study pH- 4.5, 0.1-0.6 mEq/L | These results show that Brazilian bentonite clays may be used for elimination of Zn ²⁺ through adsorption mechanisms and can replace other adsorbents more expensive. The pseudo-second-order kinetic model best represented the mechanism of interactions involved during the adsorption. The experimental data at equilibrium satisfactorily fitted the Langmuir model. |

2.16. Generation of leachate from MSW

Leachate is generated because of a cascade of chemical and biological reactions of solid waste within the landfill and produce harmful effect on the surrounding soil and groundwater if not controlled properly. Leachates are generally classified as aqueous liquids or solutions containing contaminants, which are miscible in water; non-aqueous liquids composed of organic compounds, which are immiscible in water; or mixtures of both aqueous and non-aqueous liquids that results in the formation of two separate liquid phases. An efficient and well-managed modern landfill prevents release of leachate into the environment. The liner serves as a barrier and prevents the potentially pollutant leachate from contaminating the underlying ground water resources.

2.16.1. Composition of leachate

Pollutants in MSW and industrial landfill leachate can be divided into four groups:

a) Dissolved organic matter, quantified as Chemical Oxygen Demand (COD) or Total Organic Carbon (TOC), volatile fatty acids (which accumulate during the acid phase of the

waste stabilization) (Christensen and Kjeldsen, 1989) and more refractory compounds such as fulvic-like and humic-like compounds.

b) Inorganic macro-components, which include calcium (Ca^{2+}), magnesium (Mg^{2+}), sodium (Na^+), potassium (K^+), ammonium (NH_4^+), iron (Fe^{2+}), manganese (Mn^{2+}), chloride (Cl^-), sulfate (SO_4^{2-}) and hydrogen carbonate (HCO_3^-).

c) Heavy metals, such as cadmium (Cd^{2+}), chromium (Cr^{3+}), copper (Cu^{2+}), lead (Pb^{2+}), nickel (Ni^{2+}) and zinc (Zn^{2+}).

d) Xenobiotic organic compounds (XOCs) originating from household or industrial chemicals and present in relatively low concentrations (generally less than 1.0 mg/l of individual compounds). These compounds include among others a variety of aromatic hydrocarbons, phenols, chlorinated aliphatics and pesticides.

The composition of these compounds in leachate vary due to a number of different factors such as the age and type of waste and operational practices at the site. Most of landfill leachate has high BOD, COD, ammonia, chloride, sodium, potassium, hardness and boron levels. Raw leachate contains concentrations of heavy metals in excess of the drinking water standards. Type of contaminants and their concentration depends on the nature of waste deposited in the landfills.

2.16.2. Effect of leachate on liner material

Chemicals in the landfill leachate with low dielectric constant, high electrolyte concentration, or high cation valence may cause the diffuse double layer of bentonite to shrink which in turn leads to an increase in hydraulic conductivity (Mishra et al., 2005; Olson and Mesri, 1970). Presence of various chemicals in waste could affect the contamination adsorption capacity of bentonite and in turn reduce its usefulness as barrier material. To properly design a clay barrier, it is important to understand the composition of contaminants, the extent of the accumulation of contaminants in liner material and influence on the clay structure, which in turn affect the swelling and hydraulic conductivity of the clay barrier.

2.17. Review of published works on various leachates

Ruhl and Daniel (1997) conducted experiments to determine the impact of simulated and real MSW leachate on geosynthetic clay liner (GCL). They found that the value of

hydraulic conductivity was higher in the presence of simulated MSW leachate. Vega et al. (2005) analysed the adsorption capacity of natural bentonites in presence of synthetic mine waste leachate and reported above 90% adsorption of metal ions at pH 5. Pivato and Raga (2006) investigated Ammonium attenuation from MSW landfill leachate on sorption capacity of bentonite. They found that Ammonium sorption is higher in bentonite. An impact of strong acidic leachates was analysed by Bouazza et al. (2013) on needle punched GCL and found that the value of hydraulic conductivity rises with the rise in concentration. Anna et al. (2015) investigated the impact of plating factory leachate on adsorption capacity of natural bentonite. They reported that bentonite has achieved 100% removal of Fe(II). The other ions including Zn(II), Ni(II) and Cu(II) were also removed and the removal percentages obtained were 73.78, 49.01 and 71.21%, respectively. Chen et al. (2018) examined the effect of hydraulic conductivity of Geosynthetic clay liner in presence of synthetic coal combustion product leachate and concluded that permeation with deionized (DI) water prior to permeation with leachate resulted in hydraulic conductivity up to three orders of magnitude.

Table 2.6. Summary of interaction of clay with leachates

| Sr. No | Author & Year | Leachate | Materials and Properties | Conclusion |
|---------------|--------------------------|--|---|---|
| 1. | Ruhl and Daniel (1997) | Simulated and real MSW leachate | Geosynthetic clay liner (GCL); Hydraulic conductivity | They found that the value of hydraulic conductivity was higher in the presence of simulated MSW leachate. |
| 2. | Vega et al. (2005) | Synthetic mine waste leachate | Natural Bentonites; adsorption study | They found above 90% adsorption of metal ions at pH 5. |
| 3. | Pivato and Raga (2006) | MSW landfill leachate (Ammonium attenuation) | Bentonite; Adsorption | Ammonium adsorption is higher in bentonite |
| 4. | Bouazza et al. (2013) | Strong acidic leachates | Geosynthetic clay liner | The value of hydraulic conductivity rises with the rise in concentration. |

| | | | Hydraulic conductivity | |
|----|--------------------|---|--|---|
| 5. | Anna et al. (2015) | Plating factory leachate | Natural Bentonite; Adsorption | Bentonite has achieved 100% removal of Fe. The other ions including Zn(II), Ni(II) and Cu(II) were also removed and the removal percentages obtained were 73.78, 49.01 and 71.21 %, respectively. |
| 6. | Chen et al. (2018) | Coal combustion product leachates (synthetic) | Geosynthetic clay liner; Hydraulic conductivity | Permeation with deionized (DI) water prior to permeation with trona leachate resulted in hydraulic conductivity up to three orders of magnitude. |

2.18. Summary and critical appraisal of the literature review

A review of the literature emphasized that compacted bentonite can be used as an effective adsorbent due to its high cation exchange capacity, adsorption capacity, specific surface area, and low hydraulic conductivity. The bentonite's adsorption ability is generally determined by its pore structure and chemical nature.

The utilization of swelling clays as a liner material or clay-based barriers brings attention to mechanical property changes and liner integrity when clay material interacts with different chemicals present in the leachate stream.

Leachates generated from wastes inside the landfills decrease the efficacy of the liner material. These leachates also migrate towards the surrounding environment and groundwater, thereby polluting them. Therefore, to avoid the surrounding environment and groundwater being contaminated, a low-permeable liner is provided at the bottom of the landfill to separate the waste and groundwater. The clay soil's physico-chemical characteristics–water system will alter in the presence of heavy metal ions, causing in changes in the short- and long-term chemical and mechanical behaviour of the clay soil barrier materials. The existence of heavy metals in the leachate disturbs the bentonite clay

particles' pore-fluid chemistry and affects its diffuse double layer (DDL). Due to the presence of metal ions in the leachate, the swelling behaviour and the hydraulic conductivity may get altered significantly, reducing its efficiency. Furthermore, the time of contact between the contaminants and the adsorbent is essential in designing a liner material in a waste disposal system. The rapid uptake of contaminants and attaining equilibrium in a small interval shows the efficacy of that adsorbent as a liner material for its use in the waste disposal system. Adsorption kinetics are primarily employed to define the swiftness of the adsorption process.

2.19. Research gap

For designing a liner system, the hydraulic conductivity, adsorption and shear strength are the most critical parameters for consideration. The reviewed literature highlighted that previously, limited studies were conducted to determine the potential significance of bentonites on hydraulic conductivity and adsorption behaviour in the presence of various toxic pollutants. However, no detailed studies have been reported on the investigation of the change in compressibility, consolidation parameters, shear strength, hydraulic behaviour, and the sorption and sorption kinetics of different bentonites in the presence of heavy metals and various leachates. Since the bentonite varying in their mineralogical and chemical properties performs differently with different metal contaminants, it is needed to compare the alteration in behaviour of bentonites in the presence of various metal contaminants and leachates. Furthermore, no study has been performed to compare the effect of various heavy metals and leachates on the behaviour of bentonites differing in their mineralogical composition.

2.20. Objectives of the study

The objectives of the present investigation are as follows.

- I. Studying the effect of concentrations of heavy metals (Pb^{2+} , Cu^{2+} , Zn^{2+}) on the liquid limit, free swelling, hydraulic conductivity, consolidation characteristics, shear strength and adsorption behaviours of two different bentonites.

- II. Analyzing the impacts of municipal soil waste (MSW) leachate and synthetic MSW leachates on the changes in the behaviour of the bentonites (liquid limit, free swell, consolidation, shear strength, and adsorption study)
- III. Studying the impact of leachates from fly ash, sewage sludge, and paper mill sludge on the alteration in the behaviours of both the bentonites.

2.21. Scope of the thesis

The overarching objectives of the present thesis is to utilize bentonites as a landfill liner material to prevent the surrounding environment from deteriorating due to leaching. Therefore, the scope of this thesis is to test the efficacy of bentonites for landfill use upon exposure to different types of leachates and various heavy metals present in them. To achieve the overall objective, as a first step, collection and initial characterization of the bentonites were carried out. This required performing different laboratory experiments. The learning of standard protocols and the operation of instruments were performed simultaneously. Secondly, the changes in the physico-chemical characteristics of the bentonites were observed for various concentrations of heavy metals, which was then followed by different types of leachates to test their adsorption capacity. Further, to study the effect of shear strength on the behaviour of compacted bentonites in the presence of these solutions, UCS experiments were also carried out on bentonite samples. FESEM and FTIR studies were conducted to analyse the change in surface morphology and alteration in FTIR pattern in both the bentonites before and after sorption of metals and leachates. Finally, isotherm and kinetic modelling of the adsorption study was carried out on the research data.



*Progress is impossible
without change, and
those who cannot
change their minds
cannot change anything*

- George Bernard Shaw

3

Materials and methodology

3.1. Context

This chapter explains in detail the materials used and experimental methodologies adopted to carry out the research. The methods for determining the hydraulic conductivity and swelling pressure from one-dimensional consolidation tests have also been conferred.

3.2. Design of research work

To achieve the objectives of the present investigation, the entire research work was carried out in four phases, as described below. The overall objective and its breakup into phases have been shown in Fig. 3.1.

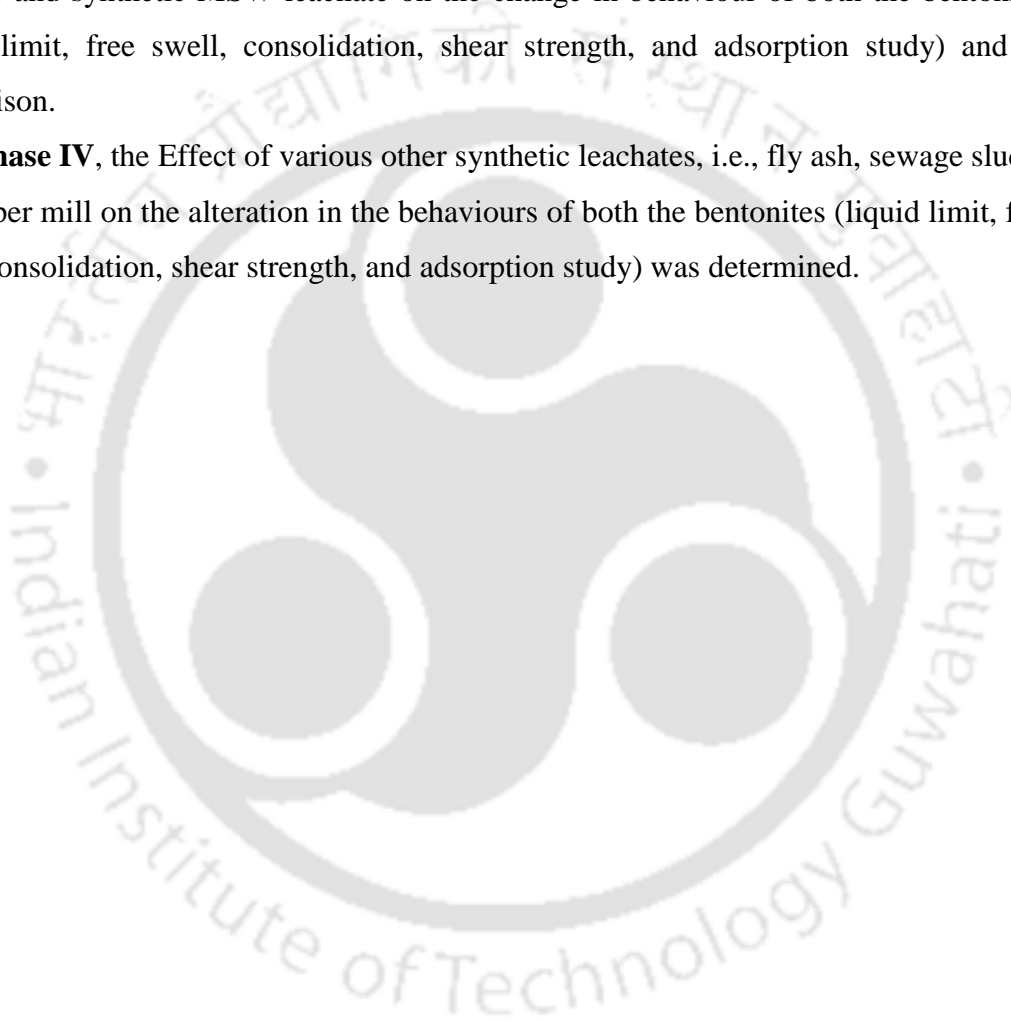
Phase I was associated with the collection of bentonites and their physical and chemical characterization.

In **Phase II**, liquid limit, free swell, and shear strength study were performed in the presence of various concentrations of Pb^{2+} , Cu^{2+} , Zn^{2+} . Some experimental parameters i.e., pH, adsorbent dose, initial concentration, and contact time has been used as a function to determine the capacity of bentonites to adsorb various metal ions. Consolidation tests were

also performed to evaluate the hydraulic conductivity and consolidation characteristics of both the bentonites. Different isotherm models were used to determine the best-fit equilibrium isotherms. Kinetic models were fitted to investigate the adsorption kinetics and mechanisms of Pb^{2+} , Cu^{2+} , and Zn^{2+} sorption on both the bentonites. The alteration in the behaviours of bentonites having diverse mineralogical and chemical characteristics was also compared in the presence of various metal contaminants.

Phase III was associated with the analysis of the impact of municipal soil waste (MSW) leachate and synthetic MSW leachate on the change in behaviour of both the bentonites (liquid limit, free swell, consolidation, shear strength, and adsorption study) and its comparison.

In **Phase IV**, the Effect of various other synthetic leachates, i.e., fly ash, sewage sludge and, paper mill on the alteration in the behaviours of both the bentonites (liquid limit, free swell, consolidation, shear strength, and adsorption study) was determined.



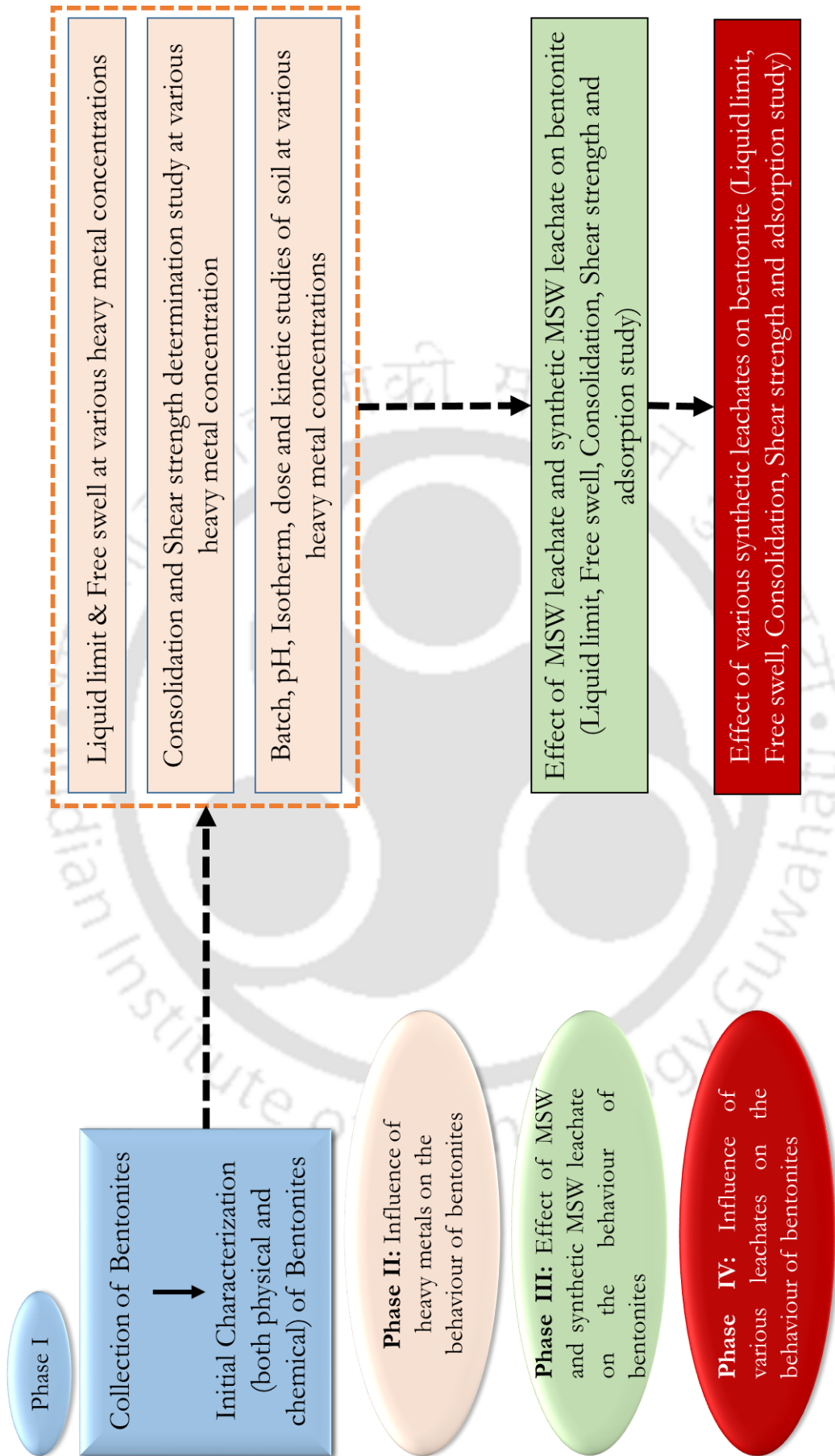


Fig. 3.1. Design of research

3.3. Procurement of bentonites and their characterization

Bentonites (Bentonite-1 and -2) were procured in powdered form from the Barmer district of the Indian state of Rajasthan (Fig. 3.2). They were subjected to various chemical and mineralogical analyses, which are listed in Table 3.1.

Ammonium acetate technique, described by Chapman (1965) and Pratt (1965), was followed for the analysis of the cation exchange capacity (CEC) of the soils. By using ASTM-D5890 (2006), the Atterberg's limits (liquid limit and plastic limit) of the soils were determined. The free swelling experiment was carried out as per ASTM-D4318 (2010). The protocol given by Cerato and Lutenegeger (2002) was used to compute the specific surface area (SSA) of both the soil. The maximum dry density (MDD) and the optimum moisture content (OMC) of both the soil were obtained by following ASTM-D698 (2012). By following ASTM-D854-92 (1994) the specific gravity of the soils was analyzed. The chemical composition of the soils listed in Table 3.2 was analyzed by using X-ray fluorescence (XRF) (AXIOS, PANalytical, Malvern, UK).

Table 3.1. Chemical and mineralogical properties of Bentonites

| Property | Bentonite-1 | Bentonite-2 |
|--|-------------|-------------|
| Liquid limit (%) | 480.0 | 305.0 |
| Plastic limit (%) | 40.0 | 39.0 |
| Plasticity index | 440.0 | 266.0 |
| Specific gravity | 2.73 | 2.70 |
| Clay content | 66.0% | 61.0% |
| Silt content | 34.0% | 39.0% |
| Cation exchange capacity (CEC) (meq/100gm) | 40.2 | 36.2 |
| Na ⁺ | 20.9 | 16.8 |
| K ⁺ | 2.2 | 2.9 |
| Ca ²⁺ | 15.2 | 14.2 |
| Mg ²⁺ | 1.9 | 2.3 |
| Specific surface area (m ² /g) | 396.3 | 340.4 |
| Optimum moisture content (OMC) | 33.0 % | 33.5 % |
| Maximum dry density (MDD) g/cc | 1.31 | 1.3 |
| pH | 8.9 | 9.2 |
| Montmorillonite content (%) | 72.0 | 64.0 |

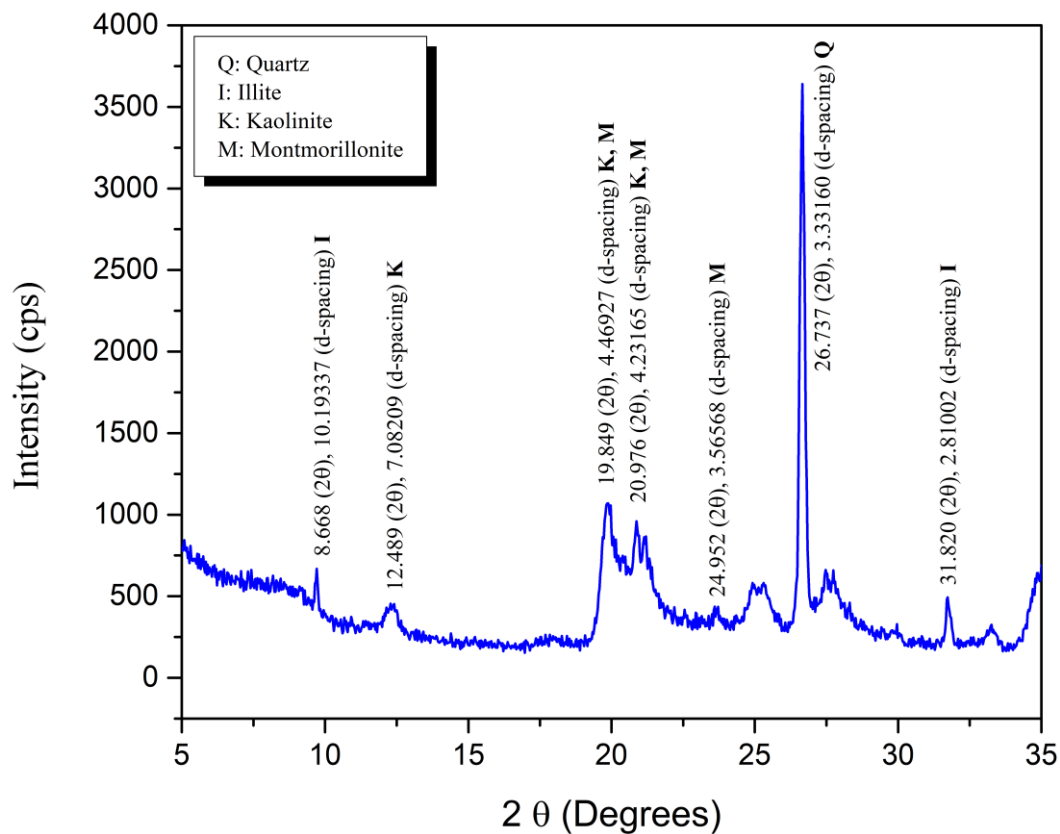
The X-ray diffraction (XRD) experiment (28 Bruker AXS D8 model, Billerica, MA) was carried out to analyze the presence of other predominant minerals like montmorillonite, illite, kaolinite, and quartz in the bentonites. Materials were scanned at 5° to 35° , through a scanning speed of $2^{\circ} 2\theta/\text{min}$ with a step size of 0.03° (Fig. 3.3 a-b). The minerals present were determined using X'Pert HighScore software.



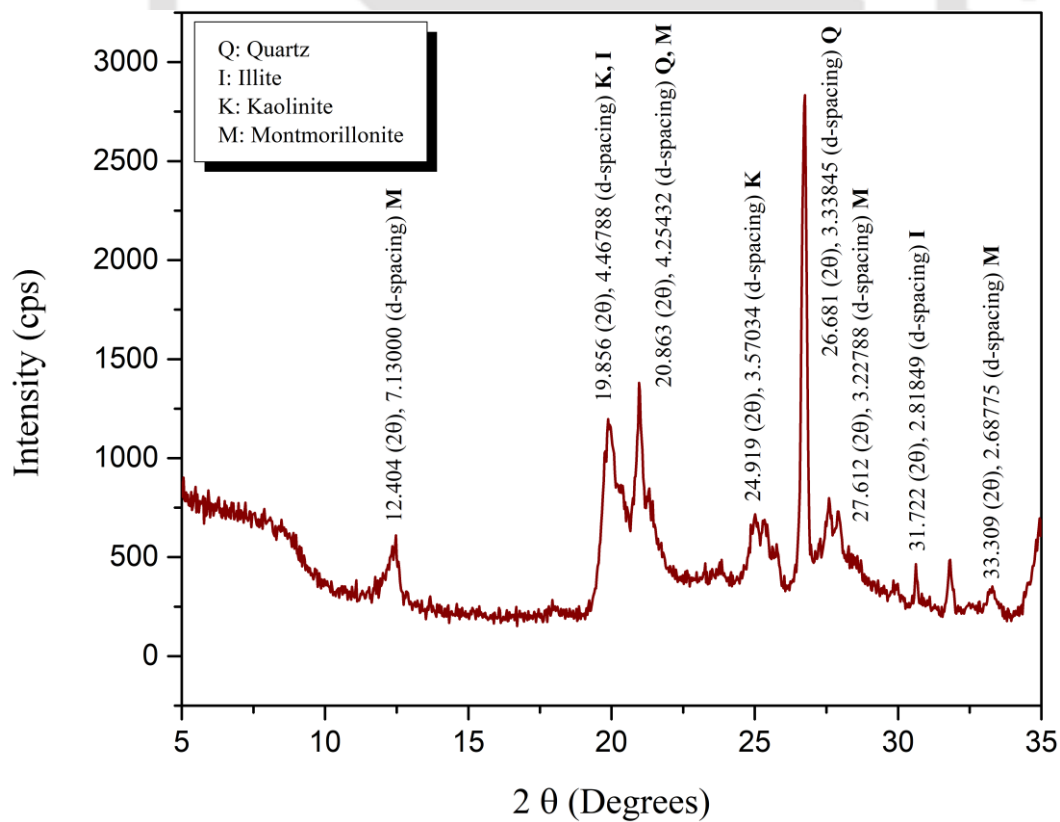
Fig. 3.2. Bentonite images: (a) Bentonite-1 (b) Bentonite-2

Table 3.2. Elemental composition expressed as weight percent of major element of both the bentonites.

| Major and minor element oxides | Bentonite-1 | Bentonite-2 |
|--------------------------------|-------------|-------------|
| SiO ₂ | 48.79 | 50.70 |
| Al ₂ O ₃ | 18.17 | 19.09 |
| Fe ₂ O ₃ | 16.16 | 16.29 |
| MnO | 0.45 | 0.31 |
| MgO | 0.94 | 1.06 |
| CaO | 1.20 | 1.10 |
| Na ₂ O | 4.67 | 3.59 |
| K ₂ O | 1.45 | 1.52 |
| TiO ₂ | 2.00 | 2.13 |
| P ₂ O ₅ | 0.18 | 0.21 |



(a)



(b)

Fig. 3.3. XRD plot for (a) Bentonite-1 and (b) Bentonite-2

Fourier transform infrared spectroscopy (FTIR) analyses were performed at room temperature following the KBr pellet method over the spectral range of 450–4000 cm^{-1} to determine the chemical functional groups present on both bentonites (PerkinElmer, Spectrum Two, Waltham, Maine). Using KBr, having a 100:1 ratio, the bentonite samples were homogeneously mixed. The stretching vibration bands were detected at 3,580–3,700 and 3,601–3,710 cm^{-1} , respectively, which shows the possibility of O–H stretching vibration of the silanol (Si-OH) groups and HO-H vibration of the water-adsorbed silica surface for Bentonites-1 and -2 (Fig. 3.4). The broad bands of Si-O were detected near 691.9, 463.3, and 523.9 cm^{-1} from the IR studies of bentonites, which indicates the presence of quartz (Karapinar and Donat, 2009).

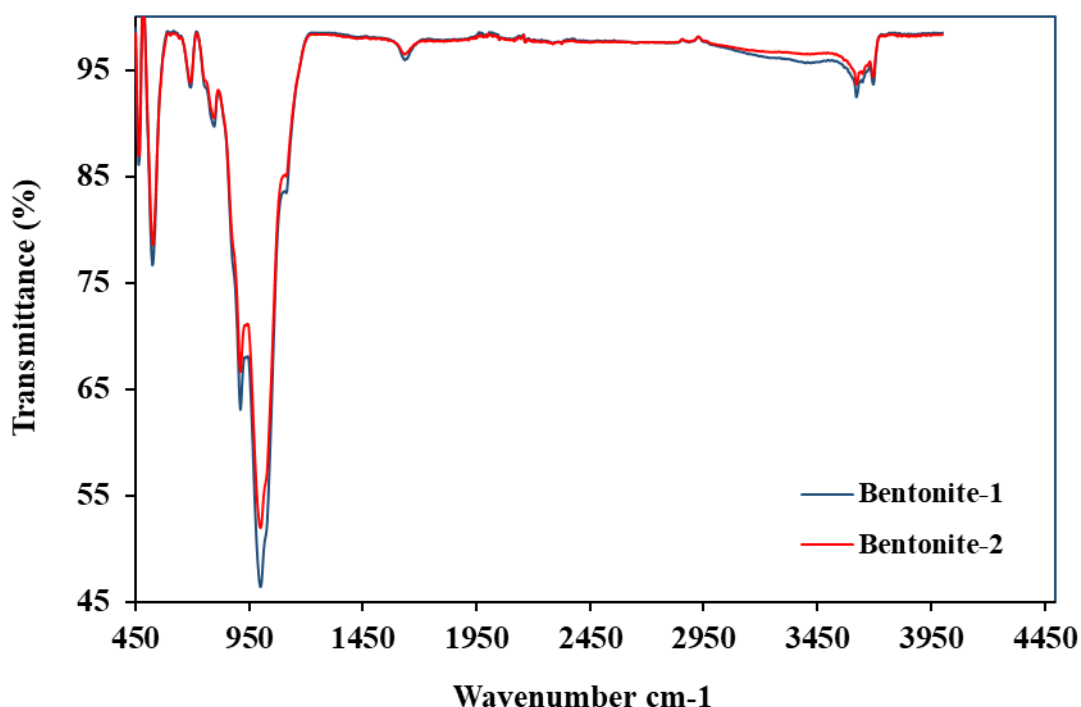


Fig. 3.4 FTIR plot of both the bentonites

Field emission scanning electron microscopy (FESEM) (Zeiss Sigma, Oberkochen, Germany) study was conducted on both the bentonites to analyse their surface morphology. The bentonite samples were oven-dried at 60°C and then crushed to fine powder forms using a pestle. Then it was sieved through a 75 μm Indian Standard (IS) sieve. The sieved samples were mounted on the aluminium stubs above double-sided carbon tape. By using a sputter coater (Quorum, SC7620, Quorum Technologies, Lewes, UK and Edwards, RV3, Czech Republic), double gold coating was done before the analysis. FESEM study was performed, and photomicrographs were obtained to visualize the surface morphology of

two bentonites. It can be seen from the Fig. 3.5 (a and b) that due to the presence of montmorillonite mineral, bentonites show a flaky dispersed structure with loose porous aggregates (Mitchell and Soga, 2005).

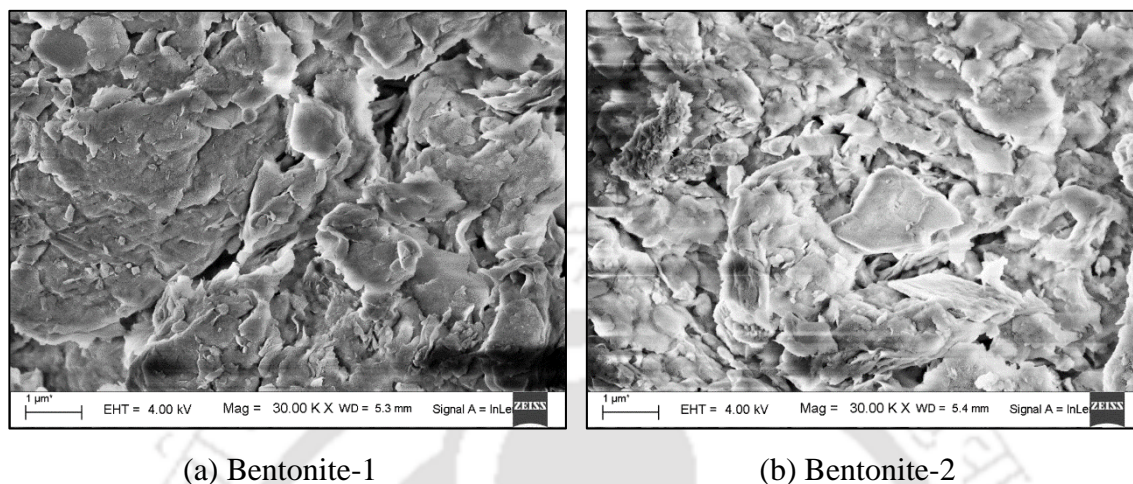


Fig. 3.5. FESEM images of the bentonites

3.4. Permeant liquid

3.4.1. Metal preparation

For this investigation, lead (Pb^{2+}), Copper (Cu^{2+}), and Zinc (Zn^{2+}) were selected, since these are the leading contaminants present in the leachate and can cause harmful effects to the human health and environment. Stock solutions of Pb^{2+} , Cu^{2+} , and Zn^{2+} were prepared by dissolving the required amount of lead nitrate [$\text{Pb}(\text{NO}_3)_2$], copper nitrate [$\text{Cu}(\text{NO}_3)_2 \cdot 3\text{H}_2\text{O}$] and zinc nitrate [$\text{Zn}(\text{NO}_3)_2 \cdot 6\text{H}_2\text{O}$] in deionized (DI) water. Different standard solutions of Pb^{2+} , Cu^{2+} , and Zn^{2+} were prepared by dissolving the desired amount of metal stock solution in DI water. Tests were carried out with bentonite in the presence of different concentrations of Pb^{2+} , Cu^{2+} , and Zn^{2+} , i.e., 100, 500, 1000, and 2000 mg/L. The present study was limited to a concentration of 2000 mg/L, as Haan (1981) and Hazarika et al. (2017) reported the maximum metal concentration of 2330 mg/L present in leachate. So, for considering the worst situation, the above concentration range has been chosen for the present study. The pH value of the individual metal solution and the metal solution with bentonites are given in Tables 3.3 and 3.4.

Table 3.3. pH values of individual metal solutions

| Heavy metal | pH | | | |
|------------------|----------|----------|-----------|-----------|
| | 100 mg/L | 500 mg/L | 1000 mg/L | 2000 mg/L |
| Pb ²⁺ | 4.75 | 4.66 | 4.08 | 3.80 |
| Cu ²⁺ | 5.31 | 4.92 | 4.65 | 4.39 |
| Zn ²⁺ | 5.78 | 5.55 | 5.47 | 5.08 |

Table 3.4. pH values of metal solutions with bentonites

| Concentration (mg/L) | pH | | | | | |
|-------------------------|------------------|------------------|------------------|------------------|------------------|------------------|
| | Bentonite-1 | | | Bentonite-2 | | |
| | Pb ²⁺ | Cu ²⁺ | Zn ²⁺ | Pb ²⁺ | Cu ²⁺ | Zn ²⁺ |
| 0 (DI water) | 8.90 | 8.90 | 8.90 | 9.20 | 9.20 | 9.20 |
| 100 | 7.80 | 6.88 | 7.56 | 7.90 | 6.75 | 7.54 |
| 500 | 6.66 | 6.36 | 6.72 | 6.53 | 5.52 | 6.62 |
| 1000 | 6.40 | 5.39 | 6.47 | 5.96 | 5.37 | 6.46 |
| 2000 | 6.13 | 5.12 | 6.02 | 5.41 | 5.08 | 5.98 |

3.4.2. Leachate preparation

(a) Municipal solid waste (MSW) leachate

A large-scale landfill simulation reactor (LSR) was fabricated under the anaerobic condition to study the behaviour of fresh MSW leachate in the landfill. The landfill reactor of 1 m³ volume (1m height, depth and length) was fabricated using an iron sheet, and the inner walls were painted with non-corrosive materials to restrict any reaction between the iron sheet and the waste material. The LSR was then filled with unshredded mixed MSW. 73% of wet waste (i.e., food waste) and 27% of dry waste (i.e., paper, plastic wood, and metals) were the major components considered in this study. The leachate was collected through a leachate collection system at the bottom of the reactor. The metal concentrations of the leachate were analysed by using an atomic absorption spectrophotometer (AAS) (55 B, Spectra AA, Agilent Technologies, Santa Clara, CA), the details of which are tabulated in Table 3.5.

(b) Synthetic leachates

There are numerous other metals, microbes, and biological species present. Here, we tried to simulate the field condition by considering heavy metals that are present in maximum concentrations in leachates. Leachates prepared by this method are called

synthetic leachates. Where actual field conditions cannot be achieved, but we try to resemble a laboratory-scale study close to real field studies of the leachates. These synthetic leachates were prepared in the laboratory by reviewing various works of literature and taking into consideration; the heavy metals found in the maximum number of respective leachates.

Four synthetic leachates, i.e., Municipal solid waste, fly ash, paper mill, and sewage sludge leachates, were selected for the present study because of their familiarity in the environment. These leachates generally consist of higher concentration of metals which can contaminate the surrounding environment and cause serious health issues. The composition of the leachates and the salts used are tabulated in Tables 3.6 – 3.9.

Table 3.6 illustrates the leachate concentration of MSW, which represents the abundance of calcium, magnesium, and Iron. However, Table 3.7 shows the leachate concentration of fly ash, which depicts the presence of zinc, lead, and copper in abundance. Paper mill leachate represents the existence of a higher amount of zinc and cadmium (Table 3.8) whereas, sewage sludge leachate confirms the presence of a higher quantity of zinc, manganese, and nickel. These synthetic leachates were prepared by dissolving the required amount of various salts in 1 L of DI water (Table 3.6 – 3.9). The pH (pH electrode, Systronics, Ahmedabad, Gujarat, India) values of all the leachates were listed in Table 3.10.

Table 3.5. Composition of MSW leachate

| Sl. No. | Constituents | Concentration (mg/L) | Salts used | Type of leachate |
|---------|------------------|----------------------|--|------------------|
| 1 | Pb ²⁺ | 2.8 | Pb(NO ₃) ₂ | MSW leachate |
| 2 | Cu ²⁺ | 1.1 | Cu(NO ₃) ₂ .3H ₂ O | |
| 3 | Zn ²⁺ | 20.6 | Zn(NO ₃) ₂ .6H ₂ O | |
| 4 | Fe ²⁺ | 150.0 | FeCl ₂ | |
| 5 | Mn ²⁺ | 19.0 | MnCl ₂ .4H ₂ O | |
| 7 | Cd ²⁺ | 47.8 | Cd(NO ₃) ₂ .4H ₂ O | |
| 8 | Ca ²⁺ | 3355.0 | CaCl ₂ .2H ₂ O | |
| 9 | Mg ²⁺ | 222.9 | MgCl ₂ .6H ₂ O | |

Table 3.6. Composition of synthetic MSW leachate

| Sl. No. | Constituents | Concentration (mg/L) | Salts used | Type of leachate & Reference |
|---------|------------------|----------------------|--|---|
| 1 | Pb ²⁺ | 2.1 | Pb(NO ₃) ₂ | Synthetic MSW leachate (Tatsi and Zouboulis, 2002) |
| 2 | Cu ²⁺ | 6.0 | Cu(NO ₃) ₂ .3H ₂ O | |
| 3 | Zn ²⁺ | 36.0 | Zn(NO ₃) ₂ .6H ₂ O | |
| 4 | Fe ²⁺ | 160.0 | FeCl ₂ | |
| 5 | Mn ²⁺ | 16.2 | MnCl ₂ .4H ₂ O | |
| 7 | Cd ²⁺ | 6.5 | Cd(NO ₃) ₂ .4H ₂ O | |
| 8 | Ca ²⁺ | 3324.0 | CaCl ₂ .2H ₂ O | |
| 9 | Mg ²⁺ | 443.0 | MgCl ₂ .6H ₂ O | |

Table 3.7. Composition of Fly ash leachate

| Sl. No. | Constituents | Concentration (mg/L) | Salts used | Type of leachate & Reference |
|---------|------------------|----------------------|--|---------------------------------------|
| 1 | Pb ²⁺ | 3655.3 | Pb(NO ₃) ₂ | Fly ash leachate (Li et al., 2007) |
| 2 | Cu ²⁺ | 886.2 | Cu(NO ₃) ₂ .3H ₂ O | |
| 3 | Zn ²⁺ | 13044.0 | Zn(NO ₃) ₂ .6H ₂ O | |
| 4 | Ni ²⁺ | 26.9 | NiCl ₂ .6H ₂ O | |
| 5 | Cd ²⁺ | 122.8 | Cd(NO ₃) ₂ .4H ₂ O | |

Table 3.8. Composition of Paper mill leachate

| Sl. No. | Constituents | Concentration (mg/L) | Salts used | Type of leachate & Reference |
|---------|------------------|----------------------|--|--|
| 1 | Pb ²⁺ | 7.5 | Pb(NO ₃) ₂ | Paper mill leachate (Hazarika et al., 2017) |
| 2 | Cu ²⁺ | 17.5 | Cu(NO ₃) ₂ .3H ₂ O | |
| 3 | Zn ²⁺ | 2366.6 | Zn(NO ₃) ₂ .6H ₂ O | |
| 4 | Fe ²⁺ | 65.4 | FeCl ₂ | |
| 5 | Mn ²⁺ | 126.0 | MnCl ₂ .4H ₂ O | |
| 6 | Ni ²⁺ | 12.7 | NiCl ₂ .6H ₂ O | |
| 7 | Cd ²⁺ | 520.8 | Cd(NO ₃) ₂ .4H ₂ O | |

Table 3.9. Composition of sewage sludge leachate

| Sl. No. | Constituents | Concentration (mg/L) | Salts used | Type of leachate & Reference |
|---------|------------------|----------------------|--|------------------------------|
| 1 | Pb ²⁺ | 130.0 | Pb(NO ₃) ₂ | |
| 2 | Cu ²⁺ | 174.0 | Cu(NO ₃) ₂ .3H ₂ O | Sewage sludge |
| 3 | Zn ²⁺ | 967.2 | Zn(NO ₃) ₂ .6H ₂ O | leachate |
| 4 | Mn ²⁺ | 355.0 | MnCl ₂ .4H ₂ O | (Nayak and |
| 5 | Ni ²⁺ | 278.0 | NiCl ₂ .6H ₂ O | Kalamdhad, 2014) |
| 6 | Cd ²⁺ | 37.0 | Cd(NO ₃) ₂ .4H ₂ O | |

Table 3.10. pH values of different leachate solutions

| Sl. No. | Type of leachate | pH |
|---------|------------------|------|
| 1 | MSW leachate | 5.21 |
| 2 | Synthetic MSW | 4.87 |
| 3 | Fly ash | 4.01 |
| 4 | Paper mill | 4.27 |
| 5 | Sewage sludge | 4.63 |

3.5. Determination of hydraulic conductivity and Consolidation characteristics

To estimate the hydraulic conductivity values, consolidation tests were performed as per the guidelines laid down in ASTM-D2435 (1996) (Fig. 3.6). The consolidation experiment is quick and provides hydraulic conductivity values at different void ratios. Several investigators (Budhu et al., 1991; Sivapullaiah et al., 2000) have followed this procedure, which offers quite satisfactory results of hydraulic conductivity as compared to the directly obtained values.

Bentonites were mixed with water at their respective optimum moisture contents and were placed in a moisture-controlled desiccator for 24 h to achieve the moisture equilibrium. The moisture-equilibrated samples were then statically compacted in oedometer rings of a diameter of 60 mm to a thickness of 15 mm to its MDD. The whole assembly was then placed in the consolidation cell and positioned in the loading frame. The specimens were swamped in the DI water or to the respective various metal concentration

under the nominal pressure of 4.9 kPa and permitted to swell. The samples were consolidated by increasing the pressure slowly by an increment ratio of 1 (i.e., increased by 4.9, 9.8, 19.6 kPa at each step) to a maximum pressure of 784.8 kPa once the swelling was analysed. Then the change in the thickness of the soil sample was measured for each pressure increment from the dial gauge readings.

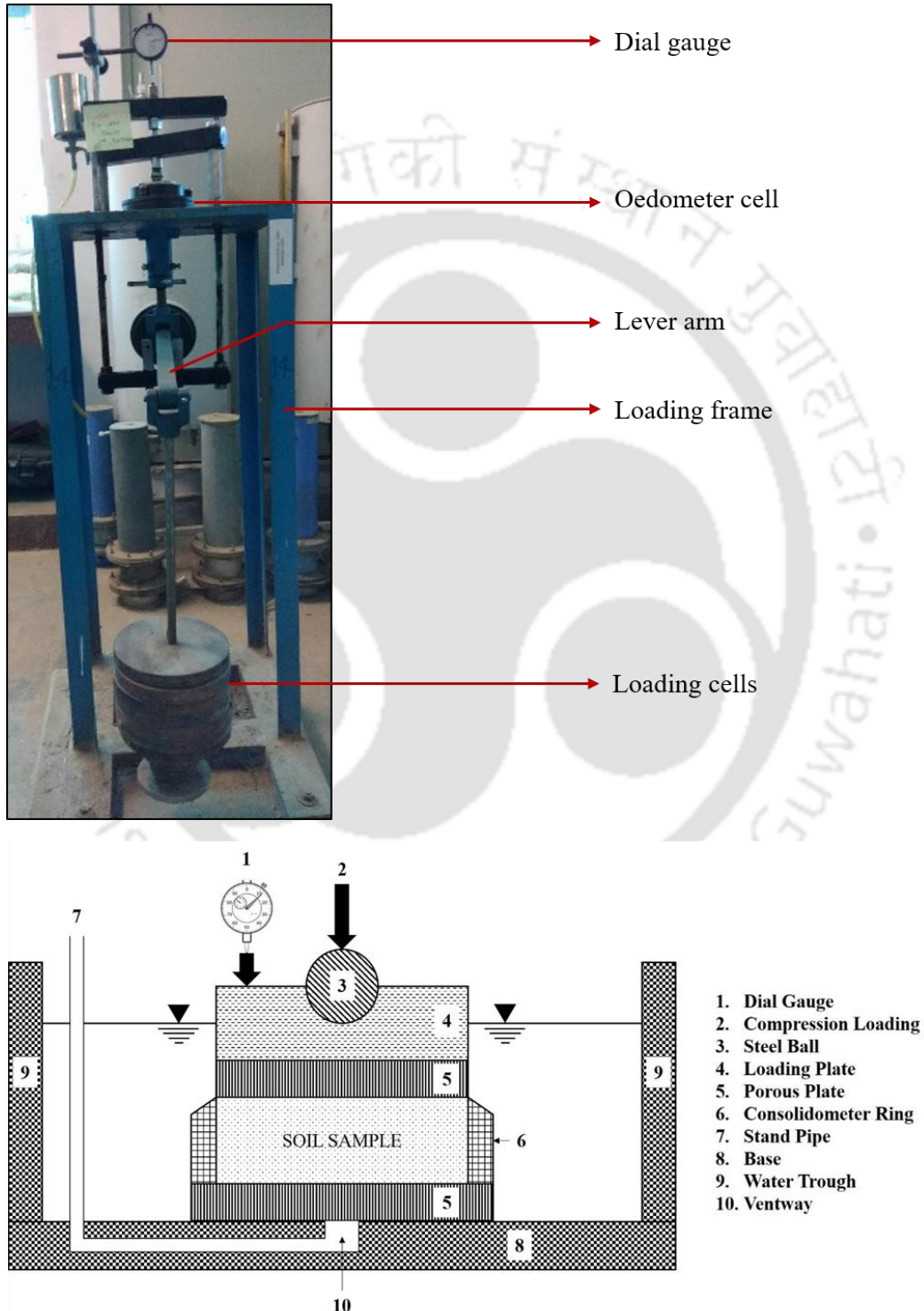


Fig. 3.6. Consolidation setup in the laboratory and its schematic diagram

The change in the void ratio corresponding to the increase in the overburden pressure was calculated as given in Eq. 3.1.

$$\Delta e = \frac{\Delta H(1 + e_0)}{H} \quad (3.1)$$

Where, e_0 indicates the initial void ratio; H represents the initial thickness of the soil sample; while the alteration in the thickness of soil sample because of the rise in overburden pressure is denoted by ΔH .

By applying Taylor square-root-of-time method (Taylor, 1948) at every load increment a time-settlement plot (example shown in Fig. 3.7) was plotted and then the coefficient of consolidation (c_v) was calculated (Eq. 3.2).

$$c_v = \frac{D^2 T_v}{t_{90}} \quad (3.2)$$

Where,

t_{90} = Time at 90% degree of consolidation (U)

U = Degree of consolidation

D = $H/2$ for double drainage

= H for single drainage

T_v = Time factor (0.848 for 90 % of consolidation).

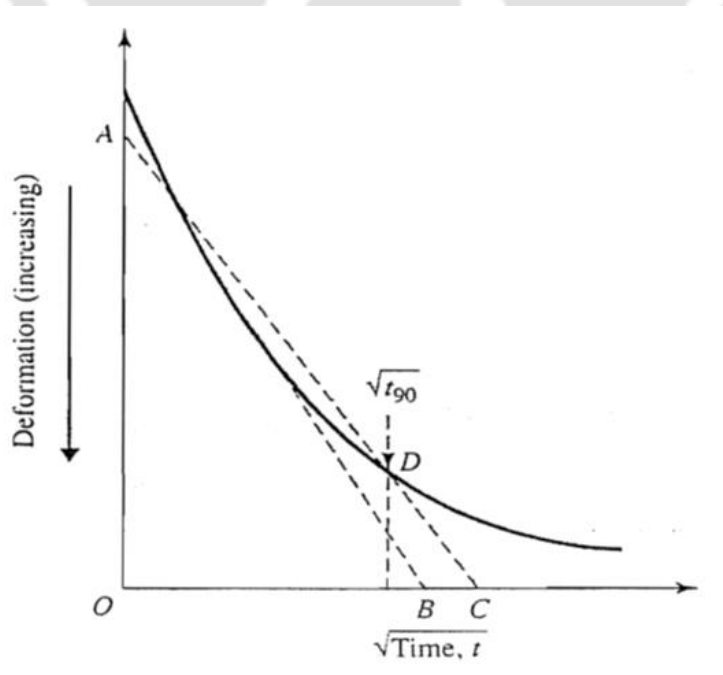


Fig. 3.7. Taylor's square root-of time fitting method (Das, 2006)

The coefficient of volume change (m_v) was computed by using Eq. 3.3,

$$m_v = - \left\{ \frac{\Delta e}{\Delta \sigma (1 + e_0)} \right\} \quad (3.3)$$

Where, the change in pressure and change in void ratio are denoted by $\Delta \sigma$ and Δe .

Terzaghi's theory of consolidation (Terzaghi, 1943) was fitted and by using the c_v and m_v , the hydraulic conductivity values (k) was computed for the increment of pressure (Eq. 3.4)

$$k = c_v m_v \gamma_w \quad (3.4)$$

Where, γ_w denotes the unit weight of the pore fluid.

The compressibility behaviour of the soil can be indicated by compression index (C_c) of a soil and was computed as the slope of the straight-line portion of the void ratio–pressure (e - $\log P$) curve as

$$C_c = \frac{e_i - e_j}{\log \frac{P_i}{P_j}} \quad (3.5)$$

Where, e_i and e_j are the void ratio corresponding to the consolidation pressure of p_i and p_j at i^{th} and j^{th} steps of loading, respectively.

3.6. Estimation of swelling pressure and swelling potential

The swelling pressure and swelling potential of the samples were obtained from the oedometer test setup. A compacted specimen under a load of 4.9 kPa was inundated with respective salt concentration. As specimens start to absorb the liquid, it starts to swell. After the completion of swelling, the sample was consolidated by adding progressive pressure beginning with 4.9 kPa and finishing with 784.5 kPa. Then, swelling pressure was determined as the pressure applied to bring back the swollen specimen to its initial volume; whereas, the swelling potential determined as the percentage increase in the volume of the soil due to swelling. Sridharan and Gurtug (2004) have explained the minutiae of this procedure.

The point SP in Fig. 3.8 corresponds to swelling pressure of the compression curve. Swelling potential (SP) for the samples was calculated as:

$$SP = \frac{\Delta e}{1 + e_0} \quad (3.6)$$

Where, Δe is the change in the void ratio of the sample due to swelling and e_0 is the initial void ratio before swelling.

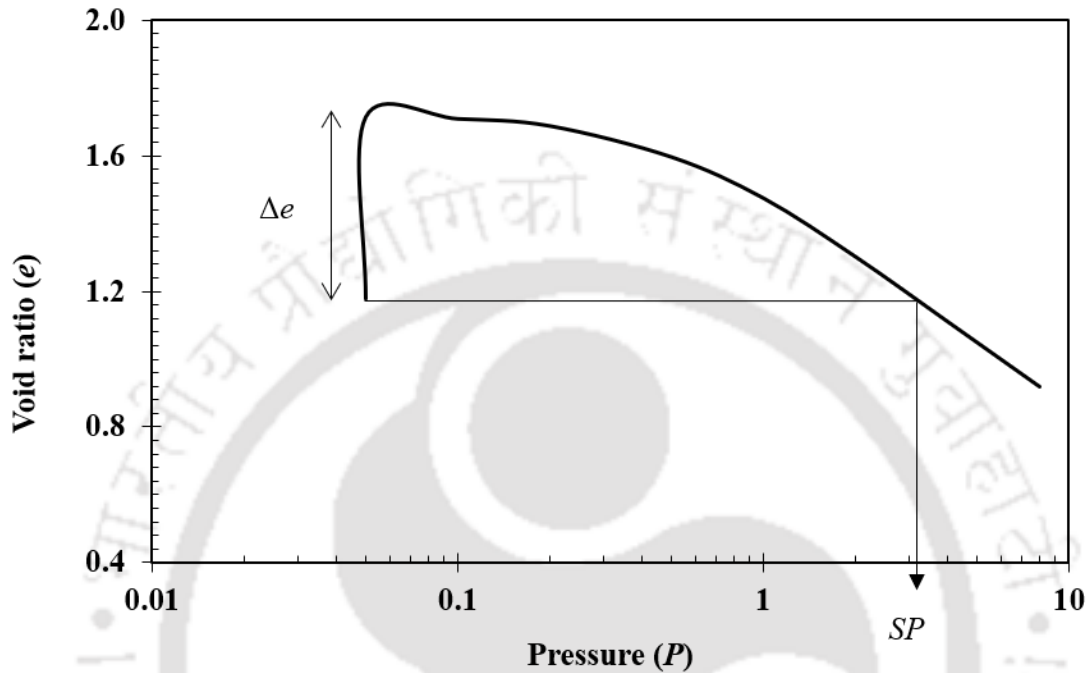


Fig. 3.8. Determination of swelling pressure and swelling potential

3.7. Unconfined compression test

Unconfined compressive strength (UCS) of the bentonite samples were performed as per ASTM-D2166 (2016). Bentonites were mixed with DI water and various permeants at OMC and MDD of DI water. Cylindrical bentonite samples of 38 mm diameter and 76 mm height were prepared. To simulate the un-drained condition, Unconfined compressive strength (σ_c) was conducted under a constant strain rate (1.25 mm/min) during the experiment. The unconfined compressive strength of the bentonite samples was analysed from the Eq. 3.7.

$$\sigma_c = \frac{P}{A} \quad (3.7)$$

Where, σ_c = Unconfined compressive strength (kPa),

P = Applied load (kN) and

A = Corresponding average cross-sectional area (mm^2)

$$A = \frac{A^{\circ}}{(1 - \varepsilon)} \quad (3.8)$$

Where, A° = Initial average cross-sectional area of the specimen (mm^2), Axial strain (%), $\varepsilon = \frac{\Delta l}{l} \times 100$, Δl = Change in length of the specimen (mm), l = The initial length of the specimen (mm).

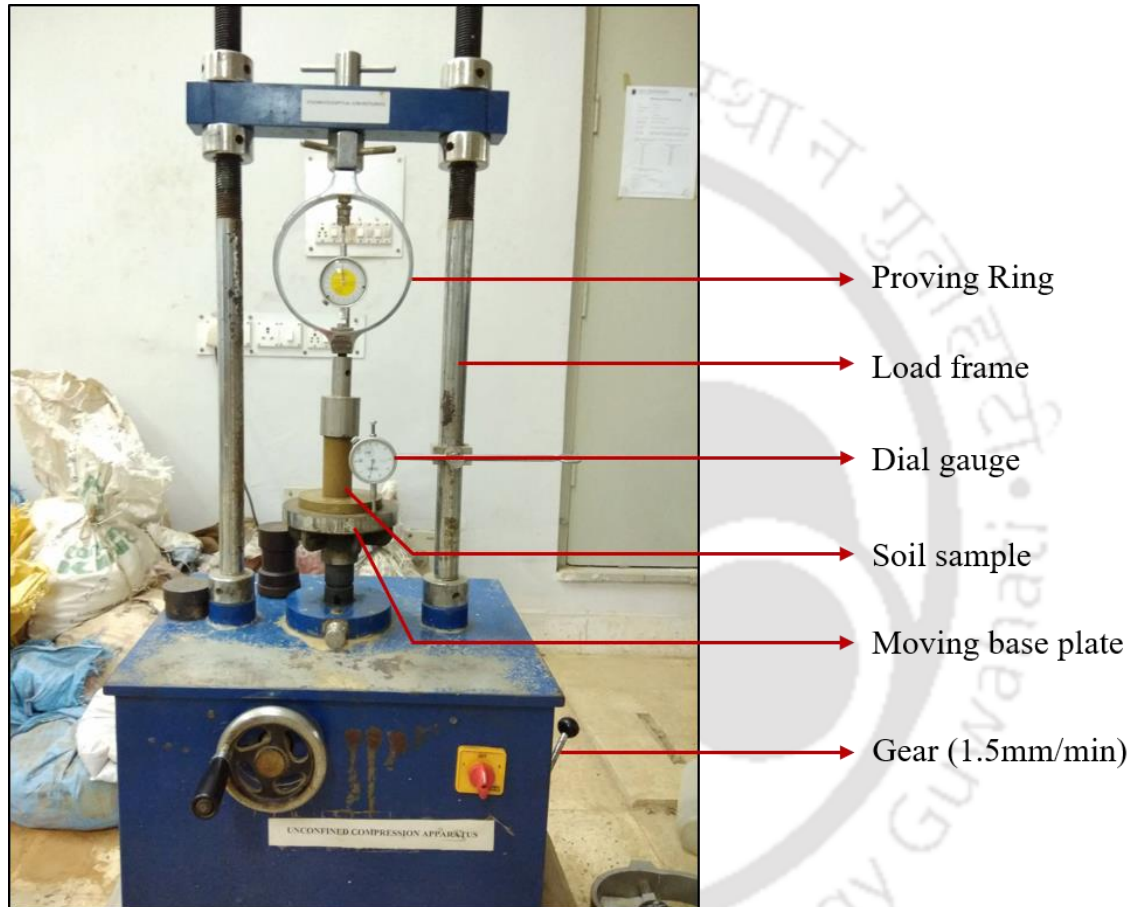


Fig. 3.9. Unconfined compressive strength (UCS) testing machine

3.8. pH Study

The process of adsorption is controlled by the pH of the mixture. The pH is an important parameter, which governs the process of adsorption. Therefore, the adsorption of various metals at pH ranges from 2-8 was examined by both the bentonites (pH electrode, Systronics, Ahmedabad, Gujarat, India). The study was performed at 28 ± 1 °C at a concentration of 1000 mg/L. Bentonite weighing 5 gm was added to a conical flask having

100 mL of metal solutions. Using 0.1M HNO₃ and 0.1NaOH, the pH of the solution was balanced. The solution was then shaken at 150 RPM using a rotary shaker. The supernatant was separated by centrifugation (10 min at 3000 rpm). By using an atomic absorption spectrophotometer (AAS), metal concentration was analyzed (55 B, Spectra AA, Agilent Technologies, Santa Clara, CA).

3.9. Batch Study

The batch study was performed as per ASTM-D4646-03 (2008) to determine the sorption capacity of metals on two different bentonites. Different concentrations of metals ranging from 100 to 2000 mg/L were prepared from the stock solutions. In a 250 mL conical flask, 5g of soil sample was mixed with 100 mL of metal solution at different initial concentrations.

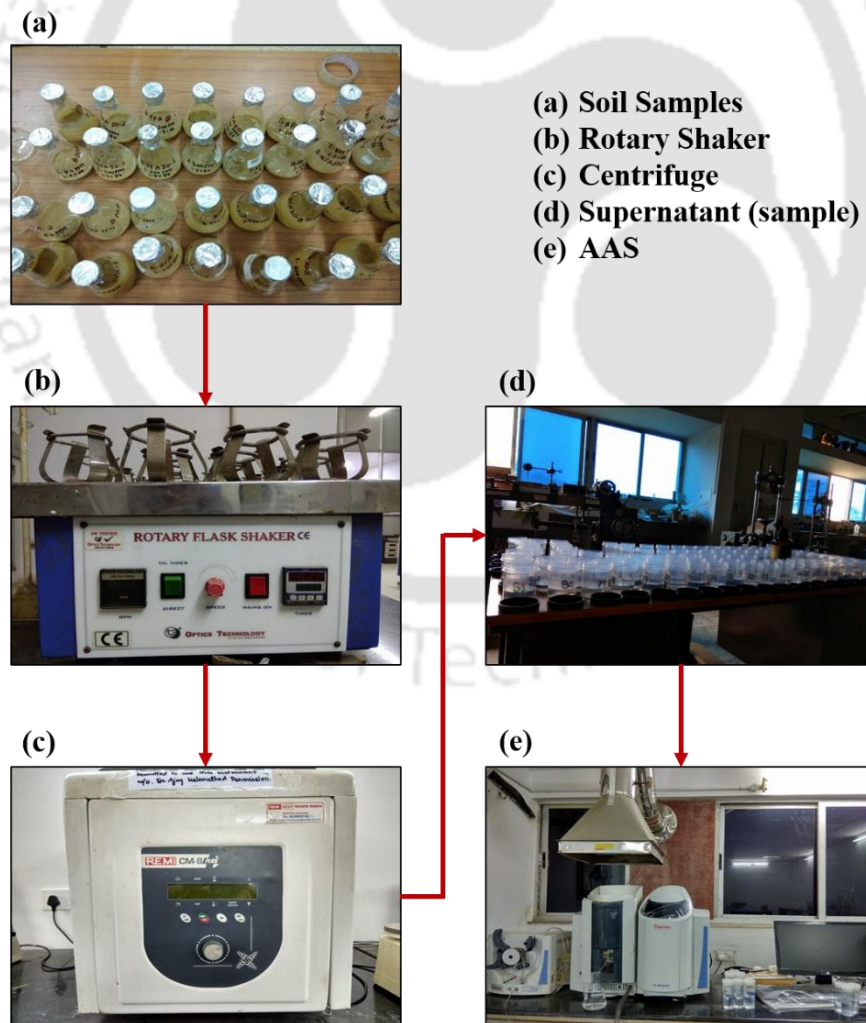


Fig. 3.10. Batch adsorption study

The pH was adjusted to 5 ± 0.1 by adding NaOH and HNO₃ of 0.1M. On a rotary shaker, the solution was agitated for 24 h at room temperature ($28 \pm 1^\circ\text{C}$). The solution was then centrifuged at 3000 rpm for 10 minutes. The supernatant obtained was then filtered using Whatman 42 filter paper, and the concentration was analyzed in AAS.

The amount of metal adsorbed on the bentonites was determined using the following equation (Eq. 3.9).

$$q_e = \frac{(C_0 - C_e)V}{m} \quad (3.9)$$

Where, q_e is the amount of metal ions adsorbed on bentonite clay (in mg/g), C_0 is the initial concentration of metal (in mg/L), C_e is the aqueous concentration of metal in equilibrium solution (in mg/L), V is the volume of metal solution (in L), and m is the mass of the adsorbent (in g). All the tests were performed in triplicates.

The percentage removal (PR) and the quantity of heavy metals adsorbed was calculated as,

$$PR = \frac{C_i - C_e}{C_i} \times 100 \quad (3.10)$$

3.10. Sorption isotherm study

Isotherm study is a noble path, to comprehend the behaviour of surface sorption. The Langmuir isotherm model (Langmuir, 1918) is a considerably followed isotherm model, which suspects monolayer adsorption on the surface incorporating a fixed number of sorption sites. Once the sites are packed, there is no additional sorption happens. The following expression represents the Langmuir isotherm model:

$$q_e = \frac{bq_{max}C_e}{1 + bC_e} \quad (3.11)$$

Where, q_{max} is the maximum quantity of contaminant sorbed per unit mass of the adsorbent (bentonite) and b is a constant related to the affinity of binding sites.

Whether the Langmuir adsorption process is favourable or not can be analyzed by using separation factor R_L .

$$R_L = \frac{1}{1 + bC_e} \quad (3.12)$$

Where, R_L is dimensionless separation factor and C_e is the maximum initial concentration of the metal ion (mg/L).

$$\text{If } \left. \begin{array}{l} R_L = 0 \\ R_L < 1 \\ R_L = 1 \\ R_L > 1 \end{array} \right\} \text{ the sorption process is } \left. \begin{array}{l} \text{Irreversible} \\ \text{Favourable} \\ \text{Linear} \\ \text{Unfavourable} \end{array} \right\}$$

The Freundlich isotherm model (Freundlich, 2002) is the frequently used model based on the assumption that the adsorption can take place on a heterogeneous surface. Freundlich model does not predict limited surface coverage. It, however, specifies the exponential distribution of active adsorption sites and their energies. The Freundlich isotherm model can be denoted by the following equation.

$$q_e = K_f C_e^{1/n} \quad (3.13)$$

Where, n and K_f are constants which denotes the retention intensity and the relative retention capacity of solid surface, respectively.

3.11. Kinetic study

In batch mode, the kinetic study was conducted on both bentonites. Five gram of bentonite soil was mixed with 100 mL of 500 mg/L of the metal solution in a conical flask. The pH of the solution was adjusted to 5 ± 0.1 by using 0.1M HNO₃ and 0.1 M NaOH solution. The test was carried out at room temperature. The solution was shaken in a rotary shaker for a shaking time ranges from 5 to 200 minutes at 150 rpm. Then the solution was centrifuged and was analyzed by AAS. It is essential to understand the mechanism of the adsorption process and the rate-controlling steps while designing adsorption systems. Numerous kinetic models are existing, and the pseudo-first-order kinetic model and pseudo-second-order kinetic model are the most extensively used for explaining the kinetic data.

Lagergren (1898), in the 19th century, proposed Pseudo-first-order kinetic model, also known as the first-order rate equation. The equation of Pseudo-first-order kinetic model can be expressed as;

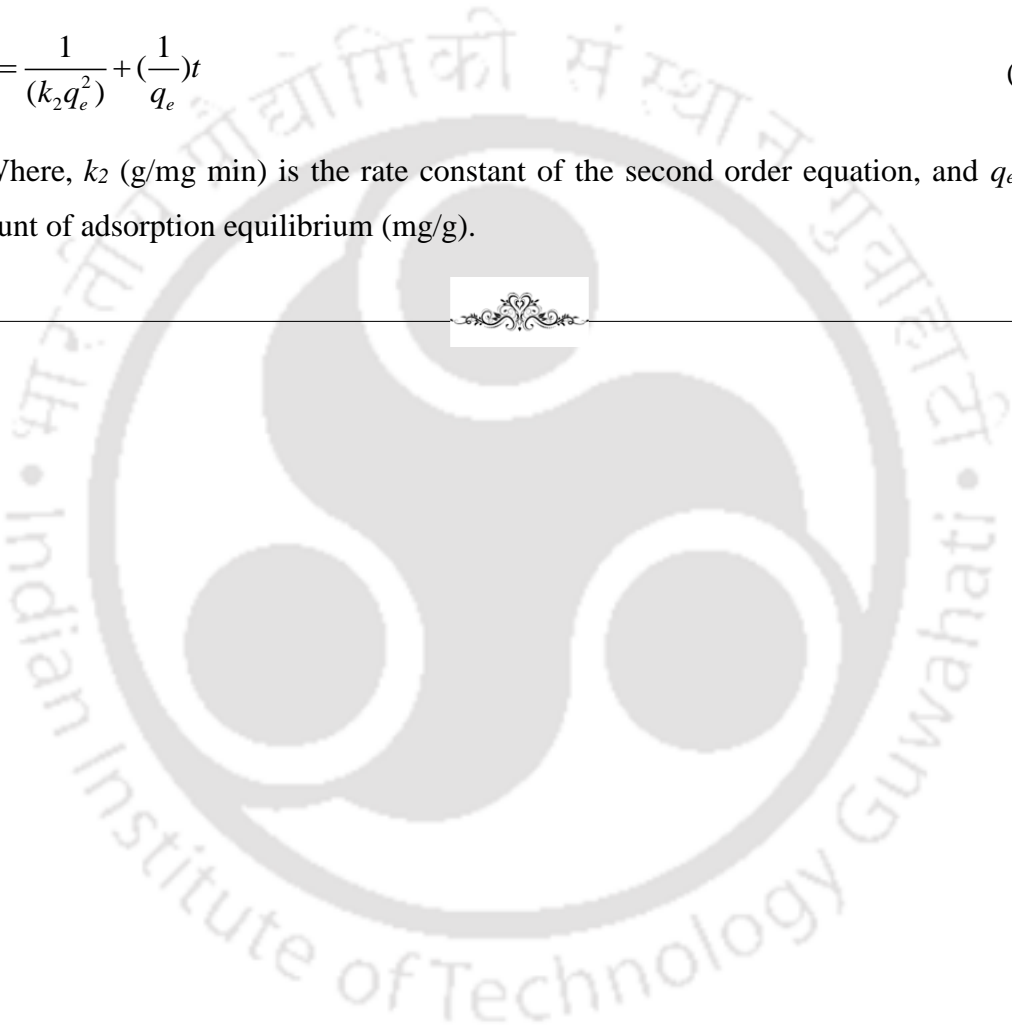
$$\ln (q_t - q_e) = \ln q_e - k_1 t \quad (3.14)$$

Where, q_t (mg/g) is adsorbed amount of metal on bentonite in contact time, t (min); k_1 is the first-order rate constant (min^{-1}).

The pseudo-second order kinetic model was first derived by Blanchard et al. (1984). The pseudo-second order kinetic model is commonly applied when overall sorption kinetics is controlled by the rate of adsorption process. The equation of pseudo-second-order kinetic model can be expressed as

$$\frac{t}{q_t} = \frac{1}{(k_2 q_e^2)} + \left(\frac{1}{q_e}\right)t \quad (3.15)$$

Where, k_2 (g/mg min) is the rate constant of the second order equation, and q_e is the amount of adsorption equilibrium (mg/g).





*Environmental pollution is
an incurable disease. It can
only be prevented.*

- Barry Commoner

4

Influence of heavy metals on the behaviour of bentonites

4.1. Introduction

Metal pollution is a serious issue worldwide due to rapid increase in industrial activity. Several toxic metals have been released in the system as industrial pollutants, triggering severe environmental pollution. Metal contaminants pollute the environment and can cause severe health issues. Some of the heavy metal like zinc, copper, nickel and iron are important for human beings in trace amounts for proper catalytic functions. However, excess use of these heavy metals may disturb the metabolism of the human being.

In many countries, the most accepted way of discarding the waste is landfilling. Leachates produced from the waste materials change the physico-chemical properties of bentonite clay that is generally considered as a liner material in a landfill. Bentonite is an extensively utilized as a liner material in landfill because of its lower hydraulic conductivity, high swelling capacity, adsorption capacity, montmorillonite content, chemical stability and low cost (Dutta and Mishra, 2016; Pawar et al., 2016). Metals present in the leachate is of most significant concern since it can cause detrimental impacts on the ecosystem. The existence of heavy-metal pollutant in the leachates disturbs the pore-fluid chemistry of the bentonite clay particles and affects its diffuse double layer (DDL). Due to

the presence of metal ions in the leachate, the swelling behaviour and consequently, the hydraulic conductivity may get altered significantly (Dutta and Mishra, 2016).

The most critical parameters which should be considered while designing a liner system for the landfill are hydraulic conductivity, compressibility, shear strength and adsorption. Harmful pollutant present inside the landfill may alter the properties of liner material, causing a reduction in efficiency. As a result, the flow path opens, and consequently, the hydraulic conductivity rises. Hence, it is crucial to investigate the variation in hydraulic behaviour along with sorption in the existence of heavy metal. Several well-documented studies have reported for effective removal of heavy metals such as Cu^{2+} (Freitas et al., 2017; Glatstein and Francisca, 2015; Karapinar and Donat, 2009), Pb^{2+} (Baylan and Meriçboyu, 2016; Deka and Sekharan, 2017; Pawar et al., 2016), Zn^{2+} (Araujo et al., 2013; Kaya and Ören, 2005; Kubilay et al., 2007) and Ni^{2+} (Futalan et al., 2011; Liu and Zhou, 2010; Vhahangwele and Mugeru, 2015; Vieira et al., 2010) employing bentonite. Numerous research groups have concentrated on the hydraulic characteristics of bentonite clays and their uses in landfills as a barrier material in the existence of several chemicals (Dutta and Mishra, 2015; Dutta and Mishra, 2016; Ören and Akar, 2017). In the past, very few investigations have been reported on the effect of various metals, leachate and mineralogical parameters on swelling, hydraulic conductivity, compressibility, shear strength and sorption behaviour of bentonite together. Since chemical and mineralogical properties in bentonite vary depending on its source of origin, its behaviour may differ considerably depending on its mineralogical composition. Hence, it is essential to compare the alteration in the characteristics of bentonites in the incidence of various metal ions.

The objective of this research was to study the hydraulic conductivity, compressibility, shear strength and adsorption characteristics of heavy metals (Pb^{2+} , Cu^{2+} , Zn^{2+}) on two different Indian bentonites having diverse mineralogical and chemical characteristics. Two bentonites with different mineralogical composition, which was reflected in their different liquid limit, CEC, montmorillonite content and free swelling value, were evaluated for their change in free swelling, liquid limits, hydraulic conductivity, swelling potential, swelling pressure and various consolidation parameters such as compression index (C_c), coefficient of consolidation (c_v) and time to complete 90% of the consolidation (t_{90}) due to the presence of various concentrations of Pb^{2+} , Cu^{2+} , and Zn^{2+} ions. Further, to study the effect of shear strength on the behaviour of compacted bentonites in the presence of these solutions, UCS experiments were also carried out on bentonite samples. Some experimental parameters, i.e. pH, bentonites dose, initial concentration and contact time have been used as a function

to determine the capacity of bentonites to adsorb metal ions. Different isotherm and kinetic model have been fitted. This investigation will be beneficial to design the practical and economic barrier system to prevent the pollutant leaching in the landfills. This study also contributes a new data set within a concentration ranges from 100 to 2000 mg/L of the metal ion.

4.2. Results and discussions

4.2.1. Influence of heavy metals on Liquid limit

The impacts of various Pb^{2+} , Cu^{2+} , and Zn^{2+} concentrations on the bentonite's liquid limit are represented in Fig. 4.1. The plot reveals that the liquid limit decreased correspondingly to an increment in the heavy metal ion concentration. The decrease was more prominent for Bentonite-1 than Bentonite-2. The liquid limit of Bentonite-2 lowered from 305.0% with DI water to 200.0%, 204.0%, and 197.0% for Zn^{2+} , Pb^{2+} , and Cu^{2+} solutions with 2000 mg/L concentration, respectively; while, for a similar increase in concentration, the liquid limit of Bentonite-1 shrank from 480.0% with DI water to 297.0%, 306.0%, and 292.0% for Zn^{2+} , Pb^{2+} , and Cu^{2+} solutions, respectively. The principal cause for this remains the development of a comparatively huge diffuse double layer (DDL) thickness for Bentonite-1 than Bentonite-2. A diminishing interparticle repulsion, attributed to an increase in metal ion concentrations, decreases the liquid limit as the particles transport freely at lesser water content or interparticle distances (Sridharan, 1975; Warkentin, 1961).

An assessment of the liquid limit values for both bentonites at the same concentration levels indicates that Bentonite-1, with greater amounts of CEC, ESP, and SSA, compared to Bentonite-2, exhibited a higher liquid limit value. Also, Bentonite with Pb^{2+} as pore fluid displayed the highest liquid limit value compared to other heavy metal ions.

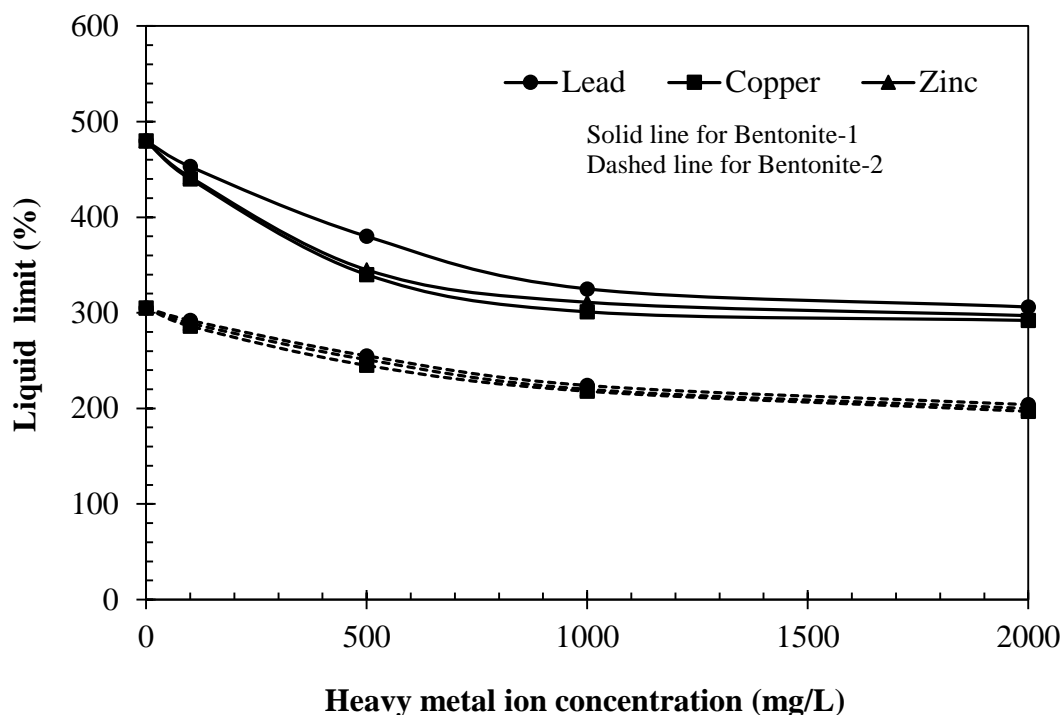


Fig. 4.1. Liquid limits of Bentonite-1 and -2 in the presence of different concentrations of heavy metals

4.2.2. Influence of heavy metals on free swelling

The influence of various concentration of lead, zinc, and copper ions on bentonites' free swelling is presented in Fig 4.2. A decline in the bentonite's free swelling corresponding to an increase in the heavy metals concentration was observed, with a steeper decline for Bentonite-1 than Bentonite-2. Furthermore, Bentonite-1 displayed an insignificant reduction for the concentration increment from 0 to 100 mg/L; however, a significant decline was observed for higher concentrations, i.e., from 100 to 2000 mg/L. For instance, for Bentonite-1, the free swelling values lowered to 31.0 mL/2g at Pb^{2+} value of 100 mg/L, from an initial amount of 32.5 mL/2g for DI water. However, when the Pb^{2+} value reached 2000 mg/L from 100 mg/L, the free swelling values decreased to 8.5 mL/2g from 31.0 mL/2g. Similarly, for Bentonite-2, the free swelling values lowered to 19.0 mL/2g at Pb^{2+} value of 100 mg/L, from an initial value of 20.0 mL/2g for Pb^{2+} value at 0 mg/L. However, when the Pb^{2+} value reached 2000 mg/L from 100 mg/L, the free swelling values decreased to 6.5 mL/2g from 19.0 mL/2g. A more significant drop in the free swelling for Bentonite-1 may be associated with a higher decline in DDL thickness, principally because of heavy

metals. The plot shows that the bentonite swelled to a higher value in the presence of Pb^{2+} solution, followed by Zn^{2+} and Cu^{2+} solutions.

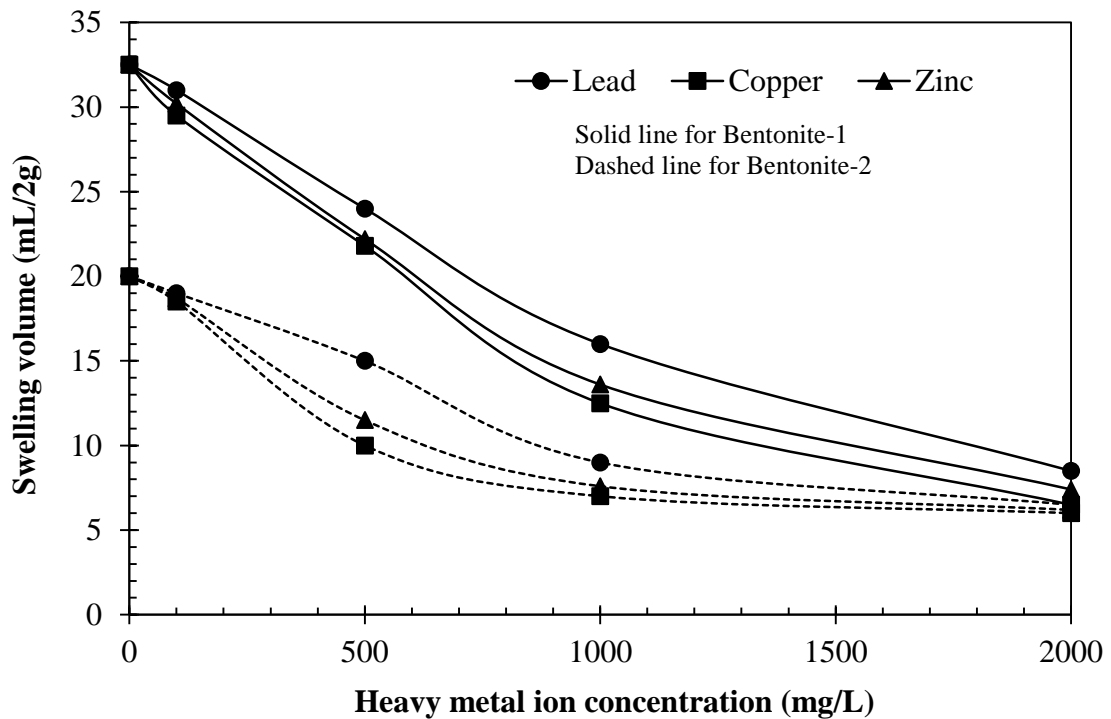


Fig. 4.2. Plots for the free swelling of Bentonite-1 and -2 in the presence of different concentrations of heavy metals

4.2.3. Influence of heavy metals on Swelling pressure

Table 4.1. Swelling Pressure of Bentonite-1 and -2 in the presence of heavy metals

| Concentration (mg/L) | Swelling Pressure (kPa) | | | | | |
|-------------------------|-------------------------|------------------|------------------|------------------|------------------|------------------|
| | Bentonite-1 | | | Bentonite-2 | | |
| | Cu^{2+} | Pb^{2+} | Zn^{2+} | Cu^{2+} | Pb^{2+} | Zn^{2+} |
| 0 (DI water) | 460.9 | 460.9 | 460.9 | 392.6 | 392.3 | 392.3 |
| 100 | 380.6 | 425.0 | 370.6 | 310.8 | 322.8 | 297.8 |
| 500 | 320.6 | 335.0 | 300.8 | 280.0 | 290.5 | 277.4 |
| 1000 | 250.2 | 270.0 | 247.6 | 244.1 | 260.8 | 240.4 |
| 2000 | 228.7 | 237.9 | 210.1 | 230.1 | 239.9 | 223.6 |

The influence of metal ion concentrations on the swelling pressure of bentonite compacted at OMC-MDD, is represented through Table 4.1, showing an inverse

relationship between the swelling pressure and metal ion concentrations in the pore fluid for both bentonites.

Similar to the free swelling and liquid limit, the swelling pressure of Bentonite-1 was also observed to have a more considerable impact than Bentonite-2 due to the presence of heavy metal ions in the pore fluid. For samples representing Bentonite-1, when compacted at OMC-MDD, a reduction in the swelling pressure from 460.9 kPa with DI water to 228.7 kPa (i.e., 50.4% reduction) due to the presence of 2000 mg/L of Cu^{2+} solution was obtained. Similarly, with an equivalent increment in concentration, Bentonite - 2's swelling pressure declined to 230.1 kPa from an initial value of 392.6 kPa (i.e., a 41.4% reduction). Since the DDL reduction as a result of metal additions was also higher for Bentonite-1 compared to Bentonite-2, a more substantial decrease in the swelling pressure was observed for Bentonite-1. Table 4.1 also reveals that Pb^{2+} ions shows higher value of swelling pressure than Cu^{2+} ions, followed by Zn^{2+} ions. Additionally, the contrast in effect was more prominently observed for 2000 mg/L compared to 100 mg/L.

4.2.4. Influence of heavy metals on Swelling potential

Table 4.2 presents the influence of heavy metals and initial water content on the bentonites' swelling potential. It was observed that the swelling potential reduced with an increment in metal concentration. A more significant swelling potential value was obtained for the solution containing Pb^{2+} than Cu^{2+} and Zn^{2+} solutions. pH conditions affect the adsorption rate, which increases as the solution becomes more acidic. The pH values of 100 mg/L Pb^{2+} , Cu^{2+} , and Zn^{2+} solutions were measured to be 4.75, 5.31, 5.78, respectively; whereas, for 2000 mg/L Pb^{2+} , Cu^{2+} , and Zn^{2+} solutions the pH were 3.80, 4.39, 5.08, respectively. The Pb^{2+} solution was found to have the highest pH among all three solutions, resulting in the least adsorption rate. Thus, when permeated with lead solution, the bentonite's swelling potential was the highest, primarily because of insufficient interaction between Pb^{2+} ions and bentonite, thus resulting in the precipitation of Pb^{2+} (Ouhadi et al., 2006). Samples representing Bentonite-2, when compacted at OMC - MDD, displayed a swelling potential value of 23.7% with DI water, further reducing to 16.0, 15.9, and 13.2% with 2000 mg/L of Pb^{2+} , Zn^{2+} , and Cu^{2+} solution, respectively. Similarly, for Bentonite-1, the samples displayed the swelling potential of 34.3% with DI water, with a further reduction to 14.3, 12.7, and 9.5% after permeation with 2000 mg/L of Pb^{2+} , Zn^{2+} , and Cu^{2+} solution, respectively.

Table 4.2 Swelling potential of Bentonite-1 and -2 in the presence of heavy metals

| Concentration (mg/L) | Swelling Potential (%) | | | | | |
|-------------------------|------------------------|------------------|------------------|------------------|------------------|------------------|
| | Bentonite-1 | | | Bentonite-2 | | |
| | Cu ²⁺ | Pb ²⁺ | Zn ²⁺ | Cu ²⁺ | Pb ²⁺ | Zn ²⁺ |
| 0 (DI water) | 34.3 | 34.3 | 34.3 | 23.7 | 23.7 | 23.7 |
| 100 | 27.0 | 32.7 | 23.2 | 22.0 | 21.5 | 23.1 |
| 500 | 20.5 | 25.7 | 21.1 | 17.9 | 20.6 | 21.1 |
| 1000 | 12.3 | 22.3 | 16.5 | 14.5 | 17.9 | 16.5 |
| 2000 | 9.5 | 14.3 | 12.7 | 13.2 | 16.0 | 15.9 |

4.2.5. Influence of heavy metals on Time swelling relationship

Fig. 4.3 - 4.8 explain the relation between bentonite swelling, denoted by percentage, and time elapsed for samples due to various Pb²⁺, Zn²⁺, and Cu²⁺ concentrations. The time-swelling plot, irrespective of initial compaction condition as well as saturating fluid, was observed to follow an “S” shaped curve, wherein the bentonite's initial swelling was gradual, followed by a steep rise and finally reached an asymptotic point. The plots show that the samples with heavy metals ions swelled in three distinct stages of swelling, i.e., initial, primary, and secondary (Mishra et al., 2009; Rao et al., 2006). Initial swelling is primarily associated with the macrostructure swelling, whereas, microstructure swellings contribute primary and secondary swellings (Rao et al., 2006).

Fig. 4.3 - 4.8 indicate a decline in the time needed to complete primary swelling with the increase in the heavy metal ion concentrations. A comparison between both bentonites showed that for the same time elapsed, the swelling percentage was more extensive for Bentonite-1 than Bentonite-2. Besides, Pb²⁺ played a more significant role in the swelling, compared to Zn²⁺ and Cu²⁺ solutions, irrespective of the bentonite types.

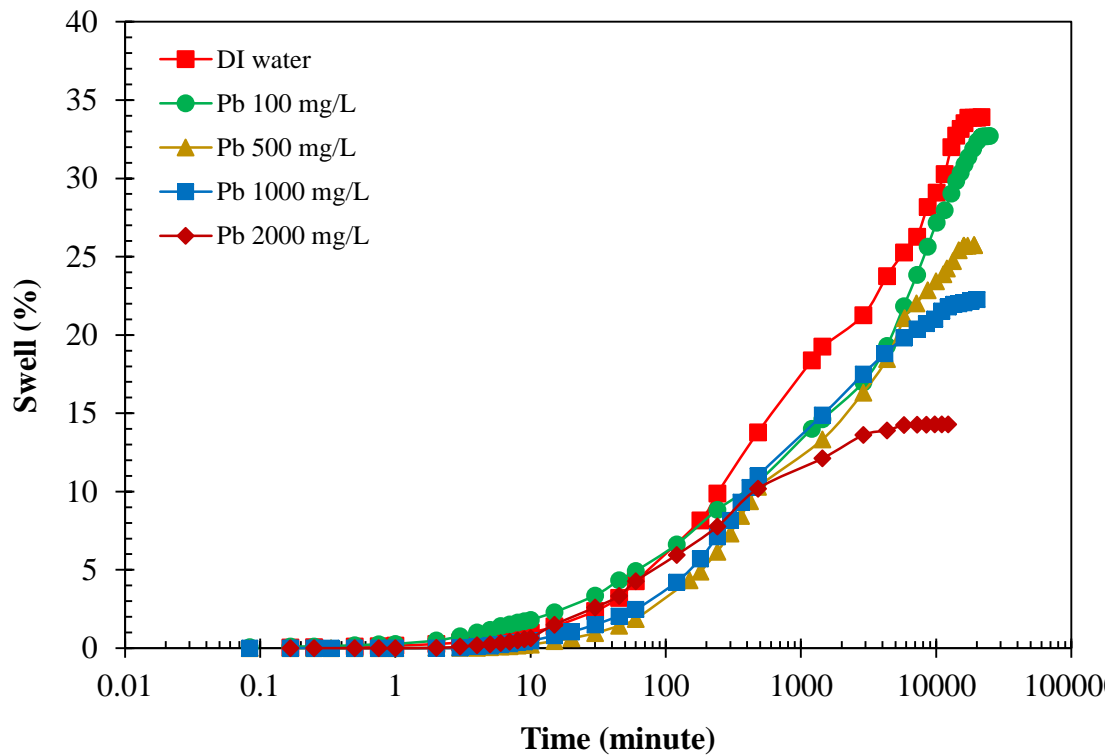


Fig. 4.3. Time–swelling plot for Bentonite-1 compacted at MDD-OMC in the presence of various Pb^{2+} concentration

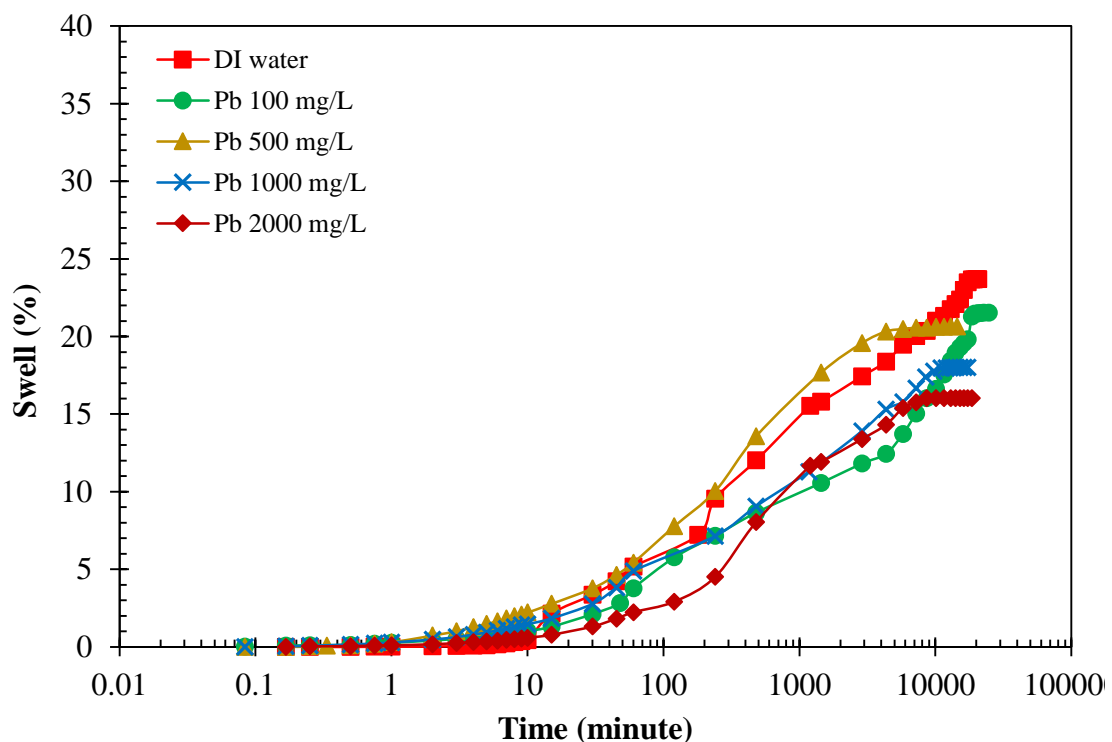


Fig. 4.4. Time–swelling plot for Bentonite-2 compacted at MDD-OMC in the presence of various Pb^{2+} concentration

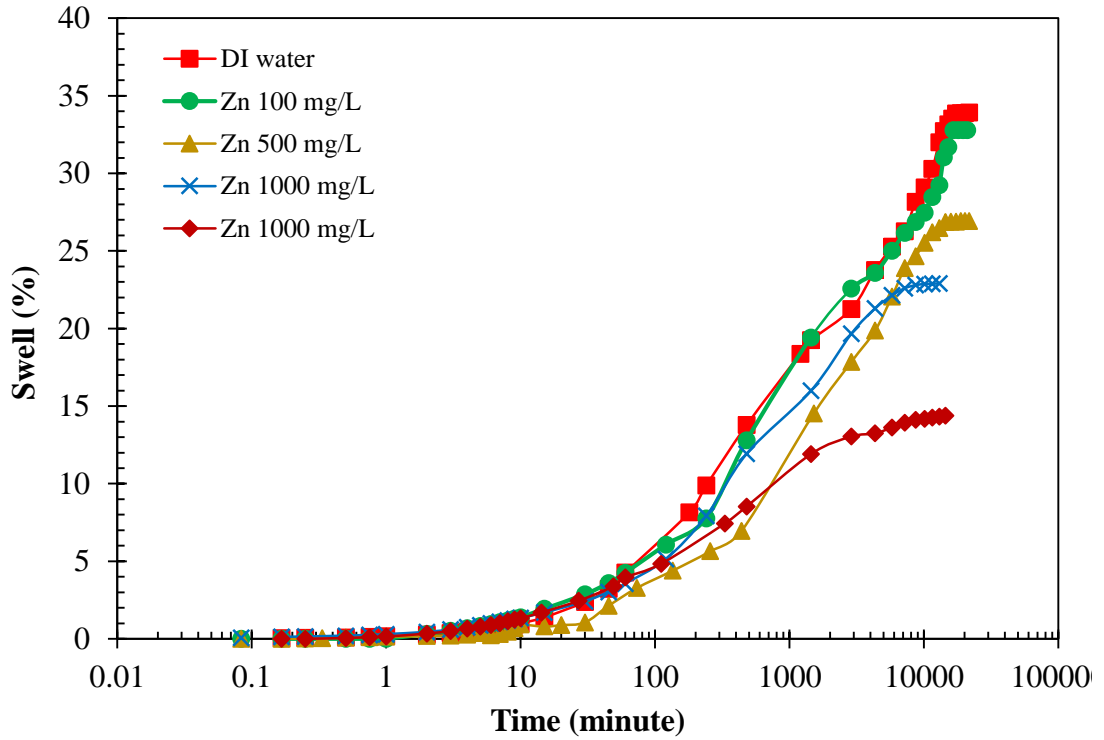


Fig. 4.5. Time–swelling plot for Bentonite-1 compacted at MDD-OMC in the presence of various Zn²⁺ concentration

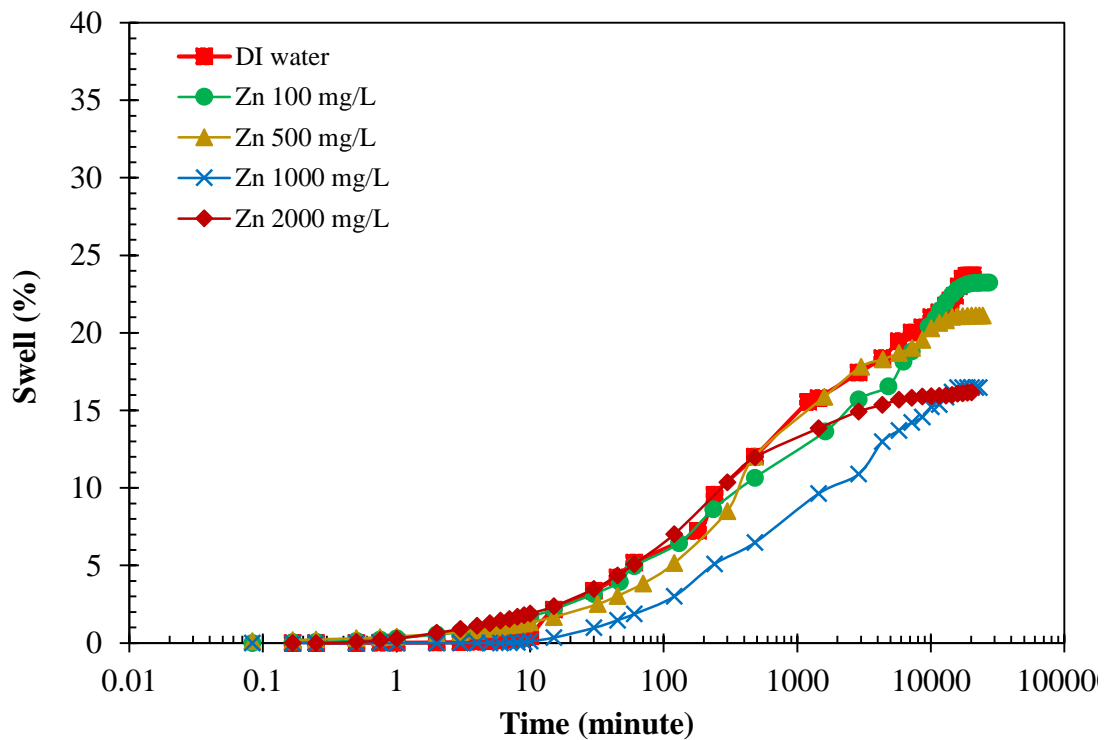


Fig. 4.6. Time–swelling plot for Bentonite-2 compacted at MDD-OMC in the presence of various Zn²⁺ concentration

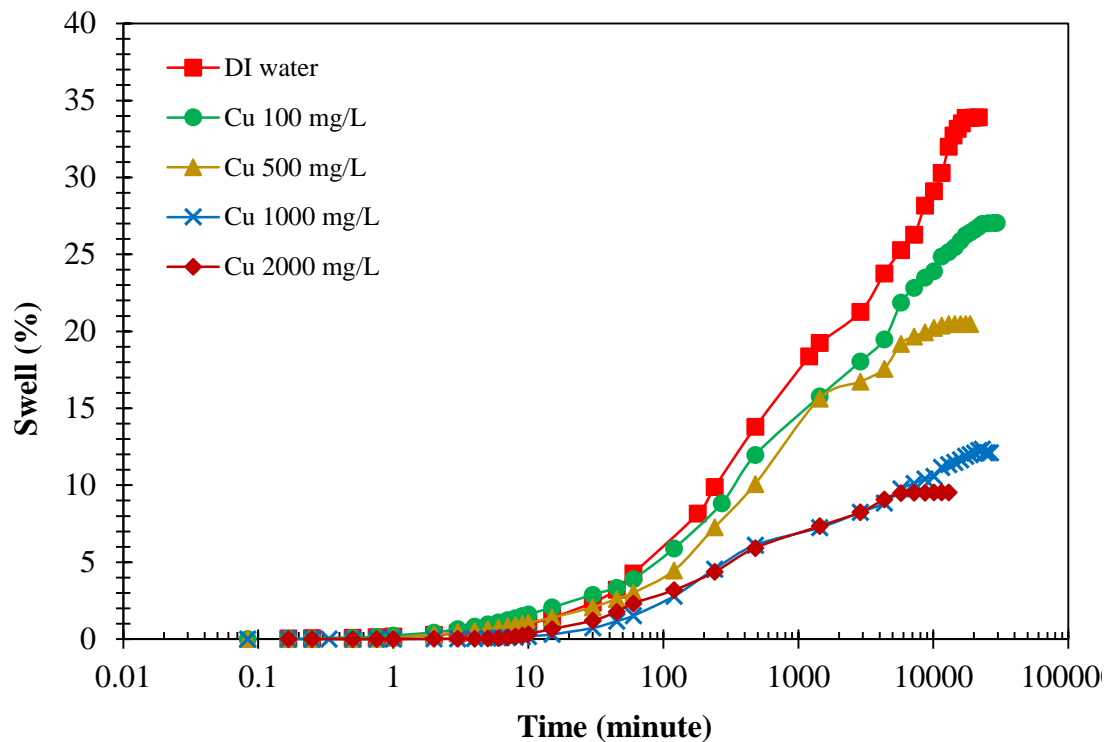


Fig. 4.7. Time-swelling plot for Bentonite-1 compacted at MDD-OMC in the presence of various Cu^{2+} concentration

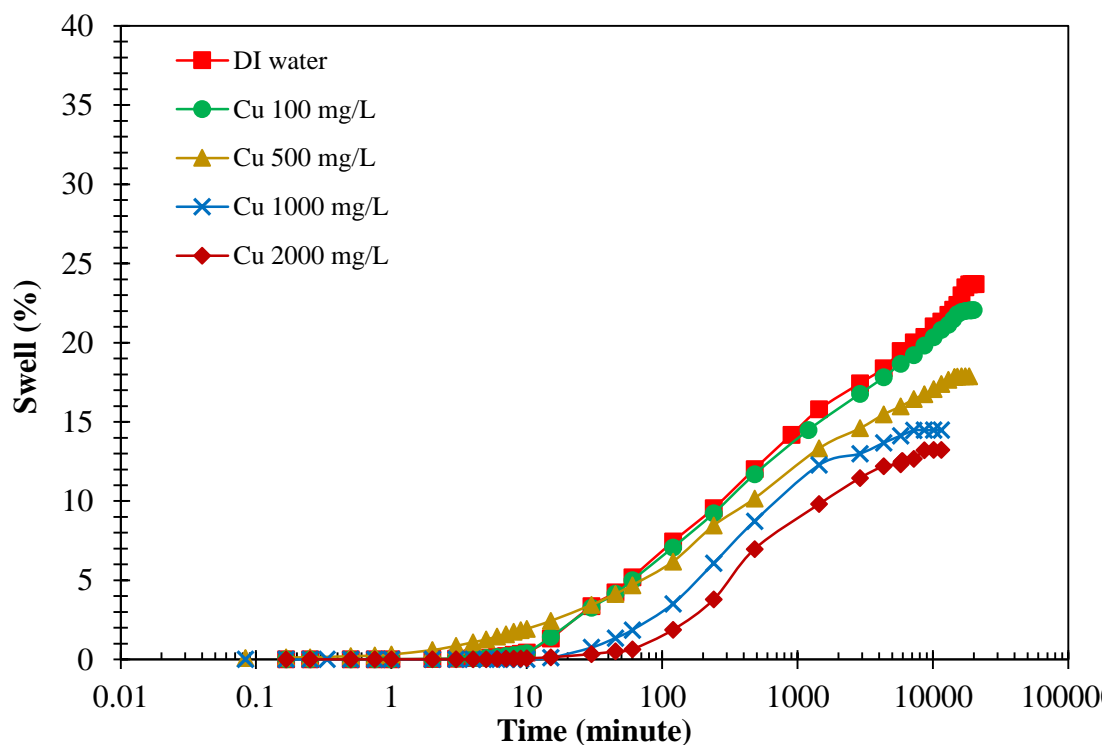


Fig. 4.8. Time-swelling plot for Bentonite-2 compacted at MDD-OMC in the presence of various Cu^{2+} concentration

4.2.6. Influence of heavy metals on Hydraulic conductivity

Several factors, such as characteristics of the permeant, soil structure, and void ratio, can affect the hydraulic conductivity of bentonites (Lambe, 1955). To investigate the effect of heavy metals (Pb^{2+} , Cu^{2+} , Zn^{2+}) on hydraulic conductivity at different void ratios, the hydraulic conductivity value of both bentonites at different void ratios were computed from the oedometer test results. The plot in Fig. 4.9 to 4.11 shows the relationship between hydraulic conductivity and void ratio of two different bentonites in the presence of heavy metal solution. It shows that the hydraulic conductivity of both the bentonites rises with the rise in heavy metal concentration. The hydraulic conductivity rises marginally when the metal concentration rises from 0 to 100 mg/L. With a further rise to 2000 mg/L, the hydraulic conductivity value increased significantly. This is primarily due to the reduction in the repulsive forces between the clay particles with the increase in metal concentration, thereby triggering a decline in the diffuse double layer thickness (Dutta and Mishra, 2016).

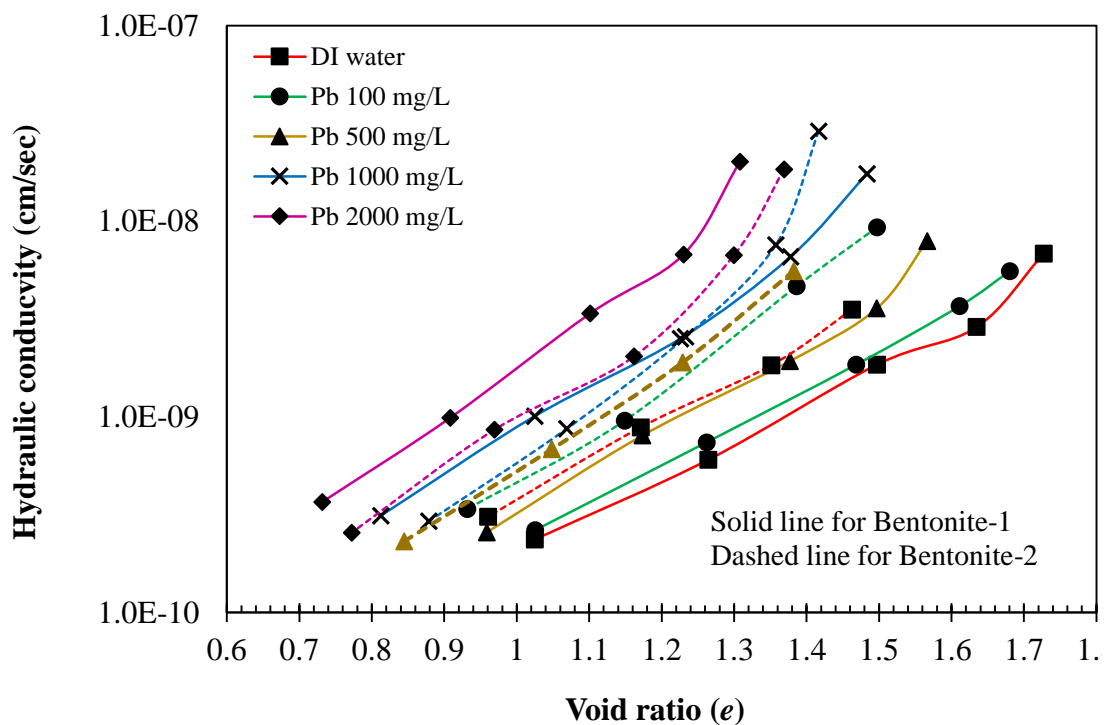


Fig. 4.9. Void ratio-hydraulic conductivity plots for Bentonite-1 and -2 compacted at MDD-OMC in presence of various concentration of Pb^{2+}

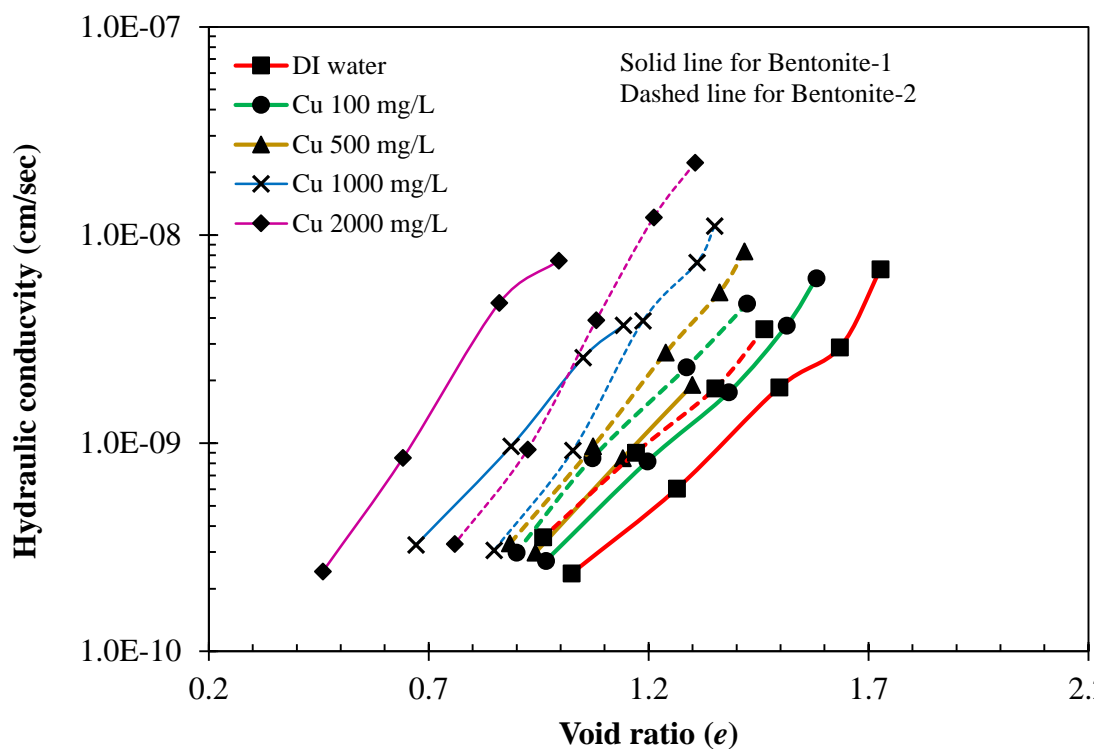


Fig. 4.10. Void ratio-hydraulic conductivity plots for Bentonite-1 and -2 compacted at MDD-OMC in presence of various concentration of Cu^{2+}

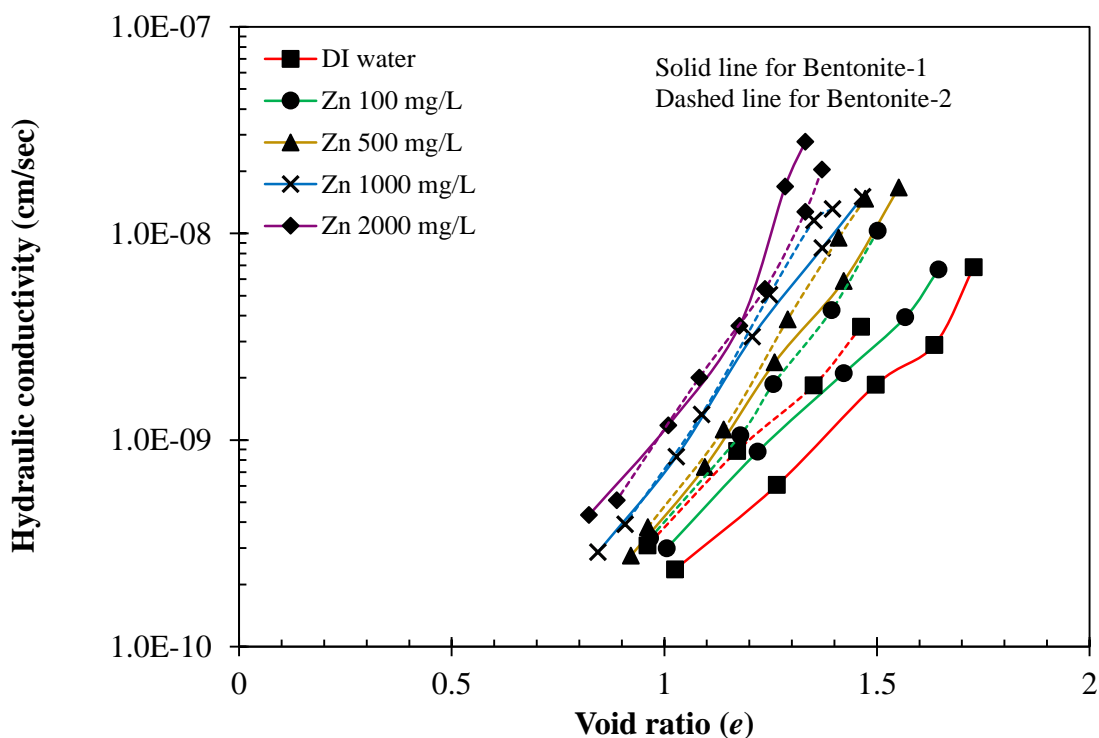


Fig. 4.11. Void ratio-hydraulic conductivity plots for Bentonite-1 and -2 compacted at MDD-OMC in the presence of various concentrations of Zn^{2+}

At a void ratio of 1.3, the hydraulic conductivity values at different Pb^{2+} and Zn^{2+} concentrations were determined and tabulated in Table 4.3 and 4.4. It can be observed from Table 4.3 that the hydraulic conductivity value is prominent at higher levels of Pb^{2+} concentration of the solution. With the increase in Pb^{2+} concentration from 0 to 100 mg/L, the hydraulic conductivity value increased from 7.10×10^{-10} to 8.76×10^{-10} cm/sec for Bentonite-1. The hydraulic conductivity value increased further to 2.09×10^{-8} cm/sec, with a further increase in the concentration to 2000 mg/L. Similarly, for Bentonite-2 with the increase in Pb^{2+} concentration from 0 to 100 mg/L, the hydraulic conductivity value increased from 1.53×10^{-9} to 2.62×10^{-9} cm/sec, but with a further rise in the concentration to 2000 mg/L, the hydraulic conductivity value increased up to a value of 7.49×10^{-10} cm/sec.

Table 4.3 Hydraulic conductivity of bentonites at a void ratio of 1.3 for Pb^{2+}

| Concentration (mg/L) | Hydraulic conductivity (cm/sec) | |
|----------------------|---------------------------------|------------------------|
| | Bentonite-1 | Bentonite -2 |
| DI Water | 7.10×10^{-10} | 1.53×10^{-09} |
| 100 | 8.76×10^{-10} | 2.62×10^{-09} |
| 500 | 1.37×10^{-09} | 3.16×10^{-09} |
| 1000 | 3.90×10^{-09} | 4.39×10^{-09} |
| 2000 | 2.09×10^{-08} | 7.49×10^{-09} |

Table 4.4. Hydraulic conductivity values of bentonites at a void ratio of 1.3 for Zn^{2+}

| Concentration (mg/L) | Hydraulic conductivity (cm/sec) | |
|----------------------|---------------------------------|------------------------|
| | Bentonite-1 | Bentonite -2 |
| DI Water | 7.10×10^{-10} | 1.53×10^{-09} |
| 100 | 1.30×10^{-09} | 2.70×10^{-09} |
| 500 | 3.30×10^{-09} | 5.00×10^{-09} |
| 1000 | 6.20×10^{-09} | 9.30×10^{-09} |
| 2000 | 2.80×10^{-08} | 1.30×10^{-08} |

Likewise, it was found that with the rise in concentration in Zn^{2+} the value of hydraulic conductivity raised from 1.53×10^{-09} to 2.70×10^{-09} cm/sec for Bentonite-2 at an initial concentration ranges from 0 to 100 mg/L; whereas, at 2000 mg/L, 1.30×10^{-08} cm/sec of hydraulic conductivity value was observed (Table 4.4). Similarly, Bentonite-1 showed that

an increment of hydraulic conductivity value from 7.10×10^{-10} to 1.30×10^{-09} cm/sec at concentration ranges from 0 to 100 mg/L and 2.80×10^{-08} cm/sec with further increase in Zn^{2+} concentration to 2000 mg/L.

Furthermore, similarly the hydraulic conductivity value was evaluated for both the bentonites permeated with different concentration of Cu^{2+} solution at a void ratio of 1.1. From Table 4.5, it can be observed that Bentonite-1 shows a hydraulic conductivity value of 5.30×10^{-10} cm/sec with the increase in Cu^{2+} concentration from 0 to 100 mg/L. With further increase in concentration to 2000 mg/L, the hydraulic conductivity value was 1.89×10^{-8} cm/sec. Similarly, Bentonite-2 shows a hydraulic conductivity value of 1.03×10^{-9} cm/sec and 5.41×10^{-9} cm/sec with the increase in Cu^{2+} concentration from 0 to 100 and 2000 mg/L, respectively.

Table 4.5. Hydraulic conductivity of bentonites at a void ratio of 1.1 for Cu^{2+}

| Concentration (mg/L) | Hydraulic conductivity (cm/sec) | |
|----------------------|---------------------------------|------------------------|
| | Bentonite-1 | Bentonite -2 |
| DI Water | 3.25×10^{-10} | 6.73×10^{-10} |
| 100 | 5.30×10^{-10} | 1.03×10^{-9} |
| 500 | 7.32×10^{-10} | 1.21×10^{-9} |
| 1000 | 3.41×10^{-9} | 1.91×10^{-9} |
| 2000 | 1.89×10^{-8} | 5.41×10^{-9} |

The two bentonites were compared for a given void ratio and concentration and the outcome depicts that, in the presence of heavy metals, Bentonite-1 indicates significant influence in comparison to Bentonite-2. With the rise in Pb^{2+} , Cu^{2+} , Zn^{2+} concentration from 0 to 100 mg/L, Bentonite-1 shows a 1.23, 1.8, 1.63 times increase in hydraulic conductivity values; whereas, for Bentonite-2 it increased by 1.71, 1.76, 1.53 times. However, with elevated concentration levels of Pb^{2+} , Cu^{2+} , Zn^{2+} from 0 to 2000 mg/L, the hydraulic conductivity was found to increase by 29.4, 39.43, 58.15 times of Bentonite-1 and 4.9, 8.50, 8.04 times for Bentonite-2, respectively.

4.2.7. Influence of heavy metals on compressibility behaviour of bentonite

The void ratio - pressure relation for both bentonites at varying heavy metal concentration levels is depicted through Fig. 4.12-4.14. Under any designated consolidation pressure, a lower value of the void ratio was observed for samples with heavy metals

compared to DI water. This reduction in the void ratio values corresponds to the higher adsorption of ions on the clay surfaces, making them closer to each other as the repulsive forces diminish, thus, eventually, decrease the DDL thickness. A marginal decrement in the void ratio was observed for Zn^{2+} and Cu^{2+} , compared to the Pb^{2+} solution.

The void ratio of Bentonite-1 was reduced to a more significant extent compared to Bentonite-2, signifying a higher compressibility value for the higher swelling bentonite in the presence of heavy metals. The higher void ratio reduction was principally attributed to the dispersion of a considerable number of cations in montmorillonite's interlayer, reducing the inter-particle counterforces.

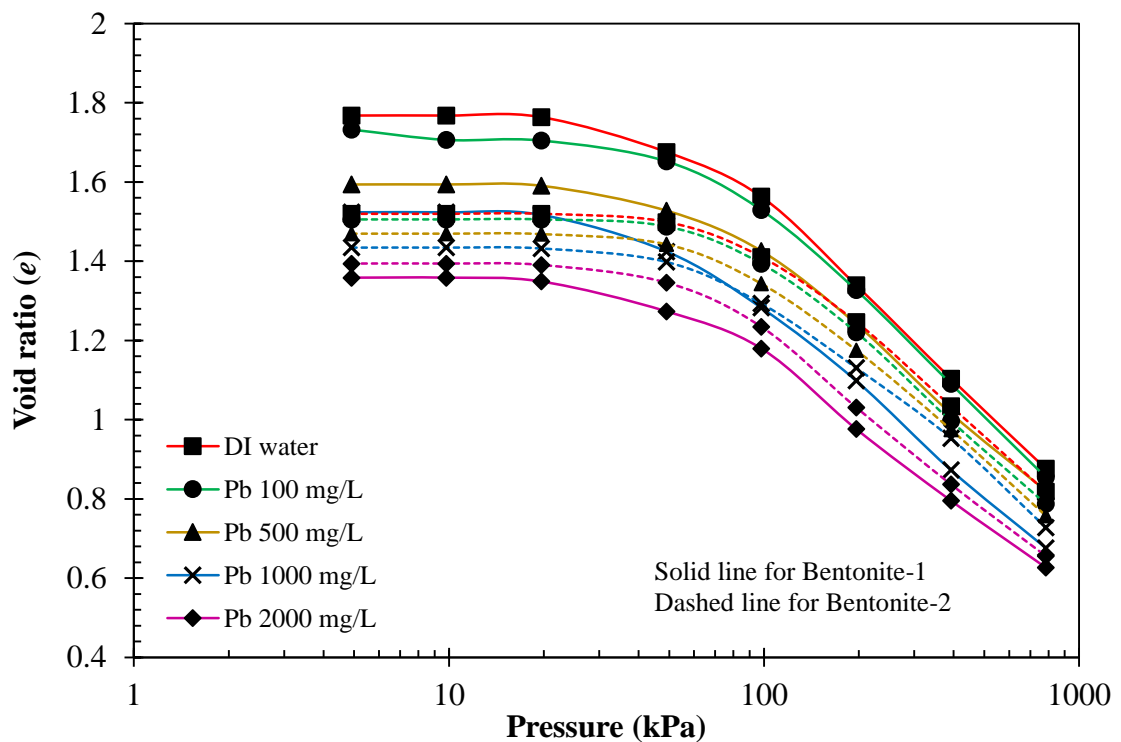


Fig. 4.12. Void ratio-pressure plots for Bentonite-1 and -2 in the presence of various Pb^{2+} concentration at OMC-MDD

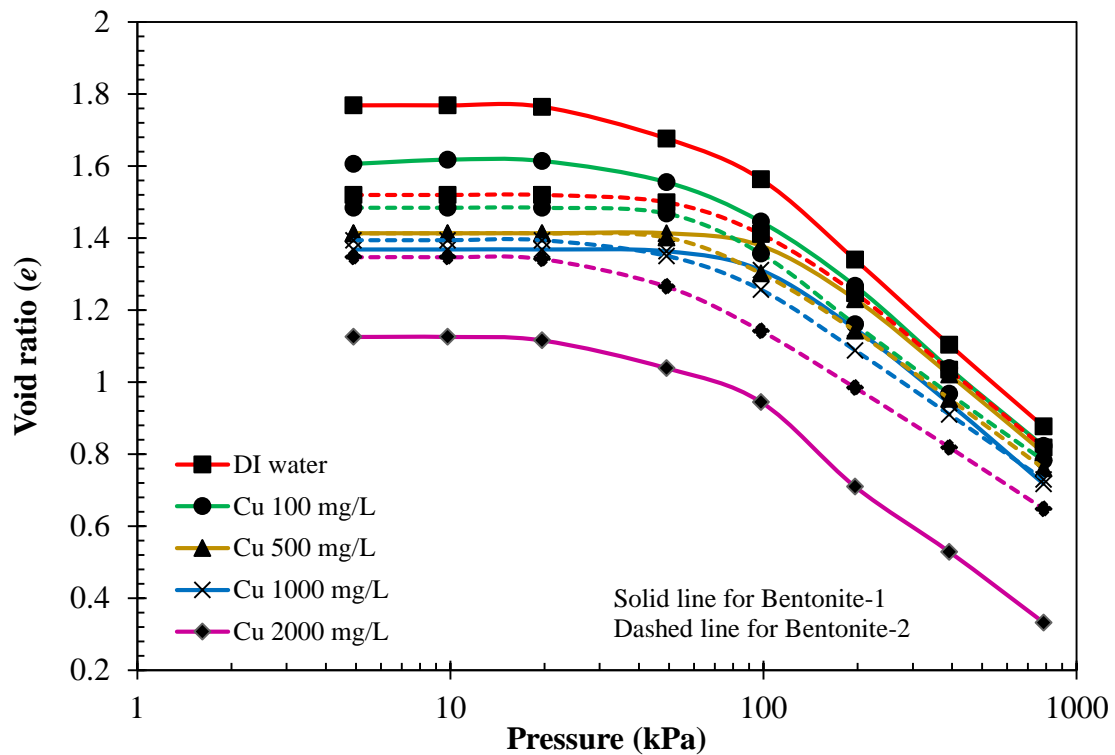


Fig. 4.13. Void ratio-pressure plots for Bentonite-1 and -2 in the presence of various Cu^{2+} concentration at OMC-MDD

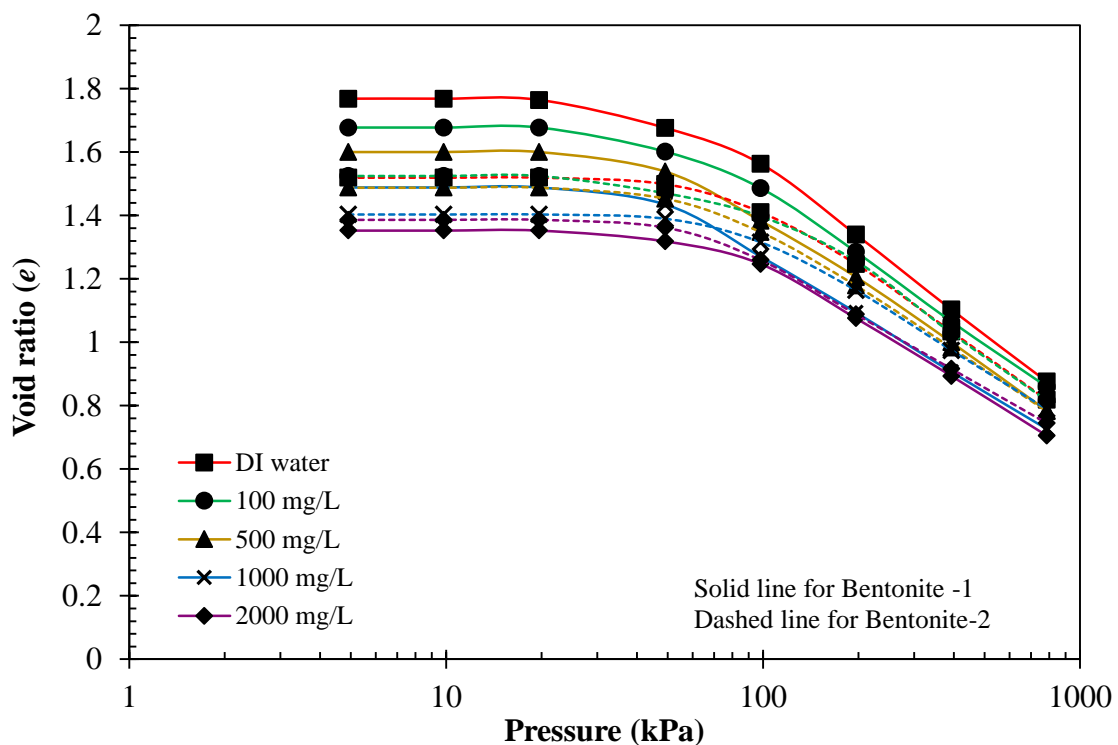


Fig. 4.14. Void ratio-pressure plots for Bentonite-1 and -2 in the presence of various Zn^{2+} concentration at OMC-MDD

4.2.8. Coefficient of consolidation (c_v)

The c_v implies the consolidation rate of a saturated specimen on the application of a surcharge load. The c_v value is used to evaluate the settlement rate and hydraulic conductivity of the soil. A higher value of c_v indicates a quicker consolidation rate and vice versa.

Fig. 4.15, 4.16 and 4.17 indicate that with a rise in the consolidating pressure, the c_v of bentonites decreases implying a slow consolidation rate at a more considerable pressure. As the pressure increases, the void ratio of the clay particles come closer to each other because of a reduction in DDL thickness and causing an increase in repulsive forces among clay particles. With a further increase in the load, the net decrease in void ratio decrease as the repulsion between the particles prevent further movement. This results in the decline in c_v value by inhibiting the further movement of the clay particles. Though, for sand-bentonite mixtures, a reverse trend was detected by Mishra et al. (2010). Fig. 4.15 to 4.17 also demonstrates that as the heavy metal concentration increases in the pore fluid, the c_v value of the bentonite also increases. The increase in the c_v with the increase in the concentration is due to a reduction in the DDL thickness. As the compressibility of the bentonite particles primarily depends upon the repulsive pressure which are controlled by physicochemical factors (Olson and Mesri, 1970), any change in these physicochemical factors such as consolidation pressure and salt concentration also brings a difference in the repulsive force. As the repulsive pressure between the particles decreases, the particles move to a closer spacing quickly on the addition of consolidating pressure causing an increase in c_v . Presence of metal ions in pore fluid, the DDL thickness is reduced, causing a reduction of a higher range of repulsive forces and as a result the settlement of the samples occurs at a faster rate. The data also indicate that the influence of different concentrations of metal ion considerably affects the decrease in c_v value with the rise in consolidation pressure.

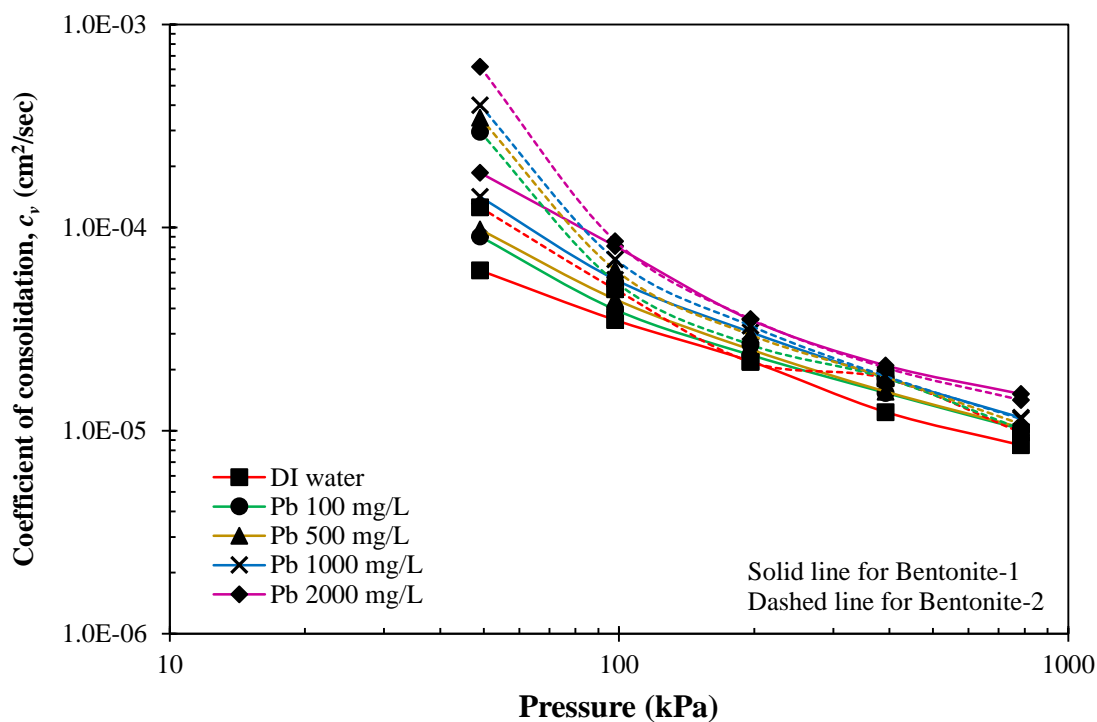


Fig. 4.15. Plot between the coefficient of consolidation and pressures of Bentonite-1 and -2 in the presence of various concentrations of Pb^{2+}

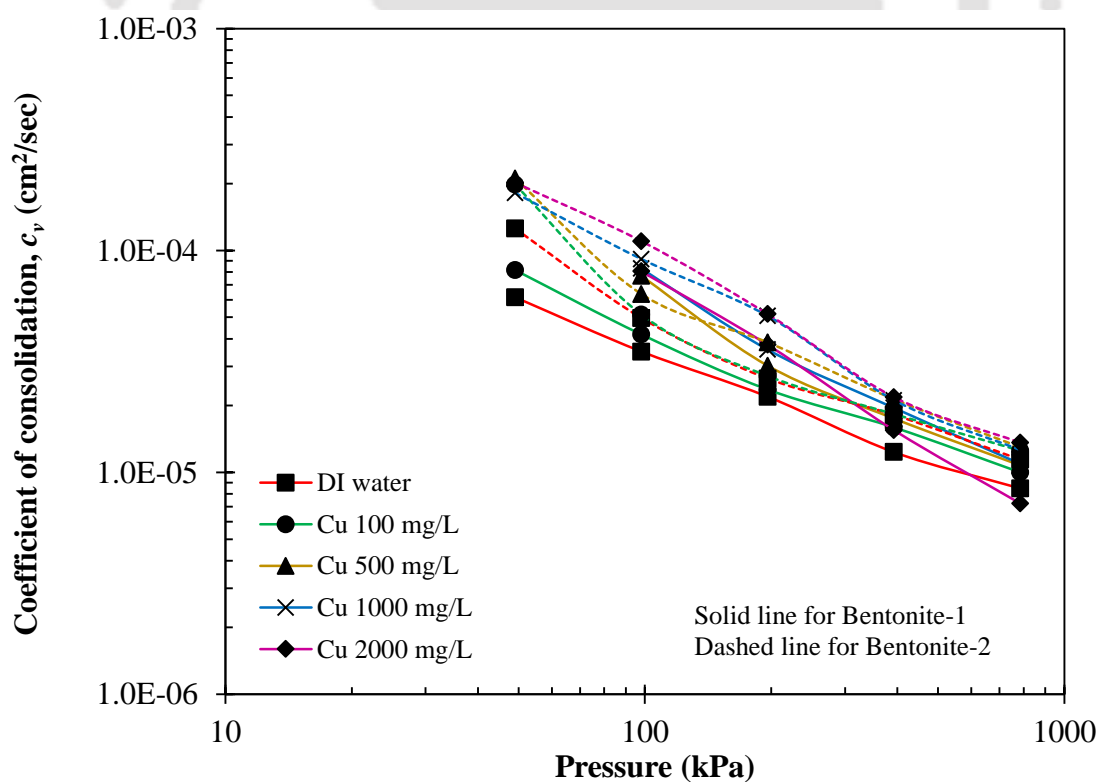


Fig. 4.16. Plot between the coefficient of consolidation and pressures of Bentonite-1 and -2 in the presence of various concentrations of Cu^{2+}

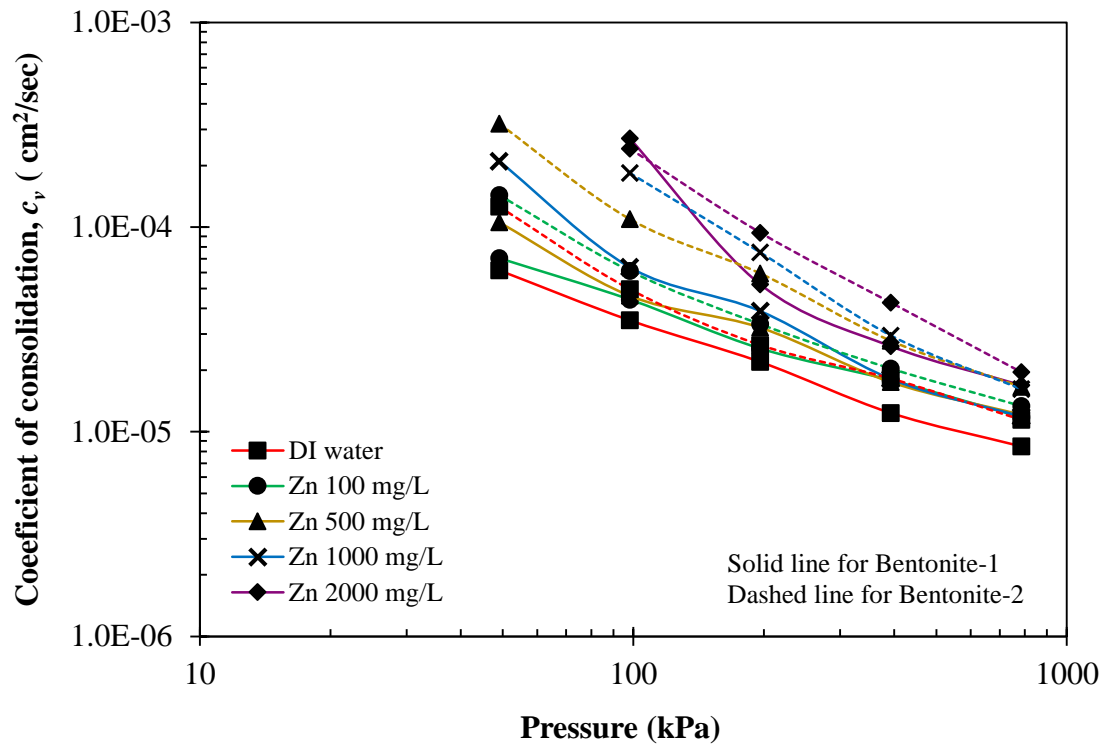


Fig. 4.17. Plot between the coefficient of consolidation and pressures of Bentonite-1 and -2 in the presence of various concentrations of Zn^{2+}

The plots demonstrate that, for Bentonite-1 and -2 infused in DI water the c_v value decreased from 3.5×10^{-5} to 8.5×10^{-6} cm^2/sec (4.1 times) and 4.9×10^{-5} to 1.1×10^{-5} cm^2/sec (4.4 times) with the increase in pressure from 98.0 kPa to 784.5 kPa. However, for soils infused with 2000 mg/L of Pb^{2+} solutions the c_v reduced from 8.4×10^{-5} to 1.5×10^{-5} cm^2/sec (5.6 times) and 6.9×10^{-5} to 1.0×10^{-5} cm^2/sec (6.9 times). Similarly, the c_v decreased from 8.1×10^{-5} to 7.3×10^{-6} cm^2/sec (11.1 times) and 1.1×10^{-4} to 1.4×10^{-5} cm^2/sec (7.8 times) when the soil samples were permeated with 2000 mg/L of Cu^{2+} solutions. Likewise, Fig. 4.17 also illustrates that the c_v declined from 2.7×10^{-4} to 1.7×10^{-5} cm^2/sec (15.9 times) and 2.4×10^{-4} to 1.9×10^{-5} cm^2/sec (12.6 times) when Bentonite-1 and -2 was permeated with 2000 mg/L of Zn^{2+} solutions.

4.2.9. Time for 90% of consolidation (t_{90})

The t_{90} of a soil sample informs about the time needed to attain 90% of consolidation at a given vertical load. The plots in Fig. 4.18, to 4.20 shows the relationship between consolidation pressure and t_{90} for the bentonite at various heavy metal concentrations. The data in the plots indicate that with the rise in pressure, the t_{90} values of both the bentonites increases. As the consolidation pressure increases, the space between the clay plates

reduces and due to that, the repulsion among clay plates increases. This will avoid further movement of the clay plates and results in a reduction in the c_v value and rise in t_{90} .

The data also indicate that the influence of concentration on the t_{90} as well. With the decrease in heavy metal concentration, the t_{90} value increased. As the concentration of heavy metal decreases, the rate of consolidation decreases, subsequently time required to complete the consolidation increases causing an increase in t_{90} .

The t_{90} value increased from 225.0 to 900.0 minutes and 96.0 to 645.2 minutes when Bentonite-1 and-2 were permeated with DI water and exposed to a consolidation pressure range from 49.0 to 784.5 kPa. However, at 2000 mg/L concentration of Pb^{2+} , it increased from 53.3 to 368.6 minutes and 35.4 to 576.0 minute. Similarly, the t_{90} rose from 12.3 to 547.56 minutes and 49.0 to 424.4 minutes in the presence of 2000 mg/L of Cu^{2+} solution. Likewise, the plot in Fig. 4.20 also reveals that for Zn^{2+} infused with 2000 mg/L of Zn^{2+} solution the t_{90} value raised from 17.6 to 368.6 minutes and 17.6 to 342.3 minutes for Bentonite-1 and -2, respectively.

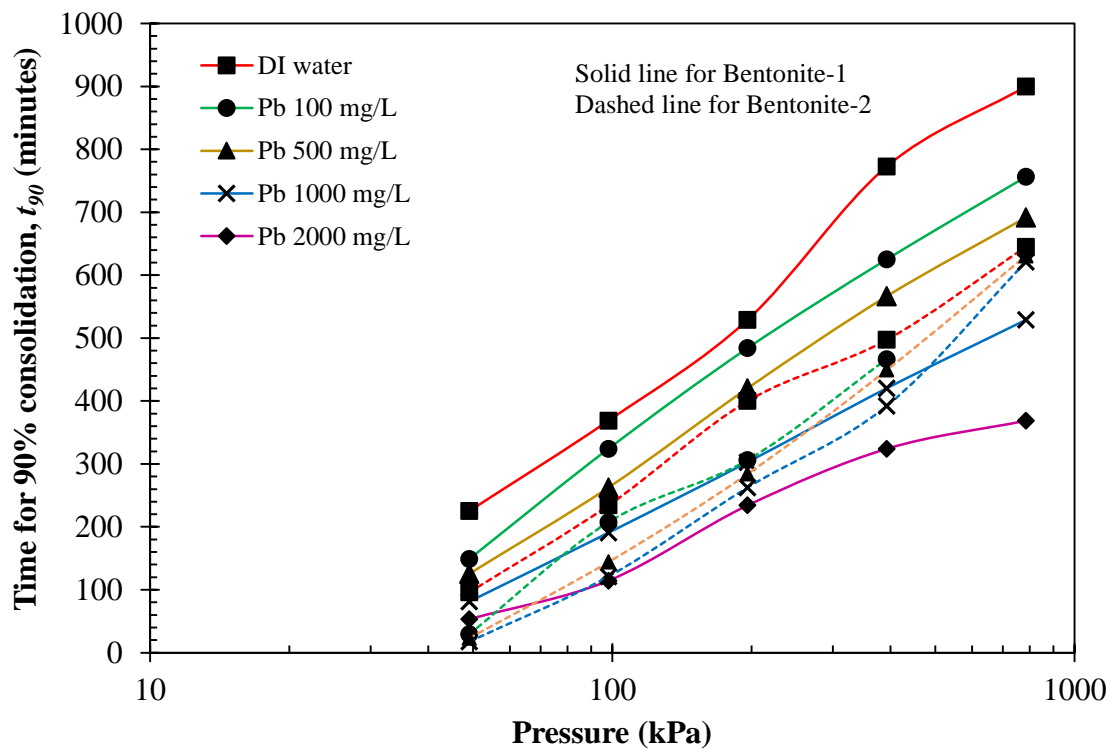


Fig. 4.18. Plot between the time for 90% of consolidation and consolidation pressures of Bentonite-1 and -2 in the presence of various concentrations of Pb^{2+}

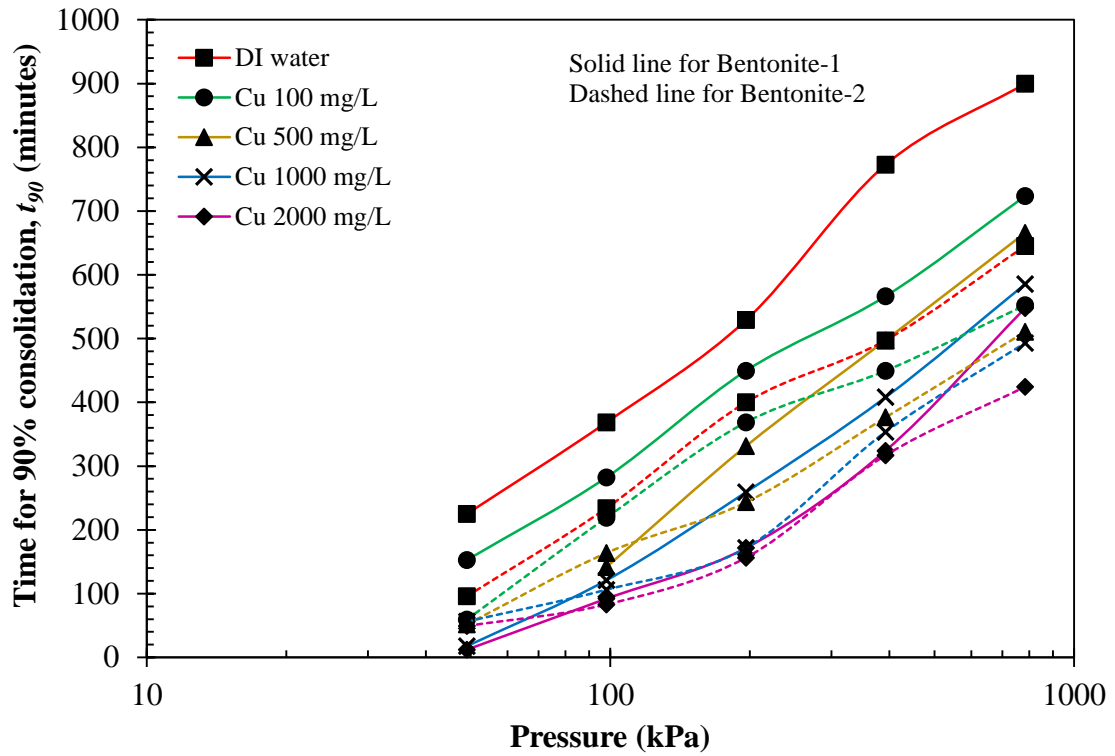


Fig. 4.19. Plot between the time for 90% of consolidation and consolidation pressures of Bentonite-1 and -2 in the presence of various concentrations of Cu^{2+}

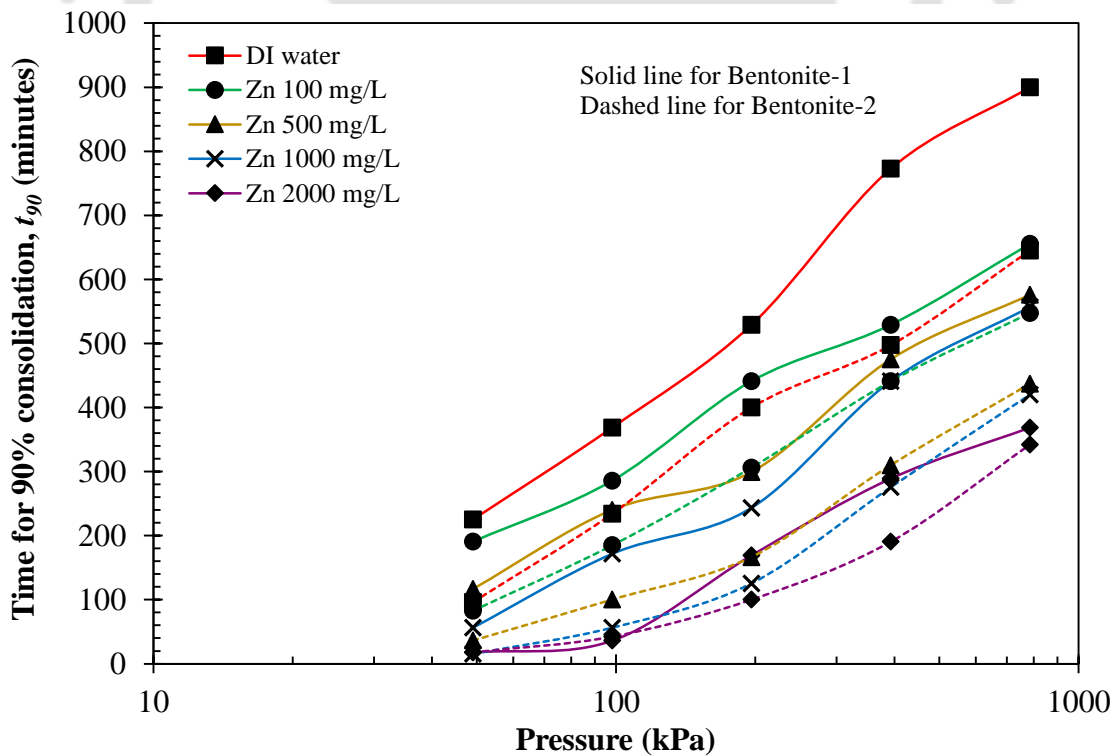


Fig. 4.20. Plot between the time for 90% of consolidation and consolidation pressures of Bentonite-1 and -2 in the presence of various concentrations of Zn^{2+}

4.2.10. Compression index (C_c)

The C_c , which indicates the compressibility nature of the soil, is used for settlement analysis of the soil sample. The impact of heavy-metal contaminants on the bentonites' compression index (C_c) is depicted in Table 4.6. The C_c of the bentonites was observed to decrease due to the infusion of heavy metals, although both bentonites displayed variations in behaviours. Bentonite-2 illustrated a decrease of C_c to 0.57, 0.60, 0.57 from 0.72 for Cu^{2+} , Pb^{2+} and Zn^{2+} concentrations from 0 to 2,000 mg/L, while a considerable abatement was observed for Bentonite-1 (from 0.79 to 0.63, 0.60, 0.60 with a similar increase in Cu^{2+} , Pb^{2+} and Zn^{2+} concentrations), respectively. With the rise in the Cu^{2+} , Pb^{2+} and Zn^{2+} concentration from 0 to 2000 mg/L, Bentonite-1 shows a 20.3, 24.1, 24.1% reduction in C_c values; whereas, for Bentonite-2 it declined by 20.8, 16.7, 20.8%. The more significant decrement in the C_c value for Bentonite-1 is attributed to a more considerate reduction in the DDL thickness with the increase in the heavy-metal concentration levels, thereby, resulting in the agglomeration of clay particles.

Table 4.6. Compression index of Bentonite-1 and -2 for various concentrations of Zn^{2+} , Cu^{2+} and Pb^{2+} solution

| Concentration (mg/L) | Compression Index (C_c) | | | | | |
|-------------------------|-----------------------------|------------------|------------------|------------------|------------------|------------------|
| | Bentonite-1 | | | Bentonite-2 | | |
| | Cu^{2+} | Pb^{2+} | Zn^{2+} | Cu^{2+} | Pb^{2+} | Zn^{2+} |
| 0 | 0.79 | 0.79 | 0.79 | 0.72 | 0.72 | 0.72 |
| 100 | 0.76 | 0.78 | 0.73 | 0.64 | 0.69 | 0.7 |
| 500 | 0.72 | 0.75 | 0.72 | 0.63 | 0.67 | 0.66 |
| 1000 | 0.69 | 0.70 | 0.62 | 0.60 | 0.66 | 0.62 |
| 2000 | 0.63 | 0.60 | 0.60 | 0.57 | 0.60 | 0.57 |

4.2.11. Unconfined compressive strength (UCS) of Bentonites

Fig. 4.21 shows the unconfined compressive strength (UCS) of Bentonite-1 and-2 in the presence of DI water and heavy metals (Cu^{2+} , Pb^{2+} , Zn^{2+}). It can be depicted that with the rise concentration level (0 to 1000 mg/L) of heavy metals, the strength of both the bentonites decreases. With a further rise in concentration level from 1000 to 2000 mg/L, the strength of both the bentonite marginally increased.

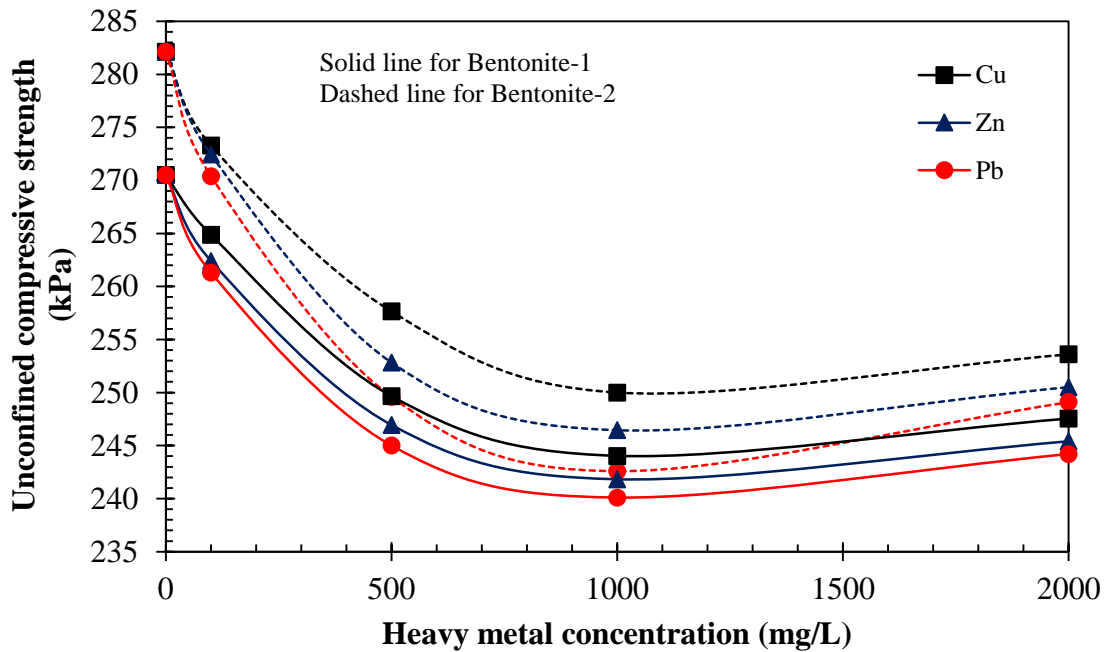


Fig. 4.21. Unconfined compressive strength (UCS) of Bentonite-1 and-2 in the presence of DI water and heavy metals

In the present study, all the samples, irrespective of permeating heavy metal types, are compacted corresponds to OMC and MDD obtained for DI water. The OMC value of bentonites mixed with heavy metal lies in the wetter side of the optimum. Therefore, soil sample permeated with heavy metal (compacted with OMC and MDD of water) exhibits lower OMC and higher MDD value (Shariatmadari et al., 2011). Thus even though the MDD value increases, the ultimate strength decreases as the water content shifted towards the wetter side. However, it can be observed that in the presence of 2000 mg/L of heavy metal solutions (Cu^{2+} , Pb^{2+} , Zn^{2+}) the UCS value marginally increased. The reason may be at higher concentration agglomeration of clay particles occurs, which results of a close interaction between the grains and consequently the effect of an increase in MDD is more than that of reduction in OMC value.

Samples prepared with Bentonite-2, when compacted at OMC – MDD of water, displayed a reduction in strength value of 10.1, 11.7 and 11.2% with the rise in concentration from 0 to 2000 mg/L of Cu^{2+} , Pb^{2+} and Zn^{2+} solution, respectively. Similarly, for Bentonite-1, the samples displayed 8.5, 9.7 and 9.3% with reduction with the increase in the concentration from 0 to 2000 mg/L of solution (Table 4.7), respectively.

Higher-strength for Bentonite-2 is observed as a result of a close interaction between the grains, which eventually leads to the lowering of liquid limit and DDL thickness values.

Table 4.7 Unconfined compression test of bentonite in presence of heavy metals

| Concentration (mg/L) | Unconfined compression test (kPa) | | | | | |
|-------------------------|-----------------------------------|------------------|------------------|------------------|------------------|------------------|
| | Bentonite-1 | | | Bentonite-2 | | |
| | Cu ²⁺ | Pb ²⁺ | Zn ²⁺ | Cu ²⁺ | Pb ²⁺ | Zn ²⁺ |
| 0 (DI water) | 270.5 | 270.5 | 270.5 | 282.1 | 282.1 | 282.1 |
| 100 | 264.9 | 261.3 | 262.4 | 273.3 | 270.4 | 272.4 |
| 500 | 249.6 | 245.0 | 246.9 | 257.6 | 249.6 | 252.9 |
| 1000 | 244.0 | 240.1 | 241.8 | 250.0 | 242.6 | 246.5 |
| 2000 | 247.5 | 244.2 | 245.4 | 253.6 | 249.1 | 250.5 |

The Fig 4.22 to 4.27 represents the stress-strain relationship of Bentonite-1 and -2 in the presence of DI water and heavy metals (Cu²⁺, Pb²⁺ and Zn²⁺). It can be depicted that, in the presence of DI water, the failure occurs at 6.32 and 5.53% of strain level for Bentonite-1 and -2, respectively. However, in the presence of 2000 mg/L of Cu²⁺, Pb²⁺ and Zn²⁺, the failure was detected at 5.2, 4.5, and 4.7% of strain level for Bentonite-1. Similarly, for Bentonite-2, the failure strain rate was found to be 5, 5 and 4.21%, respectively.

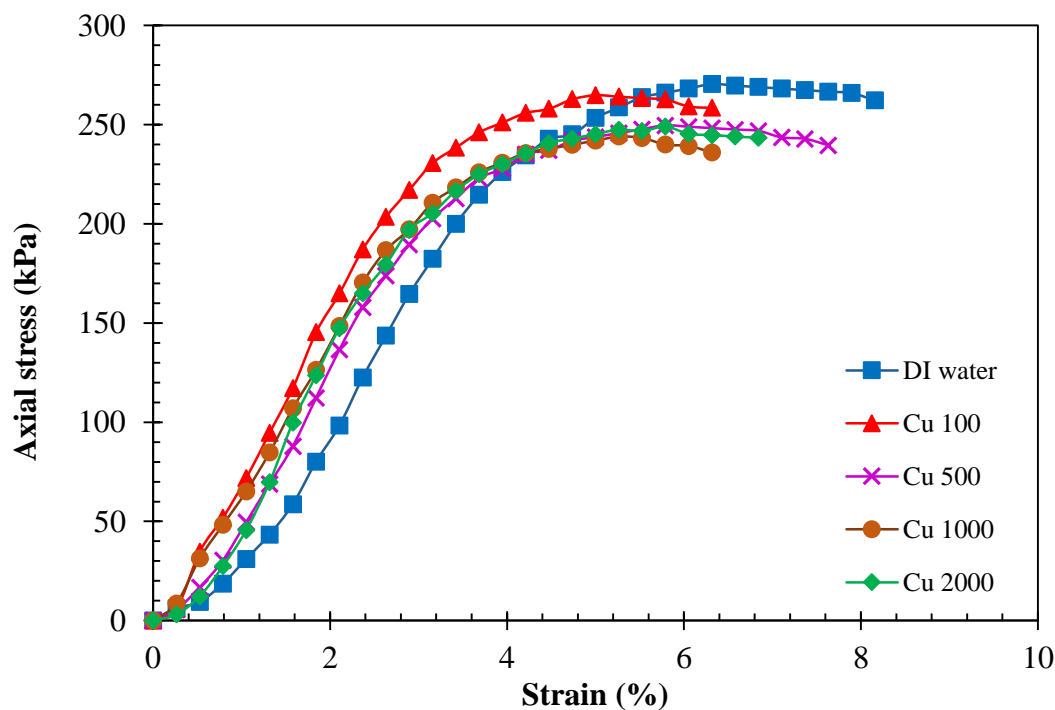


Fig. 4.22. Axial stress (kPa) vs. strain (%) relationship of the Bentonite-1 in the presence of various concentrations of Cu²⁺

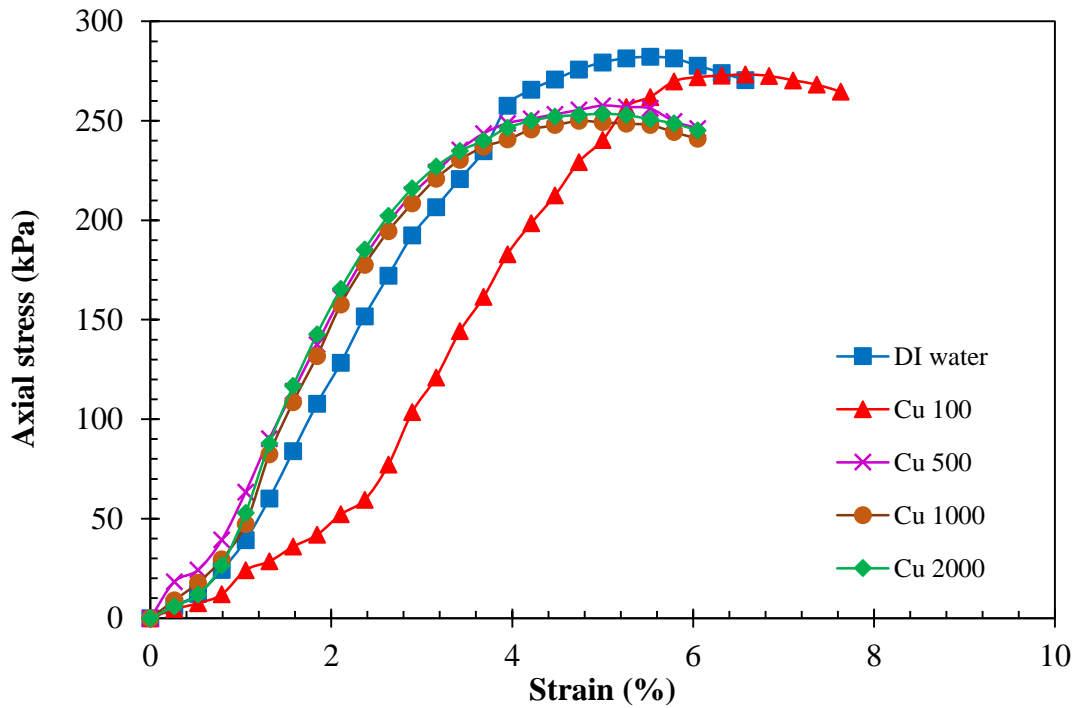


Fig. 4.23. Axial stress (kPa) vs. strain (%) relationship of the Bentonite-2 in the presence of various concentrations of Cu^{2+}

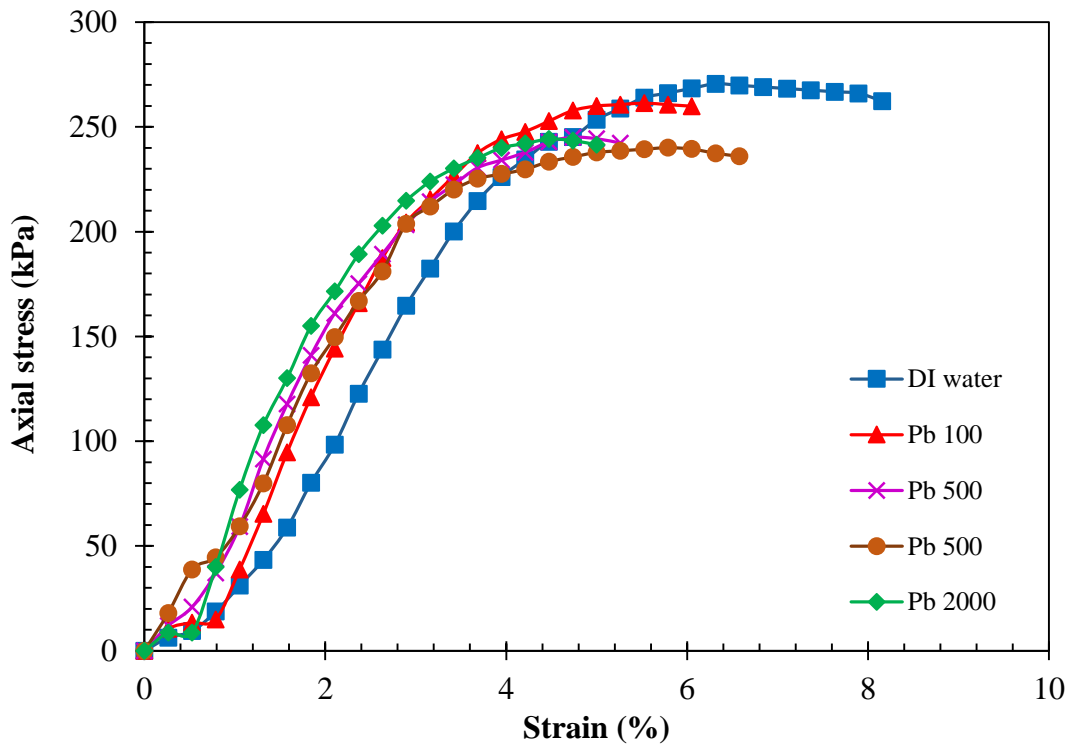


Fig. 4.24. Axial stress (kPa) vs. strain (%) relationship of the Bentonite-2 in the presence of various concentrations of Pb^{2+}

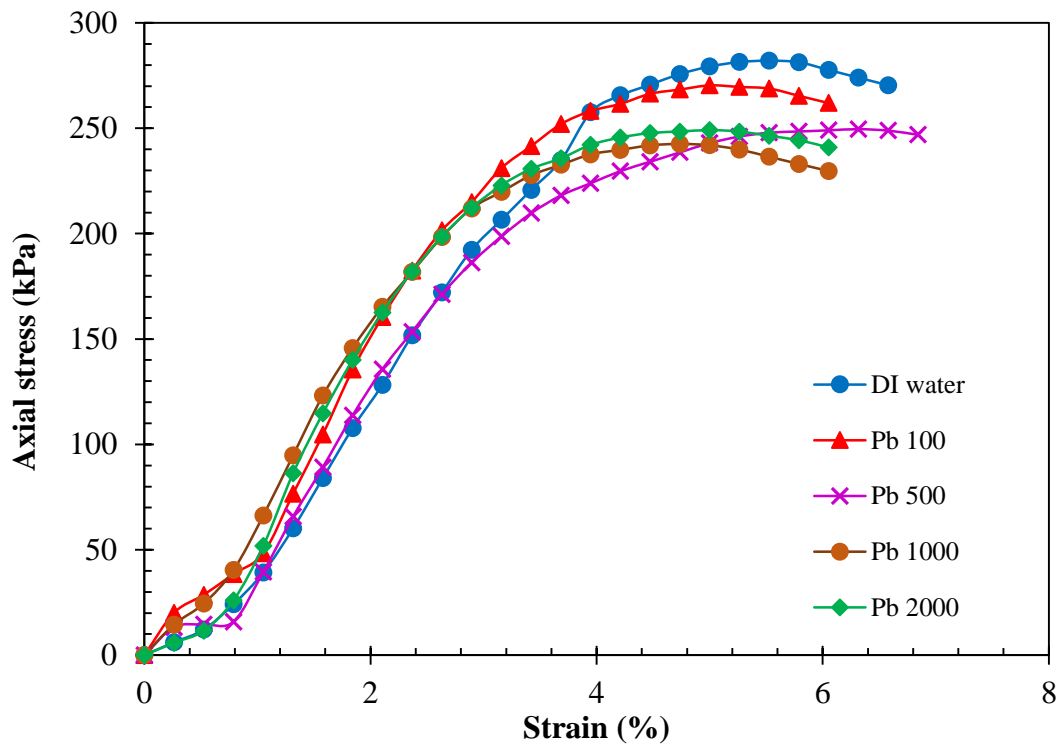


Fig. 4.25. Axial stress (kPa) vs. strain (%) relationship of the Bentonite-2 in the presence of various concentrations of Pb²⁺

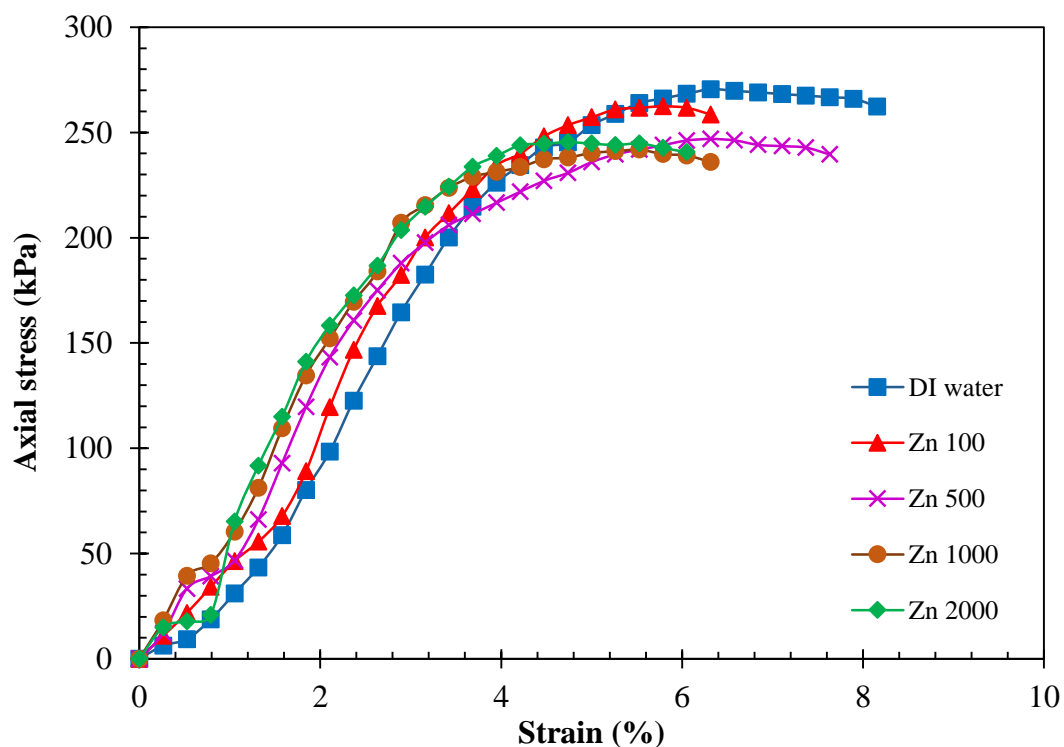


Fig. 4.26. Axial stress (kPa) vs. strain (%) relationship of the Bentonite-1 in the presence of various concentrations of Zn²⁺

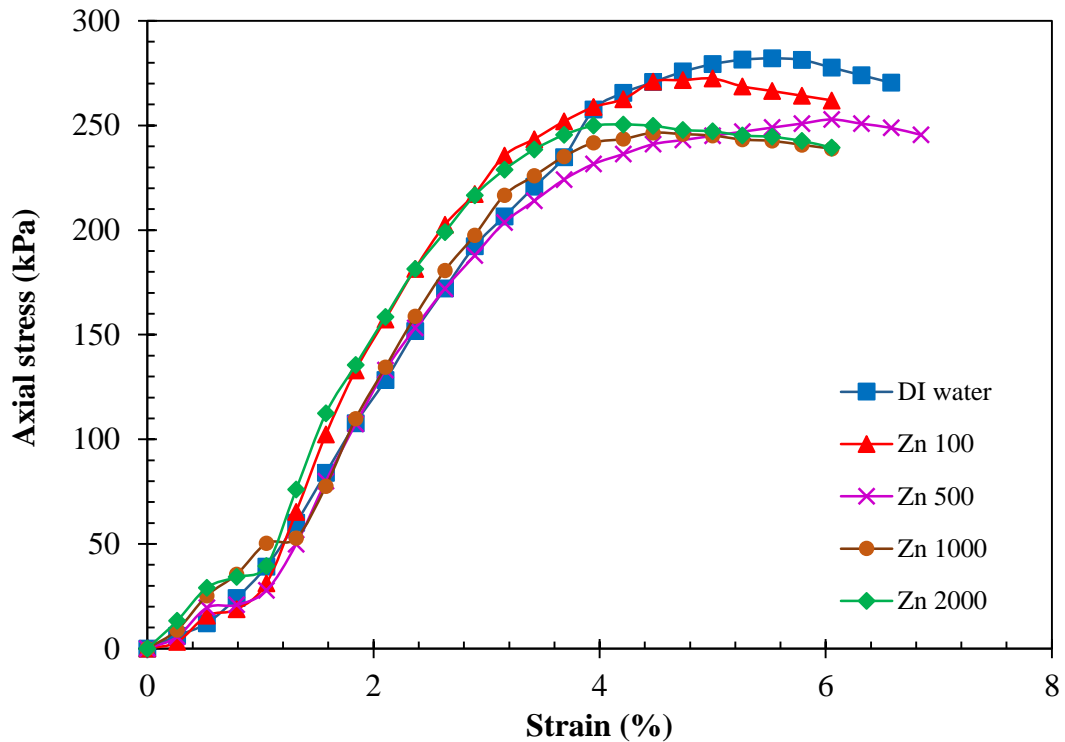


Fig. 4.27. Axial stress (kPa) vs. strain (%) relationship of the Bentonite-2 in the presence of various concentrations of Zn^{2+}

4.2.12. pH study

The plot in Fig. 4.28 to 4.30 shows the relationship between the removal percentage of heavy metal and the pH of the solution for two different bentonites. It was observed from plots that the pH of the solution, considerably affects the removal percentage of heavy metal. Fig. show that with the rise in pH of the solution, the percentage removal of metal increased.

It can be observed that the removal of Pb^{2+} was abruptly increased beyond 95% for Bentonite-1 and Bentonite-2 when the pH of the solution was 6 (Fig. 4.28). With the increase in pH from 5 to 6, the removal percentage of Pb^{2+} was increased from 90.5% to 97.3% for Bentonite-1. For Bentonite-2, the removal percentage was found to be increased from 88.2% to 96.3%, respectively. Similarly, Fig. 4.29 depicts that the removal of Cu^{2+} was abruptly increased beyond 92 and 90.2% for Bentonite-1 and -2, respectively at pH 6. Likewise, a plateau was observed at a pH ranges from 4 to 6, and a slight difference in percentage removal of Zn^{2+} was noted among this range (Fig. 4.30) Then at pH 8, the percentage removal of zinc by both the bentonites rapidly increased to 95.38 and 98.80 %.

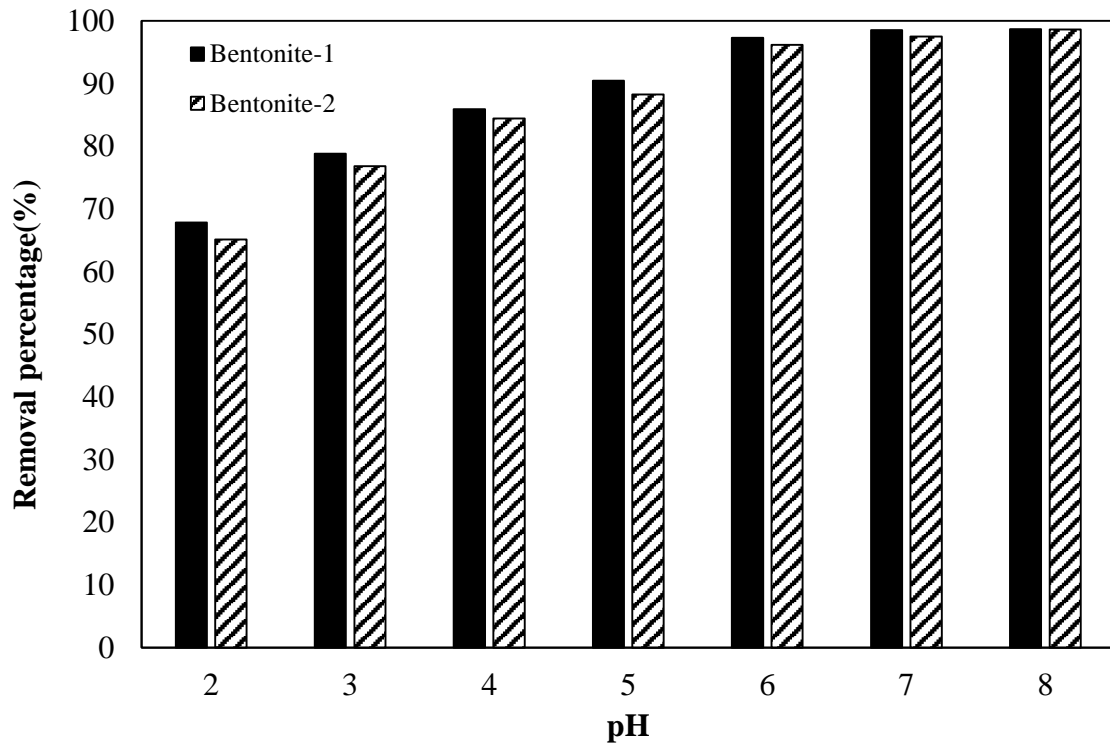


Fig. 4.28. Effect of pH on Pb²⁺ sorption on bentonites

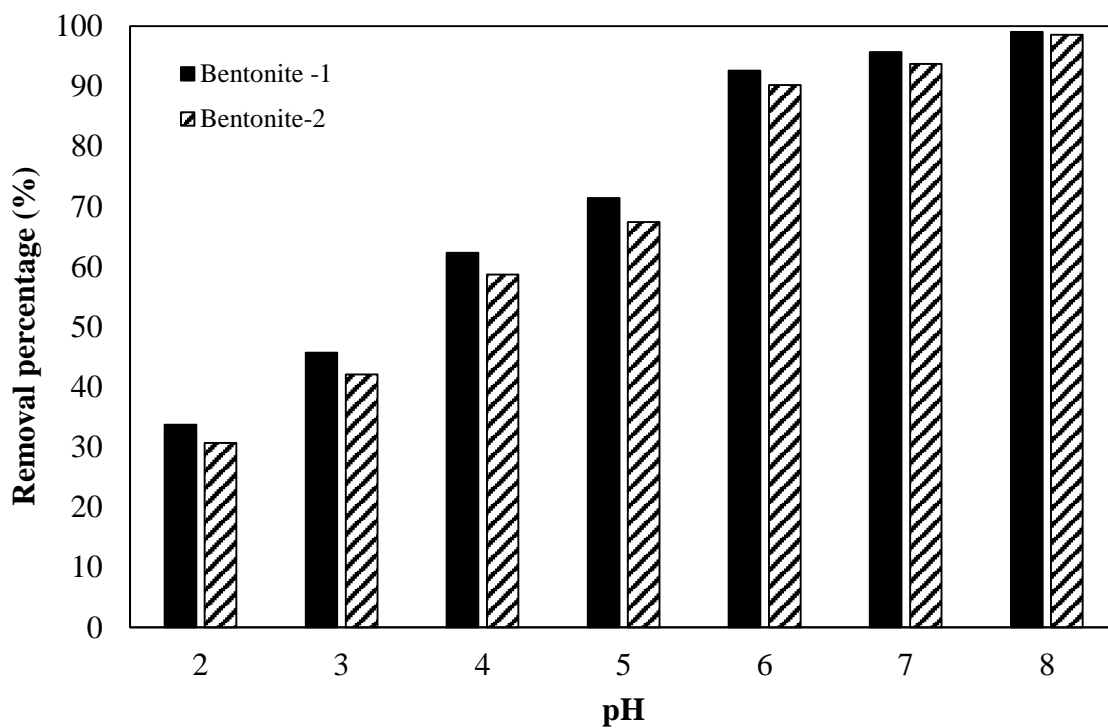


Fig. 4.29. Effect of pH on Cu²⁺ sorption on bentonites

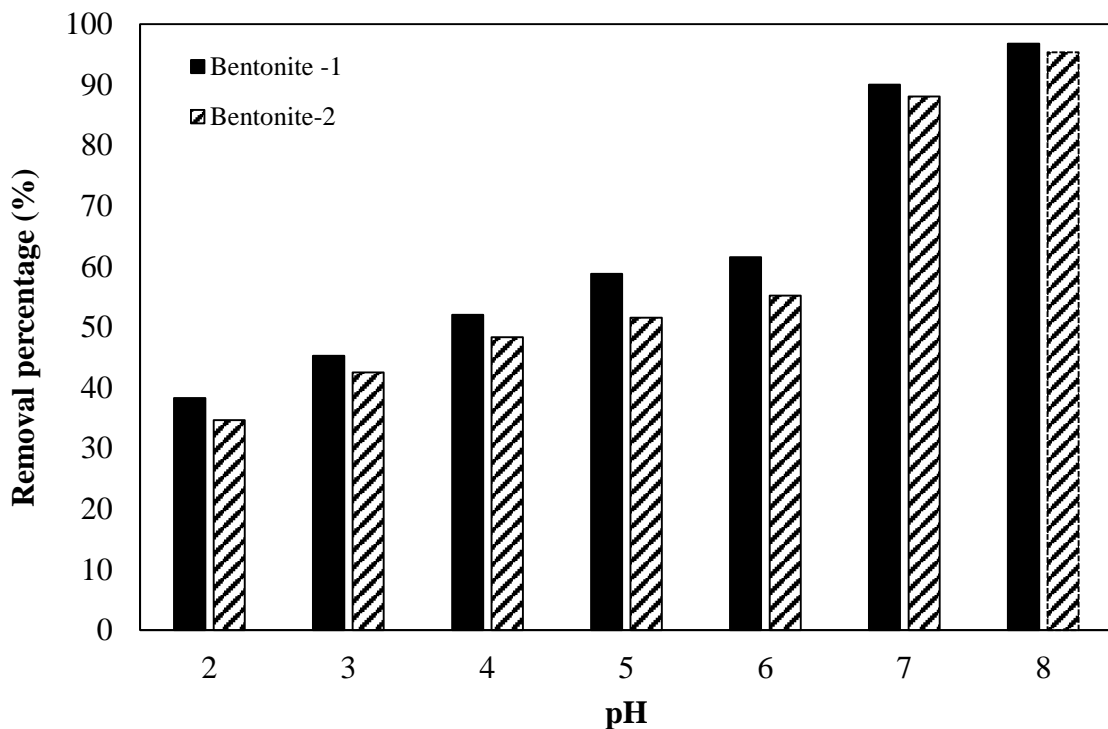


Fig. 4.30. Effect of pH on Zn^{2+} sorption on bentonites

Different mechanisms, such as dissolution, ion exchange, and precipitation, influence the adsorption of bentonite at various pH. From Figs. 4.28 to 4.30, it can be observed that at pH 2, the percentage removal of heavy metals was lowest, which can be attributed to the acidic nature of the solution. Hence, for the same adsorption site, the competition of excess H^+ ions and metal ions increased, which consequently suppressed the heavy metal adsorption. Due to acidity, the excess H^+ cations bind on the surface of bentonite, causing a decrease in the attraction between metal ions and the negatively charged bentonite surface. Therefore, the removal percentage was lower at the beginning (Hefne et al., 2008). With the gradual rise in pH of the solution, the concentration of H^+ ions reduced. This triggered the higher electrostatic attraction of metal ions to the negatively charged surface of the clay. Therefore, from pH 3, the removal percentage of heavy metals increased. From pH value, 3-5, the basic mechanism that is ion exchange and adsorption govern the adsorption properties of bentonite. At pH 4 and 5, H^+ cations were reduced, and the higher negatively charged surface became accessible for metal adsorption. Furthermore, due to the increase in pH, the OH^- increased, which increased the net negative charge on the clay surface, resulting in a further increase in the adsorption. Thus, silica present in the clay mineral attracted the positively charged metal ion by columbic forces and, therefore,

adsorption and ion exchange of the metals was favoured and removal percentage increased. Beyond pH 5, this negative charge density on the surface of bentonite decreased, resulting in the lower adsorption of metal ions (Inglezakis et al., 2007). A sharp increase in removal percentage was observed due to the formation of metal hydroxyl complexes which precipitate on the bentonite structure. Various researchers observed a similar kind of trend (Kerisit et al., 2016; Maramis et al., 2012; Pawar et al., 2016; Saha et al., 2003).

Bentonite -1 showed a higher removal rate as compared to Bentonite - 2 due to its high CEC and high SSA. The study indicates that for all metals the sorption was observed at pH ranges from 4 – 6. Therefore, to avoid precipitation, pH 5 was carefully chosen for further studies as an ideal condition. The pH study indicates that in the adsorption process pH of the solution is an essential parameter.

4.2.13. Batch adsorption study

Fig. 4.31 to 4.33 shows the relationship between the amount of heavy metals (Pb^{2+} , Cu^{2+} , Zn^{2+}) adsorbed (q_e) on both bentonites for different initial concentrations (C_i) ranging from 100 to 2,000 ppm. The plots indicate that with the rise in heavy metal concentration, the adsorption capacity of the bentonites increased. A very marginal difference in adsorption capacity was observed up to 750 mg/L of initial concentration for both the bentonites. However, with the rise in concentration beyond 750 mg/L, the adsorption capacity increased significantly. The reason can be attributed to the fact that at a lower concentration, a considerable number of sorption sites are available on the surface of bentonites. With an increase in concentration, these sorption sites are filled up. A higher amount of adsorption was observed in Bentonite-1 as compared to Bentonite-2. The maximum adsorption capacity of Pb^{2+} , Cu^{2+} and Zn^{2+} at pH 5 for Bentonite-1 was found to be 34.41, 22.80 and 15.32 mg/g for 2000 mg/L of initial concentration; however, for Bentonite-2 it was 32.20, 20.40 and 13.82 mg/g, respectively. Variation in the physical and chemical characteristics of the adsorbents such as cations associated with the exchangeable sites, swelling capacity, specific surface area (SSA), and montmorillonite content causes the difference in their sorption capacity (Deka and Sekharan, 2017; Vimonses et al., 2009). The study indicated a higher removal of Pb^{2+} , followed by Cu^{2+} and Zn^{2+} for both the bentonite. The adsorbent's affinity concerning the metal ions is considerably affected by properties of ions such as the ionic radius, hydrated ionic radius, and electronegativity.

Table 4.8 depicts the fundamental ionic properties of Pb^{2+} , Cu^{2+} and Zn^{2+} , indicating a higher ionic radius and electronegativity for Pb^{2+} , compared to Cu^{2+} and Zn^{2+} . Furthermore, a smaller hydrated ionic radius also means that the adsorbing capacity of the ions is more. This is primarily due to the ease of passage of the smaller ions having smaller hydrated ionic radius into the inner pores of the adsorbent surface. Thus, all the governing factors resulted in a more significant number of ions adsorbed on the adsorbents pertaining to Pb^{2+} , compared to Cu^{2+} and Zn^{2+} (Baylan and Meriçboyu, 2016; Milojković et al., 2014).

Table 4.8. Metal ion characteristic parameters.

| Metal ions | Electronegativity | Ionic radius (Å°) | Hydrated radius (Å°) |
|------------------|-------------------|-----------------------------------|--------------------------------------|
| Pb^{2+} | 2.33 | 1.12 | 4.01 |
| Cu^{2+} | 1.9 | 0.73 | 4.19 |
| Zn^{2+} | 1.65 | 0.74 | 4.30 |

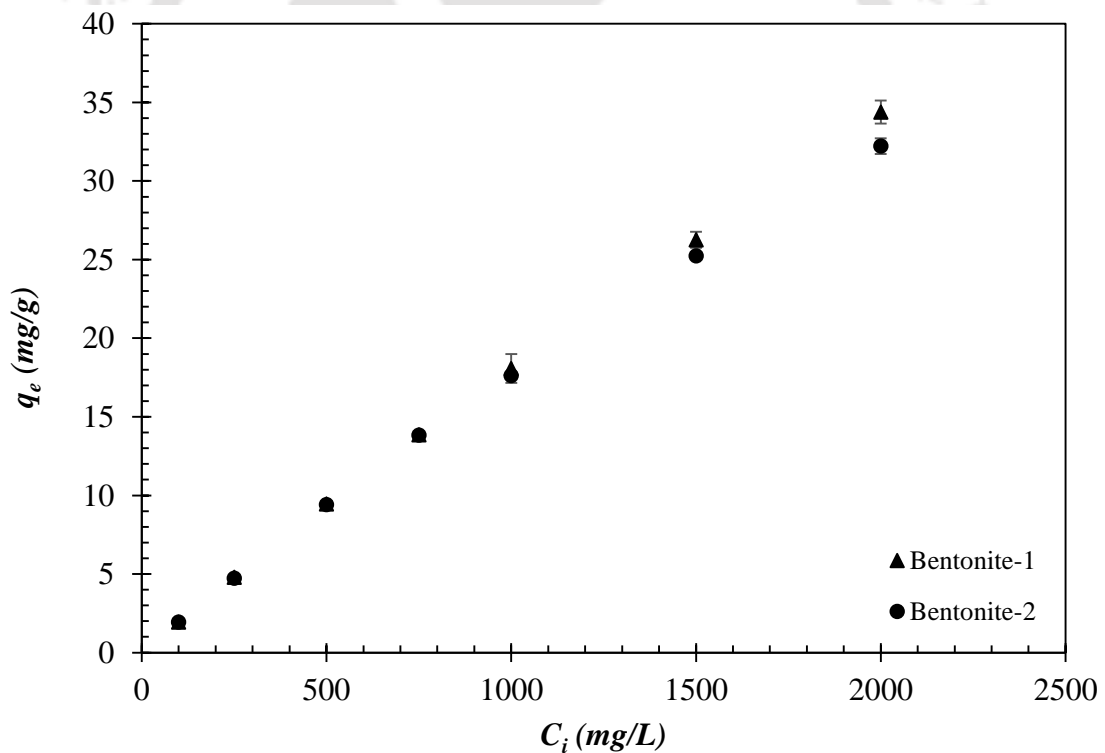


Fig. 4.31. Effect of initial concentration of Pb^{2+} on bentonites

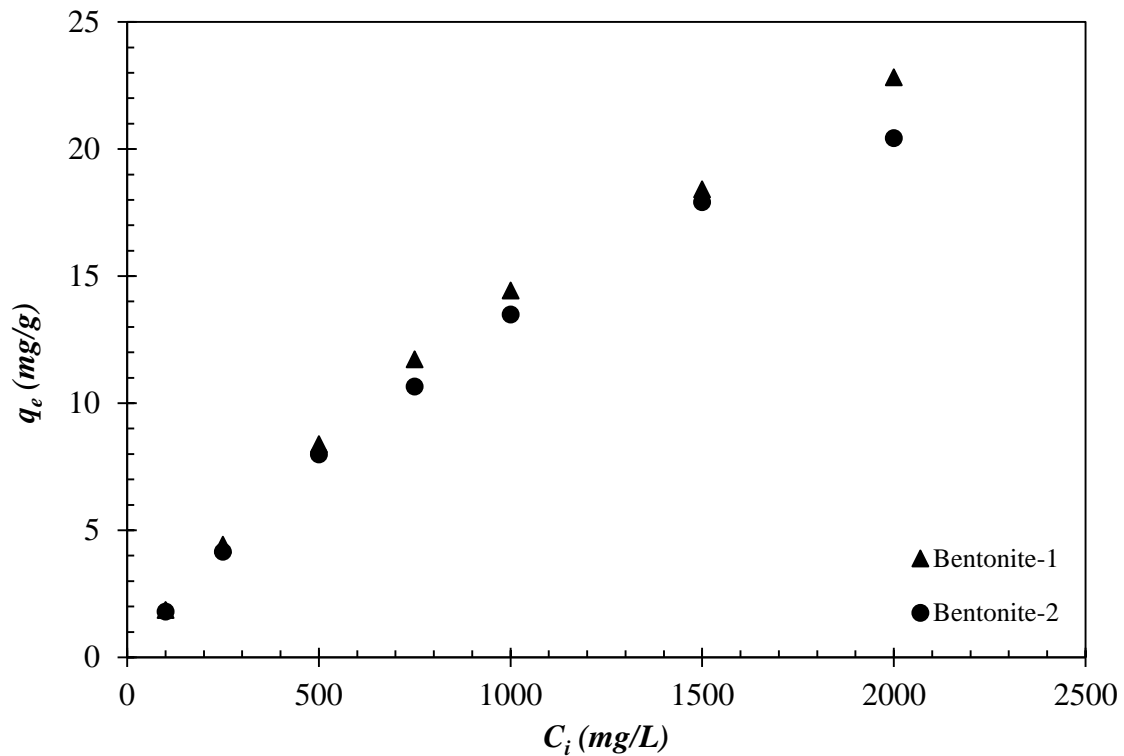


Fig. 4.32. Effect of initial concentration of Cu^{2+} on bentonites

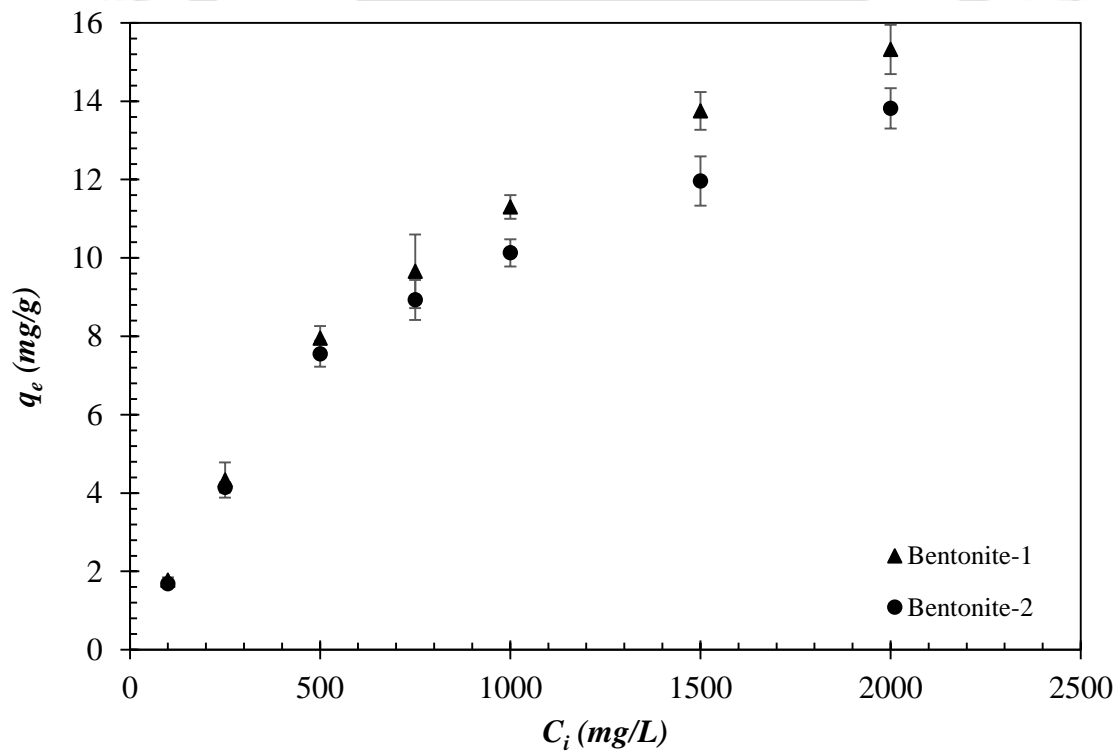


Fig. 4.33. Effect of initial concentration of Zn^{2+} on bentonites

The higher sorption capacity of bentonite clay can be clarified by important attributes of smectite mineral of montmorillonite. Montmorillonite is majorly present in bentonite, which is a clay substantial of the aluminium phyllosilicate. The significance swelling

tendency of the montmorillonite was due to its ability to adsorb water molecules between its unit layers. Montmorillonite also adsorbs various metal ions on its surface as a result of the existence of negative charge. Adsorption occurs because of the exchange of cations, and it happens by the formation of Si–O and Al–O groups on the external surfaces. Since the amount of layer charges is higher in the internal surfaces than the edge charges on the external surfaces, the cation exchange is generally found differentiated in the inward surfaces and the adsorption in outward surfaces (Baylan and Meriçboyu, 2016; Galindo et al., 2013).

In the inside surfaces, the crystal form of montmorillonite includes one octahedral and two tetrahedral layers. The central tetravalent silicon (Si^{4+}) can be reconstituted by trivalent aluminium particles (Al^{3+}) in the tetrahedral layers, and the trivalent aluminium particles (Al^{3+}) can be reconstituted by divalent cations (typically Mg^{2+} and Fe^{2+}) in the octahedral layers. Along these lines, the layers end up being negatively charged. The negatively charged layers are consistently adjusted by the hydrated cations within the surfaces. The cations being bonded by electrostatic forces for these inside surfaces can be supplanted by other cations. When the cation size resembles the pore sizes in the structure of montmorillonite, cations can be strengthened into the crystal lattice section, which eventually leads to the reduction of the negatively charged layer (Baylan and Meriçboyu, 2016). Sheta et al. (2003) investigated the sorption properties of natural zeolite and bentonite in the presence of zinc and iron and concluded that metal uptake was strongly dependent on the mineralogical properties of the soil and type of metals.

The plot in Figs. 4.34 to 4.36 depicts the removal percentage versus the initial concentration of Pb^{2+} , Cu^{2+} and Zn^{2+} . With the rise in initial metal concentration, the removal percentage declined. Primarily, at a lower concentration of heavy metals, an enormous amount of sorption sites was present on both the bentonite surfaces. With the rise in initial metal concentration, these sorption sites get occupied. Thus, the removal percentage of heavy metals declined at higher initial concentrations. The removal percentage of Pb^{2+} obtained for Bentonite-1 was 97.5% at 100 mg/L of initial concentration; however, the removal percentage was found to be 85.9% at 2000 mg/L. For Bentonite-2, the removal percentage was obtained 97.3% and 80.6% for 100 and 2000 mg/L of initial Pb^{2+} concentration, respectively. Likewise, for Cu^{2+} , it was 93.4 and 57.1 % by Bentonite-1 and 89.9 and 51.1 % by Bentonite-2 at 100 and 2000 mg/L of the initial metal concentration. Similarly, for Zn^{2+} , the removal percentage achieved was 88.8 and 38.3% for Bentonite-1 and 86.3 and 34.5 % for Bentonite-2, respectively.

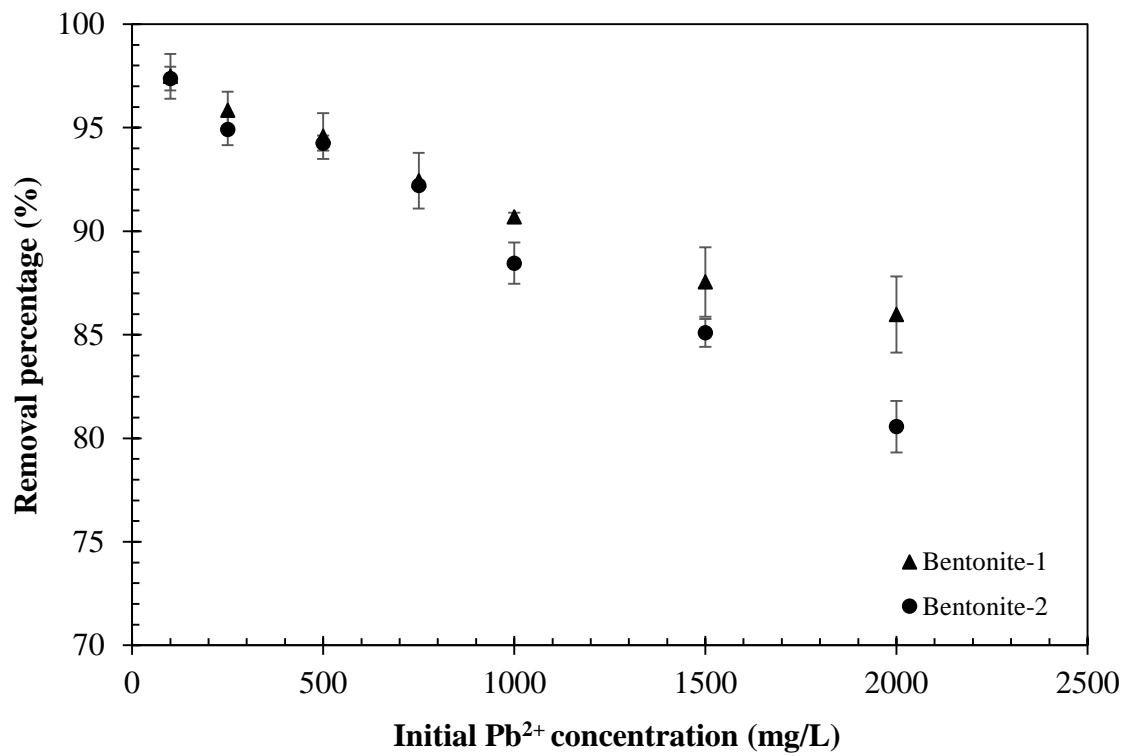


Fig. 4.34. Percentage removal of the Pb²⁺ at various initial concentrations

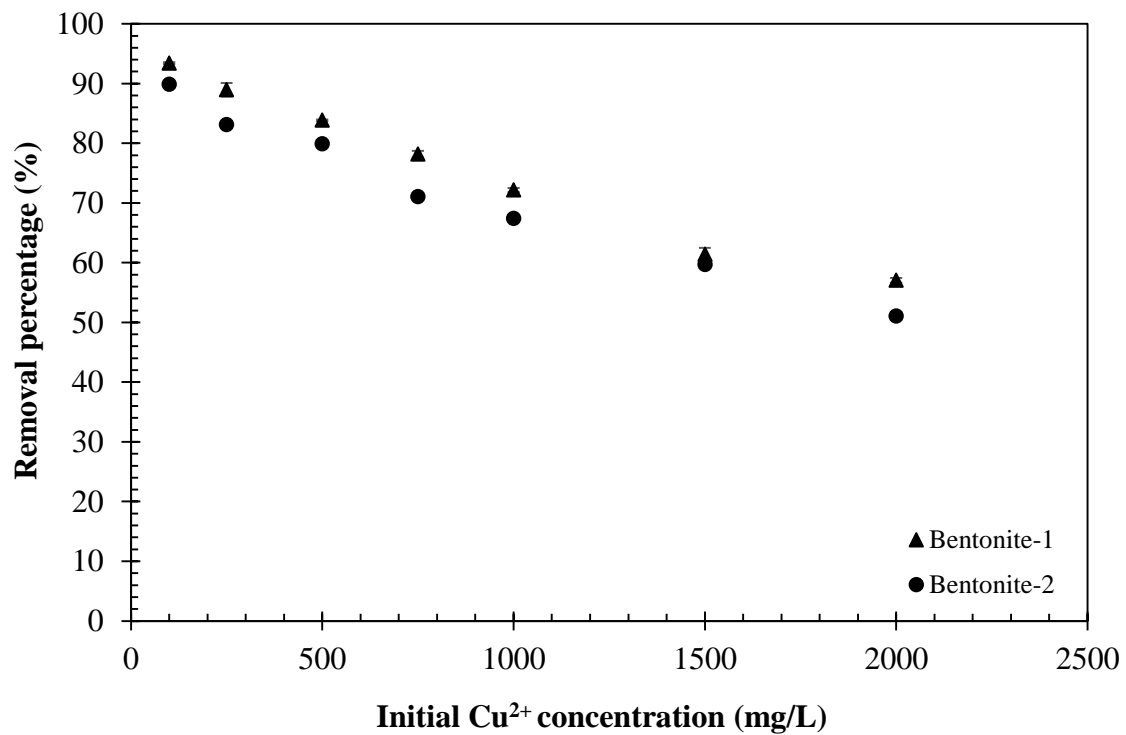


Fig. 4.35. Percentage removal of the Cu²⁺ at various initial concentrations

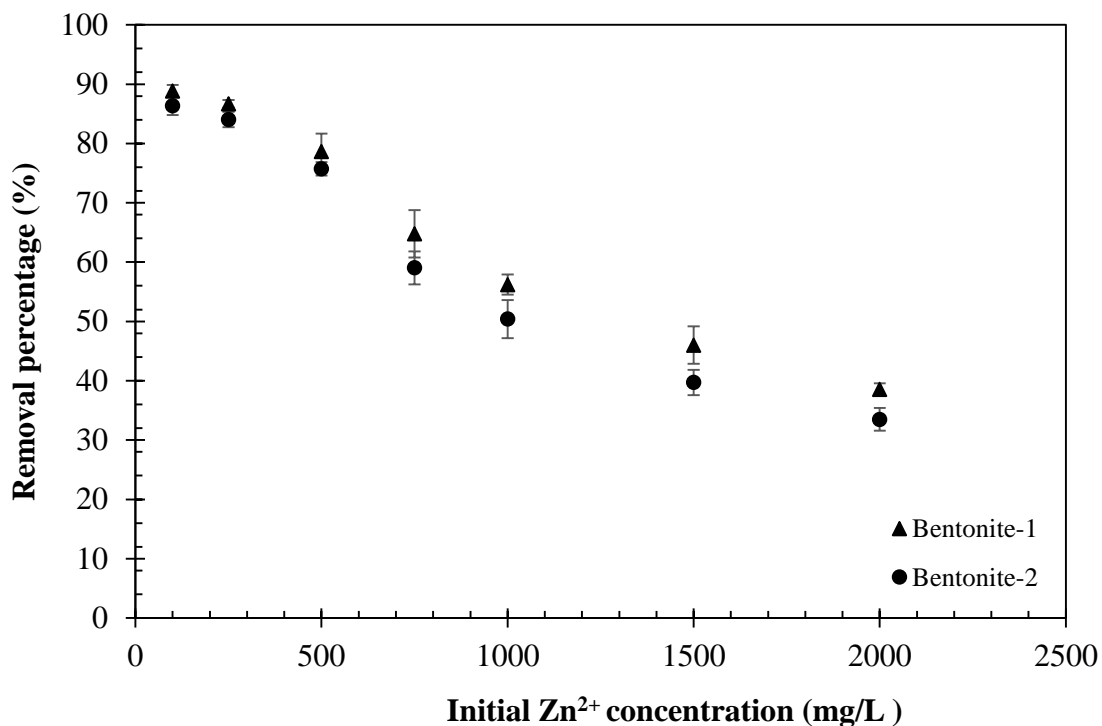


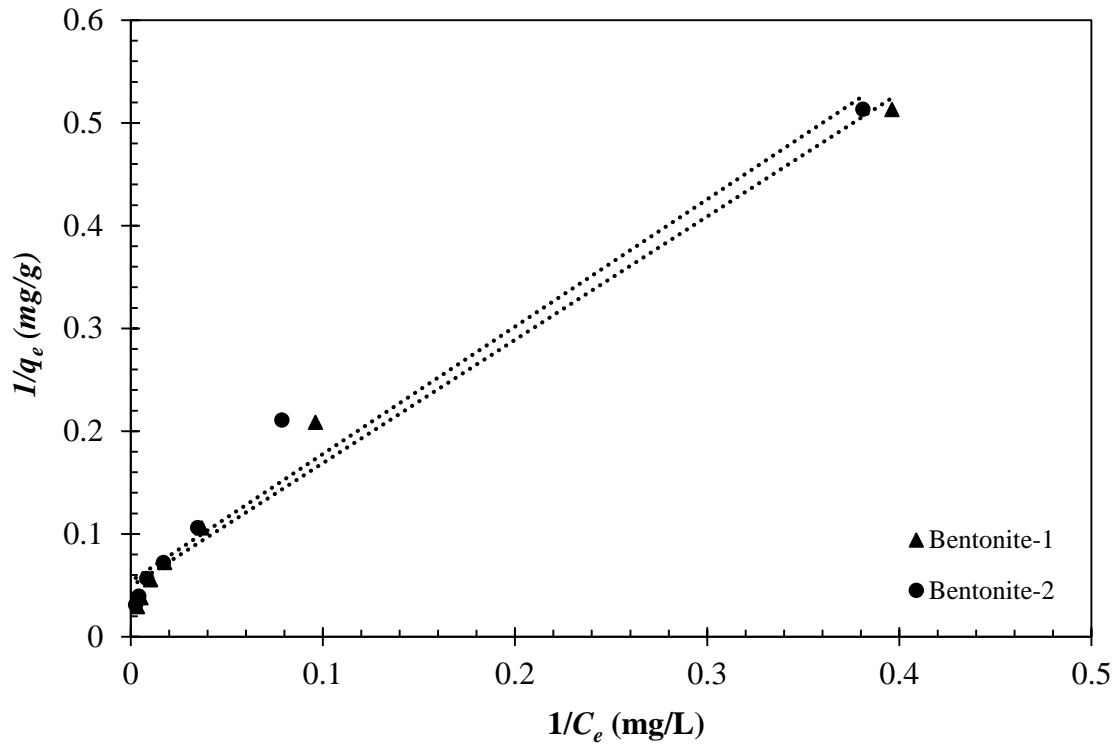
Fig. 4.36. Removal percentage of the Zn²⁺ at different initial concentrations

4.2.14. Isotherm study

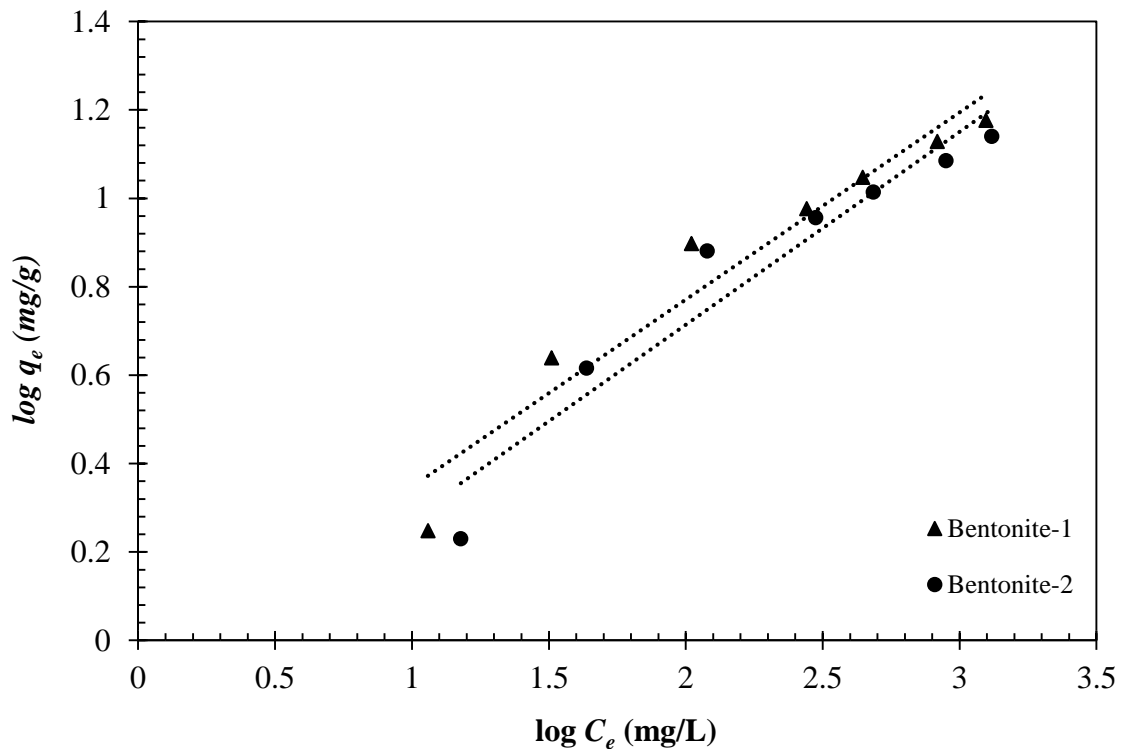
For understanding the nature of the adsorbent surface, the experimental data obtained from the batch study has been fitted by different adsorption isotherm models. Fig. 4.37 to 4.39 illustrates the data fitted to the linear form of Langmuir and Freundlich isotherm equations for both the bentonites. The computed values of the adsorption coefficients obtained from isotherm models are listed in Table 4.9. Table 4.9 shows that experimental data follows both the isotherm model.

R_L values were found to be 0.01, 0.03, 0.22 for Bentonite-1 and 0.01, 0.02, 0.21 for Bentonite-2 signifying the process of sorption is highly acceptable at higher initial Pb²⁺, Cu²⁺, Zn²⁺ concentration. The value of $1/n < 1$ indicates a favourable nature of the sorption of heavy metals on bentonites (Mall et al., 2006).

To find the best appropriate isotherm model, the regression coefficients (R^2) obtained from both the models were compared. The data in Table 4.9 indicated that for Pb²⁺ and Cu²⁺, the R^2 value of Freundlich isotherm is slightly greater than Langmuir Isotherm model for both the bentonites ($R^2 = 0.99$), which describes that, the adsorption data fitted well with the Freundlich isotherm.

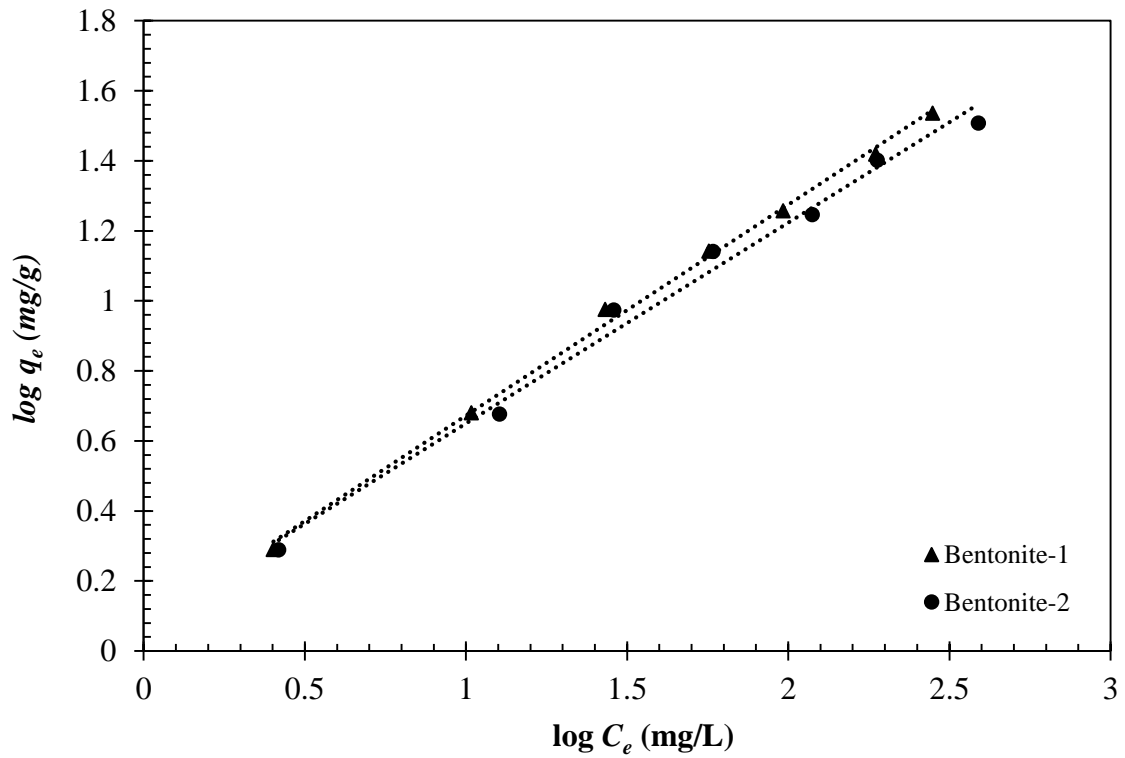


(a) Langmuir isotherm

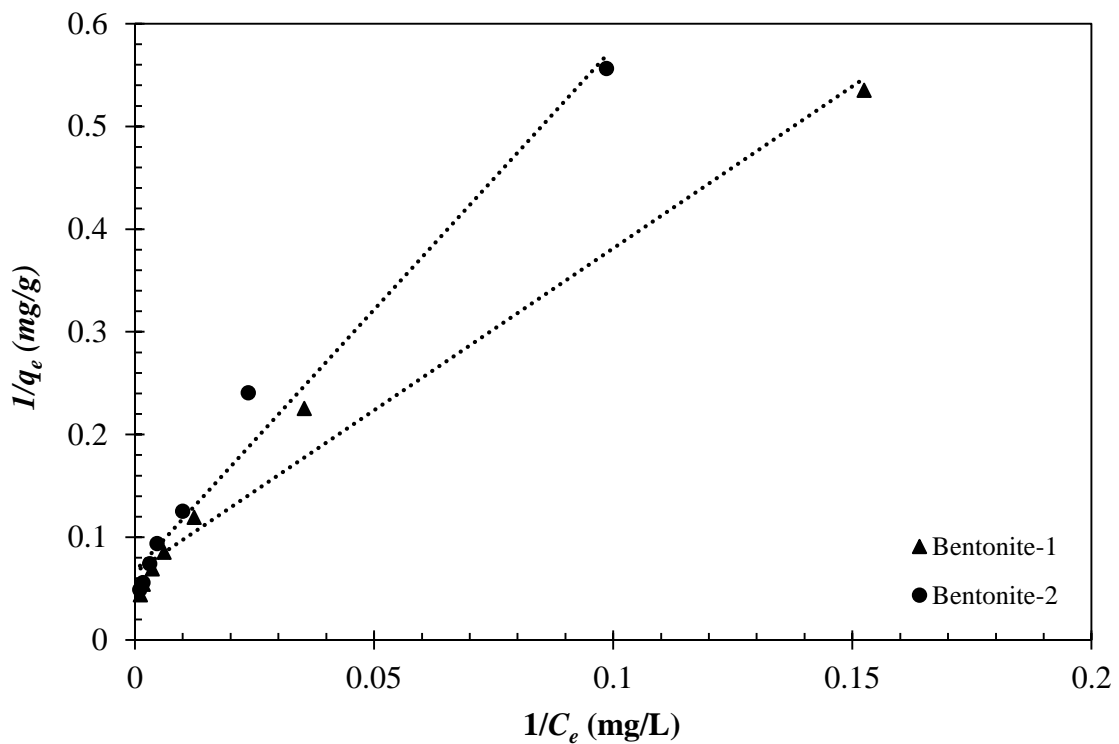


(b) Freundlich isotherm

Fig. 4.37. Linearized Langmuir and Freundlich isotherms for Pb^{2+} removal by bentonites

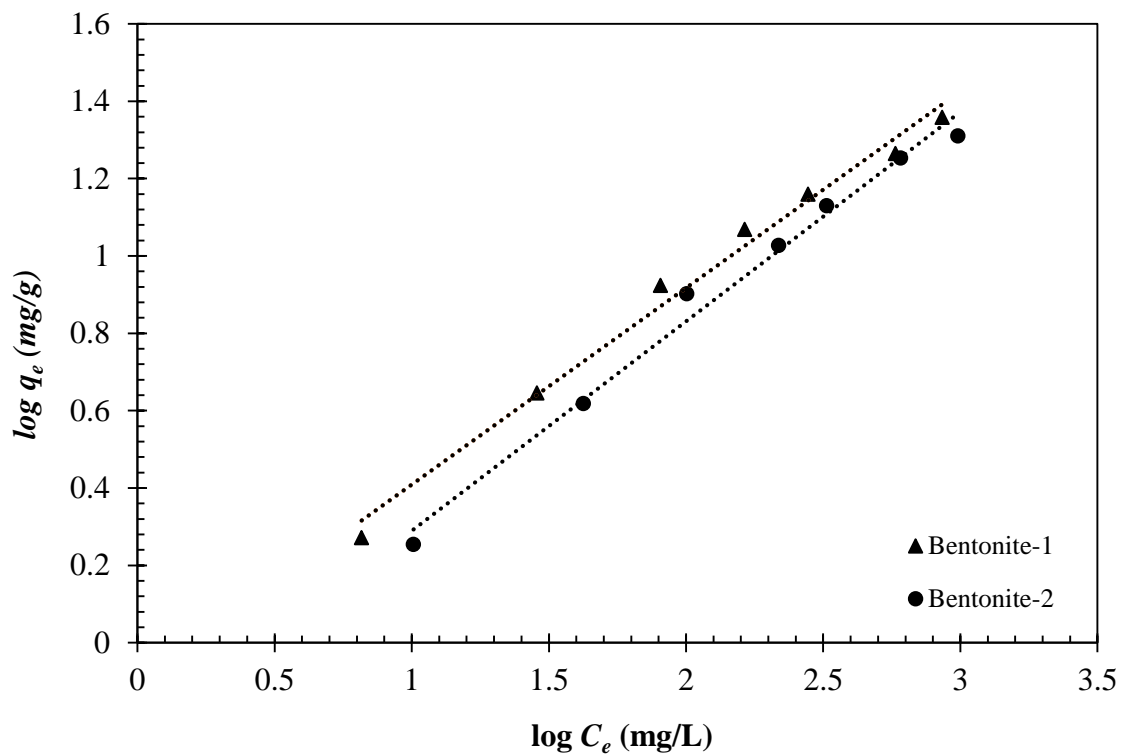


(a) Freundlich isotherm

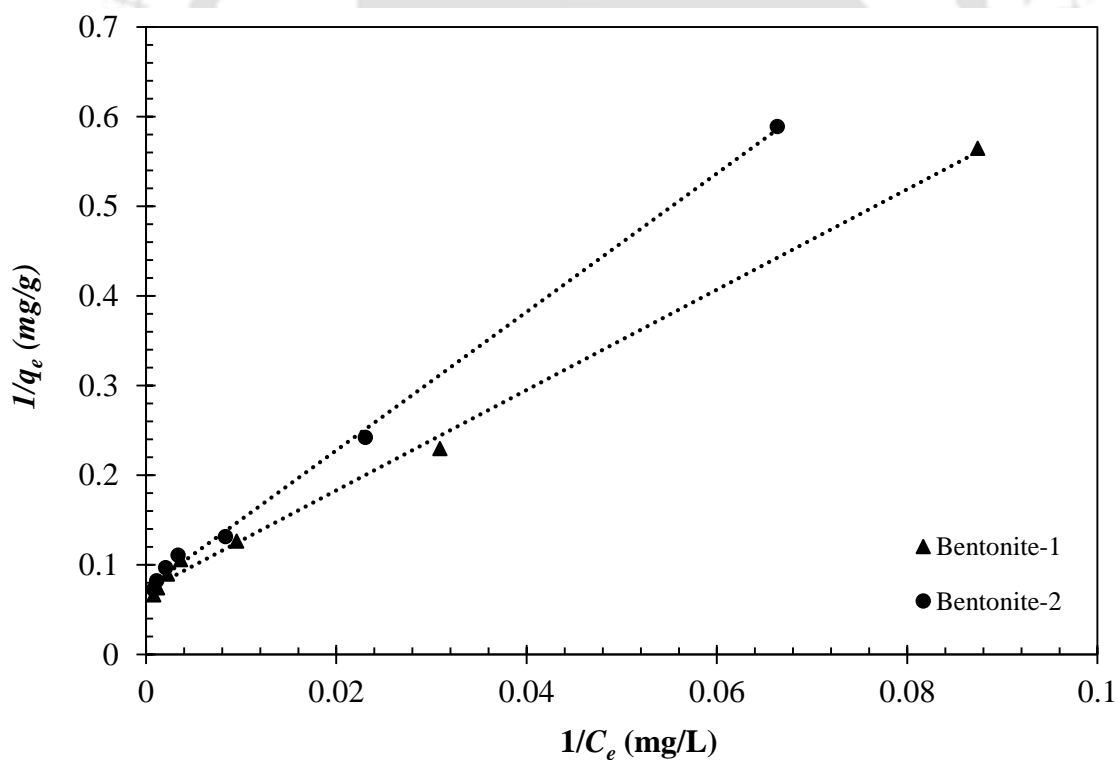


(b) Langmuir isotherm

Fig. 4.38. Linearized isotherm models for Cu²⁺ removal by bentonites



(a) Freundlich isotherm



(b) Langmuir isotherm

Fig. 4.39. Linearized isotherm models for Zn^{2+} removal by bentonites

Table 4.9. The sorption isotherms parameters for different models for Pb^{2+} , Cu^{2+} and Zn^{2+}

| Isotherm model | Parameters | Pb^{2+} | | Cu^{2+} | | Zn^{2+} | |
|---------------------|------------------|-----------|-------|-----------|-------|-----------|-------|
| | | BE-1 | BE-2 | BE-1 | BE-2 | BE-1 | BE-2 |
| Langmuir Isotherm | q_{max} (mg/g) | 20.44 | 18.55 | 15.17 | 14.94 | 14.06 | 13.64 |
| | b (L/mg) | 0.04 | 0.04 | 0.02 | 0.01 | 0.02 | 0.02 |
| | R^2 | 0.98 | 0.97 | 0.98 | 0.97 | 0.99 | 0.99 |
| | R_L | 0.01 | 0.01 | 0.03 | 0.02 | 0.22 | 0.21 |
| Freundlich Isotherm | k_f | 1.66 | 1.74 | 0.91 | 0.78 | 0.92 | 0.85 |
| | $1/n$ | 0.93 | 0.90 | 0.51 | 0.54 | 0.42 | 0.44 |
| | R^2 | 0.99 | 0.99 | 0.99 | 0.99 | 0.93 | 0.92 |

BE-1 and BE-2 indicate Bentonite 1 and 2, respectively

Hence, it specifies that sorption of Pb^{2+} and Cu^{2+} takes place in multilayer on the surface of the adsorbent and indicates infinite surface coverage. However, for Zn^{2+} , it can be observed from Table 3 that the R^2 value of the Freundlich isotherm model is lower than the Langmuir isotherm model ($R^2 = 0.99$), which indicates that the sorption data are fitted efficiently with the Langmuir isotherm. Therefore, it shows that sorption of Zn^{2+} occurs in a monolayer on the surface of the bentonite and specifies infinite surface coverage. Ayari et al. (2007) reported that for favourable sorption process $0 < R^2 < 1$; while $R^2 > 1$ indicates unfavourable adsorption, and $R^2 = 1$ signifies linear adsorption.

4.2.15. Dose study

A dose study was conducted at different bentonite dosages ranging from 0.2 to 5.0 g in 100 mL of heavy metal solution at a concentration of 100mg/L (Pb^{2+}) and 500 mg/L (Cu^{2+} and Zn^{2+}) for the contact period of 3 h at room temperature (28 ± 1 °C) maintaining an agitation speed of 150 rpm. The plot in Fig. 4.40-4.42 indicates that with the rise in the adsorbent dose, the removal rate (%) increased promptly. With the increase in bentonite dose, there was an increase in the availability of adsorption site on the bentonite surface. As the bentonite dosage increased, Fig. 4.40 demonstrated a gradual rise in Pb^{2+} removal from 50.4 to 98.0% and 28.7 to 97.3%, for Bentonite-1 and -2. Likewise, Fig. 4.41 shows that for 5 g of bentonite dose, the removal rates (%) of Cu^{2+} were 84.8 and 75.5. Similarly, the removal of Zn^{2+} raised from 25.2 to 78.9% and 24.4 to 75.8 % for Bentonite-1 and -2, respectively, with the gradual increase in bentonite dose Fig. 4.42.

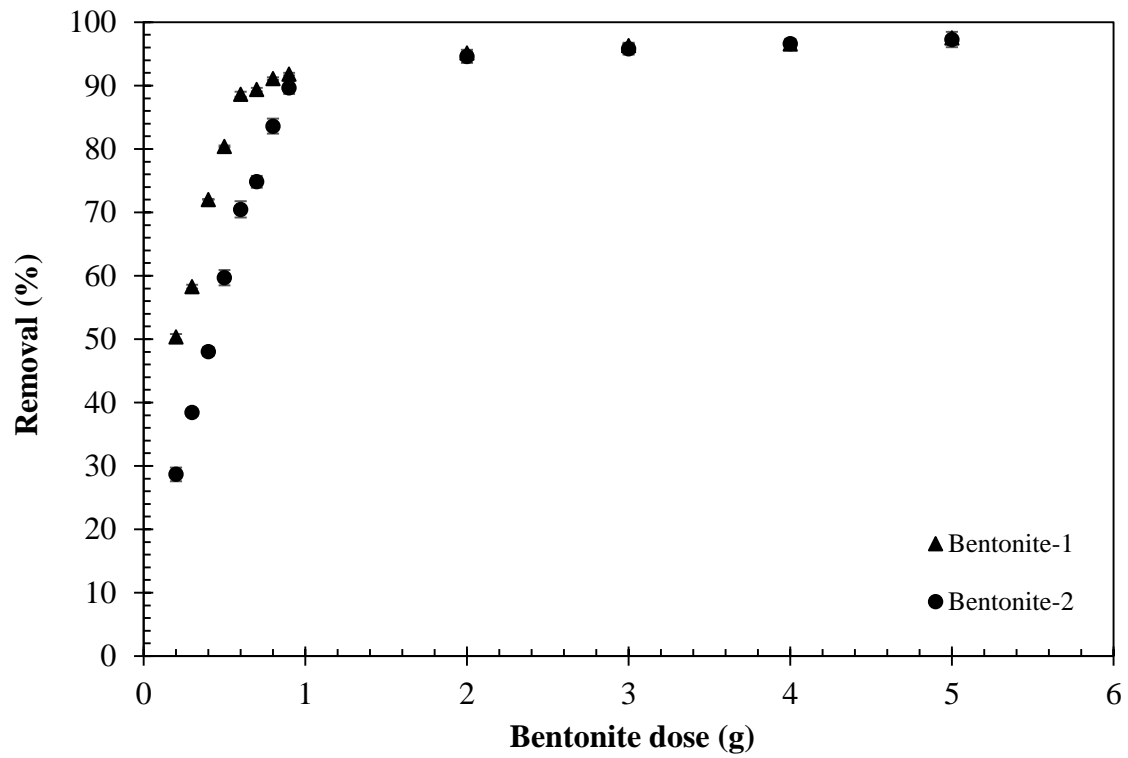


Fig. 4.40. Removal percentage of the Pb²⁺ at different bentonite dosage

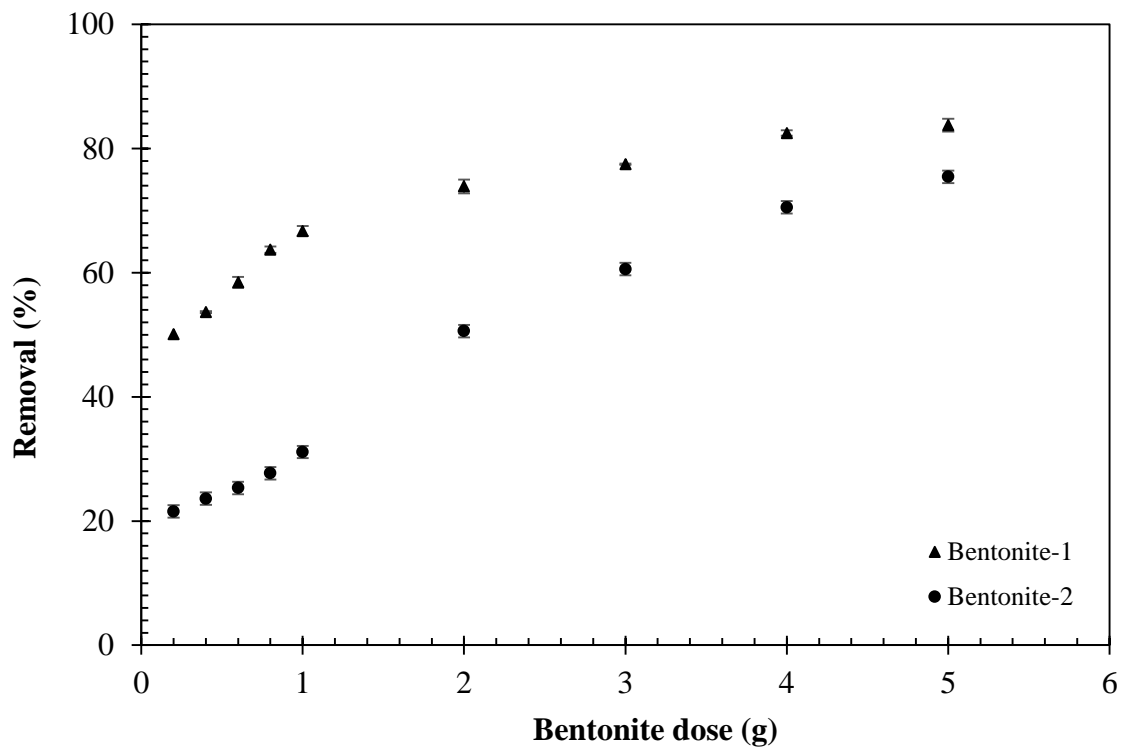


Fig. 4.41. Removal percentage of the Cu²⁺ at different bentonite dosage

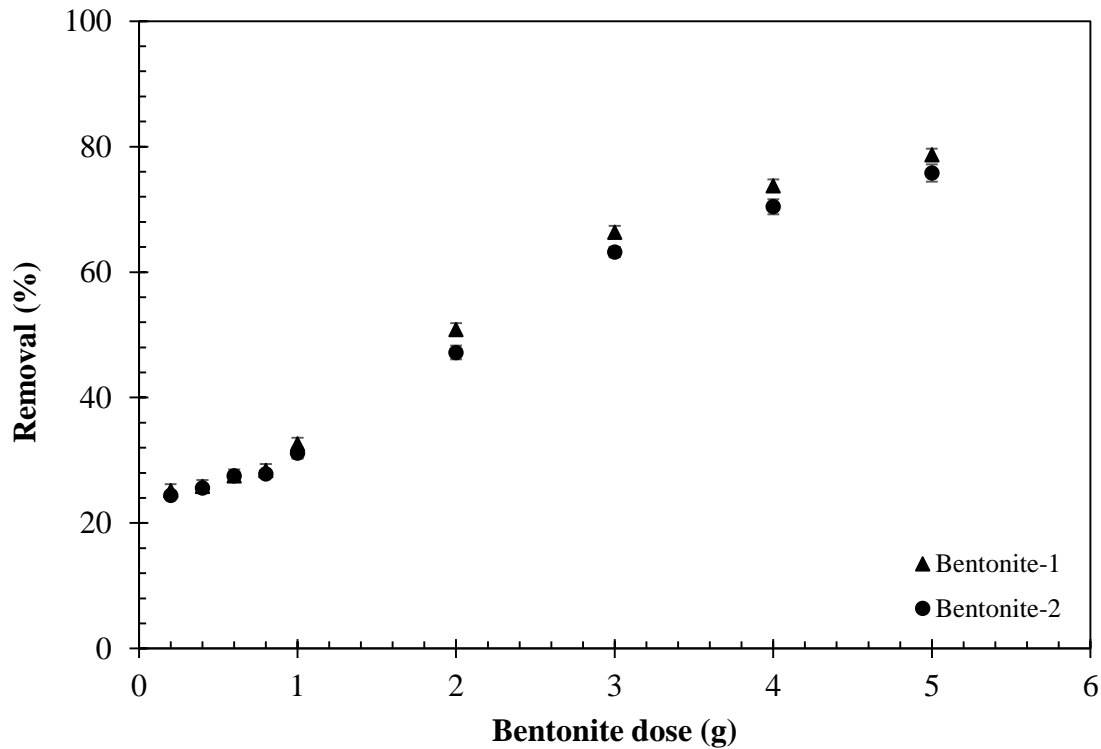


Fig. 4.42. Removal percentage of the Zn^{2+} at different bentonite dosage

However, Figs. 4.43 to 4.45 shows that the adsorption capacity of heavy metals on the bentonite decreased with the increase in bentonite dosage. With the rise in the bentonite dose, overcrowding of clay particles occurred, which led to the decrease in effective surface area; consequently, the metal ions found it hard to interact with the clay particles. Therefore, the possibility of the interaction of metal ions with clay particles gets reduced, and the sorption capacity of the bentonites decreased (Hefne et al., 2008).

The removal rate of Bentonite-1 was higher as compared to Bentonite-2 because of its high CEC montmorillonite content, SSA and swelling capacity. Vengris et al. (2001) observed a similar kind of trend on a modified clay sorbent for the adsorption of various metal ions.

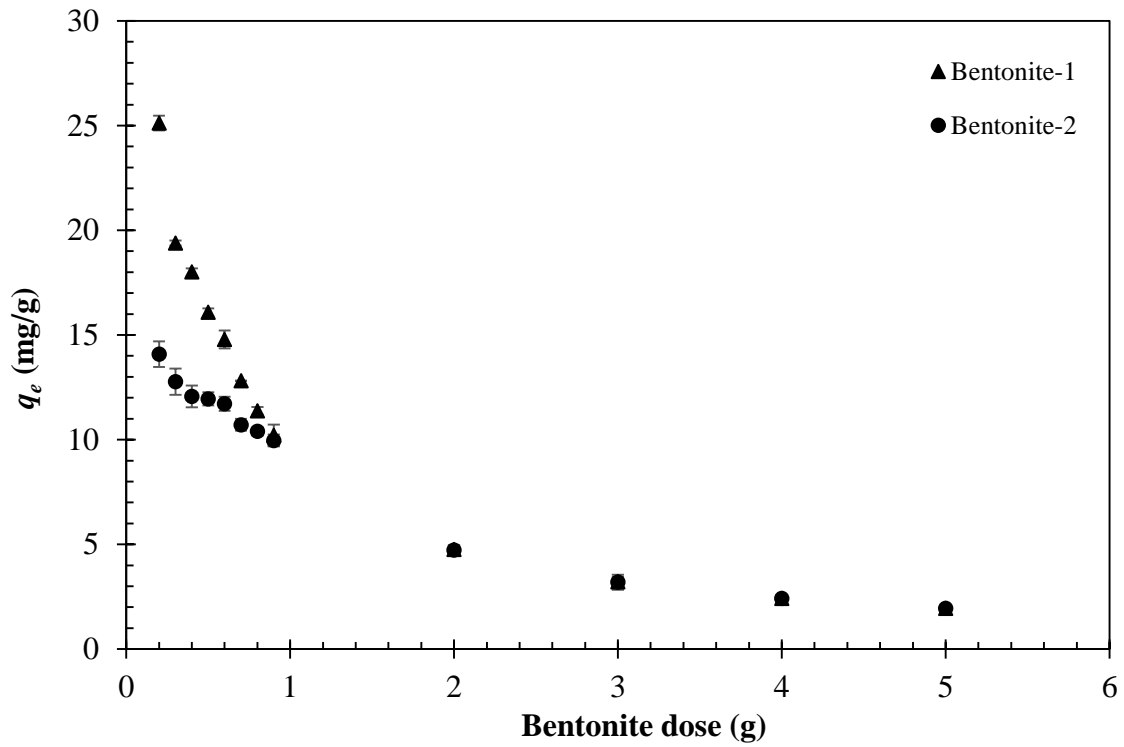


Fig. 4.43. Quantity of Pb²⁺ adsorbed at various bentonite dose

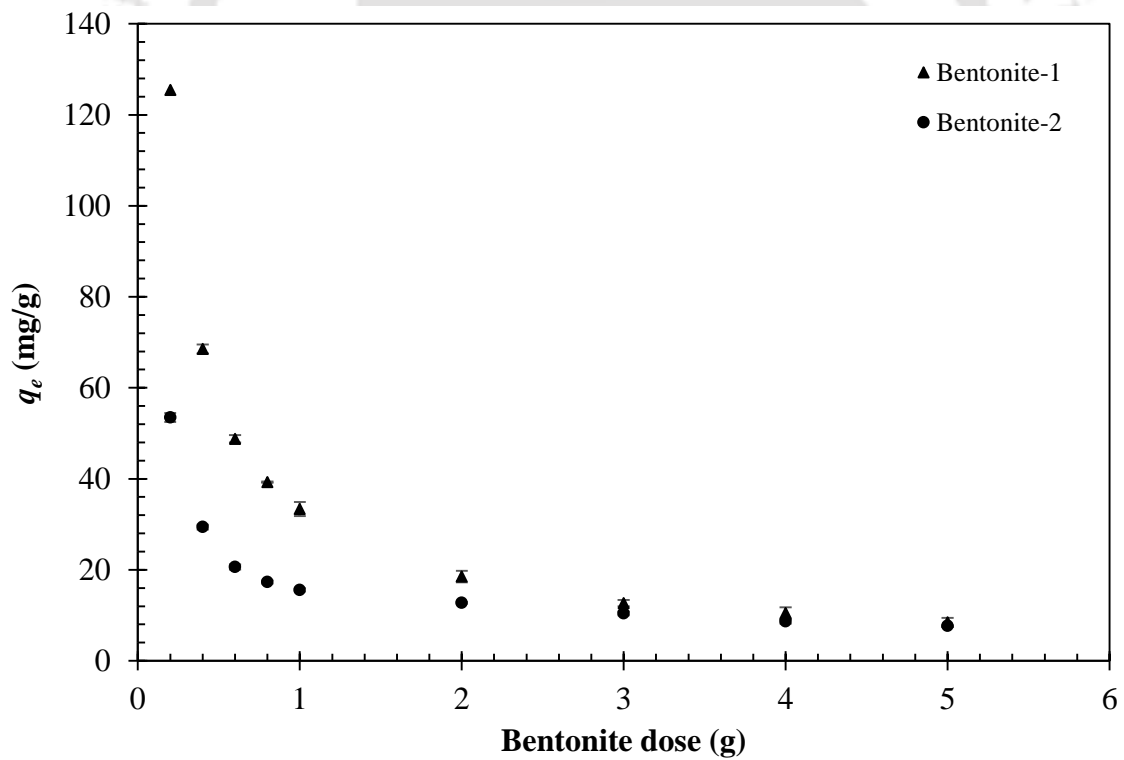


Fig. 4.44. Quantity of Cu²⁺ adsorbed at various bentonite dose

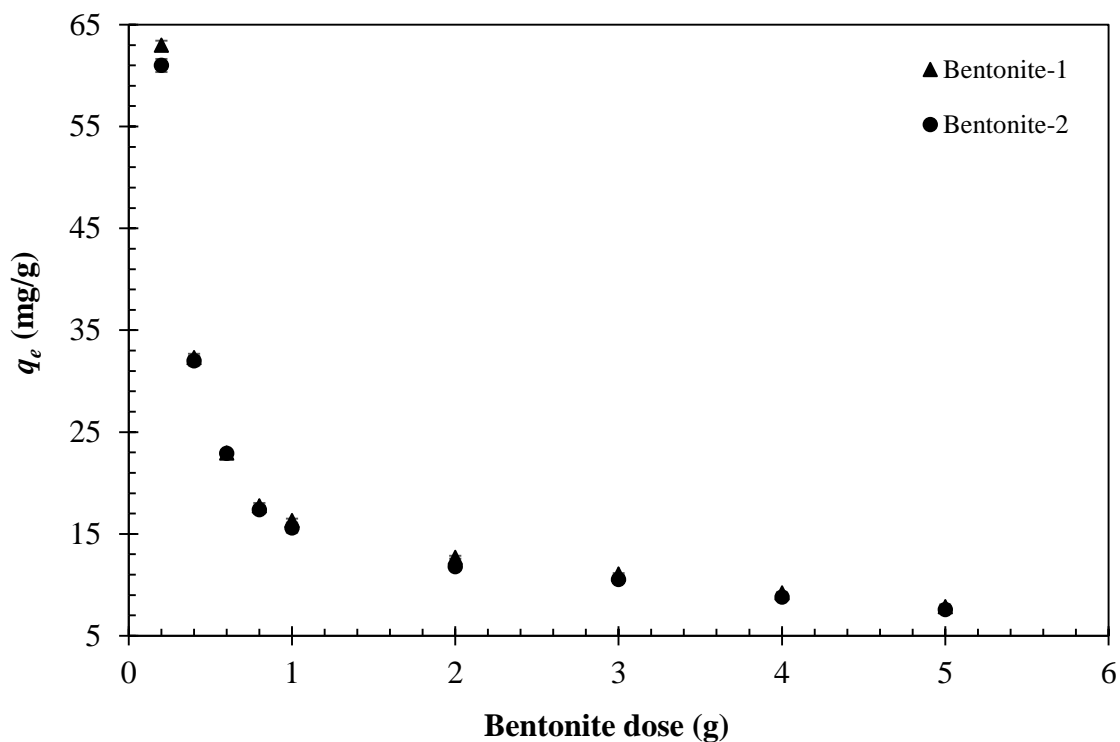


Fig. 4.45. Quantity of Zn^{2+} adsorbed at various bentonite dose

4.2.16. Contact time

The contact time among the contaminant and the adsorbent is crucial in designing a liner material in the waste disposal system. A quick uptake of contaminants and reaching of equilibrium in a short period indicates the effectiveness of that adsorbent as a liner material for its usage in the waste disposal system. The influence of contact time for the sorption of heavy metals was investigated for 3 hours for initial heavy concentrations of 500 mg/L at 28 ± 0.5 C. Bentonite dosage was 5 g/100 mL of heavy metal solution at pH 5. Fig. 4.46 to 4.48 depicts that with the increase in contact time, the amount of heavy metal adsorbed on the bentonites increased.

Fig. 4.46 shows that the removal of Pb^{2+} was fast in the first 10 minutes. After 20 minutes, the curve of contact time becomes smooth and steady-state and reaches equilibrium. From the trend, it can also be observed that initially at 5 minutes, Bentonite-1 showed 83.1% Pb^{2+} removal; whereas, Bentonite-2 showed an 81.3% removal. Likewise, Fig. 4.47 illustrates that the adsorption rate of Cu^{2+} on both bentonites reached equilibrium within 120 min. The removal percentages were found to be 83.0% and 79.1% for Bentonites-1 and -2, respectively. Similarly, it was also found that the removal of Zn^{2+} was very rapid in the first 5 minutes. The plot in Fig. 4.48 shows that 68.1 and 61.5% of removal

were obtained for Bentonite-1 and -2 in 5 minutes. After 80 minutes, the plot of contact time for both the bentonite becomes steady-state, and a plateau was observed.

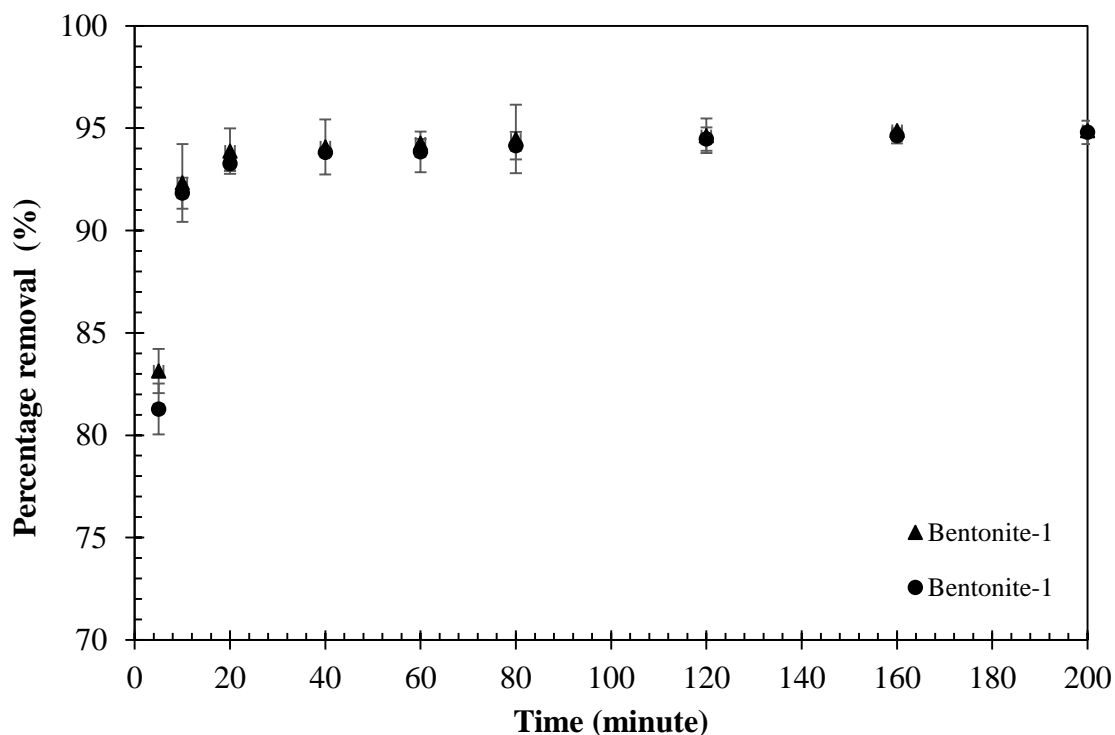


Fig. 4.46. Adsorption kinetics for Pb²⁺

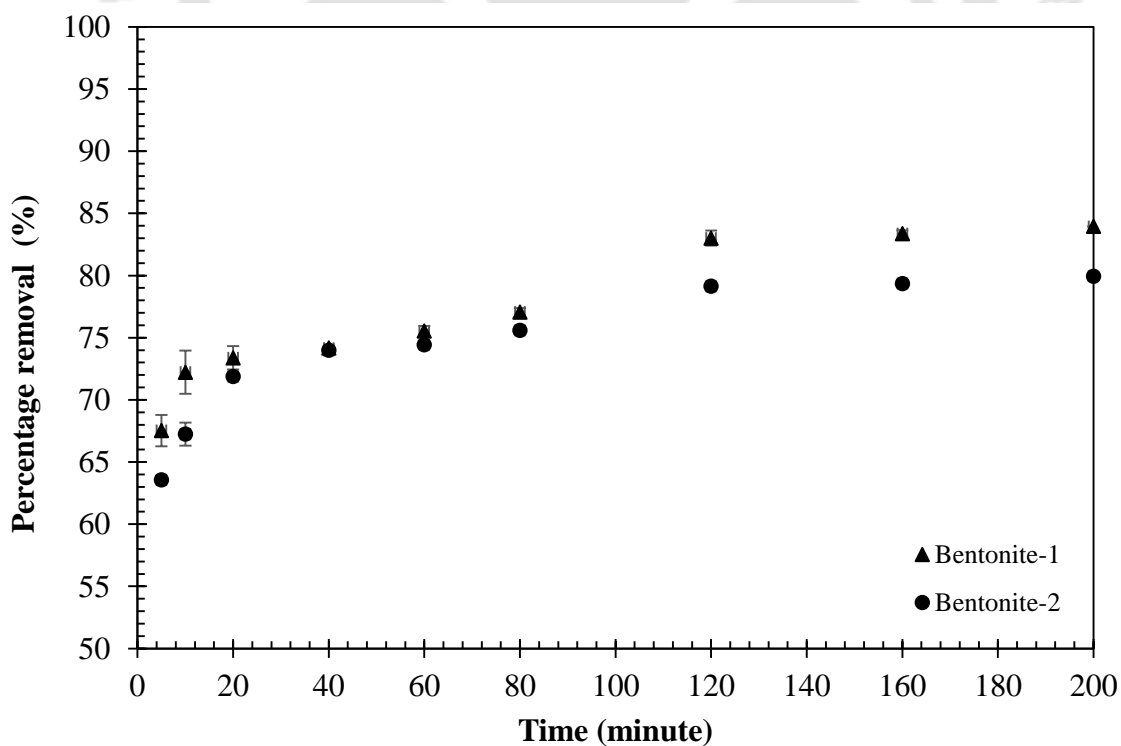


Fig. 4.47. Adsorption kinetics for Cu²⁺

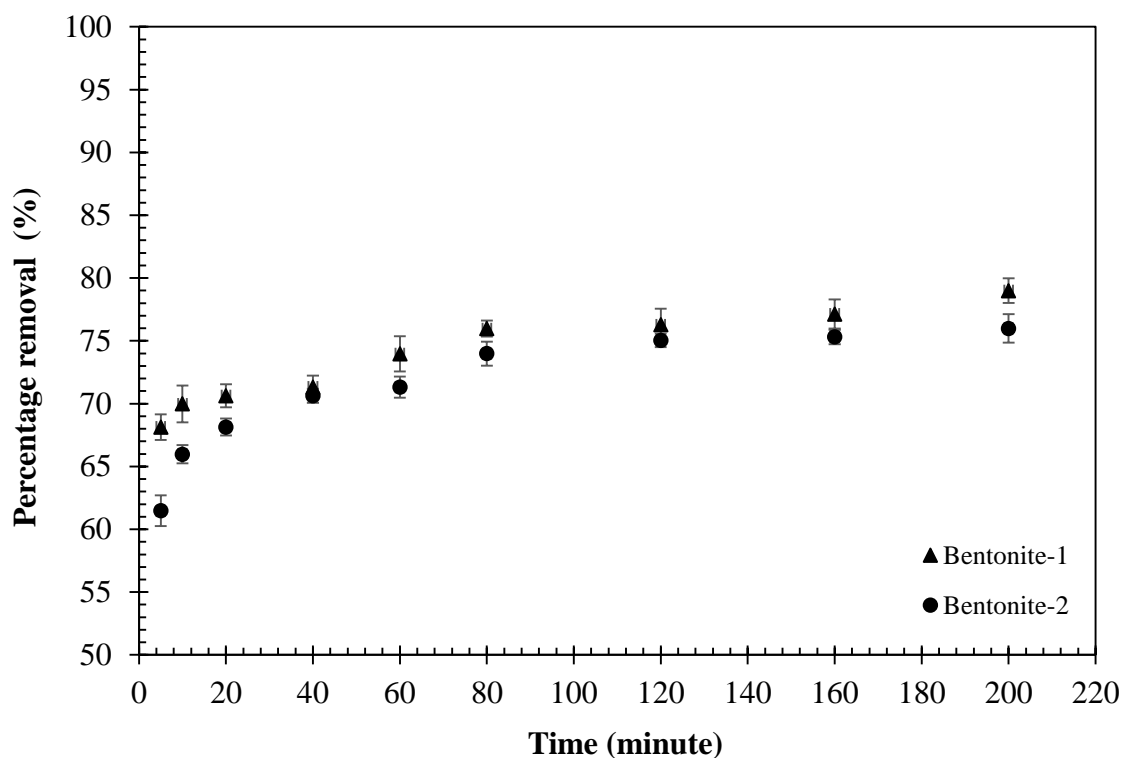


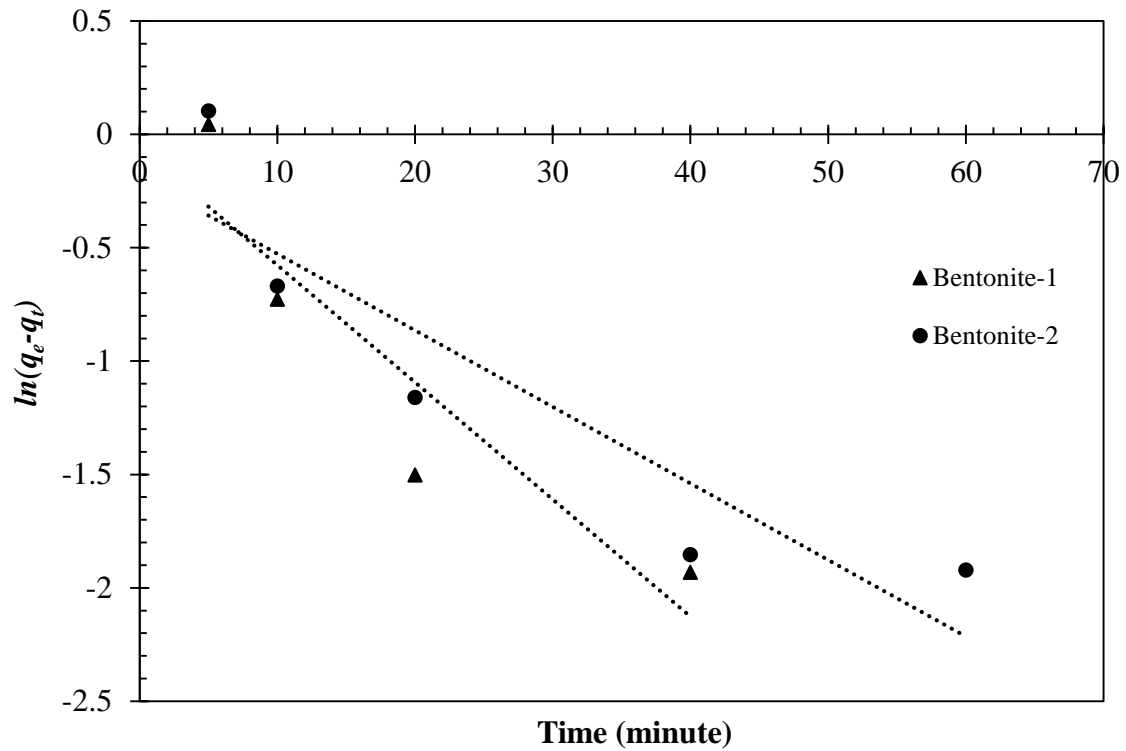
Fig. 4.48. Adsorption kinetics for Zn^{2+}

4.2.17. Kinetic study

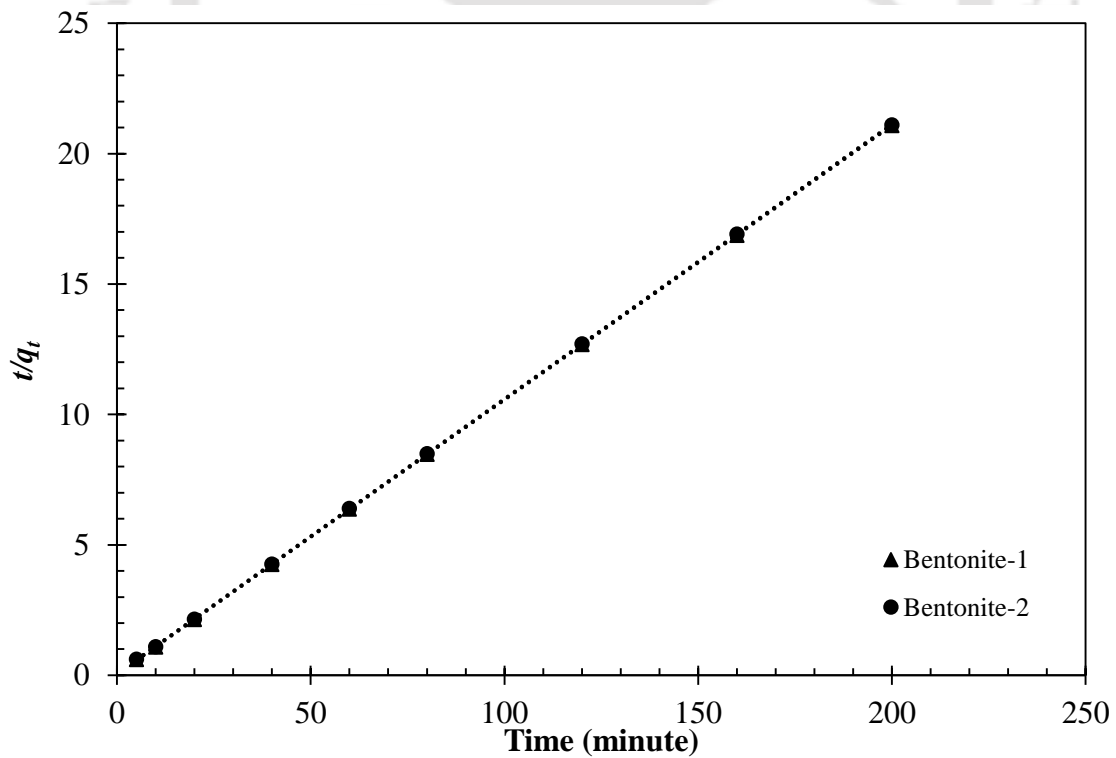
Two kinetic models were fitted comprising pseudo-first- and second-order equations to study the potential rate-controlling steps and mechanisms of adsorption. It shows the values of linear regression and kinetic constants for both bentonites. Fig. 4.49 to 4.51 displays the plot of Pseudo-first-order and Pseudo-second-order kinetics of heavy metal sorption on two different bentonites. The calculated kinetic parameters of heavy metal sorption for both the adsorbent are recorded in Table 4.10. It shows that the R^2 value for the pseudo-second-order kinetic model was more significant as compared to pseudo-first-order kinetic model for both bentonites.

The plot in Fig. 4.49 (a), 4.50 (a) and 4.51(a) shows the relationship between $\ln(q_e - q_t)$ and t for the pseudo-first-order kinetics model. It depicts that the Pseudo first-order kinetic curves of both the bentonites do not represent a straight line. The R^2 value of the model is also lower ($R^2 < 0.90$), which also suggests that the sorption of heavy metals on both the bentonites does not follow Pseudo-first order kinetic model (Table 4.10). Fig. 4.49 (b), 4.50 (b) and 4.51(b) display that plot between t/q_t versus t , which indicates a linear relationship. The Pseudo second-order kinetic model was found to be an ideal fit for both the bentonites with the significantly higher value of $R^2 > 0.99$. The calculated values of q_e were also similar

to the experimental ones, which also confirm the excellent agreement with the sorption model.

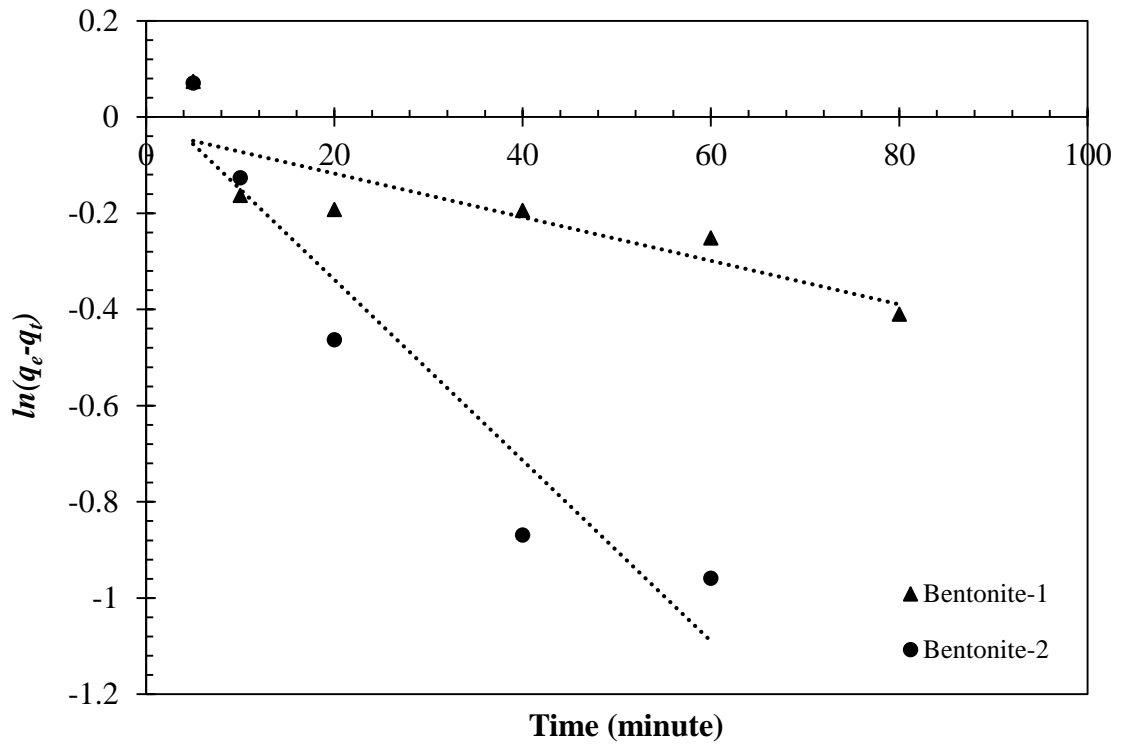


(a) Pseudo-first-order adsorption kinetics of Pb^{2+} at pH 5

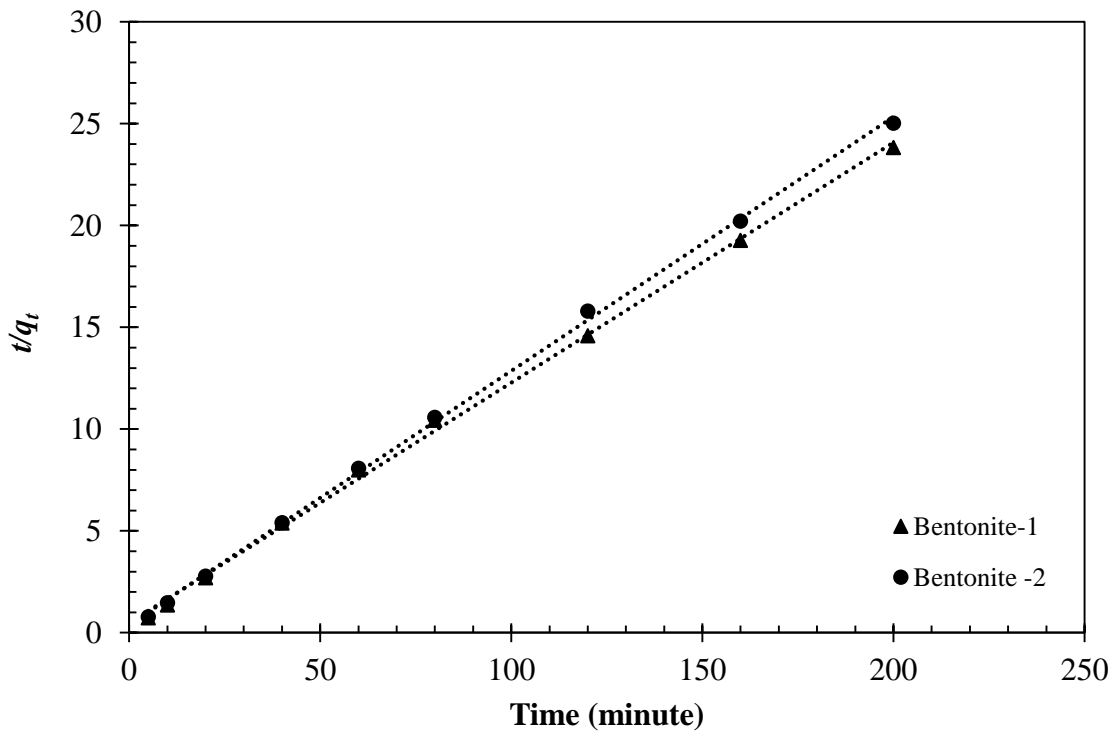


(b) Pseudo-second-order adsorption kinetics of Pb^{2+} at pH 5

Fig. 4.49. Kinetic study of bentonites in presence of Pb^{2+}

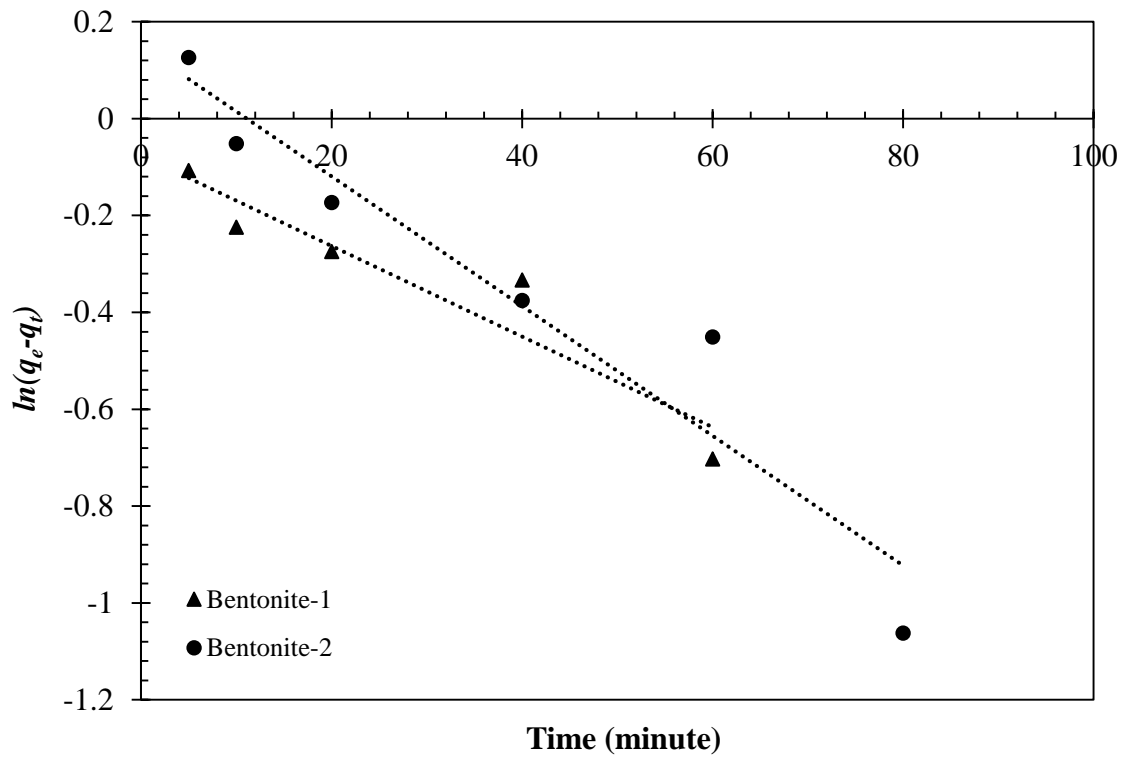


(a) Pseudo-first-order adsorption kinetics of Cu^{2+} at pH 5

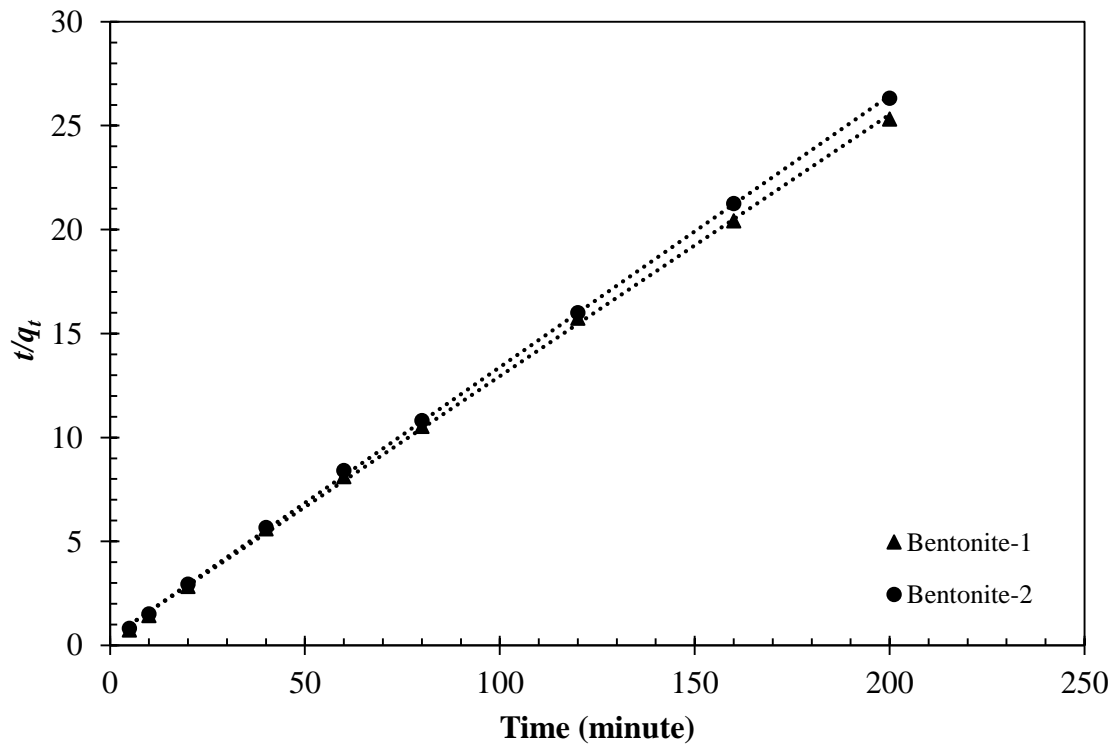


(b) Pseudo-second-order adsorption kinetics of Cu^{2+} at pH 5

Fig. 4.50. Kinetic study of bentonites in presence of Cu^{2+}



(a) Pseudo-first-order adsorption kinetics of Zn²⁺ at pH 5



(b) Pseudo-second-order adsorption kinetics of Zn²⁺ ion at pH 5

Fig. 4.51. Kinetic study of bentonites in the presence of Zn²⁺

The outcome of the study also concluded that the mechanism of the adsorption process mainly depends on adsorbent (bentonites) and adsorbate (Pb^{2+} , Cu^{2+} , and Zn^{2+}). It also concludes that the overall rate-limiting step of the metal sorption process appeared to be governed by chemisorption on both the bentonites, which comprises valence forces by exchange and sharing of the electron (Barbier et al., 2000; Vimonses et al., 2009).

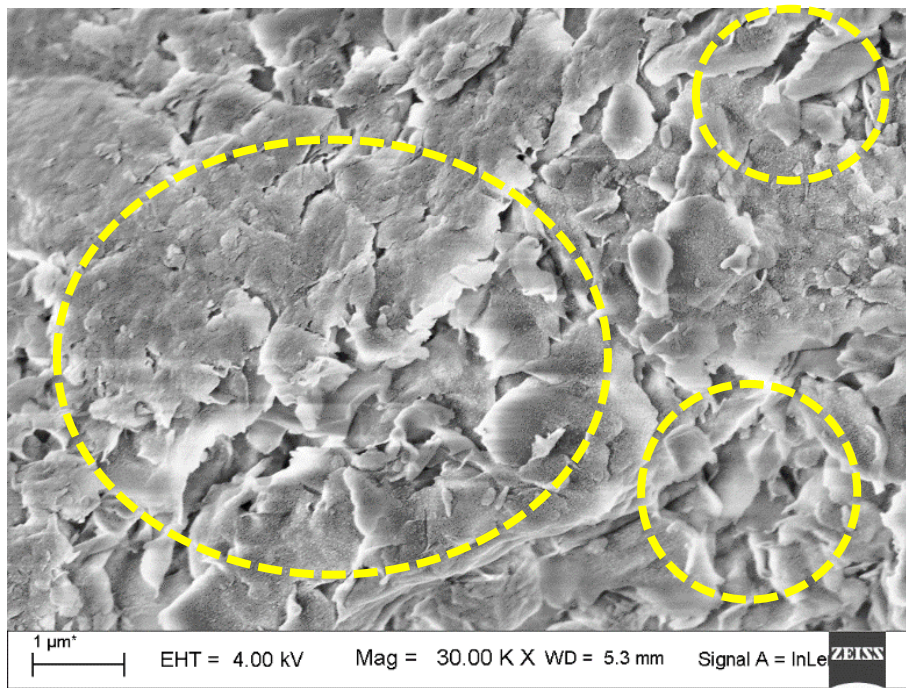
Table 4.10. Parameters for adsorption of heavy metals on Bentonites derived from the pseudo-first- and second-order kinetic models.

| Kinetic model | Parameters | Pb^{2+} | | Cu^{2+} | | Zn^{2+} | |
|---------------------------------------|-----------------------------|------------------|------|------------------|------|------------------|------|
| | | BE-1 | BE-2 | BE-1 | BE-2 | BE-1 | BE-2 |
| Pseudo 1 st order kinetics | q_e (mg/g) | 9.41 | 9.39 | 8.07 | 7.54 | 7.59 | 7.48 |
| | K_1 (min^{-1}) | 0.81 | 1.11 | 0.31 | 0.39 | 0.42 | 0.33 |
| | R^2 | 0.84 | 0.82 | 0.74 | 0.90 | 0.89 | 0.91 |
| Pseudo 2 nd order kinetics | q_e (mg/g) | 9.51 | 9.49 | 8.48 | 8.02 | 7.93 | 7.66 |
| | K_2 (g/ mg min) | 0.01 | 0.01 | 0.01 | 0.01 | 0.01 | 0.02 |
| | R^2 | 0.99 | 0.99 | 0.99 | 0.99 | 0.99 | 0.99 |

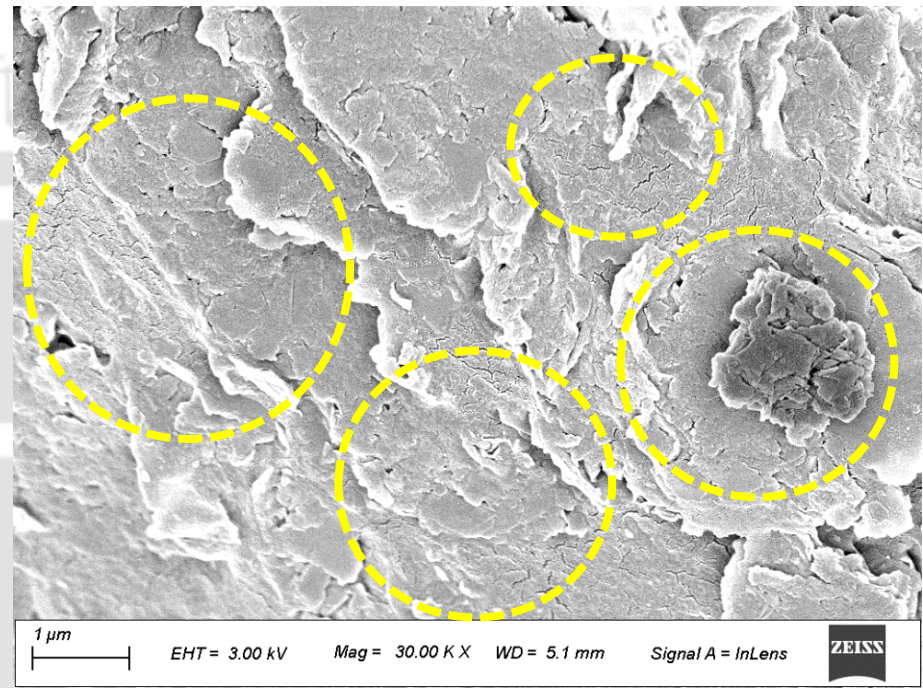
BE-1 and BE-2 indicate Bentonite-1 and -2, respectively.

4.2.18. FESEM Study

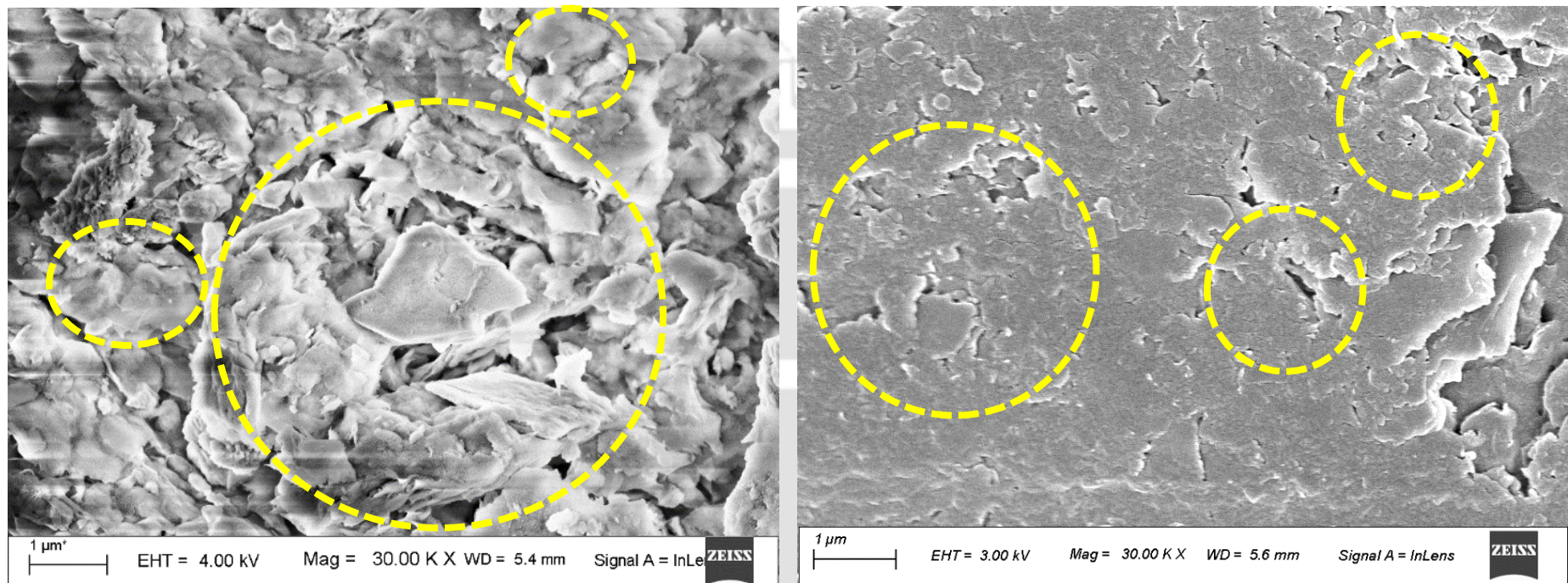
FESEM study was performed and photomicrographs were obtained to visualize the change in the surface morphology of two bentonites. It can be seen from the Figs. 4.52-4.54 [(a) and (c)] that because of the presence of montmorillonite mineral, pure bentonites show a flaky dispersed structure with loose porous aggregates (Mitchell and Soga, 2005). Fig. 4.52 - 4.54 [(b) and (d)] display the surface morphology of Cu^{2+} , Pb^{2+} and Zn^{2+} adsorbed bentonites, which shows that the pore space gradually diminishes after adsorption of heavy metals since the metal ions were adsorbed and trapped in the pore spaces of bentonites and adsorption sites presents on the bentonites gets saturated.



(a) Bentonite-1 before adsorption



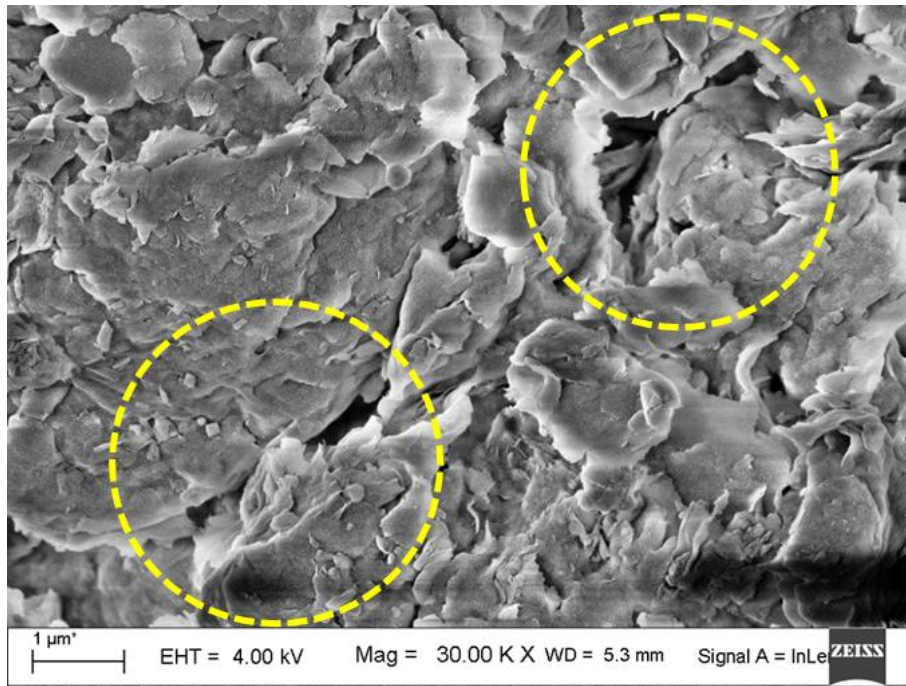
(b) Bentonite-1 after batch equilibrium study with 1000 mg/L



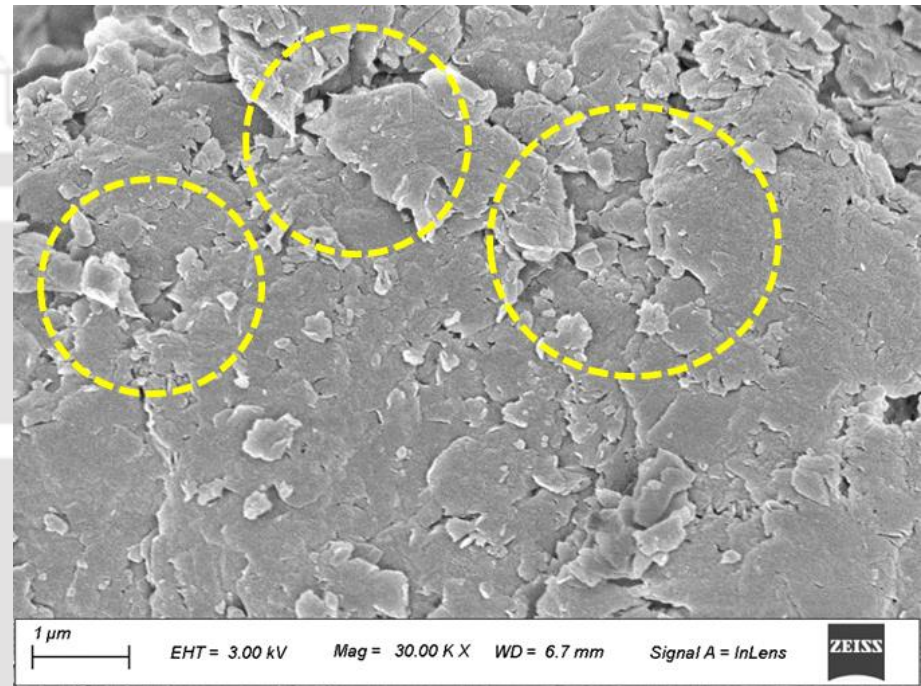
(c) Bentonite-2 before adsorption

(d) Bentonite-2 after batch equilibrium study with 1000 mg/L

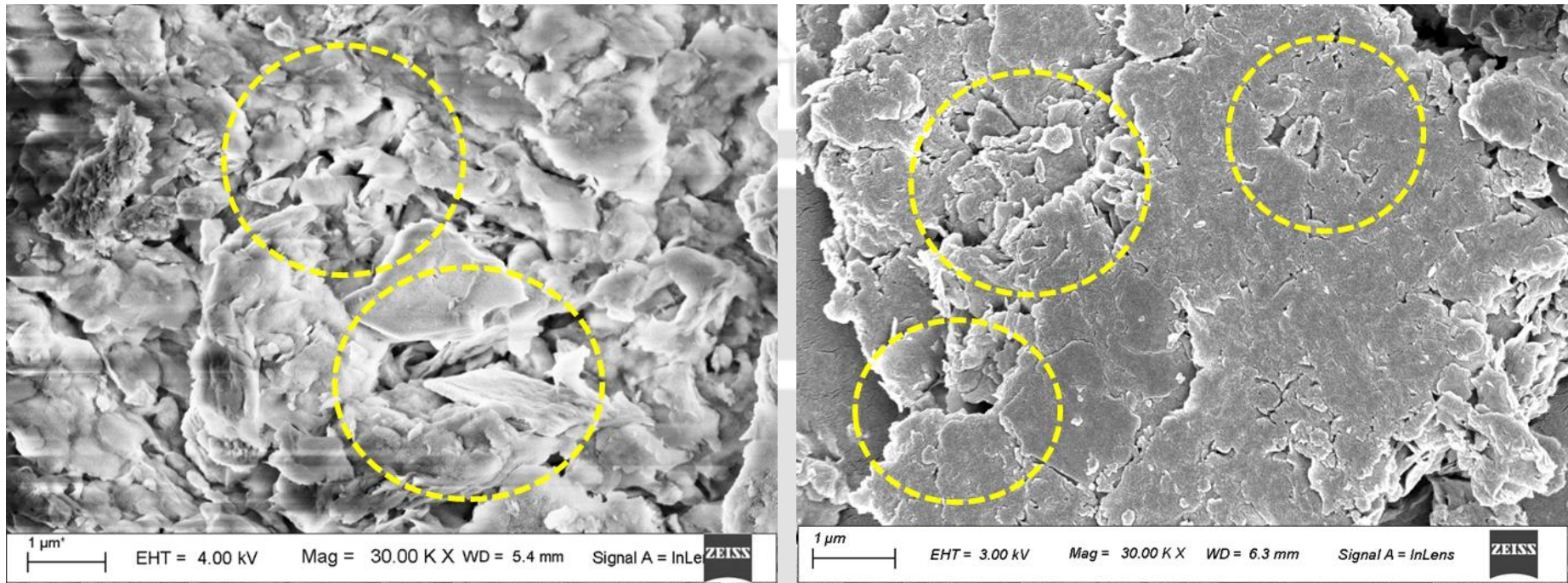
Fig. 4.52. FESEM images of bentonites in presence of Cu^{2+}



(a) Bentonite-1 before adsorption



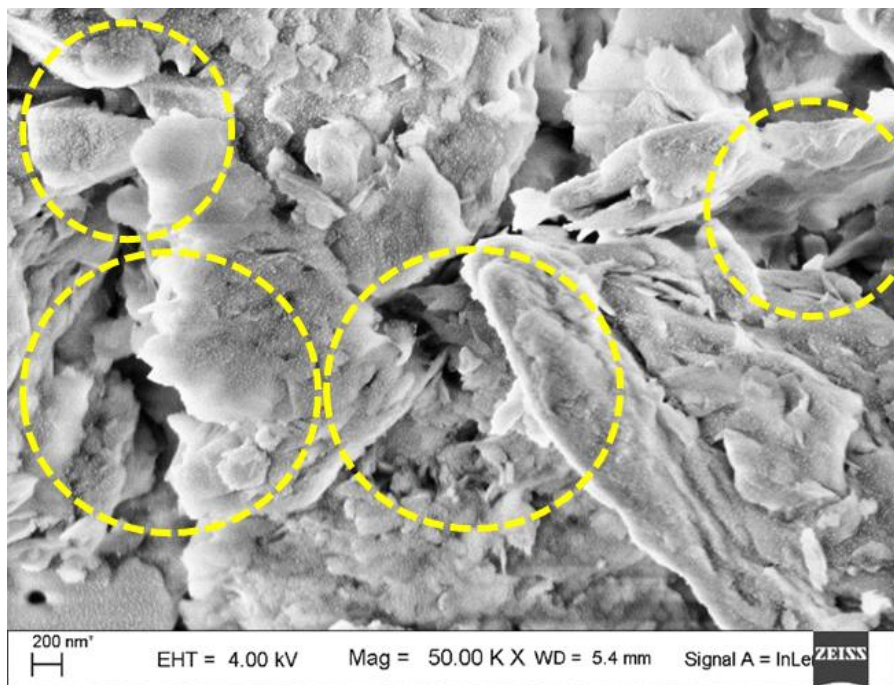
(b) Bentonite-1 after batch equilibrium study with 1000 mg/L



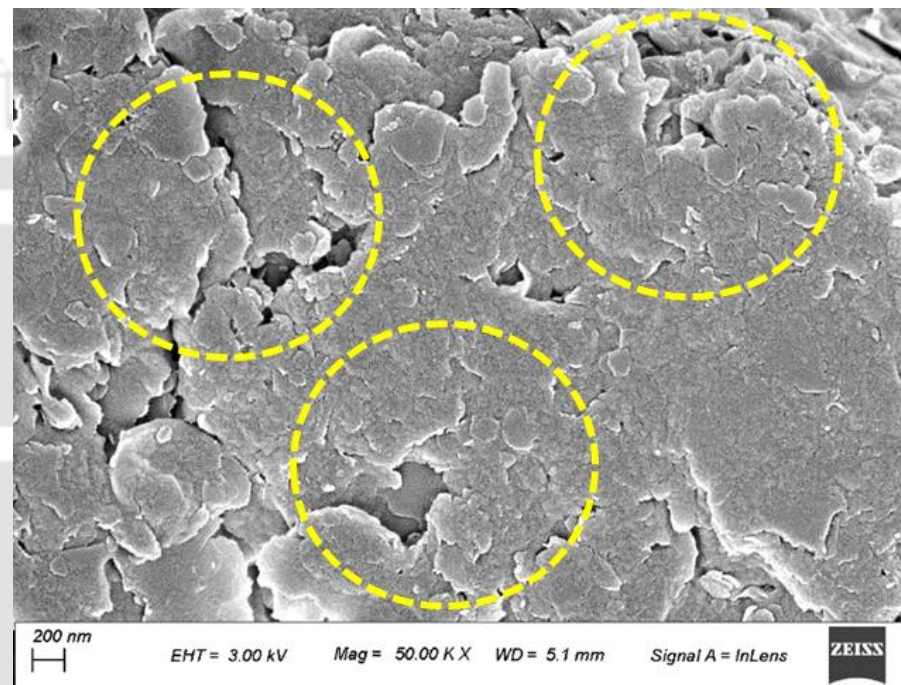
(c) Bentonite-2 before adsorption

(d) Bentonite-2 after batch equilibrium study with 1000 mg/L

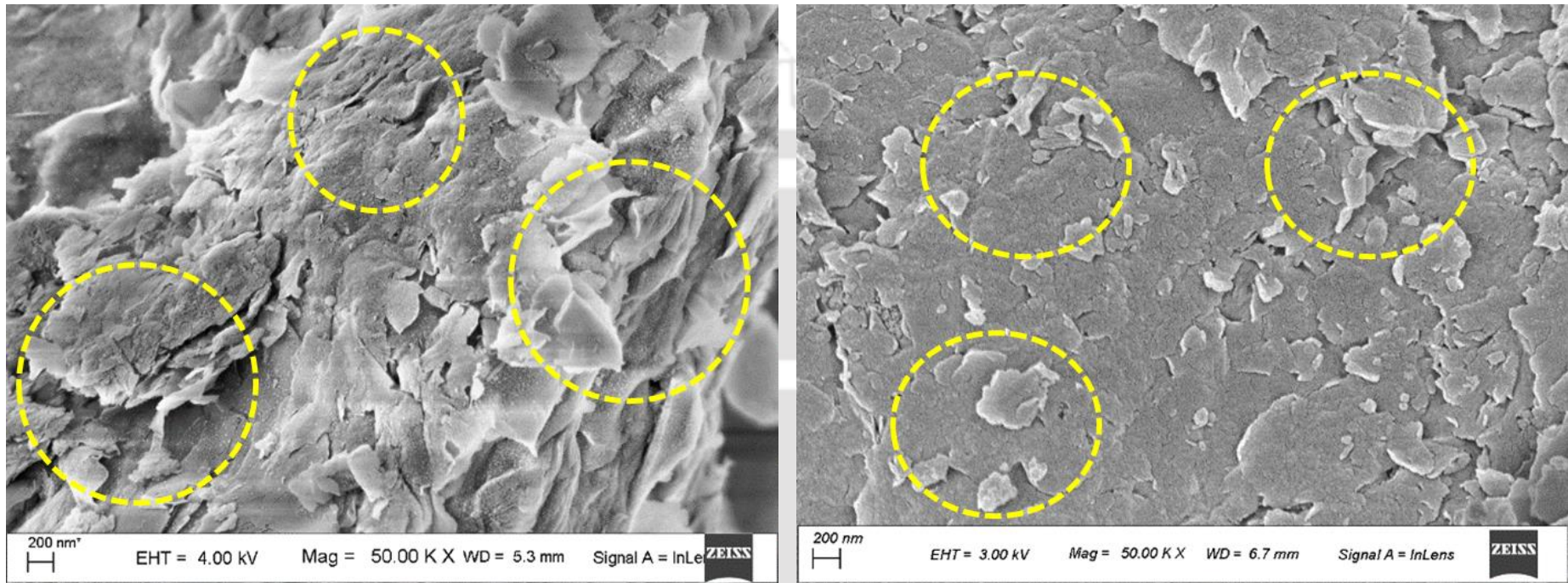
Fig. 4.53. FESEM images of bentonites in presence of Pb^{2+}



(a) Bentonite-1 before adsorption



(b) Bentonite-1 after batch equilibrium study with 1000 mg/L



(c) Bentonite-2 before adsorption

(d) Bentonite-2 after batch equilibrium study with 1000 mg/L

Fig. 4.54. FESEM images of bentonites in presence of Zn^{2+}

4.2.19. FTIR study

FTIR spectra identify the interaction among functional groups existing in the bentonites and heavy metal ions. It helps in the identification of different forms of minerals present in the clay. The FTIR spectra of both the bentonites before and after adsorption of 1000 mg/L of Cu^{2+} , Pb^{2+} and Zn^{2+} solution is displayed in Figs. 4.55-4.57 (a) and (b). A detailed band analysis is listed in Tables 4.11-4.12. The broad bands observed at 3620.49 cm^{-1} and 3620.9 cm^{-1} , which shows the possibility of O–H stretching vibration of the Silanol (Si–OH) groups and HO–H vibration of the water adsorbed silica surface for Bentonite-1 and -2 prior to adsorption. The band at 3700.0 and 3418.5 cm^{-1} for Bentonite-1 and 3706.41 and 3439.2 cm^{-1} for Bentonite-2 also resembles to the O–H stretching vibration (De Oliveira et al., 2016). A band at 1637.3 and 1636.2 cm^{-1} was observed in the FTIR spectra which is accredited to the angular vibration of the O–H group and also associated to the adsorbed water and the hydration water existing in the bentonite clay. Fig. 4.55-4.57 (a) and (b) indicate a strong band near 999.2 and 999.4 cm^{-1} and also in the region between 1131.6 and 1037.4 cm^{-1} is because of Si–O stretching vibration in tetrahedral sheets, which resembles to the characteristic band of mineral montmorillonite before adsorption. It also shows vibrational frequencies to the band correspond to 795.3 and 911.0 cm^{-1} conforming to the octahedral layers of the alumino-silicate for Bentonite-1. Similarly, for Bentonite-2, the both frequencies were observed near bands 795.8 and 910.9 cm^{-1} , respectively (Akpomie and Dawodu, 2015; De Oliveira et al., 2016; Mudasir et al., 2020). The bending vibration of Si–O–Al and Si–O was observed near 691.9 and 523.9 cm^{-1} from the IR studies of bentonites that indicates the presence of quartz (Karapinar and Donat, 2009).

However, an alteration in the pattern of FTIR was observed after adsorption study which attributed to adsorption of Cu^{2+} , Pb^{2+} and Zn^{2+} on both the bentonites [Figs. 4.55-4.57 (a) and (b)]. An alteration in the broad bands pattern was detected for Cu^{2+} [Figs. 4.55 (a) and (b)] and there were shifts in the frequency of absorption from 3700.0 to 3698.4 cm^{-1} , 3620.4 to 3616.9 cm^{-1} and 3418.5 to 3446.8 cm^{-1} for Bentonite-1. Similarly shift in the frequency of absorption from 3706.4 to 3698.7 cm^{-1} , 3620.4 to 3617.7 cm^{-1} and 3439.2 to 3450.3 cm^{-1} was observed in case of Bentonite-2. For Bentonite-1, participation of Si–O group in adsorption process can be detected by their alterations in absorption frequency from 1131.6 to 1115.8 cm^{-1} and 999.2 to 996.3 cm^{-1} . In case of Bentonite-2, shifts in absorption

frequency from 1137.4 to 1116.9 cm^{-1} and 999.4 to 996.7 cm^{-1} , respectively. Likewise, the alteration in the absorption frequency from 795.3 to 793.6 cm^{-1} , 691.9 to 686.5 cm^{-1} and 523.9 to 518.7 cm^{-1} for Bentonite-1 and 795.3 to 794.3 cm^{-1} , 691.9 to 684.8 cm^{-1} and 523.9 to 518.7 cm^{-1} for Bentonite-2 also specifies the involvement of the Si–O–Al linkage in the process of adsorption. The shifts in these adsorption bands in FTIR spectra confirm the occurrence of the adsorption of Cu^{2+} in both the bentonites (Akpomie and Dawodu, 2015; Mudasir et al., 2020). Similar to Cu^{2+} , alteration in the pattern of FTIR was observed and there were shifts in the frequency was detected in presence of Pb^{2+} and Zn^{2+} , respectively (Tables 4.11 and 4.12).

Table 4.11. FTIR spectra bands of Bentonite-1 before and after adsorption of heavy metals.

| Wavenumber (cm^{-1}) | | | | |
|---------------------------------------|---|---|---|---------------------------|
| Bentonite-1 (Before adsorption) | Bentonite-1 (After Cu^{2+} adsorption) | Bentonite-1 (After Pb^{2+} adsorption) | Bentonite-1 (After Zn^{2+} adsorption) | Attribution |
| 3700.0 | 3698.4 | 3697.4 | 3695.5 | O-H stretching |
| 3620.4 | 3616.9 | 3612.0 | 3620.2 | O-H asymmetric stretching |
| 3418.5 | 3446.8 | 3403.5 | 3378.1 | O-H asymmetric stretching |
| 1637.3 | 1633.9 | 1626.9 | 1633.8 | H-O-H Bending |
| 1131.6 | 1115.8 | 1115.8 | 1115.2 | Si-O stretching |
| 999.2 | 996.3 | 991.3 | 996.2 | Si-O stretching |
| 911.0 | 910.9 | 911.0 | 910.9 | Octahedral sheet |
| 795.3 | 793.6 | 795.0 | 790.6 | Octahedral sheet |
| 691.9 | 686.5 | 691.9 | 684.0 | Si-O-Al Bending |
| 523.9 | 518.7 | 522.9 | 517.7 | Si-O Bending |

Table 4.12. FTIR spectra bands of Bentonite-2 before and after adsorption of heavy metals.

| Wavenumber (cm ⁻¹) | | | | |
|---------------------------------------|---|---|---|------------------------------|
| Bentonite-2 (Before adsorption) | Bentonite-2 (After Cu ²⁺ adsorption) | Bentonite-2 (After Pb ²⁺ adsorption) | Bentonite-2 (After Zn ²⁺ adsorption) | Attribution |
| 3706.4 | 3698.7 | 3698.3 | 3695.5 | O-H stretching |
| 3620.9 | 3617.7 | 3616.6 | 3620.5 | O-H asymmetric stretching |
| 3439.2 | 3450.3 | 3412.7 | 3382.4 | O-H asymmetric stretching |
| 1636.2 | 1633.0 | 1623.5 | 1633.7 | H-O-H Bending |
| 1137.4 | 1116.9 | 1115.6 | 1114.3 | Si-O stretching |
| 999.4 | 996.7 | 994.7 | 996.7 | Si-O stretching |
| 910.9 | 910.9 | 910.9 | 910.0 | Octahedral sheet |
| 795.8 | 794.3 | 795.8 | 790.6 | Octahedral sheet |
| 691.9 | 684.8 | 691.9 | 688.0 | Si-O-Al Bending |
| 523.9 | 518.7 | 522.3 | 518.6 | Si-O Bending |

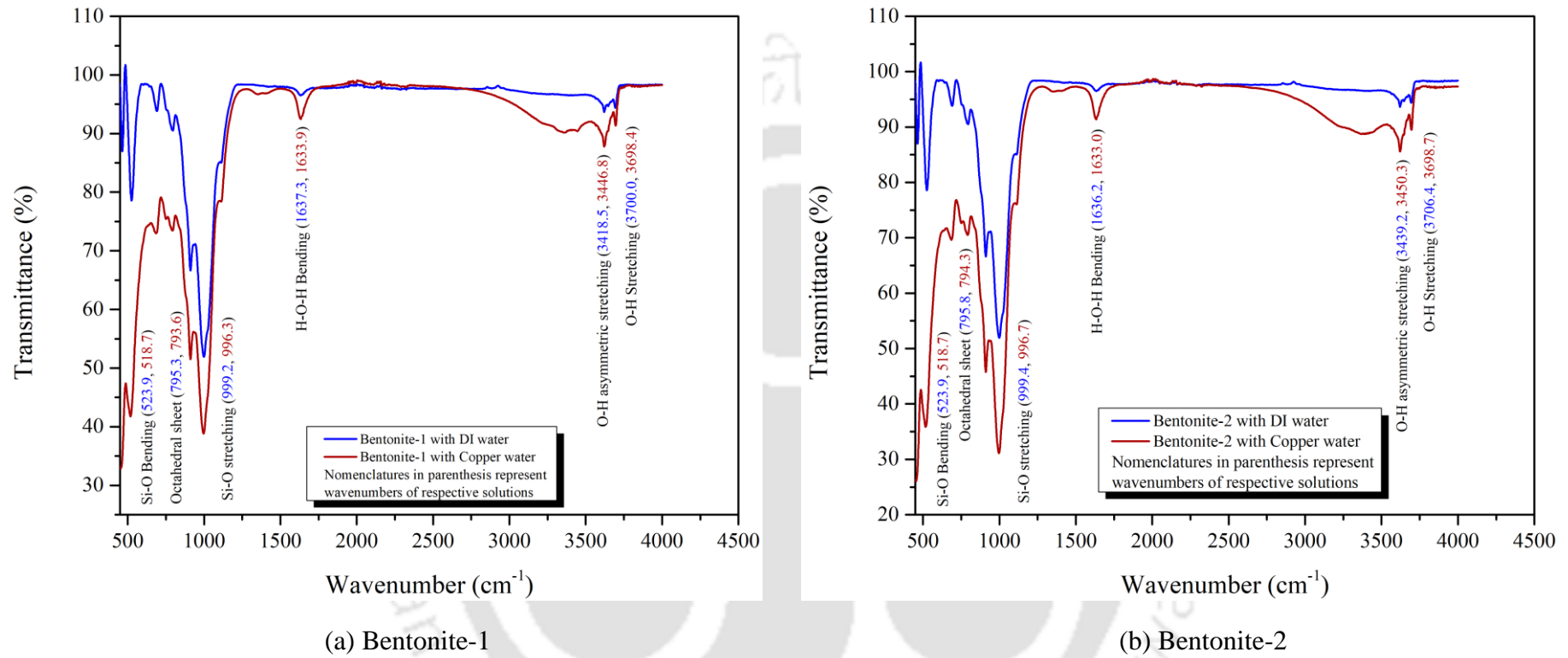


Fig. 4.55. FTIR Spectra for both bentonites in DI water and Cu²⁺ solutions

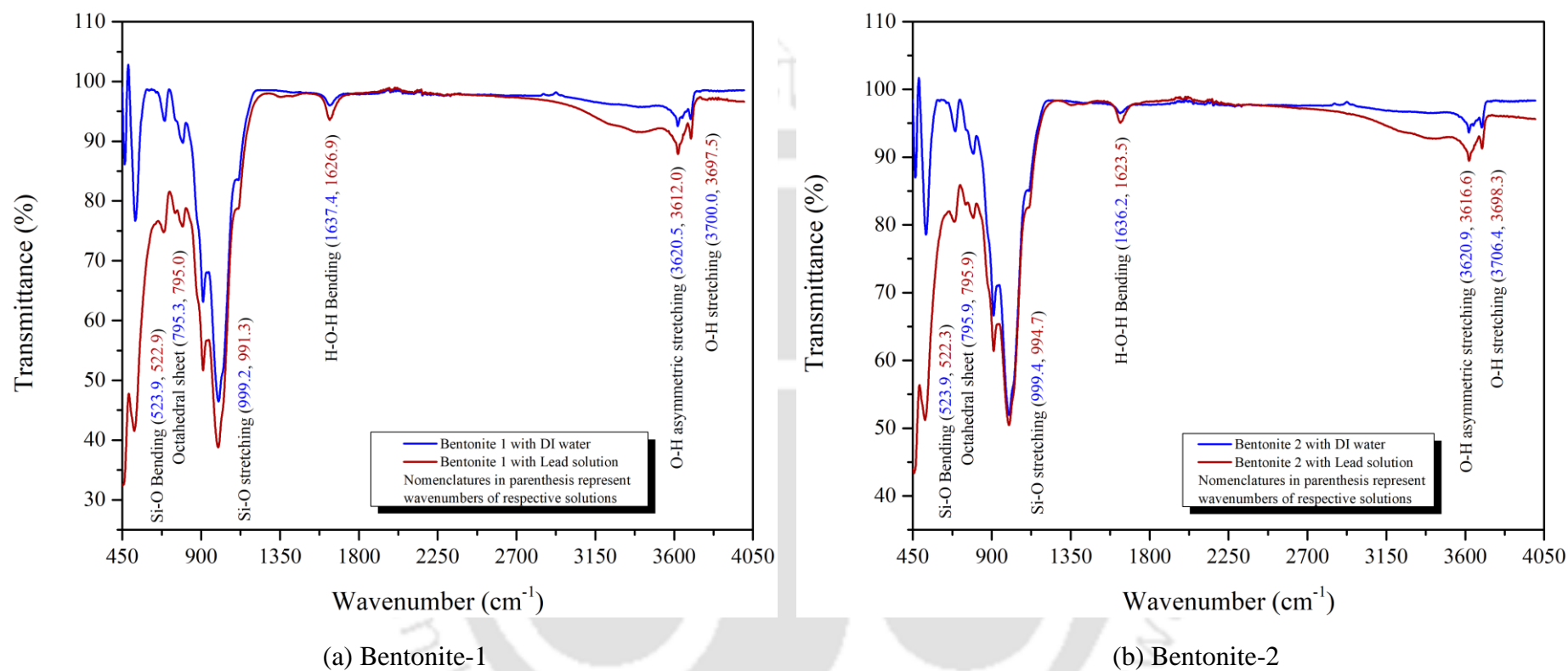


Fig. 4.56. FTIR Spectra for both bentonites in DI water and Pb^{2+} solutions

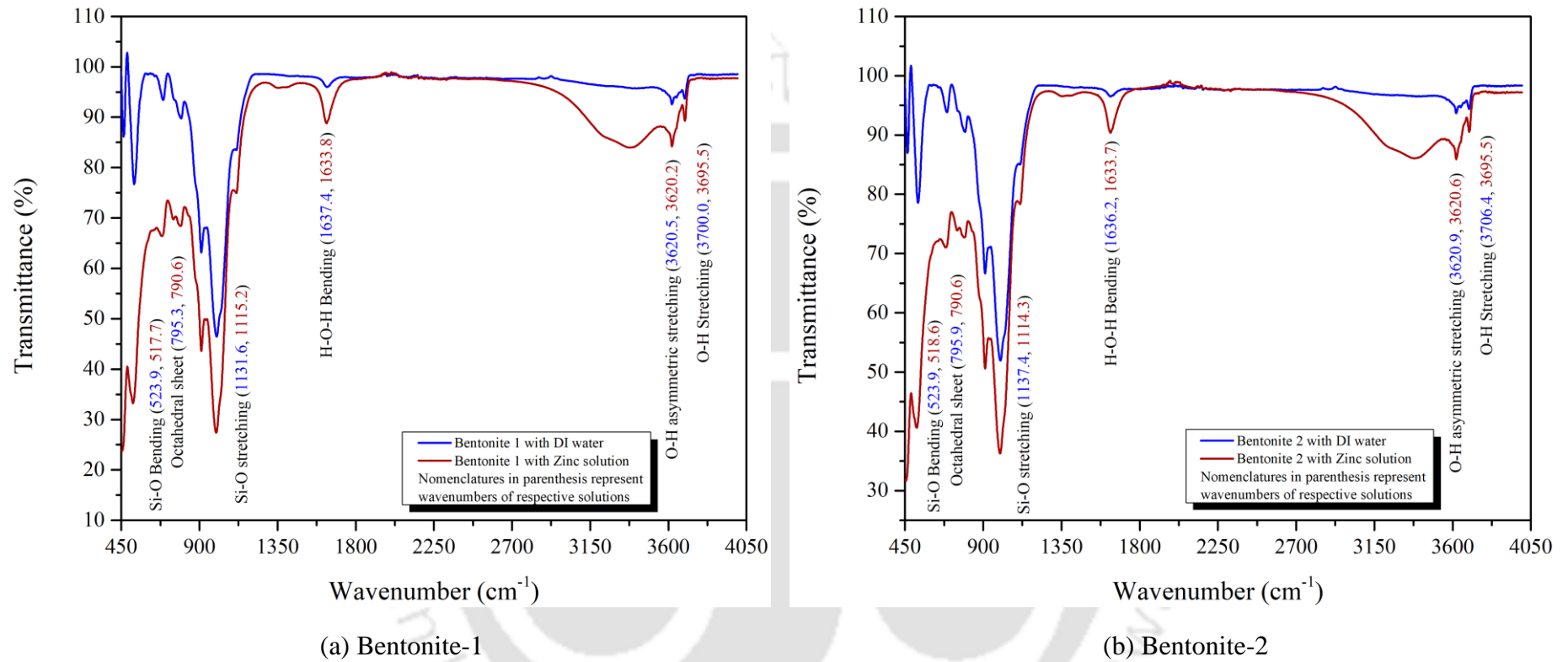


Fig. 4.57. FTIR Spectra for both bentonites in DI water and Zn²⁺ solutions

4.3. Summary

This study was carried out to investigate the effect of heavy metal ions on the behaviour of bentonites. Two bentonites with different mineralogical properties were studied for their change in the index properties, free swelling, swelling potential, swelling pressure, hydraulic conductivity, consolidation parameters and shear strength in the presence of heavy metal ions of various concentrations. Further, the investigation was conducted to analyze the influence of heavy metals on the adsorption capacity of bentonites. pH, Adsorption, dose, isotherm, contact time and kinetic studies were carried out on two bentonites. Based on the test results, the conclusions are summarised below.

- The study revealed that with the increase in heavy metal concentration, there is a decrease in Liquid limit and free swell value. The decline in free swelling and liquid limit value is caused by the substantial reduction in the DDL thickness because of the rise in metal concentration.
- The investigation showed that with a rise in heavy metal concentration, swelling potential and swelling pressure decreases. A maximum decline in the swelling potential and swelling pressure value showed with 2000 mg/L of Pb^{2+} , Cu^{2+} and Zn^{2+} solution with respect to DI water.
- The study showed that the value of the void ratio, for any given consolidation pressure, reduced with a rise in heavy metal concentration. The samples with different concentrations of Pb^{2+} , Cu^{2+} and Zn^{2+} solution revealed a lesser value of void ratio in comparison with the sample with DI water. On the surface of the clay, more Cu^{2+} ions are adsorbed due to the increase in Cu^{2+} concentration in the pore fluid. Consequently, clay particles come closer distance and repulsive force reduced, causing a reduction in DDL thickness.
- The Time - swelling relationship study indicated that, with the increase in the heavy metal concentrations, the time taken for the primary swelling reduces.
- The hydraulic conductivity value of bentonite increases with the increase in heavy metal concentration. The investigation reveals that the hydraulic conductivity rises

marginally when the Pb^{2+} concentration increases from 0 to 100 mg/L. With a further rise to 2000 mg/L, the hydraulic conductivity value increased significantly. Similar kind of trend was observed for Cu^{2+} and Zn^{2+} .

- The results indicated that with an increase in consolidation pressure, the c_v values decreased. This signifies a slow consolidation rate at a more considerable pressure. On the contrary, with the rise in heavy metal concentration, the c_v increases, which suggests a higher rate of consolidation when the soil sample is permeated with various metal solutions. With the increase in metal concentration, the thickness of DDL reduces, causing the decrease in repulsive forces between the clay particles, subsequently, soil sample consolidated more rapidly, which increases the c_v value.
- The study revealed that by the increase in the concentration of Pb^{2+} , Cu^{2+} and Zn^{2+} , t_{90} for the bentonite sample decreases. Since the c_v increases with an increase in the metal concentration, the time required to achieve the desired degree of consolidation decreases resulting in a reduction in t_{90} . On the contrary, t_{90} increase with the increase in consolidation pressure. With an increase in the consolidation pressure, the clay plates move to a closer distance because of which the repulsion between clay plates increases, which prevents further movement of the plates and results in a decrease in the c_v and increase in t_{90} .
- The C_c of the sample decreased with the rise in heavy metal concentration. This is because, with the increase in the concentration of heavy metal, the thickness of DDL is reduced. Subsequently, the clay particles come closer to each other becoming more flocculated, thus, resisting settlement of the material/liner and causing a lesser value of C_c .
- UCS value decreases due to increase in metal ion concentration up to the value to 1000 mg/L for almost all the heavy metals in both the bentonites, but at 2000 mg/L the values increased slightly.
- pH study shows that with the rise in pH of the solution, the percentage removal of heavy metal increased. The research indicates that for all metals, the sorption was observed at pH ranges from 4 – 6. Therefore, to avoid precipitation, pH 5 was carefully chosen for further studies as an ideal condition.

- The result indicates that with the rise in heavy metal concentration, the adsorption capacity of the bentonite increased. Higher adsorption of Pb^{2+} was observed, followed by Cu^{2+} and Zn^{2+} . On the contrary, the removal percentage of heavy metals decreased with the increase in initial metal concentration. The study indicated that Pb^{2+} showed higher removal, followed by Cu^{2+} and Zn^{2+} for both the bentonite. A higher amount of adsorption was observed in Bentonite-1 as compared to Bentonite-2 in the presence of all the heavy metals.
- The experimental data obtained from the batch study has been fitted by Langmuir and Freundlich isotherm models. The study showed that for Pb^{2+} and Cu^{2+} , the adsorption data fitted well with the Freundlich isotherm. However, for Zn^{2+} , the adsorption data fitted well with Langmuir Isotherm for both the bentonites.
- A dose study was conducted at different bentonite dosages ranging from 0.2 to 5.0 g in 100 mL of heavy metal solution maintaining an agitation speed of 150 rpm at 28 ± 1 °C and contact time of 3 h constant. The study showed that with the rise in adsorbent dose, the removal rate (%) increased promptly whereas, the adsorption capacity (mg/g) of all the metals reduced for both the bentonites.
- The influence of contact time for the sorption of heavy metals was investigated for a period of 3 hours for initial heavy metal concentrations of 500 mg/L at 28 ± 0.5 C. The study indicated that initially at 5 minutes, Bentonite-1 showed 83.1 and 68.1% removal for Pb^{2+} and Zn^{2+} , whereas, 81.3 and 79.1% removal was obtained for Bentonite-2 respectively. The adsorption rate of Cu^{2+} on both the bentonites reached equilibrium within 120 min. The removal percentages were found to be 83.0% and 79.1% for Bentonites-1 and -2, respectively. Bentonite-1 with higher montmorillonite content and specific surface area showed a higher adsorption rate as compared to Bentonite-2.

- Two kinetic models were fitted comprising pseudo-first- and second-order equations to study the potential rate-controlling steps and mechanisms of adsorption. For all metals, Pseudo second-order kinetic model was found to be an ideal fit for both the bentonites with the significantly higher value of $R^2 > 0.99$.
- FESEM images and FTIR studies confirm the change in surface morphology and alteration in FTIR pattern, in both the bentonites after sorption of heavy metals.





*If you set your goals
ridiculously high and
it's a failure, you will fail
above everyone else's
success*

- James Cameron

5

Effect of MSW and synthetic MSW leachate on the behaviour of bentonites

5.1. Introduction

In recent years, the world has witnessed a considerable elevation in the generation of municipal solid wastes (MSWs) as a result of enormous population growth and improvised living standards. This has increased significant pressures on the landfills, as most of the generated wastes get disposed of into them. This is primarily because landfilling is the most suitable and extensively employed technique for waste disposal (Qian et al., 2001). Over time, these wastes undergo biological as well as chemical transformations inside the landfills, thereby producing leachates (Kjeldsen et al., 2002). These leachates, when come in contact with rainwater, migrate into the sub-surface layer, thus contaminating the groundwater as well as the surrounding environment. Therefore, an impermeable liner is usually provisioned at the base of a landfill to avoid groundwater as well as soil contamination in the proximate region (Daniel, 1984).

Among the natural clays, the bentonite is found to possess massive potential as an adsorbent for removing heavy metals from aqueous solutions. Various works of literature are available, citing the relevance of the natural bentonite's efficiency as a low-cost adsorbent for eliminating trace heavy metals from water and wastewater systems (Baylan and Meriçboyu, 2016; Freitas et al., 2017). Various studies have been conducted in the past, proving bentonite as one of the most suitable landfill liner materials for preventing heavy metal percolation to the sub-surface strata (Daniel, 1984; Dutta and Mishra, 2016b; Pawar et al., 2016). Bentonite properties such as high swelling tendency, large specific surface area (SSA), lower hydraulic conductivity, massive cation exchange, and sorption capacity help achieve such high appropriateness as a liner material. Montmorillonite, consisting of phyllosilicate, forms the primary component of bentonite. It comprises one octahedral unit sandwiched between two tetrahedral units. The layers are bound together by weak van der Waals force of attraction, which allows the water to infiltrate easily, thus resulting in the formation of a diffuse double layer (DDL) followed by the swelling of bentonite (Madsen and Müller-Vonmoos, 1989; Mitchell and Soga, 2005; Norrish, 1954; Norrish and Quirk, 1954).

When found in the leachates, the non-degradable and persistent nature of the heavy metals (such as Pb, Cu, Zn, Ni, Cd, Cr, As, and Fe) mark them as a threat to the groundwater and nearby fields. This renders them as significant pollutants, the toxicity of whose is a predicament for each of the ecological, evolutionary, nutritional, and environmental reasons (Atkovska et al., 2016). The existence of heavy-metal pollutants in leachates disturbs the pore-fluid chemistry of bentonite clay particles, affecting the DDL. Besides, due to the presence of metal ions, the mineral composition of bentonite also gets altered, which consequently affects the swelling and influences the hydraulic conductivity (Dutta and Mishra, 2016a). Their toxicity is not only limited to the soil, but it has been found to have a significant impact on the water bodies (both surface and sub-surface) as well, thus rendering them a potential threat to all living entities in the natural ecosystem. Various authorities have set regulatory norms to limit the discharge of heavy metals in the environment. However, the concentrations of these elements discharged into the environment barely meet those specifications. This leads to several health hazards and environmental deterioration, necessitating the quintessential elimination of heavy metals from the water and wastewater systems.

Furthermore, estimation of the settlement of the liner material is predicted by its compressibility. The liner system gets compressed, and eventually, settle as a result of the

overloading of the wastes at the disposal sites. However, bentonite, being a highly compressible material, can get consolidated substantially. Physico-chemical and mechanical factors measure the clay particle's compressibility nature (Bolt, 1956). Short-range particle interactions such as sliding, bending, and rolling are controlled by physical properties. However, long-range particle interactions through the DDL thickness are governed by the physico-chemical properties (Mitchell and Soga, 2005). Numerous bentonite's consolidation parameters like c_v , m_v , C_c , and t_{90} are of principal concern due to their consolidation behaviour. Mishra et al. (2011) noticed a reduction in soil-bentonite mixtures' compressibility with NaCl and CaCl₂ solutions.

Moreover, hydraulic conductivity is an essential factor while designing a liner system. The liner material properties may change upon contact with leachate, which might upsurge the hydraulic conductivity value by opening the flow path and decreasing the bentonite strength as a liner material. Hence, it is quintessential to examine the variation in bentonite properties in the presence of leachate.

An extensive literature review indicates that few studies have been conducted to determine the effect of heavy metals and inorganic salts on the changes in bentonite characteristics. Most previous studies have primarily focused on the study of the hydraulic conductivity of bentonite and sorption of bentonite in the presence of various salts and metals only. Furthermore, no researches have been conducted to examine and compare the effect of fresh and synthetic MSW leachate on bentonite characteristics. As leachate produced from MSW waste comprises numerous heavy metals and inorganic salts; therefore, in comparison to single metal ions, leachate interaction will cause more complexity in the behaviour of different bentonites. Also, bentonites are observed to behave differently with the contaminants as a result of the variations in their mineralogical and chemical properties; hence, there exists a need to have a comparative assessment of their behaviours in the presence of leachates. Hence, this investigation aims at studying the effect of MSW and synthetic MSW leachates on two different bentonites possessing different chemical and mineralogical composition. Bentonites were evaluated for their liquid limit, free swell, swelling potential, swelling pressure, hydraulic conductivity, consolidation parameters, shear strength and adsorption capacity in the presence of leachates.

5.2. Results and discussion

5.2.1. Effect of MSW and synthetic MSW leachates on Liquid limit

The impact of leachates on the liquid limit of Bentonites-1 and -2 is illustrated in Fig. 5.1. The presence of leachates significantly influences the liquid limit of both the bentonites. The liquid limit decreased in the presence of synthetic MSW and MSW leachates. Bentonite-1 having a higher CEC and SSA showed a reduction in the liquid limit from 480% with DI water to 213.6% and 187.4% with Synthetic MSW and MSW leachates, respectively. However, Bentonite-2, which had a lower CEC and SSA value, the liquid limit reduced from 305 with DI water to 167.3% and 129.1% with synthetic MSW and MSW leachates, respectively. Data also illustrates that MSW leachates show a higher decrease in the value of liquid limit for both the bentonites.

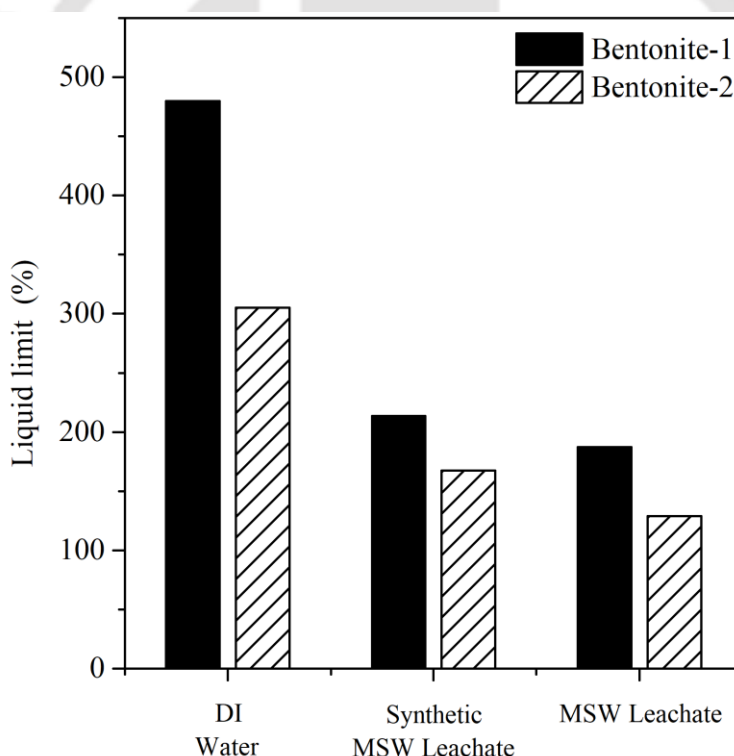


Fig. 5.1 Liquid limit of bentonites in the presence of leachates

Due to the presence of various cations in the leachates, the inter-particle repulsion force reduced, resulting in lesser inter-particle spaces and reduction in diffuse double layer thickness, causing a decline in the liquid limit. Sridharan (1975), Dutta and Mishra (2015) and Dutta and Mishra (2016b) also obtained a similar trend in the presence of various contaminants.

A comparison in the liquid limit values of both the bentonites revealed that the Bentonite-1 exhibited a higher reduction in liquid limit value in comparison to Bentonite-2 (Fig. 5.1). For Bentonite-1, a 55.5 and 65.1% decline in the liquid limit was observed for synthetic MSW and MSW leachates, respectively. However, for Bentonite-2, it was found to be 38.56 and 57.67%, respectively.

5.2.2. Effect of MSW and synthetic MSW leachates on Free swell

The influence of synthetic MSW leachate and MSW leachate on free swelling of the bentonites are illustrated in Fig. 5.2, which depicts that in the presence of both the leachates, the free swelling decreased. The higher decrease in swelling value was observed in the presence of MSW leachate for both the bentonites. Bentonite-1 showed a decline in the free swell from 32.5 mL/2g with DI water to 7.5 mL/2g and 5.5 mL/2g with synthetic MSW and MSW leachates, whereas, for Bentonite-2 it was found to be 20 mL/2g with DI water to 6.5 mL/2g and 5.0 mL/2g, respectively. Interaction of various chemicals present in the leachates with bentonites causes a decline in DDL thickness and subsequently triggering a reduction in free swell (Abd El-Aal, 2017; Dutta and Mishra, 2015; Dutta and Mishra, 2016b).

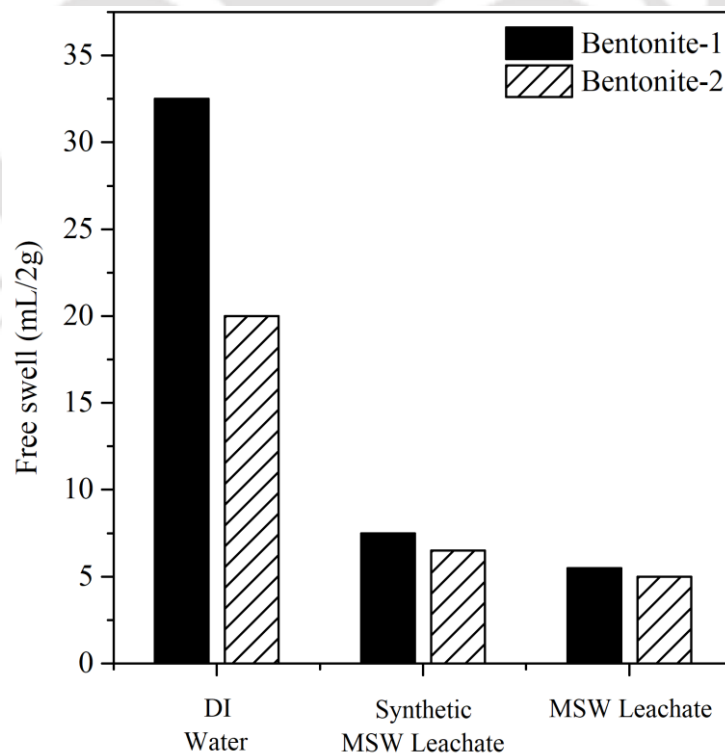


Fig. 5.2 Free swell of bentonites in presence of leachates

Bentonite-1 showed a higher reduction in swelling value as compared to Bentonite-2. A 76.9% and 83.1% decrease in the amount of free swelling was observed in the presence of synthetic MSW leachate and MSW leachate for Bentonite-1, however, for Bentonite-2 it was found to be 67.5 and 75.0%, respectively.

5.2.3. Effect of MSW and synthetic MSW leachates on swelling potential and Swelling pressure of bentonites

Table 5.1 displays the impact of synthetic MSW and MSW leachate on the swelling potential and swelling pressure of the two bentonites. It shows that both the bentonites' swelling potential reduced in the presence of both the leachates. The decline in swelling potential for leachates is owed to the decrease in DDL thickness. The swelling potential of Bentonites-1 reduced from 34.3% with DI water to 14.6 and 18.1% when permeated with synthetic MSW and MSW leachate, respectively. However, a reduction from 23.7% with DI to 13.9 and 12.7% was observed for Bentonites-2 with synthetic MSW and MSW leachate, respectively. Table 5.1 also illustrates a higher reduction in the swelling potential in the presence of both the leachates for Bentonite-1 compared to Bentonite-2.

Table 5.1. Swelling Potential and Swelling Pressure of bentonite in the presence of leachates.

| Leachates | Swelling Potential (%) | | Swelling Pressure (kPa) | |
|------------------------|------------------------|-------------|-------------------------|-------------|
| | Bentonite-1 | Bentonite-2 | Bentonite-1 | Bentonite-2 |
| DI water | 34.3 | 23.7 | 460.9 | 392.6 |
| Synthetic MSW leachate | 14.6 | 13.9 | 215.3 | 229.5 |
| MSW leachate | 18.1 | 12.6 | 201.6 | 215.0 |

Similar to the swelling potential, the swelling pressure also decreased in the presence of both the leachates (Table 5.1). In the presence of Bentonite-1, the decrease in swelling pressure was from 460.9 kPa with DI water to 215.3 kPa for synthetic MSW leachate; whereas, for Bentonite-2 it was reduced from 392.6 kPa with DI water to 229.5 kPa. Similarly, for MSW leachate, the swelling pressure decreased to 201.6 kPa and 215.0 kPa in the presence of Bentonite-1 and -2, respectively. Bentonite-1, having a higher liquid limit, CEC, and SSA experienced a higher reduction in the swelling pressure in the presence of leachates as compared to Bentonite-2. Bentonite-1 experiences swelling pressure reduction by 53.3% and 56.4% when permeated with synthetic MSW and MSW,

respectively. However, a 41.7% and 45.2% reduction was obtained for Bentonite-2 when permeated with synthetic MSW and MSW, respectively. A similar trend was obtained by Dutta and Mishra (2016b) for heavy metals (Zn^{2+} , Pb^{2+} and Cu^{2+}).

5.2.4. Effect of MSW and synthetic MSW leachates on Time swelling relationship

As the bentonite swells the inter-layer structure of the bentonite alters due to the particle–water–cation interactions. The plot in Fig. 5.3 depicts the plot between percentage swelling of bentonite and time (minute) in the presence of synthetic MSW and MSW leachate. The swelling of the expansive clay at any time was computed as the ratio of the total increase in the sample height at that time and the initial height and expressed in percentage.

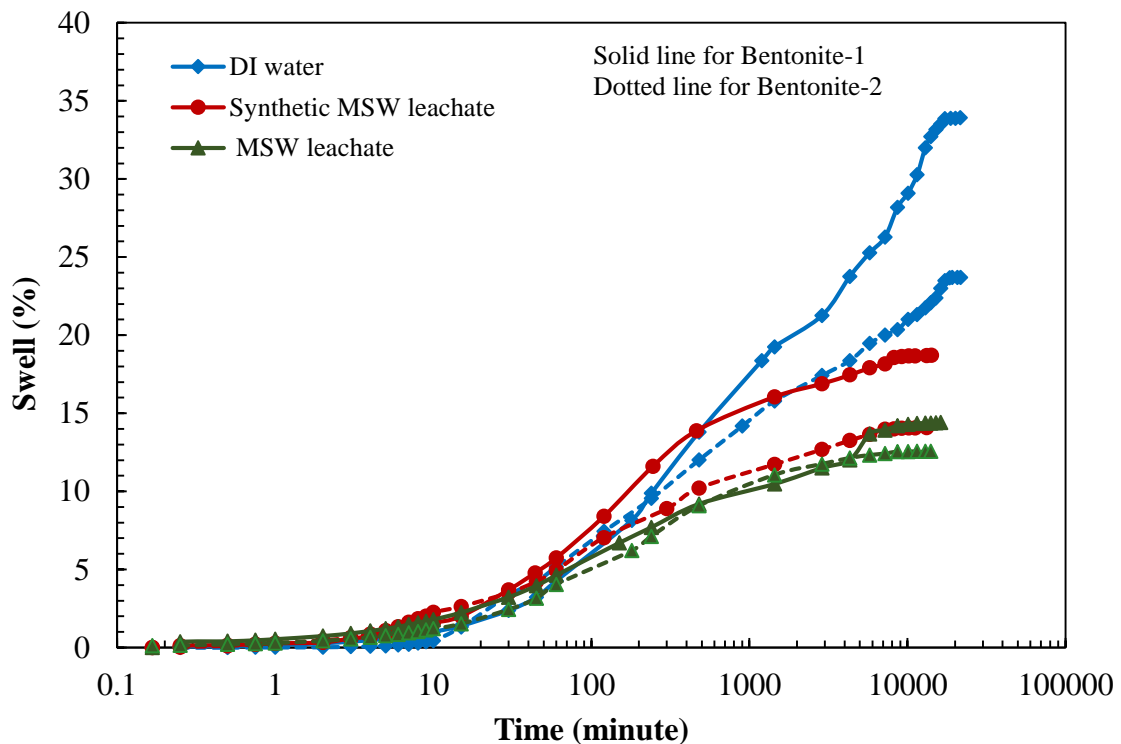


Fig. 5.3. Time–swelling plot in the presence of leachates

Regardless of the type of permeant, the plot in Fig. 5.3 followed the “S” curve. This is attributed to the fact that in the beginning, the bentonite swells gradually, and then it rises sharply and finally achieves an asymptotic value. Three stages of sample swelling, namely initial, primary, and secondary swelling (Dutta and Mishra, 2016b) were observed. The initial swelling (IS) stage comprehends only a modest increase in the swelling for all the

samples irrespective of their initial conditions, i.e., saturating liquid. On the other hand, a significant quantum of swelling was observed in the primary swelling (PS) stage. In contrast, the secondary swelling (SS) stage again witnessed marginal swelling of the samples (Fig. 5.3). The initial swelling is primarily contributed by the swelling of the macrostructure, whereas the primary and secondary swellings are attributed to the swelling of the microstructure (Dutta and Mishra, 2015). Fig. 5.3 indicates the reduction in the time taken for the initial, primary, and secondary swelling in the presence of leachates as compared to DI water.

Table 5.2. Initial swelling (IS) and Primary swelling (PS) of bentonites in the presence of leachates

| Permeant | SWELL (%) | | | | | | | |
|------------------------|-------------|---------------|--------|---------------|-------------|---------------|--------|---------------|
| | Bentonite-1 | | | | Bentonite-2 | | | |
| | IS (%) | Time (minute) | PS (%) | Time (minute) | IS (%) | Time (minute) | PS (%) | Time (minute) |
| DI water | 1 | 10 | 33.86 | 17280 | 0.42 | 10 | 23.48 | 17280 |
| Synthetic MSW leachate | 0.32 | 2 | 18.16 | 7200 | 0.27 | 1 | 14.00 | 8200 |
| MSW leachate | 0.75 | 0.46 | 14.20 | 8640 | 0.28 | 1 | 12.55 | 8640 |

Table 5.2 clearly shows that the initial swelling for synthetic MSW and MSW leachate was decreased from 10 minutes with DI water to 2 and 0.46 minutes in the presence of Bentonite-1; whereas, for Bentonite-2 it was reduced from 10 minutes with DI water to 1 minute for both leachates, respectively. Similarly, in the presence of synthetic MSW and MSW leachate, Bentonite-1 showed a reduction in the primary swelling from 17280 minutes with DI water to 7200 and 8640 minutes; however, for Bentonite-2 it was decreased from 17280 minutes with DI water to 8200 and 8640 minutes, respectively.

A comparison between both bentonites reveals that, for the same time, the swelling percentage was higher for Bentonite-1 compared to Bentonite-2 in the presence of both the leachates. This is probably due to higher CEC, SSA, and montmorillonite contents in Bentonite-1 compared to Bentonite-2.

5.2.5. Effect of MSW and synthetic MSW leachates on Hydraulic conductivity

The hydraulic conductivity has been considered as a critical parameter affecting the operation of liners and cover (Daniel and Benson, 1990). A design value of less than 1×10^{-7} cm/s for compacted clay liner has been designated by several environmental regulators (Daniel, 1984). The hydraulic conductivity of bentonites is believed to be affected by various factors, including permeant characteristics, the structure of the soil, and the void ratio (Lambe, 1958). Investigation of the hydraulic conductivity values for both the bentonites conducted at varying void ratios to determine the effects of leachates on hydraulic conductivity.

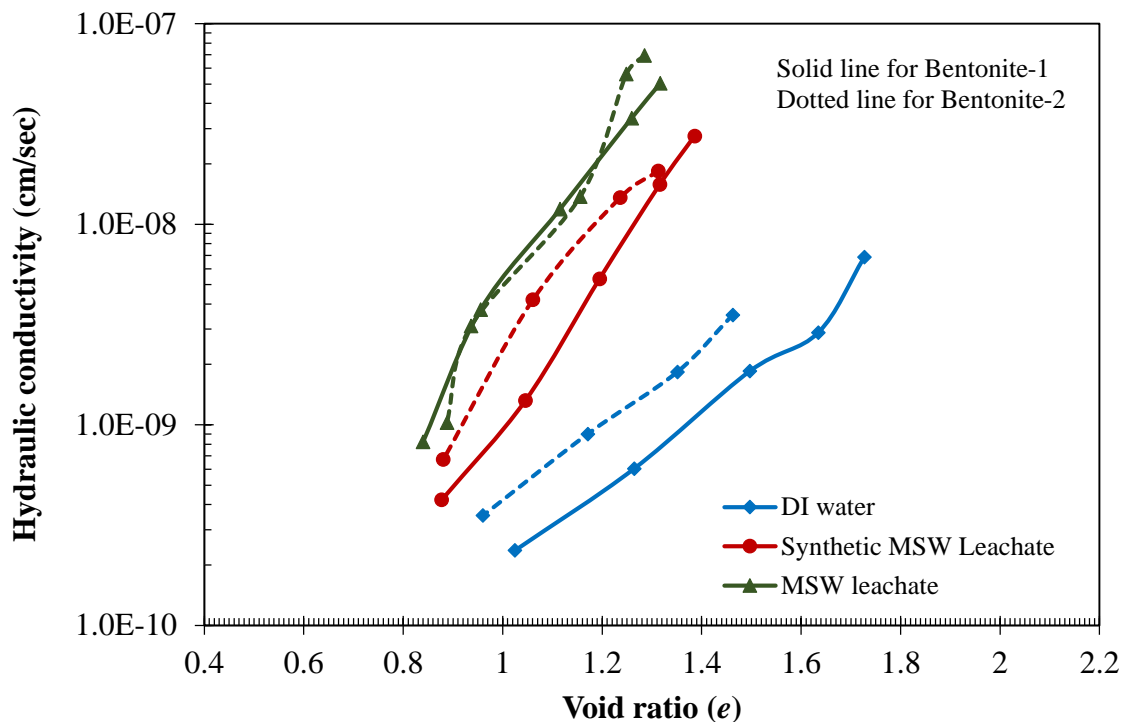


Fig. 5.4. Hydraulic conductivity of bentonites in the presence of leachates

The plot in Fig. 5.4 depicts the relationship between hydraulic conductivity and void ratio for the two bentonites in the presence of synthetic MSW and MSW leachates. The hydraulic conductivity was found to increase in the presence of both the bentonites for both the leachates. Dutta et al. (2018) observed similar kinds of trend for bentonites due to various heavy metals and salt solutions. This is attributed to a reduction in the repulsive forces among the particles of clay when it is permeated with the leachates. This decline in

the repulsive forces triggers a deterioration of the DDL thickness (Dutta and Mishra, 2016b). The plot in Fig. 5.4 depicts that the impact of leachate is more prominent in Bentonite-1. A more considerable influence of leachate on Bentonite-1 can be associated with a more significant measure of exchangeable Na^+ ions on its substitution site with respect to Bentonite-2 (Quirk and Schofield, 1955). The liquid limit, free swelling potential, and swelling pressure of both the bentonites also exhibited similar behaviours.

Furthermore, the higher value of hydraulic conductivity can be attributed to a considerable decrease in the diffuse double layer due to a higher exchange capacity of Ca^{2+} (Sposito, 1981) in the presence of MSW leachate. Bentonite pores accommodate both mobile (free to transport under the influence of hydraulic conductivity) as well as immobile water (bound by the clay layer). The increase in hydraulic conductivity as a result of the decrease in the size of the diffuse layer increases the flow of immobile water by the opening of the flow channel. This is because the amount of immobile water present depends on the thickness of the diffuse double layer of the clay surface. Hence, the reduction in the thickness in the diffuse double layer increases the hydraulic conductivity (Madsen and Mitchell, 1989; Quirk and Schofield, 1955).

Table 5.3. Hydraulic conductivity of bentonites at a void ratio of 1.2 for leachates

| Permeant | Hydraulic conductivity (cm/sec) | |
|------------------------|---------------------------------|------------------------|
| | Bentonite-1 | Bentonite-2 |
| DI Water | 4.49×10^{-10} | 1.01×10^{-09} |
| Synthetic MSW leachate | 5.86×10^{-09} | 1.15×10^{-08} |
| Fresh MSW leachate | 2.22×10^{-08} | 2.55×10^{-08} |

In order to compare both the soils in the presence of synthetic MSW and MSW leachate, hydraulic conductivity value at a void ratio of 1.2 was evaluated (Table 5.3). A comparative assessment for both the bentonite at a certain void ratio reveals that Bentonite-1 has a more significant impact than Bentonite-2. Table 5.3 indicates that for Bentonite-1 the hydraulic conductivity increased from 4.49×10^{-10} to 5.86×10^{-09} cm/sec (13.1 times) and 2.22×10^{-08} cm/sec (49.4 times) in the presence of synthetic MSW and MSW leachate; whereas, for Bentonite-2 the hydraulic conductivity value found to be increased from 1.01×10^{-09} to 1.15×10^{-08} cm/sec (11.4 times) and 2.55×10^{-08} cm/sec (25.2 times), respectively.

5.2.6 Void ratio versus pressure (e - $\log P$) relationships in the presence of leachates

The mechanical and physicochemical characteristics of the soil determine its compressibility characteristics. Physical characteristics of the soil like bending, sliding, rolling, and crushing are typically influenced by particle-to-particle interaction (Mukherjee and Mishra, 2019). The void ratio (e) and pressure (P) relationship in the presence of DI water, synthetic MSW, and MSW leachates for both the bentonite is depicted in Fig. 5.5, which reveals that the void ratio of both soils reduced with the gradual increment in pressure. The MSW leachate shows a higher reduction in the void ratio than synthetic leachate and DI water.

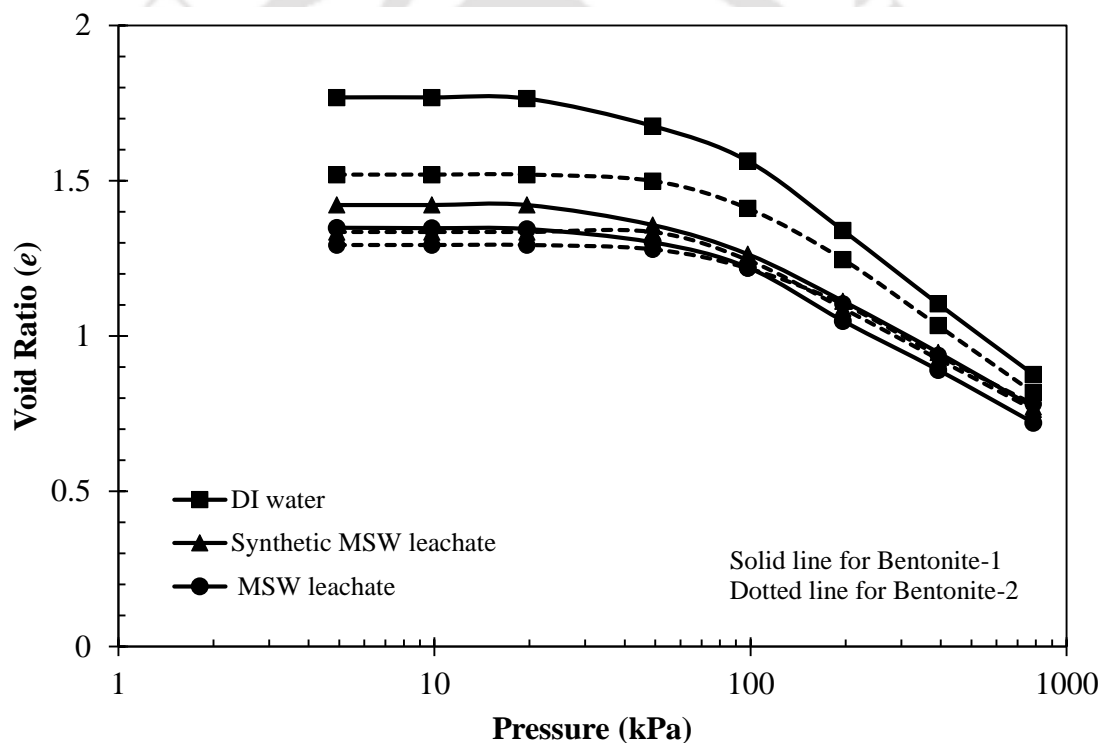


Fig. 5.5. Void ratio and Pressure relationship of bentonites in the presence of leachates

This was attributed to the inhibition of the thickness of the diffused double layer as a result of the presence of heavy metal contaminants in the leachates. The presence of pore fluid heavy metals results in more ions getting adsorbed to the clay surface, thereby, decreasing the repulsive forces. This brings the particles nearer, hence, a decline in the DDL thickness.

Comparative assessment of the compressibility of the two bentonites, as a result of the permeation of both the leachates, indicates a significant reduction in the void ratio (due to the application of pressure) for bentonite with synthetic leachate. This was primarily due to the attainment of a higher void ratio in the bentonite post saturation due to DDL growth. However, a higher concentration of heavy metals in the MSW leachate decreases the inter-particle repulsive forces, therefore, compressing the bentonite to attain a lower void ratio (Sridharan et al., 1986).

A comparative evaluation of the compressibility of the two bentonites revealed a higher void ratio reduction for Bentonite-1, compared to Bentonite-2, thus implying a higher compressibility of the superior-quality bentonite (marked by higher swelling tendency) induced by heavy-metal exposure present in the leachates. With an increase in the concentrations of the heavy metals in the pore fluid, a considerable number of cations gets dispersed in the interlayer of montmorillonite. This causes a reduction of the inter-particle counteracting forces between montmorillonite particles, resulting in the bentonite being compressed to a smaller void ratio.

5.2.7 Influence of leachates on the coefficient of consolidation (c_v)

The graph shown in Fig. 5.6 represents the relationship between the coefficient of consolidation (c_v) and consolidation pressure in the presence of leachates and DI water. Fig. 5.6 depicts that with the rise in consolidation pressure, the c_v decreases gradually. This implies a slower consolidation rate at more significant consolidating pressures. In other terms, the consolidation rate augments with the consolidation pressure application due to the existence of pore fluid heavy metals. This induces a more rapid settlement of the liner material at the waste disposal facility upon interaction with the leachate. Test results suggest that the interaction of the heavy metal ions present in the leachate with the soil pore fluid increases the degree of consolidation of the soil matrix at various loading stages.

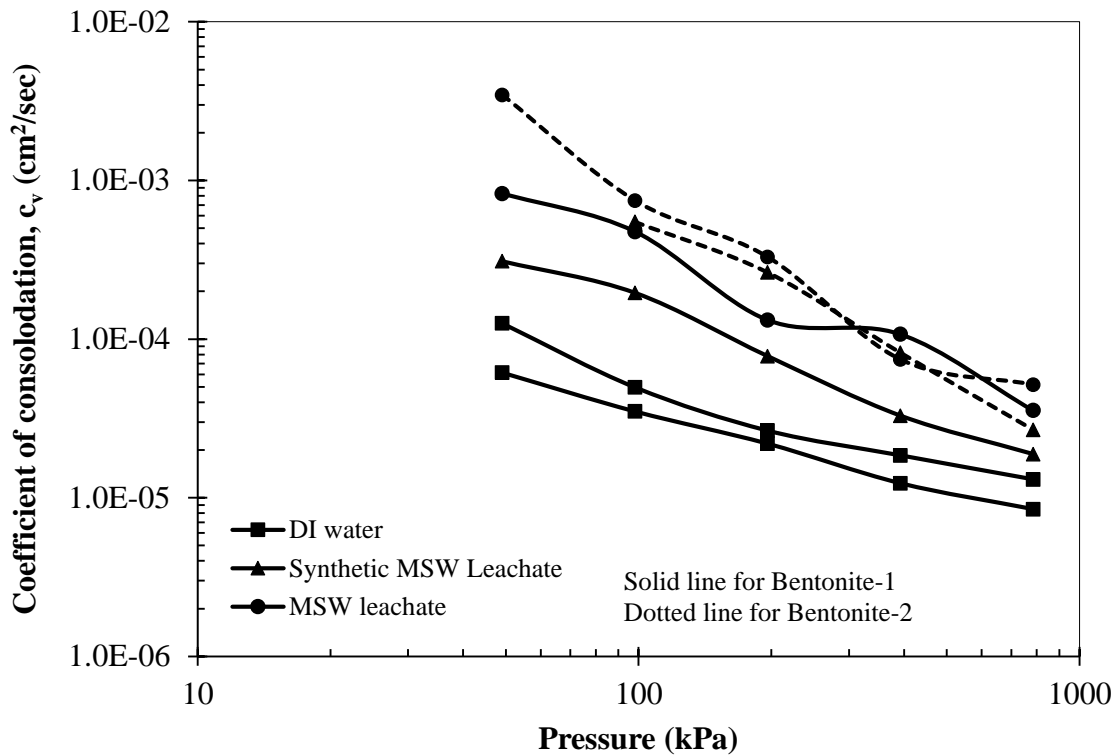


Fig. 5.6. Coefficient of consolidation (c_v) and pressure relationship for bentonites in the presence of leachates

Fig. 5.6 illustrates that, with the increase in vertical consolidation pressure from 98.1 kPa to 784.5 kPa, c_v value for Bentonite-1 and -2 permeated with DI water declined from 3.5×10^{-5} to 3.6×10^{-6} cm^2/sec (9.7 times) and 4.9×10^{-5} to 1.3×10^{-5} cm^2/sec (3.8 times). However, for Bentonite-1 & -2 the c_v value dropped from 1.9×10^{-4} to 1.8×10^{-5} cm^2/sec (10.5 times) and 5.4×10^{-4} to 2.6×10^{-5} cm^2/sec (20.8 times) in presence of synthetic MSW leachate. Similarly, for Bentonite-1 and -2 infused with MSW leachate, the c_v value reduced from 4.7×10^{-4} to 3.5×10^{-5} cm^2/sec (13.4 times) and 7.4×10^{-4} to 5.2×10^{-5} cm^2/sec (14.2 times), respectively. Physico-chemical factors of pure bentonite cause a high range of repulsive and attractive forces that control the bentonite's compressibility nature. The increase in vertical consolidation pressure results in a decrease in the DDL thickness as the clay plates come closer to each other. This closeness of the clay plates increases their repulsion, thereby, preventing further consolidation, thus decreasing the c_v value (Dutta and Mishra, 2016a).

Fig. 5.6 illustrates that the c_v value increases when the soil samples are permeated with leachates, indicating a significant rise in the consolidation rate. The DDL thickness lessens with the increase in the metal concentration, thereby reducing the clay particles' repulsive forces. This subsequently aids in the rapid consolidation of the soil samples and thus,

increasing the c_v value. A similar trend was observed by Demdoun et al. (2020) for bentonite admixtures and Dutta and Mishra (2016b) for natural bentonites. However, an utterly reverse trend was noticed by Mishra et al. (2010) for sand-bentonite mixtures.

5.2.8 Influence of leachates on Time for 90% of Consolidation (t_{90})

The graph displayed in Fig. 5.7 shows the relationship between t_{90} of different bentonites and vertical consolidation pressure in the presence of MSW and synthetic MSW leachates. It indicates that the t_{90} value rises corresponding to a rise in the vertical consolidation pressure. With the consolidation pressure increment, there is a movement of the clay plates towards each other. As the clay surface is negatively charged, this makes the clay plates repel from each other, thereby preventing any further movement, thus, decreasing the c_v values and increasing the t_{90} values Dutta and Mishra (2016b). With a rise in vertical consolidation pressure from 9.8 to 784.5 kPa, the t_{90} value rises from 51.8 to 353.4 minutes and 18.5 to 249.6 minutes for Bentonite-1 and -2 in the presence of synthetic MSW leachate. Similarly, in MSW leachate's presence, the t_{90} rises from 20.2 to 179.6 minutes and 12.9 to 132.2 minutes for Bentonite-1 and -2, respectively. The graph represents that the reduction in t_{90} value was more in the case of MSW leachate.

The graph in Fig. 5.7 also depicts that in the presence of both the leachates, t_{90} of both the bentonites reduced. Since, in the presence of leachate, c_v value rises, the time needed for accomplishing the desired degree of consolidation falls, thereby falling the t_{90} values. Dutta and Mishra (2017) observed a similar pattern in the presence of various metal ions. Comparing both bentonites reveals that Bentonite -1 is highly influenced by the presence of leachates compared to Bentonite-2. In the presence of synthetic MSW and MSW leachates, at 784.5 kPa the t_{90} value reduced from 900.0 minutes with DI water to 353.4 and 179.6 minutes (60.7% and 80.0% reduction) for Bentonite-1; whereas, for Bentonite-2 it was found to be declined from 564.1 minutes with DI water to 249.6 and 132.2 minutes (55.7% and 76.5% reduction), respectively. The graph in Fig. 5.7 illustrates that t_{90} value of the soil sample is influenced not only by the bentonite type but also on the permeants. Bentonite -1 having higher SSA, CEC, liquid limit, and montmorillonite content show a higher value of t_{90} as compared to Bentonite-2.

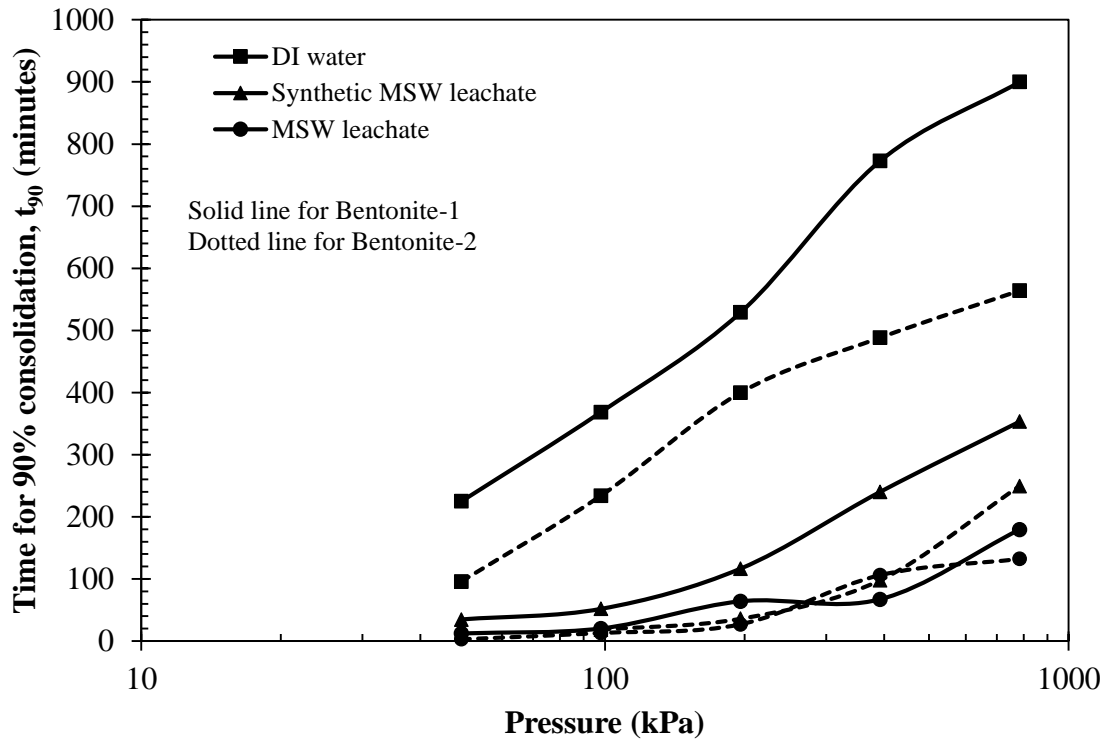


Fig. 5.7. Time for 90% consolidation (t_{90}) and pressure relationship for bentonites in the presence of leachates

5.2.9 Impact of leachate on compression index (C_c) of bentonites

Table 5.4 shows the compression index (C_c) value of the bentonites in the presence of DI water, MSW, and synthetic MSW leachates.

Table 5.4. Compression index of Bentonites-1 and -2 in presence of various leachate.

| Permeant | Compression Index (C_c) | |
|------------------------|-----------------------------|-------------|
| | Bentonite-1 | Bentonite-2 |
| DI water | 0.79 | 0.72 |
| Synthetic MSW leachate | 0.58 | 0.54 |
| MSW leachate | 0.56 | 0.52 |

Table 5.4 shows that in the presence of leachates, the C_c value is reduced. Heavy metal contaminants in leachates aid in decreasing the DDL, thereby resulting in the agglomeration of clay particles. This resists settlement, thus lowering the C_c value. Table 5.4 shows that C_c of the Bentonite-1 and -2 in the presence of DI water was found to be 0.79 and 0.72. In the presence of synthetic leachates, the C_c of Bentonite-1 and -2 are declined by 26.6% and

25.0%. However, in the presence of MSW leachate, the C_c value was reduced by 29.1% and 27.7% for Bentonite-1 and -2, respectively.

As compared to Bentonite-2, the decrease in C_c value was more prominent in the case of Bentonite-1. A higher SSA, CEC, and montmorillonite content in Bentonite-1 resulted in a thicker DDL with DI water. However, the thickness reduced considerably due to metal content in leachates, thus suppressing the clay particles to a lower void ratio.

5.2.10 Influence of leachates on unconfined compressive strength of both bentonites

The plot in Fig. 5.8 depicts the stress-strain relationship for different bentonites in the presence of DI water and leachates. It illustrates that in DI water's presence, at an extreme strain level of 6.32% and 5.53%, the failure occurs for Bentonite-1 and -2. However, in synthetic leachate, the failure was observed at 3.68% and 3.15% strain level for Bentonite-1 and -2. Similarly, for MSW leachate, the failure strain level was 3.94 and 3.95% for the bentonites, respectively.

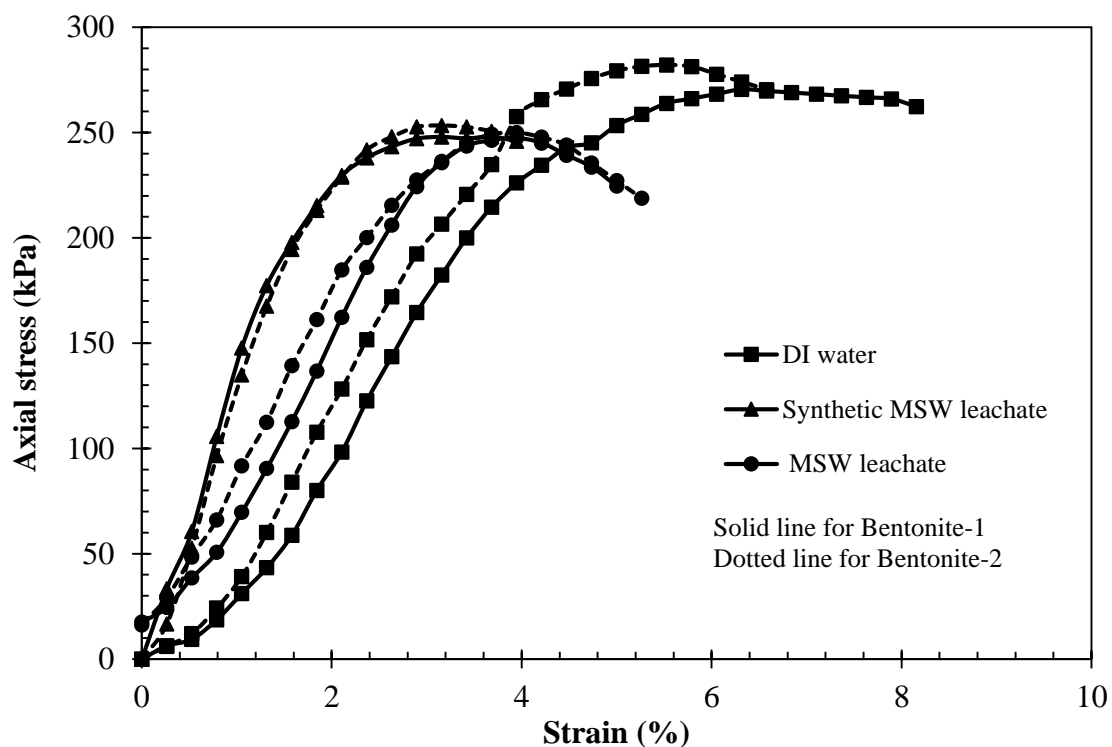


Fig. 5.8. Axial stress (kPa) vs strain (%) relationship of the bentonites in the presence of leachates

The unconfined compressive strength of both the bentonites in the presence of DI water and leachates is tabulated in Table 5.5. Table 5.5 clearly shows that the strength of the bentonite reduced in the presence of both the leachates. The strength of Bentonite-1 reduced by 8.3 and 8.5% in the presence of synthetic MSW and MSW leachate; whereas, the corresponding reduction for Bentonite-2 was 10.2 and 11.3%, respectively. The reduction in the unconfined compressive strength due to leachate can be attributed to a decrease in the density of the specimen. Since the MDD of specimen increases due to the permeation of contaminant (Abd El-Aal, 2017) and samples were compacted at MDD corresponding to DI water, the specimens permeated with leachate were in loosen state. Therefore, the unconfined compressive strength of the specimen decreased with the permeation of the leachate.

Table 5.5. Unconfined compressive strength of both bentonites in the presence of leachates.

| Permeant | Unconfined compressive strength (kPa) | |
|------------------------|---------------------------------------|-------------|
| | Bentonite-1 | Bentonite-2 |
| DI water | 270.5 | 282.1 |
| Synthetic MSW leachate | 248.0 | 253.4 |
| MSW leachate | 247.4 | 250.1 |

Higher strength for Bentonite-2 is observed. The reason is the lower liquid limit value and DDL thickness of Bentonite-2, causing a closer grain to grain contact and hence exhibits higher strength value. Table 5.5 also depicts that bentonites with MSW leachate exhibit lower strength value.

5.2.11. Adsorption of MSW and synthetic MSW leachate

In the same landfill system, a various number of heavy metals always present collectively. Thus, the adsorption behaviour of bentonites for MSW and synthetic MSW leachate was investigated in a competitive system. The composition of both the leachates is presented in Table 5.6 and 5.7.

The removal percentage of individual metal ions is depicted in Fig 5.9. In the present study, most of the metal ions present in real and synthetic leachates are found to be effectively removed by both the bentonites. Above 80% removal was observed for Pb, Cu, Fe and Mg for MSW and synthetic MSW leachate in the presence of both the bentonites. The study was conducted at a controlled temperature of $28 \pm 1^\circ\text{C}$ and at $\text{pH } 5.0 \pm 0.2$ for

MSW and synthetic MSW leachate. Highest removals were observed in Fe followed by Mg, Cu, Zn, Pb, Mn and Ca for both the bentonites (Table 5.6). Anna et al. (2015) reported that for disposed wastewater of a locally plating factory, 100% removal was obtained for Fe by using natural bentonite. They also observed a 73.7, 71.2 and 49.0% removal for Zn, Cu and Ni, respectively.

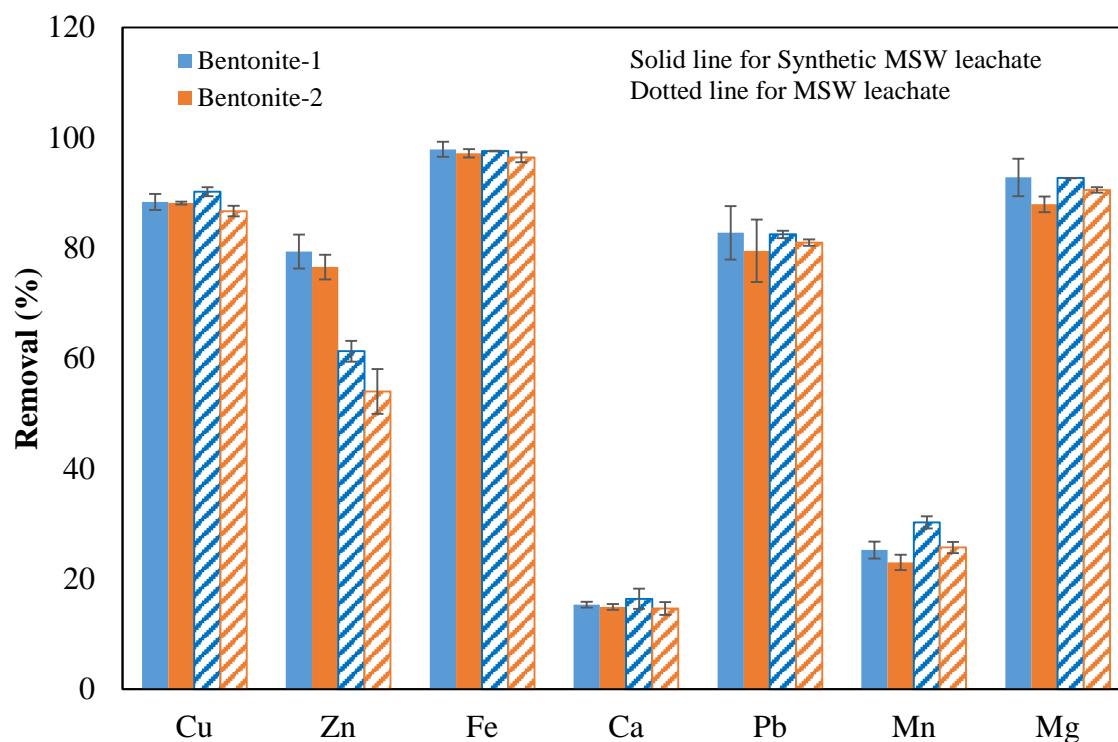


Fig. 5.9. Removal of heavy metal from MSW and synthetic MSW leachate by bentonites

In the present investigation, a higher amount of Ca was present in both the leachates, i.e., 4781 (MSW leachate) and 3324 mg/L (synthetic MSW leachate). Presence of higher concentrations of calcium may suppress other metal ions to adsorb on the surface of bentonites. It was observed that for MSW leachate, the concentrations of Ca reduced from 4781.0 mg/L to 3996.3 and 4079.9 mg/L in the presence of Bentonite -1 & 2, respectively. Likewise, for synthetic leachate, it decreased from 3324.0 mg/L to 2813.7 and 2827.7 mg/L, respectively. Fig. 5.9 depicts a 16.4 and 14.6% Ca removal for MSW leachate in the presence of Bentonite -1 and -2, respectively. Similarly, for synthetic MSW leachate 15.3 and 14.9% of removal was observed in the presence of Bentonite -1 and -2, respectively. The detailed removal of heavy metals from MSW and synthetic MSW leachate by both the bentonites are listed in Tables 5.6 and 5.7.

A higher amount of removal was observed in the presence of Bentonite-1 as compared to Bentonite-2 for synthetic and MSW leachate. The removal of Cu^{2+} , Zn^{2+} , Fe^{2+} , Ca^{2+} , Pb^{2+} , Mn^{2+} and Mg^{2+} were found to be 3.8, 11.9, 1.2, 10.6, 1.8, 14.9, and 2.3% higher for a Bentonite-1, respectively, as compared to Bentonite-2. Likewise, for synthetic leachate 0.2, 3.5, 0.7, 2.7, 3.9, 8.9, and 5.3% higher removal for Cu^{2+} , Zn^{2+} , Fe^{2+} , Ca^{2+} , Pb^{2+} , Mn^{2+} and Mg^{2+} was obtained by Bentonite-1 in comparison to Bentonite-2, respectively. The overall adsorption capacity of Bentonite-1 was found to be 17.9 and 21.4 mg/g in the presence of MSW and synthetic MSW leachate; whereas, 16.6 and 20.7 mg/g of adsorption capacity was obtained for Bentonite-2, respectively.

Table 5.6. Removal of heavy metal from MSW leachate by bentonites.

| MSW Leachate | Heavy metal | pH | Concentration (mg/L) | | Removal (%) | Adsorption capacity (mg/g) |
|--------------|-------------|---------|-----------------------|------------------|-------------|----------------------------|
| | | | Initial Concentration | After adsorption | | |
| Bentonite-1 | Cu | 5.4±0.2 | 1.14 | 0.11 | 90.2 | 0.02 |
| | Zn | | 20.62 | 7.98 | 61.3 | 0.25 |
| | Fe | | 150.00 | 3.61 | 97.6 | 2.85 |
| | Ca | | 4781.00 | 3996.31 | 16.4 | 10.68 |
| | Pb | | 2.86 | 0.50 | 82.5 | 0.05 |
| | Mn | | 19.04 | 13.28 | 30.2 | 0.11 |
| | Mg | | 222.90 | 16.26 | 92.7 | 4.02 |
| Bentonite-2 | Cu | 5.4±0.2 | 1.14 | 0.15 | 86.7 | 0.01 |
| | Zn | | 20.62 | 9.48 | 54.0 | 0.21 |
| | Fe | | 150 | 5.34 | 96.4 | 2.82 |
| | Ca | | 4781 | 4079.98 | 14.6 | 9.55 |
| | Pb | | 2.86 | 0.54 | 80.9 | 0.01 |
| | Mn | | 19.04 | 14.14 | 25.7 | 0.09 |
| | Mg | | 222.90 | 21.12 | 90.5 | 3.93 |

Variation in the physical and chemical characteristics of the adsorbents such as cations associated at the exchangeable sites, swelling capacity, specific surface area (SSA) and montmorillonite content causes the difference in their sorption capacity ((Vimonses et al., 2009). Montmorillonite adsorbs water molecules within its layers due to the higher sorption

capacity. This inherent characteristic of montmorillonite causes significant swelling of bentonite clay (aluminium phyllosilicate) for which it is a primary mineral. Various metal ions also get adsorbed on the outer and inner surfaces of the montmorillonite. Sorption through the cation exchange takes place in the internal surface of the montmorillonite; whereas, at the external surface of the montmorillonite, sorption happens due to formation Al–O and Si–O groups.

Table 5.7. Removal of heavy metals from synthetic MSW leachate by bentonites.

| Synthetic MSW Leachate | Heavy metal | pH | Concentration (mg/L) | | Removal (%) | Adsorption capacity (mg/g) |
|------------------------|-------------|---------|-----------------------|------------------|-------------|----------------------------|
| | | | Initial concentration | After adsorption | | |
| Bentonite-1 | Cu | 5.2±0.2 | 6 | 0.69 | 88.4 | 0.09 |
| | Zn | | 36 | 7.44 | 79.3 | 0.53 |
| | Fe | | 153 | 3.24 | 97.9 | 3.02 |
| | Ca | | 3324 | 2813.75 | 15.3 | 9.61 |
| | Pb | | 2.1 | 0.36 | 82.8 | 0.03 |
| | Mn | | 16.2 | 12.11 | 25.2 | 0.08 |
| | Mg | | 443 | 31.82 | 92.8 | 8.06 |
| Bentonite-2 | Cu | 5.2±0.2 | 6 | 0.71 | 88.2 | 0.09 |
| | Zn | | 36 | 8.42 | 76.6 | 0.51 |
| | Fe | | 153 | 4.32 | 97.2 | 2.99 |
| | Ca | | 3324 | 2827.68 | 14.9 | 9.35 |
| | Pb | | 2.1 | 0.43 | 79.5 | 0.03 |
| | Mn | | 16.2 | 12.48 | 22.9 | 0.07 |
| | Mg | | 443 | 53.47 | 87.9 | 7.63 |

Cation exchange is predominant in the inter surfaces due to the presence of a higher quantity of surface layer charges within the inner surfaces compared to the quantity charges on the edge of the outer surfaces. Two tetrahedral and one octahedral layer built the crystal structure of the montmorillonite where the central tetravalent silicon (Si^{4+}) within the tetrahedral layers could be swapped by trivalent aluminium ions (Al^{3+}), whereas, divalent cations like Mg^{2+} and Fe^{2+} could exchange the trivalent aluminium ions (Al^{3+}) in the octahedral layers. This phenomenon causes the negatively charged layers within the inner

surfaces, which are mainly neutralized by the hydrated cations. Electrostatic forces help to bind the cations to the internal surfaces which can be substituted with other cations. Suppose the size of the cation is alike to the pore size of the montmorillonite crystal structure. In that case, the cations bind into the crystal structure resulting reduction in the negatively charged layer (Vimonses et al., 2009).

5.2.12. Effect of MSW and synthetic MSW leachate on dose of bentonites

The adsorbent dosage studies were carried out for varying bentonite amounts, ranging from 0.2 to 5.0 g/ 100 mL leachate solution, the results of which are depicted in Fig. 5.10-5.13. It was observed that the adsorbed metal ions (i.e. their removal efficiencies) increased with increasing adsorbent dosage, primarily attributing to an increase in the clay concentration that increases the surface area of the adsorbent, which in turn, increases the number of binding sites for the same liquid volume (Anna et al., 2015; Sen and Gomez, 2011). The removal efficiency was found to be increased from 59.3 to 83.3 (Pb), 29.7 to 91.2 (Cu), 12.1 to 62.5 (Zn), 4.5 to 31.6 (Mn), 18.6 to 97.6 (Fe), 2.6 to 18.8 (Ca) and 18.9 to 92.8 (Mg) % for Bentonite-1 and 55.7 to 81.6 (Pb), 28.8 to 87.3 (Cu), 10.1 to 59.7 (Zn), 2.9 to 26.9 (Mn), 16.8 to 95.1 (Fe), 2.1 to 16.1 (Ca) and 16.7 to 90.9 (Mg) % with the gradual increase in bentonite dose of 0.2 to 5 g for MSW leachate in the presence of Bentonite-2, respectively. Likewise, for synthetic MSW leachate, the removal efficiency raised from 72.1 to 88.3 (Pb), 18.8 to 89.6 (Cu), 16.6 to 82.8 (Zn), 12.6 to 24.2 (Mn), 50.7 to 99.5 (Fe), 1.8 to 15.9 (Ca) and 31.7 to 92.2 (Mg) % in the presence of Bentonite-1 and 71.9 to 85.9 (Pb), 19.9 to 87.9 (Cu), 15.4 to 78.9 (Zn), 11.9 to 23.9 (Mn), 44.9 to 98.1 (Fe), 1.4 to 15.5 (Ca) and 30.2 to 88.4 (Mg) % for Bentonite-2, respectively. Bentonite-1 showed higher removal and adsorption capacity as compared to Bentonite-2.

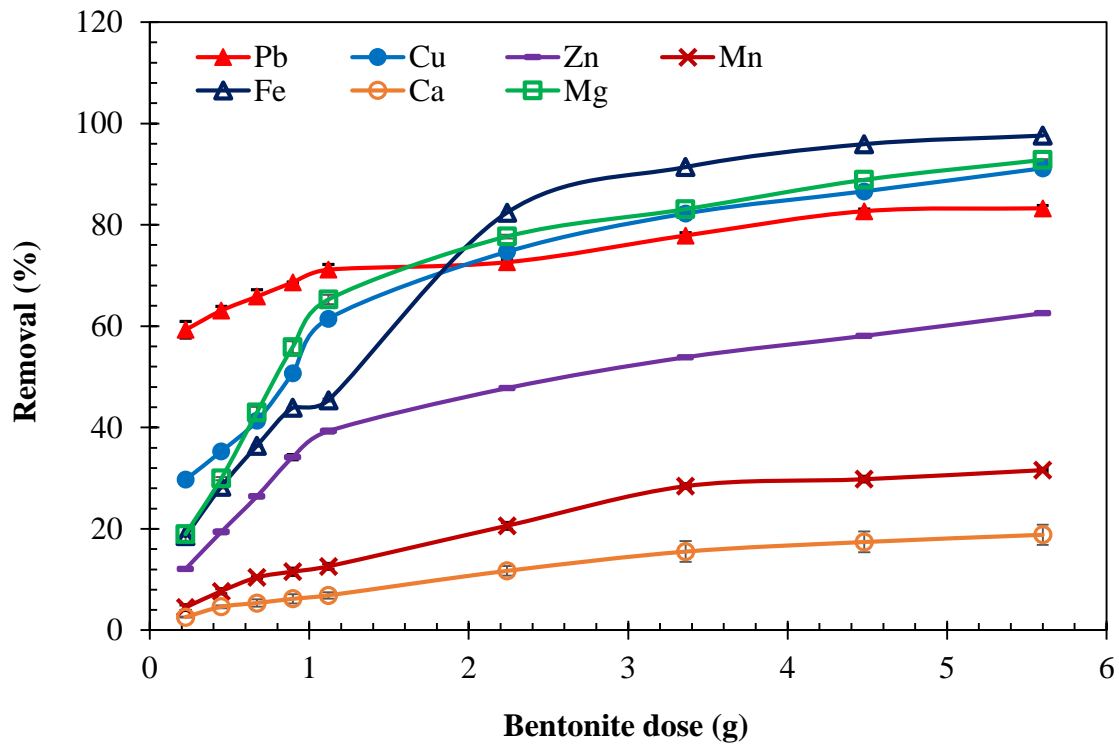


Fig. 5.10. Removal % of MSW leachate at different bentonite dosage for Bentonite-1

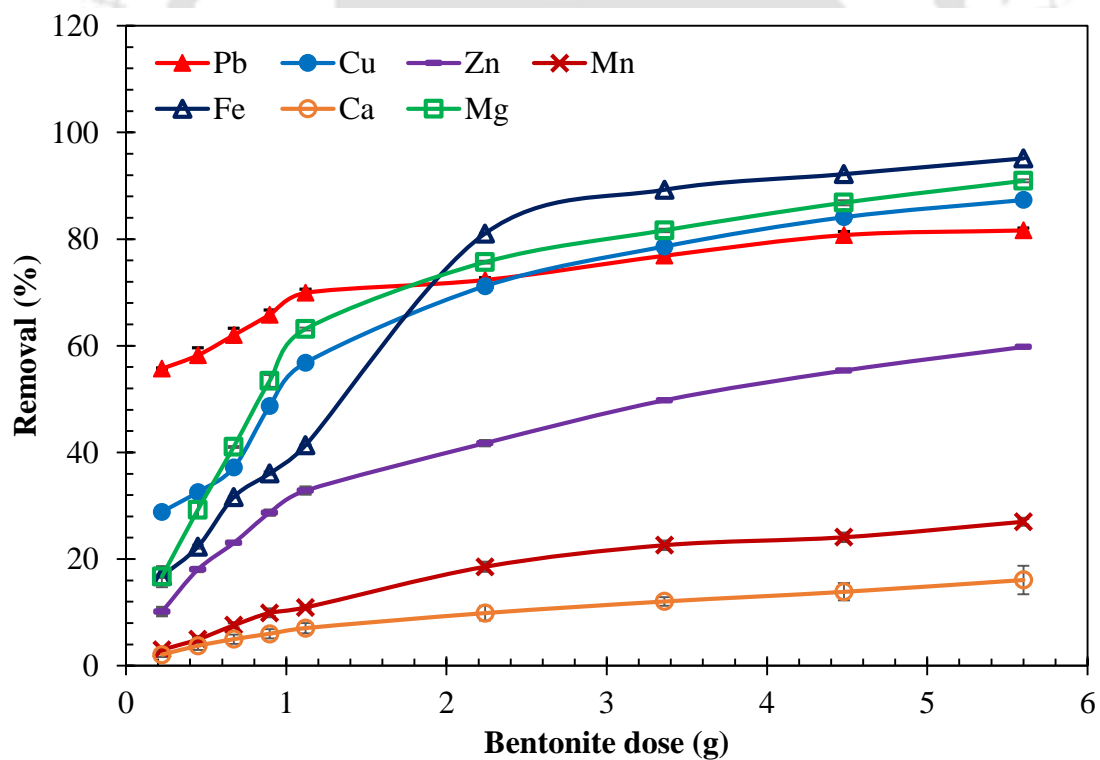


Fig. 5.11. Removal % of MSW leachate at different bentonite dosage for Bentonite-2

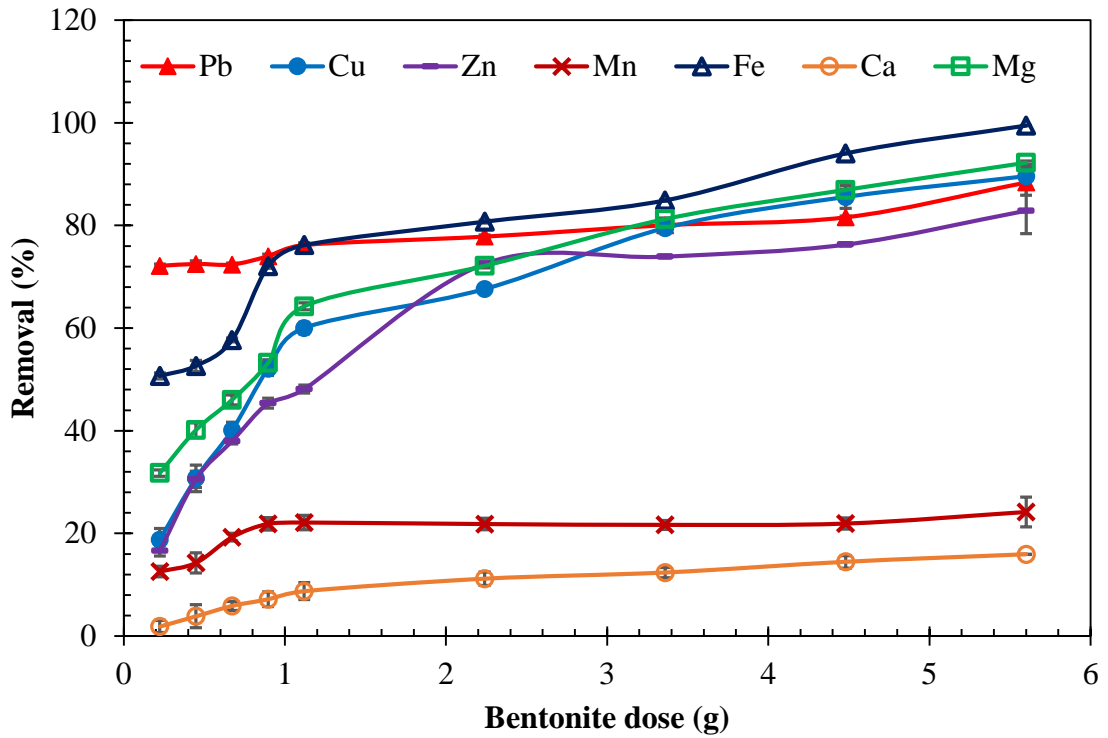


Fig. 5.12. Removal % of synthetic MSW leachate at different bentonite dosage for Bentonite-1

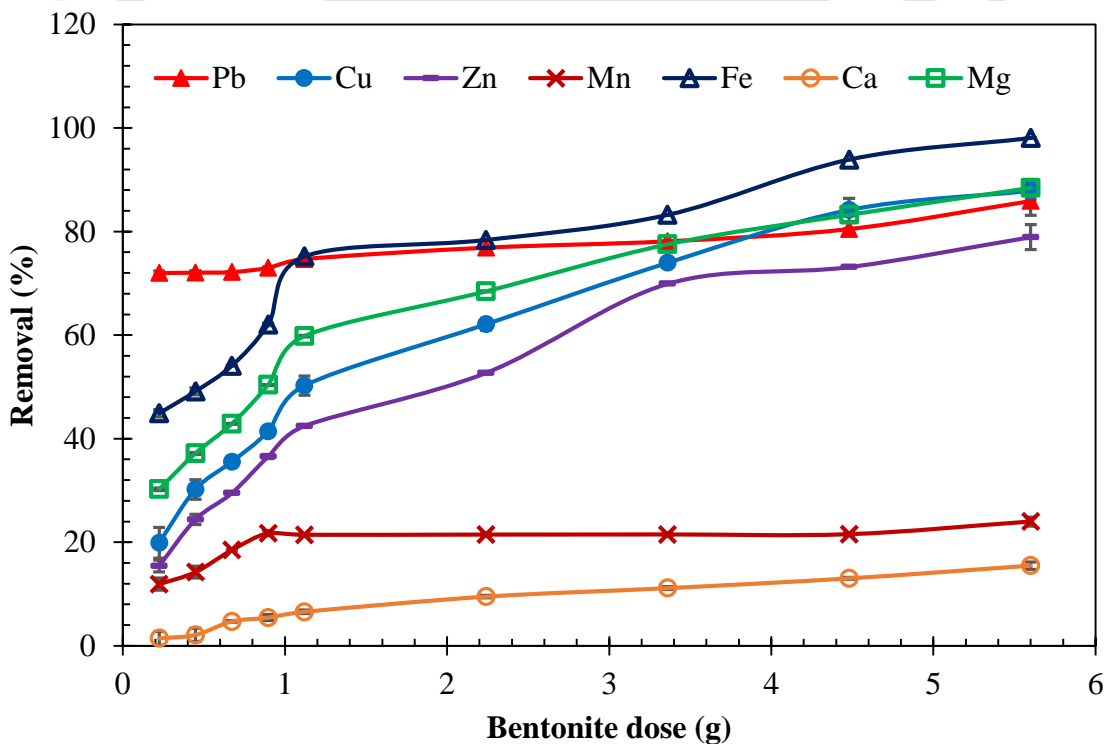
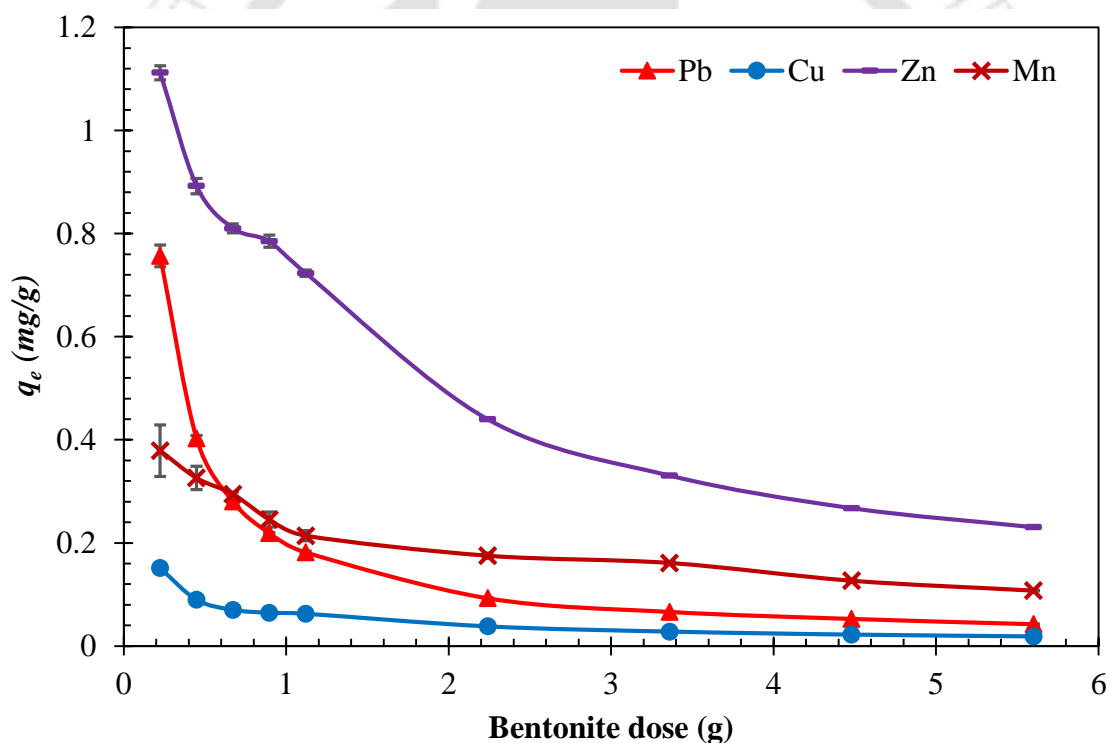
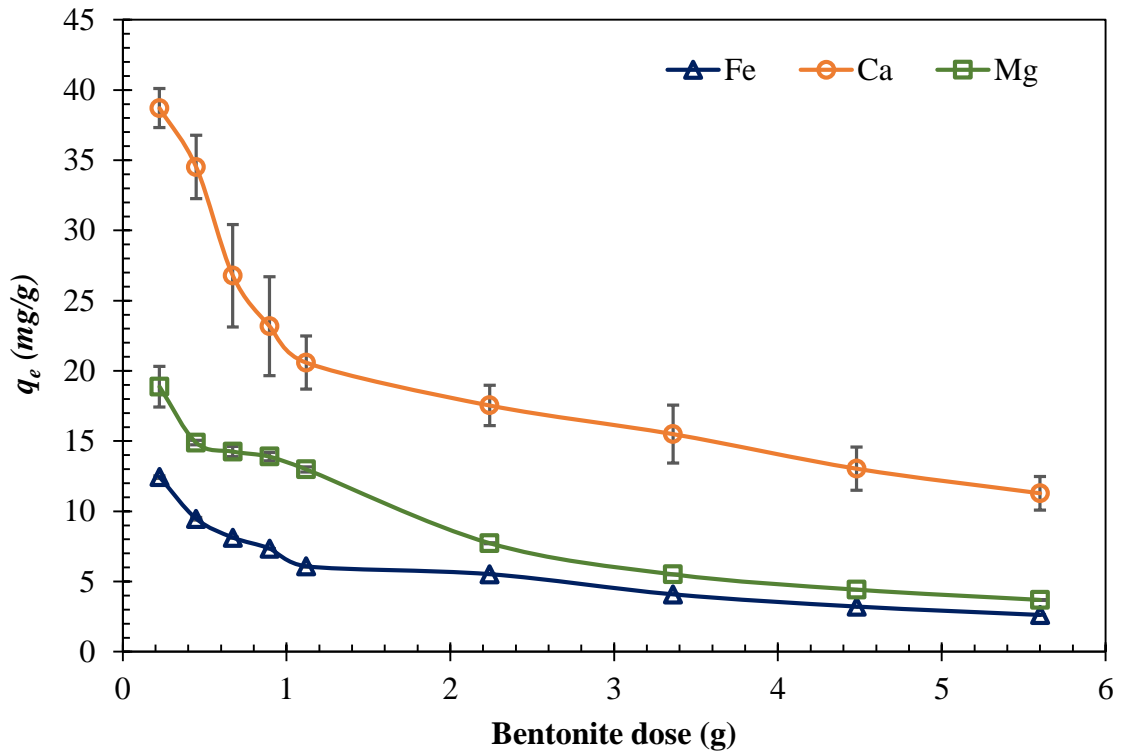


Fig. 5.13. Removal % of synthetic MSW leachate at different bentonite dosage for Bentonite-2

Furthermore, it was observed (Fig. 5.14 - 5.17) that the number of metal ions adsorbed per unit mass reduced progressively with an increase in the bentonite content. This shows that during the initial phase, a vast number of active sites are available for sorption. At high mineral concentrations, the available metal concentration is insufficient to cover the exchangeable sites on the adsorbent completely, usually resulting in low metal adsorption capacity (Anna et al., 2015; Yang et al., 2010). Besides, with an increase in the clay fraction increases the likelihood of collision between solid particles. It is, therefore, may create particle aggregation, causing a decrease in the total surface area and an increase in diffusional path length, both of which contribute to the decrease in the sorption capacity of metal ions on bentonite (Anna et al., 2015; Shukla et al., 2002). The same behaviour of other adsorbent material on metal ion adsorption has also been described (Anna et al., 2015; Chen et al., 2012; Gupta and Bhattacharyya, 2008; Vieira et al., 2010).

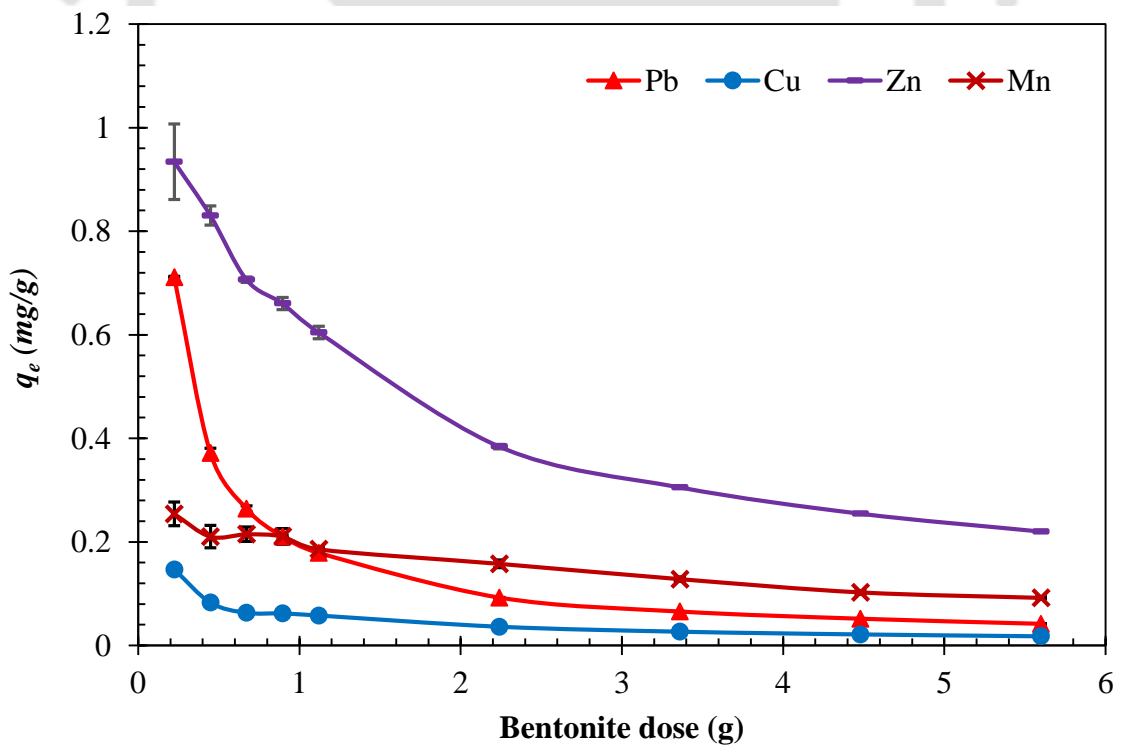


(a)

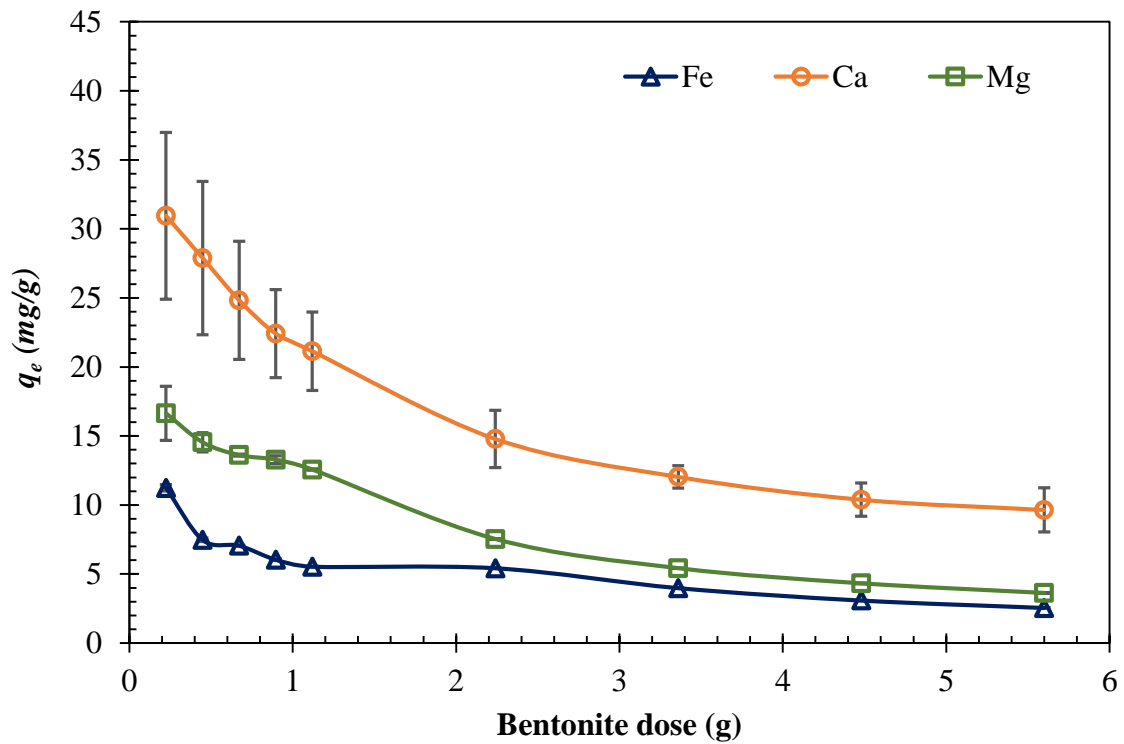


(b)

Fig. 5.14. Amount of MSW leachate adsorbed by Bentonite-1 at various bentonite dose

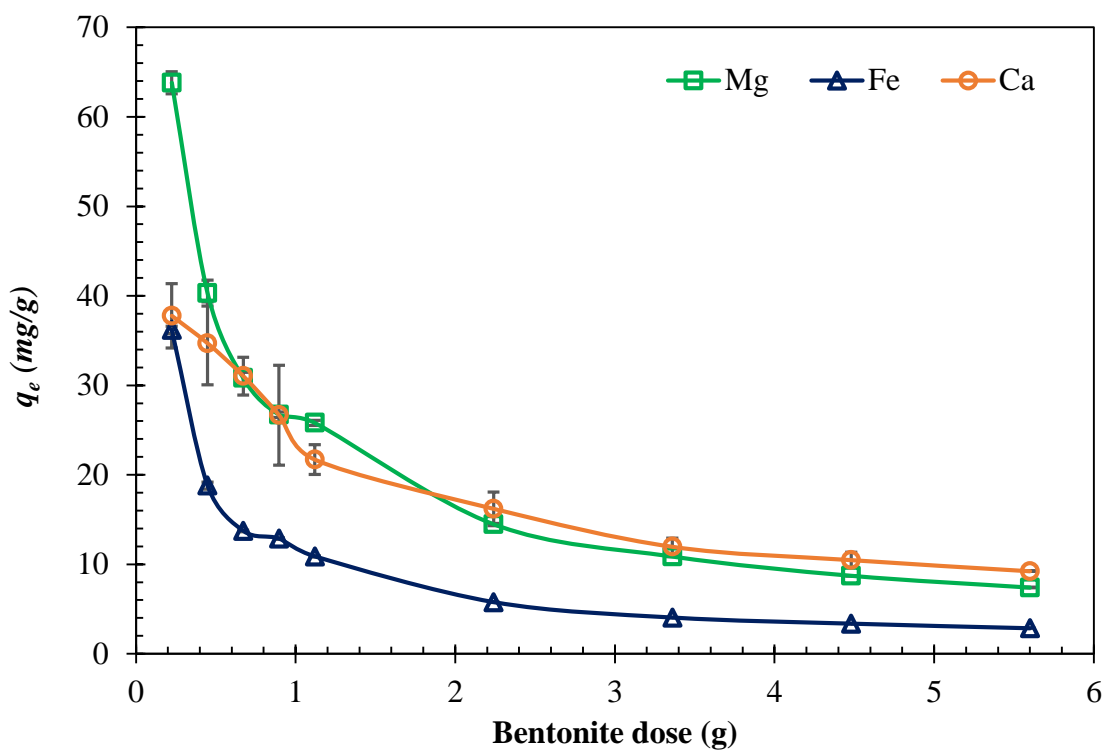


(a)

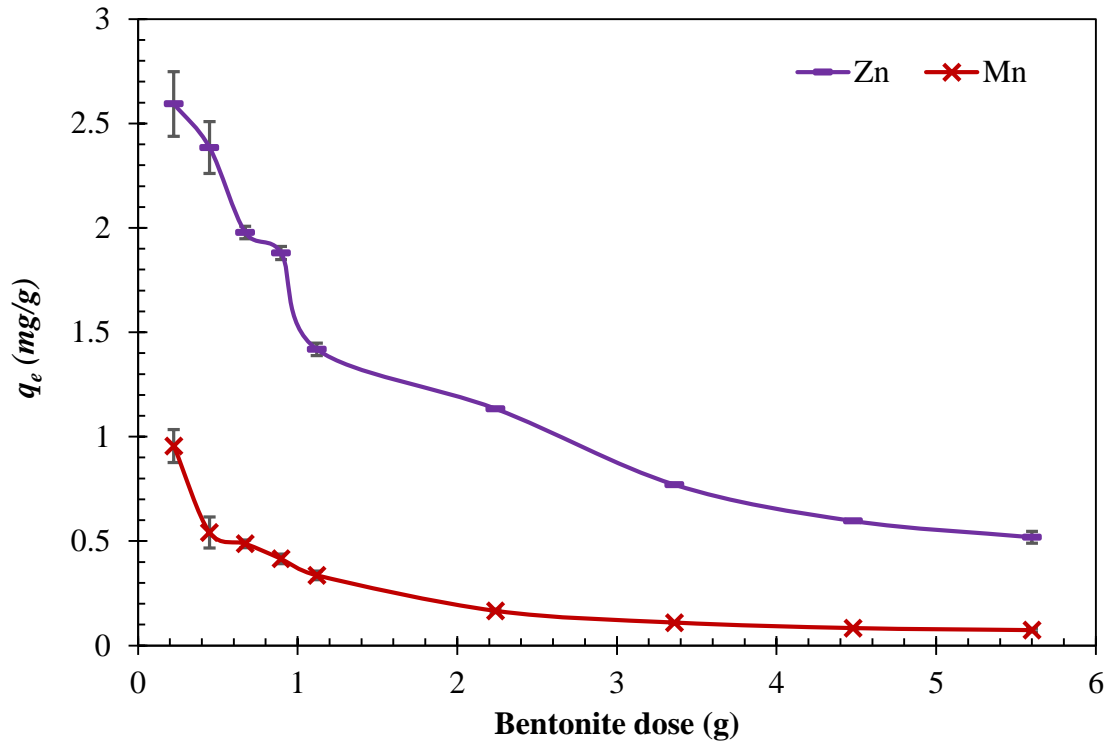


(b)

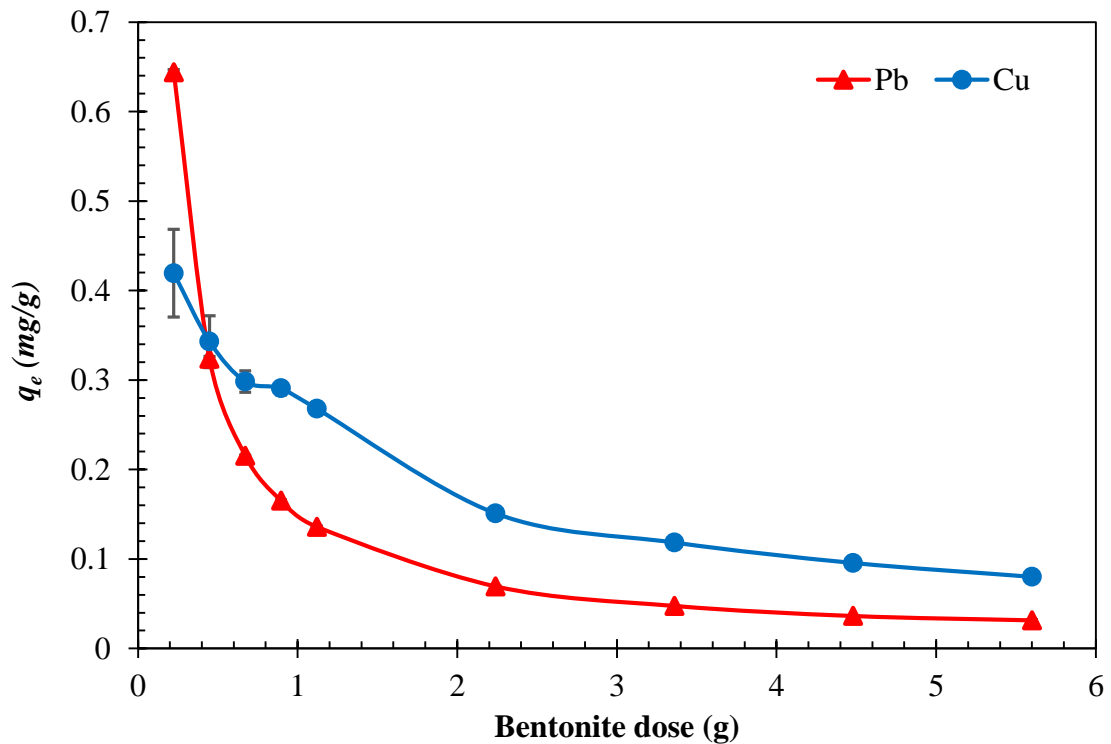
Fig. 5.15. Amount of MSW leachate adsorbed by Bentonite-2 at various bentonite dose



(a)

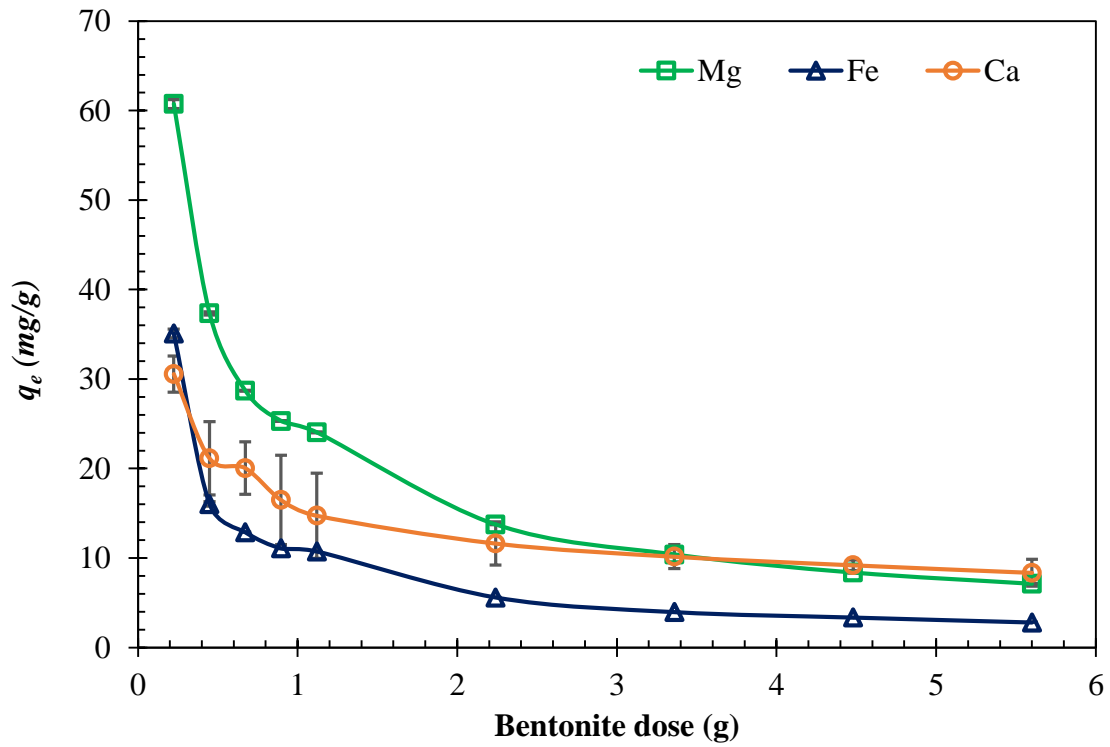


(b)

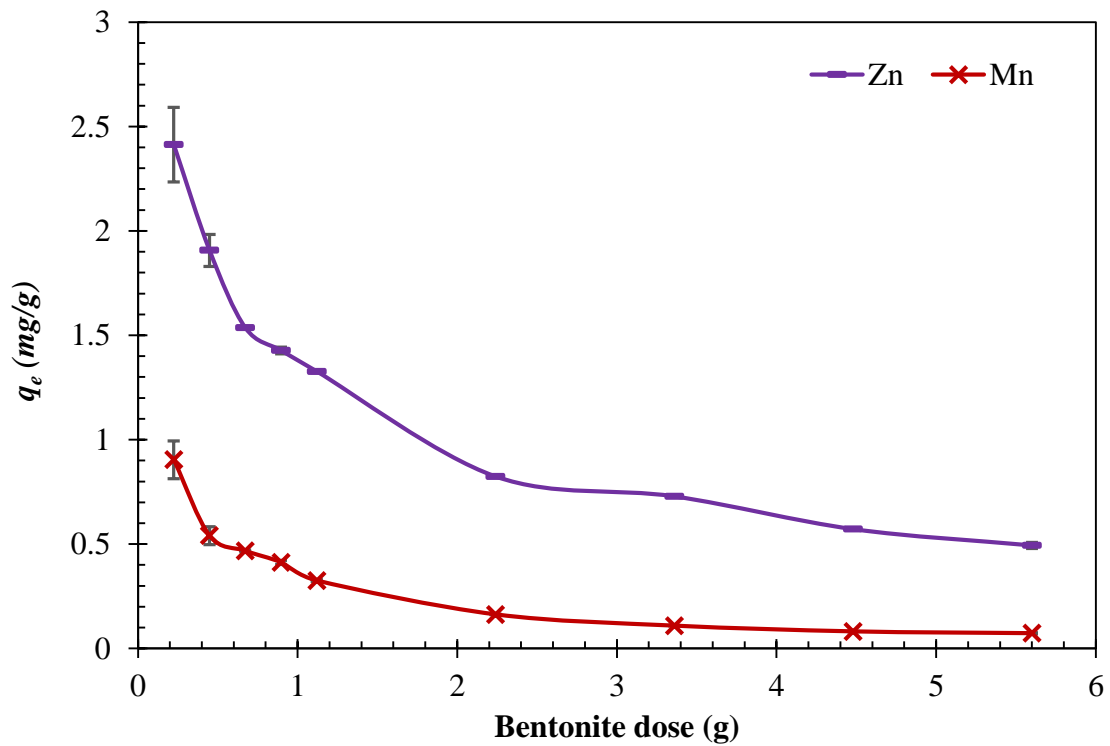


(c)

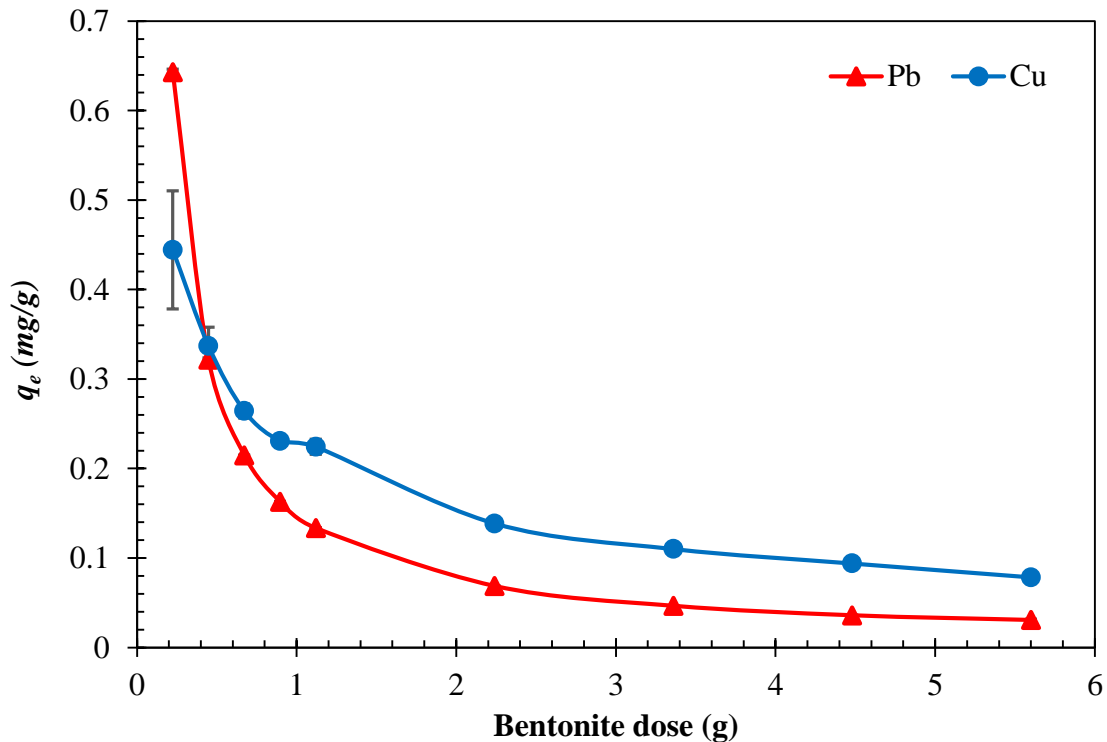
Fig. 5.16. Amount of synthetic MSW leachate adsorbed by Bentonite-1 at various bentonite dose



(a)



(b)



(c)

Fig. 5.17. Amount of synthetic MSW leachate adsorbed by Bentonite-2 at various bentonite dose

5.2.13. Kinetic study of MSW and synthetic MSW leachate

5.2.13.1. Effect of Contact time

For designing a barrier material at the waste disposal system, the time of contact between the pollutant and the adsorbent is very vital. The usefulness of the adsorbent as a barrier material for the usage in a garbage disposal system is indicated by its quick uptake of pollutants and attainment of equilibrium in a short duration. A more rapid rate of adsorption was observed for the first 20 minutes. However, to confirm the maximum removal of metal ions, the 200-minute contact time was selected in all trials conducted. Fig. 5.18 to 5.21 displays that the curve of contact time becomes smooth and steady-state, and a plateau was visible after 120 minutes. Further a rise of contact time did not result in the subsequent rise of the adsorbed heavy metal ions. For MSW leachate, the removal percentages were found to be 97.1 (Fe), 91.9 (Mg), 89.8 (Cu), 82.5 (Pb), 59.7 (Zn), 29.8 (Mn) and 13.3% (Ca) in the presence of Bentonites-1 and 96.6 (Fe), 88.9 (Mg), 86.5 (Cu), 80.4 (Pb), 50.7 (Zn), 26.1 (Mn) and 12.6% (Ca) due to Bentonite -2. Similarly, for MSW synthetic leachate, the removal was obtained 98.3 (Fe), 86.0 (Mg), 87.0 (Cu), 80.2 (Pb),

77.2 (Zn), 67.5 (Mn) and 14.1% (Ca) due to Bentonite-1 and 94.3 (Fe), 83.4 (Mg), 84.7 (Cu), 77.1 (Pb), 76.3 (Zn), 71.3 (Mn) and 13.1% (Ca) due to Bentonite-2, respectively.

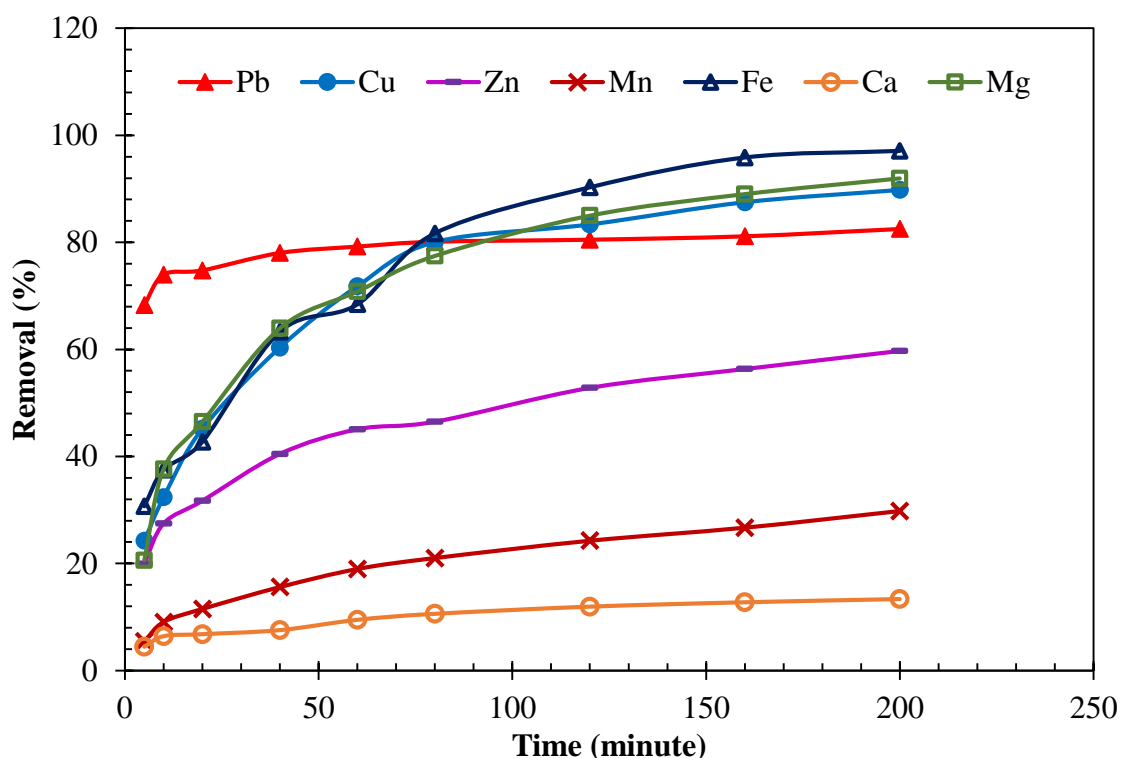


Fig. 5.18. Adsorption kinetics for MSW leachate in the presence of Bentonite-1

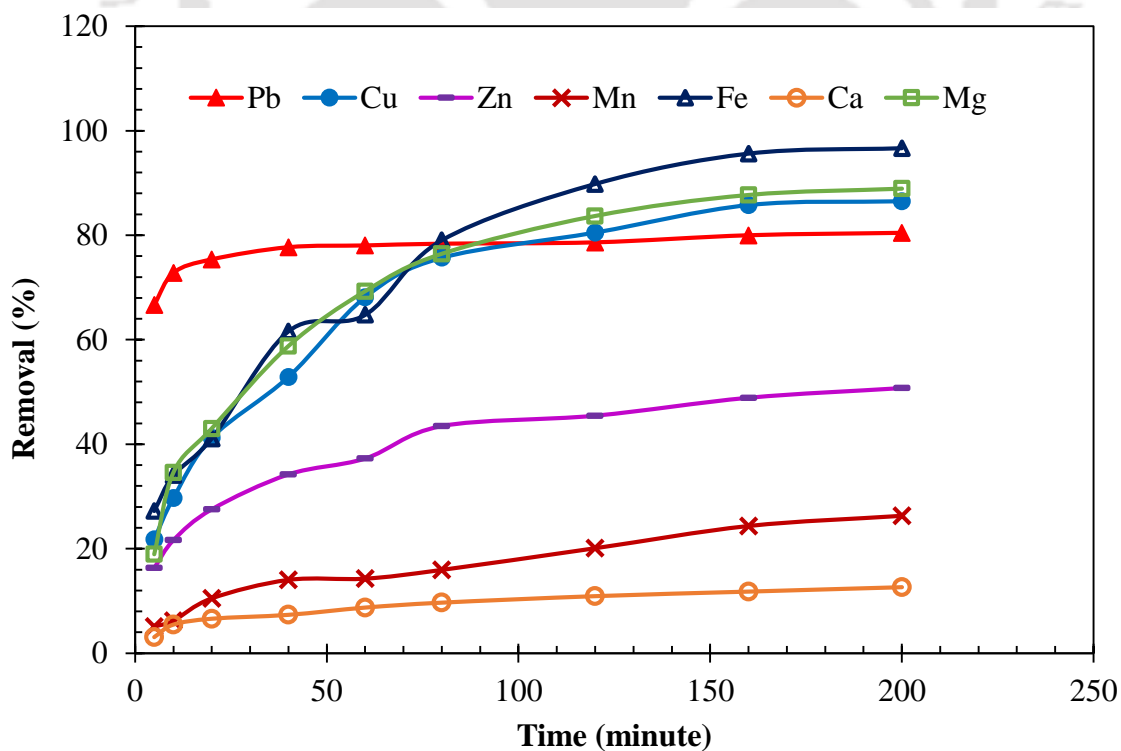


Fig. 5.19. Adsorption kinetics for MSW leachate in the presence of Bentonite-2

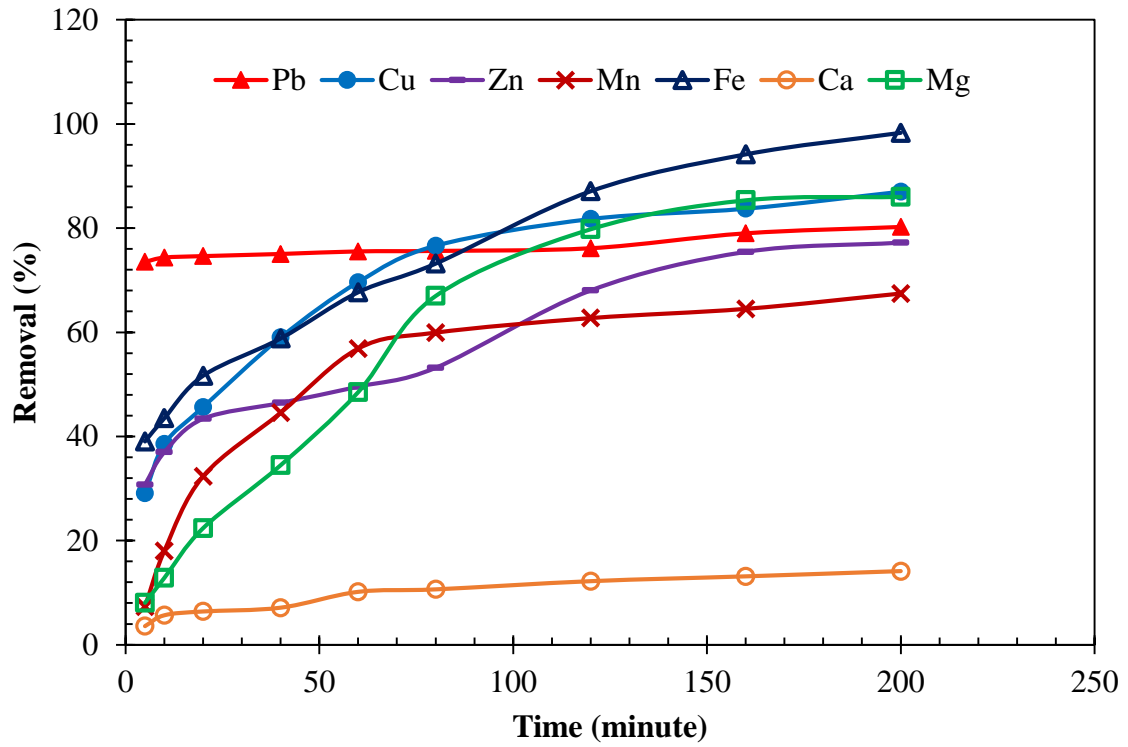


Fig. 5.20. Adsorption kinetics for synthetic MSW leachate in the presence of Bentonite-1

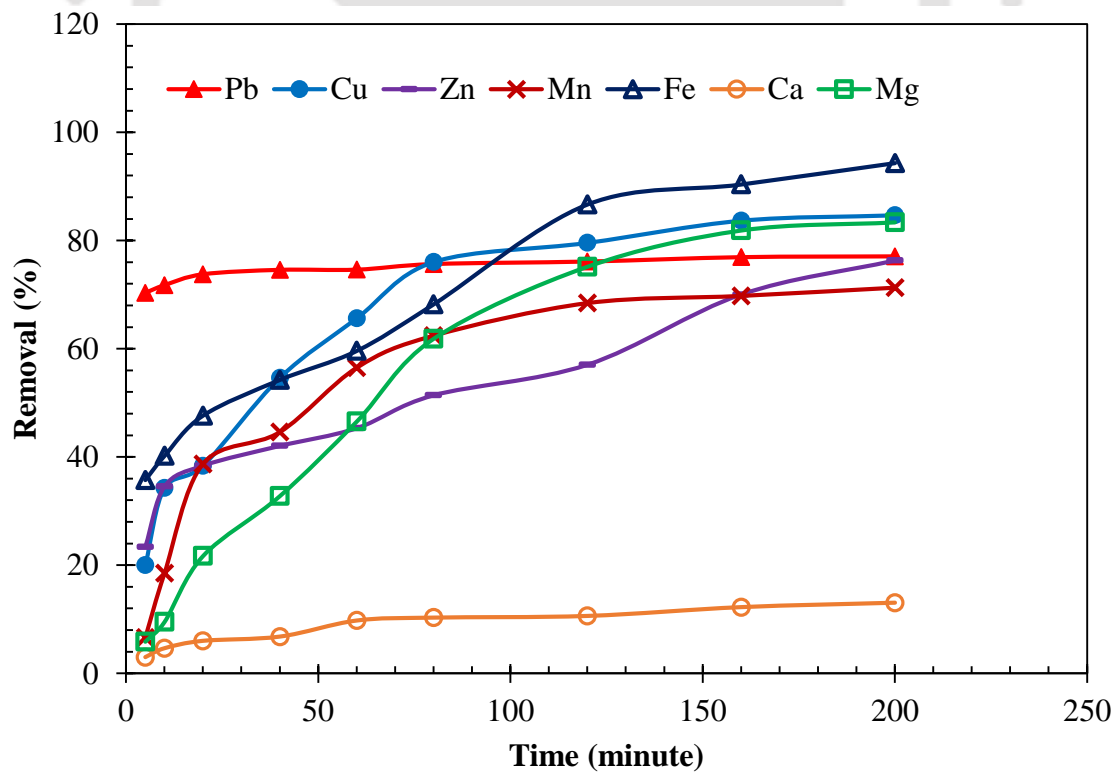
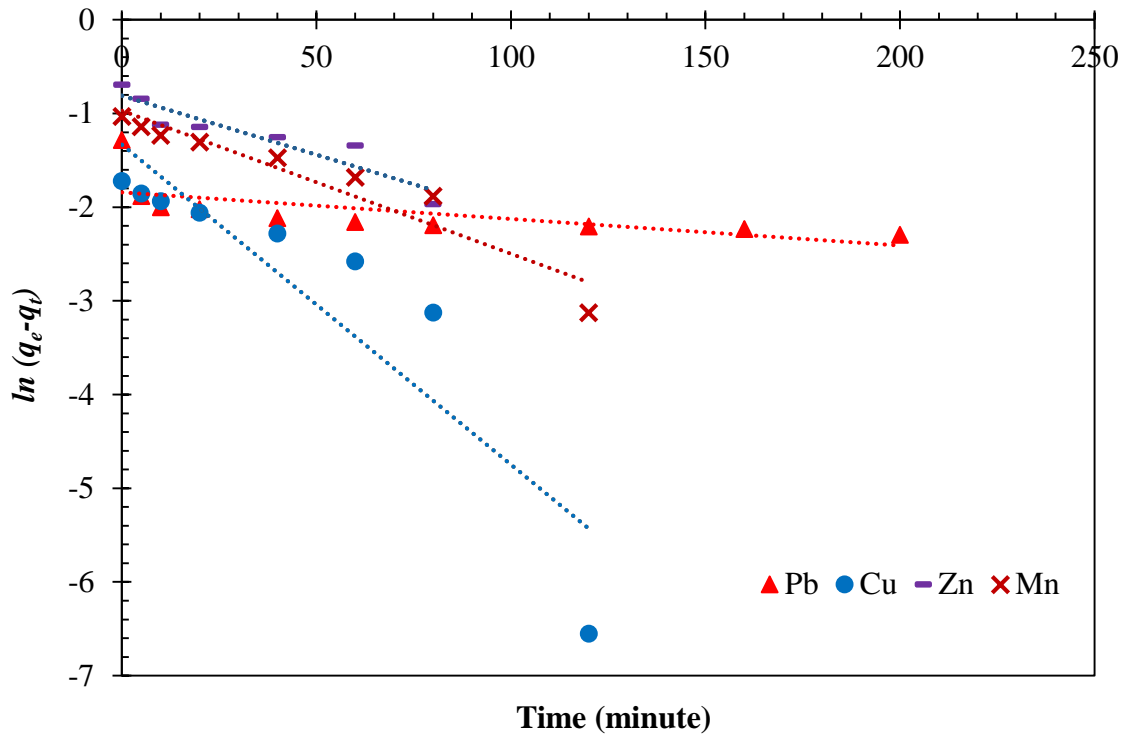


Fig. 5.21. Adsorption kinetics for synthetic MSW leachate in the presence of Bentonite-2

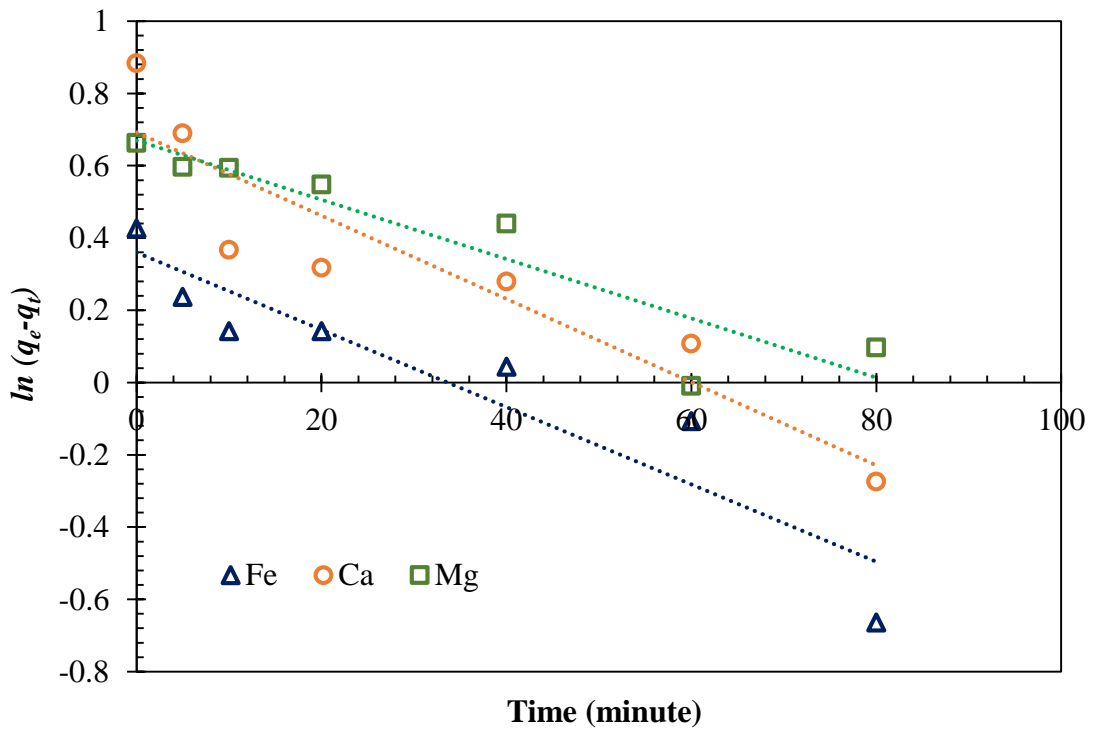
The observed results were found to comply with the previous investigations where rapid adsorption rates were reported (Anna et al., 2015; Bourliva et al., 2013; Vieira et al., 2010). A further increase in the contact time, however, did not increase the amount of adsorbed metal ions. This is because, during the initial adsorption stage, a large number of vacant sites are available, which in due course of time gets occupied and owing to the repulsive forces, filling of the remaining vacant sites becomes a challenge.

5.2.13.2. Kinetic model

Pseudo first- and second-order kinetics plot were displayed in Fig. 5.22 - 5.25. The calculated kinetic parameters of heavy metals present in MSW and synthetic MSW leachate sorption for both the bentonites are detailed in Table 5.3 and 5.4. It can be perceived from Fig. 5.22 - 5.25 that for both the bentonites, Pseudo-first-order kinetic plots do not show a straight line. The R^2 value of the model for both the soil was also lower (Table 5.8 and 5.9) signifying that sorption of heavy metals on bentonites does not fit for Pseudo-first order kinetic model. On the contrary, the R^2 values of the pseudo-second-order kinetic equation were very high ($R^2 > 0.98$ for Bentonite-1 and Bentonite-2) for both the leachates. The experimental values of q_e were also similar to the calculated values, which furthermore confirms the excellent agreement with the Pseudo-second order kinetic model. The output of the investigation directed that the process of adsorption mechanism mostly depends on adsorbate (metal ions) and adsorbent (bentonites). The study also concludes that the overall rate-limiting step of the metal sorption mechanism on both the adsorbent appeared to be ruled by chemisorption which includes valence forces by exchange and sharing of an electron.

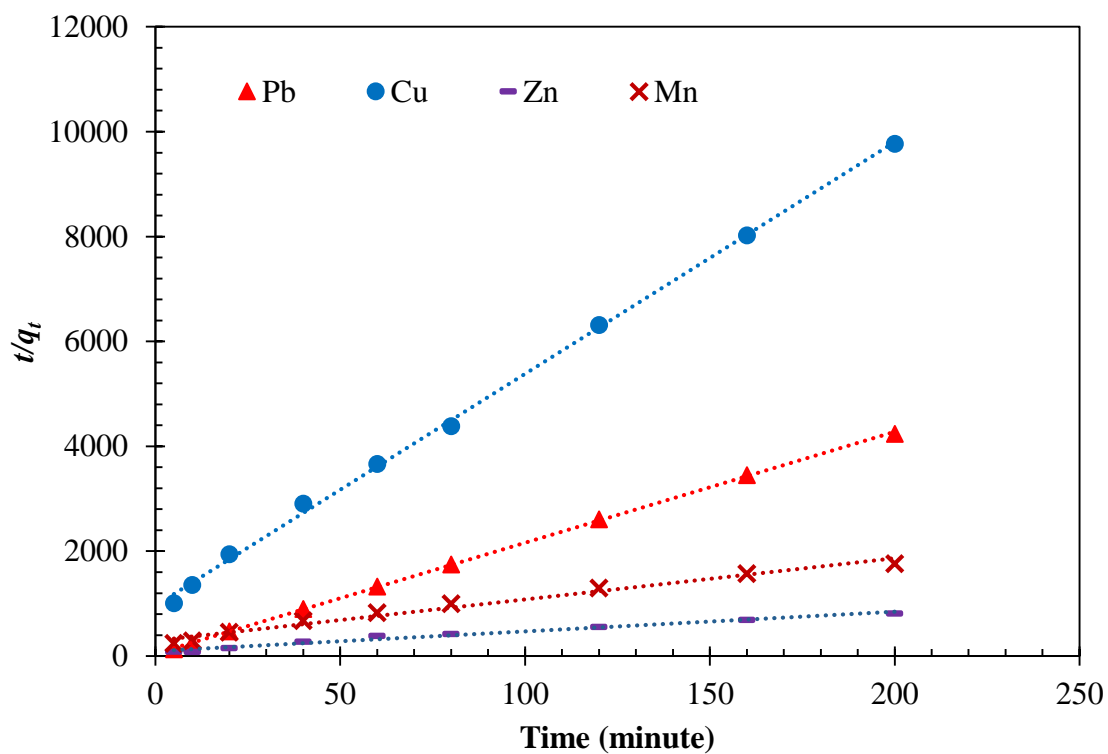


(i)

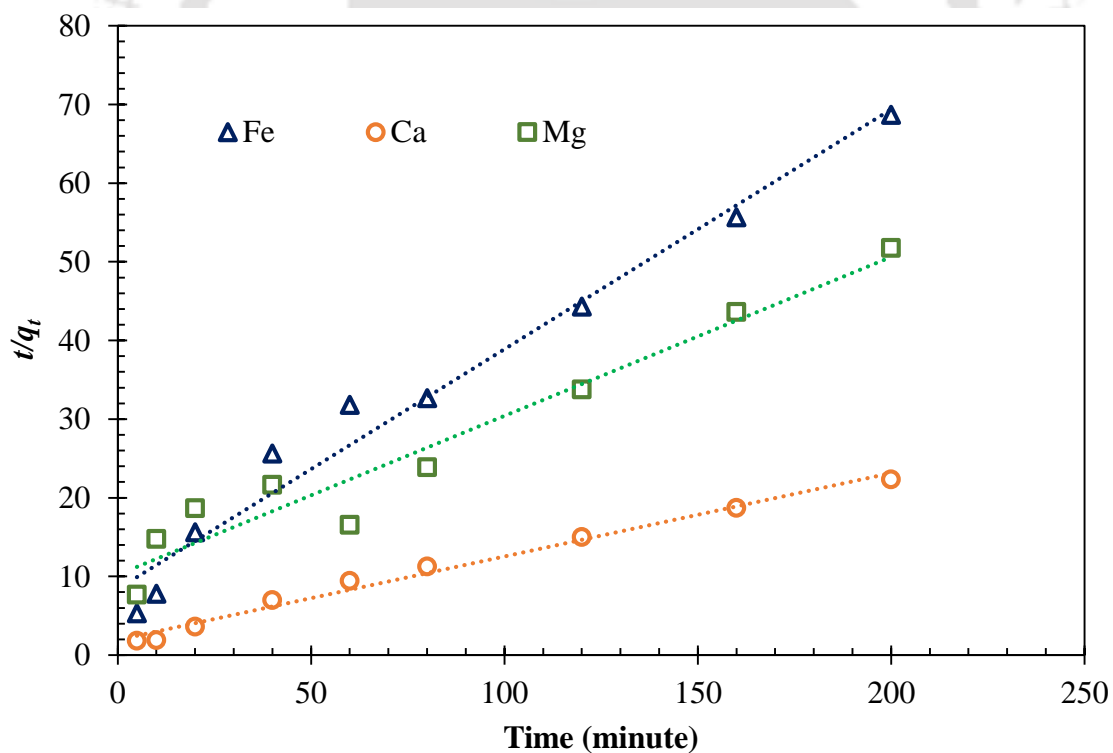


(ii)

(a) Pseudo-first-order adsorption kinetics of MSW leachate



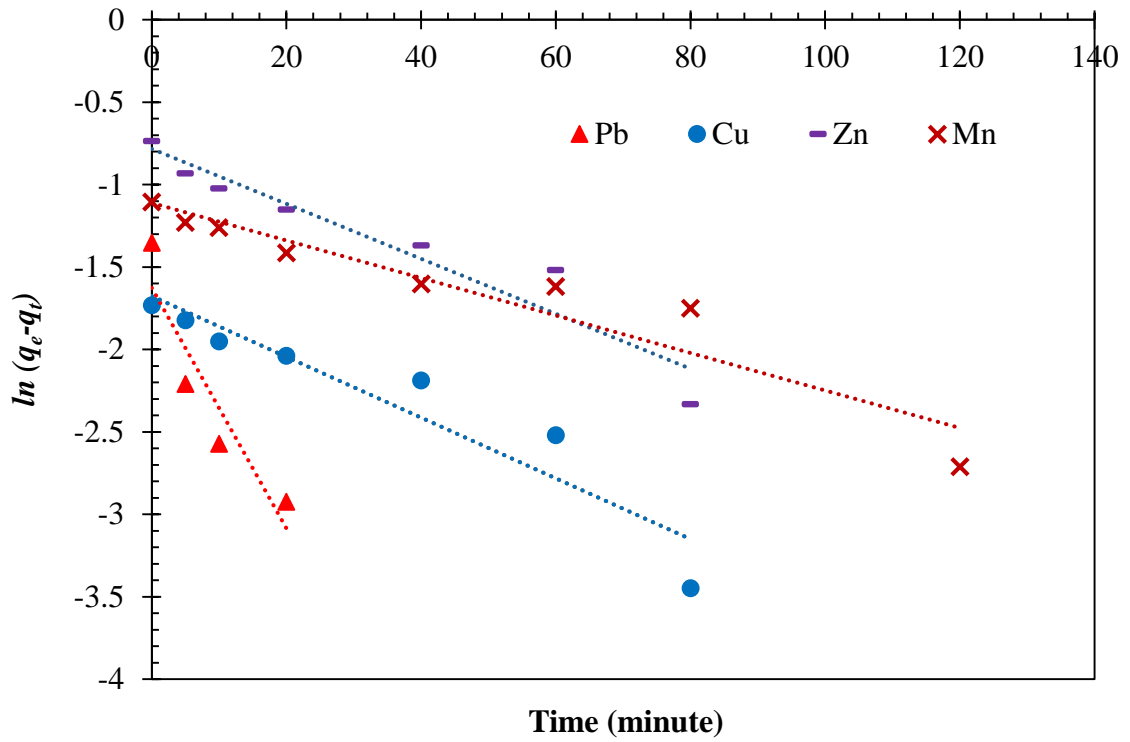
(i)



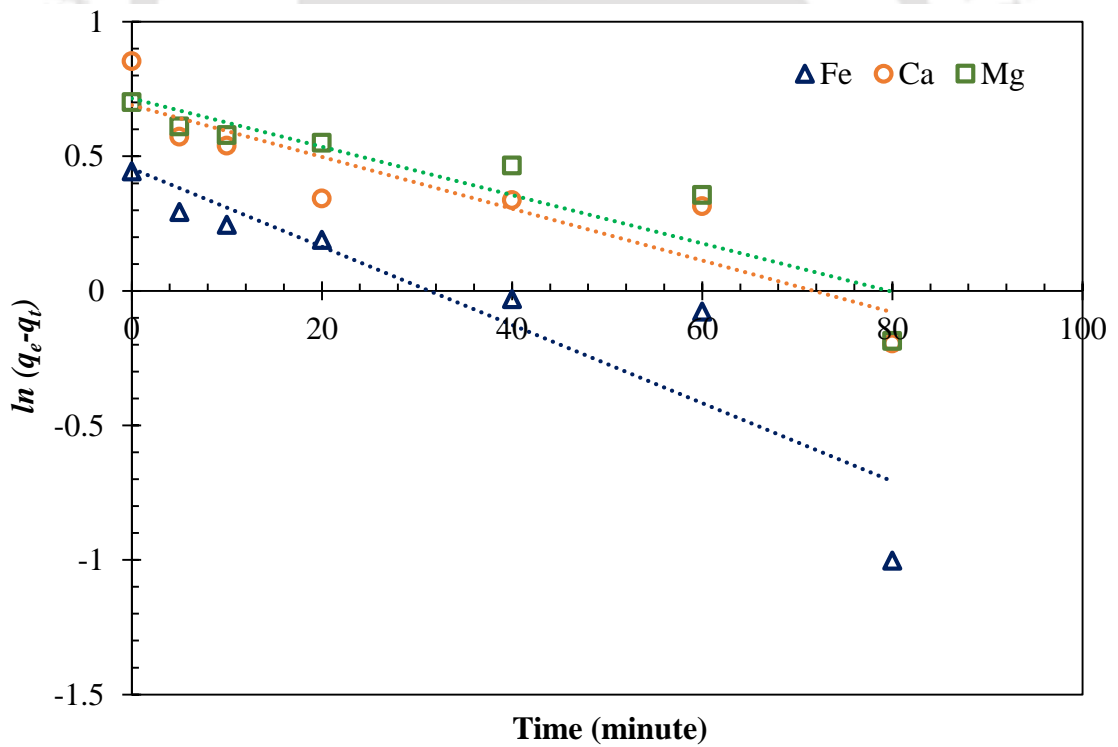
(ii)

(b) Pseudo-second-order adsorption kinetics of MSW leachate

Fig. 5.22. Kinetic study of Bentonite-1 in the presence of MSW leachate

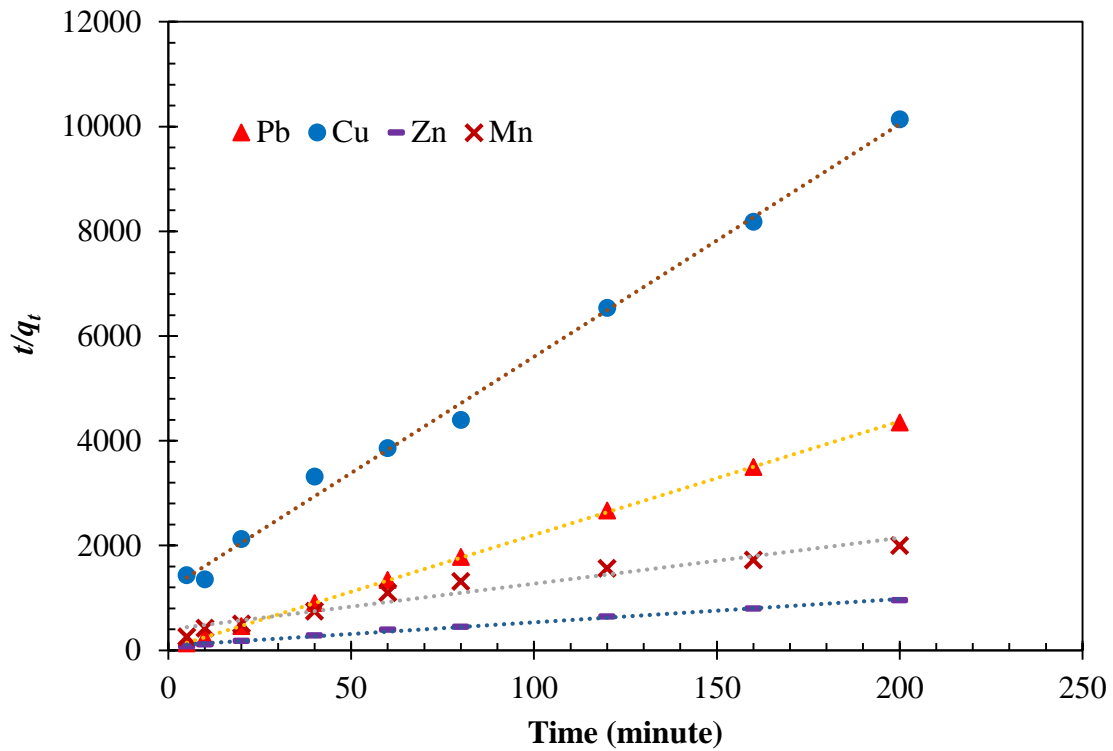


(i)

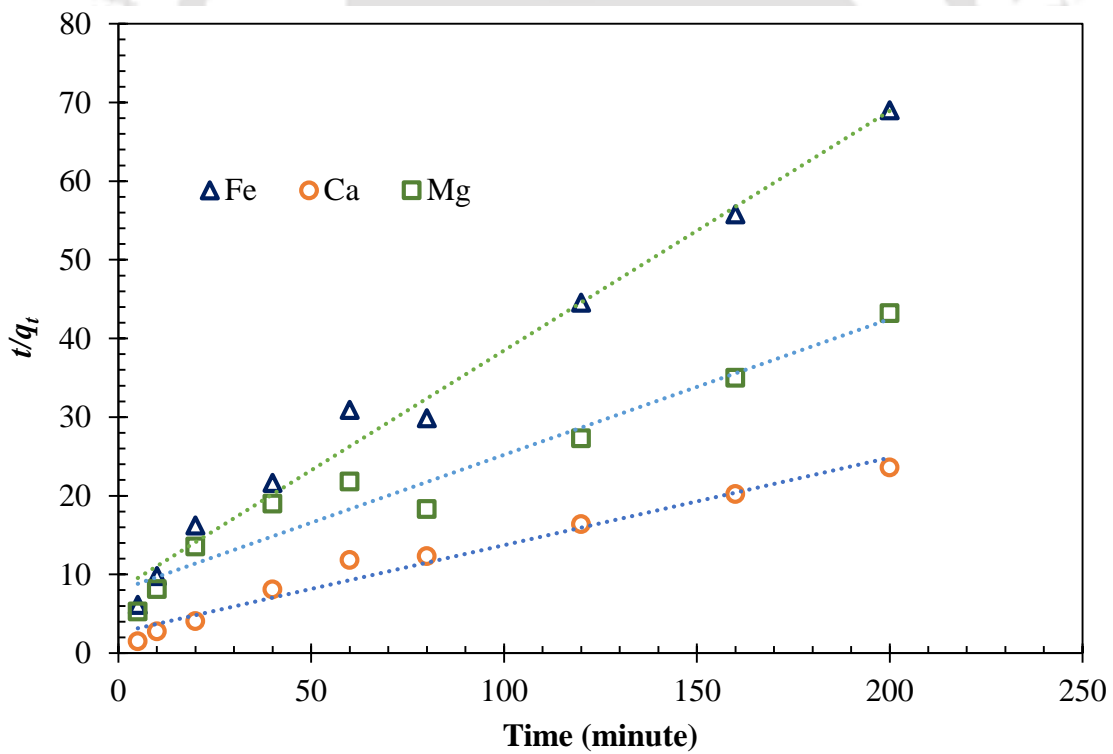


(ii)

(a) Pseudo-first-order adsorption kinetics of MSW leachate



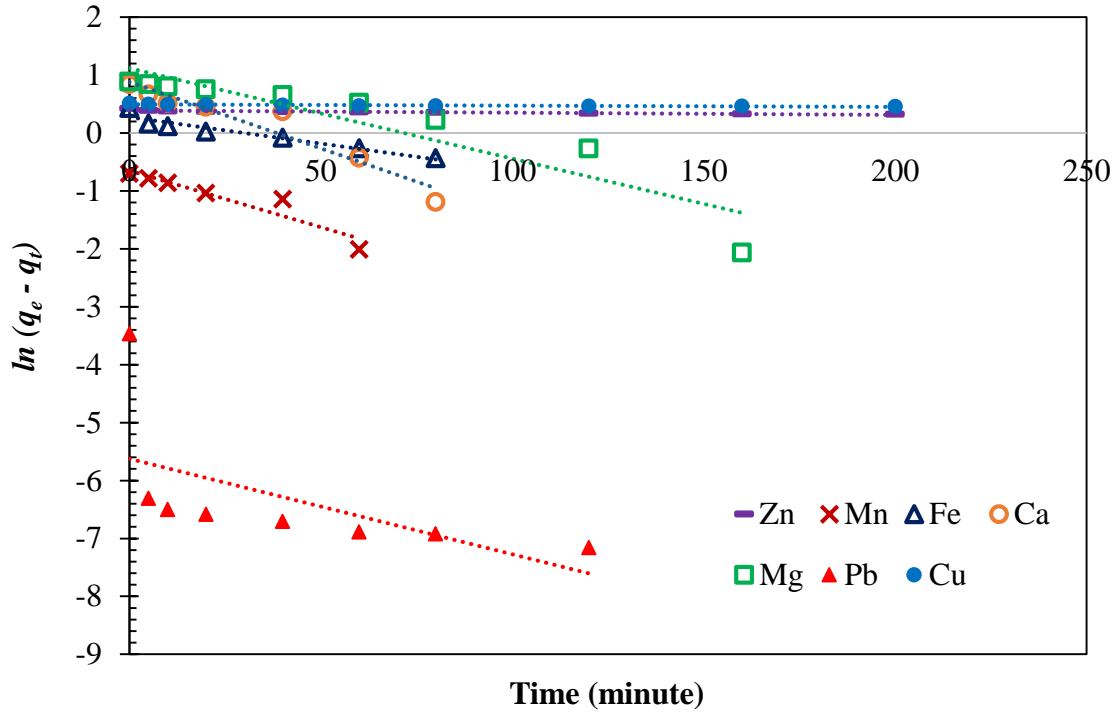
(i)



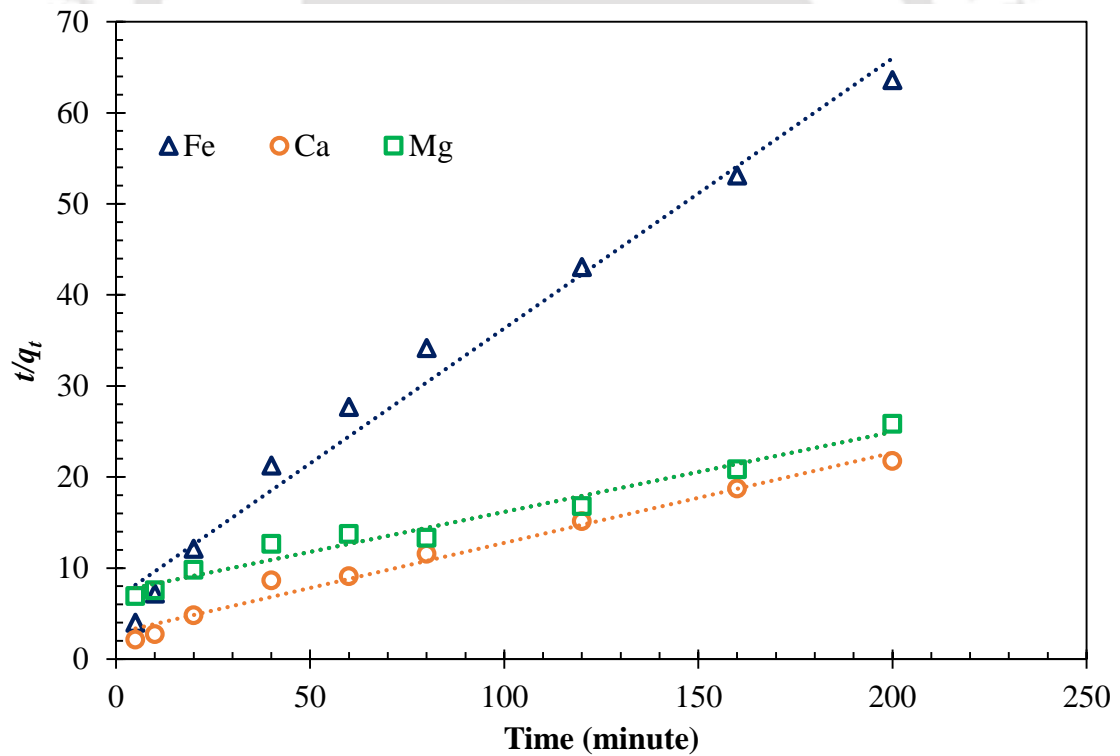
(ii)

(b) Pseudo-second-order adsorption kinetics of MSW leachate

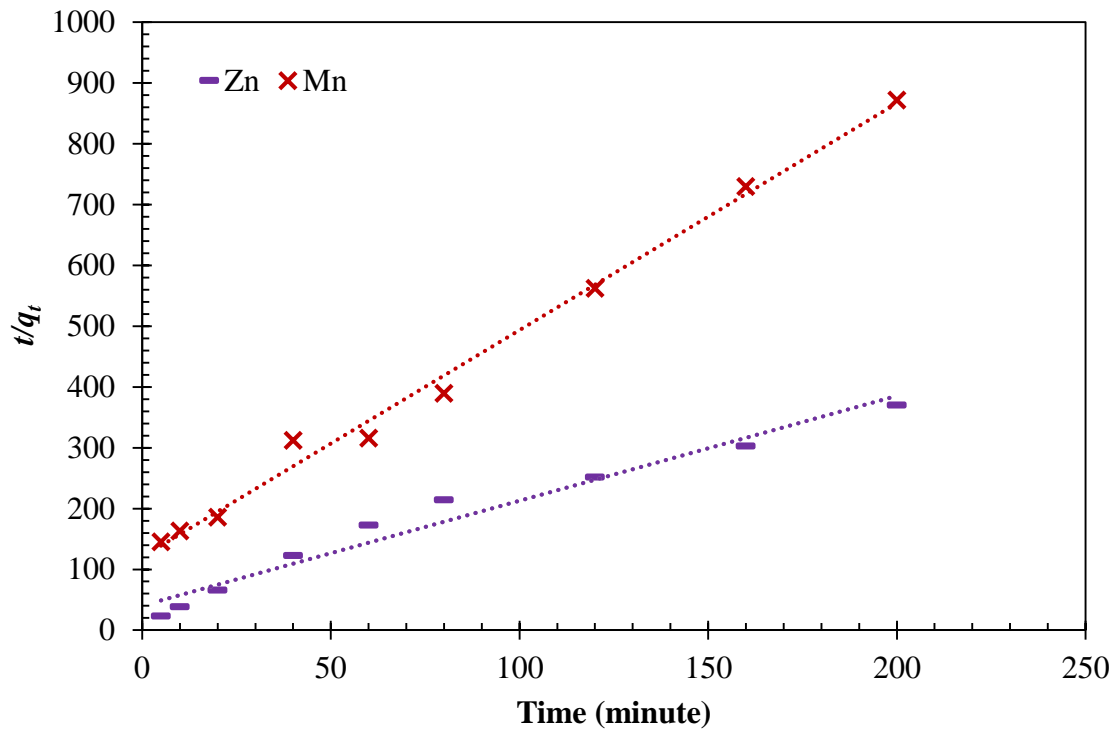
Fig. 5.23. Kinetic study of Bentonite-2 in the presence of MSW leachate



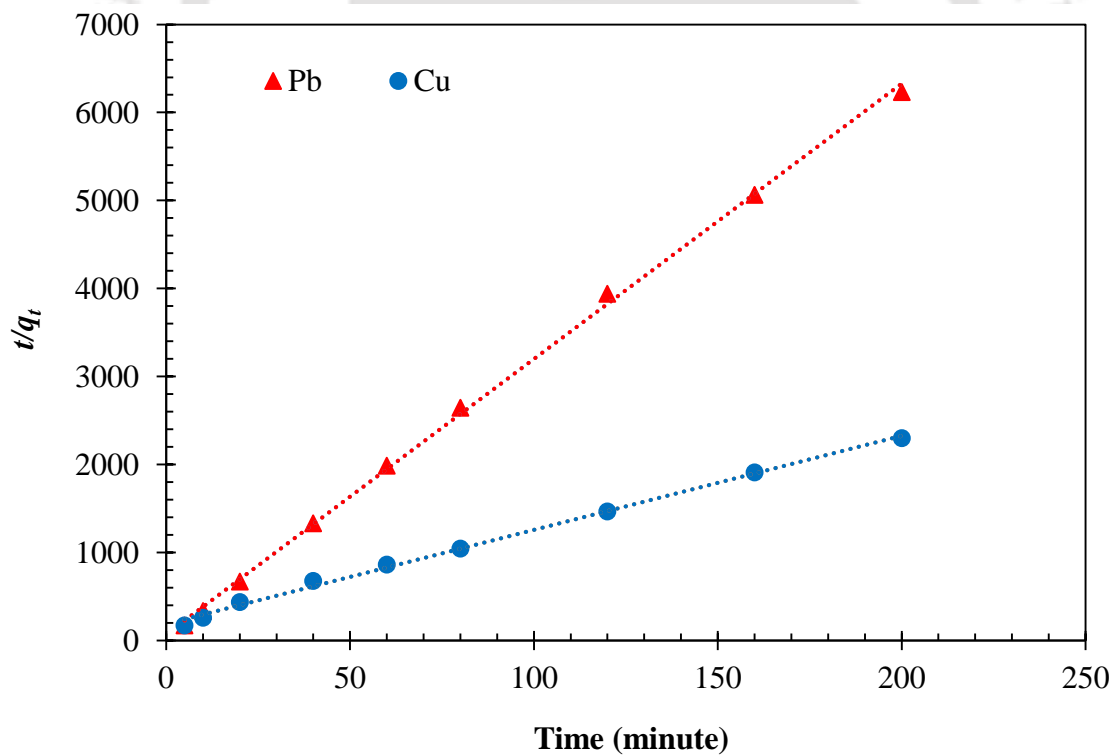
(a) Pseudo-first-order adsorption kinetics of synthetic MSW leachate



(i)



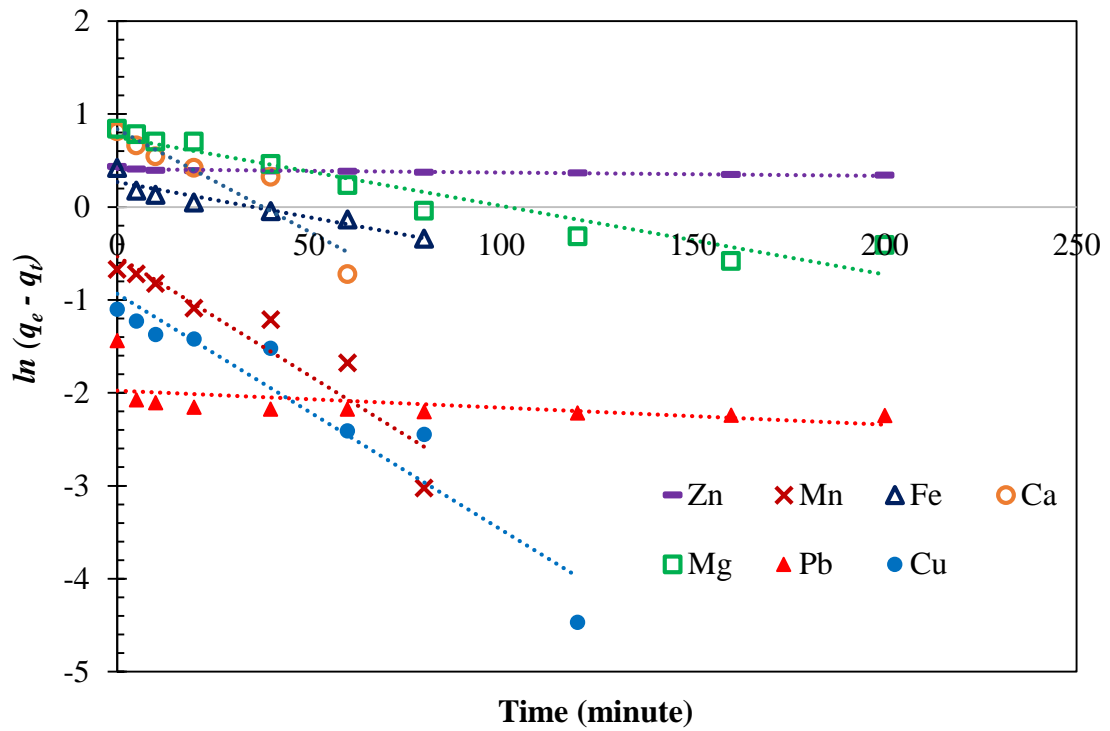
(ii)



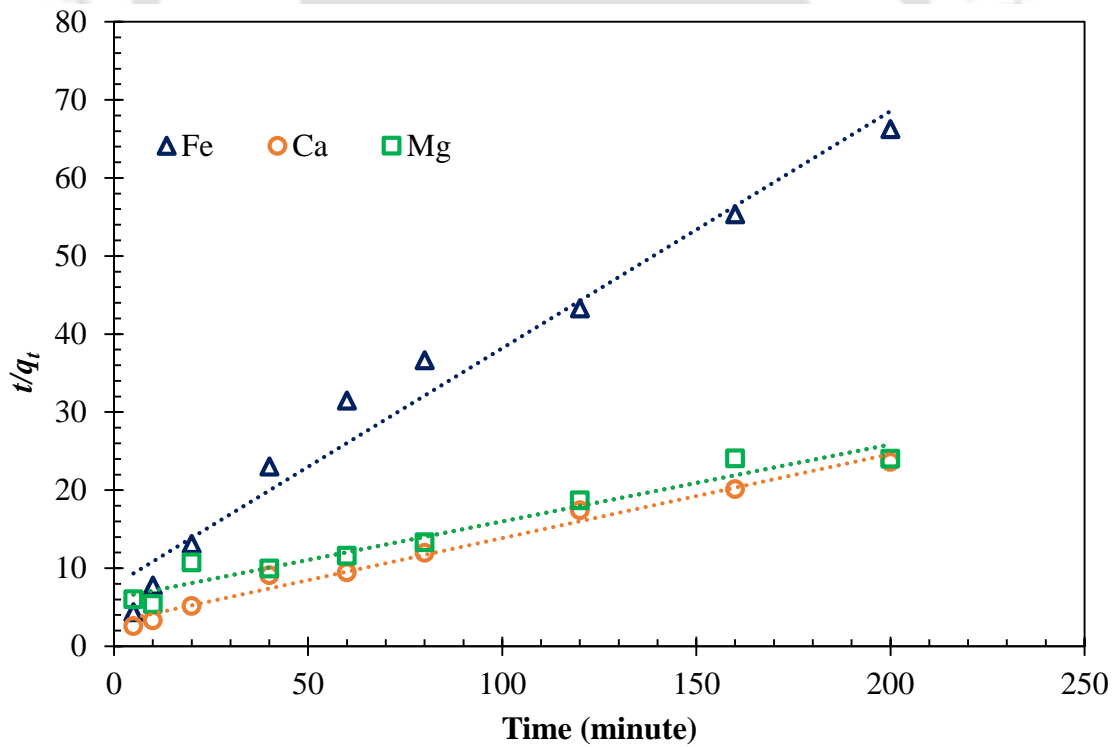
(iii)

(b) Pseudo-second-order adsorption kinetics of synthetic MSW leachate

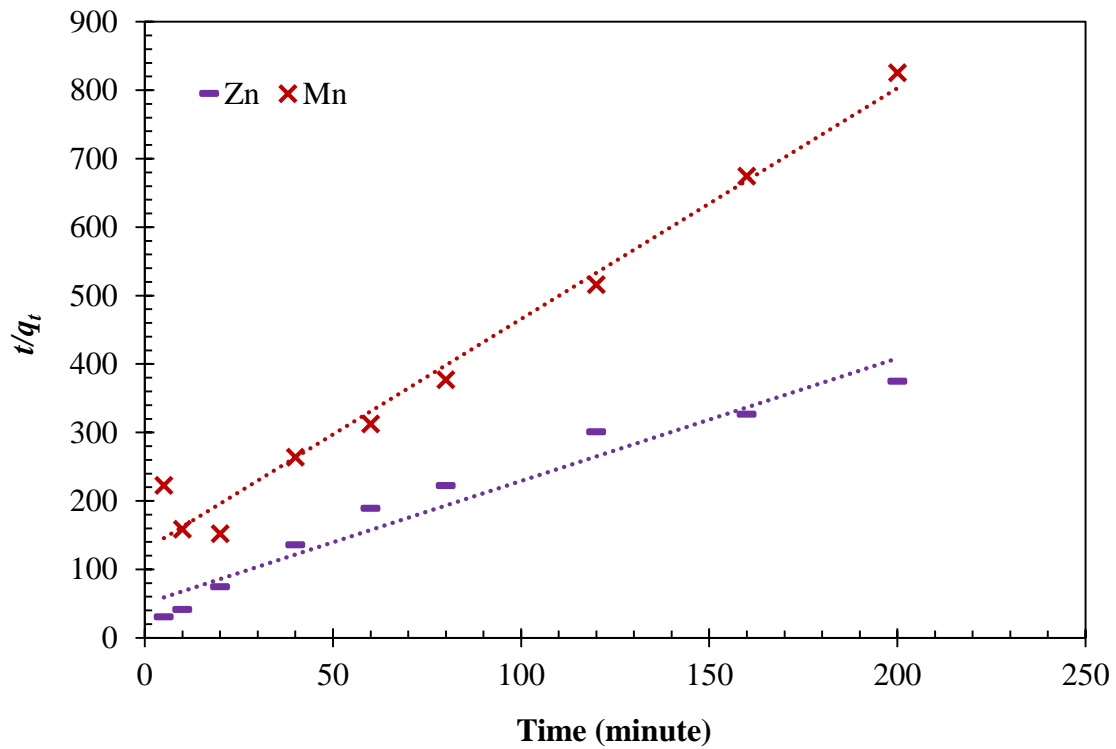
Fig. 5.24. Kinetic study of Bentonite-1 in the presence of synthetic MSW leachate



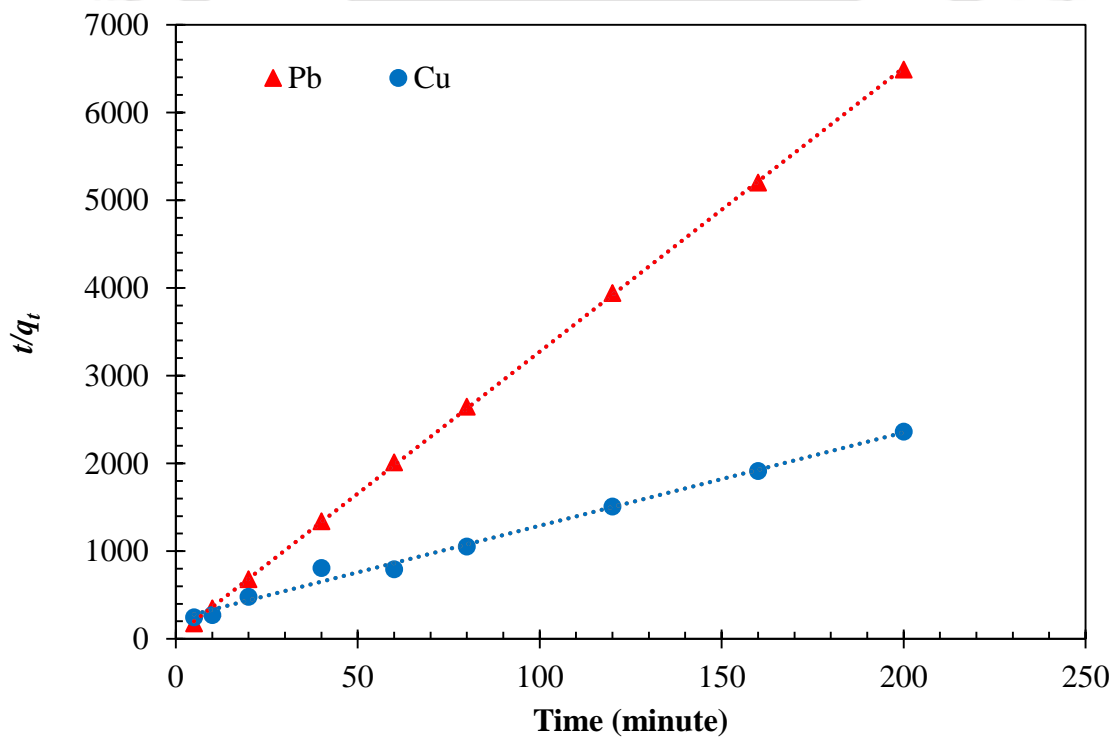
(a) Pseudo-first-order adsorption kinetics of synthetic MSW leachate



(i)



(ii)



(iii)

(b) Pseudo-second-order adsorption kinetics of synthetic MSW leachate

Fig. 5.25. Kinetic study of Bentonite-2 in the presence of synthetic MSW leachate

Table 5.8. Parameters for adsorption of heavy metals present in MSW leachate on bentonites derived from the pseudo-first- and second-order kinetic models

| Real MSW | Pseudo 1st order | | | | | | Pseudo 2nd order | | | | | |
|----------|------------------|----------------------------|-------|--------------|----------------------------|-------|------------------|------------------|-------|--------------|------------------|-------|
| | Bentonite-1 | | | Bentonite-2 | | | Bentonite-1 | | | Bentonite-2 | | |
| | q_e (mg/g) | K_1 (min ⁻¹) | R^2 | q_e (mg/g) | K_1 (min ⁻¹) | R^2 | q_e (mg/g) | K_1 (g/mg min) | R^2 | q_e (mg/g) | K_1 (g/mg min) | R^2 |
| Pb | 0.052 | 0.07 | 0.45 | 0.044 | 0.68 | 0.85 | 0.047 | 447.99 | 0.99 | 0.046 | 469.85 | 0.99 |
| Cu | 0.019 | 0.04 | 0.81 | 0.018 | 0.03 | 0.89 | 0.023 | 1952.84 | 0.99 | 0.023 | 1971.18 | 0.99 |
| Zn | 0.202 | 0.06 | 0.87 | 0.184 | 0.05 | 0.91 | 0.266 | 14.13 | 0.98 | 0.224 | 19.89 | 0.99 |
| Mn | 0.093 | 0.03 | 0.91 | 0.079 | 0.03 | 0.90 | 0.127 | 61.84 | 0.98 | 0.114 | 76.50 | 0.94 |
| Fe | 2.667 | 0.03 | 0.87 | 2.779 | 0.03 | 0.83 | 3.281 | 0.09 | 0.97 | 3.284 | 0.09 | 0.98 |
| Ca | 7.640 | 0.05 | 0.85 | 7.131 | 0.04 | 0.81 | 9.434 | 0.01 | 0.98 | 8.993 | 0.01 | 0.97 |
| Mg | 4.602 | 0.01 | 0.87 | 5.027 | 0.02 | 0.84 | 4.948 | 0.04 | 0.94 | 5.797 | 0.03 | 0.94 |

Table 5.9. Parameters for adsorption of heavy metals present in synthetic MSW leachate on bentonites derived from the pseudo-first- and second-order kinetic models.

| Synthetic MSW | Pseudo 1st order | | | | | | Pseudo 2nd order | | | | | |
|---------------|------------------|----------------------------|-------|--------------|----------------------------|-------|------------------|------------------|-------|--------------|------------------|-------|
| | Bentonite-1 | | | Bentonite-2 | | | Bentonite-1 | | | Bentonite-2 | | |
| | q_e (mg/g) | K_1 (min ⁻¹) | R^2 | q_e (mg/g) | K_1 (min ⁻¹) | R^2 | q_e (mg/g) | K_1 (g/mg min) | R^2 | q_e (mg/g) | K_1 (g/mg min) | R^2 |
| Pb | 0.031 | 0.37 | 0.34 | 0.036 | 0.06 | 0.28 | 0.032 | 978.63 | 0.99 | 0.031 | 1045.75 | 0.99 |
| Cu | 1.673 | 0.001 | 0.71 | 0.080 | 0.04 | 0.91 | 0.093 | 114.28 | 0.99 | 0.094 | 112.98 | 0.99 |
| Zn | 2.652 | 0.05 | 0.80 | 2.723 | 0.12 | 0.84 | 0.580 | 2.97 | 0.97 | 0.558 | 3.21 | 0.95 |
| Mn | 0.199 | 0.09 | 0.89 | 0.213 | 0.10 | 0.87 | 0.268 | 13.91 | 0.99 | 0.297 | 11.37 | 0.97 |
| Fe | 2.708 | 0.04 | 0.92 | 2.639 | 0.04 | 0.89 | 3.367 | 0.09 | 0.98 | 3.293 | 0.09 | 0.97 |
| Ca | 6.984 | 0.41 | 0.91 | 6.530 | 0.27 | 0.86 | 10.081 | 0.01 | 0.98 | 9.294 | 0.01 | 0.98 |
| Mg | 7.691 | 0.03 | 0.84 | 6.911 | 0.02 | 0.91 | 11.389 | 0.09 | 0.97 | 10.132 | 0.01 | 0.95 |

5.3. Summary

This investigation was conducted to study the influence of metal ions present in MSW and synthetic MSW leachate on the behaviour of bentonites. Two bentonites with different mineralogical properties were examined for their change in the index properties, free swelling, swelling potential, swelling pressure, hydraulic conductivity, consolidation parameters and shear strength in the presence of various metal ions. Further, the investigation was conducted to analyse the influence of different metals on the adsorption capacity of bentonites. Adsorption, dose, contact time and kinetic studies were carried out on two bentonites. Based on the test results, the conclusions are summarised below.

- The result indicated that liquid limit and free swelling decreased in the presence of both the leachate. MSW leachates show a higher decrease in the value of liquid limit and free swell for both the bentonites.
- The study reveals that the swelling potential of both the bentonites reduced in the presence of both the leachates. The decline in swelling potential in the presence of leachates is due to the reduction in DDL thickness. Similar to swelling potential, swelling pressure of both the bentonites decreased in the presence of both the leachates. Bentonite-1, having a higher liquid limit, high CEC, SSA experiences a higher reduction in swelling potential and swelling pressure in the presence of leachates compare to Bentonite-2.
- Comparative assessment of the compressibility of the two bentonites, as a result of the permeation of both the leachates, indicates a significant reduction in the void ratio (due to the application of pressure) for bentonite with synthetic leachate.
- Time – swelling relationship study showed that of bentonites reveals that, for the same period, the swelling percentage was higher for Bentonite-1 in comparison to Bentonite-2 in the presence of both the leachates.
- A rise in the hydraulic conductivity value was observed for both the bentonites in the presence of both the leachates. MSW leachates show a higher rise in the value of hydraulic conductivity for both the bentonites. A comparative assessment for both the bentonite at a certain void ratio reveals that Bentonite-1 has a more significant impact than Bentonite-2.
- The results indicated that with the rise in consolidation pressure, the c_v decreases gradually. Test results also suggest that the interaction of the heavy metal ion present in the leachate with the soil pore fluid increases the degree of consolidation of the soil matrix.

- The study indicated that, in the presence of both the leachates t_{90} of both the bentonites reduced. On comparing both the bentonites, it reveals that Bentonite -1 is positively influenced in the presence of leachates as compared to Bentonite-2.
- The result suggested that as compared to Bentonite-2, the decrease in C_c value was more prominent in the case of Bentonite-1.
- UCS study reveals that the strength of the bentonite reduced in the presence of both the leachates. The strength of Bentonite-1 is reduced by 8.3 and 8.5% in presence synthetic and fresh MSW leachate, whereas, the decrease in strength was found to be 1.7 and 3.9% for Bentonite-2. A higher reduction in strength was observed in the case of Bentonite-1 as compared to Bentonite-2.
- A higher amount of removal was observed in Bentonite-1 as compared to Bentonite-2 in the presence of synthetic and fresh MSW leachate. The adsorption capacity of Bentonite-1 was found to be 17.98 and 21.42 mg/g in the presence of MSW and synthetic MSW leachate, whereas, 16.62 and 20.67 mg/g of adsorption capacity was obtained for Bentonite-2 respectively.
- The dose study revealed that with the rise in adsorbent dose, the removal rate (%) increased whereas, the adsorption capacity (mg/g) of all the metals present in the leachates reduced for both the bentonites.
- Kinetic study showed that for all metals present in the leachate, Pseudo second-order kinetic model was found to be an ideal fit for both the bentonites.



*The way to get started is
to quit talking and begin
doing.*

- Walt Disney

6

Influence of various leachates on the behaviour of bentonites

6.1. Introduction

The rapid growth of human population over the past decades has also witnessed significant growth of the change in living patterns. This has led to the migration of a large population to the urban regions in search of a better way of life. With growing number of cities around the world, the problem of a growing concern of proper waste management has evolved. Nowadays, the wastes collected from the residential complexes are no longer limited to biological (kitchen/food) wastes; rather, the waste characteristics have undergone drastic changes (Yoada et al., 2014). Huge amounts of inorganic and plastic wastes, as well as electronic wastes are also generated, which eventually end up in the landfills. These wastes contain significant amounts of heavy metals and other polymer compounds, which are usually rendered toxic or in some cases, carcinogenic (Needhidasan et al., 2014).

The primary problems associated with landfills has always been leachate and gas management (Swati et al., 2018). However, leachate remains the primary concern, as the dreadful effects of leaching from the landfills can not only cause problems to the landfill, but also to the nearby environment. Furthermore, if leachates come in contact with the nearby aquifer or any surrounding surface water body, it may have a permanent detrimental

effect on them, thus making them virtually irreparable. Hence, arresting leachates from coming in contact with the surrounding soil and water body is a necessity while designing any landfill (Daniel, 1984). To serve this purpose, liners are usually provided, which act as barriers to the landfill and the surrounding environment. Several landfill liner materials are available, based on their nature, i.e., synthetic or natural. Synthetic liners include the use of HDPE materials that have proved to be excellent materials. However, they are too expensive and thus, deemed unsuitable for small landfills (Sharma and Reddy, 2004). Hence, for this purpose, natural liner materials are considered which have exceptional arresting capabilities. Among all, several studies have recommended bentonite as a landfill liner, owing to its excellent chemical stability and adsorption characteristics (Daniel, 1984; Dutta and Mishra, 2016; Nakano et al., 2008). Several studies have been conducted on various kinds of leachates (Anna et al., 2015; Chen et al., 2018; Li et al., 2015; Pivato and Raga, 2006; Vega et al., 2005). However, there exist three key leachates that are becoming increasingly dangerous with time; they are fly ash, sewage sludge, and paper mill sludge leachates.

With increasing industrialization and urbanization, space in metro cities have become a major concern. Hence, wastes are generally incinerated and the generated fly ash are disposed of to the landfills. The residues of the incinerated wastes contain various toxic chemicals such as dioxins and heavy metals which are rendered dangerous when in contact with any water source (Li et al., 2007). Furthermore, with the increasing population, the amount of wastewater generated in the form of sewage has increased manifold. This has given rise to increasing sewage treatment units in the urban regions, which generate huge quantities of sludge. This sludge is then dried and disposed of to the landfills. This destabilized sludge also possesses considerable amounts of heavy metals that are rendered harmful to the environment (Nayak and Kalamdhad, 2014). Lastly, with increasing paper consumption in the urban provinces, the generation of paper mill sludge has also seen a significant growth. The paper mill sludge is rich in heavy metal concentrations, owing to which, possess hazard to the natural environment after being disposed to the landfills (Hazarika et al., 2017).

Based on the published literature through various studies, it was seen that no study is available assessing the influence of fly ash, sewage sludge and paper mill leachates on the physical and chemical properties of bentonites. Hence, this investigation targets studying the influence of different leachates on two different bentonites possessing distinct chemical

and mineralogical composition. Bentonites were evaluated for their liquid limit, free swell, swelling potential, swelling pressure, hydraulic conductivity, consolidation parameters, shear strength and adsorption capacity in the presence of leachates.

6.2. Results and discussions

6.2.1. Impact of leachates on liquid limit and free swell

The liquid limit and free swell of bentonites are listed in Table 6.1. It was seen that in the presence of various synthetic leachates, both the parameters declined, compared to the values in the presence of DI water. In the presence of fly ash, sewage sludge and paper mill leachate the liquid limit value reduced by 73.5, 61.7 and 69.2%, respectively for Bentonite-1. In the case of Bentonite-2, it was reduced to 62.5, 46.8 and 55.6%, respectively.

It was also observed that in the presence of DI water, Bentonite-1 and -2 expanded to 32 and 20 mL/g, respectively; however, in the presence of all the leachates, the free swelling value reduced. The reduction in the free swell of Bentonite-1 was found to be 80.0, 73.8 and 76.9% in the presence of fly ash, sewage sludge and paper mill leachate, respectively. Similarly, for Bentonite-2 a decline in 75.0, 72.5 and 72.5% was obtained for fly ash, sewage sludge and paper mill leachate, respectively.

The reason can be attributed to the fact that the existence of higher concentrations of heavy metals shrinks the DDL thickness of bentonite soil (Dutta and Mishra, 2016b). Fly ash leachate showed a higher impact on both the bentonites. The reduction in DDL thickness was more significant in fly ash leachate as compared to sewage sludge and paper mill leachate due to the presence of high levels of metal concentrations. Bentonite-1 showed a higher reduction in liquid limit and free swell as compared to Bentonite-2.

Table 6.1. Liquid limit and free swell of bentonites in presence of synthetic leachates.

| Permeant | Liquid limit (%) | | Free swell (mL/2g) | |
|------------------------|------------------|-------------|--------------------|-------------|
| | Bentonite-1 | Bentonite-2 | Bentonite-1 | Bentonite-2 |
| DI water | 480.0 | 305.0 | 32.5 | 20.0 |
| Fly ash leachate | 127.2 | 114.4 | 6.5 | 5.0 |
| Sewage sludge leachate | 183.7 | 162.3 | 8.5 | 5.5 |
| Paper mill leachate | 147.6 | 135.3 | 7.5 | 5.5 |

6.2.2. Impact of leachates on swelling potential and swelling pressure

For the design of structures like liners, swelling pressure is an essential parameter, as the liners' swelling behaviour gets affected in the presence of leachates. To prevent the opening of cracks and fissures, liners must possess a high value of swelling pressure to suffice as impermeable barriers.

The data in Table 6.2 displays the consequence of the leachate on the swelling potential and swelling pressure of both the bentonites. It was seen that due to the interaction with various synthetic leachate, the swelling pressure and swelling potential of both the bentonites lessened considerably. The influence of leachate solutions on Bentonite-1 was more noteworthy as compared to Bentonite-2. The decline in swelling pressure of Bentonite-1 was from 460.9 kPa to 191.3, 208.8 and 225.6 kPa in the presence of fly ash, paper mill and sewage sludge leachate, respectively. Similarly, Bentonite-2 showed a reduction from 392.0 kPa with DI water to 210.4, 216.7 and 232.6 kPa in the presence of fly ash, paper mill and sewage sludge leachate, respectively. The fly ash leachate showed a significant effect on the swelling pressure of both the bentonites in comparison to the paper mill and sewage sludge leachate solutions indicating the presence of a higher concentration of metal solutions and its effect on swelling pressure.

Furthermore, the swelling potential of Bentonite-1 and -2 decreased in the presence of all the leachates. Bentonite-1 and -2 exhibited a swelling potential of 34.3 and 24.7% with DI water. However, due to the permeation of fly ash, paper mill and sewage sludge leachate solutions, it is declined to 13.3, 15.2 and 16.8% for Bentonite-1, respectively. Similarly, the swelling potential of Bentonite-2 was observed to be 10.7, 12.5 and 13.2% in the presence of fly ash, paper mill and sewage sludge leachate, respectively. Similar to the influence on the swelling pressure, Bentonite-1 showed higher reduction in swelling potential as compared to Bentonite-2. The percentage reduction of swelling potential in the presence of fly ash, paper mill and sewage sludge leachate with DI water was found to be 61.3, 55.7 and 51.0% for Bentonite-1, whereas, for Bentonite-2 it was 54.9, 46.9 and 44.0%, respectively. Fly ash leachate showed a higher impact for both the bentonites.

Table 6.2. Swelling Potential and Swelling Pressure of bentonites in presence of synthetic leachates.

| Permeant | Swelling Potential (%) | | Swelling Pressure (kPa) | |
|------------------------|------------------------|-------------|-------------------------|-------------|
| | Bentonite-1 | Bentonite-2 | Bentonite-1 | Bentonite-2 |
| DI water | 34.3 | 23.7 | 460.9 | 392.6 |
| Fly ash leachate | 13.3 | 10.7 | 191.3 | 210.4 |
| Sewage sludge leachate | 16.8 | 13.2 | 225.6 | 232.6 |
| Paper mill leachate | 15.2 | 12.5 | 208.8 | 216.7 |

6.2.3. Impact of synthetic leachates on Time-Swelling plot

Fig. 6.1 and 6.2 depict a standard time-swell correlation for two different bentonites in the presence of fly ash, sewage sludge and paper mill leachate. It was observed that the increase in swelling with time progressed slowly initially, then rose steeply, and finally attained an asymptomatic value. It was furthermore, observed that the time required for attaining an asymptomatic value depended mostly on the type of bentonite-clay as well as the concentration of heavy metals present in the leachates. Here, the percentage swell is computed as the ratio of the swelling amount at a particular time and the total swell of the mixture expressed as a percentage. Figure 6.1 and 6.2 describes a time vs percent swell relationship, which generally follows a standard S shape. Dakshanamurthy (1978) explained two stages of swelling; the first stage comprised of hydration of dry clay particles, wherein water gets adsorbed in successive monolayers and pushes apart the particles or the unit layers of the montmorillonite clay. The second stage includes the double-layer repulsion, where a massive volume change accompanies the swelling. However, closer inspection of the results in Fig. 6.1 and 6.2 show that the curve can be divided into three stages. In all cases the, initial swelling was less than 10% of the total swelling, essentially due to swelling of the bentonite clay particles within the voids of the coarser non-swelling fractions, which does not cause a volume increase of the sample. Primary swelling occurs when the voids no longer accommodate further swelling of the clay particles, occurring at a faster rate. After the completion of the primary swelling, the swelling further continues at a slower rate, known as the secondary swelling.

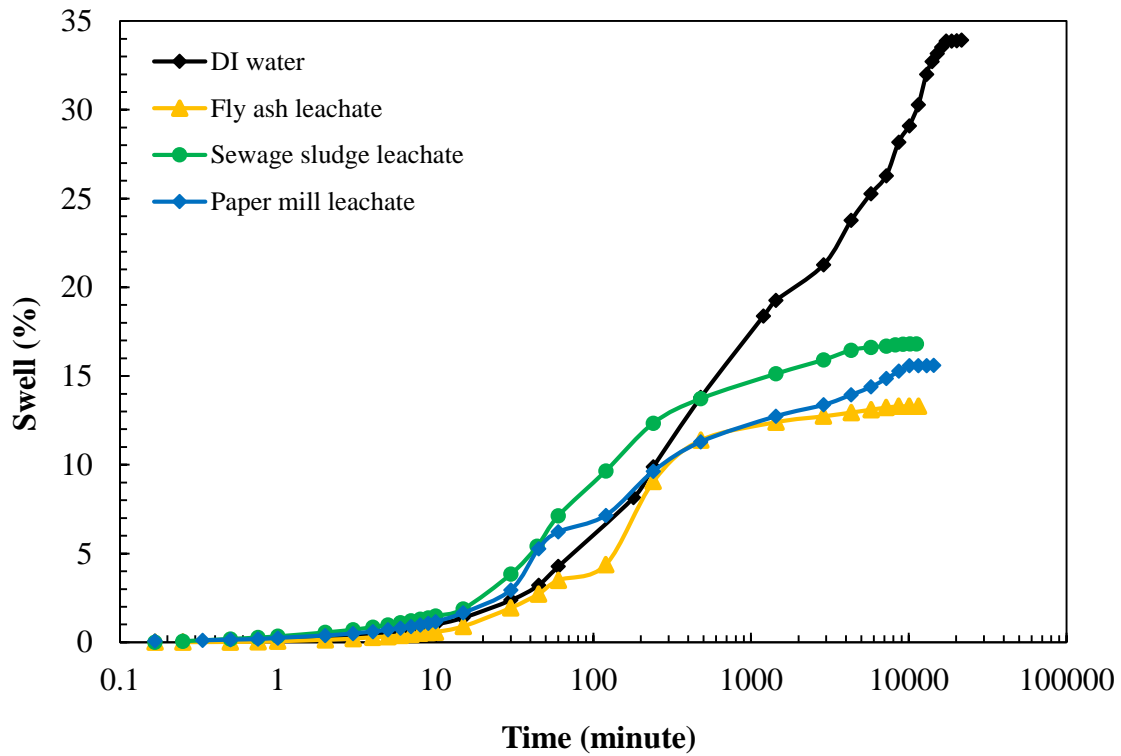


Fig. 6.1. Time–swelling plot for Bentonite-1 in presence of synthetic leachates

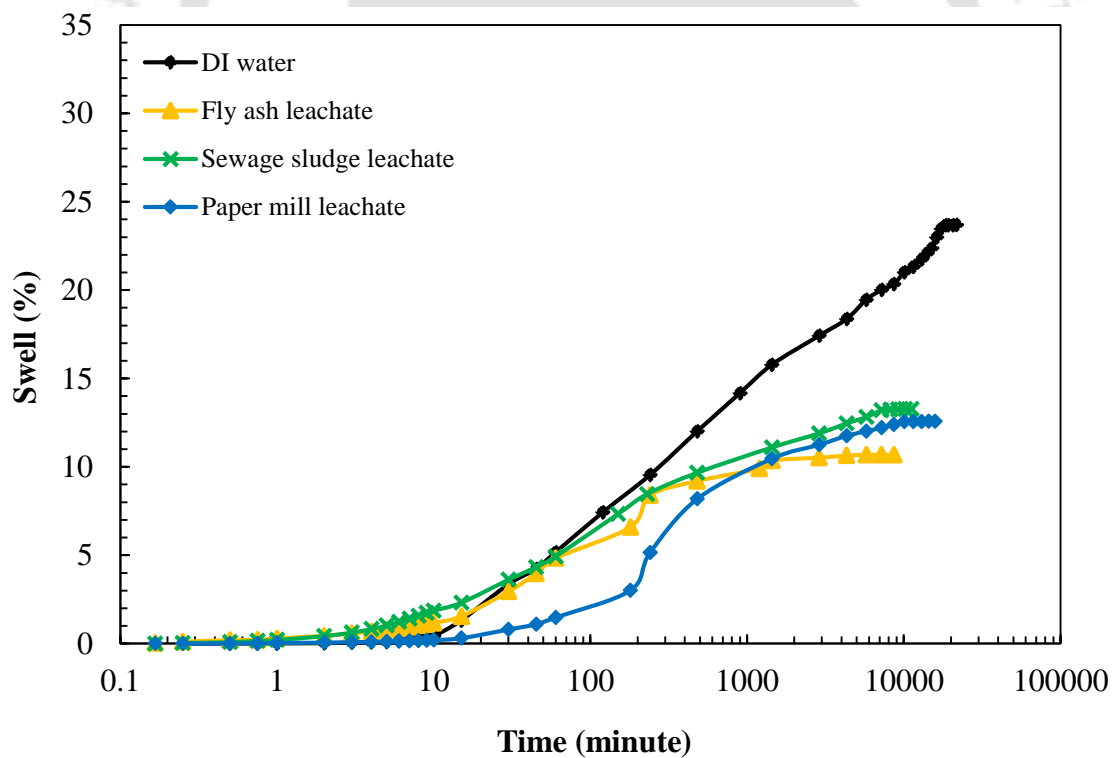


Fig. 6.2. Time–swelling plot for Bentonite-2 in presence of synthetic leachates

Table 6.3 depicts that for Bentonite-1 the initial swelling was achieved in 5, 2 and 2 minutes in the presence of fly ash, sewage sludge and paper mill leachates, respectively. Similarly, for Bentonite-2 the initial swelling was completed in 10, 1 and 15 minutes, respectively.

In the presence of synthetic fly ash, sewage sludge and paper mill leachates, Bentonite-1 achieved primary swelling in 10080, 10200 and 10080 minutes, respectively; however, for Bentonite-2 it was attained at 8640, 9200 and 8640 minutes, respectively. The swelling percentage was found to be the least in the presence of fly ash leachate, which was followed by the paper mill leachate, and sewage sludge leachate, irrespective of the bentonite quality. This is due to the presence of a higher concentration of heavy metals in the fly ash leachate, as compared to others.

A correlation between the two bentonites from the time-swelling plot revealed that for the same time elapsed, the percentage of swelling was higher for Bentonite-1 compared to Bentonite-2 in the presence of all leachates. This is because of a higher CEC, SSA, and montmorillonite content.

Table 6.3. Initial swelling (IS) and Primary swelling (PS) of bentonites in presence of leachates.

| Permeant | SWELL (%) | | | | | | | |
|------------------------|-------------|---------------|--------|---------------|-------------|---------------|--------|---------------|
| | Bentonite-1 | | | | Bentonite-2 | | | |
| | IS (%) | Time (minute) | PS (%) | Time (minute) | IS (%) | Time (minute) | PS (%) | Time (minute) |
| DI water | 1 | 10 | 33.8 | 17280 | 0.4 | 10 | 23.5 | 17280 |
| Fly ash leachate | 0.3 | 5 | 13.3 | 10080 | 0.3 | 1 | 10.7 | 8640 |
| Sewage sludge leachate | 0.5 | 2 | 16.8 | 10200 | 0.3 | 2 | 13.2 | 9200 |
| Paper mill leachate | 0.4 | 2 | 15.5 | 10080 | 0.3 | 15 | 12.4 | 8640 |

6.2.4. Impact of leachates on Hydraulic conductivity

Fig. 6.3 and 6.4 show the impact of fly ash, sewage sludge and paper mill leachates on the hydraulic conductivity of bentonites. It was observed that the hydraulic conductivity of both the bentonites was higher in the presence of various synthetic leachates.

Furthermore, it was observed that in the presence of Fly ash leachate, both the bentonites show a higher rise in hydraulic conductivity followed by Paper mill and Sewage sludge leachate. This may be due to the existence of a higher concentration of Zn^{2+} (13000 mg/L) in fly ash leachate.

Compared to the individual application of heavy metals to the bentonites, the application of leachates renders higher ionic concentrations. The binding of metal cations to the hydroxyl group in the bentonite has a direct correlation with the ionic strength of the solution. This maintains an equilibrium of both the charges on the soil surface (Sparks, 1995). Furthermore, more ions binding to the clay surface results in the shrinkage of the DDL, resulting in a higher hydraulic conductivity value and a tendency towards a more flocculated fabric. A considerable effect on the hydraulic conductivity of bentonite can also be seen due to the change in the pH of the salt solution (Mitchell and Soga, 2005). With the solution's pH increment, the net proton charge drops (Sposito, 1989), and hence, there is a higher requirement for positive ions on the clay particle surface. Thus, there is a chance of (i) an increase in hydraulic conductivity because of a rise in pore space or (ii) a decrease in hydraulic conductivity because of pore-clogging, due to the movement of particles from the acids or bases. The degree of growth in hydraulic conductivity due to the accumulation of leachates was found to be different.

A comparison study among Bentonite-1 and -2 was carried out in the presence of Fly ash, Sewage sludge and paper mill leachates. At a void ratio of 1.2, the hydraulic conductivity value was determined for both bentonites, listed in Table 6.4. It was seen that when the pore fluid comprises a higher level of different metal concentration present in fly ash leachate, the hydraulic conductivity increased about 57.5 and 61.5 times than that with DI water for Bentonite-1 and-2. Similarly, hydraulic conductivity of both the bentonites was found to be inclined by 8.6 and 7.9 times in the presence of Sewage sludge leachate. Likewise, paper mill leachate showed an increment of hydraulic conductivity by 41.1 and 9.8 times, respectively. The comparison study also revealed that because of the existence of the leachates, the hydraulic conductivity of Bentonite-1 was significantly affected as

compared to Bentonite-2. Increment in hydraulic conductivity was found to be higher in Fly ash leachate followed by the paper mill and sewage sludge leachate.

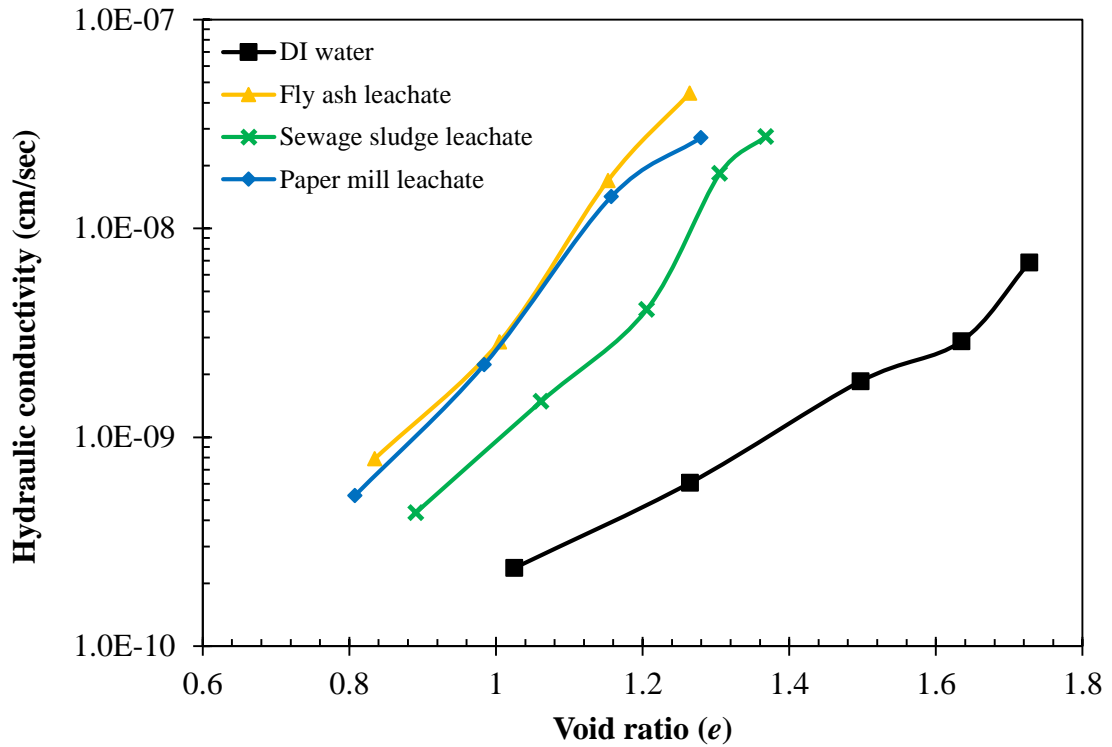


Fig. 6.3. Hydraulic conductivity of Bentonite-1 in presence of synthetic leachates

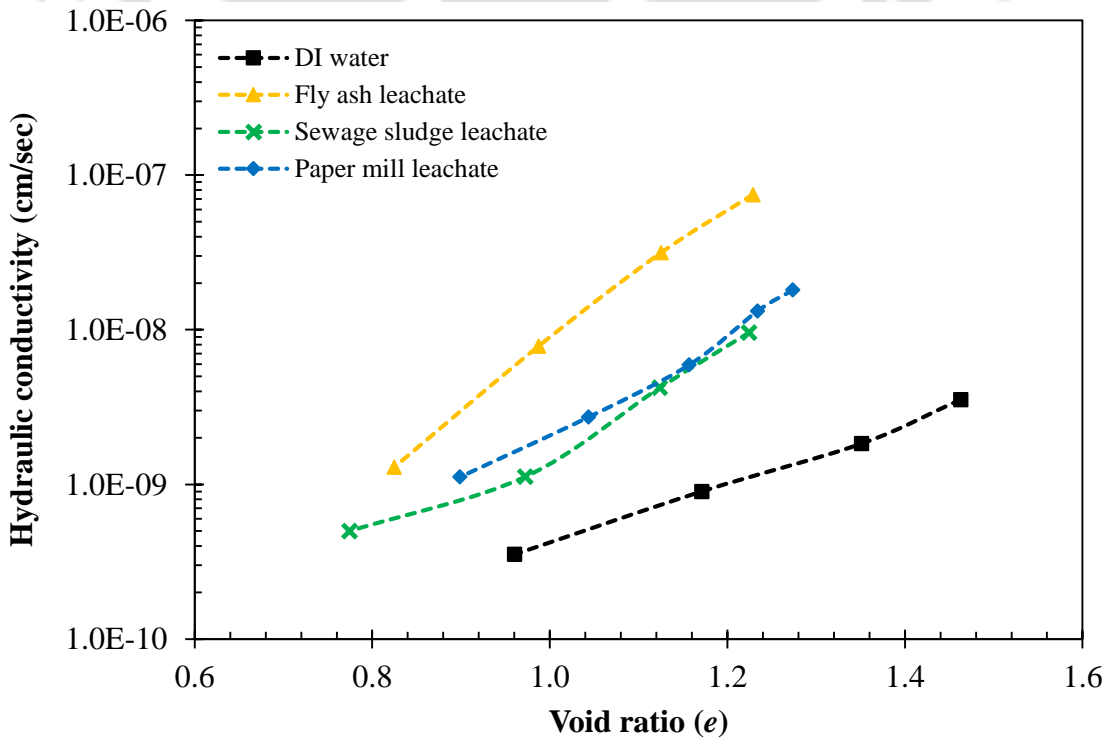


Fig. 6.4. Hydraulic conductivity of Bentonite-2 in presence of leachates

Table 6.4. Hydraulic conductivity of bentonites at a void ratio of 1.2 for synthetic leachates.

| Permeant | Hydraulic conductivity (cm/sec) at void ratio (e) 1.2 | |
|------------------------|---|------------------------|
| | Bentonite-1 | Bentonite-2 |
| DI water | 4.75×10^{-10} | 9.75×10^{-10} |
| Fly ash leachate | 2.73×10^{-8} | 6.00×10^{-8} |
| Sewage sludge leachate | 4.10×10^{-9} | 7.78×10^{-9} |
| Paper mill leachate | 1.95×10^{-8} | 9.51×10^{-9} |

6.2.5. Impact of leachates on Compressibility behaviour of bentonites

Fig. 6.5 and 6.6 depict the void ratio-pressure plots of Bentonite-1 and -2 in the existence of various synthetic leachate solutions. It was observed that there is a substantial decline in the void ratio in the presence of fly ash, sewage sludge and paper mill leachate. The compression of Bentonite-2 was less than Bentonite-1 in the presence of various synthetic leachates.

The bentonites showed a significant compressibility degree in the presence of pore fluids of lower concentrations, attributing to the generation of internal swelling forces that offer resistance against the compressive stresses. With the diffusion of various synthetic leachates containing a high level of different metal concentration into the bentonite, there is a decline in the inter-particle repulsive stresses, making the clay particles get compressed to a lower void ratio.

Reduction in the void ratio because of increment in the vertical consolidation pressure was maximum for DI water followed by sewage sludge, paper mill and fly ash leachate. The presence of combinations of the high level of metal concentrations in fly ash leachate produced the least compressibility for the bentonites. This is primarily because of the decline in diffuse double layer thickness (Mitchell and Soga, 2005; Olson and Mesri, 1970; Sridharan et al., 1986).

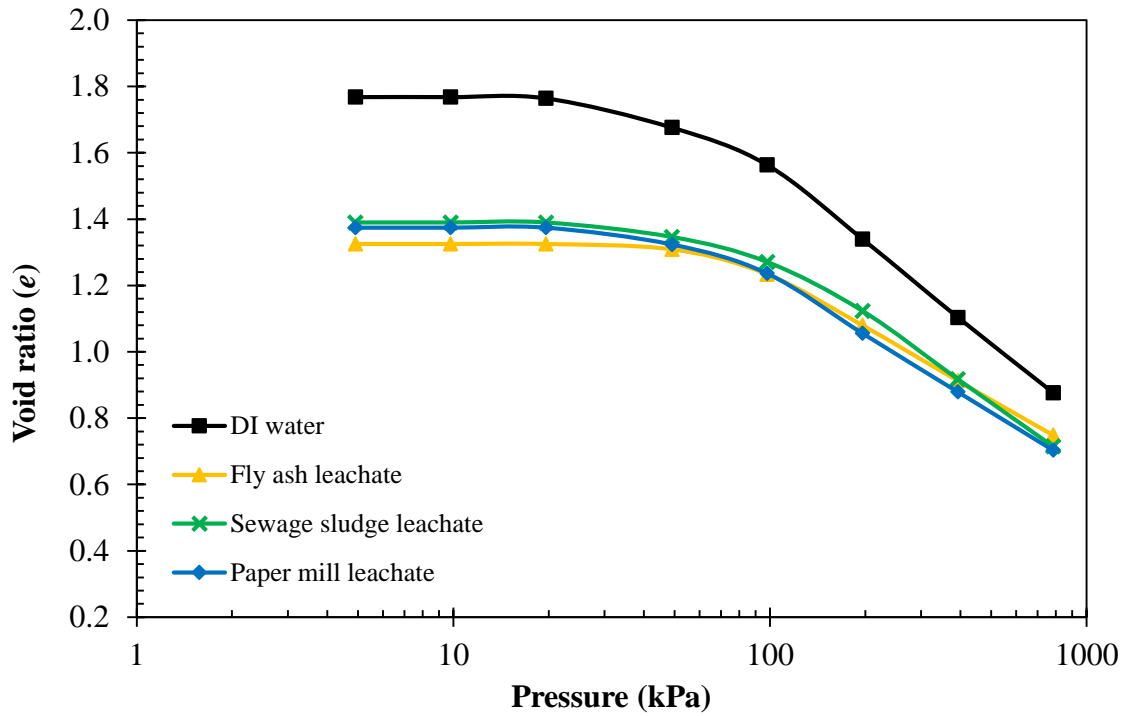


Fig. 6.5. Void ratio and Pressure relationship of bentonites in presence of leachates

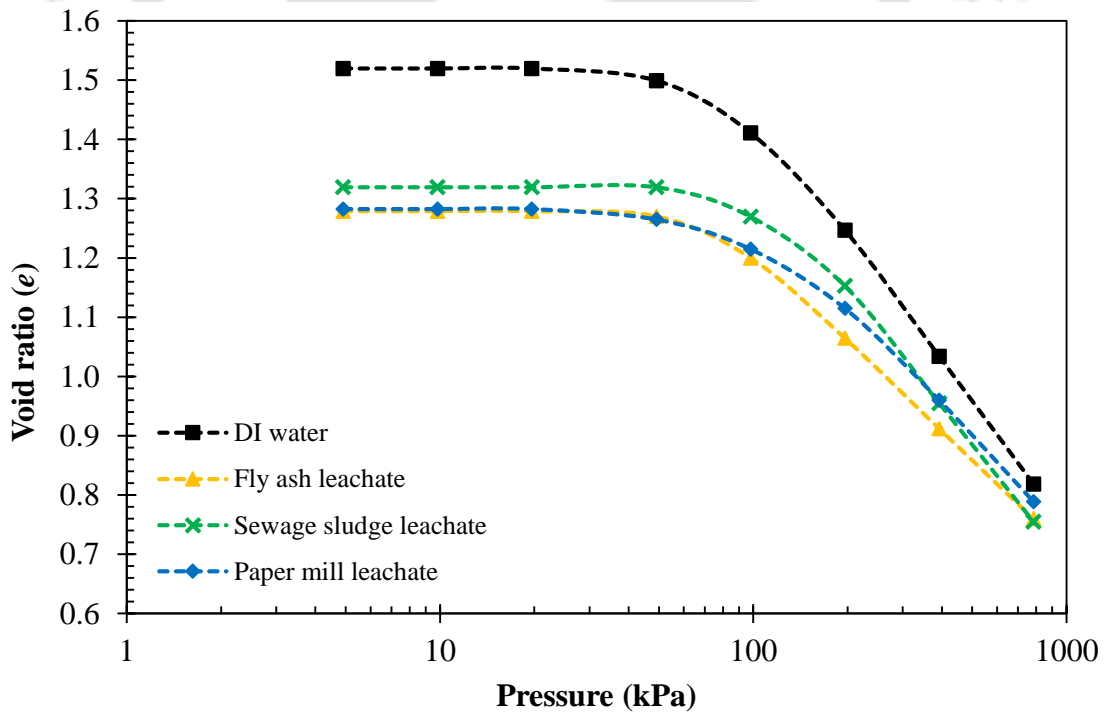


Fig. 6.6. Void ratio and Pressure relationship of bentonites in presence of leachates

6.2.6. Impact of leachates on the coefficient of consolidation (c_v) of bentonites

The relationship between the coefficient of consolidation and vertical consolidation pressures for both the bentonites in the presence of fly ash, paper mill and sewage sludge leachate is depicted in Fig. 6.7 and 6.8. It was observed that with a rise in the consolidation pressure c_v values declined. The plots also revealed that in the presence of all the synthetic leachates, the reduction of c_v value with the rise in vertical pressure significantly affected.

With DI water, the c_v for Bentonite-1 and -2 declined from 6.20×10^{-5} cm²/sec to 1.23×10^{-5} cm²/sec (5.0 times) and 4.90×10^{-5} cm²/sec to 1.31×10^{-5} cm²/sec (3.7 times), with the rise in the vertical pressure from 98.0 kPa to 784.5 kPa. However, in the presence of fly ash leachate, the c_v dropped from 6.8×10^{-4} cm²/sec to 3.3×10^{-5} cm²/sec (20.6 times) and 1.0×10^{-3} cm²/sec to 5.4×10^{-5} cm²/sec (18.5 times) for the similar range of upsurge in the vertical consolidation pressure for Bentonite-1 and -2, respectively. Similarly, for Bentonite-1 and -2 permeated with sewage sludge leachate, the c_v lessened from 2.5×10^{-4} cm²/sec to 1.92×10^{-5} cm²/sec (13.0 times) and 1.4×10^{-4} cm²/sec to 1.7×10^{-5} cm²/sec (8.2 times). Likewise, Bentonite-1 and -2 diffused with paper mill leachate showed a decline in c_v values from 4.90×10^{-4} cm²/sec to 2.18×10^{-5} cm²/sec (22.5 times) and from 2.80×10^{-4} cm²/sec to 5.4×10^{-5} cm²/sec (5.2 times), respectively.

From Fig. 6.7 and 6.8, it was also perceived that the value of c_v for both the bentonites raised in presence of all the synthetic leachates. The plot in the figure showed that at a vertical consolidation pressure of 196 kPa, c_v elevated from 3.5×10^{-5} cm²/sec with DI water to 2.6×10^{-4} cm²/sec (7.4 times), 1.7×10^{-4} cm²/sec (4.9 times) and 6.6×10^{-5} cm²/sec (1.9 times), when infused with Fly ash, Paper mill and sewage sludge leachate for Bentonite-1. However, at the same pressure for Bentonite-2, the c_v value upsurges from 2.6×10^{-5} cm²/sec in existence of DI water to 5.3×10^{-4} cm²/sec (20.4 times), 1.3×10^{-4} cm²/sec (5 times) and 7.5×10^{-5} cm²/sec (2.9 times) for the above leachates, respectively.

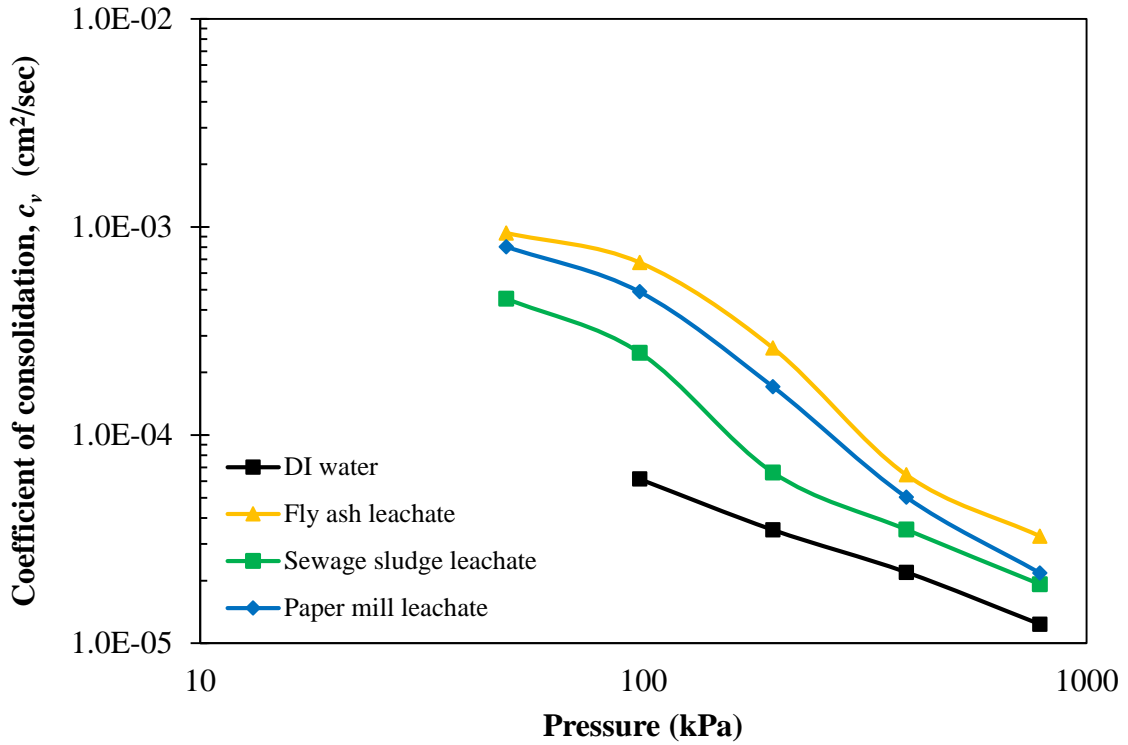


Fig. 6.7. Coefficient of consolidation (c_v) and pressure relationship for Bentonite-1 in presence of leachates

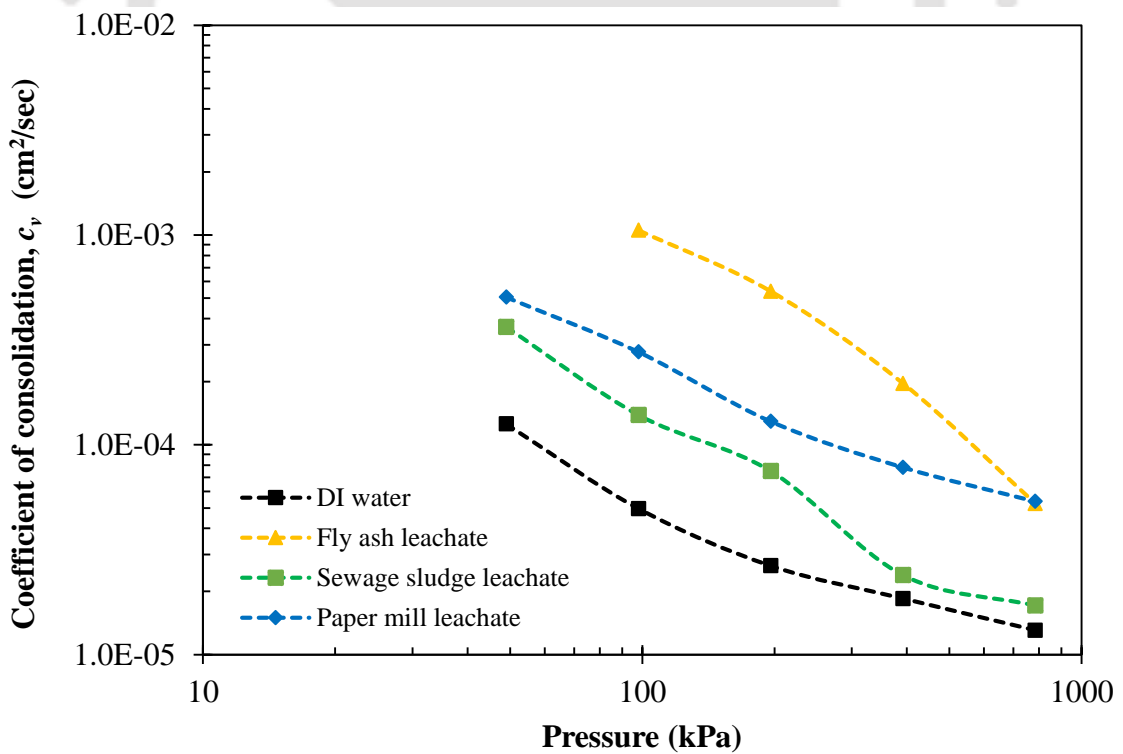


Fig. 6.8. Coefficient of consolidation (c_v) and pressure relationship for Bentonite-2 in presence of leachates

The increase in c_v value was higher for fly ash leachate followed by paper mill and sewage sludge leachate. The overall concentration was 17736.20, 3116.74 and 1941.20 mg/L for fly ash, paper mill and sewage sludge leachates, respectively. The DDL thickness of bentonite soil shrinks in existence of higher concentration of heavy metals present in the leachates causing higher hydraulic conductivity value which consequently surges the c_v value. A comparison between the c_v values for the two bentonites in presence of fly ash, sewage sludge and paper mill leachate and consolidation pressure specifies that the Bentonite-1, having higher swelling capacity, liquid limit, SSA, CEC and lower hydraulic conductivity values, revealed a lesser c_v as compared to Bentonite-2.

6.2.7. Impact of leachates on t_{90} of bentonites

Plots among consolidating pressure and time to complete 90% of consolidation (t_{90}) are shown in Fig. 6.9 and 6.10. The plots display that the t_{90} for both the bentonite samples increased in the presence of fly ash, sewage sludge and paper mill leachate solutions with the rise in the vertical consolidation pressure.

At any pressure, Bentonite-1 displayed a higher t_{90} value as compared to Bentonite-2 in the presence of all synthetic leachates. The plots also demonstrate that in the beginning, the upsurge in t_{90} with the vertical consolidation pressure was progressing slowly; however, a significant rise in the t_{90} value was observed at higher pressures. The plots also reveal that in comparison to that of DI water the upsurge in t_{90} with the consolidation pressure was not as much in presence of various synthetic leachates. The plot in Fig 6.9 and 6.10 show that the t_{90} values for the Bentonite-1 and -2 infused with DI water rose up from 368.6 to 900.0 minutes and 234.1 to 564.1 minutes with the rise in the vertical consolidation pressure from 9.8 kPa to 784.5 kPa. However, it elevated only from 14.44 minutes to 196.0 minutes and 9.0 minutes to 121.0 minutes for fly ash leachate solutions having high concentrations of heavy metals. Similarly, for sewage sludge leachate the t_{90} upraised from 39.7 minutes to 345.9 minutes and 67.2 minutes to 345.9 minutes. Likewise, on permeation with paper mill leachate it increased only from 20.3 minutes to 285.6 minutes and 33.6 minutes to 225.4 minutes respectively.

The t_{90} value seems to be lower for fly ash leachate followed by paper mill and sewage sludge leachate. This is because the metal concentration level is very high in fly ash leachate as compared to paper mill and sewage sludge leachates.

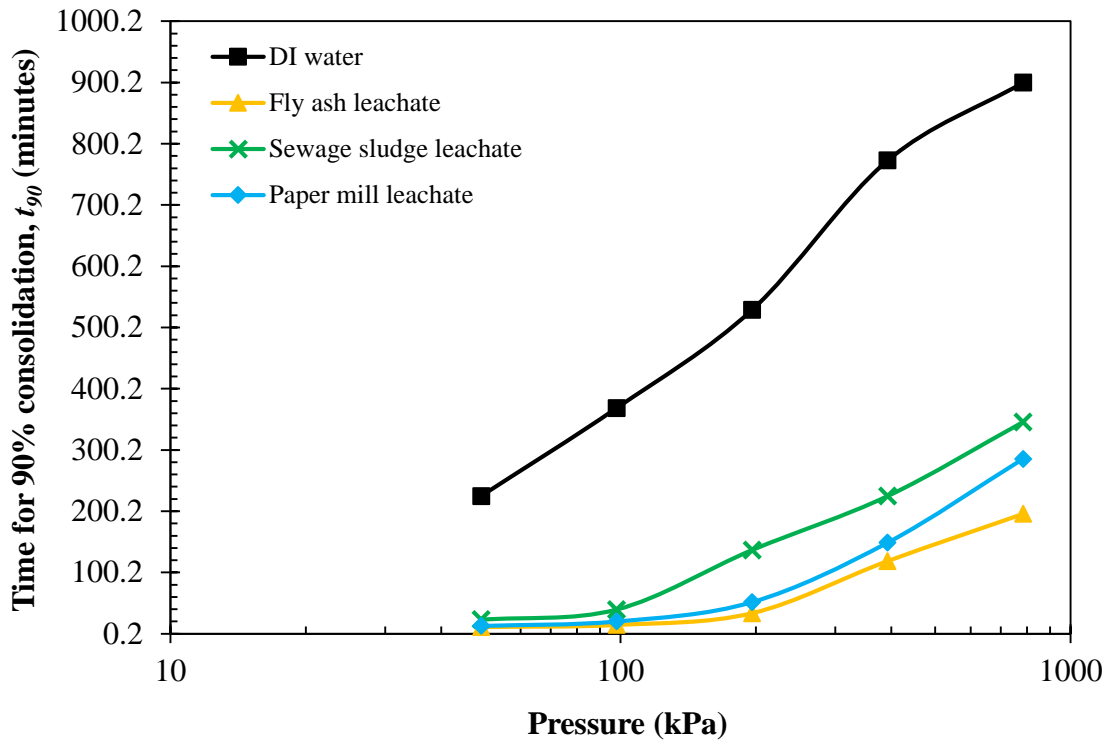


Fig. 6.9. Time for 90% consolidation (t_{90}) and pressure relationship for Bentonite-1 in presence of leachates

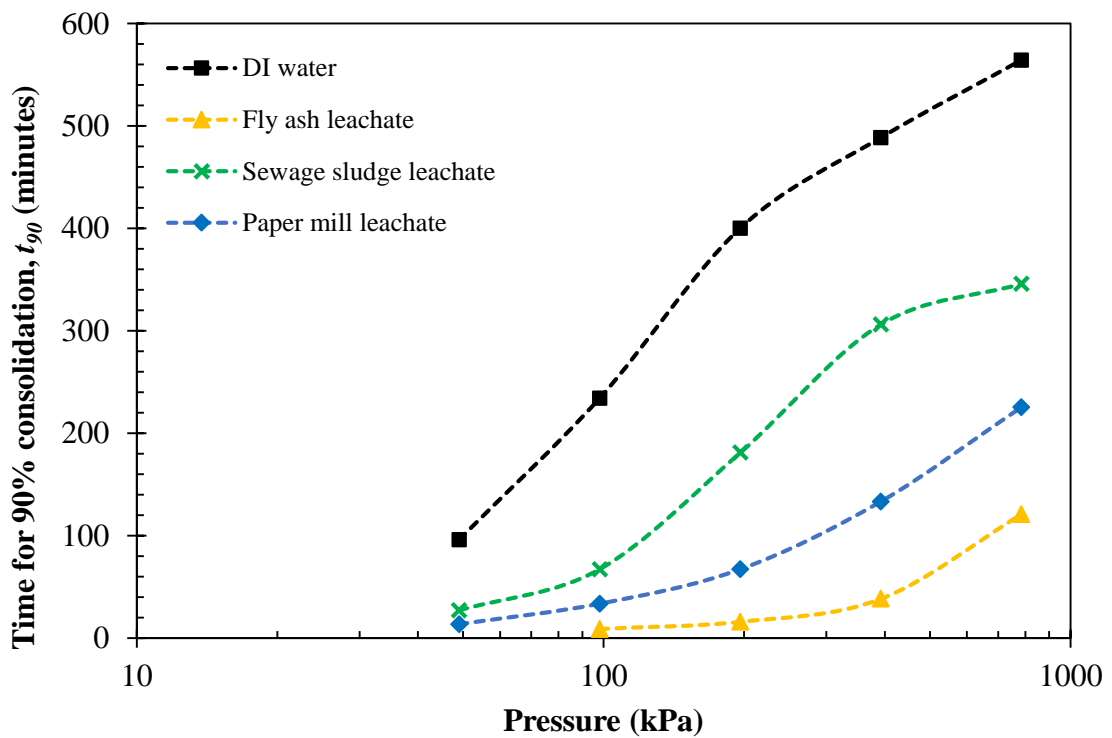


Fig. 6.10. Time for 90% consolidation (t_{90}) and pressure relationship for Bentonite-2 in presence of leachates

6.2.8. Impact of leachates on compression index (C_c) of bentonites

Like hydraulic conductivity, another important parameter that needs understanding for settlement analysis is the compression index (C_c). The C_c value of fly ash paper mill and sewage sludge leachate are listed in Table 6.5, which depicts that the C_c value of both bentonites declines in presence of leachates. For Bentonite-1 and -2, the soil samples exhibited a C_c value of 0.79 and 0.72 when infused with DI water. However, due to permeation of fly ash, sewage sludge and paper mill leachate the C_c values are declined by 31.6, 13.9 and 25.3%, respectively. Similarly, Bentonite-2 showed a reduction in C_c value of 30.6, 8.3 and 20.8% due to permeation of fly ash, sewage sludge and paper mill leachate, respectively.

Bentonite-1, having higher swelling capacity and liquid limit revealed a higher reduction in C_c as compared to Bentonite-2. Both the bentonites showed a significant reduction in C_c value in presence of Fly ash leachate.

Table 6.5. Compression index of bentonites in presence of synthetic leachates.

| Permeant | Compression Index (C_c) | |
|------------------------|-----------------------------|-------------|
| | Bentonite-1 | Bentonite-2 |
| DI water | 0.79 | 0.72 |
| Fly ash leachate | 0.54 | 0.50 |
| Sewage sludge leachate | 0.68 | 0.66 |
| Paper mill leachate | 0.59 | 0.57 |

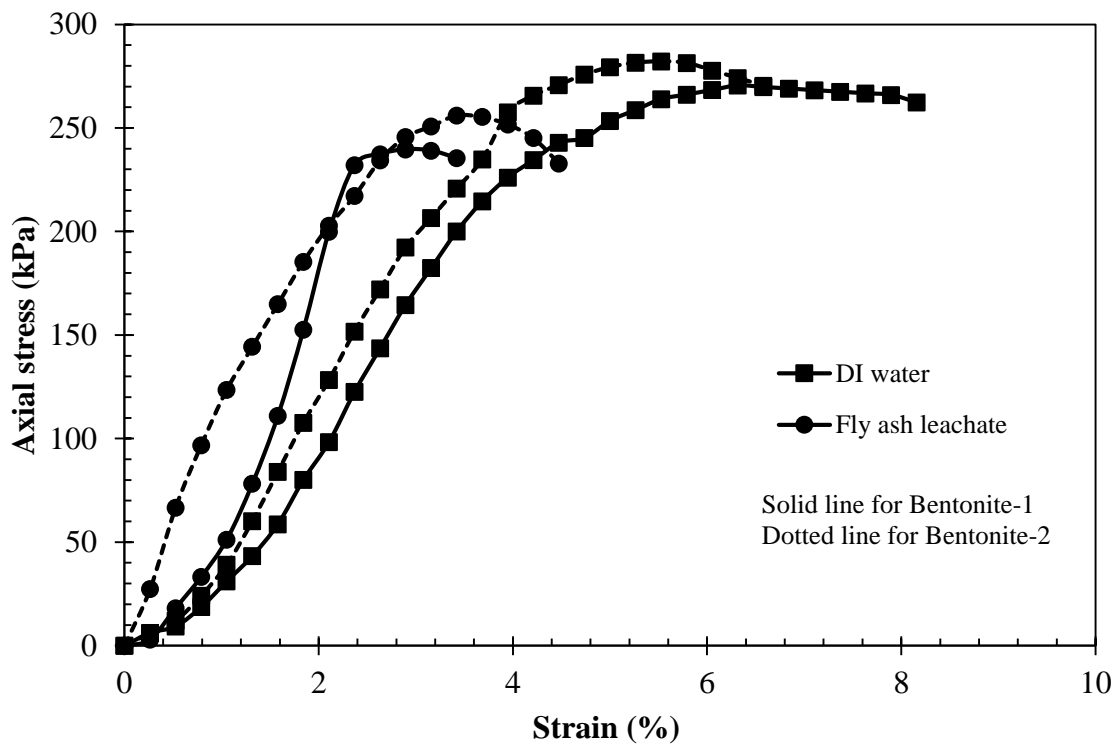
6.2.9. Impact of leachates on UCS of bentonites

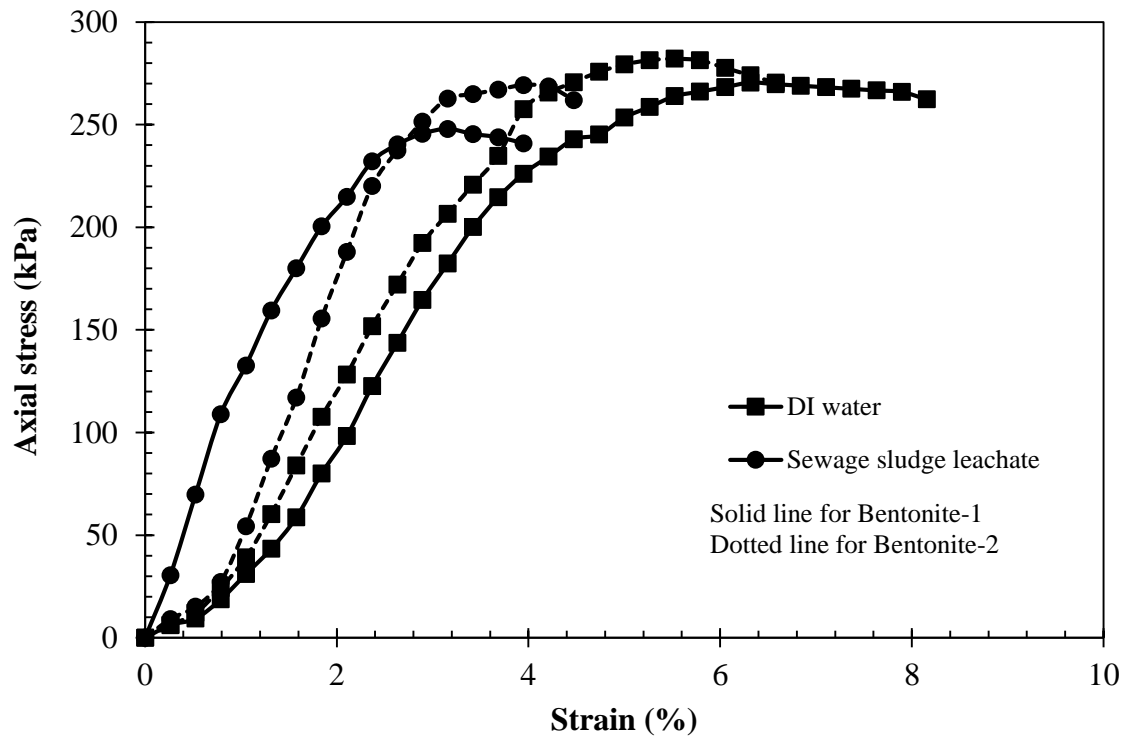
The stress-strain relationship of Bentonite-1 and -2 are depicted in Fig. 6.11 in the presence of DI water and various synthetic leachates. It explains that the failure occurs for Bentonite-1 and -2 in DI water presence at a high stress level of 6.3% and 5.5%. However, the failure was detected at 2.9 and 3.4% strain rate in the presence of Fly ash leachate for Bentonite-1 and -2, respectively. Similarly, for Sewage sludge leachate, the failure strain rate obtained was 3.7 and 3.4%. Likewise, 3.1 and 3.9% failure strain rate was noticed in case of paper mill leachate for both the bentonites, respectively.

Table 6.6. Unconfined compressive strength of bentonites in presence of synthetic leachates.

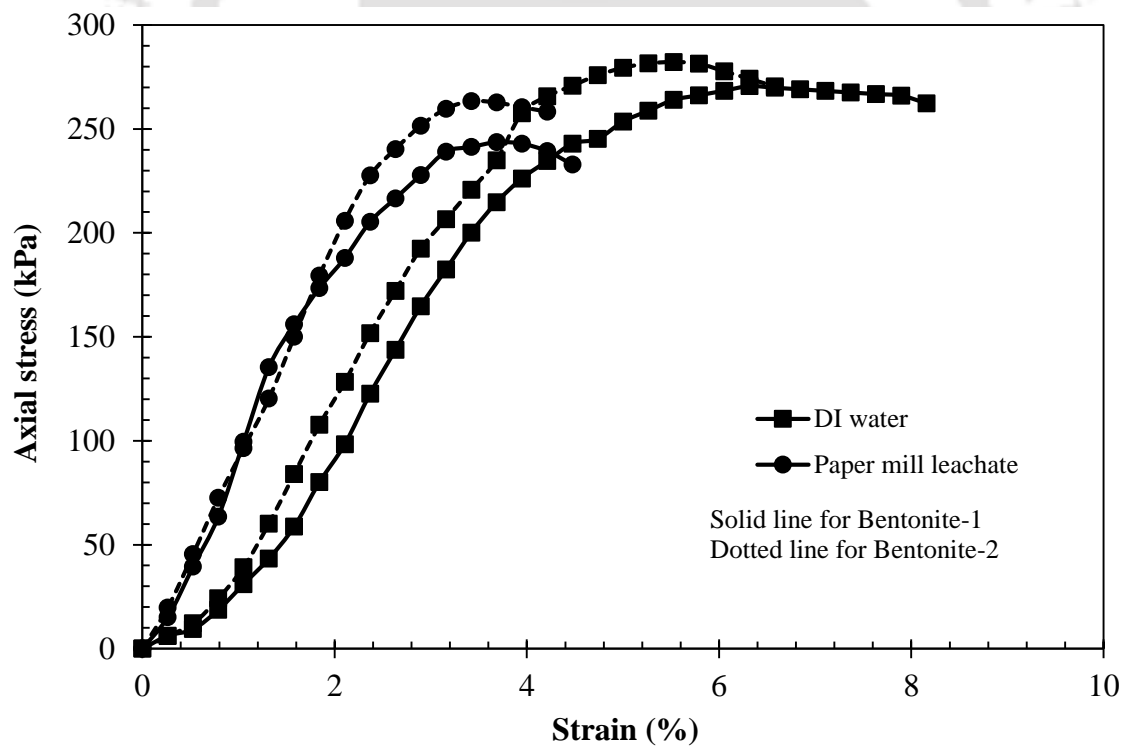
| Permeant | Unconfined compressive strength (kPa) | |
|------------------------|---------------------------------------|-------------|
| | Bentonite-1 | Bentonite-2 |
| DI water | 270.5 | 282.1 |
| Fly ash leachate | 239.7 | 256.0 |
| Sewage sludge leachate | 247.9 | 269.3 |
| Paper mill leachate | 243.6 | 263.4 |

Table 6.6 shows the unconfined compressive strength of Bentonite-1 and -2 in presence of DI water, fly ash, sewage sludge and paper mill leachate. It was observed that the strength of bentonites declined in the presence of all the leachates.





(ii) Sewage sludge leachate



(iii) Paper mill leachate

Fig. 6.11. Axial stress (kPa) vs strain (%) relationship of the bentonites in the presence of various leachates

The decline in strength of Bentonite-1 was observed by 11.4, 9.9 and 8.4% in the presence of fly ash, sewage sludge and paper mill leachate, while, for Bentonite-2 the fall in strength was found to be 9.2, 6.6 and 4.5%, respectively. This decline in strength can be attributed to the reduction in the density of the specimen. Considering the MDD of a soil specimen rises due to the diffusion of the contaminant (Abd El-Aal, 2017), and, in this case, the samples were compacted at MDD concerning DI water, the soil specimens infused with leachates were in a loosened state. Bentonite-1 exhibited a higher decline in strength in comparison to Bentonite-2. This is because of Bentonite-2's lower liquid limit and DDL thickness, thus, inducing a closer grain to grain contact and hence exhibiting a higher strength value. It is also observed that bentonites with fly ash leachate exhibit lower strength value.

6.2.10. Adsorption of various leachates on bentonites

In leachates, various numbers of metals always exist collectively. Therefore, the adsorption behaviour of bentonites for fly ash, sewage sludge and paper mill leachate were investigated in a competitive system. Fig. 6.12, 6.13 and 6.14 depict the removal of heavy metals present in fly ash, sewage sludge and paper mill leachate for both the bentonites.

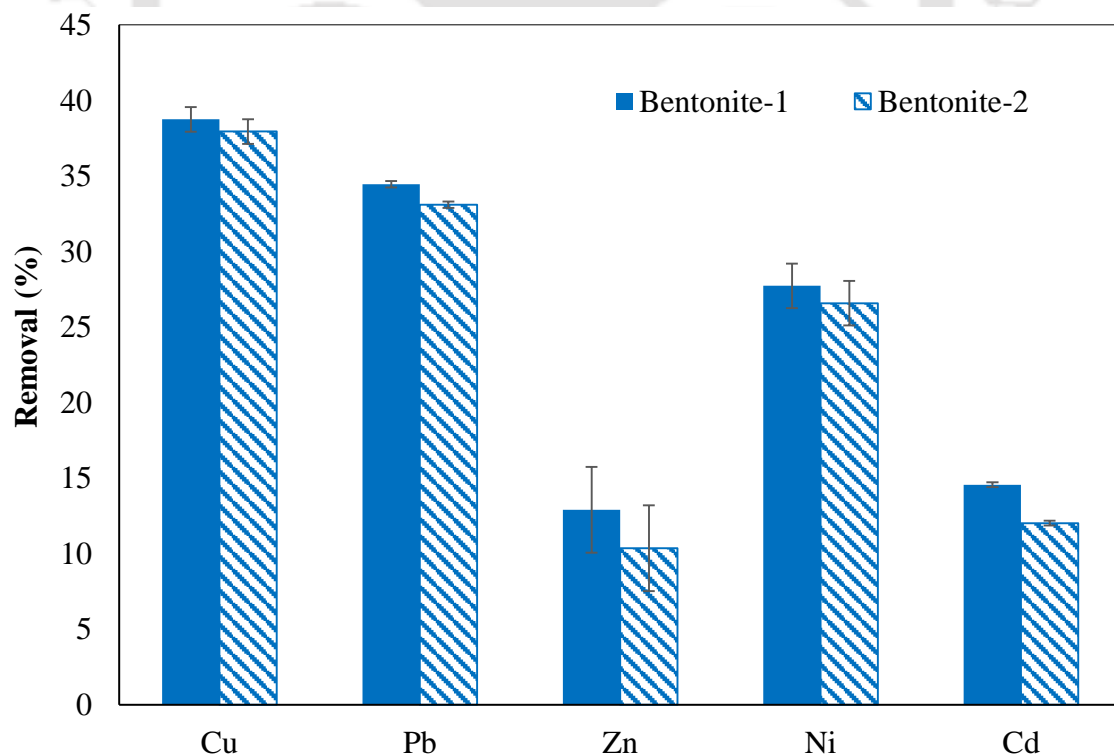


Fig. 6.12. Removal of heavy metal from fly ash leachate by bentonites

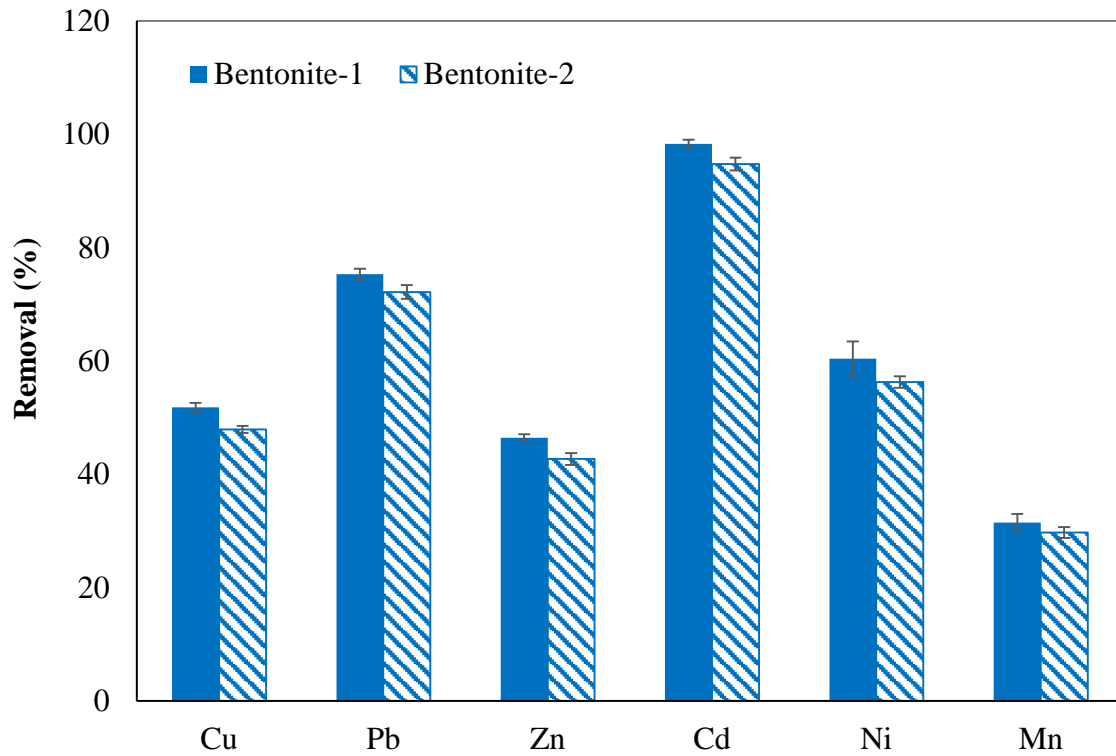


Fig. 6.13. Removal of heavy metal from sewage sludge leachate by bentonites

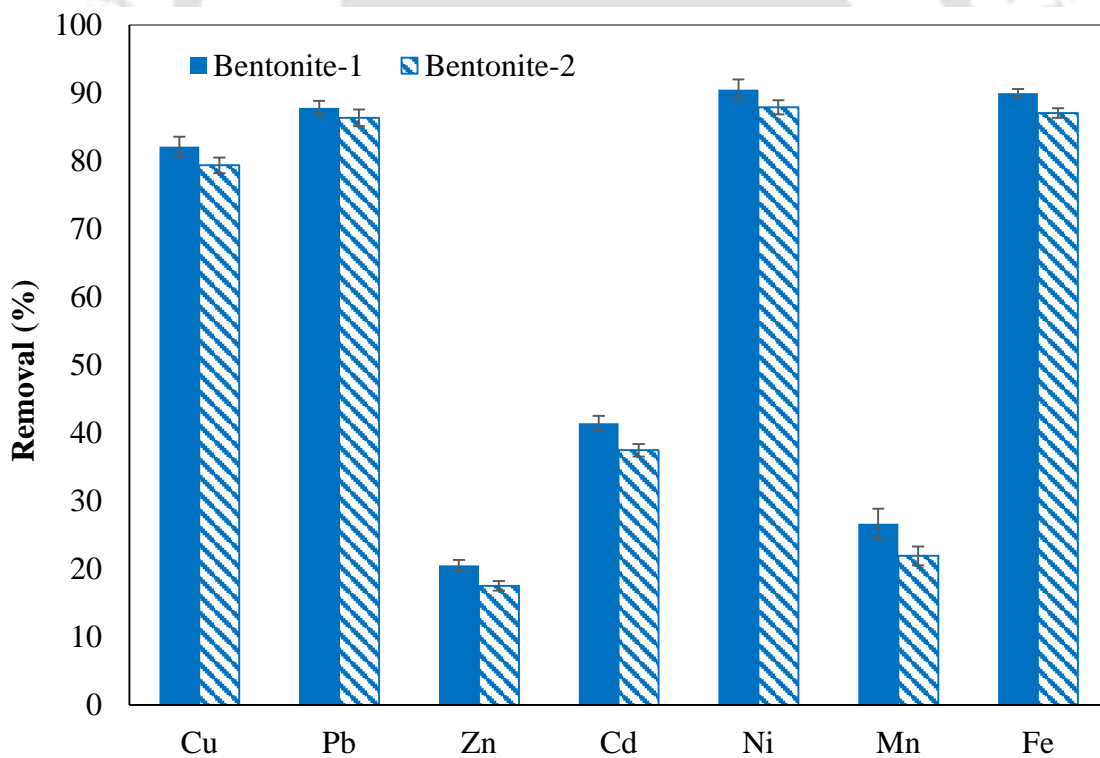


Fig. 6.14. Removal of heavy metal from paper mill leachate by bentonites

Table 6.7. Removal of heavy metal from Fly ash leachate by bentonites

| Fly-ash Leachate | Heavy metal | Final pH | Concentration (mg/L) | | Removal (%) | Adsorption capacity (mg/g) |
|---------------------|------------------|-------------|--------------------------|---------------------|----------------|----------------------------------|
| | | | Initial Concentration | After adsorption | | |
| Bentonite-1 | Cu ²⁺ | 5.6±0.2 | 886.2 | 542.8 | 38.7 | 6.8 |
| | Pb ²⁺ | | 3655.3 | 2395.7 | 34.4 | 24.3 |
| | Zn ²⁺ | | 13044.0 | 11359.8 | 12.9 | 33.7 |
| | Ni ²⁺ | | 26.9 | 19.4 | 27.7 | 0.1 |
| | Cd ²⁺ | | 123.8 | 105.7 | 14.6 | 0.3 |
| Bentonite-2 | Cu ²⁺ | 5.6±0.2 | 886.2 | 549.9 | 37.9 | 6.7 |
| | Pb ²⁺ | | 3655.3 | 2445.4 | 33.1 | 23.3 |
| | Zn ²⁺ | | 13044.0 | 11692.8 | 10.3 | 27.0 |
| | Ni ²⁺ | | 26.9 | 19.7 | 26.5 | 0.1 |
| | Cd ²⁺ | | 123.8 | 108.9 | 12.0 | 0.3 |

A higher amount of Zn²⁺ was present in fly ash leachate, i.e., 13044.0 mg/L in the present study. Existence of high level of zinc may suppress other metal ions to adsorb on the surface of both the bentonites. It was detected that due to Bentonite-1 & -2 the concentrations of Zn²⁺ reduced from 13044.0 mg/L to 11359.8 and 11692.9 mg/L for fly ash leachate. Removal of 12.9 and 10.3% was obtained for Zn²⁺ in the presence of Bentonite -1 and 2, respectively. The detailed removal of heavy metals from fly ash leachate by both the bentonites are listed in Table 6.7. The overall adsorption capacity in presence of fly ash leachate was found to be 65.3 and 57.5 mg/g for Bentonite-1 and-2, respectively.

Similarly, Tables 6.8 and 6.9 show the detailed removal of heavy metals from sewage sludge and paper mill leachate by both the bentonites. The highest removal was observed in Cd, followed by Pb, Ni, Cu, Zn, and Mn by both the bentonites for sewage sludge leachate. However, in case of paper mill leachate the maximum removal obtained for Ni subsequently by Fe, Pb, Cu, Cd, Mn, and Zn. A higher amount of removal was observed in Bentonite-1 as compared to Bentonite-2 for sewage sludge leachate. The presence of sewage sludge leachate for the removal of Cu²⁺, Pb²⁺, Zn²⁺, Cd²⁺, Ni²⁺ and Mn²⁺ was found to be 7.5, 4.2, 8.1, 3.6, 6.9, and 5.6% higher, respectively for Bentonite-1, as compared to Bentonite-2.

Table 6.8. Removal of heavy metal from sewage sludge leachate by bentonites

| Sewage sludge Leachate | Heavy metal | Final pH | Concentration (mg/L) | | Removal (%) | Adsorption capacity (mg/g) |
|------------------------------|------------------|-------------|--------------------------|---------------------|----------------|----------------------------------|
| | | | Initial Concentration | After adsorption | | |
| Bentonite-1 | Cu ²⁺ | 5.1±0.2 | 174.0 | 83.8 | 51.8 | 1.6 |
| | Pb ²⁺ | | 130.0 | 32.0 | 75.3 | 1.7 |
| | Zn ²⁺ | | 967.2 | 517.8 | 46.4 | 8.0 |
| | Cd ²⁺ | | 37.0 | 0.6 | 98.3 | 0.6 |
| | Ni ²⁺ | | 278.0 | 110.0 | 60.4 | 3.0 |
| | Mn ²⁺ | | 355.0 | 243.1 | 31.5 | 2.0 |
| Bentonite-2 | Cu ²⁺ | 5.1±0.2 | 174.0 | 90.6 | 47.9 | 1.5 |
| | Pb ²⁺ | | 130.0 | 36.2 | 72.2 | 1.7 |
| | Zn ²⁺ | | 967.2 | 554.1 | 42.7 | 7.4 |
| | Cd ²⁺ | | 37.0 | 1.9 | 94.8 | 0.6 |
| | Ni ²⁺ | | 278.0 | 121.6 | 56.2 | 3.0 |
| | Mn ²⁺ | | 355.0 | 249.4 | 29.7 | 1.8 |

Likewise, for Paper mill leachate 3.3, 1.6, 14.6, 9.6, 2.9, 17.7, and 3.3% higher removal for Cu²⁺, Pb²⁺, Zn²⁺, Cd²⁺, Ni²⁺, Mn²⁺ and Fe²⁺, respectively was obtained by Bentonite-1 in comparison to Bentonite-2. The overall uptake of sewage sludge leachate was found to be 17.0 and 16.0 mg/g in the presence of Bentonite-1 and -2, whereas, for paper mill leachate, 14.7 mg/g and 13.1 mg/g were obtained, respectively. For all the leachates, bentonites in a single system showed a higher amount of adsorption of Pb, Cu and Zn, compared to a competitive system. This is primarily attributed to competitive adsorption of different varieties of ions in the system. As there are a finite number of adsorption sites on the surface of the bentonite, each heavy metal competes for a certain site, thus attempting to be transferred from the leachate to the bentonite surface, resulting in partial sharing of the sites which reduces the adsorbed amounts.

Table 6.9. Removal of heavy metal from paper mill leachate by bentonites

| Paper mill Leachate | Heavy metal | Final pH | Concentration (mg/L) | | Removal (%) | Adsorption capacity (mg/g) |
|---------------------|------------------|----------|-----------------------|------------------|-------------|----------------------------|
| | | | Initial Concentration | After adsorption | | |
| Bentonite-1 | Cu ²⁺ | | 17.5 | 3.1 | 82.1 | 0.2 |
| | Pb ²⁺ | | 7.4 | 0.9 | 87.8 | 0.1 |
| | Zn ²⁺ | | 2366.6 | 1881.2 | 20.5 | 8.6 |
| | Cd ²⁺ | 5.0±0.2 | 520.8 | 305.0 | 41.4 | 3.8 |
| | Ni ²⁺ | | 12.7 | 1.2 | 90.5 | 0.2 |
| | Mn ²⁺ | | 126.0 | 92.4 | 26.6 | 0.6 |
| | Fe ²⁺ | | 65.4 | 6.5 | 89.9 | 1.0 |
| Bentonite-2 | Cu ²⁺ | | 17.5 | 3.6 | 79.3 | 0.2 |
| | Pb ²⁺ | | 7.4 | 1.0 | 86.3 | 0.1 |
| | Zn ²⁺ | | 2366.6 | 1951.9 | 17.5 | 7.4 |
| | Cd ²⁺ | 5.0±0.2 | 520.8 | 325.7 | 37.4 | 3.5 |
| | Ni ²⁺ | | 12.7 | 1.5 | 87.9 | 0.2 |
| | Mn ²⁺ | | 126.0 | 98.3 | 21.9 | 0.5 |
| | Fe ²⁺ | | 65.4 | 8.5 | 87.0 | 1.1 |

6.2.11. Effect of leachates on various bentonite doses

The adsorbent dosage studies were carried out for varying bentonite amounts, ranging from 0.2 to 5.0 g/100 mL leachate solutions, the results of which are depicted in Fig. 6.15-6.20. It was observed that the adsorbed metal ions (i.e. their removal efficiencies) increased with increasing adsorbent dosage, primarily attributing to an increase in the clay concentration that increases the surface area of the adsorbent, which in turn, increases the number of binding sites for the same liquid volume.

The removal efficiency was found to be increased from 3.7 to 21.6 (Cu), 2.9 to 8.2 (Ni), 5.2 to 34.8 (Pb), 1.9 to 7.6 (Zn) and 3.5 to 15.0 (Cd) % by Bentonite-1 and 3.0 to 15.7 (Cu), 1.8 to 6.2 (Ni), 4.5 to 33.2 (Pb), 1.1 to 5.9 (Zn) and 1.9 to 12.1 (Cd) % by Bentonite-2, respectively with the gradual increase in bentonite dose of 0.2 to 5.0 g for Fly ash leachate.

Likewise, for sewage sludge leachate, the removal efficiency raised from 20.7 to 53.0 (Cu), 3.9 to 27.2 (Ni), 7.7 to 35.9 (Pb), 4.8 to 30.1 (Zn), 29.2 to 98.8 (Cd) and 3.9 to 21.4

(Mn) % by Bentonite-1. However, for Bentonite-2, 20.0 to 49.0 (Cu), 3.5 to 18.3 (Ni), 4.9 to 25.9 (Pb), 2.5 to 15.9 (Zn), 23.5 to 77.0 (Cd) and 1.6 to 7.1 (Mn) % removal efficiency was obtained.

Similarly, for paper mill leachate, in presence of Bentonite-1, the removal efficiency raised from 37.8 to 82.8 (Cu), 30.1 to 90.2 (Ni), 30.1 to 89.0 (Pb), 1.8 to 15.7 (Zn), 4.5 to 26.3 (Cd), 7.5 to 28.0 (Mn) and 18.1 to 90.2 (Fe) %, respectively. Whereas, 34.9 to 79.8 (Cu), 26.7 to 86.9 (Ni), 24.3 to 86.9 (Pb), 1.3 to 11.5 (Zn), 3.5 to 23.2 (Cd), 5.6 to 23.8 (Mn) and 16.2 to 86.9 (Fe) % increase in removal was obtained by Bentonite-2.

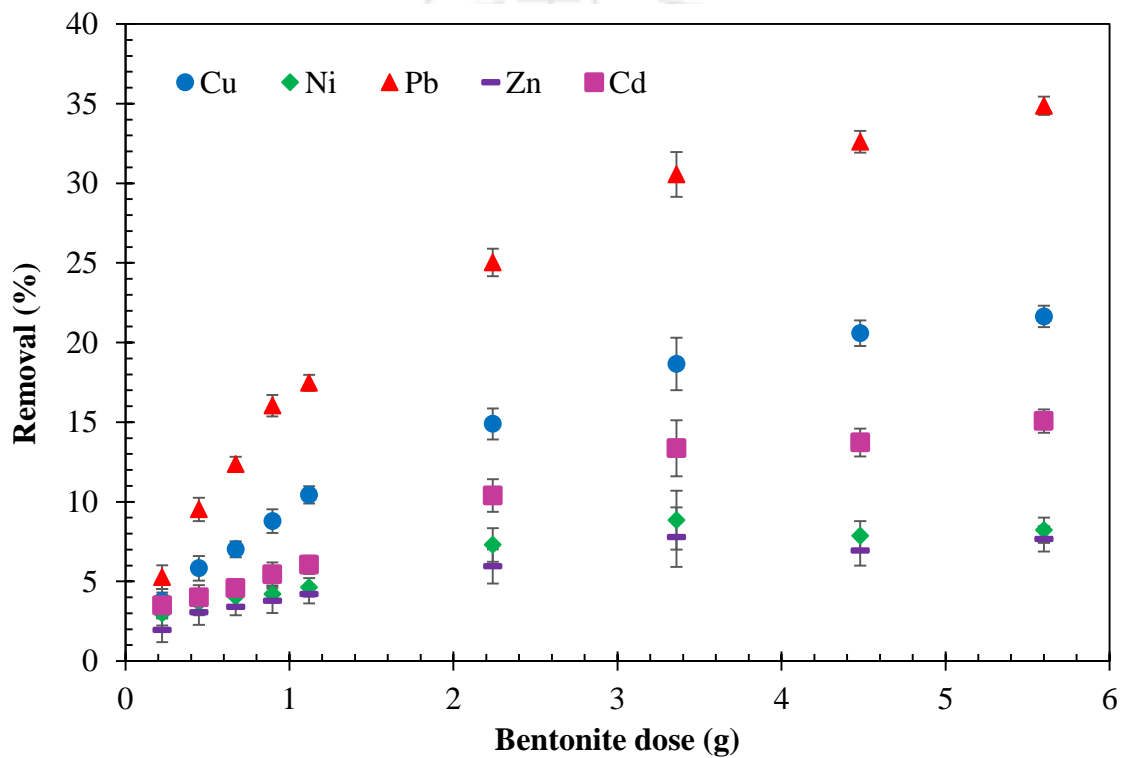


Fig. 6.15. Removal % of fly ash leachate at different bentonite dosage for Bentonite-1

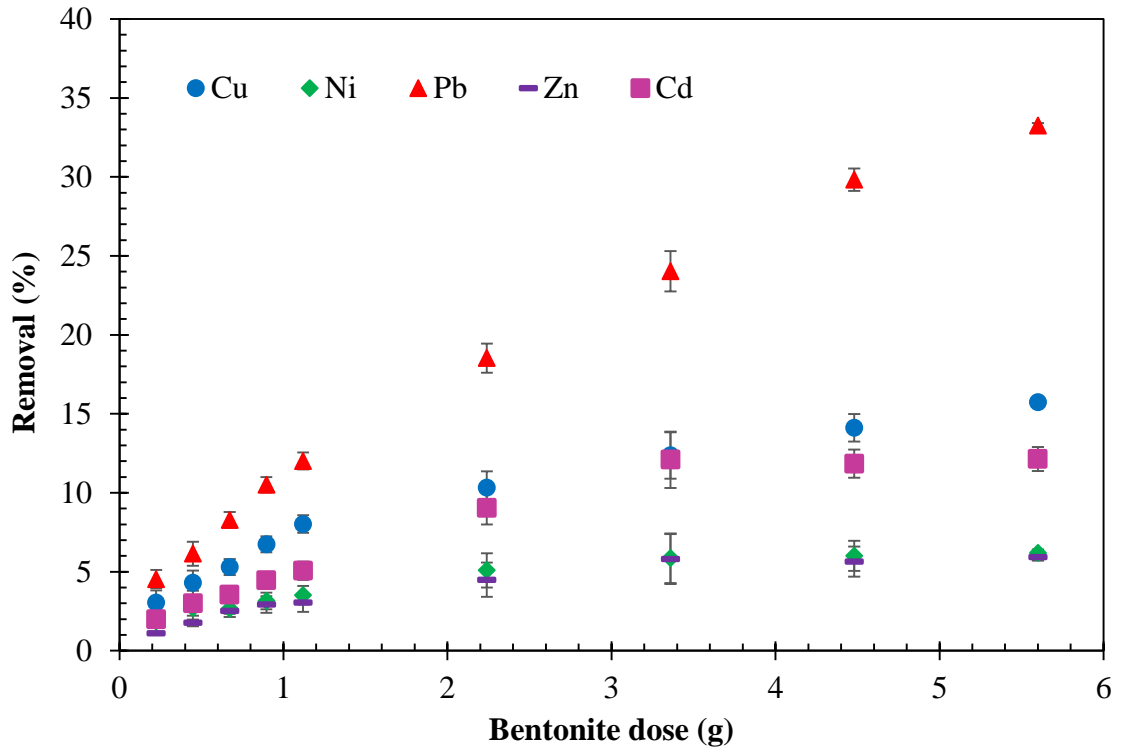
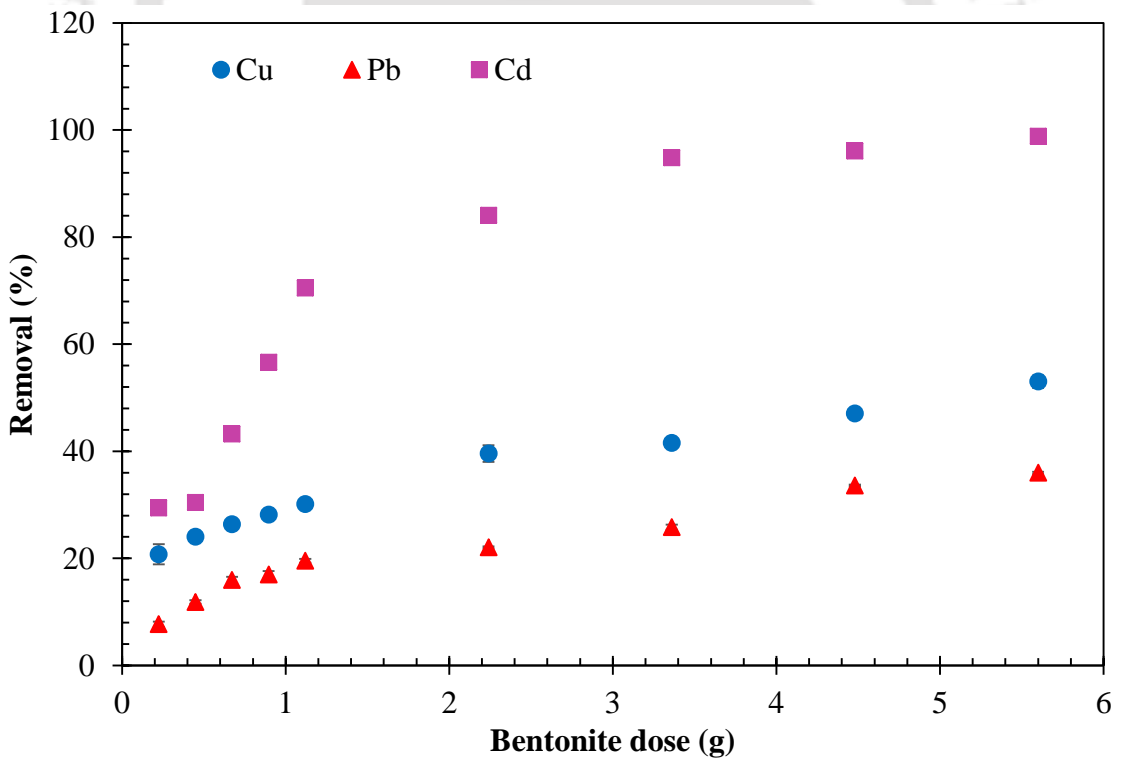
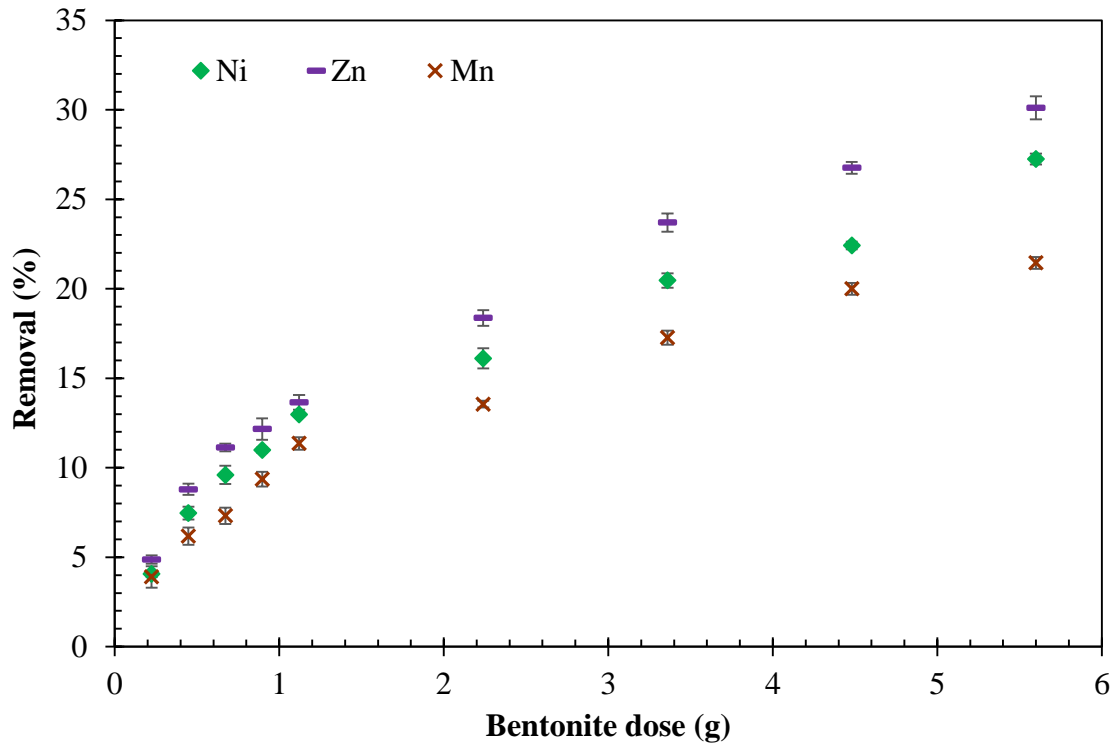


Fig. 6.16. Removal % of fly ash leachate at different bentonite dosage for Bentonite-2

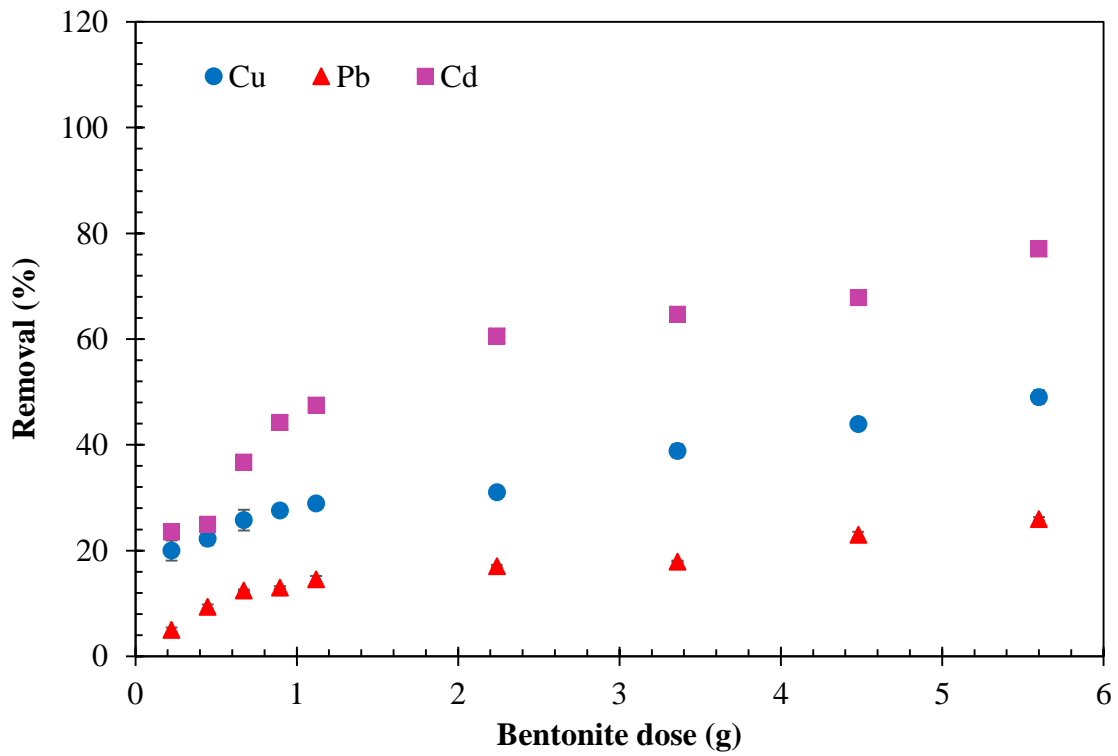


(i)

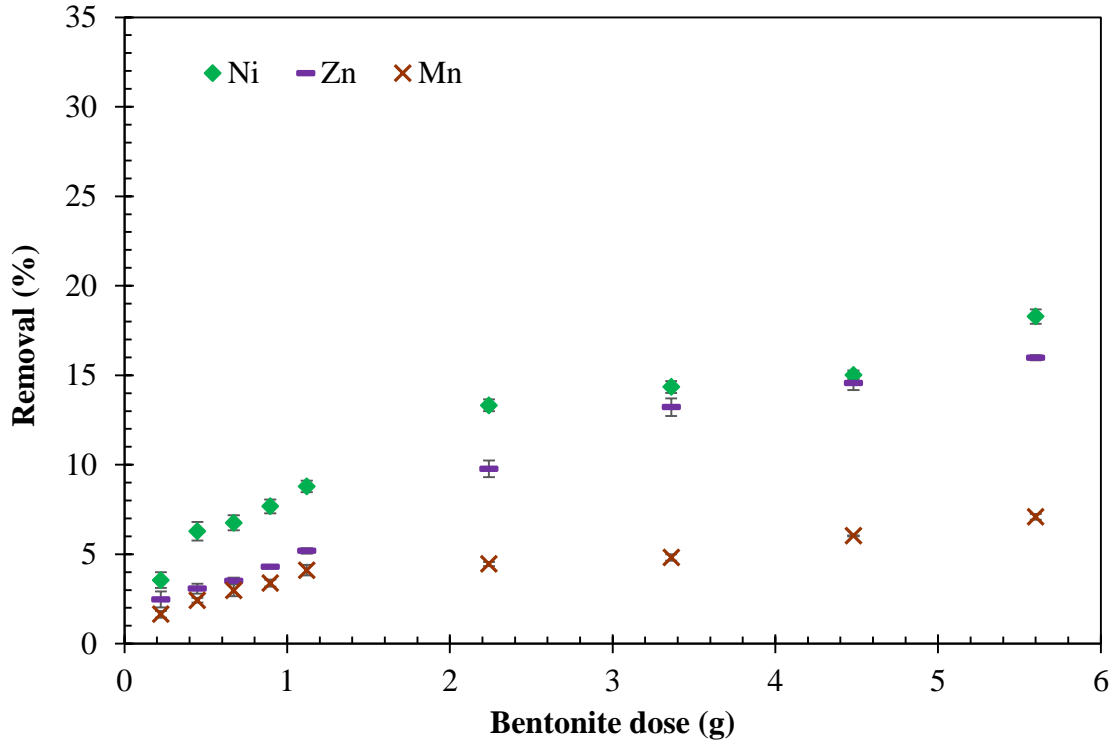


(ii)

Fig. 6.17. Removal % of sewage sludge leachate at different bentonite dosage for Bentonite-1

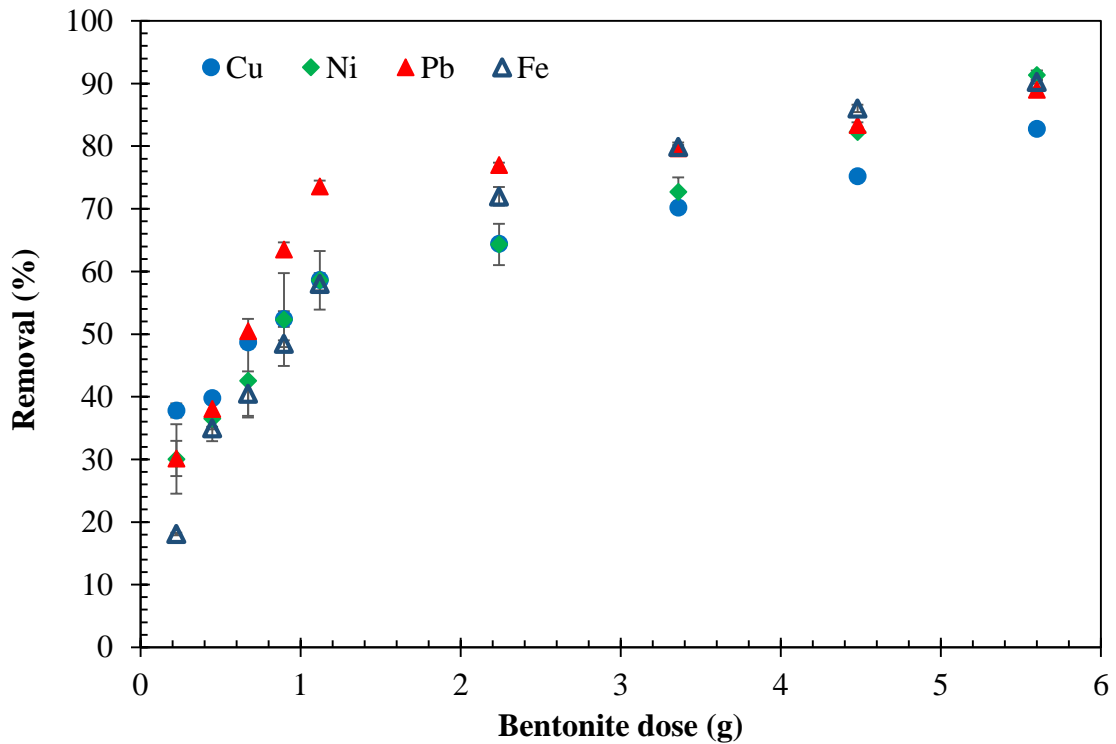


(i)

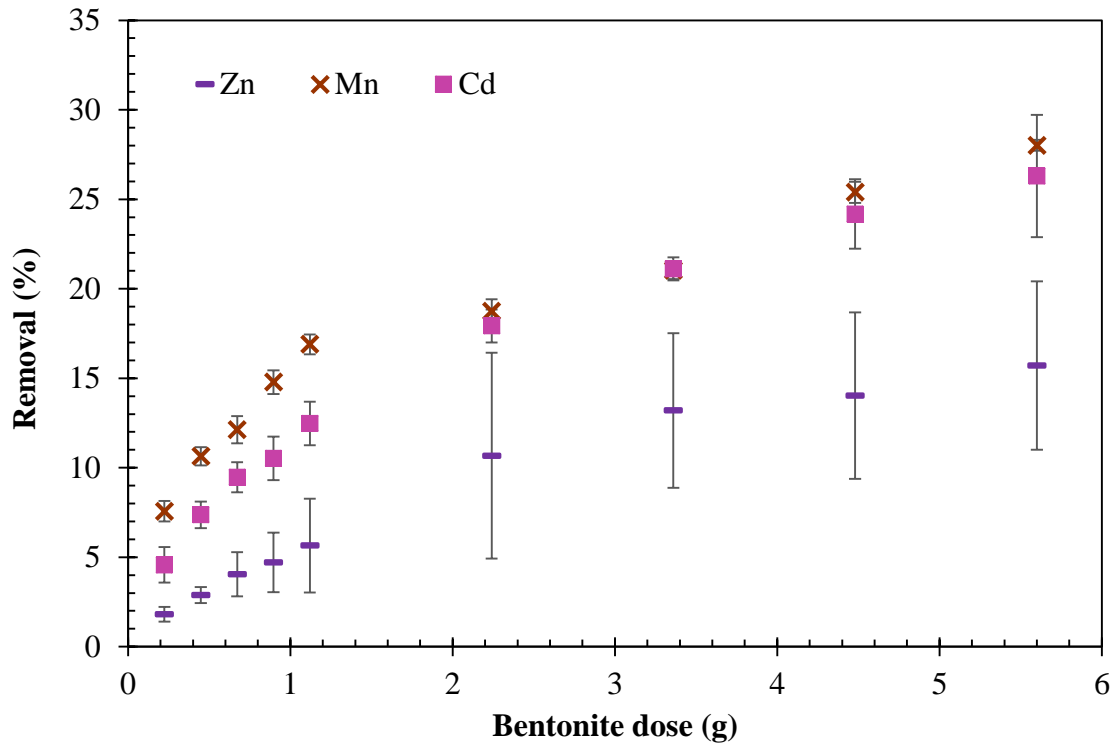


(ii)

Fig. 6.18. Removal % of sewage sludge leachate at different bentonite dosage for Bentonite-2

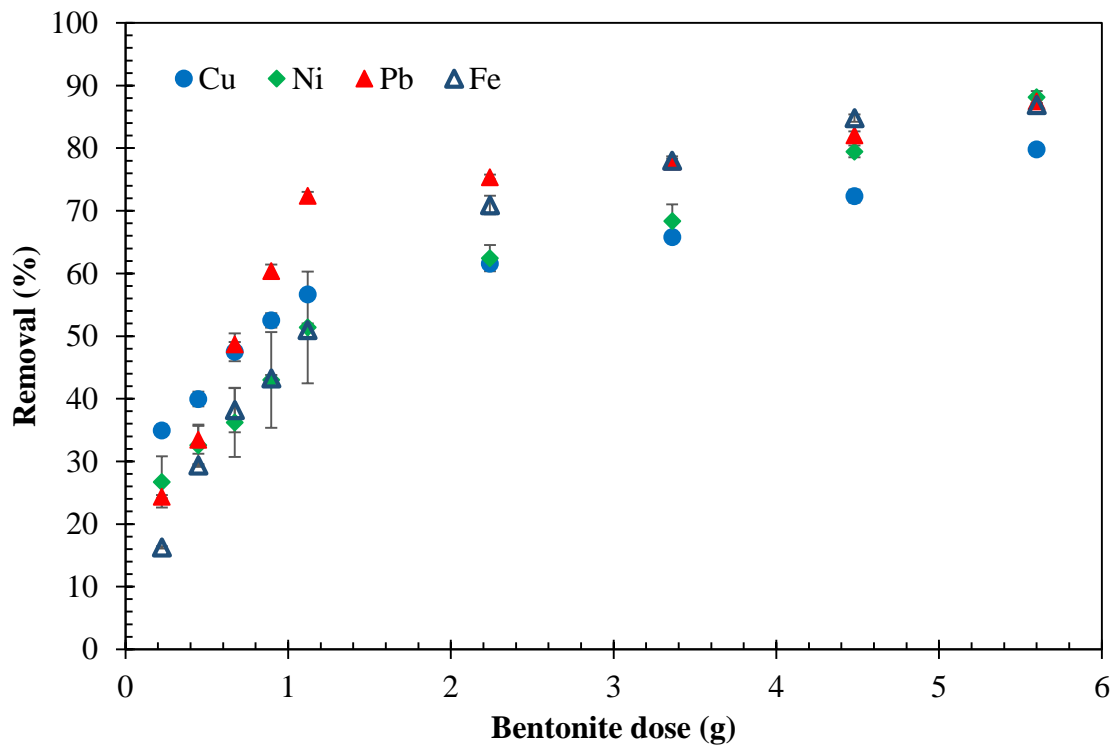


(i)

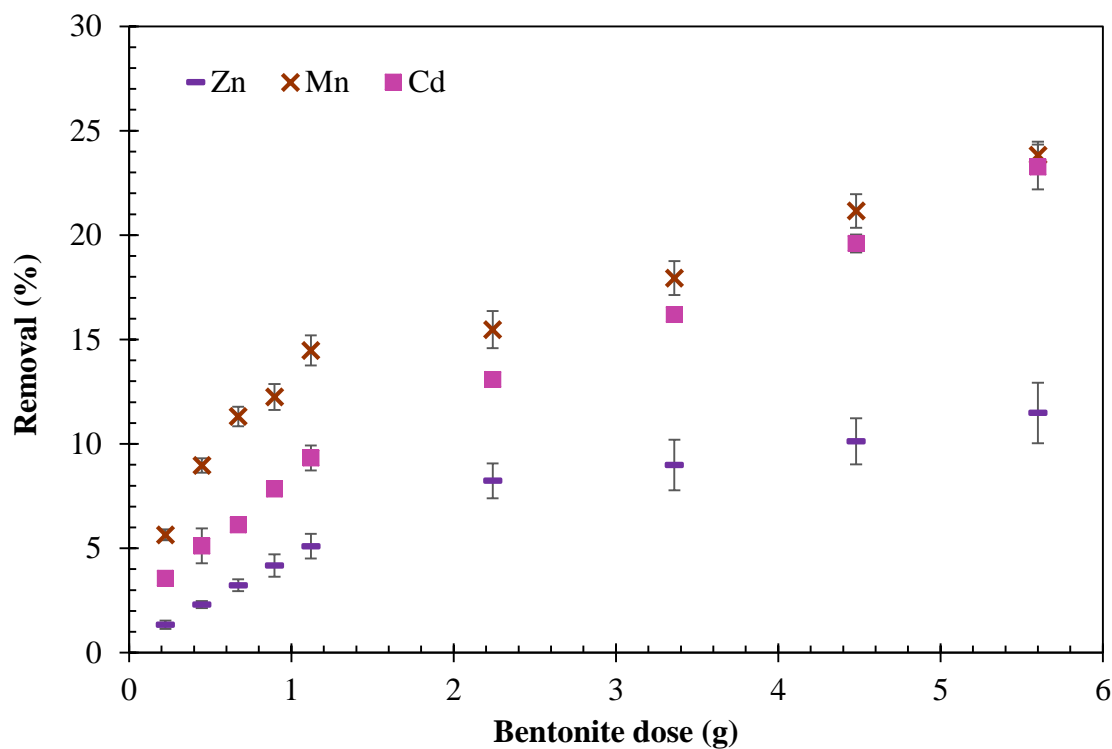


(ii)

Fig. 6.19. Removal % of paper mill leachate at different bentonite dosage for Bentonite-1



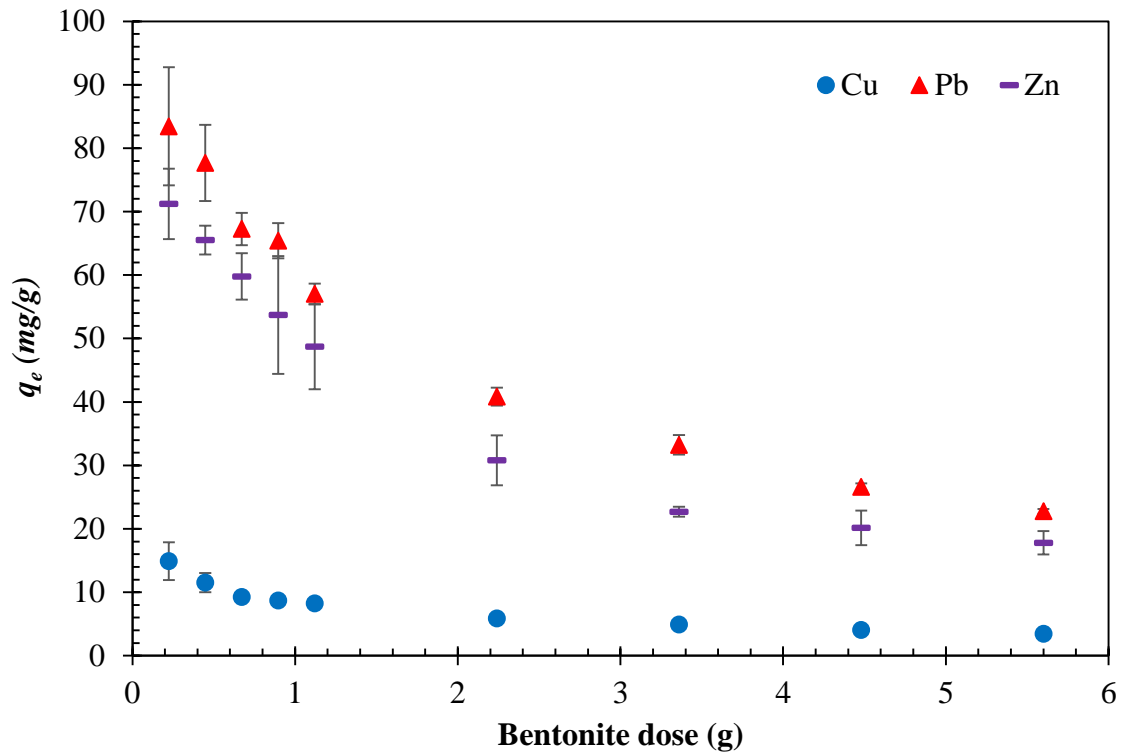
(i)



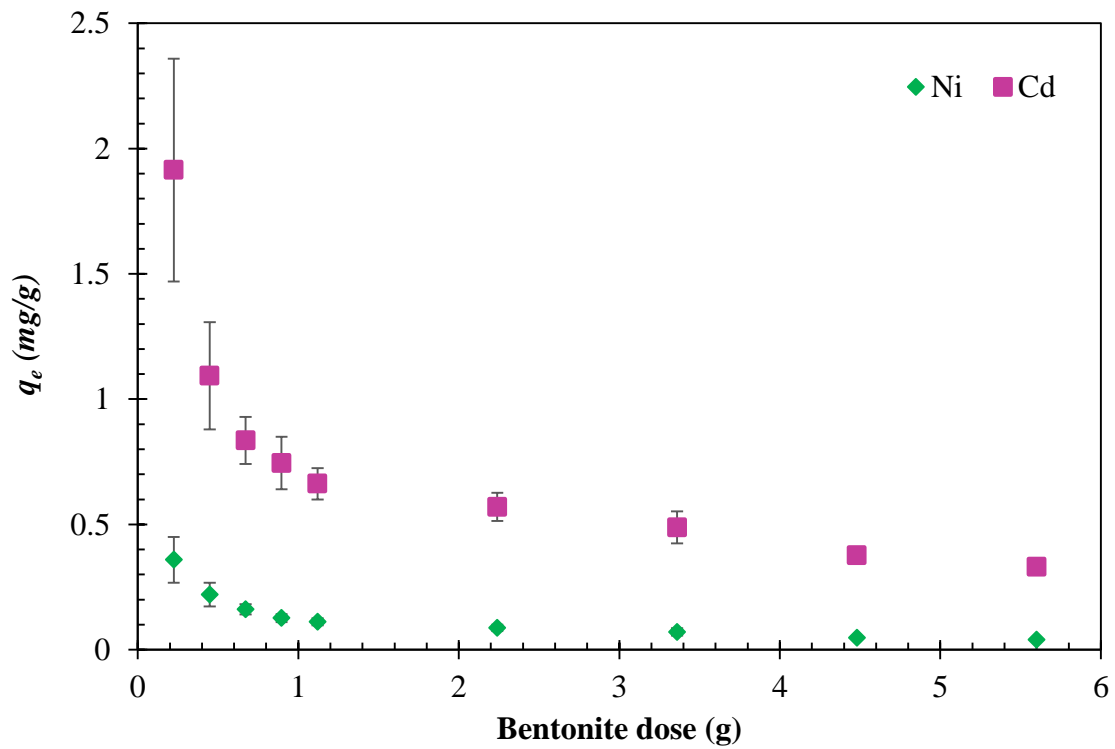
(ii)

Fig. 6.20. Removal % of paper mill leachate at different bentonite dosage for Bentonite-2

Furthermore, it was seen (Fig. 6.21 - 6.26) that the number of metal ions adsorbed per unit mass decreased progressively with an increase in the bentonite content. This shows that during the primary stage, a vast number of active sites are open for sorption. At large mineral concentrations, the available metal concentration is inadequate to cover the exchangeable sites on the adsorbent effectively, usually ending in low metal adsorption potential (Anna et al., 2015). Besides, a higher clay amount enhances the probability of collision between solid particles. It, therefore, may produce particle aggregation, causing a drop in the total surface area and an increase in diffusional path length, both of which offer a decrease in the sorption capability of metal ions on bentonites (Anna et al., 2015; Hefne et al., 2008). Similar behaviour of other adsorbent material on metal ion adsorption has also been reported (Anna et al., 2015; Chen et al., 2012; Vengris et al., 2001). Bentonite-1 showed a higher removal and adsorption capacity as compared to Bentonite-2.

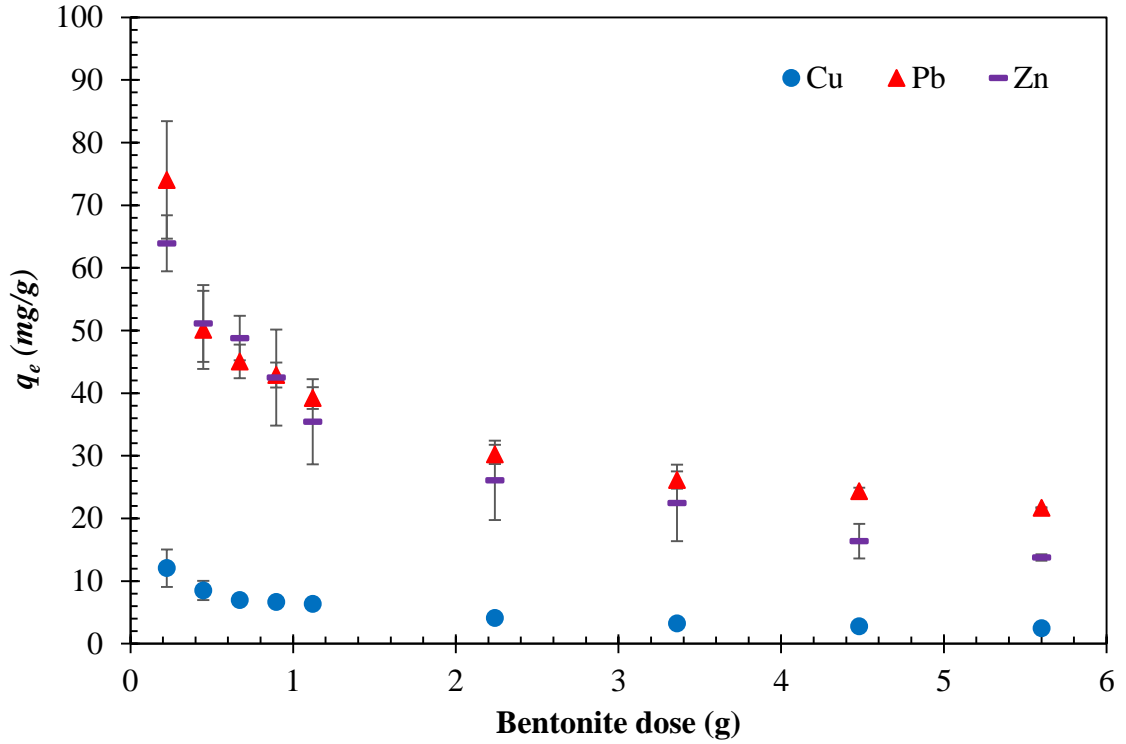


(i)

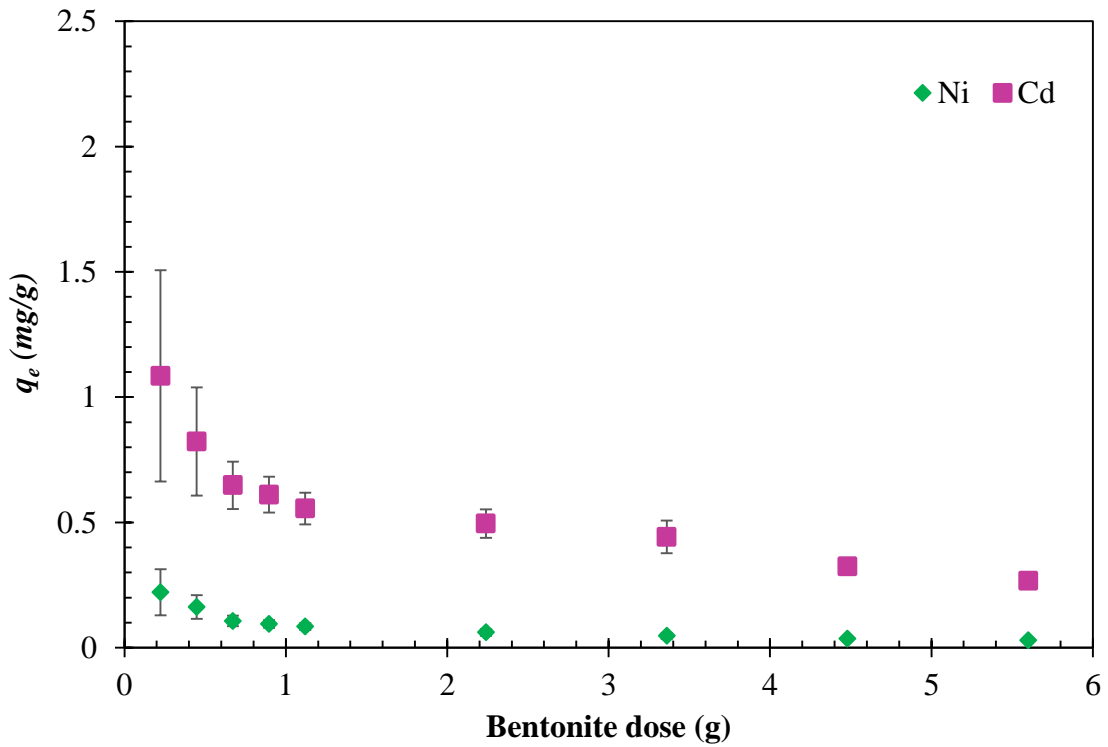


(ii)

Fig. 6.21. Amount of fly ash leachate adsorbed by Bentonite-1 at various bentonite dose

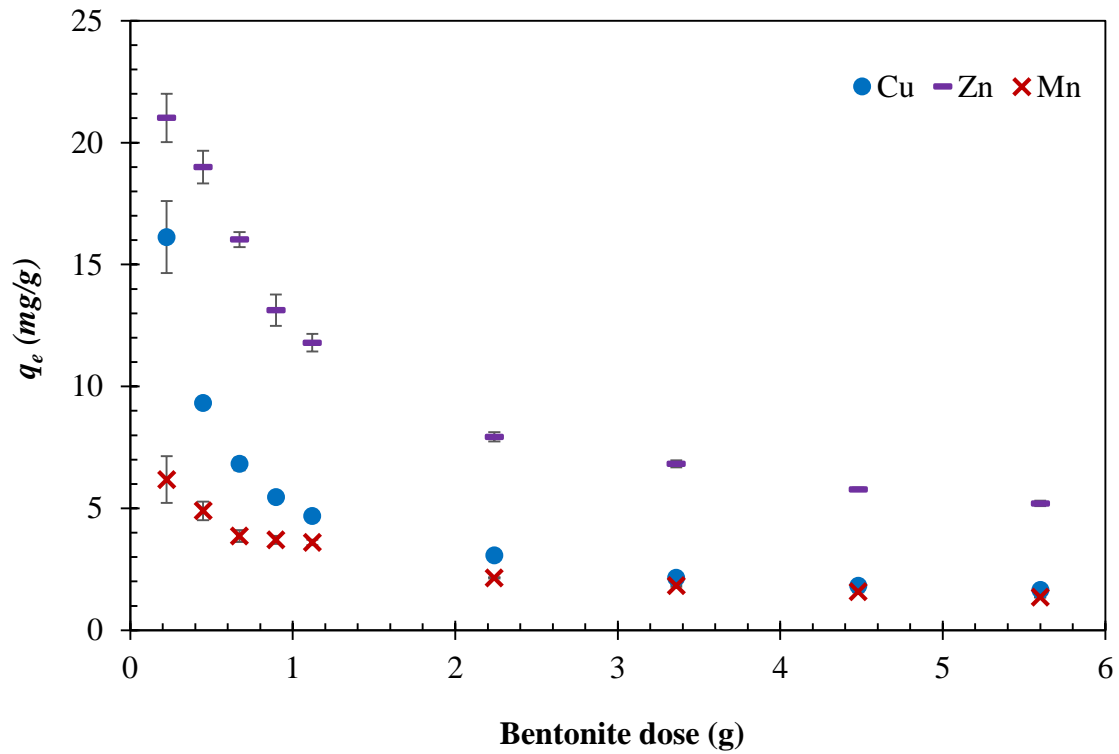


(i)

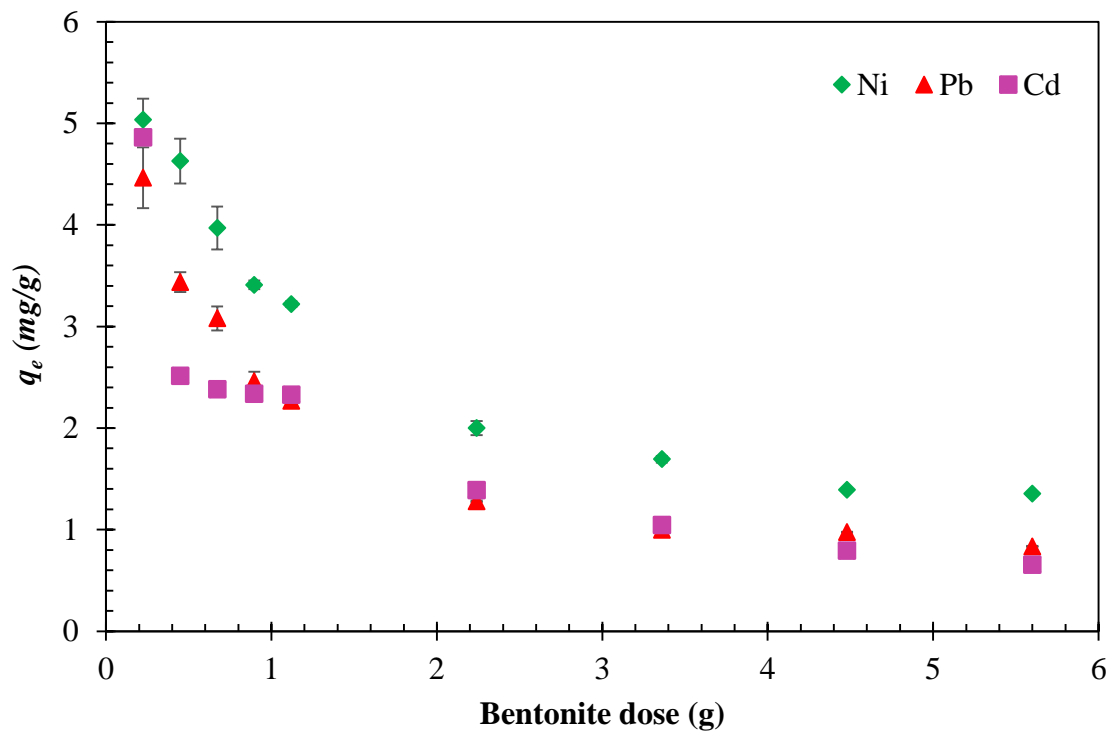


(ii)

Fig. 6.22. Amount of fly ash leachate adsorbed by Bentonite-2 at various bentonite dose

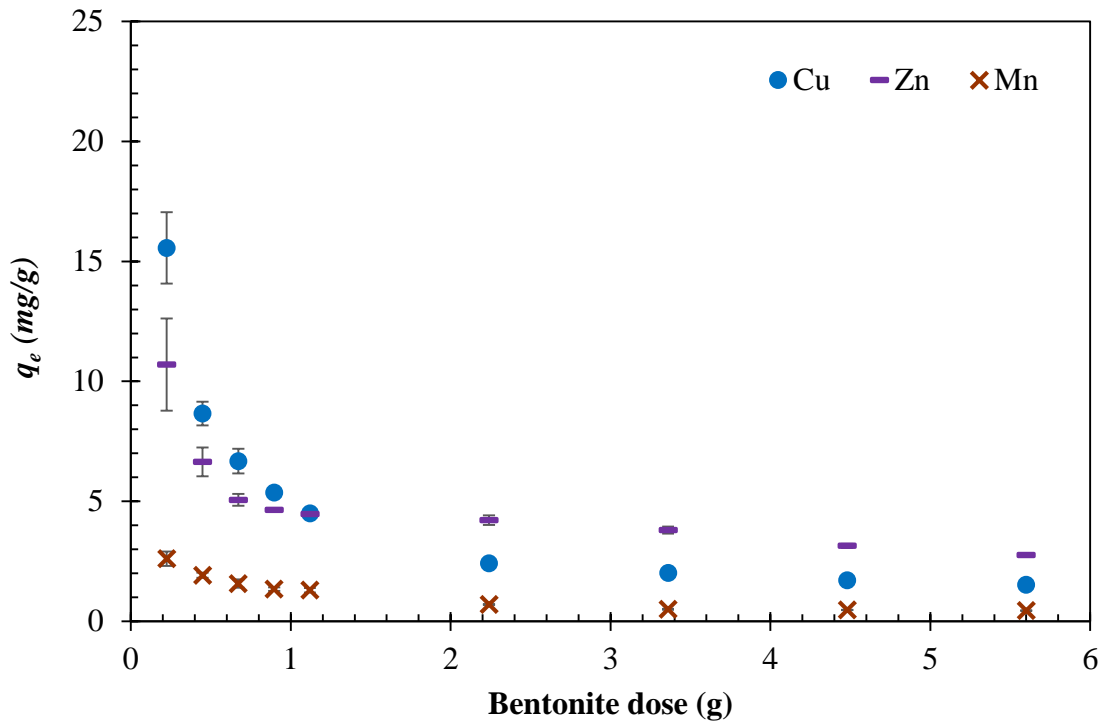


(i)

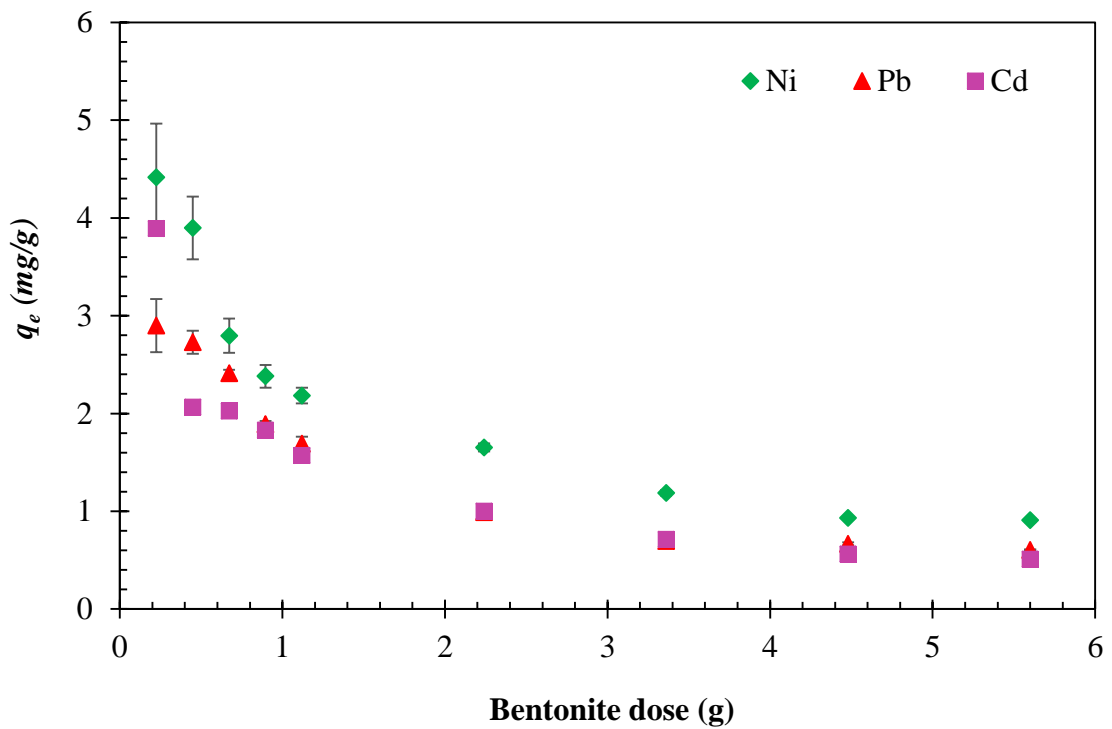


(ii)

Fig. 6.23. Amount of sewage sludge leachate adsorbed by Bentonite-1 at various bentonite dose

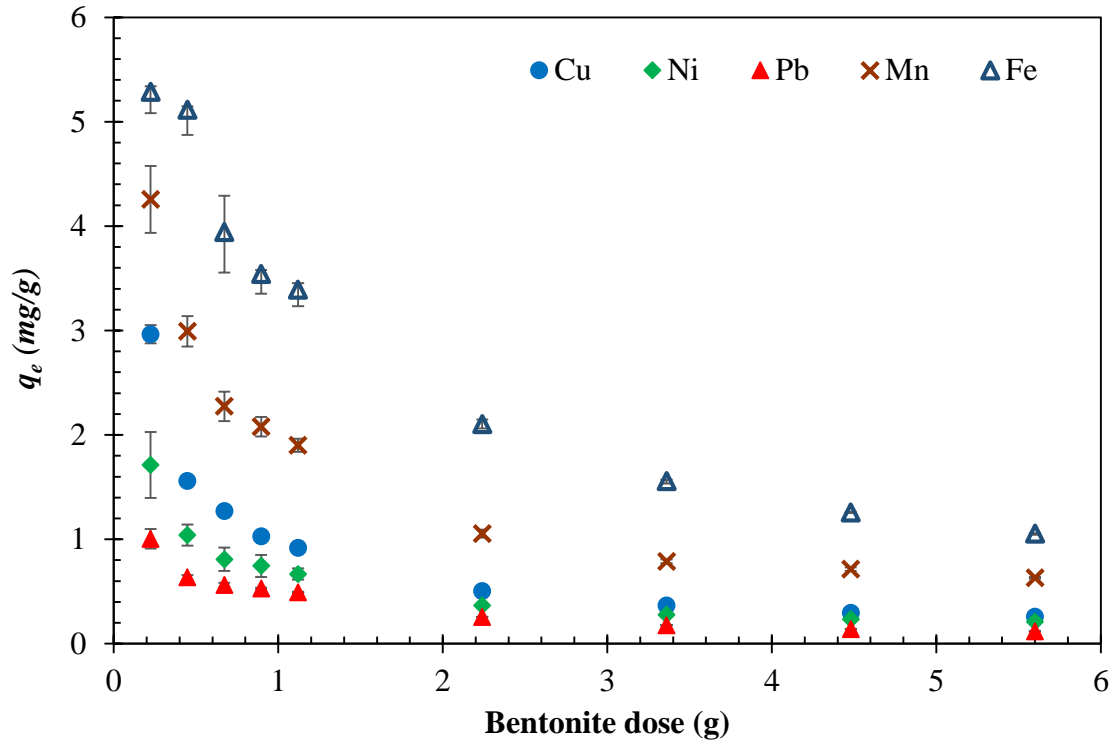


(i)

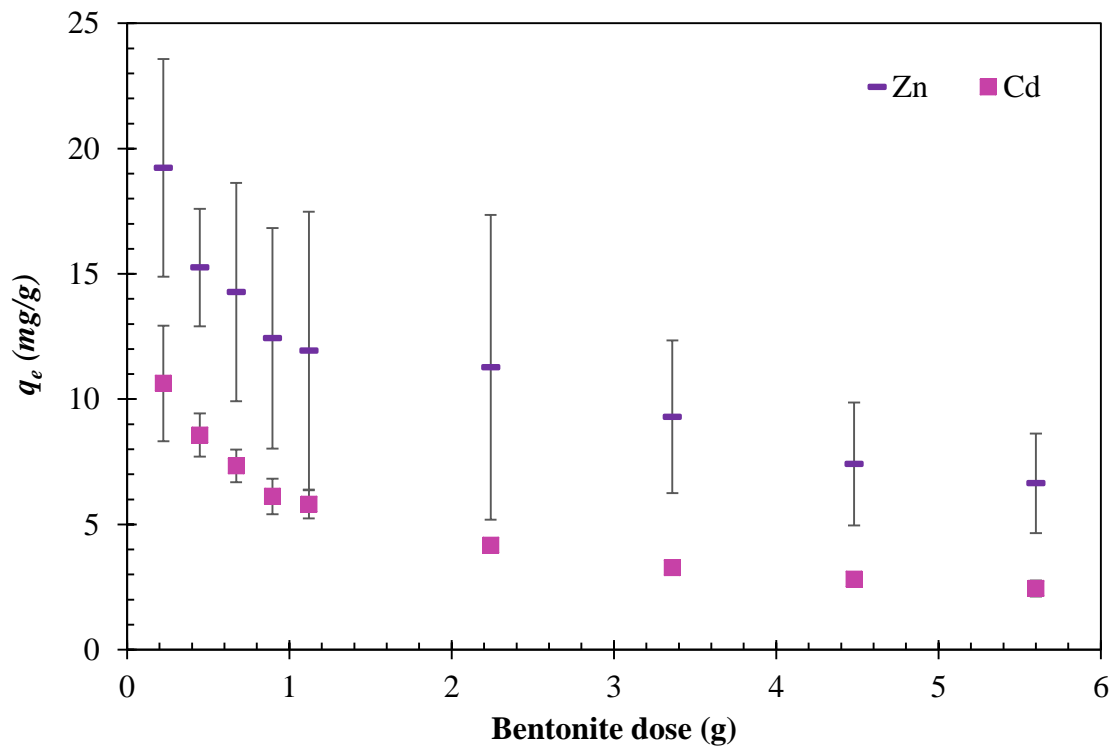


(ii)

Fig. 6.24. Amount of sewage sludge leachate adsorbed by Bentonite-2 at various bentonite dose

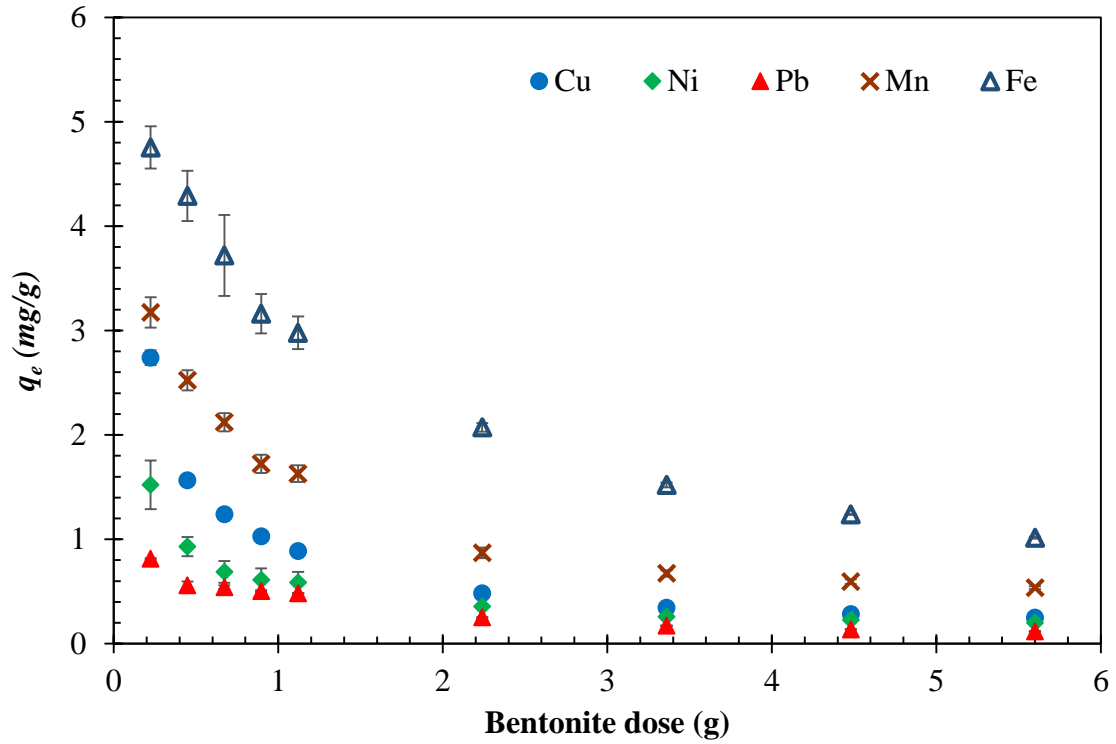


(i)

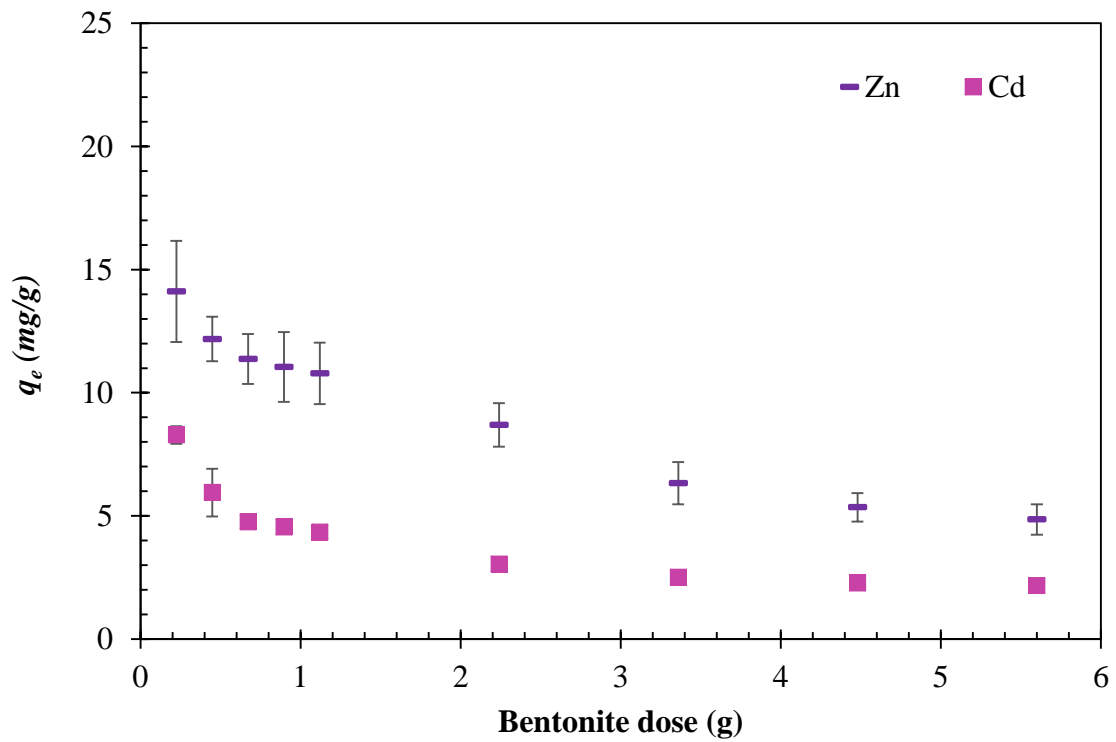


(ii)

Fig. 6.25. Amount of paper mill leachate adsorbed by Bentonite-1 at various bentonite dose



(i)



(ii)

Fig. 6.26. Amount of paper mill leachate adsorbed by Bentonite-2 at various bentonite dose

6.2.12. Kinetic study of various leachates

6.2.12.1. Effect of Contact time

The time of contact between the pollutants and the adsorbent is crucial for designing a barrier material in the garbage disposal system. The value of the adsorbent as a barrier material for usage in a garbage disposal system is symbolised by its swift uptake of pollutants and attainment of equilibrium in a short span.

The influence of contact time on the adsorption of fly ash, sewage sludge and paper mill leachates were examined at different time intervals, ranging from 5–200 minutes and the consequences are depicted in Fig. 6.27-6.32. For fly ash leachate, a quick uptake was observed for the first 20 minutes (for Zn and Cd) and 60 minutes (for Pb and Ni). A steady increase in removal was observed for Cu. Likewise, in case of sewage sludge leachate, a rapid adsorption was detected for first 20 minutes for all metal ions (Fig. 6.29-6.30). In case of paper mill leachate, speedy uptake was noticed for first 40 minutes (for Cd, Mn, Zn), 60 minutes (for Pb, Fe), and 80 minutes (for Ni, Cu) (Fig. 6.31-6.32). However, to confirm the maximum removal of metal ions, the 200 minute (fly ash leachate) and 180 minute (sewage sludge and paper mill leachates) contact time was chosen in all trials conducted. Fig. 6.27-6.32 show that the curve of contact time becomes smooth and steady-state, and a plateau was evident after 160 minutes for fly ash leachate and 120 minutes for sewage sludge and paper mill leachate respectively. A further rise of contact time did not result in a subsequent growth of the adsorbed heavy metal ions.

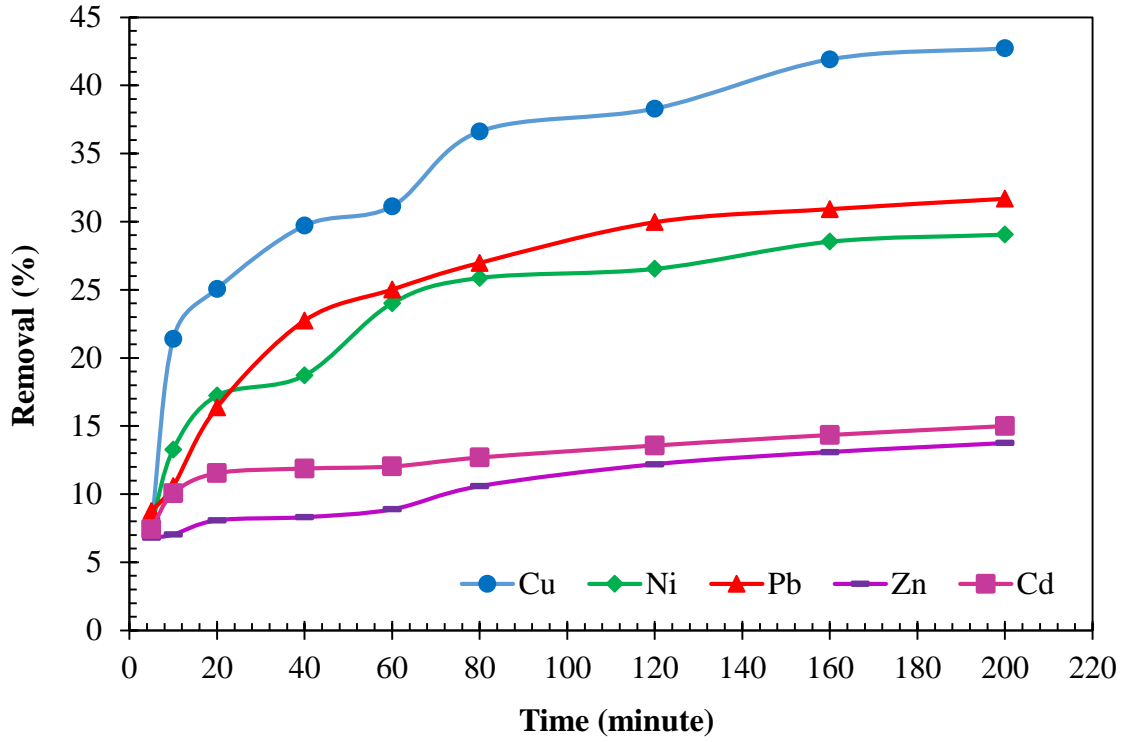


Fig. 6.27. Adsorption kinetics for fly ash leachate in presence of Bentonite-1

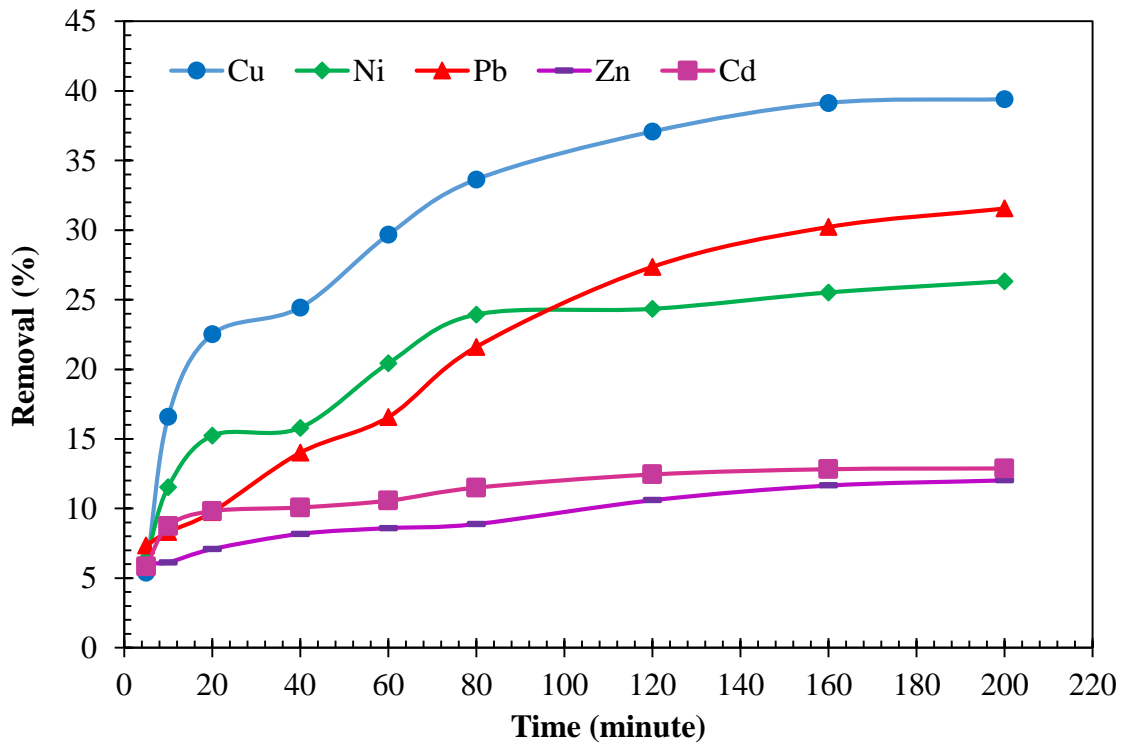


Fig. 6.28. Adsorption kinetics for fly ash leachate in presence of Bentonite-2

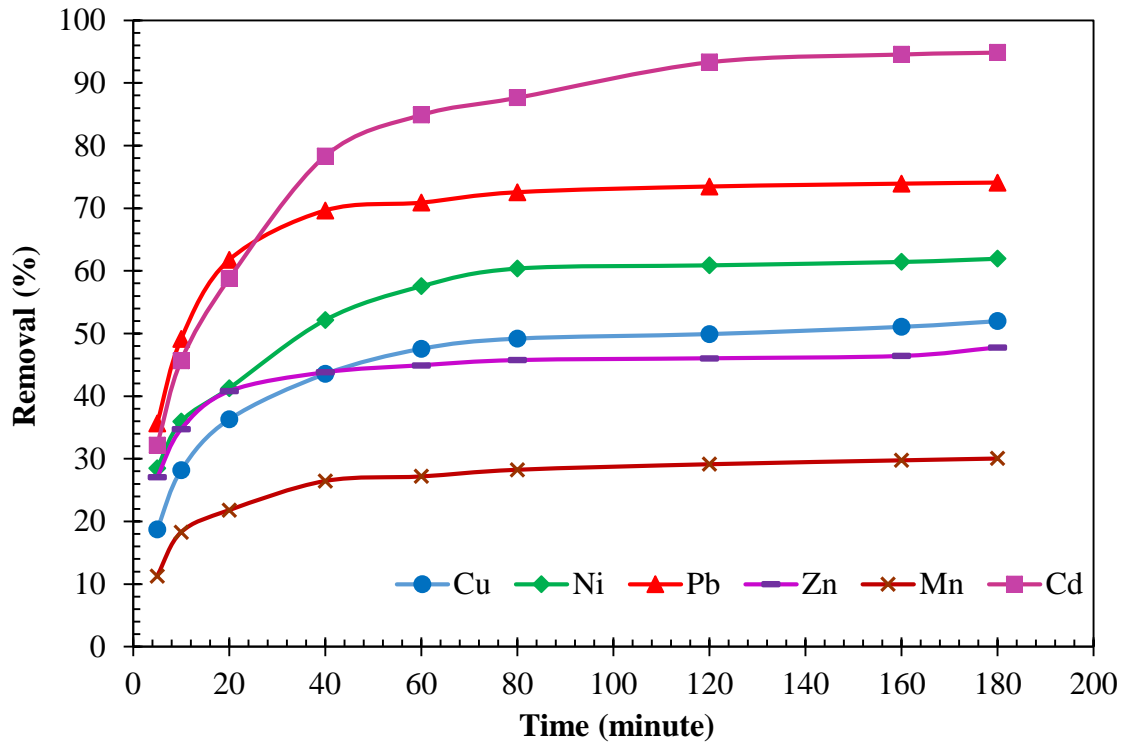


Fig. 6.29. Adsorption kinetics for sewage sludge leachate in presence of Bentonite-1

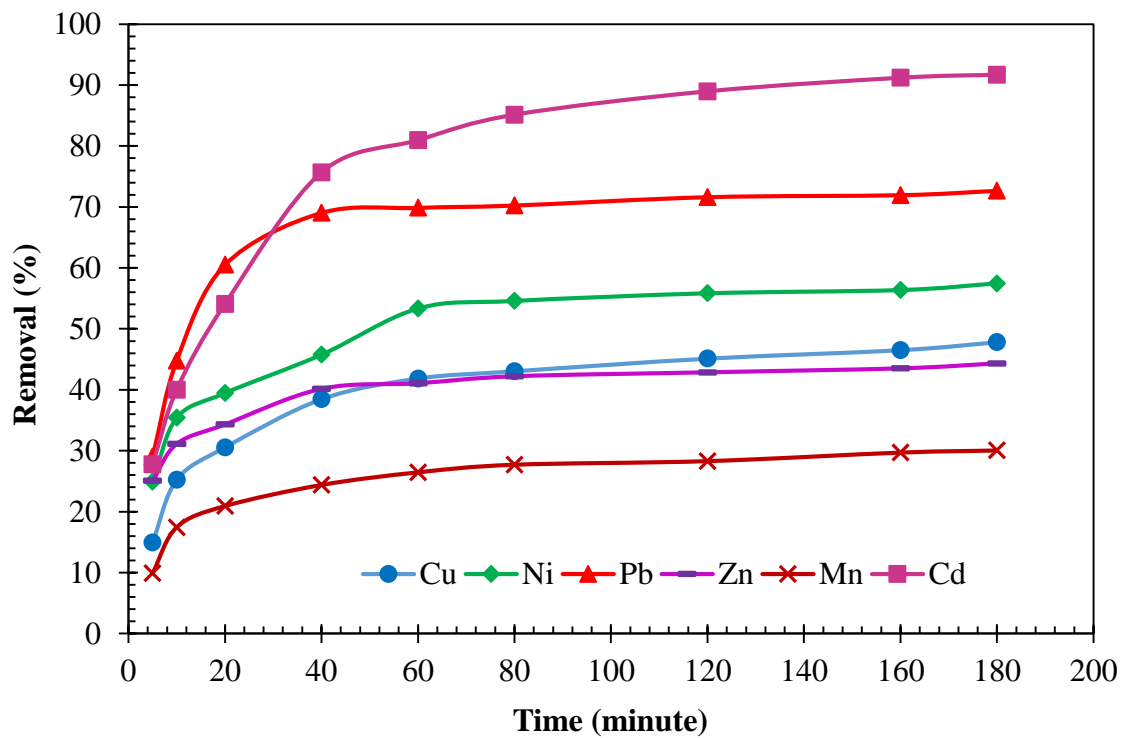


Fig. 6.30. Adsorption kinetics for sewage sludge leachate in presence of Bentonite-2

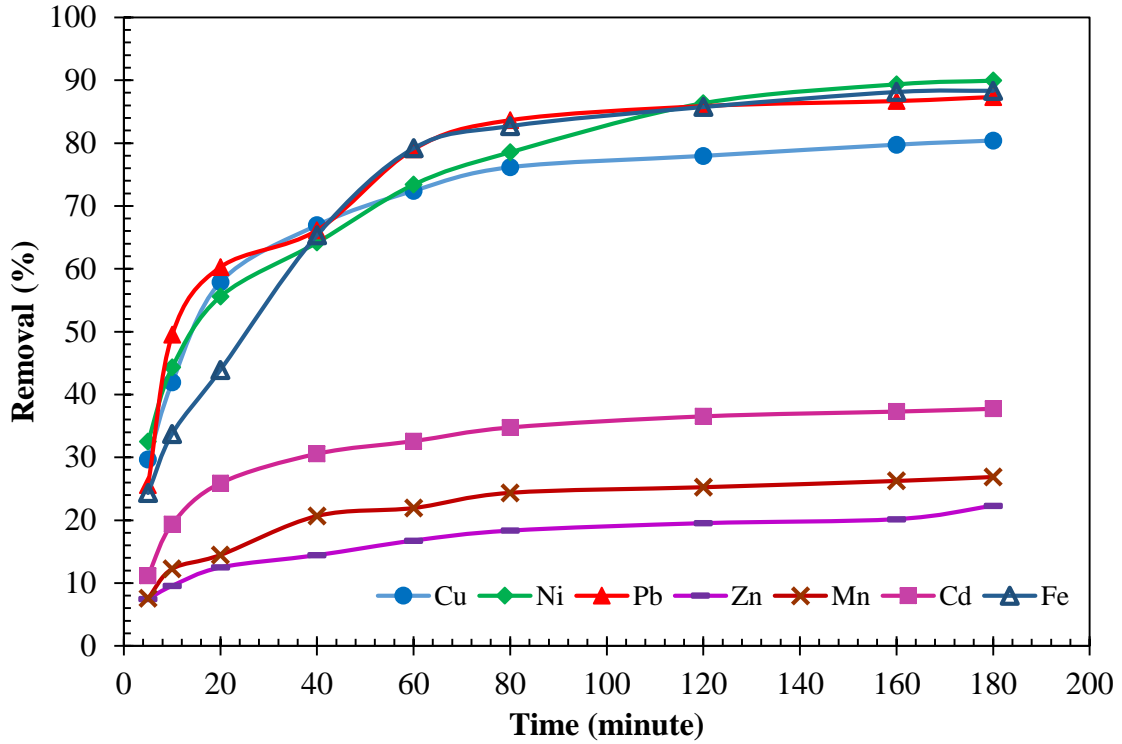


Fig. 6.31. Adsorption kinetics for paper mill leachate in presence of Bentonite-1

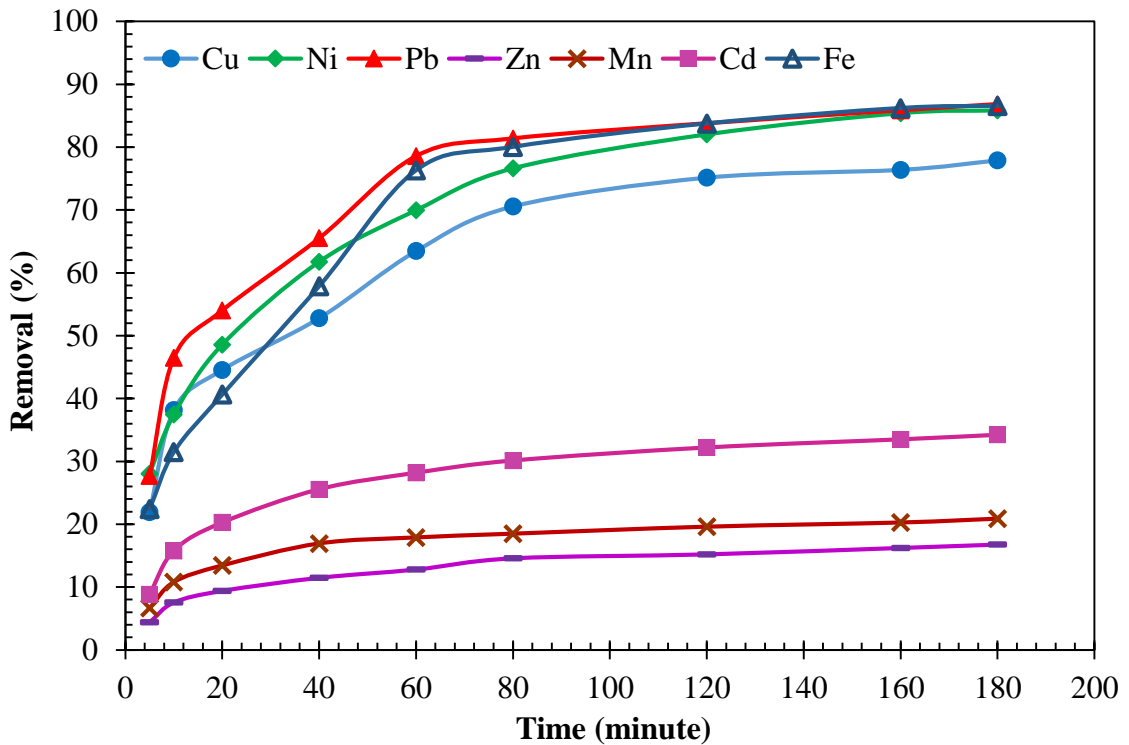


Fig. 6.32. Adsorption kinetics for paper mill leachate in presence of Bentonite-2

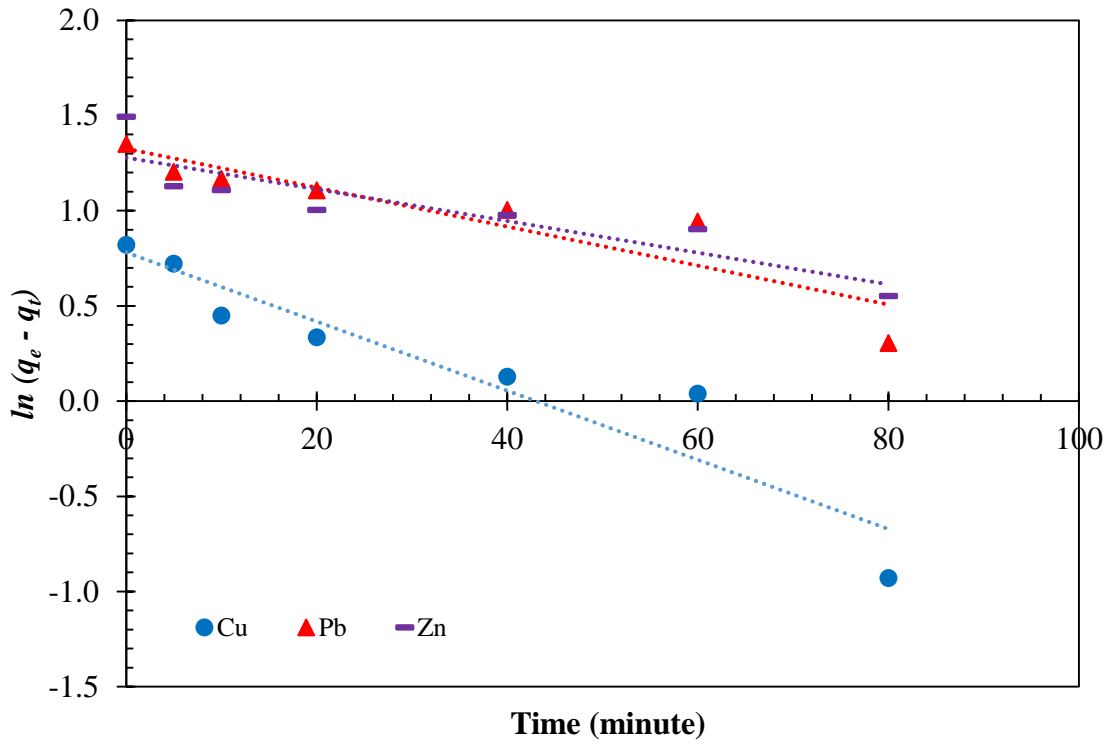
The observed results complied with the past researches where rapid adsorption rates were recorded (Anna et al., 2015; Bourliva et al., 2013; Vieira et al., 2010). A further

increment in the contact time, however, did not increase the measure of adsorbed metal ions. This is because, a vast number of unoccupied sites are available during the initial adsorption stage, which with time, gets filled up and owing to the repulsive forces, filling of the outstanding unoccupied sites becomes a test.

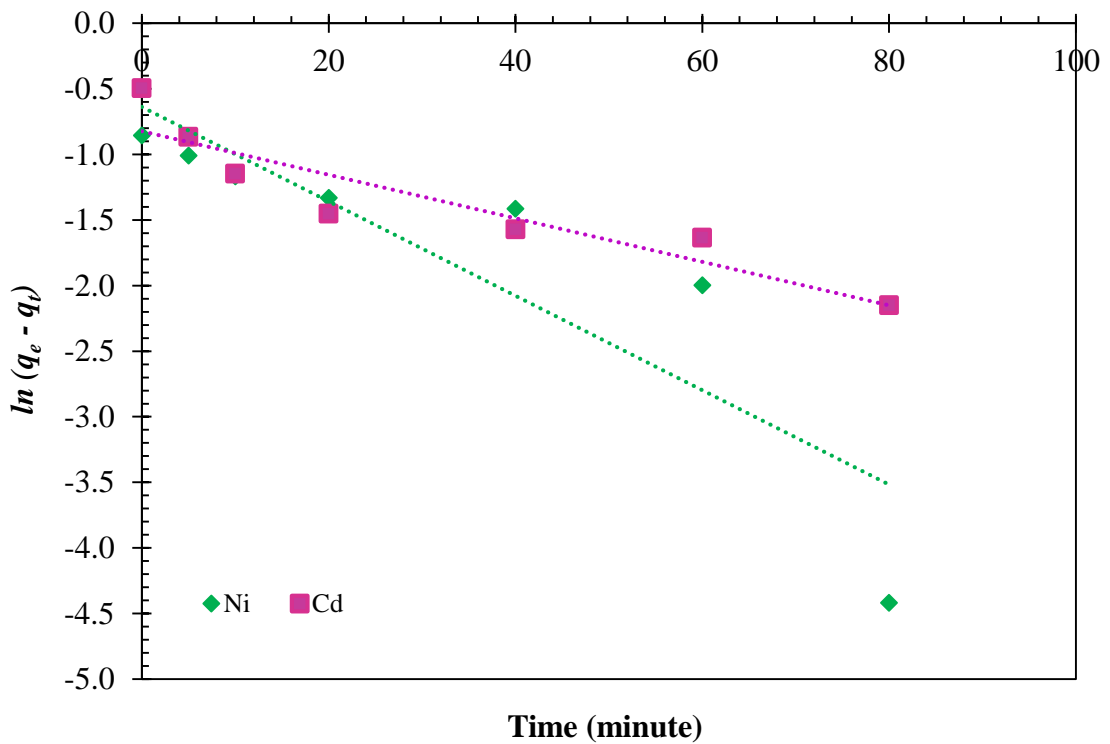
6.2.12.2. Kinetic model

Two kinetic models were fitted comprising pseudo-first and second-order equations to study the potential rate-controlling steps and mechanisms of adsorption of metal ions present in fly ash, sewage sludge and paper mill leachate. It showed the values of linear regression and kinetic constants for both bentonites.

Fig. 6.33-6.38 show plots of pseudo-first-order and pseudo-second-order adsorption kinetic of fly ash, sewage sludge and paper mill leachates, respectively. The plots show the relationship between $\ln(q_e - q_t)$ and t for the pseudo-first-order kinetics model which does not represent a straight line [Fig. 6.33-6.38 (a)]. Fig. 6.33-6.38 (b) displays the plot between t/q_t versus t , i.e., the pseudo-second-order kinetics model, which indicates a linear relationship. Tables 6.10, 6.11, and 6.12 depicts parameters for adsorption of heavy metals present in fly ash, sewage sludge and paper mill leachates on bentonites derived from the pseudo-first- and second-order kinetic models. The R^2 value of the pseudo-first-order kinetic model was lower for Bentonite-1 and-2, which recommends that the adsorption of metal ions on both the bentonites does not follow Pseudo-first order kinetic model. The data in Tables 6.10, 6.11, and 6.12 also display that the R^2 values for the pseudo-second-order kinetic model were more significant as compared to pseudo- first-order kinetic model for both bentonites in presence of all the leachates. This shows that the pseudo second-order kinetic model is more applicable, having the R^2 values greater than 0.97. In addition to this, the obtained q_e fit perfectly well with the experimental data. The results also concluded that the overall rate of the metal ions adsorption process on both bentonites seemed to be governed by the chemical process (Vimonses et al., 2009).

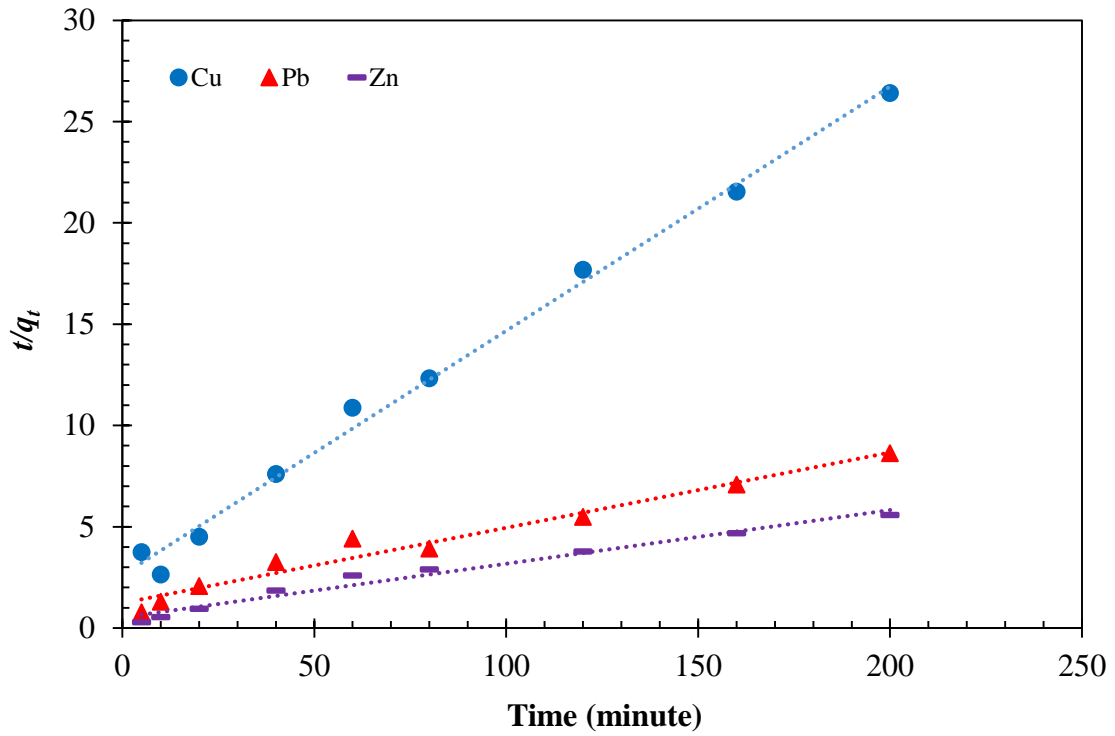


(i)

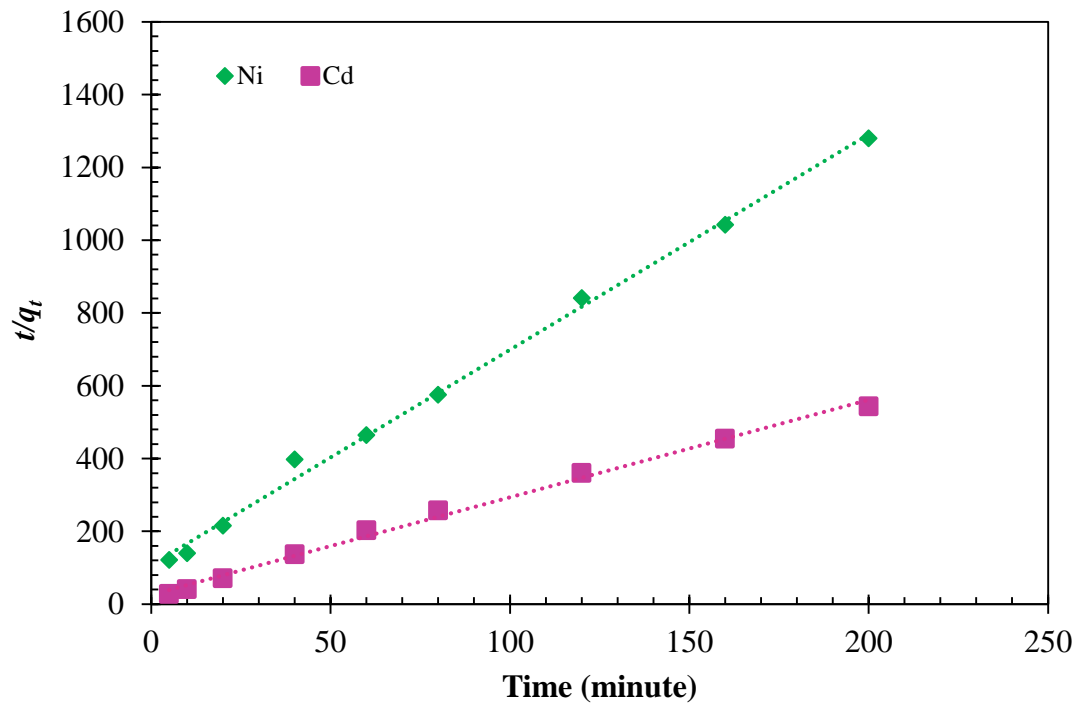


(ii)

(a) Pseudo-first-order adsorption kinetics of fly ash leachate



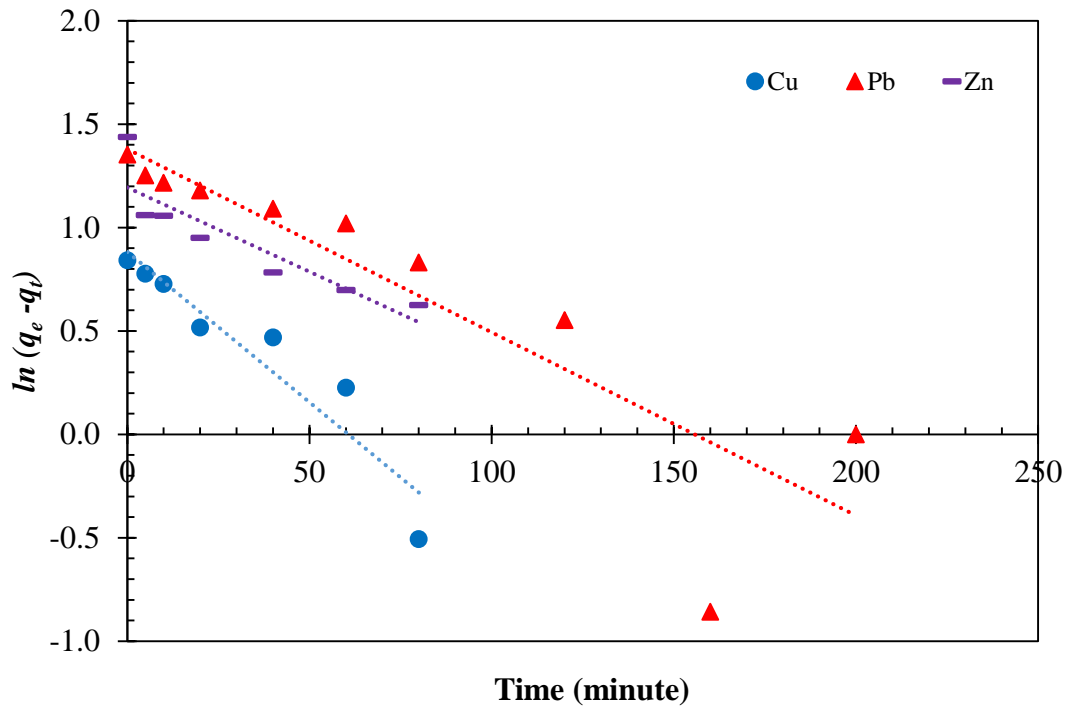
(i)



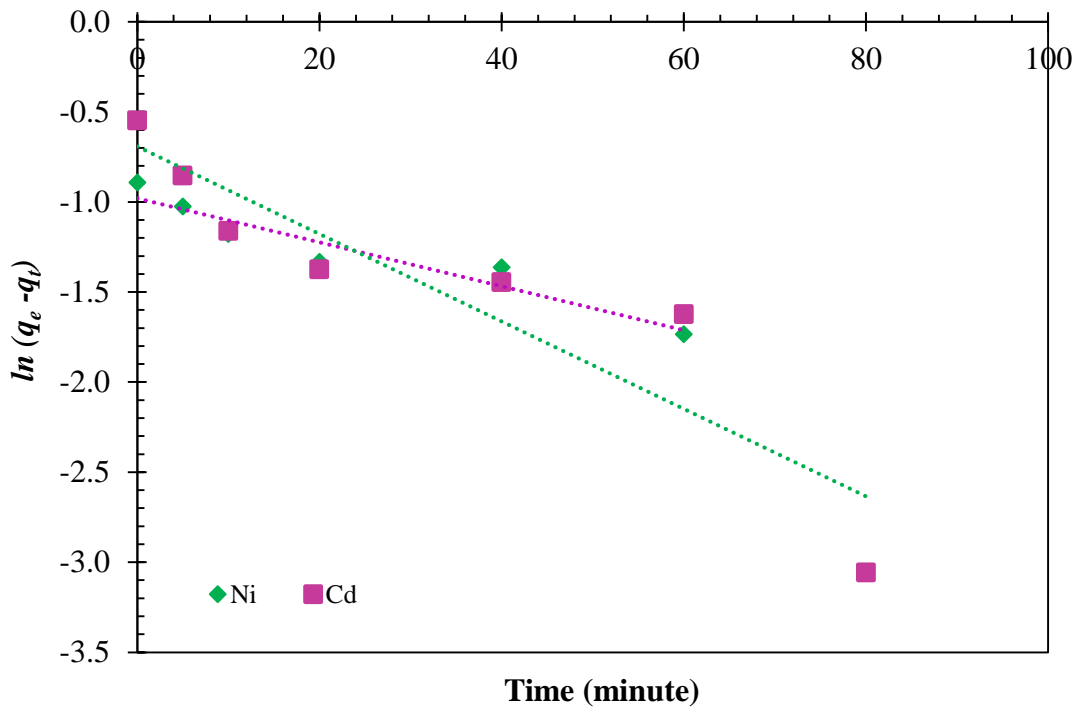
(ii)

(b) Pseudo-second-order adsorption kinetics of fly ash leachate

Fig. 6.33. Kinetic study of Bentonite-1 in presence of fly ash leachate

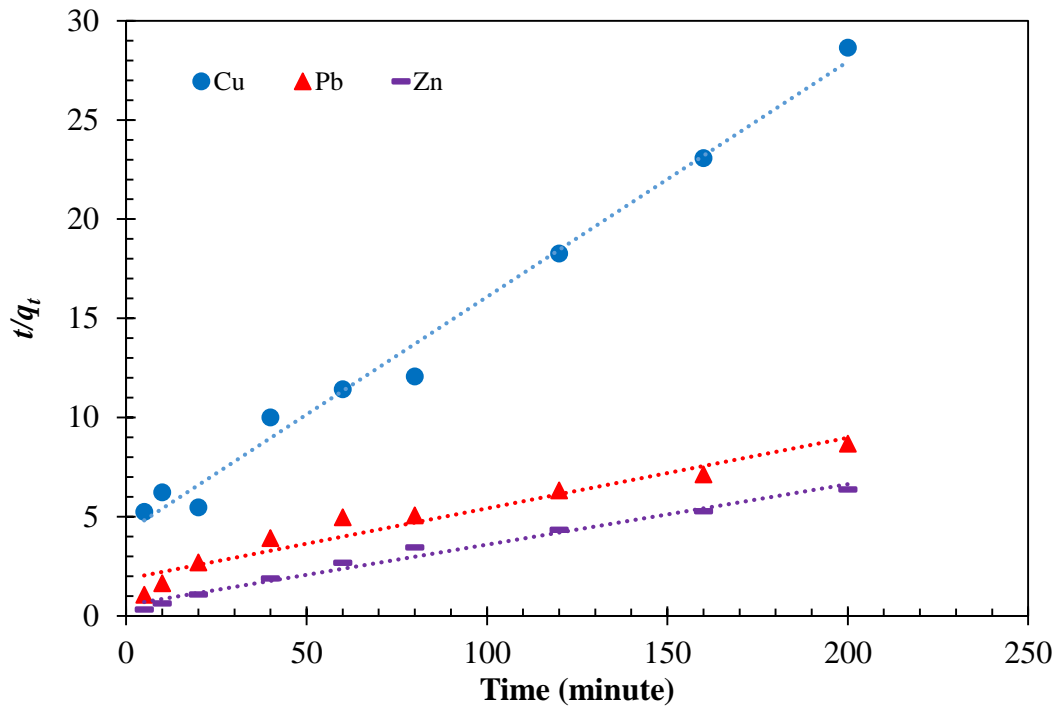


(i)

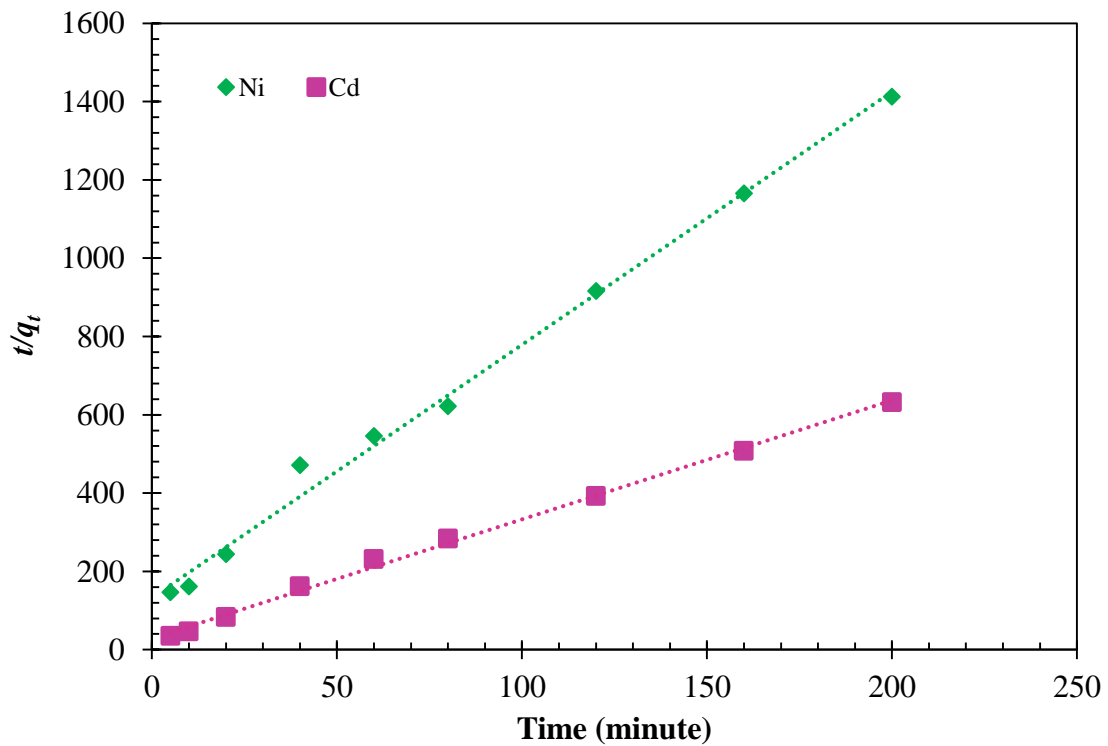


(ii)

(a) Pseudo-first-order adsorption kinetics of fly ash leachate



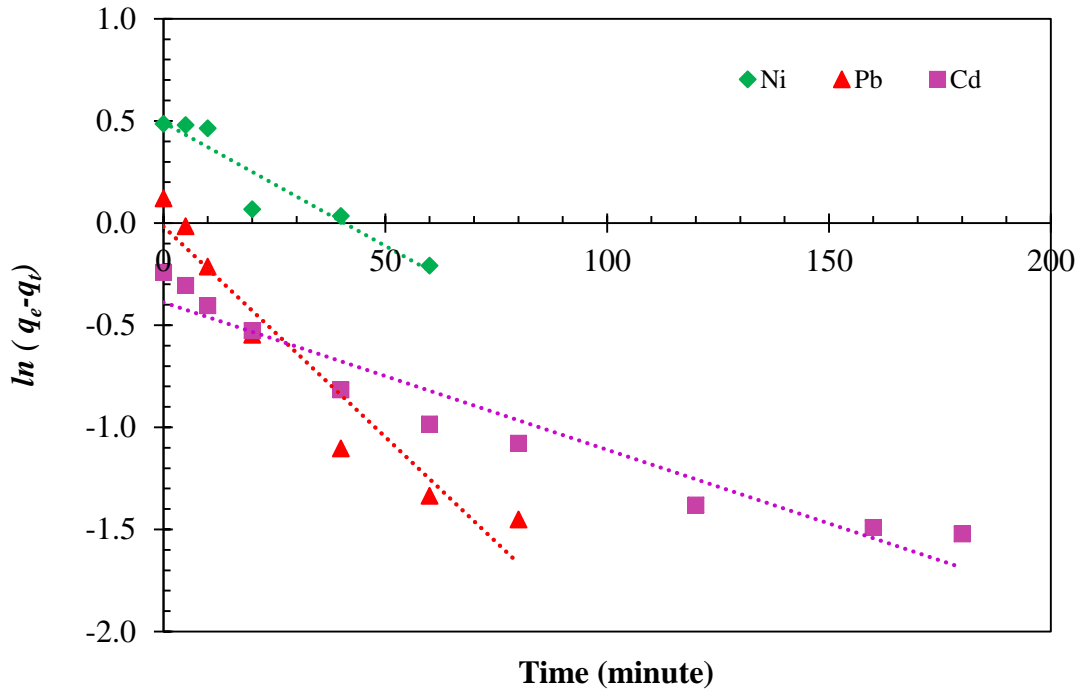
(i)



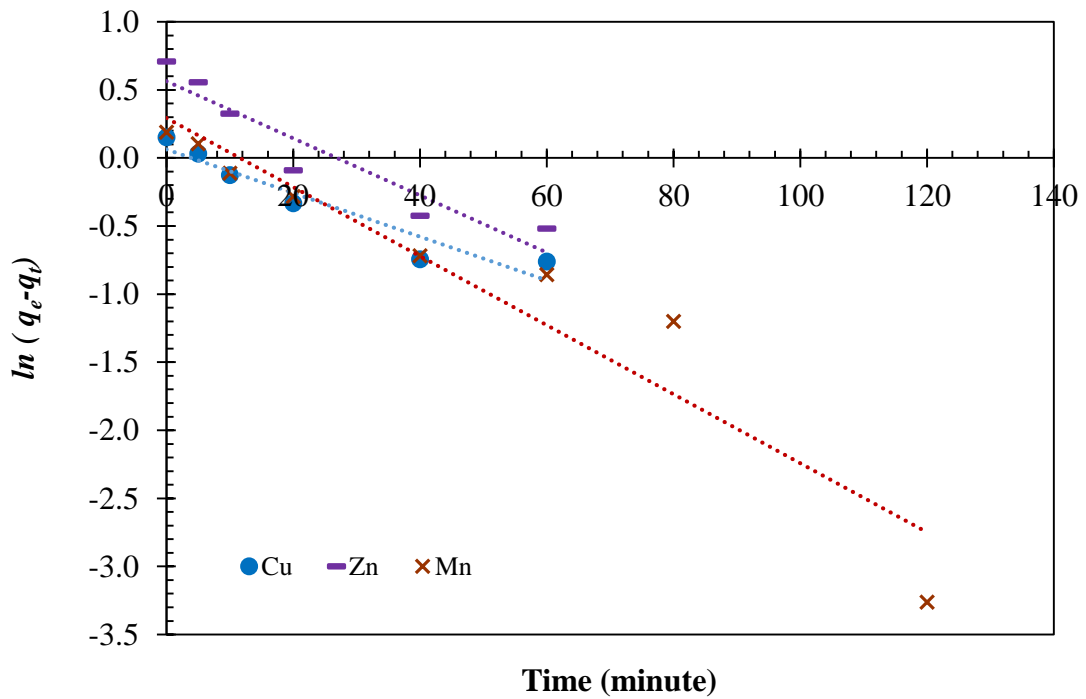
(ii)

(b) Pseudo-second-order adsorption kinetics of fly ash leachate

Fig. 6.34. Kinetic study of Bentonite-2 in presence of fly ash leachate

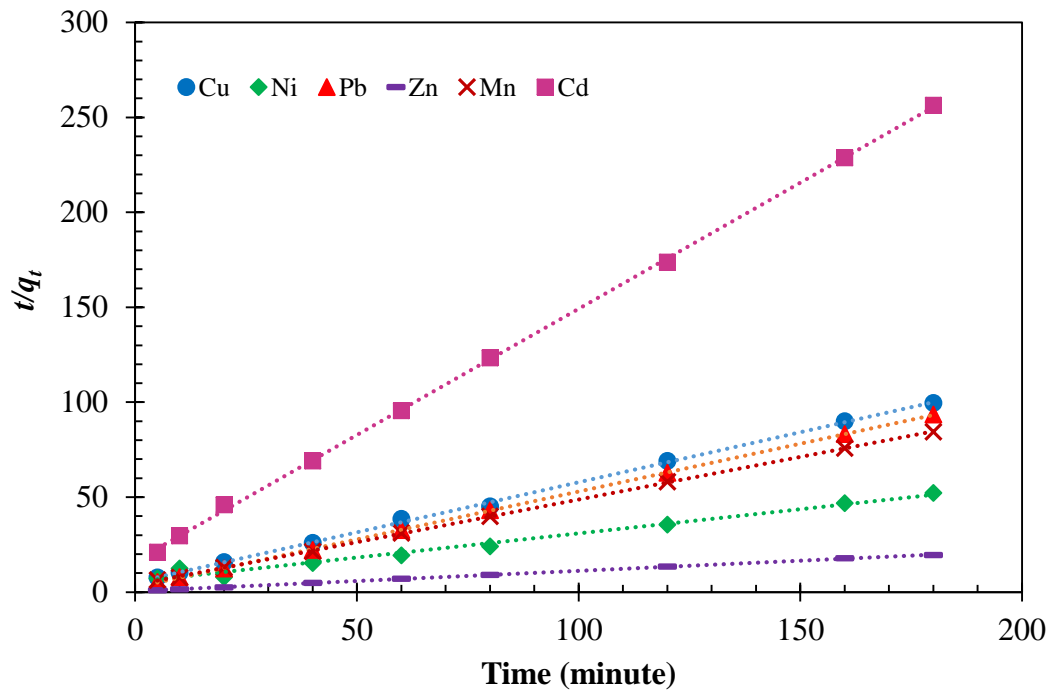


(i)



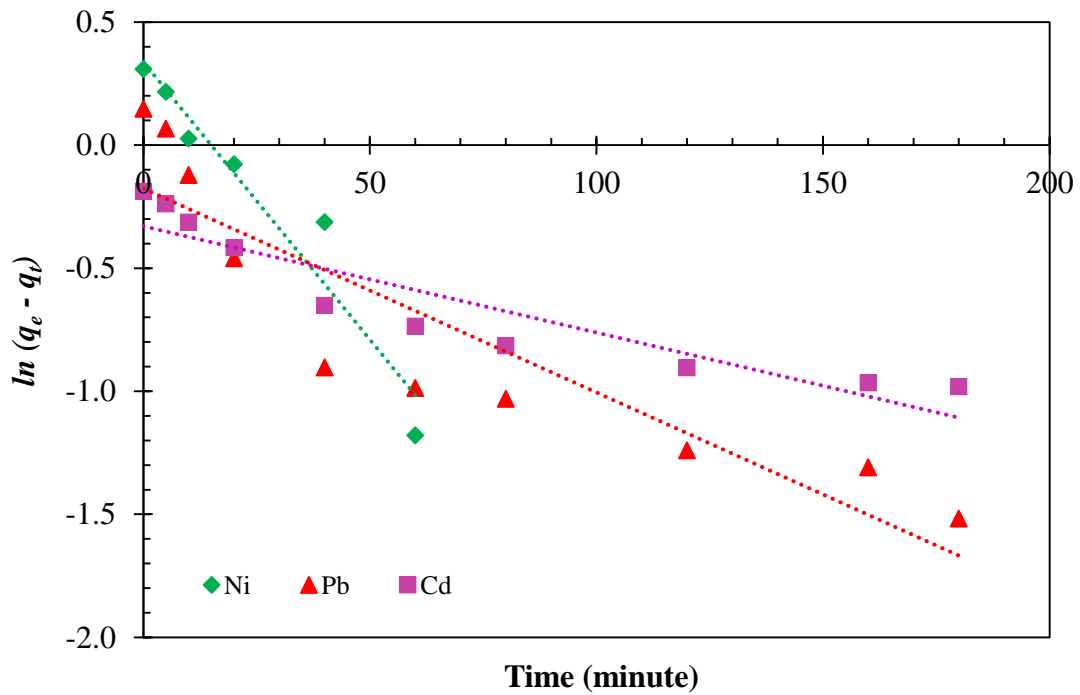
(ii)

(a) Pseudo-first-order adsorption kinetics of sewage sludge leachate

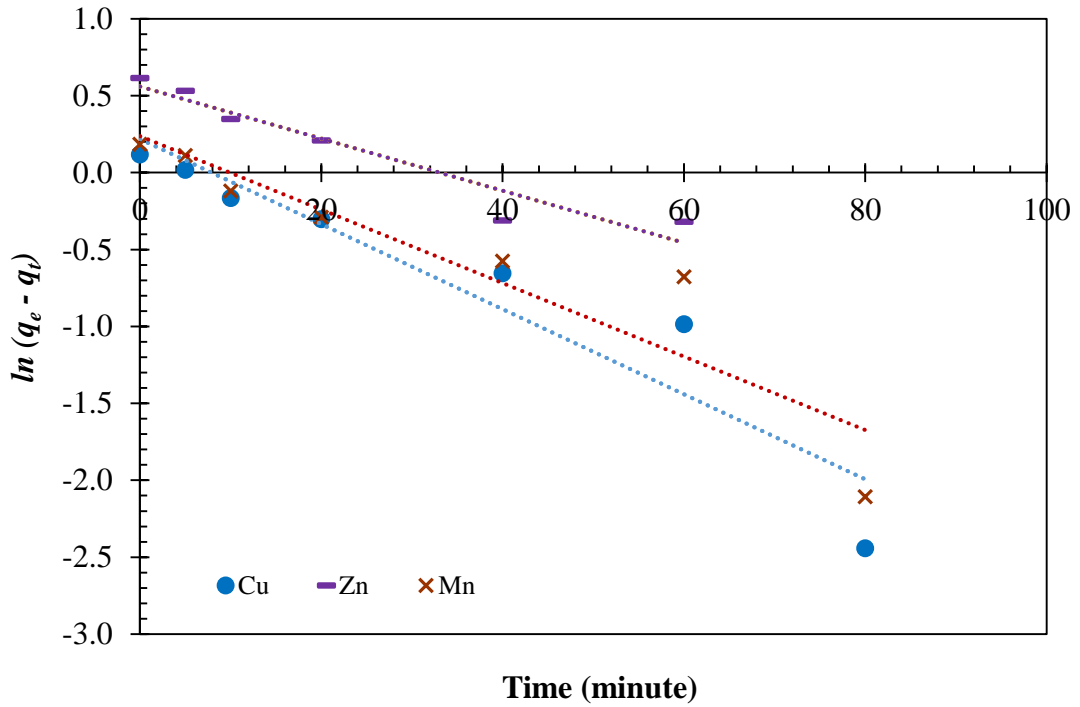


(b) Pseudo-second-order adsorption kinetics of sewage sludge leachate

Fig. 6.35. Kinetic study of Bentonite-1 in presence of sewage sludge leachate

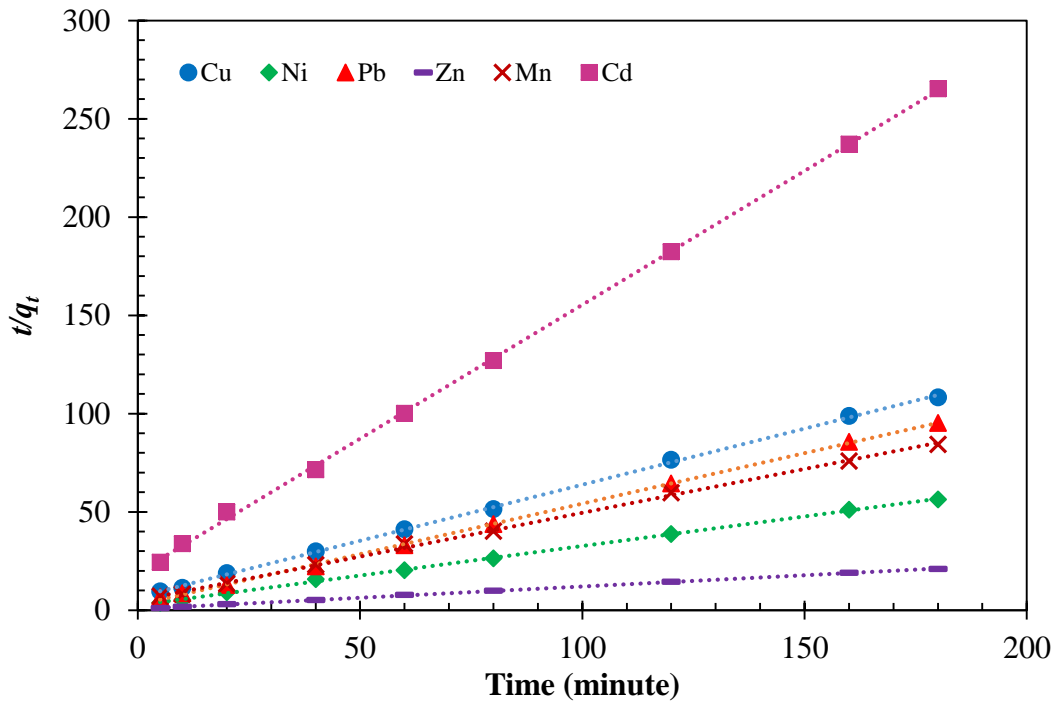


(i)



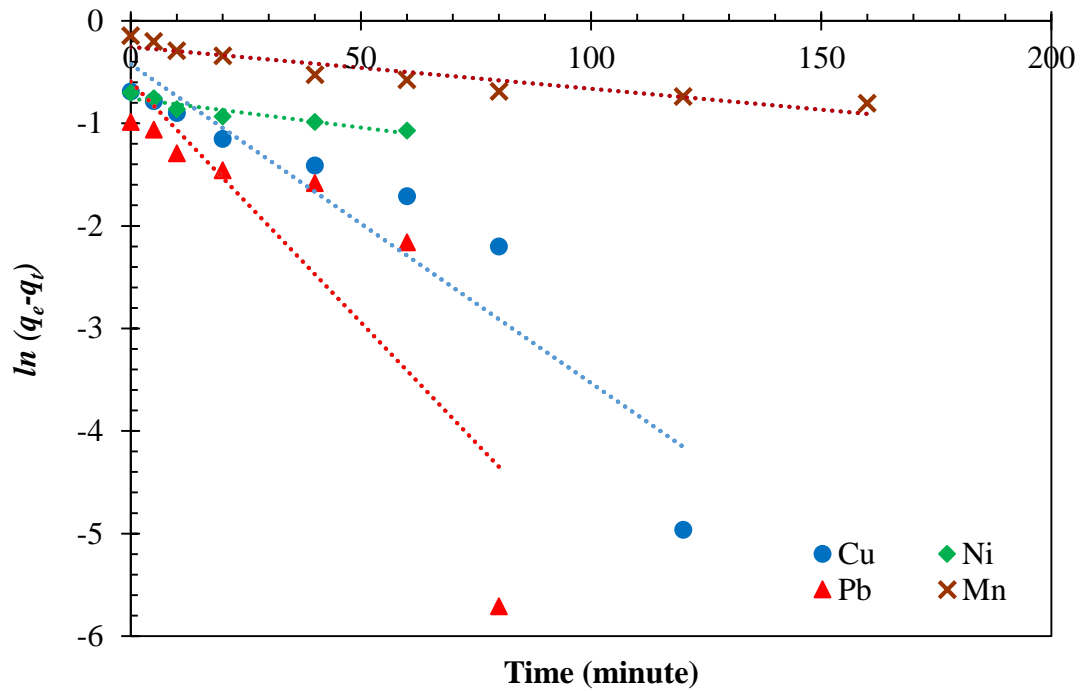
(ii)

(a) Pseudo-first-order adsorption kinetics of sewage sludge leachate

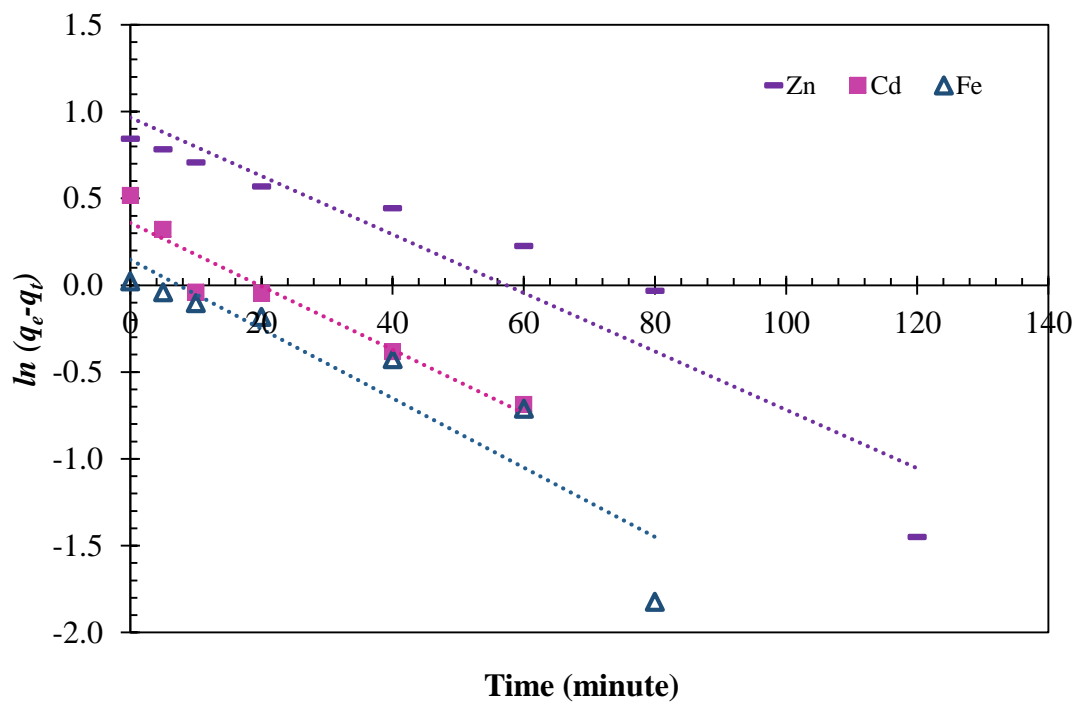


(b) Pseudo-second-order adsorption kinetics of sewage sludge leachate

Fig. 6.36. Kinetic study of Bentonite-2 in presence of sewage sludge leachate

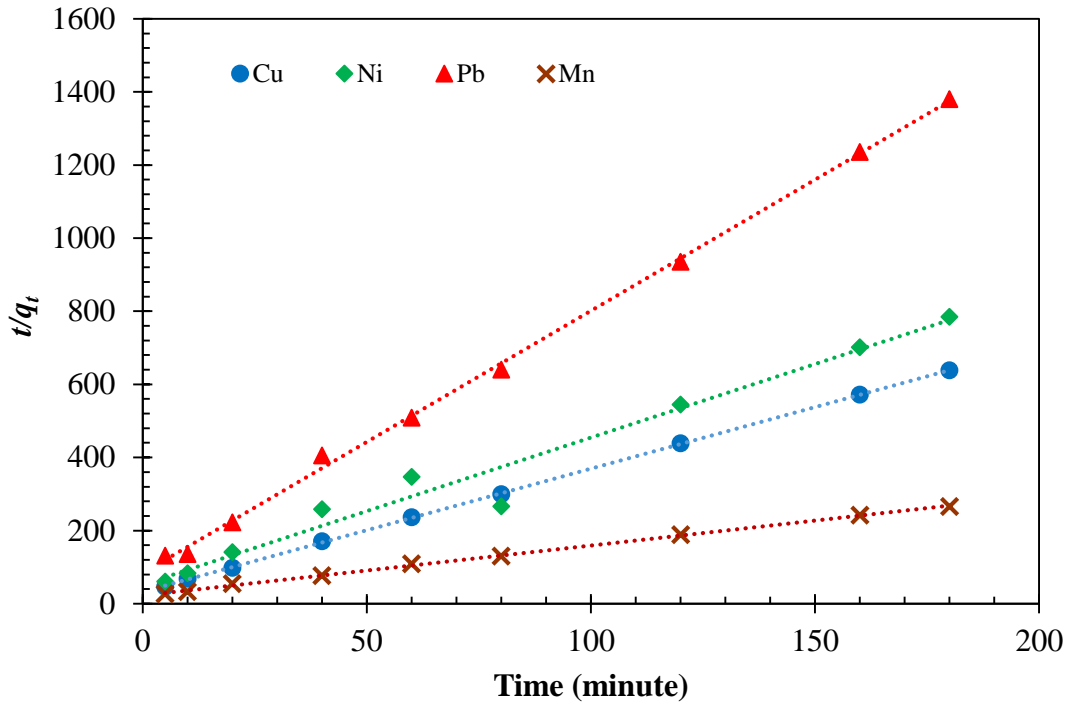


(i)

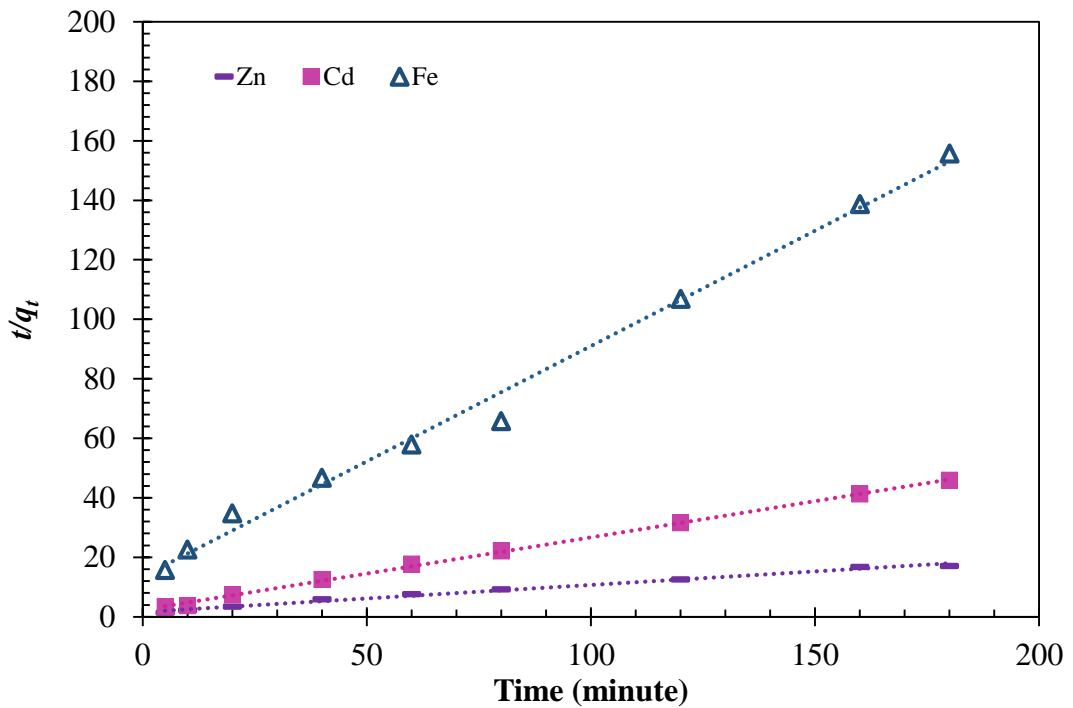


(ii)

(a) Pseudo-first-order adsorption kinetics of paper mill leachate



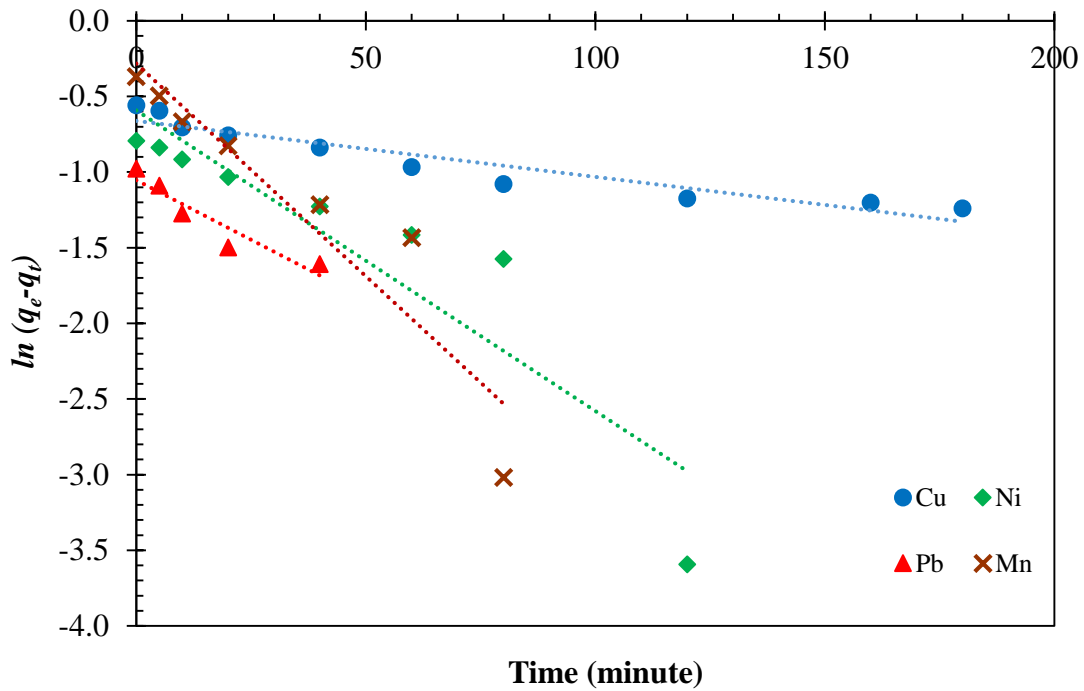
(i)



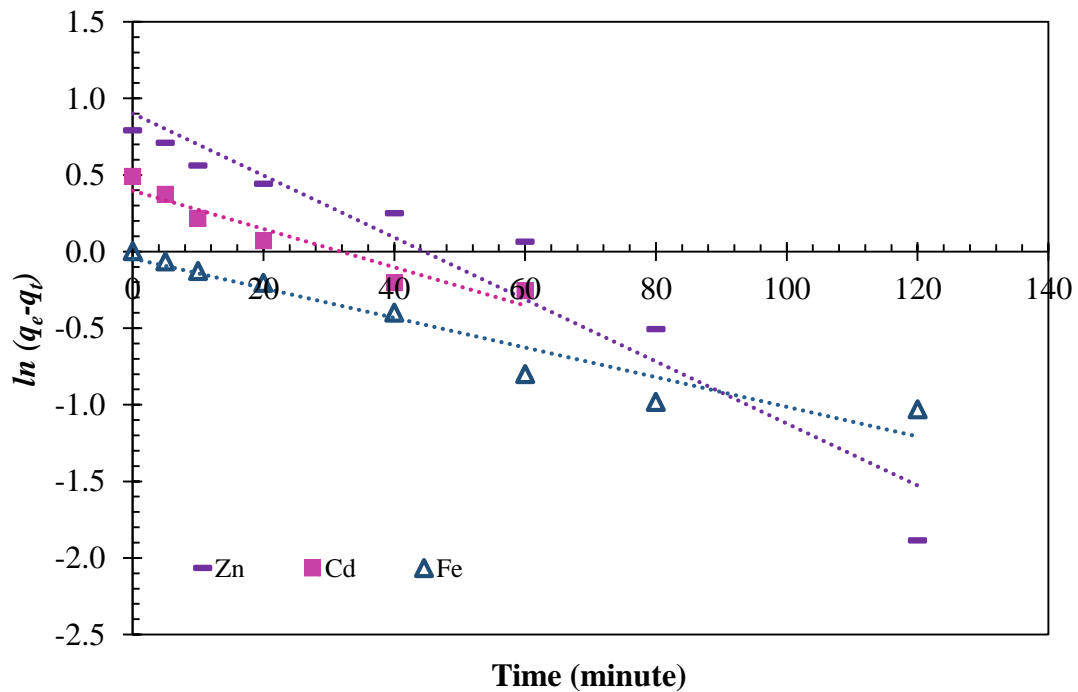
(ii)

(b) Pseudo-second-order adsorption kinetics of paper mill leachate

Fig. 6.37. Kinetic study of Bentonite-1 in presence of paper mill leachate

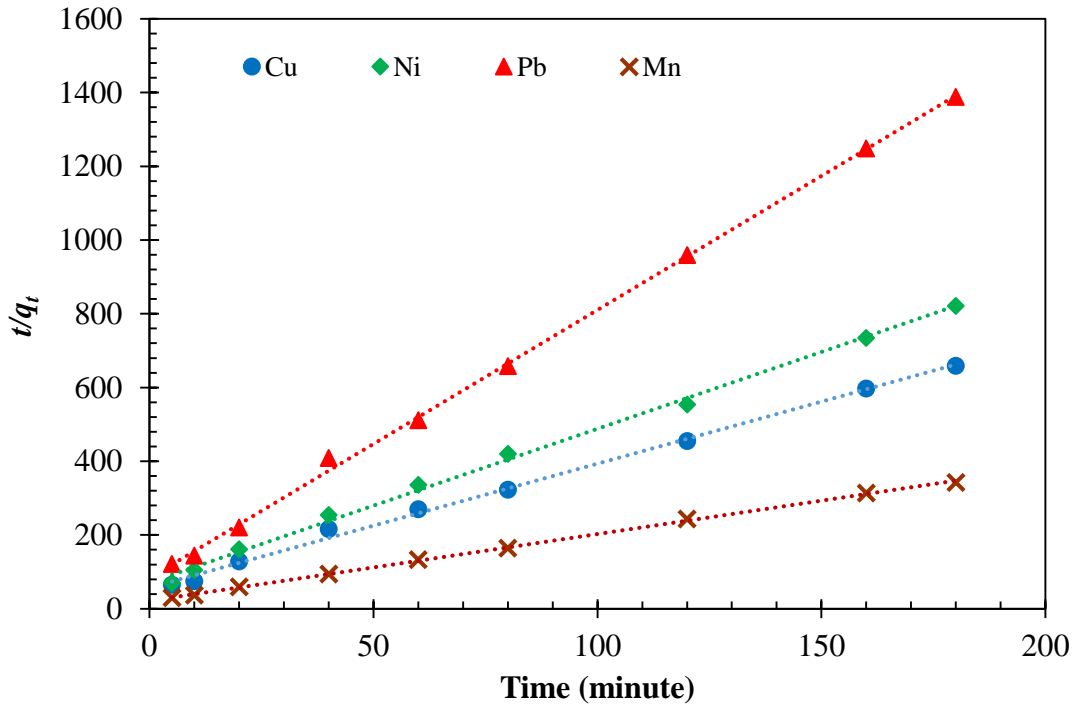


(i)

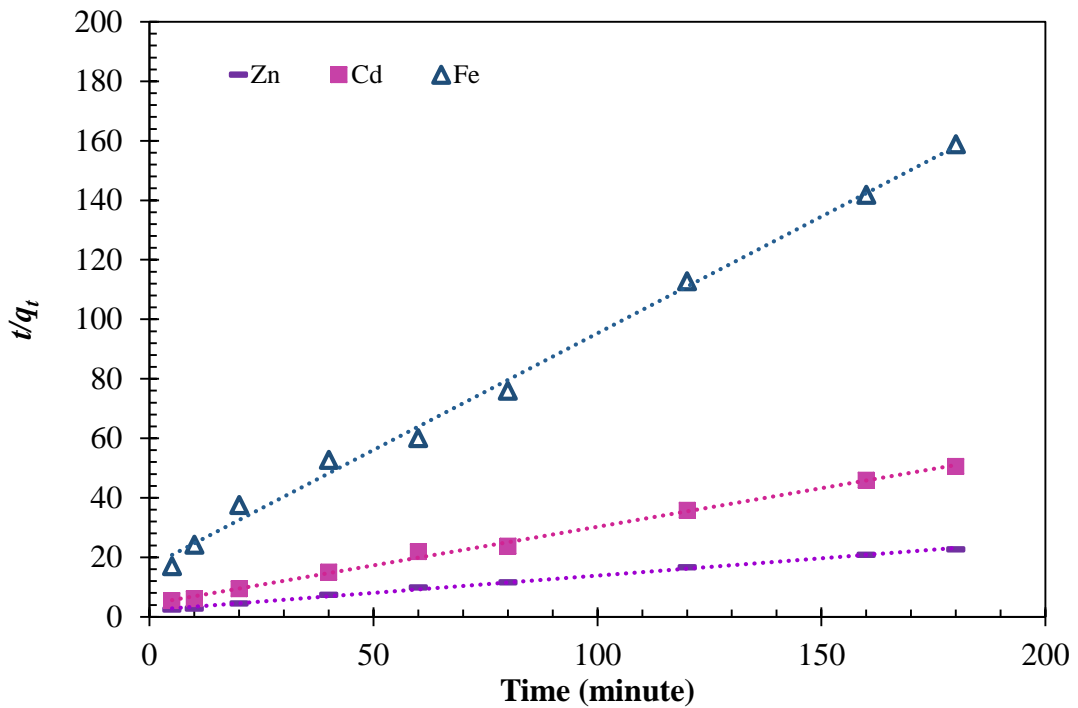


(ii)

(a) Pseudo-first-order adsorption kinetics of paper mill leachate



(i)



(ii)

(b) Pseudo-second-order adsorption kinetics of paper mill leachate

Fig. 6.38. Kinetic study of Bentonite-2 in presence of paper mill leachate

Table 6.10. Parameters for adsorption of heavy metals present in fly ash leachate on bentonites derived from the pseudo-first- and second-order kinetic models.

| Fly ash leachate | Pseudo 1st order | | | | | | Pseudo 2nd order | | | | | |
|------------------|------------------|----------------------------|-------|--------------|----------------------------|-------|------------------|------------------|-------|--------------|------------------|-------|
| | Bentonite-1 | | | Bentonite-2 | | | Bentonite-1 | | | Bentonite-2 | | |
| | q_e (mg/g) | K_1 (min ⁻¹) | R^2 | q_e (mg/g) | K_1 (min ⁻¹) | R^2 | q_e (mg/g) | K_1 (g/mg min) | R^2 | q_e (mg/g) | K_1 (g/mg min) | R^2 |
| Cu | 6.609 | 0.062 | 0.89 | 6.940 | 0.028 | 0.89 | 8.285 | 0.015 | 0.99 | 8.432 | 0.014 | 0.98 |
| Pb | 22.403 | 0.025 | 0.83 | 22.567 | 0.016 | 0.78 | 26.882 | 0.001 | 0.97 | 28.090 | 0.001 | 0.94 |
| Zn | 31.184 | 0.049 | 0.79 | 27.392 | 0.053 | 0.79 | 37.736 | 0.001 | 0.98 | 32.787 | 0.001 | 0.98 |
| Cd | 0.319 | 0.140 | 0.85 | 0.283 | 0.119 | 0.84 | 0.373 | 7.185 | 0.99 | 0.329 | 9.233 | 0.99 |
| Ni | 0.139 | 0.058 | 0.78 | 0.128 | 0.049 | 0.91 | 0.169 | 35.022 | 0.99 | 0.155 | 41.769 | 0.99 |

Table 6.11. Parameters for adsorption of heavy metals present in sewage sludge leachate on bentonites derived from the pseudo-first- and second-order kinetic models

| Sewage sludge leachate | Pseudo 1st order | | | | | | Pseudo 2nd order | | | | | |
|------------------------|------------------|----------------------------|-------|--------------|----------------------------|-------|------------------|------------------|-------|--------------|------------------|-------|
| | Bentonite-1 | | | Bentonite-2 | | | Bentonite-1 | | | Bentonite-2 | | |
| | q_e (mg/g) | K_1 (min ⁻¹) | R^2 | q_e (mg/g) | K_1 (min ⁻¹) | R^2 | q_e (mg/g) | K_1 (g/mg min) | R^2 | q_e (mg/g) | K_1 (g/mg min) | R^2 |
| Cu | 1.728 | 0.056 | 0.91 | 1.559 | 0.054 | 0.89 | 1.893 | 0.278 | 0.99 | 1.753 | 0.326 | 0.99 |
| Pb | 1.888 | 0.073 | 0.93 | 1.919 | 0.052 | 0.82 | 1.982 | 0.255 | 0.99 | 1.949 | 0.263 | 0.99 |
| Zn | 8.830 | 0.083 | 0.89 | 8.254 | 0.05 | 0.92 | 9.311 | 0.012 | 0.99 | 8.734 | 0.013 | 0.99 |
| Cd | 0.732 | 0.031 | 0.93 | 0.783 | 0.022 | 0.85 | 0.879 | 1.296 | 0.99 | 0.734 | 1.857 | 0.99 |
| Ni | 3.715 | 0.024 | 0.89 | 3.031 | 0.054 | 0.93 | 3.931 | 0.065 | 0.98 | 3.327 | 0.090 | 0.99 |
| Mn | 2.069 | 0.056 | 0.91 | 1.997 | 0.057 | 0.86 | 2.223 | 0.202 | 0.99 | 2.242 | 0.199 | 0.99 |

Table 6.12. Parameters for adsorption of heavy metals present in paper mill leachate on bentonites derived from the pseudo-first- and second-order kinetic models.

| Paper mill leachate | Pseudo 1st order | | | | | | Pseudo 2nd order | | | | | |
|---------------------|------------------|----------------------------|-------|--------------|----------------------------|-------|------------------|------------------|-------|--------------|------------------|-------|
| | Bentonite-1 | | | Bentonite-2 | | | Bentonite-1 | | | Bentonite-2 | | |
| | q_e (mg/g) | K_1 (min ⁻¹) | R^2 | q_e (mg/g) | K_1 (min ⁻¹) | R^2 | q_e (mg/g) | K_1 (g/mg min) | R^2 | q_e (mg/g) | K_1 (g/mg min) | R^2 |
| Cu | 0.273 | 0.047 | 0.87 | 0.331 | 0.027 | 0.90 | 0.297 | 11.360 | 0.99 | 0.298 | 11.293 | 0.99 |
| Pb | 0.125 | 0.056 | 0.73 | 0.122 | 0.058 | 0.87 | 0.139 | 51.508 | 0.99 | 0.138 | 52.805 | 0.99 |
| Zn | 9.60 | 0.028 | 0.89 | 7.216 | 0.041 | 0.93 | 11.001 | 0.008 | 0.99 | 8.576 | 0.014 | 0.99 |
| Cd | 3.59 | 0.09 | 0.91 | 3.286 | 0.05 | 0.91 | 4.102 | 0.059 | 0.99 | 3.858 | 0.067 | 0.99 |
| Ni | 0.26 | 0.024 | 0.88 | 0.217 | 0.026 | 0.83 | 0.249 | 16.149 | 0.97 | 0.240 | 17.346 | 0.99 |
| Fe | 1.23 | 0.03 | 0.86 | 1.157 | 0.025 | 0.92 | 1.290 | 0.601 | 0.99 | 1.274 | 0.616 | 0.99 |
| Mn | 0.82 | 0.02 | 0.87 | 0.488 | 0.058 | 0.88 | 0.732 | 1.868 | 0.99 | 0.553 | 3.275 | 0.99 |

6.3. Summary

This study was conducted to examine the impact of contaminants present in fly ash, sewage sludge and paper mill leachate on the change in behaviour of bentonites. Two bentonites with different mineralogical properties were studied for their alteration in the index properties, free swelling, swelling potential, swelling pressure, hydraulic conductivity, consolidation parameters and shear strength in the presence of various contaminants. Furthermore, the study was conducted to analyse the effects of contaminants on the adsorption capacity of the bentonites. Adsorption, dose, contact time and kinetic studies were carried out on both bentonites. Based on the test results, the critical concluding remarks are summarised below.

- Liquid limit, free swell, swelling potential, swelling pressure value was lower for fly ash leachate followed by paper mill leachate and sewage sludge leachate.
- Hydraulic conductivity value was higher for fly ash leachate followed by paper mill and sewage sludge leachate.
- Unconfined compressive strength of both the bentonites decreased in the presence of leachate. Fly ash leachate showed the least value.
- The adsorption capacity of Bentonite-1 was higher as compared to Bentonite-2 in the presence of fly ash, paper mill and sewage sludge leachates.
- For Bentonite-1, the overall adsorption capacities were found to be 65.3, 17.0 and 14.7 mg/g in presence of fly ash, paper mill and sewage sludge leachates, whereas, 57.5, 16.0 and 13.1 mg/g removal were obtained for Bentonite-2, respectively.
- Kinetic study revealed that Pseudo-second-order kinetic model was most suitable for both bentonites for all metals present in the leachate.



*It is during our darkest
moments that we must
focus to see the light.*

- Aristotle

7

Conclusion and Scope for the future work

7.1. Conclusion

This investigation aimed at studying the effects of various concentrations of heavy metals and different leachates on the swelling, hydraulic conductivity, consolidation parameters, shear strength and adsorption behaviour of bentonite. Two bentonites having different mineralogical compositions were chosen to examining their changes in the liquid limits, free swelling, swelling potential, swelling pressure, hydraulic conductivity, consolidation parameters, shear strength properties and sorption characteristics under different conditions, i.e., the presence of different heavy metals of various concentrations and for different leachates. Critical observations were made, and critical conclusions were derived, which are listed as follows:

- Bentonite having a higher liquid limit, swelling capacity, montmorillonite content, SSA and CEC undergoes a massive change in the liquid limit, free swelling, swelling potential, swelling pressure and hydraulic conductivity due to increase in the metal and leachate concentrations.
- The leachates had a considerable effect on the liquid limits, swelling pressure, and swelling potential of both the bentonites, compared to an individual heavy metal

solution, indicating an additive effect of salt on these properties. Irrespective of the bentonite quality, the swelling was found to be the least in the presence of high concentration combination solutions.

- A higher increase in the hydraulic conductivity was observed in the presence of the leachates than the single species ions.
- The study revealed that many factors such as type and concentration of metal and composition of bentonite influences the consolidation parameters (C_c , c_v , and t_{90}) of bentonite. The investigation also shows a lower void ratio exhibited when the sample was permeated with the heavy metals and leachates under any given pressure.
- The pH of the aqueous solution is an essential controlling parameter in the adsorption process. Adsorption capacity is highest for Pb^{2+} , followed by Cu^{2+} and Zn^{2+} . Bentonite-1 showed a higher adsorption capacity as compared to Bentonite-2 in the presence of metals and leachates.
- Bentonites in a single system showed a higher amount of adsorption of heavy metal (Pb^{2+} , Cu^{2+} and Zn^{2+}) compared to a competitive system (leachates).
- MSW leachate showed a higher impact on both the bentonites, compared to the synthetic leachate.
- Both bentonites showed a reduction in the unconfined compression strength (UCS) in the presence of heavy metals and leachates, however, was within the recommended value of $> 200kPa$. Bentonite-2 showed a higher Unconfined compressive strength as compared to Bentonite-1 in the presence of metals and leachates.

7.2. Scientific contributions and practical applications of the research

- The outcome of the research revealed that heavy metals coming in contact with liner for a prolonged time can cause detrimental effects on the adsorption and hydraulic behaviour of liner material. This will help the researchers and design engineers working in the area of waste disposal to understand the influence of heavy metals and leachates on bentonite in a more appropriate manner.
- The investigation provides a more comprehensive knowledge on the heavy metal effects on bentonites which will thus, prove to be of substantial help for engineers and designers.

- This study contributes to a new data set within a concentration ranges from 100 to 2000 mg/L of metal ions. The values obtained from the detailed investigation will be beneficial for engineers for designing an effective and economical barrier system liner system and choosing the most appropriate bentonite type at the waste disposal site to prevent the contamination of ground water resource and geo-environment.

7.3. Scope for the future research

The study on the behaviour of bentonites is far from being a closed issue. Further works may be concentrated in the following areas in the near future:

- In the present investigation, three individual heavy metals were used to determine the change in bentonite behaviour. However, during the literature review, it was found that other heavy metals like Nickel, Iron, Manganese etc. are also present in considerable amounts in different types of leachates. Hence, the individual effects of these heavy metals should also be investigated.
- There are other industrial leachates like coke industry, steel industry etc. which might have shown some other combinations of heavy metals and thus, can portray different results. These leachates may be considered in future investigations.
- In the actual leachate of any industry considerable numbers of heavy metals, salts, even some biological microbes are present. Here, the effects of those are not taken into consideration. Hence, these areas might also be looked upon for future research works.
- Shrinkage behaviour of these two bentonites in the presence of different heavy metals as well as different leachates may be analysed.
- As the clay liner usually comprises of layers of compacted bentonite with geosynthetic clay liners (GCL), additional studies may be carried out investigating the behaviour of bentonite in combination with GCL in the presence of salt solutions.
- Other isotherm models, such as BET and SIP isotherm models can be made use of in future investigations.
- Further studies need to be conducted to properly investigate the effects temperature, agitation speed and ionic strength.

Conclusion and Scope for the future work

- Further studies may be carried out with better interpretation with the surface charge (zeta potential) measurement of bentonites under different exposed conditions.
 - Also, geochemical modelling can be used to help better assess the results.
-



References

- Abd El-Aal, A. K. (2017). Effect of salinity of groundwater on the geotechnical properties of some Egyptian clay. *Egyptian Journal of Petroleum*, 26(3), 643-648.
<https://doi.org/10.1016/j.ejpe.2016.09.003>
- Abollino, O., Aceto, M., Malandrino, M., Sarzanini, C., & Mentasti, E. (2003). Adsorption of heavy metals on Na-montmorillonite. Effect of pH and organic substances. *Water Research*, 37(7), 1619-1627.
[https://doi.org/10.1016/S0043-1354\(02\)00524-9](https://doi.org/10.1016/S0043-1354(02)00524-9)
- Aderemi, A. O., Oriaku, A. V., Adewumi, G. A., & Otitolaju, A. A. (2011). Assessment of groundwater contamination by leachate near a municipal solid waste landfill. *African Journal of Environmental Science and Technology*, 5(11), 933-940.
<https://doi.org/10.5897/AJEST11.272>
- Adeyemo, A. A., Adeoye, I. O., & Bello, O. S. (2017). Adsorption of dyes using different types of clay: a review. *Applied Water Science*, 7(2), 543-568.
<https://doi.org/10.1007/s13201-015-0322-y>
- Agamuthu, P., & Fauziah, S. H. (2010). Heavy metal pollution in landfill environment: A Malaysian case study. In *2010 4th International Conference on Bioinformatics and Biomedical Engineering*, Granada, Spain (pp. 1-4). IEEE.
<https://doi.org/10.1109/ICBBE.2010.5516886>
- Akporomie, K. G., & Dawodu, F. A. (2015). Potential of a low-cost bentonite for heavy metal abstraction from binary component system. *Beni-suef University Journal of Basic and Applied Sciences*, 4(1), 1-13.
<https://doi.org/10.1016/j.bjbas.2015.02.002>
- Aljlil, S. A., & Alsewailem, F. D. (2014). Adsorption of Cu & Ni on bentonite clay from waste water. *Athens Journal of Natural & Formal Sciences*, 1(1), 21-30.
<https://doi.org/10.30958/ajs.1-1-2>
- Al-Qunaibit, M. H., Mekhemer, W. K., & Zaghloul, A. A. (2005). The adsorption of Cu (II) ions on bentonite—a kinetic study. *Journal of Colloid and Interface Science*, 283(2), 316-321.
<https://doi.org/10.1016/j.jcis.2004.09.022>

- Alther, G., Evans, J. C., Fang, H. Y., & Witmer, K. (1985). Influence of Inorganic Permeants upon the Permeability of Bentonite. In *Hydraulic Barriers in Soil and Rock*. ed. A. Johnson, R. Frobel, N. Cavalli, and C. Pettersson (West Conshohocken, PA: ASTM International), 64-73.
<https://doi.org/10.1520/STP34567S>
- Anna, B., Kleopas, M., Constantine, S., Anestis, F., & Maria, B. (2015). Adsorption of Cd (II), Cu (II), Ni (II) and Pb (II) onto natural bentonite: study in mono-and multi-metal systems. *Environmental Earth Sciences*, 73(9), 5435-5444.
<https://doi.org/10.1007/s12665-014-3798-0>
- Araujo, A. L. P. D., Gimenes, M. L., Barros, M. A. S. D. D., & Silva, M. G. C. D. (2013). A kinetic and equilibrium study of zinc removal by Brazilian bentonite clay. *Materials Research*, 16(1), 128-136.
<https://doi.org/10.1590/S1516-14392012005000148>
- ASTM Standard D2166-16 (2006). Standard test method for unconfined compressive strength of cohesive soil. *ASTM International*, West Conshohocken, PA.
https://doi.org/10.1520/D2166_D2166M-16
- ASTM Standard D2435-96 (1996). Test Method for One-Dimensional Consolidation Properties of Soils. *ASTM International*, West Conshohocken, PA.
<https://doi.org/10.1520/D2435-96>
- ASTM Standard D4318-10 (2010). Standard Test Methods for Liquid Limit, Plastic Limit, and Plasticity Index of Soils. *ASTM International*, West Conshohocken, PA.
<https://doi.org/10.1520/D4318-10>
- ASTM Standard D4646-03 (2008). Standard Test Method for 24-h Batch-Type Measurement of Contaminant Sorption by Soils and Sediments. *ASTM International*, West Conshohocken, PA.
<https://doi.org/10.1520/D4646-03R08>
- ASTM Standard D5890-06 (2006). Standard test method for swell index of clay mineral component of geosynthetic clay liners. *ASTM International*, West Conshohocken, PA.
<https://doi.org/10.1520/D5890-06>
- ASTM Standard D698-12 (2012). Standard Test Methods for Laboratory Compaction Characteristics of Soil Using Standard Effort (12,400 ft-lbf/ft³ (600 kN-m/m³)). *ASTM International*, West Conshohocken, PA.

- <https://doi.org/10.1520/D0698-12>
- ASTM Standard D854-14 (2014). Standard Test Methods for Specific Gravity of Soil Solids by Water Pycnometer. *ASTM International*, West Conshohocken, PA.
- <https://doi.org/10.1520/D0854-14>
- Atkovska, K., Bliznakovska, B., Ruseska, G., Bogoevski, S., Boskovski, B., & Grozdanov, A. (2016). Adsorption of Fe (II) and Zn (II) ions from landfill leachate by natural bentonite. *Journal of Chemical Technology & Metallurgy*, 51(2).
- ATSDR, U. (1999). Toxicological profile for lead. US Department of Health and Human Services. *Public Health Service, Atlanta, USA*, 582.
- ATSDR Q (2008). Draft Toxicological Profile for Cadmium. *ATSDR Agency for Toxic Substances and Disease Registry*.
- Ayari, F., Srasra, E., & Trabelsi-Ayadi, M. (2007). Removal of lead, zinc and nickel using sodium bentonite activated clay. *Asian Journal of Chemistry*, 19(5), 3325.
- Azad, F. N., Ghaedi, M., Dashtian, K., Montazerzohori, M., Hajati, S., & Alipanahpour, E. (2015). Preparation and characterization of MWCNTs functionalized by N-(3-nitrobenzylidene)-N'-trimethoxysilylpropyl-ethane-1, 2-diamine for the removal of aluminum (iii) ions via complexation with eriochrome cyanine R: spectrophotometric detection and optimization. *RSC Advances*, 5(75), 61060-61069.
- <https://doi.org/10.1039/C5RA08746E>
- Barbier, F., Duc, G., & Petit-Ramel, M. (2000). Adsorption of lead and cadmium ions from aqueous solution to the montmorillonite/water interface. *Colloids and Surfaces A: Physicochemical and Engineering Aspects*, 166(1-3), 153-159.
- [https://doi.org/10.1016/S0927-7757\(99\)00501-4](https://doi.org/10.1016/S0927-7757(99)00501-4)
- Baylan, N., & Meriçboyu, A. E. (2016). Adsorption of lead and copper on bentonite and grapeseed activated carbon in single-and binary-ion systems. *Separation Science and Technology*, 51(14), 2360-2368.
- <https://doi.org/10.1080/01496395.2016.1212888>
- Blanchard, G., Maunaye, M., & Martin, G. (1984). Removal of heavy metals from waters by means of natural zeolites. *Water Research*, 18(12), 1501-1507.
- [https://doi.org/10.1016/0043-1354\(84\)90124-6](https://doi.org/10.1016/0043-1354(84)90124-6)

- Boehme, S. E., & Panero, M. A. (2003). *Pollution prevention and management strategies for Cadmium in the New York/New Jersey Harbor*. New York Academy of Sciences, New York, USA.
- Bolt, G. H. (1956). Physico-chemical analysis of the compressibility of pure clays. *Geotechnique*, 6(2), 86-93.
<https://doi.org/10.1680/geot.1956.6.2.86>
- Bonsignore, M., Manta, D. S., Mirto, S., Quinci, E. M., Ape, F., Montalto, V., Gristina, M., Traina, A. & Sprovieri, M. (2018). Bioaccumulation of heavy metals in fish, crustaceans, molluscs and echinoderms from the Tuscany coast. *Ecotoxicology and Environmental Safety*, 162, 554-562.
<https://doi.org/10.1016/j.ecoenv.2018.07.044>
- Bouazza, A., Liu, Y., & Gates, W. P. (2013). Effect of strong acidic leachates on hydraulic conductivity of a needle punched GCL. In *Proceedings of the Heap Leach Solutions Conference* (pp. 380-389).
- Bourliva, A., Michailidis, K., Sikalidis, C., Filippidis, A., & Betsiou, M. (2013). Lead removal from aqueous solutions by natural Greek bentonites. *Clay Minerals*, 48(5), 771-787.
<https://doi.org/10.1180/claymin.2013.048.5.09>
- Bradl, H. (Ed.). (2005). *Heavy metals in the environment: origin, interaction and remediation*. Netherlands: Elsevier Science.
<https://books.google.co.in/books?id=q3P2ousSnbsC>
- Brigatti, M. F., Galan, E., & Theng, B. K. G. (2006). Structures and mineralogy of clay minerals. *Developments in Clay Science*, 1, 19-86.
[https://doi.org/10.1016/S1572-4352\(05\)01002-0](https://doi.org/10.1016/S1572-4352(05)01002-0)
- Budhu, M., Giese Jr, R. F., Campbell, G., & Baumgrass, L. (1991). The permeability of soils with organic fluids. *Canadian Geotechnical Journal*, 28(1), 140-147.
<https://doi.org/10.1139/t91-015>
- Castellanos, E., Villar, M. V., Romero, E., Lloret, A., & Gens, A. (2008). Chemical impact on the hydro-mechanical behaviour of high-density FEBEX bentonite. *Physics and Chemistry of the Earth, Parts A/B/C*, 33, S516-S526.
<https://doi.org/10.1016/j.pce.2008.10.056>

- Cerato, A. B., & Lutenecker, A. J. (2002). Determination of surface area of fine-grained soils by the ethylene glycol monoethyl ether (EGME) method. *Geotechnical Testing Journal*, 25(3), 315-321.
<https://doi.org/10.1520/GTJ11087J>
- Chai, J. C., & Miura, N. (2002). Comparing the performance of landfill liner systems. *Journal of Material Cycles and Waste Management*, 4(2), 135-142.
<https://doi.org/10.1007/s10163-002-0065-3>
- Chalmin, P., & Gaillochet, C. (2009). From waste to resource. *An Abstract of World Waste Survey, Cyclope, Veolia Environmental Services, Edition Economica, France.*
- Chandra, S., Chauhan, L. K. S., Murthy, R. C., Saxena, P. N., Pande, P. N., & Gupta, S. K. (2005). Comparative biomonitoring of leachates from hazardous solid waste of two industries using Allium test. *Science of The Total Environment*, 347(1-3), 46-52.
<https://doi.org/10.1016/j.scitotenv.2005.01.002>
- Chapman, D. L. (1913). A contribution to the theory of electrocapillarity. *The London, Edinburgh, and Dublin Philosophical Magazine and Journal of Science*, 25(148), 475-481.
<https://doi.org/10.1080/14786440408634187>
- Chapman, H. D. (1965). Cation-exchange capacity. *Methods of Soil Analysis: Part 2 Chemical and Microbiological Properties*, 9, 891-901.
<https://doi.org/10.2134/agronmonogr9.2.c6>
- Chen, J. N., Benson, C. H., & Edil, T. B. (2018). Hydraulic conductivity of geosynthetic clay liners with sodium bentonite to coal combustion product leachates. *Journal of Geotechnical and Geoenvironmental Engineering*, 144(3), 04018008.
[https://doi.org/10.1061/\(ASCE\)GT.1943-5606.0001844](https://doi.org/10.1061/(ASCE)GT.1943-5606.0001844)
- Chen, Y. G., He, Y., Ye, W. M., Lin, C. H., Zhang, X. F., & Ye, B. (2012). Removal of chromium (III) from aqueous solutions by adsorption on bentonite from Gaomiaozhi, China. *Environmental Earth Sciences*, 67(5), 1261-1268.
<https://doi.org/10.1007/s12665-012-1569-3>
- Christensen, T. H., & Kjeldsen, P. (1989). Basic biochemical processes in landfills. In *Sanitary Landfilling: Process, Technology, and Environmental Impact. Academic Press, New York. 1989. p 29-49.*
- Dakshanamurthy, V. (1978). A new method to predict swelling using a hyperbolic equation. *Geotechnical Engineering*, 9(1).

- <http://worldcat.org/issn/00465828>
- Daniel, D. E. (1984). Predicting hydraulic conductivity of clay liners. *Journal of Geotechnical Engineering*, 110(2), 285-300.
[https://doi.org/10.1061/\(ASCE\)0733-9410\(1984\)110:2\(285\)](https://doi.org/10.1061/(ASCE)0733-9410(1984)110:2(285))
- Daniel, D. E., & Benson, C. H. (1990). Water content-density criteria for compacted soil liners. *Journal of Geotechnical Engineering*, 116(12), 1811-1830.
[https://doi.org/10.1061/\(ASCE\)0733-9410\(1990\)116:12\(1811\)](https://doi.org/10.1061/(ASCE)0733-9410(1990)116:12(1811))
- Daniel, D. E., & Wu, Y. K. (1993). Compacted clay liners and covers for arid sites. *Journal of Geotechnical Engineering*, 119(2), 223-237.
[https://doi.org/10.1061/\(ASCE\)0733-9410\(1993\)119:2\(223\)](https://doi.org/10.1061/(ASCE)0733-9410(1993)119:2(223))
- Davison, A. G., Taylor, A. N., Darbyshire, J., Chettle, D. R., Guthrie, C. J. G., O'Malley, D., Mason, H.T., Fayers, P.M., Venables, K.M., Pickering, C.A.C., Franklin, D., Scott M.C., Holden, H., Wright, A.L., & Gompertz, D. (1988). Cadmium fume inhalation and emphysema. *The Lancet*, 331(8587), 663-667.
[https://doi.org/10.1016/S0140-6736\(88\)91474-2](https://doi.org/10.1016/S0140-6736(88)91474-2)
- De Oliveira, C. I. R., Rocha, M. C. G., Da Silva, A. L. N., & Bertolino, L. C. (2016). Characterization of bentonite clays from Cubati, Paraíba (Northeast of Brazil). *Cerâmica*, 62(363), 272-277.
<https://doi.org/10.1590/0366-69132016623631970>
- Deka, A., & Sekharan, S. (2017). Contaminant retention characteristics of fly ash–bentonite mixes. *Waste Management & Research*, 35(1), 40-46.
<https://doi.org/10.1177%2F0734242X16670002>
- Demdoum, A., Gueddouda, M. K., Goual, I., Souli, H., & Ghembaza, M. S. (2020). Effect of landfill leachate on the hydromechanical behavior of bentonite-geomaterials mixture. *Construction and Building Materials*, 234, 117356.
<https://doi.org/10.1016/j.conbuildmat.2019.117356>
- DING, S. L., SUN, Y. Z., YANG, C. N., & XU, B. H. (2009). Removal of copper from aqueous solutions by bentonites and the factors affecting it. *Mining Science and Technology (China)*, 19(4), 489-492.
[https://doi.org/10.1016/S1674-5264\(09\)60091-0](https://doi.org/10.1016/S1674-5264(09)60091-0)
- Dorsey, A., & Ingerman, L. (2004). Toxicological profile for copper. *U.S. Department of Health and Human Services, Public Health Service Agency for Toxic Substances and Disease Registry*.

- Du, Y. J., Fan, R. D., Reddy, K. R., Liu, S. Y., & Yang, Y. L. (2015). Impacts of presence of lead contamination in clayey soil–calcium bentonite cutoff wall backfills. *Applied Clay Science, 108*, 111-122.
<https://doi.org/10.1016/j.clay.2015.02.006>
- Dutta, J., & Mishra, A. K. (2015). A study on the influence of inorganic salts on the behaviour of compacted bentonites. *Applied Clay Science, 116*, 85-92.
<https://doi.org/10.1016/j.clay.2015.08.018>
- Dutta, J., & Mishra, A. K. (2016a). Consolidation behaviour of bentonites in the presence of salt solutions. *Applied Clay Science, 120*, 61-69.
<https://doi.org/10.1016/j.clay.2015.12.001>
- Dutta, J., & Mishra, A. K. (2016b). Influence of the presence of heavy metals on the behaviour of bentonites. *Environmental Earth Sciences, 75*(11), 1-10.
<https://doi.org/10.1007/s12665-016-5811-2>
- Dutta, J., & Mishra, A. K. (2017). Consolidation behavior of compacted bentonites in the presence of heavy metals. *Journal of Hazardous, Toxic, and Radioactive Waste, 21*(3), 04017003.
[https://doi.org/10.1061/\(ASCE\)HZ.2153-5515.0000356](https://doi.org/10.1061/(ASCE)HZ.2153-5515.0000356)
- Dutta, J., Mishra, A. K., & Das, P. (2018). Combined Effect of Inorganic Salts and Heavy Metals on the Engineering Behaviour of Compacted Bentonites. *International Journal of Geosynthetics and Ground Engineering, 4*(2), 1-11.
<https://doi.org/10.1007/s40891-018-0134-x>
- Egloffstein, T. (1997). Geosynthetic clay liners, part six: Ion exchange. *Geotechnical Fabrics Report, 15*(5).
<http://worldcat.org/issn/08824983>
- Egloffstein, T. (2020). Properties and test methods to assess bentonite used in geosynthetic clay liners. In *Geosynthetic clay liners* (pp. 51-72). CRC Press.
- Ferguson, J. E. (1990). *The Heavy Elements: Chemistry, Environmental Impact and Health Effects* (No. 628.53 F4).
- Fernández-Nava, Y., Ulmanu, M., Anger, I., Marañón, E., & Castrillón, L. (2011). Use of granular bentonite in the removal of mercury (II), cadmium (II) and lead (II) from aqueous solutions. *Water, Air, & Soil Pollution, 215*(1), 239-249.
<https://doi.org/10.1007/s11270-010-0474-1>

- Flora, S. J., Flora, G., & Saxena, G. (2006). Environmental occurrence, health effects and management of lead poisoning. In *Lead* (pp. 158-228). Elsevier Science BV.
<https://doi.org/10.1016/B978-044452945-9/50004-X>
- Freitas, E. D., Carmo, A. C. R., Neto, A. A., & Vieira, M. G. A. (2017). Binary adsorption of silver and copper on Verde-lodo bentonite: Kinetic and equilibrium study. *Applied Clay Science*, *137*, 69-76.
<https://doi.org/10.1016/j.clay.2016.12.016>
- Freundlich, H. (2002). Adsorptionstechnik. By Franz Krzil. *The Journal of Physical Chemistry*, *40*(6), 857-858.
<https://doi.org/10.1021/j150375a022>
- Futalan, C. M., Kan, C. C., Dalida, M. L., Hsien, K. J., Pascua, C., & Wan, M. W. (2011). Comparative and competitive adsorption of copper, lead, and nickel using chitosan immobilized on bentonite. *Carbohydrate Polymers*, *83*(2), 528-536.
<https://doi.org/10.1016/j.carbpol.2010.08.013>
- FWI (2001). Toxic and Hazardous Materials in Electronics; Prepared for Environment Canada. *National Office of Pollution Prevention and Industry Canada, Computers for Schools Program, Quebec, Canada.*
- Gabby, P. N. (2006). Lead: in mineral commodity summaries. Reston, VA. *US Geological Survey*, USA.
- Galindo, L. S. G., Almeida Neto, A. F. D., Silva, M. G. C. D., & Vieira, M. G. A. (2013). Removal of cadmium (II) and lead (II) ions from aqueous phase on sodic bentonite. *Materials Research*, *16*(2), 515-527.
<https://doi.org/10.1590/S1516-14392013005000007>
- Giardina, A., Larson, S. F., Wisner, B., Wheeler, J., & Chao, M. (2009). Long-term and acute effects of zinc contamination of a stream on fish mortality and physiology. *Environmental Toxicology and Chemistry: An International Journal*, *28*(2), 287-295.
<https://doi.org/10.1897/07-461.1>
- Glatstein, D. A., & Francisca, F. M. (2015). Influence of pH and ionic strength on Cd, Cu and Pb removal from water by adsorption in Na-bentonite. *Applied Clay Science*, *118*, 61-67.
<https://doi.org/10.1016/j.clay.2015.09.003>

- Gleason, M. H., Daniel, D. E., & Eykholt, G. R. (1997). Calcium and sodium bentonite for hydraulic containment applications. *Journal of Geotechnical and Geoenvironmental Engineering*, 123(5), 438-445.
[https://doi.org/10.1061/\(ASCE\)1090-0241\(1997\)123:5\(438\)](https://doi.org/10.1061/(ASCE)1090-0241(1997)123:5(438))
- Gong, R., Jin, Y., Chen, F., Chen, J., & Liu, Z. (2006). Enhanced malachite green removal from aqueous solution by citric acid modified rice straw. *Journal of Hazardous Materials*, 137(2), 865-870.
<https://doi.org/10.1016/j.jhazmat.2006.03.010>
- Gouy, M. (1910). Sur la constitution de la charge électrique à la surface d'un électrolyte. *Journal of Physics: Theories and Applications*, 9(1), 457-468.
<https://doi.org/10.1051/jphysap:019100090045700>
- Goyer, R. A., & Clarkson, T. W. (1996). Toxic effects of metals. *Casarett & Doull's Toxicology. The Basic Science of Poisons, Fifth Edition, Klaassen, CD [Ed]. McGraw-Hill Health Professions Division*, 23, 813-858.
- Graham, J., Saadat, F., Gray, M. N., Dixon, D. A., & Zhang, Q. Y. (1989). Strength and volume change behaviour of a sand-bentonite mixture. *Canadian Geotechnical Journal*, 26(2), 292-305.
<https://doi.org/10.1139/t89-038>
- Grim, R. E. (1968). *Clay Mineralogy*. 2nd edn. McGraw-Hill Book Company. New York, 185-224.
- Grim, R., & Güven, N. (1978). *Bentonites: geology, mineralogy, properties and uses: Elsevier Sci. Publ. Co., Amsterdam, Netherlands*.
- Gupta, S. S., & Bhattacharyya, K. G. (2008). Immobilization of Pb (II), Cd (II) and Ni (II) ions on kaolinite and montmorillonite surfaces from aqueous medium. *Journal of Environmental Management*, 87(1), 46-58.
<https://doi.org/10.1016/j.jenvman.2007.01.048>
- Haan, S. De (1981). Results of municipal waste compost research over more than fifty years at the Institute for Soil Fertility at Haren/Groningen, the Netherlands. *NJAS Wageningen Journal of Life Sciences*, 29(1), 49-61.
<https://doi.org/10.18174/njas.v29i1.17019>
- Hamidpour, M., Kalbasi, M., Afyuni, M., Shariatmadari, H., & Furrer, G. (2011). Sorption of lead on Iranian bentonite and zeolite: kinetics and isotherms. *Environmental Earth Sciences*, 62(3), 559-568.

- <https://doi.org/10.1007/s12665-010-0547-x>
- Harvey, B. (2002). Managing elevated blood lead levels among young children: Recommendations from the Advisory Committee on Childhood Lead Poisoning Prevention. *Atlanta: U.S. Department of Health and Human Services, Public Health Service.*
- Haug M. and Boldt-Leppin. B. (1994). Influence of Polymers on the Hydraulic Conductivity of Marginal Quality Bentonite-Sand Mixtures," In *Hydraulic Conductivity and Waste Contaminant Transport in Soil*, ed. D. Daniel and S. Trautwein (West Conshohocken, PA: ASTM International, 1994), 407-421.
<https://doi.org/10.1520/STP23900S>
- Hazarika, J., Ghosh, U., Kalamdhad, A. S., Khwairakpam, M., & Singh, J. (2017). Transformation of elemental toxic metals into immobile fractions in paper mill sludge through rotary drum composting. *Ecological Engineering*, 101, 185-192.
<https://doi.org/10.1016/j.ecoleng.2017.02.005>
- He, Z. L., Yang, X. E., & Stoffella, P. J. (2005). Trace elements in agroecosystems and impacts on the environment. *Journal of Trace elements in Medicine and Biology*, 19(2-3), 125-140.
<https://doi.org/10.1016/j.jtemb.2005.02.010>
- Hedemalm, P., Carlsson, P., & Palm, V. (1995). Waste from electrical and electronic products: a survey of the contents of materials and hazardous substances in electric and electronic products. *Nordic Council of Ministers [Nordiska ministerrådet]*.
- Hefne, J. A., Mekhemer, W. K., Al, N. M., Aldayel, O. A., & Alajyan, T. (2008). Kinetic and thermodynamic study of the adsorption of Pb (II) from aqueous solution to the natural and treated bentonite. *International Journal of Physical Sciences*, 3(11), 281-288.
<http://www.academicjournals.org/IJPS>
- Herawati, N., Suzuki, S., Hayashi, K., Rivai, I. F., & Koyama, H. (2000). Cadmium, copper, and zinc levels in rice and soil of Japan, Indonesia, and China by soil type. *Bulletin of Environmental Contamination and Toxicology*, 64(1), 33-39.
<https://doi.org/10.1007/s001289910006>
- Hiroki, M. (1992). Effects of heavy metal contamination on soil microbial population. *Soil Science and Plant Nutrition*, 38(1), 141-147.
<https://doi.org/10.1080/00380768.1992.10416961>

- Hoornweg, Daniel, Bhada-Tata, Perinaz. (2012). *What a Waste: A Global Review of Solid Waste Management. Urban development series; knowledge papers no. 15. World Bank, Washington, DC. © World Bank.*
<https://openknowledge.worldbank.org/handle/10986/17388>
- I. A. R. C. (1990). Chromium, Nickel, and Welding. IARC Monograph on the Evaluation of Carcinogenic Risks to Humans. *World Health Organization: Lyon, France.*
- Inglezakis, V. J., Stylianou, M. A., Gkantzou, D., & Loizidou, M. D. (2007). Removal of Pb (II) from aqueous solutions by using clinoptilolite and bentonite as adsorbents. *Desalination, 210(1-3)*, 248-256.
<https://doi.org/10.1016/j.desal.2006.05.049>
- Jellander, R., Marčelja, S., & Quirk, J. P. (1988). Attractive double-layer interactions between calcium clay particles. *Journal of Colloid and Interface Science, 126(1)*, 194-211.
[https://doi.org/10.1016/0021-9797\(88\)90113-0](https://doi.org/10.1016/0021-9797(88)90113-0)
- Jo, H. Y., Katsumi, T., Benson, C. H., & Edil, T. B. (2001). Hydraulic conductivity and swelling of nonprehydrated GCLs permeated with single-species salt solutions. *Journal of Geotechnical and Geoenvironmental Engineering, 127(7)*, 557-567.
[https://doi.org/10.1061/\(ASCE\)1090-0241\(2001\)127:7\(557\)](https://doi.org/10.1061/(ASCE)1090-0241(2001)127:7(557))
- Kanmani, S., & Gandhimathi, R. (2013). Assessment of heavy metal contamination in soil due to leachate migration from an open dumping site. *Applied Water Science, 3(1)*, 193-205.
<https://doi.org/10.1007/s13201-012-0072-z>
- Karapinar, N., & Donat, R. (2009). Adsorption behaviour of Cu²⁺ and Cd²⁺ onto natural bentonite. *Desalination, 249(1)*, 123-129.
<https://doi.org/10.1016/j.desal.2008.12.046>
- Kashir, M., & Yanful, E. K. (2001). Hydraulic conductivity of bentonite permeated with acid mine drainage. *Canadian Geotechnical Journal, 38(5)*, 1034-1048.
<https://doi.org/10.1139/t01-027>
- Kaya, A., & Ören, A. H. (2005). Adsorption of zinc from aqueous solutions to bentonite. *Journal of Hazardous Materials, 125(1-3)*, 183-189.
<https://doi.org/10.1016/j.jhazmat.2005.05.027>

- Kerisit, S., Okumura, M., Rosso, K. M., & Machida, M. (2016). Molecular simulation of cesium adsorption at the basal surface of phyllosilicate minerals. *Clays and Clay Minerals*, 64(4), 389-400.
<https://doi.org/10.1346/CCMN.2016.0640405>
- Khan, M. R., Hegde, R. A., & Shabiimam, M. A. (2017). Adsorption of lead by bentonite clay. *International Journal of Scientific Research and Management*, 5(7), 5800-5804.
<https://doi.org/10.18535/ijstrm/v5i7.02>
- Kittrick, J. A. (1969). Interlayer forces in montmorillonite and vermiculite. *Soil Science Society of America Journal*, 33(2), 217-222.
<https://doi.org/10.2136/sssaj1969.03615995003300020017x>
- Kjeldsen, P., Barlaz, M. A., Rooker, A. P., Baun, A., Ledin, A., & Christensen, T. H. (2002). Present and long-term composition of MSW landfill leachate: a review. *Critical Reviews in Environmental Science and Technology*, 32(4), 297-336.
<https://doi.org/10.1080/10643380290813462>
- Komine, H., & Ogata, N. (1996). Prediction for swelling characteristics of compacted bentonite. *Canadian Geotechnical Journal*, 33(1), 11-22.
<https://doi.org/10.1139/t96-021>
- Kubilay, Ş., Gürkan, R., Savran, A., & Şahan, T. (2007). Removal of Cu (II), Zn (II) and Co (II) ions from aqueous solutions by adsorption onto natural bentonite. *Adsorption*, 13(1), 41-51.
<https://doi.org/10.1007/s10450-007-9003-y>
- Kul, A. R., & Koyuncu, H. (2010). Adsorption of Pb (II) ions from aqueous solution by native and activated bentonite: kinetic, equilibrium and thermodynamic study. *Journal of Hazardous Materials*, 179(1-3), 332-339.
<https://doi.org/10.1016/j.jhazmat.2010.03.009>
- Lagergren, S. (1898). About the Theory of So-Called Adsorption of Soluble Substances. *Kungliga Svenska Vetenskapsakademiens Handlingar*, 24, 1-39.
- Laird, D. A. (1996). Model for Crystalline Swelling of 2: 1 Phyllosilicates. *Clays and Clay Minerals*, 44(4), 553-559.
<https://doi.org/10.1346/CCMN.1996.0440415>

- Laird, D. A. (2006). Influence of layer charge on swelling of smectites. *Applied clay science*, 34(1-4), 74-87.
<https://doi.org/10.1016/j.clay.2006.01.009>
- Lambe, T. (1955). The permeability of fine-grained soils. In *Symposium on Permeability of Soils. ASTM International*.
<https://doi.org/10.1520/STP46165S>
- Lambe, T. W. (1958). The engineering behavior of compacted clay. *Journal of the Soil Mechanics and Foundations Division*, 84(2), 1655-1.
<https://doi.org/10.1061/JSFEAQ.0000115>
- Langmuir, I. (1918). The adsorption of gases on plane surfaces of glass, mica and platinum. *Journal of the American Chemical society*, 40(9), 1361-1403.
- Lee, C. H., Chang, S. L., Wang, K. M., & Wen, L. C. (2000). Management of scrap computer recycling in Taiwan. *Journal of Hazardous Materials*, 73(3), 209-220.
[https://doi.org/10.1016/S0304-3894\(99\)00191-0](https://doi.org/10.1016/S0304-3894(99)00191-0)
- Lee, S. M., & Tiwari, D. (2013). Manganese oxide immobilized activated carbons in the remediation of aqueous wastes contaminated with copper (II) and lead (II). *Chemical Engineering Journal*, 225, 128-137.
<https://doi.org/10.1016/j.cej.2013.03.083>
- Li, B., Li, L. Y., & Grace, J. R. (2015). Adsorption and hydraulic conductivity of landfill-leachate perfluorinated compounds in bentonite barrier mixtures. *Journal of Environmental Management*, 156, 236-243.
<https://doi.org/10.1016/j.jenvman.2015.04.003>
- Li, L. Y. (2003). Multi-component of heavy metal contaminants adsorptivity and compatibility onto variable charge clay mineral. *Clay Science*, 12(2), 73-80.
<https://doi.org/10.11362/jcssjclayscience1960.12.73>
- Li, L. Y., & Li, F. (2001). Heavy metal sorption and hydraulic conductivity studies using three types of bentonite admixes. *Journal of Environmental Engineering*, 127(5), 420-429.
[https://doi.org/10.1061/\(ASCE\)0733-9372\(2001\)127:5\(420\)](https://doi.org/10.1061/(ASCE)0733-9372(2001)127:5(420))
- Li, L. Y., Ohtsubo, M., Higashi, T., Yamaoka, S., & Morishita, T. (2007). Leachability of municipal solid waste ashes in simulated landfill conditions. *Waste Management*, 27(7), 932-945.
<https://doi.org/10.1016/j.wasman.2006.04.014>

- Lin, L. C., & Benson, C. H. (2000). Effect of wet-dry cycling on swelling and hydraulic conductivity of GCLs. *Journal of Geotechnical and Geoenvironmental Engineering*, 126(1), 40-49.
[https://doi.org/10.1061/\(ASCE\)1090-0241\(2000\)126:1\(40\)](https://doi.org/10.1061/(ASCE)1090-0241(2000)126:1(40))
- Liu, Z. R., & Zhou, S. Q. (2010). Adsorption of copper and nickel on Na-bentonite. *Process Safety and Environmental Protection*, 88(1), 62-66.
<https://doi.org/10.1016/j.psep.2009.09.001>
- Lo, I. M., Luk, A. F., & Yang, X. (2004). Migration of heavy metals in saturated sand and bentonite/soil admixture. *Journal of Environmental Engineering*, 130(8), 906-909.
[https://doi.org/10.1061/\(ASCE\)0733-9372\(2004\)130:8\(906\)](https://doi.org/10.1061/(ASCE)0733-9372(2004)130:8(906))
- Lutz, J. F., & Kemper, W. D. (1959). Intrinsic permeability of clay as affected by clay-water interaction. *Soil Science*, 88(2), 83-90.
- Madsen, F. T., & Mitchell, J. K. (1989). Chemical effects on clay fabric and hydraulic conductivity. In *The Landfill* (pp. 201-251). Springer, Berlin, Heidelberg.
<https://doi.org/10.1007/BFb0011265>
- Madsen, F. T., & Müller-Vonmoos, M. (1989). The swelling behaviour of clays. *Applied Clay Science*, 4(2), 143-156.
[https://doi.org/10.1016/0169-1317\(89\)90005-7](https://doi.org/10.1016/0169-1317(89)90005-7)
- Mall, I. D., Srivastava, V. C., & Agarwal, N. K. (2006). Removal of Orange-G and Methyl Violet dyes by adsorption onto bagasse fly ash—kinetic study and equilibrium isotherm analyses. *Dyes and Pigments*, 69(3), 210-223.
<https://doi.org/10.1016/j.dyepig.2005.03.013>
- Maramis, V., Kurniawan, A., Ayucitra, A., Sunarso, J., & Ismadji, S. (2012). Removal of copper ions from aqueous solution by adsorption using LABORATORIES-modified bentonite (organo-bentonite). *Frontiers of Chemical Science and Engineering*, 6(1), 58-66.
<https://doi.org/10.1007/s11705-011-1160-6>
- Martin, J. P., Richards, S. J., & Pratt, P. F. (1964). Relationship of exchangeable Na percentage at different soil pH levels to hydraulic conductivity. *Soil Science Society of America Journal*, 28(5), 620-622.
<https://doi.org/10.2136/sssaj1964.03615995002800050014x>
- Mc Bride M (1994). Environmental chemistry of soils., *Oxford University Press, New York.*

- McNeal, B. L., Norvell, W. A., & Coleman, N. T. (1966). Effect of solution composition on the swelling of extracted soil clays. *Soil Science Society of America Journal*, 30(3), 313-317.
<https://doi.org/10.2136/sssaj1966.036159950030000300008x>
- Mesri, G., & Olson, R. E. (1971). Mechanisms controlling the permeability of clays. *Clays and Clay minerals*, 19(3), 151-158.
<https://doi.org/10.1346/CCMN.1971.0190303>
- Milojković, J. V., Stojanović, M. D., Mihajlović, M. L., Lopičić, Z. R., Petrović, M. S., Šoštarić, T. D., & Ristić, M. Đ. (2014). Compost of aquatic weed *Myriophyllum spicatum* as low-cost biosorbent for selected heavy metal ions. *Water, Air, & Soil Pollution*, 225(4), 1-10.
<https://doi.org/10.1007/s11270-014-1927-8>
- Mishra, A. K., Ohtsubo, M., Li, L., & Higashi, T. (2005). Effect of salt concentrations on the permeability and compressibility of soil-bentonite mixtures. *Journal of the Faculty of Agriculture, Kyushu University*, 50(2), 837-849.
- Mishra, A. K., Ohtsubo, M., Li, L., & Higashi, T. (2011). Controlling factors of the swelling of various bentonites and their correlations with the hydraulic conductivity of soil-bentonite mixtures. *Applied Clay Science*, 52(1-2), 78-84.
<https://doi.org/10.1016/j.clay.2011.01.033>
- Mishra, A. K., Ohtsubo, M., Li, L. Y., & Higashi, T. (2010). Influence of the bentonite on the consolidation behaviour of soil-bentonite mixtures. *Carbonates and Evaporites*, 25(1), 43-49.
<https://doi.org/10.1007/s13146-010-0006-5>
- Mishra, A. K., Ohtsubo, M., Li, L. Y., Higashi, T., & Park, J. (2009). Effect of salt of various concentrations on liquid limit, and hydraulic conductivity of different soil-bentonite mixtures. *Environmental Geology*, 57(5), 1145-1153.
<https://doi.org/10.1007/s00254-008-1411-0>
- Mitchell, J. K., & Jaber, M. (1990). Factors controlling the long-term properties of clay liners. In *Waste Containment Systems: Construction, Regulation, and Performance* (pp. 84-105). ASCE.
- Mitchell, J. K., & Soga, K. (2005). *Fundamentals of Soil Behavior* (Vol. 3). New York: John Wiley & Sons.

- Moffett, B. F., Nicholson, F. A., Uwakwe, N. C., Chambers, B. J., Harris, J. A., & Hill, T. C. (2003). Zinc contamination decreases the bacterial diversity of agricultural soil. *FEMS Microbiology Ecology*, *43*(1), 13-19.
<https://doi.org/10.1111/j.1574-6941.2003.tb01041.x>
- Mudasir, M., Baskara, R. A., Suratman, A., Yunita, K. S., Perdana, R., & Puspitasari, W. (2020). Simultaneous adsorption of Zn (II) and Hg (II) ions on selective adsorbent of dithizone-immobilized bentonite in the presence of Mg (II) Ion. *Journal of Environmental Chemical Engineering*, *8*(4), 104002.
<https://doi.org/10.1016/j.jece.2020.104002>
- Mukherjee, K., & Mishra, A. K. (2019). Evaluation of Hydraulic and Strength Characteristics of Sand-Bentonite Mixtures with Added Tire Fiber for Landfill Application. *Journal of Environmental Engineering*, *145*(6), 04019026.
[https://doi.org/10.1061/\(ASCE\)EE.1943-7870.0001537](https://doi.org/10.1061/(ASCE)EE.1943-7870.0001537)
- Musson, S. E., Vann, K. N., Jang, Y. C., Mutha, S., Jordan, A., Pearson, B., & Townsend, T. G. (2006). RCRA toxicity characterization of discarded electronic devices. *Environmental Science & Technology*, *40*(8), 2721-2726.
<https://doi.org/10.1021/es051557n>
- Nakano, A., Li, L. Y., Ohtsubo, M., Mishra, A. K., & Higashi, T. (2008). Lead retention mechanisms and hydraulic conductivity studies of various bentonites for geoenvironment applications. *Environmental Technology*, *29*(5), 505-514.
<https://doi.org/10.1080/09593330801984258>
- Nayak, A. K., & Kalamdhad, A. S. (2014). Feasibility of composting combinations of sewage sludge, cattle manure, and sawdust in a rotary drum reactor. *Environmental Engineering Research*, *19*(1), 47-57.
<https://doi.org/10.4491/eer.2014.19.1.047>
- Needhidasan, S., Samuel, M., & Chidambaram, R. (2014). Electronic waste—an emerging threat to the environment of urban India. *Journal of Environmental Health Science and Engineering*, *12*(1), 1-9.
<https://doi.org/10.1186/2052-336X-12-36>
- NJDEP (2002). New Jersey Mercury Task Force, Volume III, Sources of Mercury in New Jersey, p. 105. *NJDEP Division of Science, Research & Technology, Trenton, NJ*.
- Norrish, K. (1954). The swelling of montmorillonite. *Discussions of the Faraday Society*, *18*, 120-134.

- <https://doi.org/10.1039/DF9541800120>
- Norrish, K., & Quirk, J. P. (1954). Crystalline swelling of montmorillonite: Use of electrolytes to control swelling. *Nature*, *173*(4397), 255-256.
- <https://doi.org/10.1038/173255a0>
- Norseth, T. (1986). The carcinogenicity of chromium and its salts. *British Journal of Industrial Medicine*, *43*(10), 649.
- <https://dx.doi.org/10.1136%2Foem.43.10.649>
- Olphen Hv (1963). An introduction to clay colloid chemistry, for clay technologists, geologists, and soil scientists. *Interscience (Wiley), New York, 1963. xvi+ 301 pp. Illus.*
- Olson, R. E., & Mesri, G. (1970). Mechanisms controlling compressibility of clays. *Journal of Soil Mechanics & Foundations Division*, *96*(SM6).
- Olu-Owolabi, B. I., & Unuabonah, E. I. (2010). Kinetic and thermodynamics of the removal of Zn²⁺ and Cu²⁺ from aqueous solution by sulphate and phosphate-modified Bentonite clay. *Journal of Hazardous Materials*, *184*(1-3), 731-738.
- <https://doi.org/10.1016/j.jhazmat.2010.08.100>
- Onikata, M., Kondo, M., Hayashi, N., & Yamanaka, S. (1999). Complex formation of cation-exchanged montmorillonites with propylene carbonate: Osmotic swelling in aqueous electrolyte solutions. *Clays and clay minerals*, *47*(5), 672-677.
- <https://doi.org/10.1346/CCMN.1999.0470514>
- Ören, A. H., & Akar, R. Ç. (2017). Swelling and hydraulic conductivity of bentonites permeated with landfill leachates. *Applied Clay Science*, *142*, 81-89.
- <https://doi.org/10.1016/j.clay.2016.09.029>
- Ouhadi, V. R., Yong, R. N., & Sedighi, M. (2006). Influence of heavy metal contaminants at variable pH regimes on rheological behaviour of bentonite. *Applied Clay Science*, *32*(3-4), 217-231.
- <https://doi.org/10.1016/j.clay.2006.02.003>
- Pawar, R. R., Bajaj, H. C., & Lee, S. M. (2016). Activated bentonite as a low-cost adsorbent for the removal of Cu (II) and Pb (II) from aqueous solutions: Batch and column studies. *Journal of Industrial and Engineering Chemistry*, *34*, 213-223.
- <https://doi.org/10.1016/j.jiec.2015.11.014>

- Petrov, R. J., & Rowe, R. K. (1997). Geosynthetic clay liner (GCL)-chemical compatibility by hydraulic conductivity testing and factors impacting its performance. *Canadian Geotechnical Journal*, 34(6), 863-885.
<https://doi.org/10.1139/t97-055>
- Pivato, A., & Raga, R. (2006). Tests for the evaluation of ammonium attenuation in MSW landfill leachate by adsorption into bentonite in a landfill liner. *Waste Management*, 26(2), 123-132.
<https://doi.org/10.1016/j.wasman.2005.03.009>
- Plum, L. M., Rink, L., & Haase, H. (2010). The essential toxin: impact of zinc on human health. *International Journal of Environmental Research and Public Health*, 7(4), 1342-1365.
<https://doi.org/10.3390/ijerph7041342>
- Posner, A. M., & Quirk, J. P. (1964). Changes in basal spacing of montmorillonite in electrolyte solutions. *Journal of Colloid Science*, 19(9), 798-812.
[https://doi.org/10.1016/0095-8522\(64\)90056-X](https://doi.org/10.1016/0095-8522(64)90056-X)
- Pratt, P. F. (1965). Potassium. *Methods of Soil Analysis: Part 2 Chemical and Microbiological Properties*, 9, 1022-1030.
<https://doi.org/10.2134/agronmonogr9.2.c20>
- Prost, R., Koutit, T., Benchara, A., & Huard, E. (1998). State and location of water adsorbed on clay minerals: consequences of the hydration and swelling-shrinkage phenomena. *Clays and Clay Minerals*, 46(2), 117-131.
<https://doi.org/10.1346/CCMN.1998.0460201>
- Prudent, P., Domeizel, M., & Massiani, C. (1996). Chemical sequential extraction as decision-making tool: application to municipal solid waste and its individual constituents. *Science of the Total Environment*, 178(1-3), 55-61.
[https://doi.org/10.1016/0048-9697\(95\)04797-2](https://doi.org/10.1016/0048-9697(95)04797-2)
- Qian, X., Koerner, R.M. and Gray, D.H. (2002). Geotechnical Aspects of Landfill Design and Construction. *Prentice Hall*, New Jersey.
- Quirk J, Schofield R (1955). The effect of electrolyte concentration on soil permeability. *Journal of Soil Science*, 6:163-178.
- Rao, S. M., Thyagaraj, T., & Thomas, H. R. (2006). Swelling of compacted clay under osmotic gradients. *Geotechnique*, 56(10), 707-713.
<https://doi.org/10.1680/geot.2006.56.10.707>

- Rao, S. M. (2006). Identification and classification of expansive soils. *Expansive Soils Recent Advances in Characterization and Treatment*, 27-36.
- Robinson, R. G., & Allam, M. M. (1998). Effect of clay mineralogy on coefficient of consolidation. *Clays and Clay Minerals*, 46(5), 596-600.
- Ruhl, J. L., & Daniel, D. E. (1997). Geosynthetic clay liners permeated with chemical solutions and leachates. *Journal of Geotechnical and Geoenvironmental Engineering*, 123(4), 369-381.
[https://doi.org/10.1061/\(ASCE\)1090-0241\(1997\)123:4\(369\)](https://doi.org/10.1061/(ASCE)1090-0241(1997)123:4(369))
- Saha, U. K., Iwasaki, K., & Sakurai, K. (2003). Desorption behavior of Cd, Zn and Pb sorbed on hydroxy aluminum and hydroxy aluminosilicate-montmorillonite complexes. *Clays and Clay Minerals*, 51(5), 481-492.
<https://doi.org/10.1346/CCMN.2003.0510502>
- Salas JAJ, Serratos JM (1953). Compressibility of clays. *3rd International Conference of Soil Mechanics and Foundation Engineering*, Zurich. pp 192-198
- Sen, T. K., & Gomez, D. (2011). Adsorption of zinc (Zn^{2+}) from aqueous solution on natural bentonite. *Desalination*, 267(2-3), 286-294.
<https://doi.org/10.1016/j.desal.2010.09.041>
- Shackelford, C. D., Benson, C. H., Katsumi, T., Edil, T. B., & Lin, L. (2000). Evaluating the hydraulic conductivity of GCLs permeated with non-standard liquids. *Geotextiles and Geomembranes*, 18(2-4), 133-161.
[https://doi.org/10.1016/S0266-1144\(99\)00024-2](https://doi.org/10.1016/S0266-1144(99)00024-2)
- Shallari, S., Schwartz, C., Hasko, A., & Morel, J. L. (1998). Heavy metals in soils and plants of serpentine and industrial sites of Albania. *Science of the Total Environment*, 209(2-3), 133-142.
[https://doi.org/10.1016/S0048-9697\(98\)80104-6](https://doi.org/10.1016/S0048-9697(98)80104-6)
- Shariatmadari, N., & Salami, M., & Karimpour Fard, M. (2011). Effect of Inorganic Salt Solutions on Some Geotechnical Properties of Soil-Bentonite Mixtures as Barriers. *International Journal of Civil Engineering*, 9(2), 103-110.
<https://www.sid.ir/en/journal/ViewPaper.aspx?id=246544>
- Sharma, H. D., & Reddy, K. R. (2004). *Geoenvironmental engineering: site remediation, waste containment, and emerging waste management technologies*. John Wiley & Sons., Hoboken, New Jersey, USA.

- Sheta, A. S., Falatah, A. M., Al-Sewailem, M. S., Khaled, E. M., & Sallam, A. S. H. (2003). Sorption characteristics of zinc and iron by natural zeolite and bentonite. *Microporous and Mesoporous Materials*, 61(1-3), 127-136.
[https://doi.org/10.1016/S1387-1811\(03\)00360-3](https://doi.org/10.1016/S1387-1811(03)00360-3)
- Shirazi, S. M., Wiwat, S., Kazama, H., Kuwano, J., & Shaaban, M. G. (2011). Salinity effect on swelling characteristics of compacted bentonite. *Environment Protection Engineering*, 37(2), 65-74.
- Shukla, A., Zhang, Y. H., Dubey, P., Margrave, J. L., & Shukla, S. S. (2002). The role of sawdust in the removal of unwanted materials from water. *Journal of Hazardous Materials*, 95(1-2), 137-152.
[https://doi.org/10.1016/S0304-3894\(02\)00089-4](https://doi.org/10.1016/S0304-3894(02)00089-4)
- Sivapullaiah, P. V., Sridharan, A., & Stalin, V. K. (2000). Hydraulic conductivity of bentonite-sand mixtures. *Canadian Geotechnical Journal*, 37(2), 406-413.
<https://doi.org/10.1139/t99-120>
- Spalvins, E., Dubey, B., & Townsend, T. (2008). Impact of electronic waste disposal on lead concentrations in landfill leachate. *Environmental Science & Technology*, 42(19), 7452-7458.
<https://doi.org/10.1021/es8009277>
- Sparks, D. L. (1995). Sorption phenomena on soils. *Environmental Soil Chemistry*, 99-115.
<https://ci.nii.ac.jp/naid/10013147430/en/>
- Sparks, D. L. (2003). *Environmental Soil Chemistry*. Elsevier, USA.
- Sposito, G. (1981). *The Thermodynamics of Soil Solutions*. Oxford University Press, University of California, Riverside, California, USA.
- Sposito, G. (1984). *The surface chemistry of soils*. Oxford university press, New York, USA.
- Sposito G (1989). *The Chemistry of Soils*. Oxford University Press, New York, USA.
- Spurgeon, D. J., Hopkin, S. P., & Jones, D. T. (1994). Effects of cadmium, copper, lead and zinc on growth, reproduction and survival of the earthworm *Eisenia fetida* (Savigny): assessing the environmental impact of point-source metal contamination in terrestrial ecosystems. *Environmental Pollution*, 84(2), 123-130.
[https://doi.org/10.1016/0269-7491\(94\)90094-9](https://doi.org/10.1016/0269-7491(94)90094-9)

- Spurgeon, D. J., & Hopkin, S. P. (1996). The effects of metal contamination on earthworm populations around a smelting works: quantifying species effects. *Applied Soil Ecology*, 4(2), 147-160.
[https://doi.org/10.1016/0929-1393\(96\)00109-6](https://doi.org/10.1016/0929-1393(96)00109-6)
- Sridharan A (1975). Mechanisms controlling the liquid limit of clays. In *Conf. Soil Mech. Found. Eng.; Istanbul Tek. Univ.* vol. 1; pp. 65-74
- Sridharan, A., & Gurtug, Y. (2004). Swelling behaviour of compacted fine-grained soils. *Engineering Geology*, 72(1-2), 9-18.
[https://doi.org/10.1016/S0013-7952\(03\)00161-3](https://doi.org/10.1016/S0013-7952(03)00161-3)
- Sridharan, A., & Jayadeva, M. S. (1982). Double layer theory and compressibility of clays. *Geotechnique*, 32(2), 133-144.
<https://doi.org/10.1680/geot.1982.32.2.133>
- Sridharan, A. S. U. R. I., Rao, A. S., & Sivapullaiah, P. V. (1986). Swelling pressure of clays. *Geotechnical Testing Journal*, 9(1), 24-33.
<https://doi.org/10.1520/GTJ10608J>
- Sridharan, A., & Rao, G. V. (1973). Mechanisms controlling volume change of saturated clays and the role of the effective stress concept. *Geotechnique*, 23(3), 359-382.
<https://doi.org/10.1680/geot.1973.23.3.359>
- Sridharan, A., Rao, S. M., & Murthy, N. S. (1986). Compressibility behaviour of homoionized bentonites. *Geotechnique*, 36(4), 551-564.
<https://doi.org/10.1680/geot.1986.36.4.551>
- Swati, T. I., Vijay, V. K., & Ghosh, P. (2018). Scenario of landfilling in India: problems, challenges, and recommendations. *Handbook of Environmental Materials Management*. Springer, Cham, 1-16.
https://doi.org/10.1007/978-3-319-58538-3_167-1
- Tatsi, A. A., & Zouboulis, A. I. (2002). A field investigation of the quantity and quality of leachate from a municipal solid waste landfill in a Mediterranean climate (Thessaloniki, Greece). *Advances in Environmental Research*, 6(3), 207-219.
[https://doi.org/10.1016/S1093-0191\(01\)00052-1](https://doi.org/10.1016/S1093-0191(01)00052-1)
- Taylor D (1948). *Fundamentals of Soil Mechanics*. John Wiley & Sons, New York, USA.
- Tchobanoglous G, Theisen H, Vigil S (1993). *Integrated solid waste management: Engineering principles and management issues*. McGraw-Hill, New York, USA.

- Tchounwou, P. B., Newsome, C., Williams, J., & Glass, K. (2008). Copper-induced cytotoxicity and transcriptional activation of stress genes in human liver carcinoma (HepG₂) cells. In *Metal ions in Biology and Medicine: Proceedings of the International Symposium on Metal Ions in Biology and Medicine held at Les ions metalliques en biologie et en medecine. Symposium international sur les ions metalliques*. (Vol. 10, p. 285). NIH Public Access.
- Tchounwou, P. B., Yedjou, C. G., Patlolla, A. K., & Sutton, D. J. (2012). Heavy metal toxicity and the environment. *Molecular, Clinical and Environmental Toxicology*, 133-164.
https://doi.org/10.1007/978-3-7643-8340-4_6
- Terzaghi K (1943). *Theoretical Soil Mechanics*, John Wiley & Sons, New York, USA.
- Thammathiwat, A., & Chim-oye, W. (2010). Effect of permeant liquid on the swell volume and permeability of geosynthetic clay liners. *Electronic Journal of Geotechnical Engineering*, 15, 1183-1197.
- Thangavel P, Rajannan G, Ramasamy K (2002). Evidence of hexavalent chromium in tannery waste contaminated soil. *Journal of Ecotoxicology & Environmental Monitoring*, 12:291-297.
- Themelis, N. J., & Mussche, C. (2013). Municipal solid waste management and waste-to-energy in the United States, China and Japan. In *2nd International Academic Symposium on Enhanced Landfill Mining, Houthalen-Helchteren* (pp. 14-16).
- USEPA (1989). *Characterization of Products Containing Lead and Cadmium in Municipal Solid Waste in the United States, 1970 to 2000*; EPA/530-SW-89-015B. Office of Solid Waste: Washington, DC
- Van Olphen, H. (1965). Thermodynamics of interlayer adsorption of water in clays. I.— Sodium vermiculite. *Journal of Colloid Science*, 20(8), 822-837.
[https://doi.org/10.1016/0095-8522\(65\)90055-3](https://doi.org/10.1016/0095-8522(65)90055-3)
- Vega, J. L., Ayala, J., Loreda, J., & Iglesias, J. G. (2005). Bentonites as adsorbents of heavy metals ions from mine waste leachates: Experimental data. In *9th International Mine Water Congress*, Oviedo, Spain (pp. 603-609).
- Vengris, T., Binkien, R., & Sveikauskait, A. (2001). Nickel, copper and zinc removal from waste water by a modified clay sorbent. *Applied Clay Science*, 18(3-4), 183-190.
[https://doi.org/10.1016/S0169-1317\(00\)00036-3](https://doi.org/10.1016/S0169-1317(00)00036-3)

- Vhahangwele, M., & Mugeru, G. W. (2015). The potential of ball-milled South African bentonite clay for attenuation of heavy metals from acidic wastewaters: Simultaneous sorption of Co^{2+} , Cu^{2+} , Ni^{2+} , Pb^{2+} , and Zn^{2+} ions. *Journal of Environmental Chemical Engineering*, 3(4), 2416-2425.
<https://doi.org/10.1016/j.jece.2015.08.016>
- Vieira, M. G. A., Neto, A. A., Gimenes, M. L., & Da Silva, M. G. C. (2010). Sorption kinetics and equilibrium for the removal of nickel ions from aqueous phase on calcined Bofe bentonite clay. *Journal of Hazardous Materials*, 177(1-3), 362-371.
<https://doi.org/10.1016/j.jhazmat.2009.12.040>
- Vimonses, V., Lei, S., Jin, B., Chow, C. W., & Saint, C. (2009). Kinetic study and equilibrium isotherm analysis of Congo Red adsorption by clay materials. *Chemical Engineering Journal*, 148(2-3), 354-364.
<https://doi.org/10.1016/j.cej.2008.09.009>
- Wan, A. W. L., Graham, J., & Gray, M. N. (1990). Influence of soil structure on the stress-strain behavior of sand-bentonite mixtures. *Geotechnical Testing Journal*, 13(3), 179-187.
<https://doi.org/10.1520/GTJ10156J>
- Warkentin, B. P. (1961). Interpretation of the upper plastic limit of clays. *Nature*, 190(4772), 287-288.
<https://doi.org/10.1038/190287a0>
- Weimin, M. Y., Zhang, F., Chen, B., Chen, Y. G., Wang, Q., & Cui, Y. J. (2014). Effects of salt solutions on the hydro-mechanical behavior of compacted GMZ01 bentonite. *Environmental Earth Sciences*, 72(7), 2621-2630.
<https://doi.org/10.1007/s12665-014-3169-x>
- WHO/FAO/IAEA (1996). *Trace elements in human nutrition and health*. World Health Organization, Geneva, Switzerland
- Widmer, R., Oswald-Krapf, H., Sinha-Khetriwal, D., Schnellmann, M., & Böni, H. (2005). Global perspectives on e-waste. *Environmental Impact Assessment Review*, 25(5), 436-458.
<https://doi.org/10.1016/j.eiar.2005.04.001>
- Wilson, D. N. (1988). Cadmium-market trends and influences. In *Cadmium 87. Proceedings of the 6th International Cadmium Conference, London, Cadmium Association* (Vol. 9, p. 16).

- Wong, C. S., Wu, S. C., Duzgoren-Aydin, N. S., Aydin, A., & Wong, M. H. (2007). Trace metal contamination of sediments in an e-waste processing village in China. *Environmental Pollution*, *145*(2), 434-442.
<https://doi.org/10.1016/j.envpol.2006.05.017>
- Xue, Q., Zhang, Q., & Liu, L. (2012). Impact of high concentration solutions on hydraulic properties of geosynthetic clay liner materials. *Materials*, *5*(11), 2326-2341.
<https://doi.org/10.3390/ma5112326>
- Yang, S., Zhao, D., Zhang, H., Lu, S., Chen, L., & Yu, X. (2010). Impact of environmental conditions on the sorption behavior of Pb (II) in Na-bentonite suspensions. *Journal of Hazardous Materials*, *183*(1-3), 632-640.
<https://doi.org/10.1016/j.jhazmat.2010.07.072>
- Yoda, R. M., Chirawurah, D., & Adongo, P. B. (2014). Domestic waste disposal practice and perceptions of private sector waste management in urban Accra. *BMC Public Health*, *14*(1), 1-10.
<https://doi.org/10.1186/1471-2458-14-697>
- Yong, R. N., & Di Perno, N. (1991). Sources and characteristics of waste-with specific reference to Canada. *Geotechnical Research Centre, McGill University, Montreal, Quebec, Canada*.
- Yoshida, M., Ahmed, S., Nebil, S., & Ahmed, G. (2002). Characterization of leachate from Henchir El Yahoudia close landfill. *Water Waste Environ Res*, *1*(2), 129-42.
- Young, R. (2012). *Soil properties and behaviour* (Vol. 5). Elsevier Scientific Company, Amsterdam, The Netherlands.
- Zai, M., Ferchichi, M., Ismaï, A., Jenayeh, M., & Hammami, H. (2004). Rehabilitation of El Yahoudia dumping site, Tunisia. *Waste Management*, *24*(10), 1023-1034.
<https://doi.org/10.1016/j.wasman.2004.07.002>
- Zhang, F., Low, P. F., & Roth, C. B. (1995). Effects of monovalent, exchangeable cations and electrolytes on the relation between swelling pressure and interlayer distance in montmorillonite. *Journal of Colloid and Interface Science*, *173*(1), 34-41.
<https://doi.org/10.1006/jcis.1995.1293>
- Zhang, S. Q., & Hou, W. G. (2008). Adsorption behavior of Pb (II) on montmorillonite. *Colloids and Surfaces A: Physicochemical and Engineering Aspects*, *320*(1-3), 92-97.
<https://doi.org/10.1016/j.colsurfa.2008.01.038>

- Zhu, C. M., Ye, W. M., Chen, Y. G., Chen, B., & Cui, Y. J. (2013). Influence of salt solutions on the swelling pressure and hydraulic conductivity of compacted GMZ01 bentonite. *Engineering Geology*, 166, 74-80.
<https://doi.org/10.1016/j.enggeo.2013.09.001>
- Zhu, S., & Qin, Y. (2017). Adsorption of Lead from Aqueous Solutions to Bentonite and Composite. In *Characterization of Minerals, Metals, and Materials 2017* (pp. 91-100). Springer, Cham.
https://doi.org/10.1007/978-3-319-51382-9_11





Publications

INTERNATIONAL JOURNALS (Published)

1. **Ray S., Mishra A.K., Kalamdhad A.S.** 2021. Influence of Synthetic and Fresh municipal solid waste leachate on consolidation parameters of bentonites. *Environmental Science and Pollution Research*. [I.F. 3.06, Q2].
DOI: <https://doi.org/10.1007/s11356-021-12863-4>
2. **Ray, S., Mishra, A.K. and Kalamdhad, A. S.** 2021. Adsorption and hydraulic conductivity studies on bentonites in presence of Copper Solutions. *Journal of Hazardous, Toxic, and Radioactive Waste* 25(2), 06020007. [I.F. 1.44, Q3].
DOI: [https://doi.org/10.1061/\(ASCE\)HZ.2153-5515.0000588](https://doi.org/10.1061/(ASCE)HZ.2153-5515.0000588)
3. **Ray, S., Kalamdhad, A. S. and Mishra, A.K.** 2020. Bentonites as a Copper Adsorbent: Equilibrium, pH, Agitation, Dose, and Kinetic Effect Studies. *Journal of Hazardous, Toxic, and Radioactive Waste*, 24(1), 04019027. [I.F. 1.44, Q3].
DOI: [https://doi.org/10.1061/\(ASCE\)HZ.2153-5515.0000476](https://doi.org/10.1061/(ASCE)HZ.2153-5515.0000476)
4. **Ray, S., Mishra, A.K. and Kalamdhad, A. S.** 2020. Equilibrium, kinetic and hydraulic study of different Indian bentonites in presence of lead. *European Journal of Environmental and Civil Engineering*. [I.F. 2.52, Q2].
DOI: <https://doi.org/10.1080/19648189.2020.1754297>
5. **Ray, S., Mishra, A.K. and Kalamdhad, A.** 2019. Influence of various concentration of lead on consolidation parameters of bentonite. *International Journal of Geotechnical Engineering*. [I.F. 1.74, Q2].
DOI: <https://doi.org/10.1080/19386362.2019.1618029>

INTERNATIONAL JOURNALS (Under Review)

1. **Ray, S., Mishra, A.K. and Kalamdhad, A. S.** Evaluation of Equilibrium, Kinetic and Hydraulic Characteristics of Indian Bentonites in Presence of Heavy metal for Landfill Application. *Journal of Cleaner Production*. (**Review Comments Submitted**). [I.F. 7.25, Q1].
2. **Ray S., Mishra A.K., Kalamdhad A.S.** Impact of Real and Simulated Municipal Solid Waste Leachates on the Hydraulic and Swelling Behaviour of Bentonites for Landfill Application. *Environmental Monitoring and Assessment*. (**Review Comments Submitted**). [I.F. 1.90, Q2].
3. **Ray S., Mishra A.K., Kalamdhad A.S.** Effect of lead, copper and zinc on the change in behaviour of bentonites. *Environmental Technology*.

4. **Ray S.**, Mishra A.K., Kalamdhad A.S. Hydraulic performance, consolidation characteristics and shear strength analysis of bentonites in the presence of fly-ash, sewage sludge and paper-mill leachate for landfill application. *Journal of Environmental Management*.

BOOK CHAPTERS (Published/Accepted for Publication)

1. **Ray S.**, Chowdhury B.R., Mishra A.K., Kalamdhad A.S. 2021 Influence of the Presence of Zinc on the Behaviour of Bentonite. In: *Problematic Soils and Geoenvironmental Concerns* vol. 88. (pp. 295 -306) Springer, Singapore.
DOI: https://doi.org/10.1007/978-981-15-6237-2_25
2. **Ray, S.**, Mishra, A.K. and Kalamdhad, A.S. 2020. Adsorption and Hydraulic Conductivity Studies on Bentonites in the Presence of Zinc. In: *Advances in Computer Methods and Geomechanics* (pp. 489-500). Springer, Singapore.
DOI: https://doi.org/10.1007/978-981-15-0886-8_40
3. **Ray, S.**, Mishra, A.K. and Kalamdhad, A.S. 2020. Impact on Bentonite Due to the Presence of Various Concentrations of Lead and Copper Solutions. In: *Sustainable Environmental Geotechnics* (pp. 323-331). Springer, Cham.
DOI: https://doi.org/10.1007/978-3-030-51350-4_33
4. **Ray, S.**, Chowdhury, B.R., Mishra, A.K. and Kalamdhad, A.S. October 2018. Impact of Heavy Metals on Consolidation Properties of Bentonite. In: *The International Congress on Environmental Geotechnics* (pp. 567-574). Springer, Singapore.
DOI: https://doi.org/10.1007/978-981-13-2224-2_70
5. **Ray, S.**, Mishra, A.K. and Kalamdhad, A.S., 2021. Removal of lead and copper by using bentonite as an adsorbent. In: *Integrated Approaches Towards Solid Waste Management*. *(Accepted for Publication)*.
DOI: In Press
6. **Ray, S.**, Mishra, A.K. and Kalamdhad, A.S., 2021. Influence of lead and copper on behavioural changes of compacted bentonite. In: *Japanese Geotechnical Society Special Publication*. *(Accepted for Publication)*.
DOI: In Press

CONFERENCE PROCEEDINGS (International conferences)

1. **Ray, S.**, Mishra, A.K. and Kalamdhad, A.S. 2020. Adsorption and Hydraulic Conductivity Studies on Bentonites in the Presence of Zinc., *International IACMAG Symposium*, Gandhinagar, India.

2. **Ray S.**, Mishra A.K., Kalamdhad A.S. 2020. Removal of lead and copper by using bentonite as an adsorbent. *RECYCLE 2020*, Guwahati, India.
3. **Ray S.**, Mishra A.K., Kalamdhad A.S. 2019. Impact of bentonite in presence of various concentration of lead and copper solution, *2nd International Conference on Environmental Geotechnology, Recycled Waste Material and Sustainable Engineering*, UIC, Chicago.
4. **Ray S.**, Chowdhury B.R., Mishra A.K., Kalamdhad A.S. 2018. Impact of Heavy Metals on Consolidation Properties of Bentonite, *8th International Congress on Environmental Geotechnics*, Hangzhou, China.
5. **Ray S.**, Mishra A.K., Kalamdhad A.S., Chowdhury B.R. 2018. Influence of the presence of lead on the behaviour of bentonites, *RECYCLE 2018*, Guwahati, India
6. Chowdhury B.R., **Ray S.**, Mishra A.K., Kalamdhad A.S. 2018. Influence of bentonite in presence of various concentration of copper solution. *RECYCLE 2018*, Guwahati, India
7. **Ray S.**, Mishra A.K., Kalamdhad A.S. 2020. Influence of Lead and Copper on behavioural changes of Compacted Bentonite. *CPEG*, Kyoto, Japan. (*Accepted for Presentation*).

CONFERENCE PROCEEDINGS (National conferences)

1. **Ray, S.**, Chowdhury, B.R., Mishra, A.K., and Kalamdhad, A.S. 2018. Influence of the presence of Zinc on the behaviour of bentonite, *Indian Geotechnical Conference*, Bangalore, India.
2. **Ray, S.**, Mishra, A.K., and Kalamdhad, A.S. 2017. Behaviour of bentonite in presence of heavy metal, *Indian Geotechnical Conference*, Guwahati, India.

WORKSHOP ATTENDED

International Workshop on Promoting Sustainable Protection and Restoration of Soil, Groundwater and Water Environment conducted by Taiwan Ministry of Science and Technology (MOST) in National Cheng Kung University, Tainan from September 22 to 29, 2019.

AWARDS

Best Poster presentation titled “**Beneficial Conversion of Domestic Bio-waste**” in 1st International Conference on Waste Management, jointly organised by Waste Management Research Group and Association of Civil Engineers, held at IIT Guwahati.

